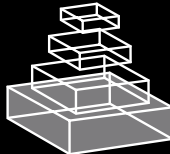


frontiers RESEARCH TOPICS

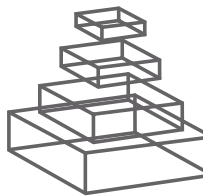
INTRA- AND INTER-SPECIES
INTERACTIONS IN MICROBIAL
COMMUNITIES

Topic Editors

Luis R. Comolli, Birgit Luef and
Manfred Auer



frontiers in
MICROBIOLOGY



FRONTIERS COPYRIGHT STATEMENT

© Copyright 2007-2015
Frontiers Media SA.
All rights reserved.

All content included on this site, such as text, graphics, logos, button icons, images, video/audio clips, downloads, data compilations and software, is the property of or is licensed to Frontiers Media SA ("Frontiers") or its licensees and/or subcontractors. The copyright in the text of individual articles is the property of their respective authors, subject to a license granted to Frontiers.

The compilation of articles constituting this e-book, wherever published, as well as the compilation of all other content on this site, is the exclusive property of Frontiers. For the conditions for downloading and copying of e-books from Frontiers' website, please see the Terms for Website Use. If purchasing Frontiers e-books from other websites or sources, the conditions of the website concerned apply.

Images and graphics not forming part of user-contributed materials may not be downloaded or copied without permission.

Individual articles may be downloaded and reproduced in accordance with the principles of the CC-BY licence subject to any copyright or other notices. They may not be re-sold as an e-book.

As author or other contributor you grant a CC-BY licence to others to reproduce your articles, including any graphics and third-party materials supplied by you, in accordance with the Conditions for Website Use and subject to any copyright notices which you include in connection with your articles and materials.

All copyright, and all rights therein, are protected by national and international copyright laws.

The above represents a summary only. For the full conditions see the Conditions for Authors and the Conditions for Website Use.

ISSN 1664-8714
ISBN 978-2-88919-449-0
DOI 10.3389/978-2-88919-449-0

ABOUT FRONTIERS

Frontiers is more than just an open-access publisher of scholarly articles: it is a pioneering approach to the world of academia, radically improving the way scholarly research is managed. The grand vision of Frontiers is a world where all people have an equal opportunity to seek, share and generate knowledge. Frontiers provides immediate and permanent online open access to all its publications, but this alone is not enough to realize our grand goals.

FRONTIERS JOURNAL SERIES

The Frontiers Journal Series is a multi-tier and interdisciplinary set of open-access, online journals, promising a paradigm shift from the current review, selection and dissemination processes in academic publishing.

All Frontiers journals are driven by researchers for researchers; therefore, they constitute a service to the scholarly community. At the same time, the Frontiers Journal Series operates on a revolutionary invention, the tiered publishing system, initially addressing specific communities of scholars, and gradually climbing up to broader public understanding, thus serving the interests of the lay society, too.

DEDICATION TO QUALITY

Each Frontiers article is a landmark of the highest quality, thanks to genuinely collaborative interactions between authors and review editors, who include some of the world's best academicians. Research must be certified by peers before entering a stream of knowledge that may eventually reach the public - and shape society; therefore, Frontiers only applies the most rigorous and unbiased reviews.

Frontiers revolutionizes research publishing by freely delivering the most outstanding research, evaluated with no bias from both the academic and social point of view.

By applying the most advanced information technologies, Frontiers is catapulting scholarly publishing into a new generation.

WHAT ARE FRONTIERS RESEARCH TOPICS?

Frontiers Research Topics are very popular trademarks of the Frontiers Journals Series: they are collections of at least ten articles, all centered on a particular subject. With their unique mix of varied contributions from Original Research to Review Articles, Frontiers Research Topics unify the most influential researchers, the latest key findings and historical advances in a hot research area!

Find out more on how to host your own Frontiers Research Topic or contribute to one as an author by contacting the Frontiers Editorial Office: researchtopics@frontiersin.org

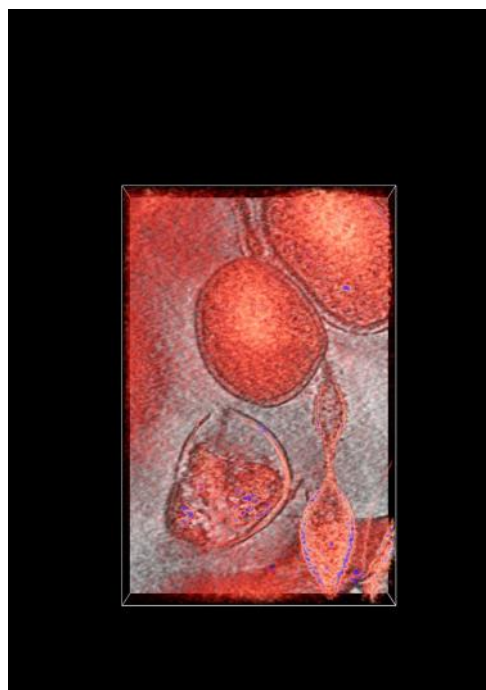
INTRA- AND INTER-SPECIES INTERACTIONS IN MICROBIAL COMMUNITIES

Topic Editors:

Luis R. Comolli, Lawrence Berkeley National Laboratory, USA

Birgit Luef, Norwegian University of Science and Technology, Norway

Manfred Auer, Lawrence Berkeley National Laboratory, USA



Inter-species interconnections in environmental microbial communities. We are looking at an approximately 50-voxel-thick slice through a tomographic reconstruction on top of a one-voxel-thick slice in grey scale. There is thus a depth to the view as our eyes project part of the volume, indicated by the box, onto the plane. There is a round ARMAN cell at the center and what appears to be an extension from a different cell type into it, pinching through the cell wall. This cell is a Thermoplasmata. The Thermoplasmatales are an order of the Thermoplasmata, a class of the Euryarchaeota. All are acidophiles, growing optimally at pH below 2. Many of these organisms do not contain a cell wall, as is the case for the Plasma shown in this image. They adopt various shapes, and tend to form buds that are freed from the main organism. This can be clearly seen happening in the cell on the right.

Recent developments in various “OMICs” fields have revolutionized our understanding of the vast diversity and ubiquity of microbes in the biosphere. However, most of the current paradigms of microbial cell biology, and our view of how microbes live and what they are capable of, are derived from *in vitro* experiments on isolated strains. Even the co-culturing of mixed species to interrogate community behavior is relatively new. But the majority of microorganisms lives in complex communities in natural environments, under varying conditions, and often cannot be cultivated. Unless we obtain a detailed understanding of the near-native 3D ultrastructure of individual community members, the 3D spatial community organization, their metabolic interdependences, coordinated gene expression and the spatial organization of their macromolecular machines inventories as well as their communication strategies, we won’t be able to truly understand microbial community life.

How spatial and also temporal organization in cell–cell interactions are achieved remains largely elusive. For example, a key question in microbial ecology is what mechanisms microbes employ to respond when faced with prey, competitors or predators, and changes in external factors. Specifically, to what degree do bacterial cells in biofilms act individually or with coordinated responses? What are the spatial extent and coherence of coordinated responses? In addition, networks linking organisms across a dynamic range of physical constraints and connections should provide the basis for linked evolutionary changes under pressure from a changing environment. Therefore, we need to investigate microbial responses to altered or adverse environmental conditions (including phages, predators, and competitors) and their macromolecular, metabolic responses according to their spatial organization.

We envision a diverse set of tools, including optical, spectroscopical, chemical and ultrastructural imaging techniques that will be utilized to address questions regarding e.g. intra- and inter-organism interactions linked to ultrastructure, and correlated adaptive responses in gene expression, physiological and metabolic states as a consequence of the alterations of their environment. Clearly strategies for co-evolution and in general the display of adaptive strategies of a microbial network as a response to the altered environment are of high interest. While a special focus will be placed on terrestrial sole-species or mixed biofilms, we are also interested in aquatic systems, biofilms in general and microbes living in symbiosis.

In this Research Topic, we wish to summarize and review results investigating interactions and possibly networks between microbes of the same or different species, their co-occurrence, as well as spatiotemporal patterns of distribution. Our goal is to include a broad spectrum of experimental and theoretical contributions, from research and review articles to hypothesis and theory, aiming at understanding microbial interactions at a systems level.

Table of Contents

- 06 Intra- and Inter-Species Interactions in Microbial Communities**
Luis R. Comolli
- 09 The Lethal Cargo of *Myxococcus Xanthus* Outer Membrane Vesicles**
James E. Berleman, Simon Allen, Megan A. Danielewicz, Jonathan P. Remis, Amita Gorur, Jack Cunha, Masood Z. Hadi, David R. Zusman, Trent R. Northen, H.Ewa Witkowska and Manfred Auer
- 20 Phage–Host Interplay: Examples From Tailed Phages and Gram-Negative Bacterial Pathogens**
Soraya Chaturongakul and Puey Ounjai
- 28 Emergence of Microbial Networks as Response to Hostile Environments**
Dario Madeo, Luis R. Comolli and Chiara Mocenni
- 41 Methane Production From Protozoan Endosymbionts Following Stimulation of Microbial Metabolism Within Subsurface Sediments**
Dawn E. Holmes, Ludovic Giloteaux, Roberto Orellana, Kenneth H. Williams, Mark J. Robbins and Derek R. Lovley
- 50 Grappling Archaea: Ultrastructural Analyses of an Uncultivated, Cold-Loving Archaeon, and its Biofilm**
Alexandra K. Perras, Gerhard Wanner, Andreas Klingl, Maximilian Mora, Anna K. Auerbach, Veronika Heinz, Alexander J. Probst, Harald Huber, Reinhard Rachel, Sandra Meck and Christine Moissl-Eichinger
- 60 Identification of a Cyclic-di-GMP-Modulating Response Regulator that Impacts Biofilm Formation in a Model Sulfate Reducing Bacterium**
Lara Rajeev, Eric G. Luning, Sara Altenburg, Grant M. Zane, Edward E. K. Baidoo, Michela Catena, Jay D. Keasling, Judy D. Wall, Matthew W. Fields and Aindrila Mukhopadhyay
- 73 Inter-Species Interconnections in Acid Mine Drainage Microbial Communities**
Luis R. Comolli and Jill F. Banfield
- 81 Temporal Dynamics of Fibrolytic and Methanogenic Rumen Microorganisms During in Situ Incubation of Switchgrass Determined by 16S rRNA Gene Profiling**
Hailan Piao, Medora Lachman, Stephanie Malfatti, Alexander Sczyrba, Bernhard Knierim, Manfred Auer, Susannah G.Tringe, Roderick I. Mackie, Carl J. Yeoman and Matthias Hess
- 92 Persistence in the Shadow of Killers**
Robert M. Sinclair
- 97 Nutrient Cross-Feeding in the Microbial World**
Erica C. Seth and Michiko E. Taga

- 103 Variations in the Identity and Complexity of Endosymbiont Combinations in Whitefly Hosts**
Einat Zchori-Fein, Tamar Lahav and Shiri Freilich
- 111 Intercellular Communications in Multispecies Oral Microbial Communities**
Lihong Guo, Xuesong He and Wenyuan Shi
- 124 Volatile-Mediated Interactions Between Phylogenetically Different Soil Bacteria**
Paolina Garbeva, Cornelis Hordijk, Saskia Gerards and Wietse de Boer
- 133 Planctomycetes and Macroalgae, a Striking Association**
Olga M. Lage and Joana Bondoso
- 142 Plugging in or Goin Wireless: Strategies for Interspecies Electron Transfer**
Pravin Malla Shrestha and Amelia-Elena Rotaru



Intra- and inter-species interactions in microbial communities

Luis R. Comolli *

Beamline 4.2.2, Advanced Light Source, ALS-Molecular Biology Consortium, Berkeley, CA, USA

*Correspondence: lrc.comolli@gmail.com

Edited by:

Lisa Y. Stein, University of Alberta, Canada

Reviewed by:

Jay T. Lennon, Indiana University, USA

Keywords: archaea, microbial communities, inter-species interactions, uncultivated biofilms, microbial networks

In this Special Topic we explore some of the novel mechanisms interconnecting microbes within and across species, and to their physical environment, across vastly different scales.

As developments in various “OMICs” fields have revolutionized our understanding of the vast diversity and ubiquity of microbes in the biosphere, we have also developed new holistic ways of thinking about them. Human microbiome scientists are currently thinking about the whole set of microorganisms in the human intestine as a single entity or as one organism (Li, 2014). In the confined environment of the human body and subjected to a tight interaction with the host, this conceptual shift from individual microbes and “species” to their integrated set of inputs and outputs may seem natural. Individual microbes react individually to the host environment in the context of other microbes and their mutual interactions, producing as a result an integrated collective behavior. The human body in turn processes and reacts to this aggregated result, the behavior and actions of the whole microbial community. Thus, while individual bacteria interactions occur at the nanoscale size range, bacterial communities are shaped by landscape structures from the microscale or larger and produce collective behavior at such a scale as well.

More open systems are potentially more complex, at least in terms of having variable or open physical boundaries and a less tightly regulated dynamic range of local properties. Nonetheless, across a wide range of diverse environments (soils, lakes, coral reefs, hot and acidic extreme environments, subsurface aquifers, and living organisms from plants to animals), whole populations of microorganisms have developed system-wide homeostatic adaptations to external factors (Fernandez et al., 2014 and references therein; Karatan and Watnick, 2009). The chemical transmissions of information underlying collective behaviors such as in quorum sensing have been recognized for a long time (Ryan and Dow, 2008 and references therein), but we are referring here to more intimate relationships. In the case of biofilms it is natural to compare them with tissues (Hall-Stoodley et al., 2004; Karatan and Watnick, 2009; Subbiahdoss et al., 2009), with various cell types and the extracellular substances as a matrix holding the whole together. Genomics data increasingly point toward the co-existence of metabolically incomplete individual “species” across environments, including microorganisms within planktonic systems such as subsurface aquifers (Wrighton et al.,

2012; Castelle et al., 2013). There seems to be a wide range of phenomena beyond the use of chemical signals to synchronize behavior across entire populations.

The type and extent of microbe-microbe and microbe-host nutritional interactions will determine the metabolism of the entire community in a given environment. We would expect the choice between biofilm formation and planktonic growth to be accurately regulated. Indeed, Rajeev et al. (2014) report on two diguanylate cyclases (DGCs) in the bacterium *Desulfovibrio vulgaris* Hildenborough that function as part of two-component signaling pathway, each one specific for one choice of growth fate. Once the fate has been committed, the type of interactions, topological relationships and constraints, and the physical means to establish them determine metabolic strategies. Nutrient sharing and electron transfer among microbes are reviewed by Seth and Taga (2014), and Shrestha and Rotaru (2014), respectively. Microbial community members can also gather energy cooperatively, from chemical reactions no single species can catalyze. Two types of electron transfer between microorganisms are recognized: the transfer of chemical intermediate in redox reactions and direct electron transfer. These and possibly other modes of nutrient and energy sharing between microbes are just starting to be investigated through mechanistic and structural studies.

The physical means used by microbes to form networks or affect other microbes at a distance are surprising and somewhat counter-intuitive within old paradigms of species. Perras et al. (2014) examined uncultivated biofilms taken directly from a natural sulfidic marsh (Sippenauer Moor near Regensburg, Bavaria, Germany) by transmission and scanning electron microscopy (TEM and SEM). The dominant *SM1 Euryarchaeon* uses thin appendages to connect to other cells of the same species forming a network in which each cell has an average of six connections, but also connects to cells of other species. In fact, the archaeal cells appear to connect to bacteria, establishing an interaction across two kingdoms of life. Comolli and Banfield (2014) linked cryogenic TEM with genomics and proteomics to show a range of physical interactions and connections between archaeal cells of different species, including “synapse-like” and tubular connections through cell wall openings. The inner diameters of some of these connections are large enough to enable the exchange of the largest cytoplasmic macromolecules and

molecular machines. Berleman et al. (2014) used conventional TEM, Mass Spectrometry analysis and biochemistry to investigate outer membrane vesicles (OMV) produced by *Myxococcus xanthus*, a bacterial micro-predator known for hunting other microbes. They analyzed the protein and small molecule cargo of OMVs conclusively proving that they are associated with antibiotic activity, including the product of gene *mepA*, an M36 protease homolog. Taken together these three contributions show physical means used by microbes to affect other microbes within their environment but at a distance: how they establish vast networks with new physical properties than those of individual microbes; how they interconnect across species physically, in principle enabling the exchange of gene products; and releasing enzymatic cargo.

Given a set of experimental observations, models allow us to explore the minimal set of rules and relationships that could account for the data; numerical simulations and models also serve to generate new hypothesis or extend questions beyond the available experimental data (Silva, 2011). In this Special topic Madeo et al. (2014) apply game theory in a first model that accounts for the observed patterns of inter-species interconnections in imaging data. Sinclair (2014) shows the counter-intuitive possibility of killer and prey co-existence, an insight of potentially wide impact. As more extensive imaging data across modalities shows us patterns and relationships for different types of microbial communities, and highly-resolved metabolomics capabilities resolving essential co-dependencies are developed, a new generation of modeling efforts of increasing power and sophistication will play a key role. New models will likely incorporate dozens to hundreds of secreted chemicals and metabolites that modulate the behavior, survival, and differentiation of members of the community, extending our ability to formulate new testable hypothesis.

We argue above that microbial communities in defined relationships or environments should be thought of holistically, and four papers in this Special Topic do just that. Holmes and co-authors investigated symbiotic associations of protozoa and endosymbiotic methanogens in groundwater communities (Holmes et al., 2014). They show how under certain conditions, the protozoa hosting endosymbionts become important members of the microbial community. As they feed on moribund biomass and produce methane, their system-wide conclusions are relevant for engineered bioremediation approaches in general. Hess and co-workers (Piao et al., 2014) used 16S rRNA gene profiling analysis of the cow cellulose-digesting anaerobic rumen ecosystem, where microbial-mediated fermentation degrades a complex mixture of cellulosic fibers. They show how diverse microbial taxonomic groups change in time, such that complete degradation is the results of their synergistic activity. Gathering an impressive dataset, Freilich and co-authors (Zchori-Fein et al., 2014) studied variations in the bacterial symbiotic communities of the sweet potato whitefly *Bemisia tabaci* (Hemiptera: Aleyrodidae). Compiling a dataset of over 2000 individuals derived from several independent screenings, the dataset is unprecedented in number of individuals as well as the geographical range and habitat diversity. Their work adds compelling evidence that facultative endosymbionts complement partial metabolic pathways in the

host, thus modulating their distribution patterns. Guo et al. (2014) allow us to expand our framework from terrestrial microbiology to human oral microbial communities whose synergistic activities can be pathogenic to us. They surveyed evidence of cell contact-dependent physical interactions, metabolic interdependencies, and synchronizing signaling systems which are used to maintain a balanced microbial community but also induce pathogenic pathways if we do not control them. Mechanisms conferring robustness, adaptability, and integrated responses are present in microbial communities from habitats that may seem inhospitable to us, to microbial communities common in human environments.

Perhaps conceptual aspects of the “holobiont” play a role at an entirely more subtle level, as volatile-mediated interactions can be expected to play an important role in information sharing, synchronization, and competition among physically separated microbes. Garbeva et al. (2014) report the first experimental study indeed proving antibiotic production levels and gene expression changes in one bacterial species, *Pseudomonas fluorescens Pf0-1*, as a consequence of the exposure to volatiles produced by four different species. In these cases microbes are in direct contact, confined in a structured space, which they can alter to some degree, and to which they must adapt too. We can thus reason that these physical aspects inevitably lead to networks and interactions. However, in the case of microbes distributed in space at non-obligatory short distances, indeed long variable distances, the emergence of communications and networks through volatile chemicals seems to more forcefully challenge the idea of “single individuals” or “single species.” This work contributes to expanding how we think of the concept “holobiont.”

Microorganisms with unique positions in the kingdom of life and the complex web of interactions they participate in are of great interest, as they can show us either evolutionary remnants or novel ways to solve the same problems. Lage and Bondoso review the relatively understudied interactions between Planctomycetes and macroalgae in the context of complex microbial biofilms (Lage and Bondoso, 2014). Planctomycetes share certain features with archaea, such as proteinaceous cell walls without peptidoglycan, and some distinctive characteristics with eukaryotes such as a complex system of endomembranes forming a unique cell plan. Completing our survey, Ounjai and Chaturongakul review how bacteriophages affect host gene expression (Chaturongakul and Ounjai, 2014). As microbes are under evolutionary pressure to improve environmental fitness, bacteriophages need to dynamically adapt to alter gene expression for their own survival. Microbes in turn can use part of the bacteriophages machinery as part of their tool box to compete with other microbes. They argue that imaging and structural work hold the key to further elucidating this complex evolutionary relationship.

We have presented a comprehensive survey showing physical interactions and connections between microbes of different species, co-occurrence patterns of distribution, and a range of metabolic interdependences across environments. As stated in the opening of this Special Topic, we believe there is a compelling need for imaging data across modalities, providing physical characterizations linking metagenomics and metaproteomics to microbial patterns of distribution and networks. We also look

forward for the development of novel imaging instrumentation and measurement technologies supporting an integrated analysis of communication among cytoplasmic compartments, between individual microbial cells, and within multicellular communities and biofilms.

REFERENCES

- Berleman, J. E., Allen, S., Danielewicz, M. A., Remis, J. P., Gorur, A., and Auer, M. (2014). The lethal cargo of *Myxococcus xanthus* outer membrane vesicles. *Front. Microbiol.* 5:474. doi: 10.3389/fmicb.2014.00474
- Castelle, C. J., Hug, L. A., Wrighton, K. C., Thomas, B. C., Williams, K. H., Wu, D., et al. (2013). Extraordinary phylogenetic diversity and metabolic versatility in aquifer sediment. *Nat. Commun.* 4, 2120. doi: 10.1038/ncomms3120
- Chaturongakul, S., and Ounjai, P. (2014). Phage–host interplay: examples from tailed phages and Gram-negative bacterial pathogens. *Front. Microbiol.* 5:442. doi: 10.3389/fmicb.2014.00442
- Comolli, L. R., and Banfield, J. F. (2014). Inter-species interconnections in acid mine drainage microbial communities. *Front. Microbiol.* 5:367. doi: 10.3389/fmicb.2014.00367
- Fernandez, L., Mercader, J. M., Planas-Félix, M., and Torrents, D. (2014). Adaptation to environmental factors shapes the organization of regulatory regions in microbial communities. *BMC Genomics* 15:877. doi: 10.1186/1471-2164-15-877
- Garbeva, P., Hordijk, C., Gerards, S., and de Boer, W. (2014). Volatile-mediated interactions between phylogenetically different soil bacteria. *Front. Microbiol.* 5:289. doi: 10.3389/fmicb.2014.00289
- Guo, L., He, X., and Shi, W. (2014). Intercellular communications in multispecies oral microbial communities. *Front. Microbiol.* 5:328. doi: 10.3389/fmicb.2014.00328
- Hall-Stoodley, L., Costerton, J. W., and Stoodley, P. (2004). Bacterial biofilms: from the natural environment to infectious diseases. *Nat. Rev. Microbiol.* 2, 95–108. doi: 10.1038/nrmicro821
- Holmes, D. E., Giloteaux, L., Orellana, R., Williams, K. H., Robbins, M. J., and Lovley, D. (2014). Methane production from protozoan endosymbionts following stimulation of microbial metabolism within subsurface sediments. *Front. Microbiol.* 5:366. doi: 10.3389/fmicb.2014.00366
- Karatan, E., and Watnick, P. (2009). Signals, regulatory networks, and materials that build and break bacterial biofilms. *Microbiol. Mol. Biol. Rev.* 73, 310. doi: 10.1128/MMBR.00041-08
- Lage, O. M., and Bondoso, J. (2014). Planctomycetes and macroalgae, a striking association. *Front. Microbiol.* 5:267. doi: 10.3389/fmicb.2014.00267
- Li, Y. (2014). “Genomics and BGI, today and tomorrow,” in *Life Sciences Division Seminar* (Berkeley, CA: Lawrence Berkeley National Laboratory, LBNL).
- Madeo, D., Comolli, L. R., and Mocenni, C. (2014). Emergence of microbial networks as a response to hostile environments. *Front. Microbiol.* 5:407. doi: 10.3389/fmicb.2014.00407
- Perras, A. K., Wanner, G., Klingl, A., Mora, M., Auerbach, A. K., Heinz, V., et al. (2014). Grappling archaea: ultrastructural analyses of an uncultivated, cold-loving archaeon, and its biofilm. *Front. Microbiol.* 5:397. doi: 10.3389/fmicb.2014.00397
- Piao, H., Lachman, M., Malfatti, S., Sczryba, A., Knierim, B., Auer, M., et al. (2014). Temporal dynamics of fibrolytic and methanogenic rumen microorganisms during in situ incubation of switchgrass determined by 16S rRNA gene profiling. *Front. Microbiol.* 5:307. doi: 10.3389/fmicb.2014.00307
- Rajeev, L., Luning, E. G., Altenburg, S., Zane, G. Z., Baidoo, E. E., Catena, M., et al. (2014). Identification of a cyclic-di-GMP-modulating response regulator that impacts biofilm formation in a model sulfate reducing bacterium. *Front. Microbiol.* 5:382. doi: 10.3389/fmicb.2014.00382
- Ryan, R. P., and Dow, M. J. (2008). Diffusible signals and interspecies communication in bacteria. *Microbiology* 154, 1845–1858. doi: 10.1099/mic.0.2008/017871-0
- Seth, E. C., and Taga, M. E. (2014). Nutrient cross-feeding in the microbial world. *Front. Microbiol.* 5:350. doi: 10.3389/fmicb.2014.00350
- Shrestha, P. M., and Rotaru, A.-E. (2014). Plugging in or going wireless: strategies for interspecies electron transfer. *Front. Microbiol.* 5:237. doi: 10.3389/fmicb.2014.00237
- Silva, G. A. (2011). The need for the emergence of mathematical neuroscience: beyond computation and simulation. *Front. Comput. Neurosci.* 5:51. doi: 10.3389/fncom.2011.00051
- Sinclair, R. (2014). Persistence in the shadow of killers. *Front. Microbiol.* 5:342. doi: 10.3389/fmicb.2014.00342
- Subbiahdoss, G., Kuijper, R., Grijpma, D. W., van der Mei, H. C., and Busscher, H. J. (2009). Microbial biofilm growth vs. tissue integration: “The race for the surface” experimentally studied. *Acta Biomater.* 5, 1399–1404. doi: 10.1016/j.actbio.2008.12.011
- Wrighton, K. C., Thomas, B. C., Sharon, I., Miller, C. S., Castelle, C. J., VerBerkmoes, N. C., et al. (2012). Fermentation, hydrogen, and sulfur metabolism in multiple uncultivated bacterial phyla. *Science* 337, 1661–1665. doi: 10.1126/science.1224041
- Zchori-Fein, E., Lahav, T., and Freilich, S. (2014). Variations in the identity and complexity of endosymbiont combinations in whitefly hosts. *Front. Microbiol.* 5:310. doi: 10.3389/fmicb.2014.00310

Conflict of Interest Statement: The author declares that the research was conducted in the absence of any commercial or financial relationships that could be construed as a potential conflict of interest.

Received: 10 October 2014; accepted: 03 November 2014; published online: 24 November 2014.

*Citation: Comolli LR (2014) Intra- and inter-species interactions in microbial communities. *Front. Microbiol.* 5:629. doi: 10.3389/fmicb.2014.00629*

*This article was submitted to Terrestrial Microbiology, a section of the journal *Frontiers in Microbiology*.*

Copyright © 2014 Comolli. This is an open-access article distributed under the terms of the Creative Commons Attribution License (CC BY). The use, distribution or reproduction in other forums is permitted, provided the original author(s) or licensor are credited and that the original publication in this journal is cited, in accordance with accepted academic practice. No use, distribution or reproduction is permitted which does not comply with these terms.



The lethal cargo of *Myxococcus xanthus* outer membrane vesicles

James E. Berleman^{1,2,3}, Simon Allen⁴, Megan A. Danielewicz¹, Jonathan P. Remis¹, Amita Gorur¹, Jack Cunha¹, Masood Z. Hadi^{1,5,6}, David R. Zusman², Trent R. Northen¹, H. Ewa Witkowska⁴ and Manfred Auer^{1*}

¹ Life Sciences Division, Lawrence Berkeley National Laboratory, Berkeley, CA, USA

² Department of Molecular and Cell Biology, University of California, Berkeley, Berkeley, CA, USA

³ School of Biology, St. Mary's College, Moraga, CA, USA

⁴ Department of Obstetrics, Gynecology and Reproductive Science, UCSF Sandler-Moore Mass Spectrometry Core Facility, San Francisco, CA, USA

⁵ Space Biosciences Division, Synthetic Biology Program, NASA Ames Research Center, Moffett Field, CA, USA

⁶ Physical Biosciences Division, Lawrence Berkeley National Laboratory, Berkeley, CA, USA

Edited by:

Lisa Y. Stein, University of Alberta, Canada

Reviewed by:

Deborah R. Yoder-Himes, University of Louisville, USA

Garret Suen, University of Wisconsin-Madison, USA

Sharon Grayer Wolf, Weizmann Institute of Science, Israel

***Correspondence:**

Manfred Auer, Life Sciences Division, Lawrence Berkeley National Laboratory, Berkeley, CA 94720, USA

e-mail: mauer@lbl.gov

Myxococcus xanthus is a bacterial micro-predator known for hunting other microbes in a wolf pack-like manner. Outer membrane vesicles (OMVs) are produced in large quantities by *M. xanthus* and have a highly organized structure in the extracellular milieu, sometimes occurring in chains that link neighboring cells within a biofilm. OMVs may be a vehicle for mediating wolf pack activity by delivering hydrolytic enzymes and antibiotics aimed at killing prey microbes. Here, both the protein and small molecule cargo of the OMV and membrane fractions of *M. xanthus* were characterized and compared. Our analysis indicates a number of proteins that are OMV-specific or OMV-enriched, including several with putative hydrolytic function. Secondary metabolite profiling of OMVs identifies 16 molecules, many associated with antibiotic activities. Several hydrolytic enzyme homologs were identified, including the protein encoded by MXAN_3564 (*mepA*), an M36 protease homolog. Genetic disruption of *mepA* leads to a significant reduction in extracellular protease activity suggesting MepA is part of the long-predicted (yet to date undetermined) extracellular protease suite of *M. xanthus*.

Keywords: predation, fruiting body, predatory rippling, predator-prey interactions, secondary metabolism and enzymes

INTRODUCTION

The outer membrane (OM) of bacteria plays a crucial role in mediating cell-cell interactions for symbiotic and pathogenic relationships (Marshall, 2005; Cross, 2014). The OM provides a permeable barrier with important functions in transport and protection for the cell envelope of Gram-negative bacteria (Nikaido, 2003; Cornejo et al., 2014). Though the OM is often generalized, there is a great deal of diversity in this envelope structure that may help inform us on the evolutionary origin of the OM and the functional capacity of this structure (Vollmer, 2012; Jiang et al., 2014). One example of this OM diversity is the biosynthesis by some bacteria of OM vesicles (OMVs) (Beveridge, 1999; Mashburn-Warren et al., 2008), and more recently vesicle chains and tubes (Remis et al., 2014). OMVs provide a variety of additional functions to bacterial cells that go beyond the traditional concept of the OM, including the exchange of beneficial cell-cell communication signals, delivery of harmful toxins in pathogenesis and microbial competition (Kesty et al., 2004; Mashburn and Whiteley, 2005; Evans et al., 2012). The larger, more complex chain and tube structures can also provide a network function analogous to mycelia and filamentous multicellular organizations (Wei et al., 2011; Remis et al., 2014).

Here, we examine the OMV cargo of *Myxococcus xanthus*, a delta-proteobacterium that produces copious amounts of

OM-derived structures. *M. xanthus* is a common soil bacterium that displays complex social behavior through the formation of multicellular structures that facilitate surface colonization during vegetative swarming, segregation of cell types through aggregation into fruiting bodies for differentiation into spores as well as predation of prey microorganisms (Berleman et al., 2006; Pelling et al., 2006; Velicer and Vos, 2009). The “wolf pack” predatory behavior of *M. xanthus* is of particular interest as cells are able to distinguish between self and non-self even when attacking other Gram-negative bacteria such as *E. coli* by lysing prey bacteria without the aid of phagocytosis (Berleman et al., 2008; Pan et al., 2013). The “wolf pack” response is observed during predation, where the judicious oscillation of cell reversals directs *M. xanthus* cell movement through prey colonies. The killing of *E. coli* cells has long been thought to depend on the secretion of antibiotics and proteolytic exoenzymes (Rosenberg et al., 1977). Here, we utilize liquid chromatography-mass spectrometry (LC-MS) approaches to define the molecular cargo that mediates the wolf pack predatory ability of *M. xanthus*.

The *M. xanthus* genome is large for bacteria, with 7331 predicted protein coding loci (Goldman et al., 2006). The large genome size is due in part to a large reservoir of genes coding for hydrolytic enzymes and secondary metabolite pathways, both of which are thought to benefit the predatory life style of

this microbe. A wide variety of secondary metabolites have been identified from *M. xanthus* and related organisms including natural products with antibiotic, antifungal and anti-tumor activity (Gerth et al., 1983; Krug et al., 2008; Li et al., 2014). Myxovirescin (also called antibiotic TA), the myxochelins and the myxalamids produced by *M. xanthus* all have antibiotic properties, but their expression and native function are not well understood (Gerth et al., 1983; Li et al., 2008; Xiao et al., 2012). The extracellular proteins that localize to matrix polysaccharides have previously been profiled, with one locus identified that is required for fruiting body development in certain backgrounds (Curtis et al., 2007). The protein profile of OMVs has been shown to differ between high nutrient and low nutrient conditions (Kahnt et al., 2010), but there is still little known about extracellular enzymatic activity in *M. xanthus*. Here, we identify a protease in *M. xanthus* similar to M36 fungalysins utilized by fungi for extracellular hydrolytic activity (Lilly et al., 2008).

RESULTS

FRACTIONATION OF VESICLES FROM OUTER MEMBRANES OF *M. XANTHUS*

OMV structures have been observed in a number of bacteria, but the full extent of their function(s) remains a topic of study. Lab cultures of *M. xanthus* produce OMVs, some of which remain tethered to the cell surface, whereas others are secreted into the extracellular environment (Palsdottir et al., 2009). The chemical composition of OMVs has been shown to include lipid, carbohydrate and protein macromolecules (Kahnt et al., 2010; Evans et al., 2012; Remis et al., 2014), all of which likely play a critical role in OMV organization and possibly in fusion of OMVs to other cells. To determine the secondary metabolite and protein

cargo of OMVs we isolated and purified OM and OMV fractions, respectively, from wild type cells using ultracentrifugation and serial filtration (Figure 1A). The presence of OMVs structures were confirmed by both transmission electron microscopy (TEM) of whole cells (Figure 1B) and after OMV purification (see Figures 1C,D) and normalized via quantifying incorporation of the lipophilic dye FM4-64 as described previously (Remis et al., 2014). This confirmed that the integrity of the vesicle structures was maintained throughout the preparation (see Figures 1C,D). SDS-PAGE analysis of our OMV preparations indicates a large number of proteins in this fraction, in agreement with previous studies on extracellular fractionation (Kahnt et al., 2010).

MASS SPECTROMETRY OF CELL FRACTIONS IDENTIFIED A UNIQUE OMV PROTEIN CARGO

To determine the protein cargo of each cell fraction, proteins isolated from purified vesicles and whole cell membranes were digested with trypsin and proteolytic peptides examined by reversed phase (RP) liquid chromatography (LC) mass spectrometry (MS). RP LCMS analysis of three OMV and membrane fractions from independent cultures delivered consistent results in terms of a number of matched peptides and identified proteins, summarized in Tables S1 and S2 (Supplement Data S1). The MS evidence for all protein identification in all samples based on peptides matched above the peptide identify threshold is shown in Supplement Data S2. A total of 287 and 786 proteins were identified in OMV and OM, respectively (Figure 2 and Table 1). Of these proteins, 88 proteins were detected only in the OMV fraction (S3), 199 were detected in both cell fractions (Table S4), and 583 proteins were detected only in the membrane fractions (S5). This comparison suggests that there is a protein

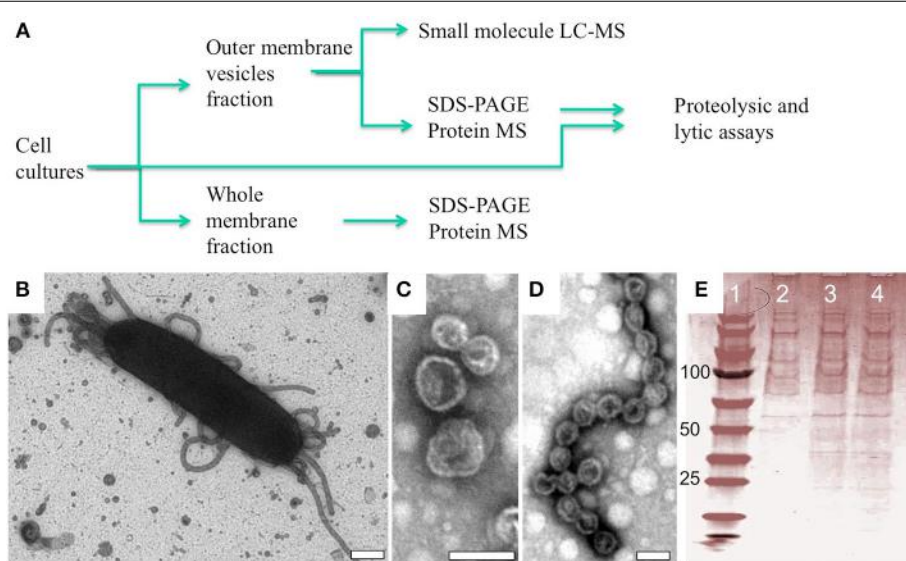


FIGURE 1 | OMV structures observed *in situ* and after purification.

(A) Flow chart of experimental procedure with representative analytics (B–E). (B) Negative staining EM of an *M. xanthus* wild type DZ2 cell showing a mixture of extracellular structures associated with the cell including isolated vesicles and vesicle chains (Scale bar = 200 nm).

After purification, these structures maintain their distinctive shape as (C) vesicles and (D) vesicle chains (Scale bars = 40 nm). (E) SDS-PAGE analysis showing consistency of protein profiles in OMV fractions used for protein MS: lane 1 standards, lane 2–4 OMV fractions from 3 independent cultures.

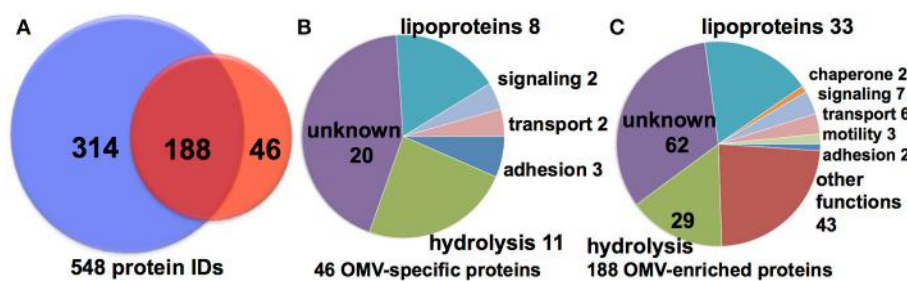


FIGURE 2 | Cell fraction comparison and predicted function. (A) Conservative set of 548 (46 OMV only, 188 shared, 314 OM only) protein IDs from MS analysis of >10,000 peptides. Putative function binning of (B) 46 OMV-specific and (C) 188 OMV-enriched proteins.

cargo that is unique to OMVs. There are 7331 total predicted proteins in the *M. xanthus* complete genome (Goldman et al., 2006), indicating that we have detected 12 % of the total genomic potential in these two fractions. To limit further analysis to proteins that were identified with the highest stringency, we reduced this pool by considering only proteins that were identified in at least two samples on the basis of at least two distinct peptides. This analysis yields a conservative set of 46 OMV-specific, 188 OMV-contained, and 314 membrane proteins, or 7.5 % of the total genome prediction (Figure 2A). (Nudelman et al., 2005; Ducret et al., 2013; Wei et al., 2014).

A majority of the identified OMV-specific proteins (20 of 46) are listed as uncharacterized hypothetical proteins, making functional prediction difficult (Figure 2B, Table 1). Of the remaining proteins identified in the purified OMV fraction, 8 are listed as putative lipoproteins and 11 have a putative hydrolytic activity. The latter include 7 proteins predicted to have peptidase or protease activity (MXAN_0587, MXAN_0805, MXAN_1650, MXAN_1967, MXAN_2760, MXAN_5454, and MXAN_5970). Chitinase (MXAN_4534), phosphoesterase (MXAN_3577), hydratase (MXAN_3162), and nuclease (MXAN_0366) enzymatic functions are also predicted. We also found several proteins predicted to be involved in extracellular functions, such as MXAN_0362 (putative pilus protein), MXAN_0889 (RCC1 repeat beta-propeller fold), and adhesins (MXAN_0510, and MXAN_4914). A similar distribution of functions was observed if we expand our analysis to the 234 OMV-enriched proteins (46 specific, 188 shared with membrane) detected (Figure 2C), with more hydrolytic functions, particularly peptidase and protease homologs. We also detected A-motility proteins, CglB, AgmO, and AgmV, supporting a role for OMVs in intra-species sharing of motility components, although it is still subject to debate whether OMVs are directly involved in the transfer of motility components between *M. xanthus* cells (Nudelman et al., 2005; Ducret et al., 2013; Wei et al., 2014). The detection of Agm motility proteins in membrane fractions supports previous findings (Luciano et al., 2011).

Of the 7331 predicted proteins in the total *M. xanthus* proteome, cellular localization programs (e.g., PSORTb), give expected localization for ~66% of the proteome, with most proteins predicted to reside in the cytoplasm or cytoplasmic membrane (see Figure 3). By comparison, the proteins detected in the OMV fraction are enriched for proteins with “unknown

localization.” While the membrane preparations are also enriched for OM and IM proteins, it is important to note that proteins we have identified in the OMV fraction come from all cell fractions based on the current predictions. This may be due to several factors: ubiquitous localization (e.g., proteins may localize to more than one fraction), misannotation (imperfect prediction algorithms), or contamination of a few proteins from another cell fraction during the purification process. However, the most abundant cytoplasmic proteins that are common artifacts of other cell fractions, e.g., ribosomal proteins (Choi et al., 2011), were rarely detected in our samples, indicating that cross contamination is least likely, and that this data will help to improve prediction programs.

ABUNDANCE OF OMV PROTEINS

The relative abundance of each protein in the samples was approximated by calculating its contribution to a sum of the exponentially modified protein indices (emPAI) assigned to each sample component (mol %) (Ishihama et al., 2005). Thus, generated (mol %) value estimates of relative protein abundances in each sample were then compared across the samples (Table 2, Tables S2–S4). Out of six proteins found in OMV at relative abundance above 2%, four appeared at a higher relative level in OMV than in the corresponding OM samples, i.e., lipoproteins (MXAN_6367 and MXAN_7333), a hydrolase (MXAN_0201) and a hypothetical protein (MXAN_5453). The other two, chaperonins GroEL1 (MXAN_4895) and GroEL2 (MXAN_4467) ranked as the first and third most abundant protein in OMV, albeit were present at ~50% level of the observed in OM. Nineteen proteins were enriched by more than 10-fold in OMV compared with membrane (OM) samples. Of those, nine have unknown function (leading with MXAN_1365 at >75 fold excess), five are lipoproteins (leading with MXAN_2277 at >30 fold excess), and three are hydrolases (an alpha/beta fold hydrolase, MXAN_0201, an M36 peptidase, MXAN_3564, and metal dependent amidohydrolase, MXAN_0886, the latter at >65 fold excess). Of note, three TonB-dependent receptor related proteins were found in OMV fractions (MXAN_6911, MXAN_4559, and MXAN_1450). The presence of two GroEL chaperone homologs coded for in the *M. xanthus* genome have been investigated previously, and GroEL1 has been shown to be essential for fruiting body development and sporulation, whereas GroEL2 plays a role in antibiotic production and predation (Li et al., 2010; Wang et al.,

Table 1 | MS analysis of purified vesicles and purified membrane fraction.

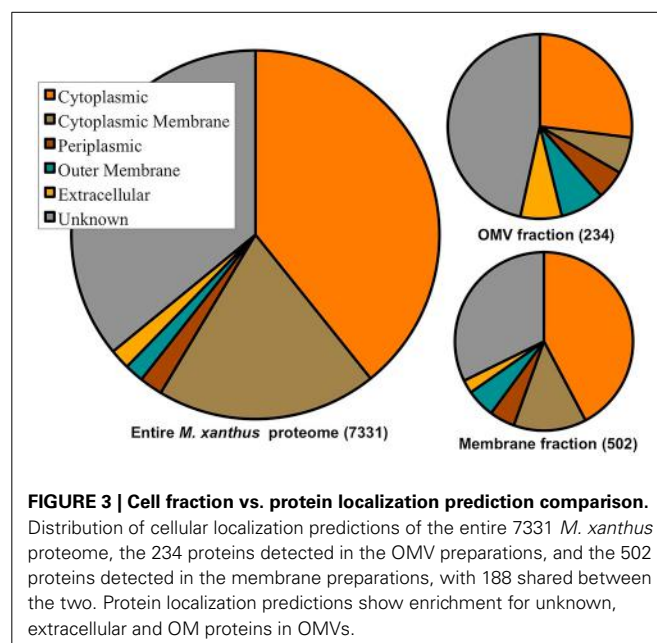
Loci	Putative functions
OMV SPECIFIC	
20 loci	Hypothetical proteins
8 loci	Putative lipoproteins
MXAN_0366	Endonuclease/exonuclease/phosphatase family protein
MXAN_0587	Trypsin domain protein
MXAN_0805	Peptidase, M10A/M12A subfamilies
MXAN_1650	Peptidase, S1A (chymotrypsin) subfamily
MXAN_1967	Putative peptidase, S8 (subtilisin) family
MXAN_2760	Peptidase, M28E family
MXAN_3162	Fumarate hydratase, class I
MXAN_3577	Metallophosphoesterase
MXAN_4534	Chitinase, class I
MXAN_5454	Peptidase, M36 (fungalsin) family
MXAN_5970	Peptidase, S8 (subtilisin) family
MXAN_0510	Putative cell wall surface anchor family protein
MXAN_4914	F5/8 type C domain protein
MXAN_5098	Putative Ig domain protein
MXAN_1668	Serine/threonine kinase associate protein
MXAN_5229	Putative GTP-binding protein
MXAN_0362	Putative pilus biogenesis operon protein
MXAN_0889	RCC1 repeat domain protein
OMV ENRICHED	
62 loci	Unknown
38 loci	Putative lipoproteins
43 loci	Other functions
MXAN_0201	Hydrolase, alpha/beta fold family
MXAN_0533	NAD dependent epimerase/dehydratase family
MXAN_0886	Metal dependent amidohydrolase
MXAN_1389	Putative alkaline phosphatase
MXAN_1394	Metallo-beta-lactamase family protein
MXAN_1564	Alkyl hydroperoxide reductase C
MXAN_1623	Peptidase, M16 (pitrylsin) family
MXAN_1624	Peptidase, M16 (pitrylsin) family
MXAN_2016	Prolyl endopeptidase precursor
MXAN_2382	Peptidase, M18 (aminopeptidase I) family
MXAN_2519	Peptidase U62
MXAN_2787	Homogentisate 1,2-dioxygenase
MXAN_2814	Putative N-acetyl muramoyl-Lalanine amidase
MXAN_2906	Penicillin acylase family protein
MXAN_3042	Glycine dehydrogenase
MXAN_3160	Peptidase, M13 (neprilysin) family
MXAN_3465	Histidine ammonia-lyase
MXAN_3564	Peptidase, M36 (fungalsin) family
MXAN_4146	Alanine dehydrogenase
MXAN_4327	Glu/Leu/Phe/Val dehydrogenase
MXAN_5040	Aldehyde dehydrogenase
MXAN_5326	Putative phytase
MXAN_5933	Peptidase, M48 (Ste24 endopeptidase) family
MXAN_6106	Matrix-associated zinc metalloprotease FibA
MXAN_6266	Putative 2,3-cyclic-nucleotide 2-phosphodiesterase
MXAN_6516	Adenosylhomocysteinase
MXAN_6539	Extracellular protease domain protein

(Continued)

Table 1 | Continued

Loci	Putative functions
MXAN_6601	Peptidase, S9C (acylaminocyl-peptidase) subfamily
MXAN_4796	Fibronectin type III domain protein
MXAN_4467	Chaperonin GroEL1
MXAN_4895	Chaperonin GroEL2
MXAN_2538	Adventurous gliding motility protein AgmO
MXAN_3060	Adventurous gliding motility protein CglB
MXAN_4865	Adventurous gliding motility protein AgmV
MXAN_1450	TonB-dependent receptor
MXAN_4559	TonB dependent receptor
MXAN_5766	TPR domain protein
MXAN_6248	Cyclic nucleotide-binding domain protein
MXAN_6911	TonB-dependent receptor
MXAN_5042	OmpA domain protein
MXAN_5598	OmpA domain protein
MXAN_6665	Putative branched chain amino acid ABC transporter

Vesicle protein cargo can be broken down into two groups, proteins that are consistently detected in the OMV purified samples, but not the membrane samples (OMV specific) and proteins are consistently detected and shared between the two cell fractions (OMV enriched). Data was collected from 3 independent vesicle purifications and membrane purifications. Pertinent data is shown here, full data set is available in Supplement Data S1.

**FIGURE 3 | Cell fraction vs. protein localization prediction comparison.**

Distribution of cellular localization predictions of the entire 7331 *M. xanthus* proteome, the 234 proteins detected in the OMV preparations, and the 502 proteins detected in the membrane preparations, with 188 shared between the two. Protein localization predictions show enrichment for unknown, extracellular and OM proteins in OMVs.

2014). The abundance of GroEL chaperonins in the OMV fraction suggests the possibility that OMV proteins may require proper protein folding after export into OMV structures. Also, GroEL proteins are known to function in large tetradecamer complexes, which may in part explain the high frequency of detection. The presence of TonB-dependent receptor proteins and a large number of hydrolytic enzymes suggests that OMVs contain transport and catalytic functions.

Table 2 | Relative abundance of proteins detected in vesicles through semi-quantitative MS analysis.

Prot_acc	Putative function	OMV Avg Score	OMV mol %	OM Avg Score	OM mol %	Relative ratio OMV/OM
MXAN_1365	Hypothetical protein	4448 ± 1517	1.3 ± 0.6	414 ± 62	0.02 ± 0.001	77.5
MXAN_4895	Chaperonin GroEL 2	4350 ± 908	8.2 ± 3.8	70526 ± 9769	16.3 ± 4.6	0.5
MXAN_1450	TonB-dependent receptor	3583 ± 875	1.6 ± 0.4	7244 ± 904	1 ± 0.2	1.6
MXAN_0962	Putative lipoprotein	3533 ± 628	1.2 ± 0.1	2760 ± 100	0.2 ± 0.01	5.8
MXAN_0201	Hydrolase, alpha/beta fold family	3272 ± 1094	2.6 ± 0.7	376 ± 313	0.2 ± 0.1	14.1
MXAN_5453	Hypothetical protein	2938 ± 979	2.6 ± 0.7	1368 ± 817	0.3 ± 0.2	9.4
MXAN_4467	Chaperonin GroEL 1	2515 ± 769	3.4 ± 1.1	33949 ± 6097	6.4 ± 1.6	0.5
MXAN_3564	Peptidase, M36 (fungalsin) family	2471 ± 737	0.4 ± 0.1	643 ± 430	0.04 ± 0.03	11.0
MXAN_4860	Hypothetical protein	2379 ± 383	0.8 ± 0.3	1162 ± 231	0.2 ± 0.01	3.7
MXAN_7199	Putative lipoprotein	1800 ± 711	0.4 ± 0.1	677 ± 95	0.1 ± 0.01	4.5

Table 3 | Secondary metabolites identified in OMV fractions.

Name	Putative function	RT	m/z	Mass	Molecular formula	Compound ID
Cittilin A	Antibiotic	4.5	631.275	630.268	C34H38N4O8	N/A
Dkxanthene 492 - 574	Yellow pigment	6.1–8.1	493.248–597.168*	492.238–574.280	C27H32N4O5-C32H38N4O6	N/A
Myxalamid A	Antibiotic	12.6	416.317	415.305	C26H41NO3	6440913
Myxalamid B	Antibiotic	11.7	402.301	401.291	C25H39NO3	5282085
Myxalamid C	Antibiotic	11.1	388.285	387.275	C24H37NO3	6439800
Myxochelin A	Chelating agent	4.7	405.167	404.16	C20H24N2O7	16093504
Myxochelin B	Chelating agent	2.7	404.183	403.177	C20H25N3O6	10873133
Myxovirescin A	Antibiotic	11.9	624.448	623.438	C35H61NO8	6450484

Metabolites were identified by LC MS analysis of OMV cell fractions, putative structures are shown in **Figure 3** and detailed tandem MS data in Supplement Data S2. m/z values indicate [M+H]⁺ except when noted; * denotes [M+Na]⁺.

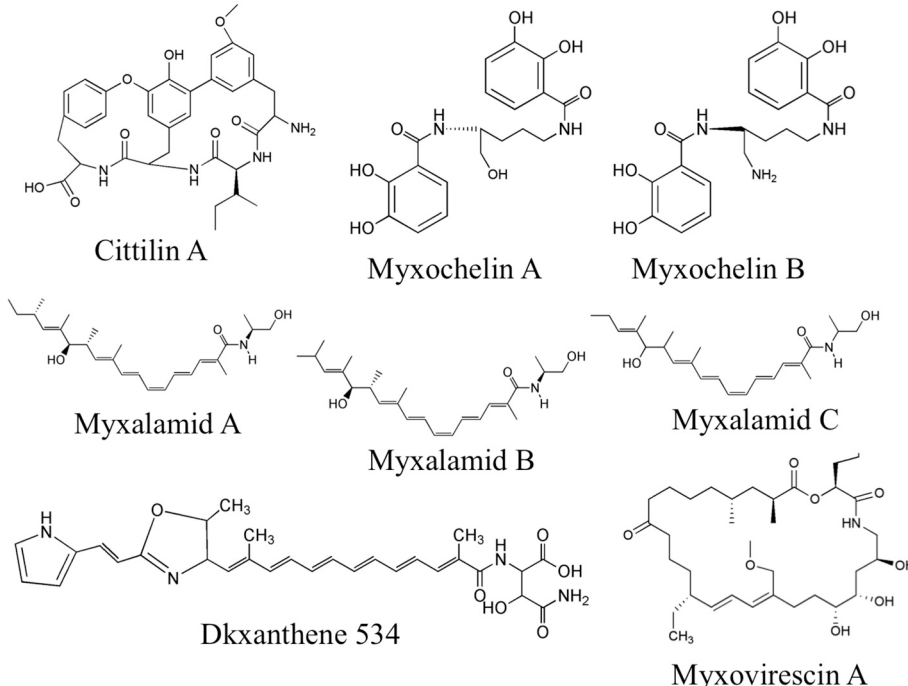
MASS SPECTROMETRY ANALYSIS OF SMALL MOLECULES IN OMVs

Purified OMV fractions of *M. xanthus* cultures were also prepared for analysis by Liquid Chromatography Mass spectrometry (LC/MS) for determination of secondary metabolites. Profiling was performed via targeted searches for known *M. xanthus* secondary metabolites (Krug et al., 2008; Kim et al., 2009; Weissman and Müller, 2010). Tandem MS (MS/MS) was performed to help identify 16 molecules from five chemical families based on accurate mass and MS/MS (Supplement Data S2). We detected and confirmed the presence in OMV fractions for two myxochelins (m/z of 404.183 and 405.167, respectively), three myxalamids (m/z of 416.317, 402.301, and 388.285, respectively), and nine dkxanthenes (m/z values ranging from 493.248 to 597.168) (**Table 3** for MS details, **Figure 4** for predicted structures). Myxochelins are iron chelating siderophores that have been shown, when purified, to have some antibacterial properties as well (Weissman and Müller, 2010). Myxochelin A can be synthesized from two molecules of 2,3-dihydroxybenzoic acid condensed with the amine groups of a lysine residue (Li et al., 2008). The myxalamids have desaturated linear or branched carbon backbones (C17–18 long), with hydroxyl residues at one end. The myxalamids have antibiotic properties by inhibiting the cytochrome I NADH:ubiquinone oxidoreductase (Gerth et al., 1983). Dkxanthenes have a common chemical backbone with many different R group potentials, resulting in a family of nine distinct, but related structures detected. The dkxanthenes are essential for viable-spore formation, and are also the major

yellow pigment present in myxobacteria (Meiser et al., 2006). In addition, cittilin A (m/z of 631.275) and myxovirescin (m/z of 624.448), both non-ribosomal peptide secondary metabolites, were detected. Cittilin A is a peptide antibiotic with a structure derived from three tyrosines and an isoleucine residue, with no known cellular target (Grabley and Thiericke, 1999). Myxovirescin A (also called TA) has a macrocyclic structure and is an antibiotic that inhibits type II signal peptidases during protein secretion (Xiao et al., 2012).

MepA IS A METALLOPROTEASE WITH EXTRACELLULAR ACTIVITY

The presence of an M36 metalloprotease homolog (locus MXAN_3564), which we will subsequently refer to as *mepA*, at high abundance in OMV fractions led to the hypothesis that this protein could be the long-predicted, but to date elusive enzyme for enabling extracellular digestion of protein during wolf pack predatory behavior. This hypothesis prompted us to construct an *mepA* insertion mutant, disrupting *MepA* function. The *mepA* insertion mutant strain was subjected to thorough physiological analysis (see below). The *mepA* gene is located downstream of MXAN_3563, a putative nucleoside epimerase predicted to be involved in membrane biogenesis (note that MXAN_3563 was not detected here in either OMV or OM fractions) and upstream of MXAN_3565 a hypothetical protein coded for on the opposite DNA strand. The *mepA* mutant construct was cultured and analyzed for social behaviors by observing growth at high density on low nutrient CFL media. Fruiting bodies were

**FIGURE 4 | Secondary metabolites detected in OMV fractions.**

Representative structures from tandem MS analysis of *M. xanthus* OMV fractions are shown, based on comparison to known *M. xanthus* products. Six chemical families were identified, most of

which have some antibiotic activity. Note that for the dkxanthene chemical family, nine distinct members were detected but only DKxanthene534 is shown. Further detail can be found in **Table 3** and Supplement Table 2.

observed to form with normal shape, distribution and timing in the *mepA* mutant, as expected (**Figures 5A,B**). When incubated in co-culture with *E. coli* prey on CFL media, the *mepA* mutant was observed to invade and lyse prey cells with normal timing and rippling behavior, indicating that it is not required for motility or lysis of prey (**Figures 5C,D**). We also examined *mepA* mutant cell cultures with SEM and TEM microscopy and observed the presence of OMV structures surrounding and attached to cells (**Figures 5E,F**).

To examine the putative proteolytic activity of the MepA protein, OMVs were isolated from both the *mepA* mutant and wild type DZ2. Using a resorufin labeled-casein protein substrate, we compared the protease activity of whole cells and purified OMVs in both strains (**Figure 5G**). Both whole cells and the OMV fractions of wild type showed rapid proteolytic activity, whereas the *mepA* mutant was deficient in both cases. The *mepA* mutant strain displayed only ~33 % of the rate of proteolysis compared to the wild type, suggesting that the *mepA* locus is an important part of the proposed extracellular protease cocktail produced by *M. xanthus*. It is unclear if this greatly reduced activity is due solely to MepA enzymatic activity or if loss of MepA has pleiotropic effects on other exoproteases of *M. xanthus*. It has previously been shown that OMVs mediate the killing of *E. coli* prey cells through the delivery of toxic proteins or antibiotics (Evans et al., 2012; Remis et al., 2014). Examination of these strains for lytic activity through incubation with mCherry-labeled *E. coli* cells indicated no difference between the rate of *E. coli* cell lysis by wild type *M. xanthus* and the *mepA* strain, suggesting that the protease

activity of *mepA* is utilized only as a secondary factor during predation, by breaking down protein released by already lysed cells (**Figure 5H**).

DISCUSSION

In addition to the paradigm that Gram-negative cells have cellular compartments consisting of cytoplasm, inner membrane, periplasm, and outer membrane, our data suggests that *M. xanthus* cells possess another distinct compartment, i.e., outer membrane vesicles. We find that OMVs contain a unique protein cargo, distinguished from proteins found in the membranes, that predict extracellular hydrolytic functions for OMVs. This is in agreement with data showing functional activity associated with OMV fractions (Evans et al., 2012; Remis et al., 2014). The detection of OMV-enriched and OMV-specific proteins suggests the ability of *M. xanthus* to sort proteins into OMVs, but further study is required to determine if there is a protein sorting mechanism for OMVs of proteobacteria analogous to the COPII vesicle trafficking in eukaryotic cells (Zanetti et al., 2012). Bhat et al., have proposed that a lysine residue at position +7 in the N-terminal sequence directs proteins to the extracellular matrix (ECM), whereas a lysine residue at position +2 directs proteins to the IM (Bhat et al., 2011). No similarly conserved signal has yet been identified for OM proteins or OMV proteins, nor do we know the mechanism by which OMV structures are produced, but this data set should help focus future studies on OMV formation in *M. xanthus*. Previous studies indicate that *M. xanthus* OMV biogenesis occurs anywhere along the cell resulting either

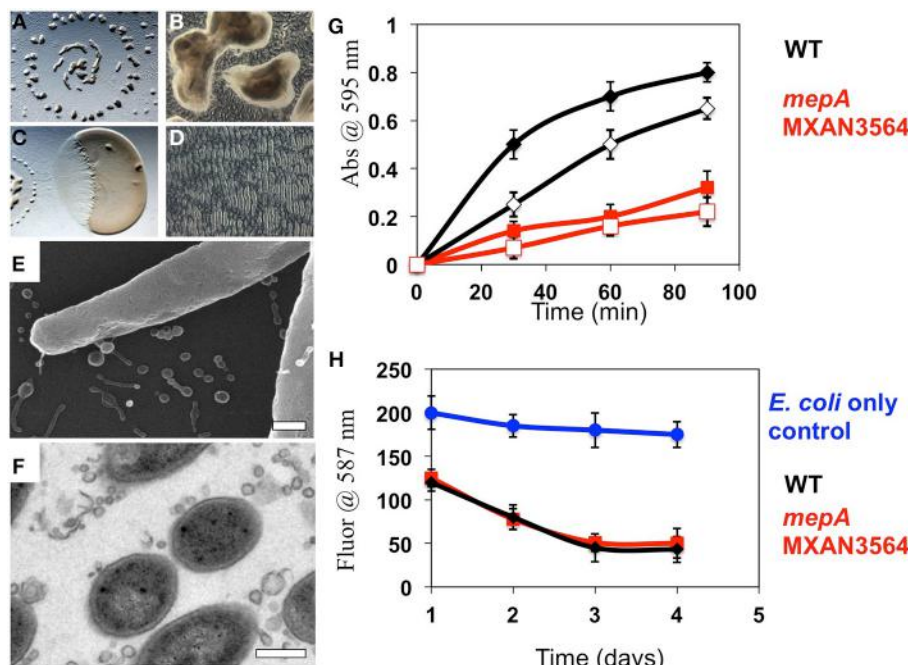


FIGURE 5 | Physiological analysis of a *mepA* metalloprotease mutant. **(A,B)** 72 h incubation of a 10 μ l aliquot of *mepA* cells induced to form fruiting bodies on CFL media. Normal fruiting body timing, distribution **(A)** and sporulation **(B)** were observed. **(C,D)** 48 h incubation of a 2 μ l aliquot of *mepA* cells incubated adjacent to a 5 μ l aliquot of *E. coli* on CFL media for observation of predatory behavior. Both clearing **(C)** and rippling **(D)** were observed. Electron microscopy of *mepA* cells shows the presence of vesicles with both **(E)** Scanning electron microscopy and **(F)** Transmission electron microscopy. **(G)** Resorufin-conjugated Casein was incubated with

whole cell (solid marks) and vesicle preparations (open marks) of wild type DZ2 (black) and *mepA* (red) and proteolysis measured by the colorimetric release of soluble resorufin over 90 min, relative to control with no addition. *mepA* whole cells and OMV fractions show reduced proteolytic activity. **(H)** Analysis of prey cell lysis of mCherry expressing fluorescent *E. coli* cells by wild type DZ2 (black) and *mepA* (red) shows that both strains reduce fluorescent signal with similar kinetics, relative to the *E. coli* only control (blue). Error bars represent standard deviation from 3 independent assays, scale bars are 0.5 microns.

in pinching off single OMVs or long chains that stay attached to cells (Palsdottir et al., 2009; Remis et al., 2014). As our understanding of OMV content is refined we may be able to predict OMV-directed proteins in unstudied or understudied organisms.

OM and OMV compartments are likely critical to cell-cell signaling processes in both intraspecies and interspecies interactions (Krug et al., 2008; Mashburn-Warren et al., 2008; Evans et al., 2012). Several features are particularly striking, such as the presence of the MepA metalloprotease that, when disrupted, results in reduced exoenzyme proteolytic activity. Since there is still some exoprotease activity (33% of wildtype levels) detected in OMVs isolated from the *mepA* mutant, we expect that some of the other hydrolytic enzymes identified are also involved in macromolecule degradation. Since predation by bacteria requires both extracellular lysis of prey and acquisition of the nutrients released, we suggest that the MepA protein is likely involved in acquiring nutrients from released extracellular protein, but not in prey cell lysis. In addition, the high abundance of two GroEL chaperonin homologs within OMVs is intriguing. The importance of the two GroEL homologs in social behaviors such as fruiting body formation (Li et al., 2010) and antibiotic production (Wang et al., 2014) suggests that both proteins may exert these functions through localization to OMV organelles, and suggest that they are involved in ensuring proper folding of exoproteins after export. In

addition, proteins involved in motility were detected in both the membrane and the OMV proteomes and, while supporting the idea that OMVs may play a role in the complex motility systems of *M. xanthus*.

The proteomics study employed a shotgun workflow that is based on a stochastic selection of precursor ions for tandem MS (MS/MS) upon which peptide/protein identification is based (McDonald and Yates, 2002). While very powerful as a proteomics discovery tool, the shotgun analytical format suffers from undersampling (Frahm et al., 2006), thus limiting the achievable level of technical reproducibility (Tabb et al., 2010). When analyzing high complexity samples, a failure to detect/identify a protein under LCMS shotgun conditions does not preclude its presence in the sample but rather it suggests that a species might be present at a relatively low level. With this caveat in mind, a number of proteins were repeatedly identified in the same sample type, i.e., 45 and 31% of all OMV and membrane proteins, respectively were matched by at least two distinct peptides across all samples of a given category. We have assessed consistency of our data by evaluating two analytical attributes of the protein identification evidence, i.e., relative abundance (mol %) and a number of distinct peptides for their inter-sample variability. To this end, we used 128 and 242 OMV and membrane proteins, respectively, that were detected in three biological replicates by at least two distinct

peptides. As shown in graphs 2A and 2B in S1, the CVs of relative abundances and distinct peptides numbers were below 0.6 for more than 90% of OMV and 70–90% OM identifications, suggesting high similarity among the samples. Likewise, we evaluated consistency of analysis of proteins between the sample types in the same biological replicate, this time comparing ratios between relative abundances and distinct peptide numbers in membrane and OMV fractions isolated from the same culture. Since in this case the results were affected by the analysis of twice as many samples (6 vs. 3), a larger spread of values was observed. Nevertheless, error factors remain below a two-fold level for more than 70% and ~90% of shared proteins when evaluating differences in relative abundances and numbers of distinct peptides, respectively (graph 2C in S1). Of note, a higher level of reproducibility was observed in the analysis of vesicles vs. membrane proteome, possibly due to the lower complexity of the former sample. While the above analyses highlight the significant similarity among the analyzed samples, targeted MS assays (Jaffe et al., 2008; Addona et al., 2009; Schmidt et al., 2009; Boja and Rodriguez, 2012) are required to validate the data presented here with a larger number of samples.

A diversity of secondary metabolites was also detected in the OMVs, many of which are thought to have antibiotic properties. These may assist in killing prey bacteria and also inhibiting the growth of competing microbes. Further study on the localization of these molecules is needed, but unlike classic antibiotic producers such as *Penicillium notatum*, *M. xanthus* typically kills upon cell-cell contact (Berleman and Kirby, 2009). The detection of several molecules with antibiotic properties leads to the hypothesis that targeted delivery of antibiotics through OMVs mediates prey cell lysis on contact. Such a mechanism would have the benefit that expensive secondary metabolites are not lost through diffusion. Furthermore, the packaging of several antibiotics and hydrolytic enzymes in a nano-scale package may provide a lethal cocktail that prevents the selection for single mutation resistance in the bacterial species that *M. xanthus* feeds on. If this holds true, then OMVs may be a powerful tool in the fight against multi-drug resistant pathogenic bacteria. Perhaps OMVs can be engineered to form a new generation of antibiotics—where susceptible cells are overwhelmed by a targeted cargo of multiple antibacterial molecules and hydrolytic enzymes. Further study of the protein and small molecule content on OMVs should improve our understanding of these organelles and their capacity to act as vehicles for intercellular delivery.

METHODS

CELL GROWTH AND MUTANTS

M. xanthus DZ2 (wild type) was grown in liquid culture shaking at 200 rpm, 32°C in CYE media consisting of 5 mM MOPS pH 7.6, 2 mM MgSO₄, 0.5% (w/w) Bacto Casitone, 0.25% (w/w) Bacto Yeast Extract or on 1.5% agar plates with the same components.

OMV AND MEMBRANE PURIFICATION

To obtain OMV and membrane cell fractions, 25 mL liquid *M. xanthus* cultures were first vortexed for 30 s to shear OMV structures from cells as before (Remis et al., 2014). The vortexed

culture was then centrifuged for 10 min at 5000 × G to pellet the cells prior to decanting the OMV containing supernatant. The supernatant was then passed sequentially through a 0.45 μm filter followed by a 0.22 μm syringe filter to remove cellular debris that did not pellet with previous step. Finally the cell free liquid was centrifuged at 140,000 × G for 1 h and the resulting pellet resuspended in 1 mL of PBS to obtain OMV-fractions. For membrane fractions, the cell pellets were resuspended in PBS with 5 mg DNase I according to previous methods (Thein et al., 2010). The suspension was lysed by sonication, and centrifuged at 5000 × G to remove incompletely lysed cells. The suspension was centrifuged at 140,000 × G for 1 h and washed 3 times with PBS. Sample aliquots were subjected to electron microscopy analysis to monitor the presence and purity as well as possible contamination levels. All samples were resuspended and vesicles were purified as described above five independent times. Samples were mixed with lipid dye FM 4–64 (Molecular Probes) and using a microplate (Greiner Bio-One North America, Inc., Monroe, NC) and plate-reader (Tecan, Vission-100, AFAB Lab, LLC, Frederick, MD) relative concentration of vesicle sample was determined.

TRYPTIC DIGESTION AND PROTEIN IDENTIFICATION BY LCMS

OMV and OM samples were digested using a method adopted from Papac et al. (1998), modified as previously described (Chhabra et al., 2011). A 5 μL aliquot of sample was then loaded onto a trapping cartridge (Dionex) and the sample washed for 10 min with 2% acetonitrile in 0.1% formic acid (10 μL/min). The trapping cartridge was then moved “in-line” with a C18 column analytical column (Dionex PepMap 75 μm i.d. × 150 mm) and peptide separation carried out using a 45-min linear gradient from 2 to 40% B at a flow rate of 600 nL/min (A: 2% acetonitrile (HPLC grade, Burdick and Jackson)/0.1% formic acid (Pierce Scientific); B: 98% acetonitrile/0.1% formic acid). The nano-LC-ESI-MSMS analysis utilized a 2D ultra NanoLC system (Eksigent) interfaced with a Thermo Scientific LTQ Orbitrap Velos (Waltham, MA) via an Advance CaptiveSpray Ionization source (Michrom BioResources, Auburn, CA) fitted with a Michrom BioResources CaptiveSpray 20 μm i.d. tapered tip. Nanospray was performed at a spray voltage of 1.5 kV. Precursor scans were acquired in the Orbitrap over the mass range of *m/z* 300–1500 with a resolution of 30,000, with lock mass enabled. Twleve data-dependent MS/MS scans were performed per precursor scan using the LTQ. Charge state screening and monoisotopic precursor selection were enabled, and peptides with 1+ charge state and unassigned charge states were rejected. MS/MS were collected utilizing an isolation width of 3 Da, normalized collision energy of 30 eV, an activation Q of 0.250 and an activation time of 10 ms. The mass spectrometer was routinely calibrated with a solution of caffeine, MRFA peptide and Ultramark 1621 according to the manufacturer’s instructions. MS/MS data were converted to a mascot generic format (.mgf) by Mascot Daemon software and Mascot v 2.2 search engine (Matrix Science) was employed to search the data against a custom *M. xanthus* protein sequence database (downloaded from UniProt) with common contaminants appended; a reversed version was concatenated to the database to follow false discovery rate (14862 sequences; 5626671 residues). Peaklists were

generated with the Mascot Daemon (Matrix Sciences) using the “ThermoFinigan LCQ/DECA RAW file” (Thermo Fisher) data import filter; search was limited to doubly- and triply-charged precursors. The following search parameters were utilized: precursor mass tolerance 5 ppm; fragment mass tolerance 0.8 Da; tryptic digestion; 1 missed cleavage; fixed modification: Cys-carbamidomethyl; variable modifications: deamidation (Asn and Gln), Met-sulfoxide and Pyro-glu (N-term Gln). Average FDR values were 2.0 and 0.8% for OM and OMV samples, respectively. Proteins that were identified with at least one peptide scoring above the Mascot calculated identity threshold in at least one of the six analyzed samples are reported; no manual verification of MS/MS data was performed. Relative protein abundances were approximated by the protein molar fractions (mol %) that are based on the exponentially modified protein abundance index (emPAI) values that were automatically calculated by the Mascot search engine as described at the vendor’s website <http://www.matrixscience.com/help/quant_empai_help.html> (Ishihama et al., 2005).

MASS SPECTROMETRY OF SMALL MOLECULES

OMV fractions were frozen and lyophilized overnight. The remaining powder was then collected in separate glass scintillation vials and 5 mL of a solvent mixture of 3:3:2 IPA:MeOH:H₂O was added. The samples were then vortexed, and the liquid decanted to fresh Eppendorf tubes and dried down via speed vacuum. The extract was then reconstituted to 1 mL of the same solvent mixture. Precipitates were pelleted and liquid decanted to a new Eppendorf tube. These were once again speed vacuumed to dryness, reconstituted in 400 μL in the same solvent mixture, and filtered with 0.2 um filters. These samples were run on an Agilent 6550 mass spectrometer coupled with an Agilent UPLC Eclipse C18 column. A 21 min method was used with a C-18 column. Solvent A was LC MS grade water with 0.1% formic acid, and Solvent B was LC MS grade acetonitrile with 0.1% formic acid. Vesicle extract was diluted by 50% with solvent mixture, and 1 μL was injected. At a flow rate of 0.6 mL/min, the gradient used was 1 min at 5% Solvent B, and then a 19 min gradient to 95% Solvent B, followed by 1 min holding at 95% Solvent B. Metabolite profiling was performed via targeted searches for known *M. xanthus* secondary metabolites using Mass Hunter software (Agilent Technologies, Santa Rosa, CA). Ions matching known *M. xanthus* metabolites within 5 ppm were subjected to tandem MS to further support their identification by matching two or more known fragments.

MUTANT CONSTRUCTION

Gene specific primers (Forward: 5'-CAGGCTTCACC-gene specific region-3' and Reverse: 3'-AAAGCTGGGTC- gene specific region-5') were designed to amplify ~500–600 bp of genomic coding region from genomic DNA. A second PCR was performed using Gateway® compatible primers (Forward: 5'-GGGGACAAGTTGTACAAAAAGCAGGCTTCACC-3' and Reverse: 3'-GGGGACCACTTGTACAAGAAAGCTGGGTC-5'). PCR products were run on a 1.5% agarose gel and excised under UV lamp. The gel, containing amplified genomic region were purified using QIAquick PCR purification kit (Qiagen).

Purified DNA fragments were cloned into pDONR™201 using BP Clonase® II Enzyme Mix according to manufacturer’s instructions (Life Technologies, USA) and incubated overnight at room temperature before transforming into chemical competent cells. DNA sequencing of the inserted gene was performed using flanking primers by Quintara Biosciences, USA.

ELECTRON MICROSCOPY

Negative-staining by TEM. *M. xanthus* cultures were fixed in 10% glutaraldehyde for 30 min and resuspended gently. 3 μL of this cell suspension was added to a formavar coated copper mesh grid (Electron Microscopy Sciences, Hatfield, PA) and then stained with 2 % uranyl acetate (3 μL) for 2 min. Excess cell suspension was adsorbed onto filter paper and washed with 3.5 μL ddH₂O between additions. Whole mount negative stained samples were imaged at 60 kV on a JEOL 1200-EX transmission electron microscope.

SCANNING ELECTRON MICROSCOPY

Cultures were grown on poly-lysine coated silicon wafers in 2 ml CYE submerged cultures for 18 h at 32°C. Wafers were harvested and fixed with 2.5% Glutaraldehyde in Sodium Cacodylate buffer pH 7.2. Post-fixation was done on ice using 1% Osmium Tetroxide in Sodium Cacodylate buffer pH 7.2 for 1 h. Samples were dehydrated using a graded ethanol series (20, 40, 60, 80, 90, 100% × 3) at 10 min per step. Critical point drying was performed with a Tousimis AutoSamdri 815 Critical Point Dryer (Tousimis, Rockville, MD 20851, USA). Samples were then sputter coated with gold-palladium using a Tousimis Sputter Coater (Tousimis, Rockville, MD 20851, USA) to prevent charging in the microscope. Images were collected using the Hitachi S5000 Scanning Electron Microscope (Hitachi High Technologies America Inc, Pleasanton, CA 94588, USA).

Thin section TEM. *M. xanthus* colonies were grown for 4 days on CYE agar plates in 40 mm diameter aluminum weighing pans and prepared as before (Remis et al., 2014). Briefly, samples were fixed with 2.5% Glutaraldehyde for 1 h, post-fixed with 1% Osmium Tetroxide for and stained with 5 mM Ruthenium Red. Dehydration was performed using a graded ethanol series, followed by a step-wise infiltration with epon resin and polymerized in an 80°C oven. Sample blocks were sectioned at 90 nm using a Leica EM UC6 microtome (Leica Microsystems Inc. Buffalo Grove, IL). Sections were collected on slot grids and stained with 2% uranyl acetate and Reynolds lead citrate. Imaging was performed with an FEI Tecnai 12 transmission electron microscope (FEI, Hillsboro, OR).

PHYSIOLOGICAL STUDIES

Rapid fruiting body induction of *M. xanthus* and predation of *E. coli* strain β2155 were performed as before Berleman and Kirby (2007) by adding washed cells to CFL media and incubating at 32°C for 3–5 d. CFL contains 10 mM MOPS, pH 7.6, 1 mM KH₂PO₄, 8 mM MgSO₄, 0.02% (NH₄)₂SO₄, 0.002% Na Citrate, 0.01% Casitone and 0.002% Na Pyruvate. Images were captured using a Nikon SMZ1000 dissecting microscope (Nikon Instruments Inc., Melville, NY). Assays were performed at least three times, with representative images selected. For quantitative

assays, *E. coli* strain β2155 harboring a constitutively expressed mCherry protein was utilized (Remis et al., 2014). Black Corning 96 well Polystyrol plate (Corning Life Sciences, Tewksbury, MA), with 200 μl of CFL agar were used for incubation and fluorescence measurement. 10 μl aliquots of *E. coli* cells were added and allowed to dry before adding 10 μl aliquots of *M. xanthus* DZ2 or *mepA* pipetted directly on the *E. coli*. Fluorescent measurements were acquired 1, 2, 3, and 4 days after plating with a Tecan Infinite M1000 microplate reader (Tecan Systems, Inc., San Jose, CA). Averaged readings across multiple samples were used to determine lytic rate.

Proteolysis of protein was determined using colorimetric detection of at $\text{abs} = 574 \text{ nm}$ of released resorufin-labeled casein protein (Roche, Inc., Mannheim, Germany). *M. xanthus* cultures or purified vesicles were incubated in 50 mM Tris-HCl pH7.8, 5 mM CaCl₂ for 60 min at 37°C. To measure absorbance, aliquots were removed at the times indicated and proteolysis stopped through addition of 5 % Trichloroacetic acid. Remaining protein was pelleted through centrifugation and the supernatant assayed for released peptides. After 60 min incubation, An abs value of 0.2 is equivalent to 100 ng of trypsin hydrolysis.

ACKNOWLEDGMENTS

We thank Dr. Emilia Mauriello, for her advice and discussion and Marcin Zemla for technical assistance. We would also like to thank the Auer Lab for helpful discussions. This work was supported by the National Institutes of Health (5R01GM020509 and 3R01GM020509-36S1 to David R. Zusman), by Lab directed research development funds from the Office of Biological and Environmental Research of the US Department of Energy under contract number DE-AC02-05CH11231 (to Manfred Auer and Trent R. Northen) and the US Department of Energy VFP program (James E. Berleman). Mass spectrometry analysis was performed by the UCSF Sandler-Moore Mass Spectrometry Core Facility, which acknowledges support from the Sandler Family Foundation, the Gordon and Betty Moore Foundation, and NIH/NCI Cancer Center Support Grant P30 CA082103.

SUPPLEMENTARY MATERIAL

The Supplementary Material for this article can be found online at: <http://www.frontiersin.org/journal/10.3389/fmcb.2014.00474/abstract>

REFERENCES

- Addona, T. A., Abbatangelo, S. E., Schilling, B., Skates, S. J., Mani, D. R., Bunk, D. M., et al. (2009). Multi-site assessment of the precision and reproducibility of multiple reaction monitoring-based measurements of proteins in plasma. *Nat. Biotechnol.* 27, 633–641. doi: 10.1038/nbt.1546
- Berleman, J. E., Chumley, T., Cheung, P., and Kirby, J. R. (2006). Rippling is a predatory behavior in *Myxococcus xanthus*. *J. Bacteriol.* 188, 5888–5895. doi: 10.1128/JB.00559-06
- Berleman, J. E., and Kirby, J. R. (2007). Multicellular development in *Myxococcus xanthus* is stimulated by predator-prey interactions. *J. Bacteriol.* 189, 5675–5682. doi: 10.1128/JB.00544-07
- Berleman, J. E., and Kirby, J. R. (2009). Deciphering the hunting strategy of a bacterial wolfpack. *FEMS Microbiol. Rev.* 33, 942–957. doi: 10.1111/j.1574-6976.2009.00185.x
- Berleman, J. E., Scott, J., Chumley, T., and Kirby, J. R. (2008). Predatrix behavior in *Myxococcus xanthus*. *Proc. Natl. Acad. Sci. U.S.A.* 105, 17127–17132. doi: 10.1073/pnas.0804387105
- Beveridge, T. J. (1999). Structures of gram-negative cell walls and their derived membrane vesicles. *J. Bacteriol.* 181, 4725–4733.
- Bhat, S., Zhu, X., Patel, R. P., Orlando, R., and Shimkets, L. J. (2011). Identification and localization of *Myxococcus xanthus* porins and lipoproteins. *PLoS ONE* 6:e27475. doi: 10.1371/journal.pone.0027475
- Boja, E. S., and Rodriguez, H. (2012). Mass spectrometry-based targeted quantitative proteomics: achieving sensitive and reproducible detection of proteins. *Proteomics* 12, 1093–1110. doi: 10.1002/pmic.201100387
- Chhabra, S. R., Butland, G., Elias, D. A., Chandonia, J.-M., Fok, O.-Y., Juba, T. R., et al. (2011). Generalized schemes for high-throughput manipulation of the Desulfobivibrio vulgaris genome. *Appl. Environ. Microbiol.* 77, 7595–7604. doi: 10.1128/AEM.05495-11
- Choi, D.-S., Kim, D.-K., Choi, S. J., Lee, J., Choi, J.-P., Rho, S., et al. (2011). Proteomic analysis of outer membrane vesicles derived from *Pseudomonas aeruginosa*. *Proteomics* 11, 3424–3429. doi: 10.1002/pmic.201000212
- Cornejo, E., Abreu, N., and Komeili, A. (2014). Compartmentalization and organelle formation in bacteria. *Curr. Opin. Cell Biol.* 26, 132–138. doi: 10.1016/j.celb.2013.12.007
- Cross, A. S. (2014). Anti-endotoxin vaccines: back to the future. *Virulence* 5, 219–225. doi: 10.4161/viru.25965
- Curtis, P. D., Atwood, J. 3rd., Orlando, R., and Shimkets, L. J. (2007). Proteins associated with the *Myxococcus xanthus* extracellular matrix. *J. Bacteriol.* 189, 7634–7642. doi: 10.1128/JB.01007-07
- Ducret, A., Fleuchot, B., Bergam, P., and Mignot, T. (2013). Direct live imaging of cell-cell protein transfer by transient outer membrane fusion in *Myxococcus xanthus*. *Elife* 2:e00868. doi: 10.7554/elife.00868
- Evans, A. G. L., Davey, H. M., Cookson, A., Currinn, H., Cooke-Fox, G., Stanczyk, P. J., et al. (2012). Predatory activity of *Myxococcus xanthus* outer-membrane vesicles and properties of their hydrolase cargo. *Microbiology* 158, 2742–2752. doi: 10.1099/mic.0.060343-0
- Frahm, J. L., Howard, B. E., Heber, S., and Muddiman, D. C. (2006). Accessible proteomics space and its implications for peak capacity for zero-, one- and two-dimensional separations coupled with FT-ICR and TOF mass spectrometry. *J. Mass Spectrom.* 41, 281–288. doi: 10.1002/jms.1024
- Gerth, K., Jansen, R., Reifenstahl, G., Höfle, G., Irschik, H., Kunze, B., et al. (1983). The myxalamids, new antibiotics from *Myxococcus xanthus* (Myxobacterales). I. Production, physico-chemical and biological properties, and mechanism of action. *J. Antibiot. (Tokyo)* 36, 1150–1156. doi: 10.7164/antibiotics.36.1150
- Goldman, B. S., Nierman, W. C., Kaiser, D., Slater, S. C., Durkin, A. S., Eisen, J. A., et al. (2006). Evolution of sensory complexity recorded in a myxobacterial genome. *Proc. Natl. Acad. Sci. U.S.A.* 103, 15200–15205. doi: 10.1073/pnas.0607335103
- Grabley, S., and Thiericke, R. (1999). *Drug Discovery from Nature*. Berlin; Heidelberg: Springer.
- Ishihama, Y., Oda, Y., Tabata, T., Sato, T., Nagasu, T., Rappaport, J., et al. (2005). Exponentially modified protein abundance index (emPAI) for estimation of absolute protein amount in proteomics by the number of sequenced peptides per protein. *Mol. Cell. Proteomics* 4, 1265–1272. doi: 10.1074/mcp.M500061-MCP200
- Jaffe, J. D., Keshishian, H., Chang, B., Addona, T. A., Gillette, M. A., and Carr, S. A. (2008). Accurate inclusion mass screening: a bridge from unbiased discovery to targeted assay development for biomarker verification. *Mol. Cell. Proteomics* 7, 1952–1962. doi: 10.1074/mcp.M800218-MCP200
- Jiang, C., Brown, P. J. B., Ducret, A., and Brun, Y. V. (2014). Sequential evolution of bacterial morphology by co-option of a developmental regulator. *Nature* 506, 489–493. doi: 10.1038/nature12900
- Kahnt, J., Aguiluz, K., Koch, J., Treuner-Lange, A., Konovalova, A., Huntley, S., et al. (2010). Profiling the outer membrane proteome during growth and development of the social bacterium *Myxococcus xanthus* by selective biotinylation and analyses of outer membrane vesicles. *J. Proteome Res.* 9, 5197–5208. doi: 10.1021/pr1004983
- Kesty, N. C., Mason, K. M., Reedy, M., Miller, S. E., and Kuehn, M. J. (2004). Enterotoxigenic Escherichia coli vesicles target toxin delivery into mammalian cells. *EMBO J.* 23, 4538–4549. doi: 10.1038/sj.emboj.7600471
- Kim, J., Choi, J. N., Kim, P., Sok, D.-E., Nam, S.-W., and Lee, C. H. (2009). LC-MS/MS profiling-based secondary metabolite screening of *Myxococcus xanthus*. *J. Microbiol. Biotechnol.* 19, 51–54. doi: 10.4014/jmb.0711.775

- Krug, D., Zurek, G., Revermann, O., Vos, M., Velicer, G. J., and Müller, R. (2008). Discovering the hidden secondary metabolome of *Myxococcus xanthus*: a study of intraspecific diversity. *Appl. Environ. Microbiol.* 74, 3058–3068. doi: 10.1128/AEM.02863-07
- Li, J., Wang, Y., Zhang, C., Zhang, W., Jiang, D., Wu, Z., et al. (2010). *Myxococcus xanthus* viability depends on groEL supplied by either of two genes, but the paralogs have different functions during heat shock, predation, and development. *J. Bacteriol.* 192, 1875–1881. doi: 10.1128/JB.01458-09
- Li, S.-G., Zhao, L., Han, K., Li, P.-F., Li, Z.-F., Hu, W., et al. (2014). Diversity of epothilone producers among Sorangium strains in producer-positive soil habitats. *Microb. Biotechnol.* 7, 130–141. doi: 10.1111/1751-7915.12103
- Li, Y., Weissman, K. J., and Müller, R. (2008). Myxochelin biosynthesis: direct evidence for two- and four-electron reduction of a carrier protein-bound thioester. *J. Am. Chem. Soc.* 130, 7554–7555. doi: 10.1021/ja8025278
- Lilly, W. W., Stajich, J. E., Pukkila, P. J., Wilke, S. K., Inoguchi, N., and Gathman, A. C. (2008). An expanded family of fungalsin extracellular metallopeptidases of *Coprinopsis cinerea*. *Mycol. Res.* 112, 389–398. doi: 10.1016/j.mycres.2007.11.013
- Luciano, J., Agrebi, R., Le Gall, A. V., Warrel, M., Fiegna, F., Ducret, A., et al. (2011). Emergence and modular evolution of a novel motility machinery in bacteria. *PLoS Genet.* 7:e1002268. doi: 10.1371/journal.pgen.1002268
- Marshall, J. C. (2005). Lipopolysaccharide: an endotoxin or an exogenous hormone? *Clin. Infect. Dis. Off. Publ. Infect. Dis. Soc. Am.* 41(Suppl. 7), S470–S480. doi: 10.1086/432000
- Mashburn, L. M., and Whiteley, M. (2005). Membrane vesicles traffic signals and facilitate group activities in a prokaryote. *Nature* 437, 422–425. doi: 10.1038/nature03925
- Mashburn-Warren, L., McLean, R. J. C., and Whiteley, M. (2008). Gram-negative outer membrane vesicles: beyond the cell surface. *Geobiology* 6, 214–219. doi: 10.1111/j.1472-4669.2008.00157.x
- McDonald, W. H., and Yates, J. R. (2002). Shotgun proteomics and biomarker discovery. *Dis. Markers* 18, 99–105. doi: 10.1155/2002/505397
- Meiser, P., Bode, H. B., and Müller, R. (2006). The unique DKxanthene secondary metabolite family from the myxobacterium *Myxococcus xanthus* is required for developmental sporulation. *Proc. Natl. Acad. Sci. U.S.A.* 103, 19128–19133. doi: 10.1073/pnas.0606039103
- Nikaido, H. (2003). Molecular basis of bacterial outer membrane permeability revisited. *Microbiol. Mol. Biol. Rev.* 67, 593–656. doi: 10.1128/MMBR.67.4.593-656.2003
- Nudelman, E., Wall, D., and Kaiser, D. (2005). Cell-to-Cell transfer of bacterial outer membrane lipoproteins. *Science* 309, 125–127. doi: 10.1126/science.1112440
- Paldottir, H., Remis, J. P., Schaudinn, C., O'Toole, E., Lux, R., Shi, W., et al. (2009). Three-dimensional macromolecular organization of cryofixed *Myxococcus xanthus* biofilms as revealed by electron microscopic tomography. *J. Bacteriol.* 191, 2077–2082. doi: 10.1128/JB.01333-08
- Pan, H., He, X., Lux, R., Luan, J., and Shi, W. (2013). Killing of *Escherichia coli* by *Myxococcus xanthus* in aqueous environments requires exopolysaccharide-dependent physical contact. *Microb. Ecol.* 66, 630–638. doi: 10.1007/s00248-013-0252-x
- Papac, D. I., Briggs, J. B., Chin, E. T., and Jones, A. J. (1998). A high-throughput microscale method to release N-linked oligosaccharides from glycoproteins for matrix-assisted laser desorption/ionization time-of-flight mass spectrometric analysis. *Glycobiology* 8, 445–454. doi: 10.1093/glycob/8.5.445
- Pelling, A. E., Li, Y., Cross, S. E., Castaneda, S., Shi, W., and Gimzewski, J. K. (2006). Self-organized and highly ordered domain structures within swarms of *Myxococcus xanthus*. *Cell Motil. Cytoskeleton* 63, 141–148. doi: 10.1002/cm.20112
- Remis, J. P., Wei, D., Gorur, A., Zemla, M., Haraga, J., Allen, S., et al. (2014). Bacterial social networks: structure and composition of *Myxococcus xanthus* outer membrane vesicle chains. *Environ. Microbiol.* 16, 598–610. doi: 10.1111/1462-2920.12187
- Rosenberg, E., Keller, K. H., and Dworkin, M. (1977). Cell density-dependent growth of *Myxococcus xanthus* on casein. *J. Bacteriol.* 129, 770–777.
- Schmidt, A., Claassen, M., and Aebersold, R. (2009). Directed mass spectrometry: towards hypothesis-driven proteomics. *Curr. Opin. Chem. Biol.* 13, 510–517. doi: 10.1016/j.cbpa.2009.08.016
- Tabb, D. L., Vega-Montoto, L., Rudnick, P. A., Variath, A. M., Ham, A.-J. L., Bunk, D. M., et al. (2010). Repeatability and reproducibility in proteomic identifications by liquid chromatography-tandem mass spectrometry. *J. Proteome Res.* 9, 761–776. doi: 10.1021/pr9006365
- Thein, M., Sauer, G., Paramasivam, N., Grin, I., and Linke, D. (2010). Efficient subfractionation of gram-negative bacteria for proteomics studies. *J. Proteome Res.* 9, 6135–6147. doi: 10.1021/pr1002438
- Velicer, G. J., and Vos, M. (2009). Sociobiology of the myxobacteria. *Annu. Rev. Microbiol.* 63, 599–623. doi: 10.1146/annurev.micro.091208.073158
- Vollmer, W. (2012). Bacterial outer membrane evolution via sporulation? *Nat. Chem. Biol.* 8, 14–18. doi: 10.1038/nchembio.748
- Wang, Y., Li, X., Zhang, W., Zhou, X., and Li, Y. (2014). The groEL2 gene, but not groEL1, is required for biosynthesis of the secondary metabolite myxovirescin in *Myxococcus xanthus* DK1622. *Microbiology* 160, 488–495. doi: 10.1099/mic.0.065862-0
- Wei, X., Pathak, D. T., and Wall, D. (2011). Heterologous protein transfer within structured myxobacteria biofilms. *Mol. Microbiol.* 81, 315–326. doi: 10.1111/j.1365-2958.2011.07710.x
- Wei, X., Vassallo, C. N., Pathak, D. T., and Wall, D. (2014). Myxobacteria produce outer membrane-enclosed tubes in unstructured environments. *J. Bacteriol.* 196, 1807–1814. doi: 10.1128/JB.00850-13
- Weissman, K. J., and Müller, R. (2010). Myxobacterial secondary metabolites: bioactivities and modes-of-action. *Nat. Prod. Rep.* 27, 1276–1295. doi: 10.1039/c001260m
- Xiao, Y., Gerth, K., Müller, R., and Wall, D. (2012). Myxobacteria antibiotic TA (myxovirescin) inhibits type II signal peptidase. *Antimicrob. Agents Chemother.* 56, 2014–2021. doi: 10.1128/AAC.06148-11
- Zanetti, G., Pahuja, K. B., Studer, S., Shim, S., and Schekman, R. (2012). COPII and the regulation of protein sorting in mammals. *Nat. Cell Biol.* 14, 20–28. doi: 10.1038/ncb2390

Conflict of Interest Statement: The authors declare that the research was conducted in the absence of any commercial or financial relationships that could be construed as a potential conflict of interest.

Received: 19 June 2014; accepted: 22 August 2014; published online: 09 September 2014.

*Citation: Berleman JE, Allen S, Danielewicz MA, Remis JP, Gorur A, Cunha J, Hadi MZ, Zusman DR, Northen TR, Witkowska HE and Auer M (2014) The lethal cargo of *Myxococcus xanthus* outer membrane vesicles. Front. Microbiol. 5:474. doi: 10.3389/fmicb.2014.00474*

This article was submitted to Terrestrial Microbiology, a section of the journal Frontiers in Microbiology.

Copyright © 2014 Berleman, Allen, Danielewicz, Remis, Gorur, Cunha, Hadi, Zusman, Northen, Witkowska and Auer. This is an open-access article distributed under the terms of the Creative Commons Attribution License (CC BY). The use, distribution or reproduction in other forums is permitted, provided the original author(s) or licensor are credited and that the original publication in this journal is cited, in accordance with accepted academic practice. No use, distribution or reproduction is permitted which does not comply with these terms.



Phage–host interplay: examples from tailed phages and Gram-negative bacterial pathogens

Soraya Chaturongakul^{1,2} and Puey Ounjai^{3*}

¹ Department of Microbiology, Faculty of Science, Mahidol University, Bangkok, Thailand

² Center for Emerging Bacterial Infections, Faculty of Science, Mahidol University, Bangkok, Thailand

³ Department of Biology, Faculty of Science, Mahidol University, Bangkok, Thailand

Edited by:

Luis Raul Comolli, Lawrence Berkeley National Laboratory, USA

Reviewed by:

Steven Ripp, University of Tennessee, USA

Joanne B. Emerson, University of California, Berkeley, USA

***Correspondence:**

Puey Ounjai, Department of Biology, Faculty of Science, Mahidol University, 272 Rama VI Road, Ratchathewi, Bangkok 10400, Thailand
e-mail: puey.oun@mahidol.ac.th

Complex interactions between bacteriophages and their bacterial hosts play significant roles in shaping the structure of environmental microbial communities, not only by genetic transduction but also by modification of bacterial gene expression patterns. Survival of phages solely depends on their ability to infect their bacterial hosts, most importantly during phage entry. Successful dynamic adaptation of bacteriophages when facing selective pressures, such as host adaptation and resistance, dictates their abundance and diversification. Co-evolution of the phage tail fibers and bacterial receptors determine bacterial host ranges, mechanisms of phage entry, and other infection parameters. This review summarizes the current knowledge about the physical interactions between tailed bacteriophages and bacterial pathogens (e.g., *Salmonella enterica* and *Pseudomonas aeruginosa*) and the influences of the phage on host gene expression. Understanding these interactions can offer insights into phage–host dynamics and suggest novel strategies for the design of bacterial pathogen biological controls.

Keywords: bacteriophage, host–phage interaction, phage resistance mechanism, host–phage dynamics, microbial community

INTRODUCTION

Bacteriophages (or phages) are the most abundant and most diversified microorganisms on Earth. Acting as obligate bacterial predators, phage can be found in all reservoirs populated by bacterial hosts, e.g., in soil (Marsh and Wellington, 1994; Kimura et al., 2008), in aquatic environments (Bergh et al., 1989; Suttle, 2007), and even in the human gut (Breitbart et al., 2003; Mills et al., 2013). The evolutionary success of bacteriophages, estimated at approximately an order of magnitude and up to a 25-fold greater abundance in comparison with their bacterial hosts (Fuhrman, 1999), indicates remarkable dynamic adaptability of phages in nature.

In natural habitats, phages and bacteria are in a constant arms race that proceeds in continuous cycles of co-evolution (Thingstad and Lignell, 1997). As bacteria develop mechanisms to prevent phage infection, e.g., bacterial receptor modification and degradation of invading phage DNA (Labrie et al., 2010), phages can circumvent the resistance and evolve mechanisms to target such resistant bacteria (Samson et al., 2013). This arms race continues and become one of the major forces to both expand global genetic diversity and maintain balance within microbial communities.

Previous reviews of phage–bacteria interaction mainly focused on model organisms such as *Escherichia coli* phages (or coliphages) and bacterial CRISPR/Cas immunity systems against phage genome replication. The focal points of this review, however, are physical interactions between tailed phages and other Gram-negative bacterial pathogens, specifically *Salmonella enterica* and *Pseudomonas aeruginosa*, and the influences of phage–host interactions on the gene expression of these clinically important bacteria and, more generally, on microbial diversity.

PHYSICAL INTERACTIONS BETWEEN TAILED PHAGES AND THEIR HOSTS

To initiate infection, phages need to adsorb to the host surfaces, penetrate cell walls and inject genetic materials into the host. Mechanisms used to initiate the connection to bacterial hosts prior to phage genome injection are referred to as tails. Ackermann and Prangishvili (2012) demonstrates that over ninety percent of approximately 6,200 phages examined by electron microscopy (EM) are tailed phages in the *Caudovirales* order (i.e., siphophages, myophages, and podophages). As the name implies, the adsorption machinery dedicated for specific host recognition is localized at the tail-end, varying from a simple tail tip to a complex base plate. Such mechanisms appear to be well-correlated with host adsorption strategies (Veesler and Cambillau, 2011; Fokine and Rossmann, 2014). Some tail structures can be quite complex and include extra-structures including tail spikes and tail fibers (Fokine and Rossmann, 2014). This adsorption machinery is the most rapidly evolving part of the tailed phage genome (Hendrix et al., 1999). Tail proteins of these phages are diverse and capable of recognizing almost every host surface component (Figure 1), including surface proteins, polysaccharides and lipopolysaccharides (LPS; Lindberg, 1973).

The interactions between phages and hosts occur between phage tail proteins and bacterial receptors, which are proteins or LPS. These interactions determine host specificity and range. Known receptors (Table 1) of *Salmonella* phages are flagella proteins (e.g., FliC and FljB, Shin et al., 2012; and FliK, Choi et al., 2013), outer membrane porin or osmoregulatory protein OmpC (Ho and Slauch, 2001; Marti et al., 2013), outer membrane protein for vitamin B₁₂ uptake BtuB (Kim and Ryu,

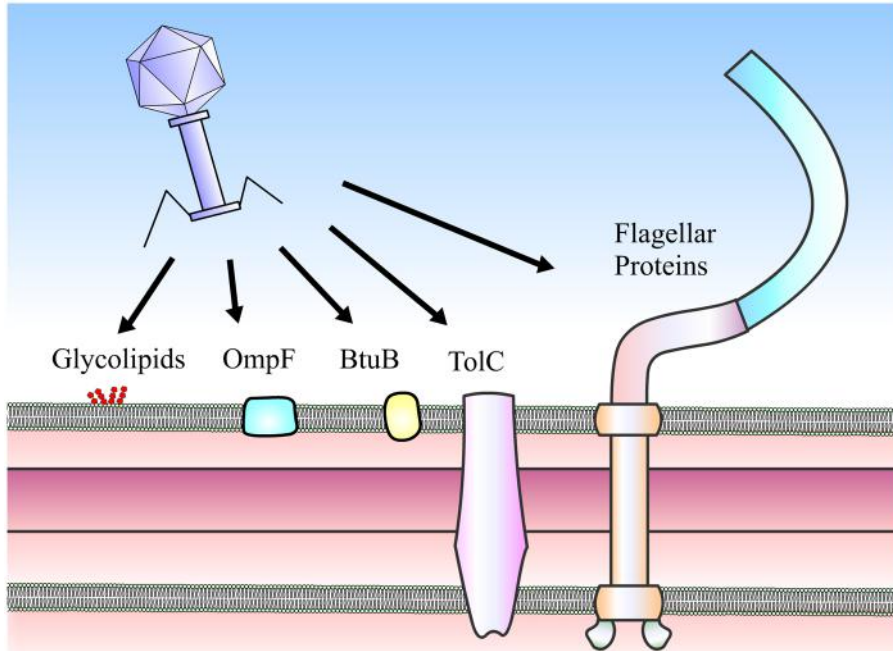


FIGURE 1 | Receptors of *Salmonella* phages. Phages can use a number of cell surface moieties as receptors, including glycolipids (O- and Vi-antigens), integral membrane proteins (e.g., OmpF, BtuB, and TolC) and flagella proteins (FliC, FliB, and FliK).

2011), outer membrane protein for drug efflux pump TolC (Ricci and Piddock, 2010), outer membrane transport protein FhuA (Casjens et al., 2005), O-antigen of LPS (Shin et al., 2012), and Vi capsular antigen (Pickard et al., 2010). On the other hand, known phage receptors in *P. aeruginosa* are type IV pili (Heo et al., 2007; Bae and Cho, 2013) and O-antigen of LPS (Le et al., 2013).

The protein–protein interactions between phage tail fiber proteins and bacterial flagella filaments are specific and strong. Such flagellotropic phages adsorb to the bacterial hosts via flagellin proteins, i.e., phase 1 antigen FliC, phase 2 antigen FljB, or flagella hook FliK (Shin et al., 2012; Choi et al., 2013). The preference for each flagella receptor varies among phages. *Salmonella* siphophages can use only FliC or both FliC and FljB as receptors (Shin et al., 2012). The latter is more prevalent as variety in host receptors leads to wider possible host ranges. In addition to being flagellotropic, host adsorption in some phages is also dependent upon motility and the directional rotation of the flagella themselves. For instance, *Salmonella* phage iEPS5 requires adsorption to either FliC or FljB flagellin and successful host infection only occurs if the flagella are rotating counter-clockwise in the presence of flagella torque protein MotA and hook protein FliK (Choi et al., 2013). The evidence also suggests that, alongside the adsorption step, injection of iEPS5 DNA is also flagella-dependent, possibly through the flagellin channel (Choi et al., 2013). In addition to adsorption through flagella, phages can also attach through the pili. Specifically, *P. aeruginosa* phage MPK7 and M22 utilize type IV pili as their receptors. *P. aeruginosa* hosts lacking *pilA* gene are resistant to infection by these phages (Heo et al., 2007; Bae and Cho, 2013).

Besides motility apparatus such as flagella and pili, outer membrane proteins are also targets for phage adsorption. OmpC porin is used as a receptor by *Salmonella* Gifsy and T4-like phages (Ho and Slauch, 2001; Marti et al., 2013), while vitamin B₁₂ uptake protein BtuB is used by T5-like phages (Kim and Ryu, 2011). Although resistance to BtuB-targeting phages can develop in *Salmonella*, the trait is not heritable and bacterial daughter cells can revert and become susceptible to these phages again (Kim and Ryu, 2011). Additionally, a conserved innate efflux pump TolC is used by *Salmonella* phage as a receptor (Ricci and Piddock, 2010). TolC has also been shown to be a colonization factor of *S. Typhimurium*, in which a *tolC* null strain is virulence attenuated (Webber et al., 2009). Therefore, application of TolC targeting phages is expected to have dual advantages, as the phages themselves can directly infect the bacterial host and can also drive the emergence of TolC-deficient *Salmonella*, which is incapable of colonization and incapable of spreading infection. Like coliphages, *Salmonella* phages use ferrichrome transport protein FhuA as a receptor (Casjens et al., 2005).

Bacteriophages also use surface antigens such as O-and Vi-antigens as receptors. In both *S. enterica* and *P. aeruginosa*, O-antigens of LPS are phage receptors. In *Salmonella*, tail spike proteins of the typical siphophages or podophages not only recognize but also hydrolyze the O-antigen, allowing the phage to penetrate through the 100-nm O-antigen layer during infection (Andres et al., 2012). Siphophage SSU5, however, uses core oligosaccharides of LPS as receptors (Kim et al., 2014), making SSU5 a beneficial addition to the phage cocktail against insensitive

Table 1 | Specific host receptors for *Salmonella* and *P. aeruginosa* phages.

	Specific host receptors	Reference
<i>S. enterica</i>	<i>Flagellar proteins</i>	
	FliC and FljB	Shin et al. (2012)
	FliK	Choi et al. (2013)
	<i>Outermembrane proteins</i>	
	OmpC	Ho and Slauch (2001), Marti et al. (2013)
	BtuB	Kim and Ryu (2011)
	TolC	Ricci and Piddock (2010)
	FhuA	Casjens et al. (2005)
	<i>Surface antigens</i>	
	O-antigen	Shin et al. (2012)
	Vi-antigen	Pickard et al. (2010)
<i>P. aeruginosa</i>	<i>Surface antigens</i>	
	O-antigen	Le et al. (2013)
	Vi-antigen	Temple et al. (1986), Hanlon et al. (2001)
	<i>Type IV pili</i>	
	PilA	Bae and Cho (2013), Heo et al. (2007)

Salmonella populations capable of O-antigen glucosylation (Kim and Ryu, 2012). Other than O-antigens, Vi capsular antigens of *S. Typhi* are also targets for recognition by phage tail protein, specifically at a conserved acyl esterase domain (Pickard et al., 2010). On the other hand, phages of *P. aeruginosa* recognize O-antigens of LPS using tail fibers (Le et al., 2013). Interestingly, extracellular matrix-like structures such as alginate glycopolysaccharide layers are also found in *Pseudomonas* spp. The role of these layers is to physically alter phage accessibility. Phage F116 of *Pseudomonas* can produce alginate lyase which dissolves the alginate layer and facilitates penetration and dispersion of phages in such a matrix (Hanlon et al., 2001). However, alteration in alginate production renders *Pseudomonas* insensitive to phage2 and φPLS-I, thus revealing the role of alginate in adhesion (Temple et al., 1986).

It is important to note that interactions between phages and host bacteria are not exclusive to single types of phage protein-receptor recognition. Shin et al. (2012) demonstrated cross-infection and cross-resistance among phages recognizing different targets on *S. enterica*, e.g., bacterial hosts that are resistant to flagellatropic phages are sensitive to phages targeting BtuB and LPS. Conversely, due to possible interactions between BtuB and LPS targets, bacterial strains that are resistant to BtuB-targeting and LPS-targeting phages are susceptible to flagellatropic phages (Shin et al., 2012). According to the “killing the winner” hypothesis (Thingstad and Lignell, 1997), cross-infection by different types of phages naturally limits the abundance of successful strains and thereby increases bacterial diversity. Although a vast variations of

phage tails and other adsorption structures have been observed by EM (Ackermann and Prangishvili, 2012), the X-ray structures of phage tail proteins including Dif and gp27-like proteins from various phages demonstrate remarkable structural similarities which suggest a common evolutionary origin for phage tail proteins (Veesler and Cambillau, 2011).

PHAGE-BACTERIA: GENETIC GIVE-AND-TAKE

Rapid reciprocal evolutionary competition between bacteria and phages (and even among phages with common bacterial hosts in a shared environment) creates high selective pressure, forcing diversification of the attachment-related structures and the emergence of various phage infection tactics (as reviewed in Veesler and Cambillau, 2011). However, success in infection is apparently not sufficient for phage survival in nature. As an obligate parasite, phages are dependent upon the survival of their host population. Thus, the availability of hosts is at least as important in determining the environmental fitness of phages. Phages must also modulate the gene expression of host cells to prevent superinfection by other phages.

In a lysogenic life cycle, phage integrates its genome and replicates along with its host. Not only the host survival is sustained, the presence of prophages has also been repeatedly shown to be beneficial. Prophages can provide their host population with immunity against secondary infection or superinfection by other incoming phages. In lysogenic *S. enterica*, expression of podophage P22-encoded proteins SieA and SieB exclude superinfection through degradation of the superinfecting phage genome (Susskind et al., 1974a) and induce lysis of superinfected host cells, protecting the whole host population (Susskind et al., 1974b). Similarly, the expression of siphophage HK97-encoded protein gp15 protein excludes superinfection by other HK97 phages via inhibition of phage genome entry (Cumby et al., 2012).

Beyond superinfection exclusion, prophages can also enhance the fitness of their hosts in the environment. A recent study in *P. aeruginosa* PAO1 has shown that infection with LPS-targeting E79 myophage for 4 days gave rise to E79-immune variants that, while exhibiting slower growth than control PAO1 and impairment of twitching, swimming and swarming abilities, produced more virulence factor pyocyanin and were less frequently internalized by J774 macrophages (Hosseiniidoust et al., 2013). In addition, several lines of evidence demonstrate extensive genetic circulation amongst phage and host communities. In fact, approximately 20% of the extant genetic content of a given bacterial species are acquired (Gogarten et al., 2002). These acquired genetic materials include so-called mobile genetic elements, including several bacterial pathogenicity islands which can potentially be horizontally transferred across species boundaries. Some phage-related chromosomal islands use phages as transduction vectors (Novick et al., 2010). This phage-mediated horizontal transfer of genetic material is of extreme importance as it acts as an active driving force behind bacterial evolution. Classic examples are the *P. aeruginosa* gigantic bacteriocin called R- and F-type pyocins which are utilized to combat other microbes in the community (Nakayama et al., 2000). High sequence similarities and striking structural parallels between the phage tail structures and bacterial pyocins reveal a

clear evolutionary connection between these complex molecular devices (Nakayama et al., 2000). Another phage-like structure found in bacteria including *P. aeruginosa* is a dynamic bacterial type VI secretion system (T6SS) used for translocation of virulence factors into target cells: the same mechanism the phage uses to transfer its genome to the host (Basler et al., 2012). Moreover, a recent report has shown that phage tail-like structures produced by marine bacterium *Pseudoalteromonas luteoviolacea* can trigger metamorphosis of a marine tubeworm, providing novel insights into the intricate interaction between phage, bacterium and animal (Shikuma et al., 2014).

Taken together, it is clear that phages play key roles in shaping the evolution of bacteria and vice versa. Phages not only manipulate expression of bacterial genes but also provide competitiveness for their hosts to thrive in the ecosystem as that would mutually be beneficial for both parties. Substantial structural and mechanistic analogies among bacterial puncturing devices, pyocins and secretion systems indicate an intimate evolutionary relationship between phages and their hosts.

PHAGES IN MICROBIAL ECOSYSTEMS

Extensive *in vitro* characterization of host–phage relationships indicates short-term arms races are run between hosts and parasites (Hall et al., 2011); however, in natural habitats the interaction continues over extended time-periods. A recent study proposed that the co-evolution of phages and soil microbial communities is more likely driven by fluctuating selection dynamics, which can continue indefinitely (Gómez and Buckling, 2011). In a large ecosystem, an immune bacterial population gains benefit from the bactericidal effects of phages that act against other competitive species in the same pool and selectively enrich the ecosystem. It may therefore be better to view phage–host relationships as not merely parasitic but as mutualistic (Williams, 2013).

In an attempt to better understand phage–bacteria population dynamics, extensive metagenomic studies have been performed to characterize microbial communities in various niches, including marine, soil, and animal hosts. Metagenomic studies of human feces have demonstrated high abundance and diversity of phages (Minot et al., 2011, 2013). Barr et al. (2013) demonstrated that the abundance of phages on mucosal surfaces of epithelial cells can provide defense against bacterial infection, suggesting a plausible model for phage therapy against host mucosal infection such as foodborne infection by *S. enterica* or lung infection by *P. aeruginosa*.

As naturally designed predators to balance bacterial ecology, and at a time when multi-drug resistant bacteria are becoming widespread, phages have been identified as potential antimicrobial agents for biocontrol applications in various applications: medical therapy, agribusiness, and food safety. In the case of *S. enterica*, there have been reports of the use of phages as antimicrobial testing agents in areas ranging from food-producing animals to ready-to-eat foods (Wall et al., 2010; Guenther et al., 2012). In the case of *P. aeruginosa* phages, many reports have suggested that phages can be used to treat *P. aeruginosa* infected wounds and to disrupt the bacterial biofilm (recently reviewed in Wittebole et al., 2014). Nonetheless, it is crucial to remain aware of host–phage dynamics when developing phage therapies. The typical structure

of phage–host populations in fluctuating selection dynamics is that immune bacteria are present in high abundance and are infected by wide host range phages while sensitive bacteria are much less abundant and are infected by both wide and narrow host range phages (Flores et al., 2011). Narrow host range phages are needed and must be carefully selected to ensure that the low abundance bacterial population has no chance at resurgence.

NEW RESEARCH APPROACHES IN PHAGE–HOST INTERACTION

In terms of host–phage interaction, structural biology and microbiology are counterparts. Although several detailed structures of bacteriophages have been determined at near atomic resolution by cryoEM and image analysis (e.g., **Figures 2A,B**; Lander et al., 2012; Guo et al., 2013; Zhang et al., 2013), concern has been raised regarding poor data quality in EM of bacteriophages (Ackermann, 2014). It is also important to keep in mind that identified host–phage interactions are based on a limited number of microbial systems. It is indeed a challenge to catch the action of bacteriophages in their native niches. The invention of a small portable cryo-plunger for cryoEM that allows vitrification of environmental sample on site has opened new opportunities to merge the strengths of metagenomics and of cryoEM (Comolli et al., 2012; Luef et al., 2013). Combining metagenomics and cryogenic electron tomography (cryoET), an imaging technique suitable for visualizing the 3D organization of a pleiomorphic structure at moderate resolution, will reveal unexplored worlds within the microbial community. In fact, cryoET has been used to capture the extensive structural rearrangement of virus particles and their molecular machineries, e.g., during T7 phage infection (**Figure 2C**; Hu et al., 2013), the assembly of cyanophage (Dai et al., 2013) and the formation of virus-associated pyramids (VAPs) for the egression of archaeal virus (Daum et al., 2014).

In addition, the cryoEM 3D reconstruction of phages and virus can be vastly improved by averaging taking advantage of the icosahedral symmetry of the virus (Guo et al., 2013; Li et al., 2013; Zhang et al., 2013). Unfortunately, applying symmetry will completely mask all the unique non-symmetrical features such as base plates and tails. Of interest, a new type of extremely sensitive complementary metal oxide semiconductor (CMOS) detector has recently been developed (McMullan et al., 2009). This detector allows correction for drift and beam-induced motions of the specimen, thus images can be acquired at higher resolution. Bai et al. (2013) were able to reconstruct the 3D asymmetrical structure of ribosome at near atomic resolution using only 30,000 particles. Currently, more routine image processing and data acquisition protocols are being refined for advanced single particle analysis (Bai et al., 2013; Li et al., 2013). Combining single particle EM with biochemical experiments, 3D snapshots of bacteriophages trapped in various states can potentially be achievable at near atomic resolution.

Moreover, an electron-optical equivalent of “phase contrast” light microscopy called “phase plate” is being developed. Various prototypical versions of phase plate have been shown to improve contrast in EM significantly (Daney and Nagayama, 2011; Glaeser, 2013). Glaeser et al. (2013) showed that, with phase plate, small proteins such as individual streptavidin tetramers

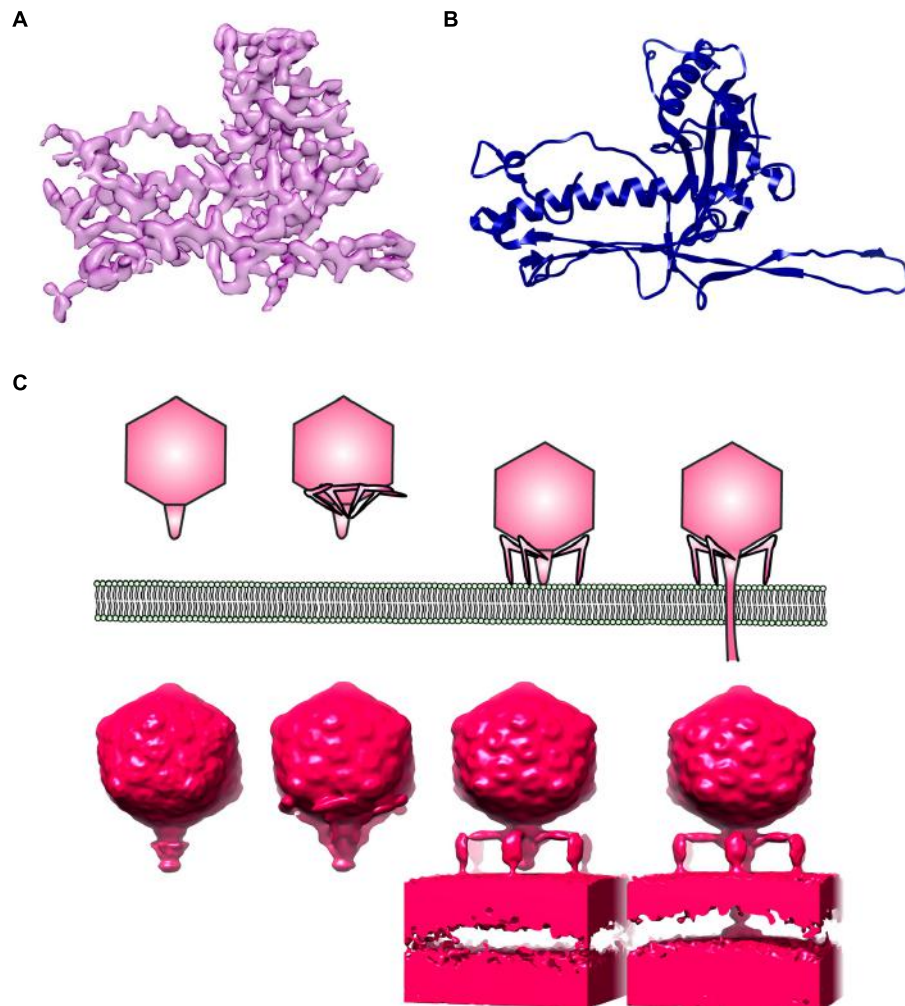


FIGURE 2 | Electron microscopy (EM) of phages. **(A)** An electron density map of a major capsid protein (MCP) from *Bordetella pertussis* phage BPP1 determined by single particle reconstruction at 3.5 Ångstrom resolution. **(B)** A ribbon model of BPP1 MCP (Image rendered from deposited structure, EMD-5766 and PDB ID 3J4U; Zhang et al., 2013). **(C)** A top cartoon shows

different stages of T7 phage infection derived from electron cryotomography based on Hu et al. (2013); bottom shows surface rendition of electron density map generated from electron cryotomography and subtomogram averaging (Images rendered from deposited EMD structures, EMD-5534, EMD-5535, EMD-5536, EMD-5537; Hu et al., 2013).

can be clearly distinguished in cryo. Furthermore, using phase contrast cryoEM, the 3D structure of epsilon15 bacteriophage can be resolved at nanometer resolution even with no symmetry imposed (Murata et al., 2010). Remarkably, structural details such as the tail and capsid of an individual phage can be directly delineated by electron cryo-tomographic reconstruction (Murata et al., 2010). Once these elaborate EM instruments are in place, they will enable not only a relatively routine 3D rendition of phages at high resolution using single particle analysis, but will also elucidate phage structural dynamics in the physiological environment.

Advances in metagenomics analyses and sequencing technologies have not only led to a much better appreciation of the abundance of uncultivable environmental microbial populations, but they have also enabled the monitoring of community dynamics (Breitbart and Rohwer, 2005; Edwards and Rohwer, 2005; Suttle,

2005; Rosario and Breitbart, 2011; Breitbart, 2012; Duhaime and Sullivan, 2012). However, only a handful of insights on the novel phage species can be gained through such techniques. Combining metagenomic analysis with correlative light-EM, which allows visualization of the same sample with both fluorescent and EM (Knierim et al., 2012; Luef et al., 2013; Chang et al., 2014; Schorb and Briggs, 2014), will lead to a “visual metagenomics” that will drive the genomic identification and structural characterization of novel uncultivable phages. Clearly, this is just the beginning of a new era of phage research.

CONCLUSIONS AND PERSPECTIVES

In this review, we summarize the physical interactions between tailed phages and commonly found Gram-negative bacterial pathogens, specifically *S. enterica* and *P. aeruginosa*, which can be used as models, for other pathogens in the development

of phage therapeutic strategy. The ongoing evolutionary battles between phages and bacteria continue to shape microbial communities. As the co-evolution continues, bacteria develop resistance and exploit phage machinery to fight other bacteria in order to increase environmental fitness while phages manipulate host behaviors by alteration of bacterial gene expression. Recent advances in metagenomic analysis open new doors to the vast resources of genetic diversity of viromes from various habitats, while cryoET gives much clearer pictures of how phages and hosts interact at the molecular level. Functional characterization of phages in the laboratory, combined with cryoET and subtomogram averaging, provide snapshots of different stages in phage infection. Furthermore, recent developments in direct-electron detection technology, phase plate and single particle EM provide routine protocols for determination of 3D structures of phages at near-atomic resolution. These could potentially revolutionize our understanding of the complex interplay between phages and hosts in their natural ecosystems, which is of fundamental importance in phage use in biocontrol and therapeutic strategies.

ACKNOWLEDGMENTS

Soraya Chaturongakul acknowledges the support by the Center of Excellence on Environmental Health, Toxicology and Management of Chemicals (ETM). Puey Ounjai acknowledges support from the Talent Management Program of Mahidol University.

REFERENCES

- Ackermann, H. W. (2014). Sad state of phage electron microscopy. Please shoot the messenger. *Microorganisms* 2, 1–10. doi: 10.3390/microorganisms2010001
- Ackermann, H. W., and Prangishvili, D. (2012). Prokaryote viruses studied by electron microscopy. *Arch. Virol.* 157, 1843–1849. doi: 10.1007/s00705-012-1383-y
- Andres, D., Roske, Y., Doering, C., Heinemann, U., Seckler, R., and Barbirz, S. (2012). Tail morphology controls DNA release in two *Salmonella* phages with one lipopolysaccharide receptor recognition system. *Mol. Microbiol.* 83, 1244–1253. doi: 10.1111/j.1365-2958.2012.08006.x
- Bae, H., and Cho, Y. (2013). Complete genome sequence of *Pseudomonas aeruginosa* podophage MPK7, which requires type IV pili for infection. *Genome Announc.* 1, e00744–e00813. doi: 10.1128/genomeA.00744-13
- Bai, X. C., Fernandez, I. S., McMullan, G., and Scheres, S. H. W. (2013). Ribosome structures to near-atomic resolution from thirty thousand cryo-EM particles. *Elife* 2, e00461. doi: 10.7554/elife.00461
- Barr, J. J., Auro, R., Furlan, M., Whiteson, K. L., Erb, M. L., Pogliano, J., et al. (2013). Bacteriophage adhering to mucus provide a non-host-derived immunity. *Proc. Natl. Acad. Sci. U.S.A.* 110, 10771–10776. doi: 10.1073/pnas.1305923110
- Basler, M., Pilhofer, M., Henderson, G. P., Jensen, G. J., and Mekalanos, J. J. (2012). Type VI secretion requires a dynamic contractile phage tail-like structure. *Nature* 483, 182–186. doi: 10.1038/nature10846
- Bergh, O., Borsheim, K. Y., Bratbak, G., and Heldal, M. (1989). High abundance of viruses found in aquatic environments. *Nature* 340, 467–468. doi: 10.1038/340467a0
- Breitbart, M. (2012). Marine viruses: truth or dare. *Ann. Rev. Mar. Sci.* 4, 425–448. doi: 10.1146/annurev-marine-120709-142805
- Breitbart, M., Hewson, I., Felts, B., Mahaffy, J. M., Nulton, J., Salamon, P., and Rohwer, F. (2003). Bacteriophages, transposons, and plasmids: metagenomic analyses of an uncultured viral community from human feces. *J. Bacteriol.* 185, 6220–6223. doi: 10.1128/JB.185.20.6220-6223.2003
- Breitbart, M., and Rohwer, F. (2005). Here a virus, there a virus, everywhere the same virus? *Trends Microbiol.* 13, 278–284. doi: 10.1016/j.tim.2005.04.003
- Casjens, S. R., Gilcrease, E. B., Winn-Stapley, D. A., Schicklmaier, P., Schmieger, H., Pedulla, M. L., et al. (2005). The generalized transducing *Salmonella* bacteriophage es18: complete genome sequence and DNA packaging strategy. *J. Bacteriol.* 187, 1091–1104. doi: 10.1128/JB.187.3.1091-1104.2005
- Chang, Y. W., Chen, S., Tocheva, E. I., Treuner-Lange, A., Löbach, S., Søgaard-Andersen, L., et al. (2014). Correlated cryogenic photoactivated localization microscopy and cryo-electron tomography. *Nat. Methods* 11, 737–739. doi: 10.1038/nmeth.2961
- Choi, Y., Shin, H., Lee, J., and Ryu, S. (2013). Identification and characterization of a novel flagellum-dependent *Salmonella*-infecting bacteriophage, iEPS5. *Appl. Environ. Microbiol.* 79, 164829–164837. doi: 10.1128/AEM.00706-13
- Comolli, L. R., Duarte, R., Baum, D., Luef, B., Downing, K. H., Larson, D. M., et al. (2012). A portable cryo-plunger for on-site intact cryogenic microscopy sample preparation in natural environments. *Microsc. Res. Tech.* 75, 829–836. doi: 10.1002/jemt.22201
- Cumby, N., Edwards, A. M., Davidson, A. R., and Maxwell, K. L. (2012). The bacteriophage HK97 gp15 moron element encoded a novel superinfection exclusion protein. *J. Bacteriol.* 194, 5012–5019. doi: 10.1128/JB.00843-12
- Dai, W., Fu, C., Raytcheva, D., Flanagan, J., Khant, H. A., Liu, X., et al. (2013). Visualizing virus assembly intermediates inside marine cyanobacteria. *Nature* 502, 707–710. doi: 10.1038/nature12604
- Danev, R., and Nagayama, K. (2011). Optimizing the phase shift and the cut-on periodicity of phase plates for TEM. *Ultramicroscopy* 111, 1305–1315. doi: 10.1016/j.ultramic.2011.04.004
- Daum, B., Quax, T. E. F., Sachse, M., Mills, D. J., Reimann, J., Yıldız, Ö., et al. (2014). Self-assembly of the general membrane remodeling protein PVAP into sevenfold virus associated pyramids. *Proc. Natl. Acad. Sci. U.S.A.* 111, 3829–3834. doi: 10.1073/pnas.1319245111
- Duhame, M. B., and Sullivan, M. B. (2012). Ocean viruses: rigorously evaluating the metagenomic sample-to-sequence pipeline. *Virology* 434, 181–186. doi: 10.1016/j.virol.2012.09.036
- Edwards, R. A., and Rohwer, F. (2005). Viral metagenomics. *Nat. Rev. Microbiol.* 3, 504–510. doi: 10.1038/nrmicro1163
- Flores, C. O., Meyer, J. R., Valverde, S., Farr, L., and Weitz, J. S. (2011). Statistical structure of host-phage interactions. *Proc. Natl. Acad. Sci. U.S.A.* 108, E288–E297. doi: 10.1073/pnas.1101595108
- Fokine, A., and Rossman, M. G. (2014). Molecular architecture of tailed double-stranded DNA phages. *Bacteriophage* 4, e28281. doi: 10.104161/bact.28281
- Fuhrman, J. A. (1999). Marine viruses and their biogeochemical and ecological effects. *Nature* 399, 541–548. doi: 10.1038/21119
- Glaeser, R. M. (2013). Methods for imaging weak-phase objects in electron microscopy. *Rev. Sci. Instrum.* 84, 111101. doi: 10.1063/1.4830355
- Glaeser, R. M., Sassolini, S., Cambie, R., Jin, J., Cabrini, S., Schmid, A. K., et al. (2013). Minimizing electrostatic charging of an aperture used to produce in-focus phase contrast in the TEM. *Ultramicroscopy* 135, 6–15. doi: 10.1016/j.ultramic.2013.05.023
- Gogarten, J. P., Doolittle, W. F., and Lawrence, J. G. (2002). Prokaryotic evolution in light of gene transfer. *Mol. Biol. Evol.* 19, 2226–2238. doi: 10.1093/oxfordjournals.molbev.a004046
- Gómez, P., and Buckling, A. (2011). Bacteria-phage antagonistic coevolution in soil. *Science* 332, 106–109. doi: 10.1126/science.1198767
- Guenther, S., Herzig, O., Fieseler, L., Klumpp, J., and Loessner, M. J. (2012). Biocontrol of *Salmonella Typhimurium* in RTE foods with bacteriophage FO1-E2. *Int. J. Food Microbiol.* 154, 66–72. doi: 10.1016/j.ijfoodmicro.2011.12.023
- Guo, F., Liu, Z., Vago, F., Ren, Y., Wu, W., Wright, E. T., et al. (2013). Visualization of uncorrelated, tandem symmetry mismatches in the internal genome packaging apparatus of bacteriophage T7. *Proc. Natl. Acad. Sci.* 110, 6811–6816. doi: 10.1073/pnas.1215563110
- Hall, A. R., Scanlan, P. D., Morgan, A. D., and Buckling, A. (2011). Host-parasite coevolutionary arms races give way to fluctuating selection. *Ecol. Lett.* 14, 634–642. doi: 10.1111/j.1461-0248.2011.01624.x
- Hanlon, G. W., Denyer, S. P., Olliff, C. J., and Ibrahim, L. J. (2001). Reduction in exopolysaccharide viscosity as an aid to bacteriophage penetration through

- Pseudomonas aeruginosa* biofilms. *Appl. Environ. Microbiol.* 67, 2746–2753. doi: 10.1128/AEM.67.6.2746-2753.2001
- Hendrix, R. W., Smith, M. C., Burns, R. N., Ford, M. E., and Hatfull, G. F. (1999). Evolutionary relationships among diverse bacteriophages and prophages: all the world's a phage. *Proc. Natl. Acad. Sci. U.S.A.* 96, 2192–2197. doi: 10.1073/pnas.96.5.2192
- Heo, Y., Chung, I., Choi, K. B., Lau, G. W., and Cho, Y. (2007). Genome sequence comparison and superinfection between two related *Pseudomonas aeruginosa* phages, D3112 and MP22. *Microbiology* 153, 2885–2895. doi: 10.1099/mic.0.2007/007260-0
- Ho, T. D., and Slouch, J. M. (2001). OmpC is the receptor for Gifsy-1 and Gifsy-2 bacteriophages of *Salmonella*. *J. Bacteriol.* 183, 1495–1498. doi: 10.1128/JB.183.4.1495-1498.2001
- Hosseinioust, Z., Tufenkji, N., and van de Ven, T. G. M. (2013). Predation in homogeneous and heterogeneous phage environments affects virulence determinants of *Pseudomonas aeruginosa*. *Appl. Environ. Microbiol.* 79, 2862–2871. doi: 10.1128/AEM.03817-12
- Hu, B., Margolin, W., Molineux, I. J., and Liu, J. (2013). The bacteriophage T7 virion undergoes extensive structural remodeling during infection. *Science* 339, 576–579. doi: 10.1126/science.1231887
- Kim, M., Kim, S., Park, B., and Ryu, S. (2014). Core lipopolysaccharide-specific phage SSU5 as an auxiliary component of a phage cocktail for *Salmonella* biocontrol. *Appl. Environ. Microbiol.* 80, 1026–1034. doi: 10.1128/AEM.03494-13
- Kim, M., and Ryu, S. (2011). Characterization of a T5-like coliphage, SPC35, and differential development of resistance to SPC35 in *Salmonella enterica* serovar *Typhimurium* and *Escherichia coli*. *Appl. Environ. Microbiol.* 77, 2042–2050. doi: 10.1128/AEM.02504-10
- Kim, M., and Ryu, S. (2012). Spontaneous and transient defence against bacteriophage by phase-variable glucosylation of O-antigen in *Salmonella enterica* serovar *Typhimurium*. *Mol. Microbiol.* 86, 411–425. doi: 10.1111/j.1365-2958.2012.08202.x
- Kimura, M., Jia, Z., Nakayama, N., and Asakawa, S. (2008). Ecology of viruses in soils: past, present and future perspectives. *Soil Sci. Plant Nutr.* 54, 1–32. doi: 10.1111/j.1747-0765.2007.00197.x
- Knierim, B., Luef, B., Wilmes, P., Webb, R. I., Auer, M., Comolli, L. R., et al. (2012). Correlative microscopy for phylogenetic and ultrastructural characterization of microbial communities. *Environ. Microbiol. Rep.* 4, 36–41. doi: 10.1111/j.1758-2229.2011.00275.x
- Labrie, S. J., Samson, J. E., and Moineau, S. (2010). Bacteriophage resistance mechanisms. *Nat. Rev. Microbiol.* 8, 817–827. doi: 10.1038/nrmicro2315
- Lander, G. C., Baudoux, A. C., Azam, F., Potter, C. S., Carragher, B., and Johnson, J. E. (2012). Capsomer dynamics and stabilization in the T = 12 marine bacteriophage SIO-2 and its procapsid studied by CryoEM. *Structure* 20, 498–503. doi: 10.1016/j.str.2012.01.007
- Le, S., He, X., Tan, Y., Huang, G., Zhang, L., Lux, R., et al. (2013). Mapping the tail fiber as the receptor binding protein responsible for differential host specificity of *Pseudomonas aeruginosa* bacteriophages PaP1 and JG004. *PLoS ONE* 8:e68562. doi: 10.1371/journal.pone.0068562
- Li, X., Mooney, P., Zheng, S., Booth, C., Braunfeld, M. B., Gubbens, S., et al. (2013). Electron counting and beam-induced motion correction enable near atomic resolution single particle cryoEM. *Nat. Methods* 10, 584–590. doi: 10.1038/nmeth.2472
- Lindberg, A. A. (1973). Bacteriophage receptors. *Annu. Rev. Microbiol.* 27, 205–241. doi: 10.1146/annurev.mi.27.100173.001225
- Luef, B., Fakra, S. C., Csencsits, R., Wrighton, K. C., Williams, K. H., Wilkins, M. J., et al. (2013). Iron-reducing bacteria accumulate ferric oxyhydroxide nanoparticle aggregates that may support planktonic growth. *ISME J.* 7, 338–350. doi: 10.1038/ismej.2012.103
- Marsh, P., and Wellington, E. M. (1994). Phage-host interaction in soil. *FEMS Microbiol. Ecol.* 15, 99–108. doi: 10.1111/j.1574-6941.1994.tb00234.x
- Marti, R., Zurfluh, K., Hagens, S., Pianezzi, J., Klumpp, J., and Loessner, M. J. (2013). Long tail fibres of the novel broad-host-range T-even bacteriophage S16 specifically recognize *Salmonella* OmpC. *Mol. Microbiol.* 87, 818–834. doi: 10.1111/mmi.12134
- McMullan, G., Faruqi, A. R., Henderson, R., Guerrini, N., Turchetta, R., and van Hoften, G. (2009). Experimental observation of the improvement in MTF from backthinning a CMOS direct electron detector. *Ultramicroscopy* 109, 1144–1147. doi: 10.1016/j.ultramic.2009.05.005
- Mills, S., Shanahan, F., Stanton, C., Hill, C., Coffey, A., and Ross, R. P. (2013). Movers and shakers: influence of bacteriophages in shaping the mammalian gut microbiota. *Gut Microbes* 4, 4–16. doi: 10.4161/gmic.22371
- Minot, S., Bryson, A., Chehoud, C., Wu, G. D., Lewis, J. D., and Bushman, F. D. (2013). Rapid evolution of the human gut virome. *Proc. Natl. Acad. Sci. U.S.A.* 110, 12450–12455. doi: 10.1073/pnas.1300833110
- Minot, S., Sinha, R., Chen, J., Li, H., Keilbaugh, S. A., Wu, G. D., et al. (2011). The human gut virome: inter-individual variation and dynamic response to diet. *Genome Res.* 21, 1616–1625. doi: 10.1101/gr.122705.111
- Murata, K., Liu, X., Danev, R., Jakana, J., Schmid, M. F., King, J., et al. (2010). Zernike phase contrast cryo-electron microscopy and tomography for structure determination at nanometer and subnanometer resolutions. *Structure* 18, 903–912. doi: 10.1016/j.str.2010.06.006
- Nakayama, K., Takashima, K., Ishihara, H., Shinomiya, T., Kageyama, M., Kanaya, S., et al. (2000). The R-type pyocin of *Pseudomonas aeruginosa* is related to P2 phage, and the F-type is related to lambda phage. *Mol. Microbiol.* 38, 213–231. doi: 10.1046/j.1365-2958.2000.02135.x
- Novick, R. P., Christie, G. E., and Penades, J. R. (2010). The phage-related chromosomal islands of gram-positive bacteria. *Nat. Rev. Microbiol.* 8, 541–551. doi: 10.1038/nrmicro2393
- Pickard, D., Toribio, A. L., Petty, N. K., de Tonder, A., Yu, L., Goulding, D., et al. (2010). A conserved acetyl esterase domain targets diverse bacteriophage to the Vi capsular receptor of *Salmonella enterica* serovar *Typhi*. *J. Bacteriol.* 192, 5746–5754. doi: 10.1128/JB.00659-10
- Ricci, V., and Piddock, L. J. V. (2010). Exploiting the role of TolC in pathogenicity: identification of a bacteriophage for eradication of *Salmonella* serovars from poultry. *Appl. Environ. Microbiol.* 76, 1704–1706. doi: 10.1128/AEM.02681-09
- Rosario, K., and Breitbart, M. (2011). Exploring the viral world through metagenomics. *Curr. Opin. Virol.* 1, 289–297. doi: 10.1016/j.coviro.2011.06.004
- Samson, J. E., Magadan, A. H., Sabri, M., and Moineau, S. (2013). Revenge of the phages: defeating bacterial defences. *Nat. Rev. Microbiol.* 11, 675–687. doi: 10.1038/nrmicro3096
- Schorb, M., and Briggs, J. A. (2014). Correlated cryo-fluorescence and cryo-electron microscopy with high spatial precision and improved sensitivity. *Ultramicroscopy* 143, 24–32. doi: 10.1016/j.ultramic.2013.10.015
- Shikuma, N. J., Pilhofer, M., Weiss, G. L., Hadfield, M. G., Jensen, G. J., and Newman, D. K. (2014). Marine tapeworm metamorphosis induced by arrays of bacterial phage tail-like structures. *Science* 343, 529–533. doi: 10.1126/science.1246794
- Shin, H., Lee, J., Kim, H., Choi, Y., Heu, S., and Ryu, S. (2012). Receptor diversity and host interaction of bacteriophages infecting *Salmonella enterica* serovar *Typhimurium*. *PLoS ONE* 7:e43392. doi: 10.1371/journal.pone.0043392
- Susskind, M. M., Botstein, D., and Wright, A. (1974a). Superinfection exclusion by P22 prophage in lysogens of *Salmonella typhimurium*. III. Failure of superinfecting phage DNA to enter sieA+ lysogens. *Virology* 62, 350–366. doi: 10.1016/0042-6822(74)90398-5
- Susskind, M. M., Wright, A., and Botstein, D. (1974b). Superinfection exclusion by P22 prophage in lysogens of *Salmonella typhimurium*. IV. Genetics and physiology of sieB exclusion. *Virology* 62, 367–384. doi: 10.1016/0042-6822(74)90399-7
- Suttle, C. A. (2005). Viruses in the sea. *Nature* 437, 356–361. doi: 10.1038/nature04160
- Suttle, C. A. (2007). Marine viruses-major players in the global ecosystem. *Nat. Rev. Microbiol.* 5, 801–812. doi: 10.1038/nrmicro1750
- Temple, G. S., Ayling, P. D., and Wilkinson, S. G. (1986). Isolation and characterization of a lipopolysaccharide-specific bacteriophage of *Pseudomonas aeruginosa*. *Microbiol. Microbiol.* 45, 81–91. doi: 10.1099/0022-1317-33-1-99
- Thingstad, T. F., and Lignell, R. (1997). Theoretical models for the control of bacterial growth rate, abundance, diversity and carbon demand. *Aquat. Microb. Ecol.* 13, 19–27. doi: 10.3354/ame013019
- Veesler, D., and Cambillau, C. (2011). A common evolutionary origin for tailed-bacteriophage functional modules and bacterial machineries. *Microbiol. Mol. Biol. Rev.* 75, 423–433. doi: 10.1128/MMBR.00014-11

- Wall, S. K., Zhang, J., Rostagno, M. H., and Ebner, P. D. (2010). Phage therapy to reduce preprocessing *Salmonella* infections in market-weight swine. *Appl. Environ. Microbiol.* 76, 48–53. doi: 10.1128/AEM.00785-09
- Webber, M. A., Bailey, A. M., Blair, J. M. A., Morgan, E., Stevens, M. P., Hinton, J. C. D., et al. (2009). The global consequence of disruption of the AcrAB-TolC efflux pump in *Salmonella enterica* includes reduced expression of SPI-1 and other attributes required to infect the host. *J. Bacteriol.* 191, 4276–4285. doi: 10.1128/JB.00363-09
- Williams, H. T. P. (2013). Phage-induced diversification improves host evolvability. *BMC Evol. Biol.* 13:17. doi: 10.1186/1471-2148-13-17
- Wittebole, X., De Roock, S., and Opal, S. M. (2014). A historical overview of bacteriophage therapy as an alternative to antibiotics for the treatment of bacterial pathogens. *Virulence* 5, 225–235. doi: 10.4161/viru.25991
- Zhang, X., Guo, H., Jin, L., Czornyj, E., Hodes, A., Hui, W. H., et al. (2013). A new topology of the HK97-like fold revealed in *Bordetella* bacteriophage by cryoEM at 3.5 Å resolution. *Elife* 2, e01299. doi: 10.7554/elife.01299

Conflict of Interest Statement: The authors declare that the research was conducted in the absence of any commercial or financial relationships that could be construed as a potential conflict of interest.

Received: 30 April 2014; accepted: 04 August 2014; published online: 20 August 2014.
Citation: Chaturongakul S and Ounjai P (2014) Phage-host interplay: examples from tailed phages and Gram-negative bacterial pathogens. *Front. Microbiol.* 5:442. doi: 10.3389/fmicb.2014.00442

This article was submitted to Terrestrial Microbiology, a section of the journal *Frontiers in Microbiology*.

Copyright © 2014 Chaturongakul and Ounjai. This is an open-access article distributed under the terms of the Creative Commons Attribution License (CC BY). The use, distribution or reproduction in other forums is permitted, provided the original author(s) or licensor are credited and that the original publication in this journal is cited, in accordance with accepted academic practice. No use, distribution or reproduction is permitted which does not comply with these terms.



Emergence of microbial networks as response to hostile environments

Dario Madeo¹, Luis R. Comolli² and Chiara Mocenni^{1*}

¹ Department of Information Engineering and Mathematics, University of Siena, Siena, Italy

² Structural Biology and Imaging Department, Life Sciences Division, Lawrence Berkeley National Laboratory, Berkeley, CA, USA

Edited by:

Lisa Y. Stein, University of Alberta, Canada

Reviewed by:

Elisa Michelin, University of Bologna, Italy

Jorge Passamani Zubelli, IMPA, Brazil

***Correspondence:**

Chiara Mocenni, Department of Information Engineering and Mathematics, University of Siena, via Roma 56, 53100 Siena, Italy
e-mail: mocenni@dii.unisi.it

The majority of microorganisms live in complex communities under varying conditions. One pivotal question in evolutionary biology is the emergence of cooperative traits and their sustainment in altered environments or in the presence of free-riders. Co-occurrence patterns in the spatial distribution of biofilms can help define species' identities, and systems biology tools are revealing networks of interacting microorganisms. However, networks of inter-dependencies involving micro-organisms in the planktonic phase may be just as important, with the added complexity that they are not bounded in space. An integrated approach linking imaging, "Omics" and modeling has the potential to enable new hypothesis and working models. In order to understand how cooperation can emerge and be maintained without abilities like memory or recognition we use evolutionary game theory as the natural framework to model cell-cell interactions arising from evolutive decisions. We consider a finite population distributed in a spatial domain (biofilm), and divided into two interacting classes with different traits. This interaction can be weighted by distance, and produces physical connections between two elements allowing them to exchange finite amounts of energy and matter. Available strategies to each individual of one class in the population are the propensities or "willingness" to connect any individual of the other class. Following evolutionary game theory, we propose a mathematical model which explains the patterns of connections which emerge when individuals are able to find connection strategies that asymptotically optimize their fitness. The process explains the formation of a network for efficiently exchanging energy and matter among individuals and thus ensuring their survival in hostile environments.

Keywords: microbial communities, bacterial social networks, evolutionary games, graph theory, evolutive decisions, hostile environmental conditions

1. INTRODUCTION

How spatial and temporal organization in cell-cell interactions are achieved remains largely elusive. The central hypothesis of this unique topic is that a broad range of interactions and connections forming networks across species define strategies for co-evolution, and the display of adaptive strategies from microbial networks as a response to altered environments (Ben-Jacob and Cohen, 1997; Ben-Jacob et al., 2000; Dwyer et al., 2008). These are questions of great interest in a rapidly evolving area of science.

Surfaces concentrate nutrients, and it is generally assumed that planktonic cells were the first to take advantage of the catalytic and protective advantages offered by surfaces—a first step in the development of biofilms. Likely the first complex systems to achieve homeostasis in response to fluctuations in the primitive Earth environment, biofilms facilitated the development of complex interactions between individual cells and the development of signaling pathways and chemotactic motility (Hall-Stoodley et al., 2004; Fuhrman, 2009; Gure, 2009; Shimoyama et al., 2009). Interactions between two species of microbes that affect their coexistence and evolution have been studied in a laboratory system of two species (Hansen et al., 2009). Direct cell-cell

interspecies interactions have been reported for laboratory cultures (Dubey and Ben-Yehuda, 2011) and for intact microbes in natural communities (Comolli and Banfield, 2014).

New metagenomics data from environmental microbial communities (e.g., Wrighton et al., 2012; Kantor et al., 2013) is showing that novel, small microorganisms lack the full metabolic potential to have a truly independent lifestyle. In other work (Baker et al., 2010; Comolli and Banfield, 2014) linking genomics and imaging, one novel nanoarchaea named ARMAN has been found establishing connections with archaea of different species. Therefore, we start with microbes of different classes or species assuming they lack the full metabolic potential necessary for survival under certain conditions; we also assume the two species complement the needs of each other, so that individual of one species seek the complement provided by individuals of the other species.

Evolutionary game theory (Weibull, 1995; Hofbauer and Sigmund, 1998; Nowak, 2006b) provides a rather intuitive framework to model interactions and decisions among co-evolving members of a population. It has been successfully used to describe relevant mechanisms of cooperation in biology (Nowak, 2006a; Frey, 2010) as the result of collective behavior induced by

altruistic decisions, which allows a population to increase its own fitness.

The present study is an attempt to model the activation of connections among the members of a population of microorganisms accounting for the new findings on microbial communities formation. Starting from evolutionary game theory we are interested in understanding the conditions (for the simplified variables and parameters of our model) allowing the onset of cooperative interaction between two or more individuals, and their sustainment in the most efficient networks. Specifically the formation of suitable physical connections will eventually allow them to exchange a certain amount of energy and matter. The activation of links among microorganisms gives rise to the formation of a network, which increases the probability that any single individual and the whole population will survive.

The proposed approach is based on a recent paper (Madeo and Mocenni, under revision) where evolutionary game theory is extended to model the behavior of a finite population in which members are organized according to a network of relationships between them, such as friendship, spatial proximity, sharing, etc. The model introduced in that paper describes decisions of single individuals rather than average strategies of the whole population, and provides a natural tool to deal with the problem of connection formation among couples of bacteria from a single-cell fitness perspective—we will use the term “bacteria” for simplicity, but they could also be archaea or protists. The main idea motivating the present paper is that two microorganisms establish a connection when it provides a significant gain to both. This paradigm assumes that two classes of bacteria with different biological characteristics are present in the system, and under averse environmental conditions members of one class may need to access resources that only the individuals of the other class are able to produce, and viceversa.

In terms of game theory the propensity of a bacterium to establish a connection with another one is a behavioral strategy, namely a *game strategy*. Each strategy provides a certain payoff which accounts for natural constraints, such as distance and available energy. A connection strategy becomes effective if both involved individuals take an enough great advantage from it. This process can be described as a game where available strategies to the players are decisions to connect. Evolutionary games and the replicator equations introduced in Madeo and Mocenni (under revision) provide the mathematical models allowing us to follow the system dynamics of connections of a single bacterium and network formation at a global level. As a result, if the environmental conditions are favorable, the bacteria spend their energy only on surviving and reproducing. To the contrary, under averse conditions they acquire/transfer a certain amount of available energy from/to the connected bacteria. A similar phenomenon is the well known mechanism of coordinated motion and aggregation shown by the starving amoeba *Dictyostelium discoideum* (Eichinger and Noegel, 2003). Moreover, we assume that the bacteria are not allowed to move. Indeed, in the present work we are mainly focused on introducing a methodology that will be leverage in future works, and where the models will be compared with experimental data.

The approach proposed in this paper implicitly incorporates mechanisms of cell-cell recognition underlying interspecies interactions, and uses theory and modeling to show the emergence of counterintuitive patterns resulting, for example, from long term communication mechanisms. Our results show that the formed networks optimize the use of the available energy produced and exchanged between microorganisms. We also find conditions or regions of the parameter space which clearly enable or prevent efficient outcomes.

The paper is organized as follows: Section 2 describes the components of the mathematical model, such as bacteria, decisions and payoffs, the model equations, and the basic mechanisms of network formation. In Section 3 theoretical and experimental results are reported. The results obtained are discussed in Section 4. Finally, Section 5. reports a detailed technical description of the evolutionary game which is assumed to be the basis of system dynamics.

2. MATERIALS AND METHODS

In this section we introduce the mathematical model describing the mechanism for which the individuals of a population of bacteria are able to make the decision of establishing reciprocal connections aimed at maximizing their probability of survival in a hostile environment. More precisely, cooperation yields the activation of a physical connection between two or more organisms, such as the extensions visible in **Figure 1** where the Cryogenic-electron microscopy image of a biofilm revealing the existence of connections among archaea of different species are reported.

2.1. INDIVIDUALS, STRATEGIES, DECISIONS, AND REWARDS

We assume that a population of N bacteria is located in a spatial domain and that it is composed of two subclasses. The classes differ only for genetic and phenotypic characteristics, and not for their members behavior or decisions. Elements of different classes can create links to exchange genetic material, proteins, metabolic intermediates, etc. The formation of links is assumed to stem from the need to obtain elements allowing bacteria to better resist hostile external conditions (Ben-Jacob et al., 2000). Analogously two elements of the same class are not allowed to create any link. The original conditions are restored once the external situation becomes favorable again and the bacteria are able to reproduce.

In order to be willing to create a link, a microorganism must have enough (finite) available energy to exchange with one or more organisms of another class. The level of energy that bacteria decide to share depends on how averse the environmental conditions are. Moreover, energy transfer is dissipative, because a part of the energy is lost due to distance and effort of linking.

The model developed in this paper assumes that the connections are bilateral; although, one can allow monodirectional links as explained in Section 2.3.

The processes and assumptions described above can be modeled by introducing the following variables:

- \mathcal{V} is the set of all considered bacteria ($|\mathcal{V}| = N$);
- $\mathcal{V}_1 \subset \mathcal{V}$ and $\mathcal{V}_2 \subset \mathcal{V}$ are the subclasses, where $\mathcal{V} = \mathcal{V}_1 \cup \mathcal{V}_2$ and $\mathcal{V}_1 \cap \mathcal{V}_2 = \emptyset$;

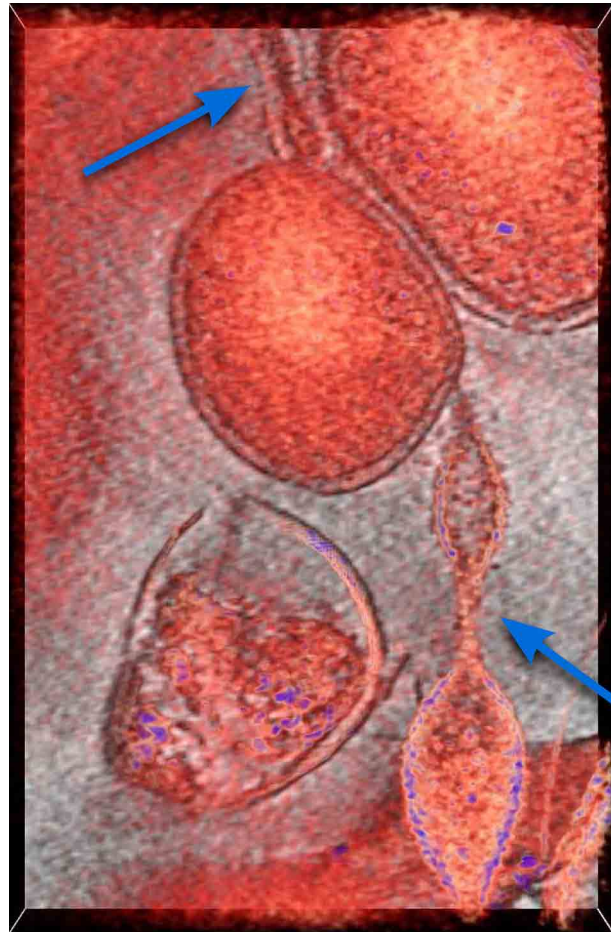


FIGURE 1 | Cryogenic-electron microscopy image of a small region of a biofilm. In red, a 50-voxel-thick slice through a tomographic reconstruction overlaid onto a one-voxel-thick slice in gray scale. There is a round cell at the center and what appears to be an extension from a different cell type into it from the bottom, and another at the top. Previous work (see Baker et al., 2010 and references therein) established they belong to different species of archaea. Arrows indicate tubular extensions or appendages connecting the microbial cell in the center to microbial cells of different species. This is established by their typical, clearly different cell walls. For more information see Comolli and Banfield (2014) in this Special Topic.

- $\rho_{v,w} > 0$ is the distance between bacteria v and w ;
- $T_v > 0$ is the maximum amount of energy that organism v can transfer to others.

The decision of an individual to establish a connection with other individuals is modeled using an evolutive game. In the game the players (bacteria) are allowed to choose a strategy in set \mathcal{S} . The strategies available to each player consist of the will of being connected to another player. The number of feasible strategies to each player is N and we can state a relationship of equivalence between players and strategies. For simplicity of notation, we indicate players and strategies by means of their labels, thus $\mathcal{V} = \mathcal{S} = \{1, \dots, N\}$, and, when needed, players will be labeled by the letters v, w, \dots and their strategies by the symbols s_v, s_w, \dots . For example, if player $v \in \mathcal{V}$ uses strategy $s_v \in \mathcal{S}$ with $v \neq s_v$, he wishes to connect to player $w \in \mathcal{V}$, which is such that

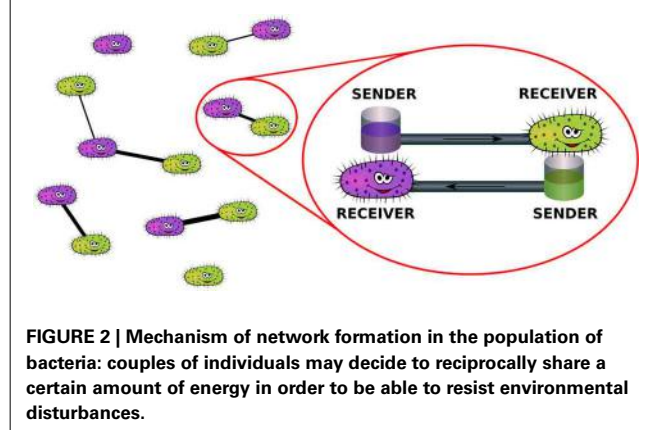


FIGURE 2 | Mechanism of network formation in the population of bacteria: couples of individuals may decide to reciprocally share a certain amount of energy in order to be able to resist environmental disturbances.

$w = s_v$. On the contrary, if $v = s_v$, then v is connected only to himself. Since self energy transfers are not meaningful, circular connections correspond to the activation of any connection.

Consider two individuals, $v \in \mathcal{V}_1$ and $w \in \mathcal{V}_2$, and suppose that v chooses pure strategy $s_v \in \mathcal{S}$ and w chooses pure strategy $s_w \in \mathcal{S}$. At this point, v will receive energy from w if and only if $s_v = w$ and $s_w = v$. The same holds for w . This means that individual v is effectively connected to w if and only if w is also willing to be connected to v .

A pictorial representation of the physical mechanisms described by the model is reported in **Figure 2**.

The effective energy $\mathcal{E}(w, v)$ received by v when it is connected to w depends on the reciprocal decisions of the two individuals to be connected and on their physical distance. More specifically, energy is defined by:

$$\mathcal{E}(w, v) = T_w \gamma(\rho_{v,w}), \quad (1)$$

where $\gamma(\rho)$ is a monotonically decreasing function allowing to quantify the effective available energy after dissipation due to distance. Although multiple specifications are possible, the properties that $\gamma(\rho)$ should satisfy are the following:

- (i) $\gamma(\rho) \geq 0 \forall \rho \in [0, +\infty)$;
- (ii) $\gamma'(\rho) \leq 0 \forall \rho \in [0, +\infty)$;
- (iii) $\gamma(0) = 1$;
- (iv) $\gamma(+\infty) = 0$.

Moreover, $\mathcal{E}(w, v) = 0$ if v and w belong to the same set.

Notice that since T_v is generally different from T_w , $\mathcal{E}(w, v)$ can be different from $\mathcal{E}(v, w)$, i.e., the two individuals may earn different rewards from connection.

To develop the model equations describing the biological mechanism of cooperation, we assume that the members of the population are allowed to play suitable games, the strategies of which are the propensity to form connections. The members of the population will be interchangeably called individuals, bacteria or players.

2.2. THE REPLICATOR EQUATION OF CONNECTIONS

The state variable of the model is the propensity x_{v,s_v} of a player to connect to another player. More specifically, the quantity x_{v,s_v} can

be read as a percentage indicating the share of energy that player v is available to transfer to player w . According to our previous notation, we can also indicate the second player w as the strategy that player v adopts when he is looking for a connection with him ($w = s_v$). The distribution of strategies of a single individual v of the population is accounted by vector

$$\mathbf{x}_v = (x_{v,1}, \dots, x_{v,N}),$$

where

$$\sum_{s_v=1}^N x_{v,s_v} = 1 \wedge x_{v,s_v} \in [0, 1] \forall v, s_v.$$

In general, $x_{v,s_v} \neq x_{s_v,v}$, because two individuals starting the process of connection are allowed to independently choose the amount of sharable energy—although both are required to share a minimum energy to make effective connections.

An individual can decide to share his energy with more than one, at which point the vector representing strategy distribution \mathbf{x}_v may include components strictly less than 1. In this case, it is called *mixed strategy* distribution. On the other hand, solutions with $N - 1$ null and only one unitary component are called *pure strategies* in the underlying game. It is clear to see that mixed strategies include pure strategies.

From a biological point of view pure and mixed strategies indicate that an individual is willing to connect with strictly one or more bacteria, respectively.

The complete distribution of the chosen strategies for the whole population is represented by the variable

$$\mathbf{X} = (\mathbf{x}_1, \dots, \mathbf{x}_N),$$

which includes N^2 components, namely x_{v,s_v} . There are N components for each bacterium belonging to each of the two classes \mathcal{V}_1 and \mathcal{V}_2 .

The above statements allowed us to define the reward, or payoff, p_{v,s_v}^G , obtained by player v when it connects to s_v , as follows:

$$p_{v,s_v}^G = \mathcal{E}(s_v, v)x_{s_v,v}, \quad (2)$$

where the superscript G indicates the presence of a graph. Consequently, the average payoff for player v over the graph is:

$$\phi_v^G = \sum_{s_v=1}^N x_{v,s_v} p_{v,s_v}^G. \quad (3)$$

According to the well known theory on evolutionary games (Weibull, 1995; Hofbauer and Sigmund, 1998) and to the same theory extended to networked populations (Madeo and Mocenni, under revision), we can write the *replicator equation* of the game accounting for the graph under construction by bacteria. This equation describes the evolution over time of the distribution of pure/mixed strategy vectors \mathbf{x}_v , and reads as follows:

$$\dot{x}_{v,s_v} = x_{v,s_v} (p_{v,s_v}^G - \phi_v^G). \quad (4)$$

The corresponding Cauchy problem can be obtained from Equation (4) by setting an additional constraint on initial conditions, namely $x_{v,s_v}(t=0) = x_{v,s_v}^0$. It is well known from the theory on ordinary differential equations (ODEs), that this problem has a unique solution, $x_{v,s_v}(t)$, $t \in [0, T]$. In the specific system developed here this solution represents the evolution over time of the distribution of the propensities of each bacterium to be connected to any other bacterium present in the systems. Some examples of the evolution of these variables over time are shown in **Figure 6** reported below and in Supplementary Movie 1.

2.3. THE GRAPH TOPOLOGY

The solution $\mathbf{X}(t) = (\mathbf{x}_1, \dots, \mathbf{x}_N)$ of Equation (4) allows us to calculate the *effective connection graph* $\mathcal{G}^E(t)$, by defining its adjacency matrix $\mathbf{A}^E(t) = \{a_{v,w}^E(t)\}_{v,w \in \mathcal{V}}$ as follows:

$$a_{v,w}^E(t) = \begin{cases} 1 & \text{if } x_{v,s_v}(t) > \eta \wedge x_{w,s_w}(t) > \eta \\ 0 & \text{otherwise} \end{cases}, \quad (5)$$

where $s_v = w$, $s_w = v$ and $\eta \in [0, 1]$ is a given threshold.

The model can also be developed assuming that the effective connection graph $\mathcal{G}^E(t)$ is directed, in order to take into account monodirectional connections, arising, for example, when bacterium v shares energy with w , but w does not send anything back. Indeed, one can rewrite graph (5) as follows:

$$a_{v,w}^E(t) = \begin{cases} 1 & \text{if } x_{v,s_v}(t) > \eta \\ 0 & \text{otherwise} \end{cases}, \quad (6)$$

where $s_v = w$. The latter approach goes beyond the scope of the present study, and in the following we only use the bidirectional graph defined by Equation (5).

The parameter η in Equation (5) represents the threshold above which the will to connect becomes an effective link. From a mathematical point of view η is a way of selecting optimal connections, but it also has an interesting biological interpretation because it is correlated to the maximum number of connections that a bacteria is allowed to have. Suppose that bacterium v is the most connected in the graph, and let n_v be the number of its connections. Then there are at least n_v components x_{v,s_v} of vector \mathbf{x}_v greater than η . Since the sum of all these components is at most 1, each of them is at least $\frac{1}{n_v}$ and hence $\eta < \frac{1}{n_v}$. Thus, η is inversely correlated to the number of connections of the most connected bacterium in the graph.

In order to ease the explanation of the model and the mechanism of link formation we report a schematic representation of possible connections and state variables for a prototypical system composed by the two sets $V_1 = \{v_1\}$ and $V_2 = \{w_1, w_2\}$ in **Figure 3A**. This system is deeply analyzed in the following Subsection 2.3.1.

2.3.1. The system of equations for a simple case

Here we report some theoretical results obtained by developing the mathematical model for a simple example involving $N = 3$ bacteria divided into 2 classes, in particular, $\mathcal{V}_1 = \{v_1\}$ and $\mathcal{V}_2 = \{w_1, w_2\}$, as shown by **Figure 3**. For the sake of simplicity in the following equations the individuals are simply enumerated from 1

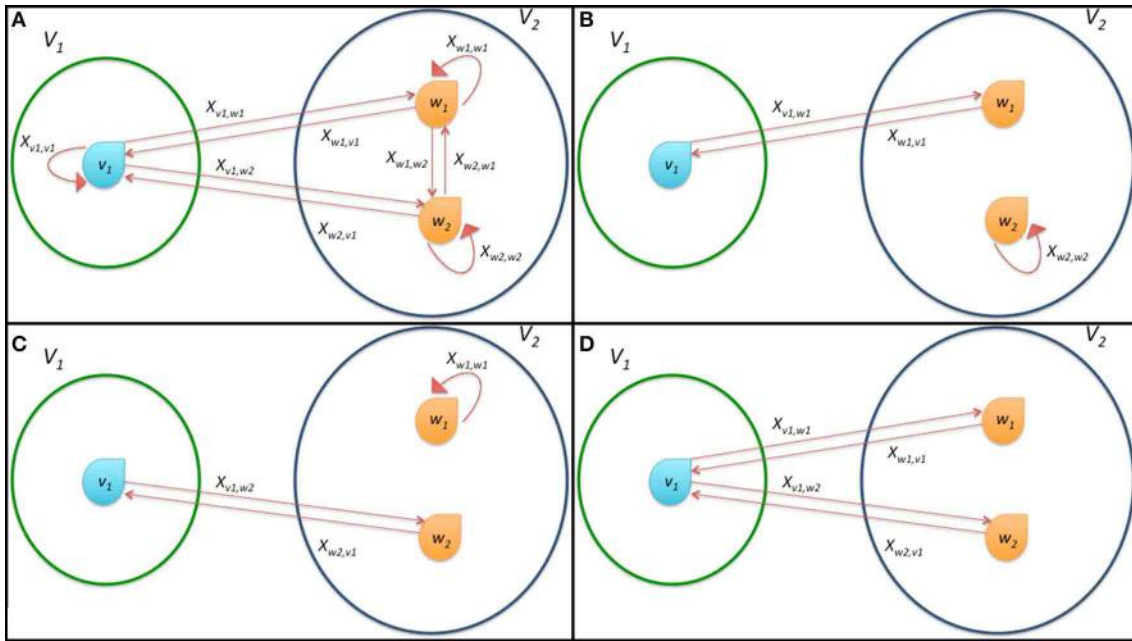


FIGURE 3 | Schematic representation of the connections among the bacteria in a simple system composed by only three microorganisms divided in the two classes \mathcal{V}_1 and \mathcal{V}_2 . (A) shows all possible connections, (B,C) report the effective

formation of a single connection and (D) represents the onset of multiple connections. The state variables $x_{v,w}$ describing the dynamics of the system according to Equation (7) are also reported as labels of arcs of the graph.

to 3, specifically $\mathcal{V}_1 = \{1\}$ and $\mathcal{V}_2 = \{2, 3\}$. In this case the system is composed of $N^2 = 9$ ordinary differential equations:

$$\left\{ \begin{array}{l} \dot{x}_{1,1} = -x_{1,1}\phi_1^G \\ \dot{x}_{1,2} = x_{1,2}(x_{2,1}\mathcal{E}(2,1) - \phi_1^G) \\ \dot{x}_{1,3} = x_{1,3}(x_{3,1}\mathcal{E}(3,1) - \phi_1^G) \\ \\ \dot{x}_{2,1} = x_{2,1}(1 - x_{2,1})x_{1,2}\mathcal{E}(1,2) \\ \dot{x}_{2,2} = -x_{2,2}x_{2,1}x_{1,2}\mathcal{E}(1,2) \\ \dot{x}_{2,3} = -x_{2,3}x_{2,1}x_{1,2}\mathcal{E}(1,2) \\ \\ \dot{x}_{3,1} = x_{3,1}(1 - x_{3,1})x_{1,3}\mathcal{E}(1,3) \\ \dot{x}_{3,2} = -x_{3,2}x_{3,1}x_{1,3}\mathcal{E}(1,3) \\ \dot{x}_{3,3} = -x_{3,3}x_{3,1}x_{1,3}\mathcal{E}(1,3) \end{array} \right. , \quad (7)$$

where $\phi_1^G = (x_{1,2}x_{2,1}\mathcal{E}(2,1) + x_{1,3}x_{3,1}\mathcal{E}(3,1))$.

As described in Madeo and Mocenni (under revision), pure strategy profiles are always stationary points for system (7). In particular, concerning players 2 and 3, the strategies $\mathbf{x}_2^* = \mathbf{x}_3^* = [1 \ 0 \ 0]^T$ are attractive, since $\dot{x}_{2,1} \geq 0$, $\dot{x}_{3,1} \geq 0$, $\dot{x}_{2,2} \leq 0$, $\dot{x}_{2,3} \leq 0$ and $\dot{x}_{3,2} \leq 0$, $\dot{x}_{3,3} \leq 0 \ \forall \mathbf{x}$. As expected, both players 2 and 3 naturally want to connect to player 1. Moreover, $\phi_1^G \geq 0$ and hence $\dot{x}_{1,1} \leq 0$. This means that $x_{1,1}^* = 0$ is attractive and $x_{1,2}^* + x_{1,3}^* = 1$. Using these stationary state values, we can rewrite the second and third equations as follows:

$$\left\{ \begin{array}{l} \dot{x}_{1,2} = x_{1,2}^*(1 - x_{1,2}^*)(\mathcal{E}(2,1) - \mathcal{E}(3,1)) \\ \dot{x}_{1,3} = x_{1,2}^*(1 - x_{1,2}^*)(\mathcal{E}(3,1) - \mathcal{E}(2,1)) \end{array} \right. . \quad (8)$$

Clearly, $\mathbf{x}_1^* = [0 \ 1 \ 0]^T$ and $\mathbf{x}_1^* = [0 \ 0 \ 1]^T$ are stationary points. These two cases represent situations in which bacterium 1 connects only to bacterium 2 or 3, respectively (see Figures 3B,C). If $\mathcal{E}(2,1) = \mathcal{E}(3,1)$, then $\mathbf{x}_1^* = [0 \ x_{1,2}^* \ 1 - x_{1,2}^*]^T$ represents an infinite set of stationary points, with $x_{1,2}^* \in (0, 1)$ and $1 - x_{1,2}^* \in (0, 1)$. This means that player 1 can potentially establish connections with both players 2 and 3. This happens when $x_{1,2}^*$ and $1 - x_{1,2}^*$ are also greater than η . This result shows that in the particular case in which there are players able to transfer the same amount of energy to a single bacterium, multiple connections are allowed (see Figure 3D).

3. RESULTS

In this section we provide some numerical simulation results of the model developed in this paper.

As described in the Materials and Methods Section, the function γ in Equation (1) accounts for the assumption that the mechanism of connection formation depends on the distance between bacteria. The simulations reported in this section have been obtained by using the following specification of γ :

$$\gamma(\rho) = \begin{cases} 1 - \frac{\rho}{\mu} & 0 \leq \rho \leq \mu \\ 0 & \rho > \mu \end{cases} . \quad (9)$$

According to Equation (9), in the definition of γ the parameter μ represents a distance threshold for feasible connections; indeed, for each couple of bacteria v and w that are separated by a distance $\rho_{v,w} > \mu$, $\gamma(\rho_{v,w}) = 0$ and hence $\mathcal{E}(w, v) = 0$. In other words,

connections over distances greater than μ do not allow any energy exchange and are thus not convenient.

In order to evaluate quantitatively the simulation results we introduce the following indicator of efficiency:

$$\mathcal{I}^G(t) = \frac{\sum_{\bar{v}=1}^N \sum_{\bar{s}_v=1}^N p_{\bar{v}, \bar{s}_v}^G}{\sum_{\bar{v}=1}^N \max_z \mathcal{E}(\bar{v}, z)}, \quad (10)$$

where \bar{v} s are all the connected bacteria and z are all bacteria. The indicator evaluates the instantaneous ratio between the total payoff of connected bacteria and the total energy available to bacteria for establishing connections. Notice that the \mathcal{I}^G changes over time. The payoff and the number of connected bacteria vary in time.

3.1. EXPERIMENTAL RESULTS

The results of several numerical experiments developed over a population of 30 bacteria organized into two different classes are reported. The energy available to each bacterium is assigned randomly at the beginning of the simulation.

The net energy \mathcal{E} that each bacterium is available to share with other bacteria is initial energy T scaled by distance through γ . In other words, this quantity represents the energy that each

bacterium is available to send (sender) to another bacterium (receiver). Sender and receiver bacteria are reported as rows and columns of the grid shown in **Figure 4**, respectively. The stars indicate the presence of a connection among bacteria that has been permanently established according to the mechanisms described by Equation (5).

It is interesting to note that effective connections are possible only when both linked bacteria have enough available energy to share with the other. The antisymmetric parts of the matrix are not involved in the mechanism of energy sharing because the connections are allowed only among individuals belonging to different classes.

When the steady state is reached, we find the presence of effective stable connections reported in **Figure 5** for a run with 30 bacteria over 100 time steps. The colors of the nodes correspond to the value of the payoff described by Equation (2), calculated at the steady state. With parameter values $\eta = 0.2$ and $\mu = 0.2$, we can see that some bacteria are able to activate multiple connections. Connections involving more than 3 bacteria are also possible for different values of the parameters, as reported by the following figures. The interplay between **Figures 4** and **5** is shown by Supplementary Movie 1, where the dynamics is reproduced, and the onset of links can be followed over time (left inset of the

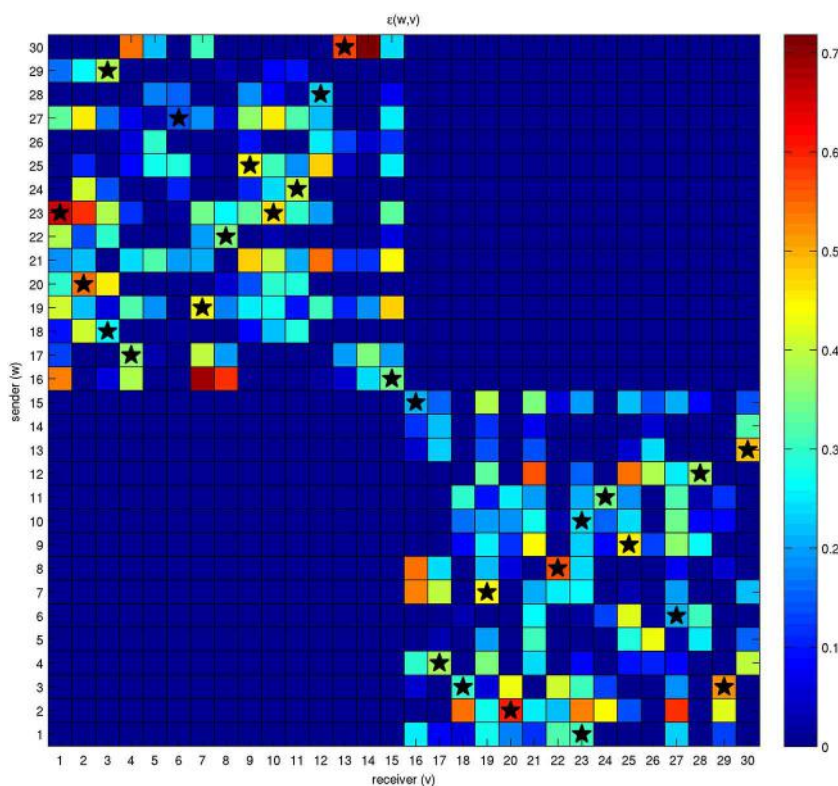


FIGURE 4 | Energy initially available for exchange among a network of 30 bacteria.

Each bacterium has a quantity of energy available it wants to transfer to the others and it will be allowed to receive an amount of energy from them. These two energies are represented by different colors in the rows and columns of the grid. For example, bacterium 23 wants to share a large amount of energy with bacterium

1; on the contrary, the quantity of energy that bacterium 1 is available to transfer to bacterium 23 is much lower. Nonetheless, the two bacteria will be able to establish an effective connection, although with different intensities, because the corresponding state variables $x_{1,23}$ and $x_{23,1}$ lie above threshold η . The stars correspond to effective connections and energy exchanges.

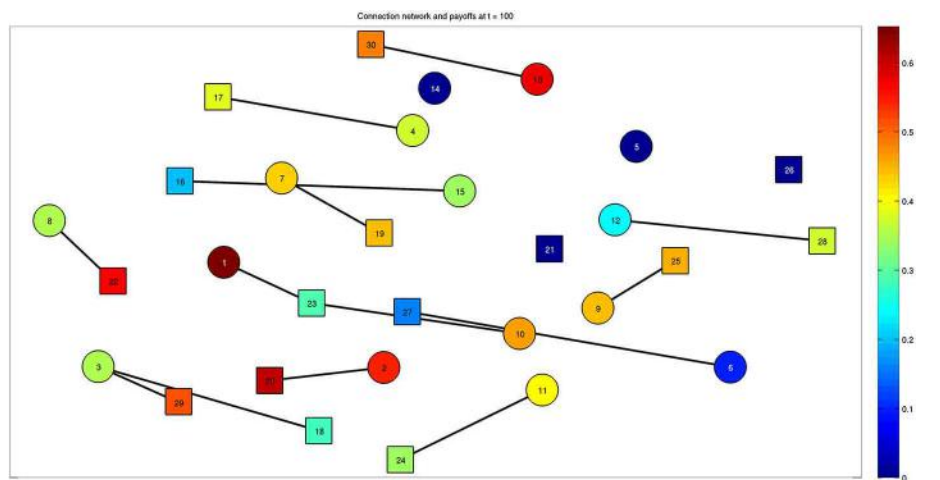


FIGURE 5 | Final configuration of the network composed of 30 bacteria at steady state ($t = 100$). Bacteria belonging to the two classes are represented by different shapes, such as squares and circles. The color associated to each bacterium represents the effective quantity of energy it

receives thanks to the established connections. Multiple connections are present, for example bacteria 3 and 23 established connections with bacteria 29–18 and 1–10, respectively. See also Supplementary Movie 1, which reports the whole dynamics and provides the connection between **Figures 4 and 5**.

movie). The inset on the right part of the movie reports the state variable $x_{v,w}$ for each bacterium.

Furthermore, the complete dynamics of the energy received by each bacterium is reported in **Figure 6**.

Figure 7 shows the values of the efficiency indicator (10) and the number of connections arising in the evolutive process. Both efficiency and number of connections have a monotonically increasing and saturating dynamics, showing that the process reaches a steady state quite fast.

More details on the state variables and solutions of Equation (4) are provided in **Figure 8**. In particular, the time course of the dynamics of two bacteria is reported and compared to threshold η . One can observe that the first link between the two bacteria is formed at approximately $t = 70$, when both variables exceed threshold η . Nevertheless, the connection is removed later on at approximately $t = 125$, when one of the two components falls below the threshold. It is interesting to note that the bacteria try to activate several connections before they are able to reach a steady state, i.e., a stable and permanent configuration.

Figure 9 shows the time course of the efficiency indicator on a time interval of 400 time instants for different values of parameter η . The increase of efficiency over time indicates that the system is moving toward a more efficient state. Moreover, for small values of μ (solid lines) efficiency is higher for larger η s, while for large values of μ (dashed lines) the asymptotic values reached by efficiency are independent of η . Recall that μ is related to the amplitude of the spatial region to which each bacterium is allowed to look for connections with others. The independence of the final configuration of the network on parameter η spontaneously resulting from the model is very important because there are presently no guidelines for choosing appropriate values of the threshold η .

Another significant result emerging from the inspection of **Figure 9** is that for small μ s values of η exist for which efficiency

increases more quickly. In particular, for $\eta = 0.5$, the asymptotic value of efficiency is reached much faster than for any other value.

The inset of **Figure 9** reports the histogram of the different kinds of connections that can be established by bacteria with respect to η and for different μ . As one can see, for small μ multiple connections are feasible while for high μ s only one to one connections are effectively possible. As mentioned system efficiency reduces for small values of μ the system efficiency reduces. This result confirms that single connections are more efficient and robust. One should also consider that in these present simulations we assume to have only two classes of bacteria, and multiple connections would involve more than one bacterium belonging to the same class, i.e., providing the same information content. In this sense, it seems obvious that single connections are more efficient than multiple ones. Future works will be devoted to compare the solution provided by the proposed model with optimal connection networks.

In **Figure 10** the values of efficiency are reported as a function of time for different values of parameter μ . Notice that in this case both the efficiency and its derivative are independent on parameter μ except for $\mu = 0.1$. The curves have the same dynamics for $\mu = \{0.3, 0.5, 0.6\}$, while for $\mu = 0.1$ the system takes more time to reach steady state. This mechanism is even stronger for smaller η s, reported as solid lines in the figure. Moreover, in the latter case, the inset of **Figure 10** shows that for small η bacteria are allowed to establish multiple connections with approximately the same efficiency.

Figure 11 reports the time course of the number of connections for different values of η and μ , where solid lines correspond to small and dashed lines to large values of μ , respectively. It is worthwhile to note that the number of connections is independent on both parameters η and μ except for the case of $\eta = 0.01$ and $\mu = 0.1$. In this case the number of connections is higher,

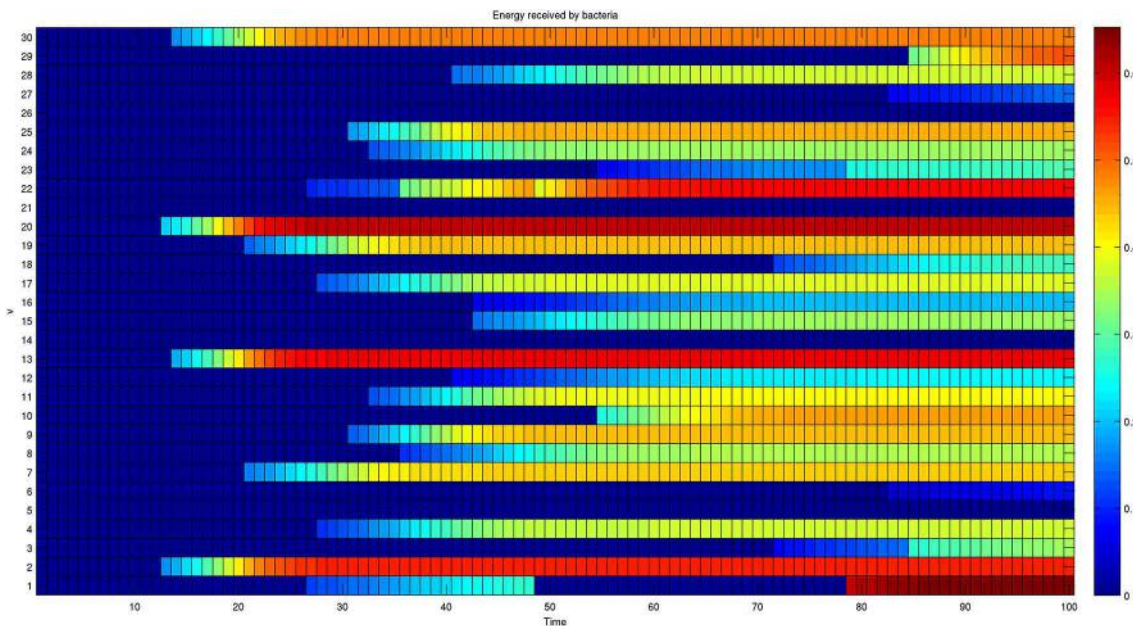


FIGURE 6 | Dynamics of the energy received by each member of a network composed of 30 bacteria. The colors reported in each row represent the energy received by a single bacterium over time. The energy

received initially is null for all bacteria. The presence of oscillating behaviors, such as the one shown by bacterium 1, shows that the final configuration is also the result of transient activated/deactivated connections.

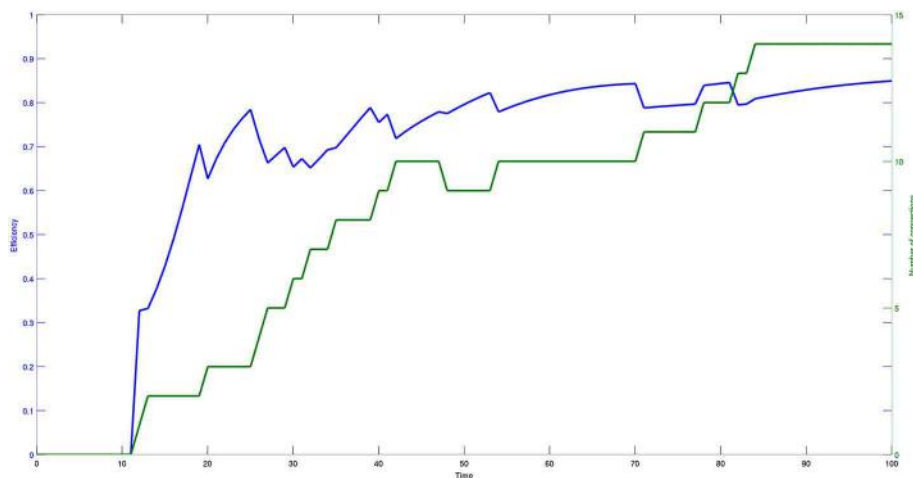


FIGURE 7 | Time course of efficiency (blue) and number of effective connections (green) of a network composed of 30 bacteria. The data are plotted with different scales and the model parameters are set as follows: $\eta = 0.2$ and $\mu = 0.2$.

even though efficiency is lower, shown by the solid red line of **Figure 9**. A small value of η means that almost any connection is possible and a small value of μ means that the spatial horizon where the bacteria are allowed to look for connections is also very small. Thus, the bacteria will be only allowed to establish multiple one to one short range connections and probably lose the more efficient ones.

Notice that for small values of η some connections already exist at $t = 0$. In fact, the initial values of the state variables assigned randomly to some couples of bacteria may fall below the threshold from the beginning.

In **Figure 12** we report the same results of **Figure 11**, but with respect to parameter μ . The most important thing to notice in this case is that the number of connections for small μ and any η is less than any other parameter value. A further significant result is the transient behavior occurring for $\eta = 0.1$ and $\mu = \{0.3, 0.5, 0.6\}$, where groups of bacteria experiment with connections after which they can decide to regress.

4. DISCUSSION

This paper is the first attempt to develop a mathematical model describing the activation of suitable physical connections among

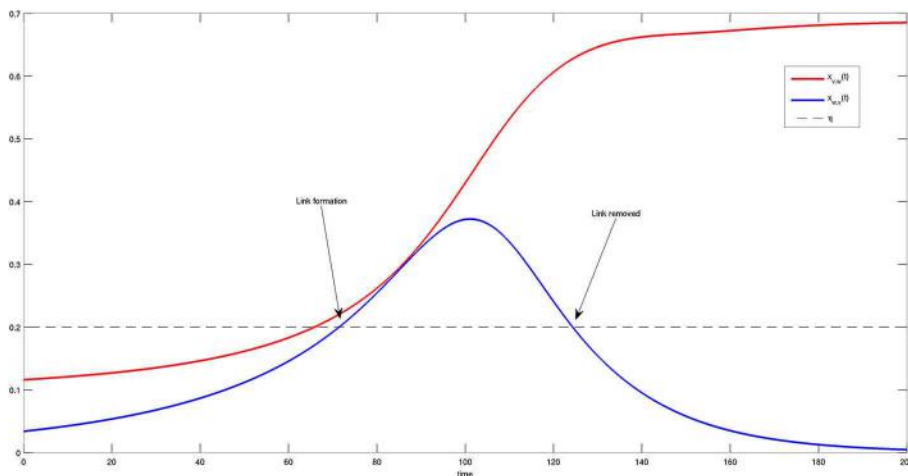


FIGURE 8 | Time course of two components $x_{v,w}(t)$ (red) and $x_{w,v}(t)$ (blue) of the system state $X(t)$. When both components are greater than η (dashed black line), a link between v and w is

formed. The link disappears when component $x_{v,w}(t)$ falls below the threshold η . This transient behavior is in agreement with the results shown in **Figure 6**.

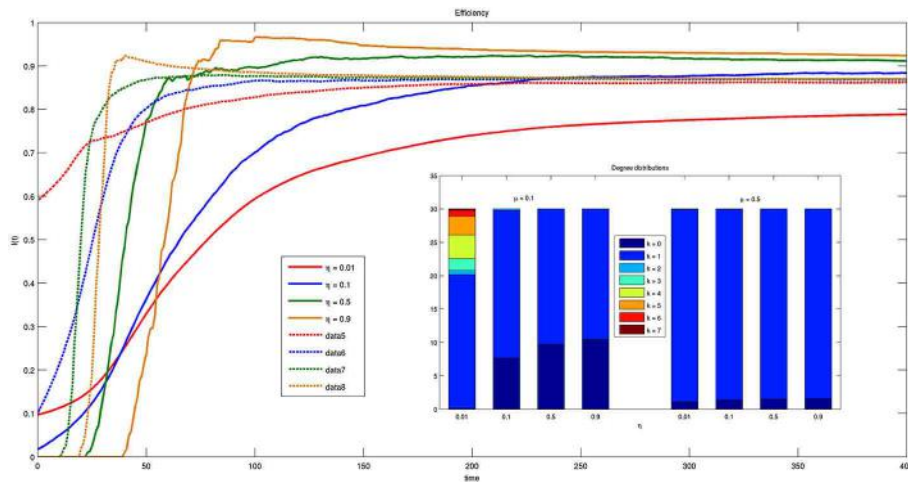


FIGURE 9 | Time course of efficiency for different values of threshold $\eta = \{0.01, 0.1, 0.5, 0.9\}$ and parameter $\mu = \{0.1, 0.5\}$. Solid lines correspond to $\mu = 0.1$ and dashed lines to $\mu = 0.5$. The inset reports the histogram of connections for $\mu = 0.1$ and $\mu = 0.5$ at $t = 200$.

two or more bacteria experiencing hostile environmental conditions. Contrary to standard ways of interpreting collaboration and clustering among groups or subgroups of bacteria, the model proposed in this study describes a mechanism based on the strategies of individual players. Instead of interpreting patterns as a result of macroscopic and collective behavior involving a large part of the population of bacteria, our model allows two or more bacteria to make the decision of connecting to another specific bacterium of a different species.

An important result of this work is that bacteria (microorganisms) prefer one to one rather than multiple connections because the first ones are more efficient, optimal and robust. This fact reproduces what has been experimentally observed in biofilms, where interspecies interactions do not produce a “common good” such as the constituents of biofilm architecture, but

all associations are cell-to-cell (see Comolli and Banfield, 2014). In our framework, these connections result from spontaneous co-evolutive dynamics of groups of bacteria, and are the natural consequence of the basic assumptions under evolutionary game theory. Thus, the fact that we did not need to include any additional a priori assumption or information in the model to obtain the above results suggests our model captures a fundamental aspect of microbial life within biofilms.

When environmental conditions are very averse, and microorganisms need the recruitment of diversified biological components such as metabolites, proteins, defense mechanisms, nucleic acids, etc. (see Mitri et al., 2011), we may suppose that each component is provided by a bacterium belonging to a particular class. At this point, we expect that multiple connections will be more efficient than one-to-one. The present work can be powerfully

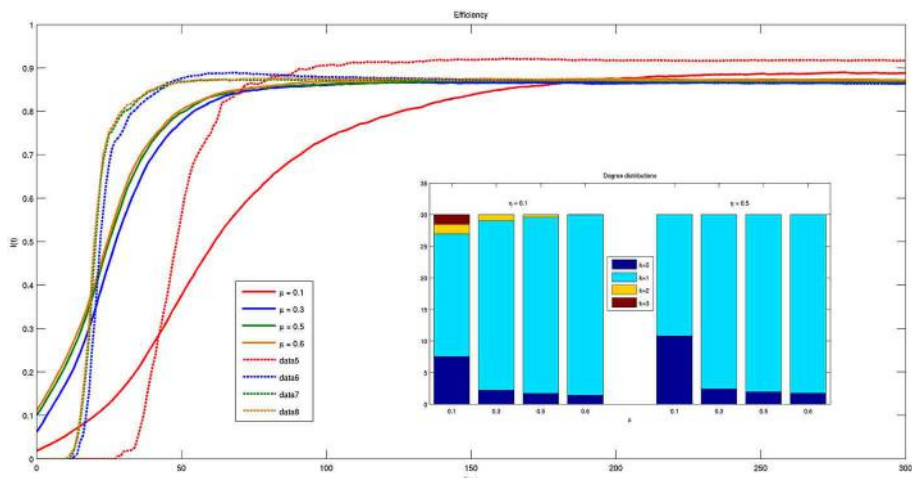


FIGURE 10 | Time course of efficiency for different values of parameter $\mu = \{0.1, 0.3, 0.5, 0.6\}$ and threshold $\eta = \{0.1, 0.5\}$. Solid lines correspond to $\eta = 0.1$ and dashed lines to $\eta = 0.5$. The inset reports the histogram of connections for $\eta = 0.1$ and $\eta = 0.5$ at $t = 300$.

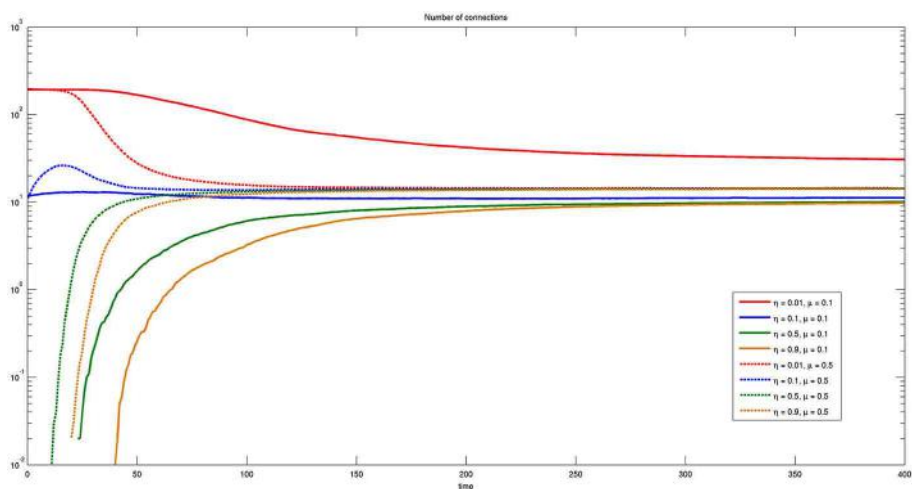


FIGURE 11 | Time course of the number of connections for different values of η and μ . Here $\eta = \{0.01, 0.1, 0.5, 0.9\}$ and $\mu = \{0.1, 0.5\}$. Some connections are present at the initial time when the threshold η is sufficiently low.

extended to account for the presence of more than two subclasses of bacteria, and hence more than two kinds of energies available for exchanges.

An additional significant result of the paper is that the asymptotic values of efficiency at the global level, and number of connections are almost independent of the connection activating threshold η and distance threshold μ . Recall that two bacteria belonging to different classes establish a link when they are both willing to connect, i.e., their state variables are greater than parameter η . The connection mechanism dissipates a certain amount of energy and allows the system to reach a certain level of efficiency. On the other hand, parameter μ mostly influences the total number of connections, even though at steady state the same level of efficiency is reached. Put together, the above results indicate that the model has a

globally attractive steady state, which is optimum with respect to the strategies' distribution of the underlying game. Nevertheless, parameter η significantly influences how fast the above steady state is reached during the first phases of the process of network formation.

The recruitment of the optimal network configuration needs deeper investigation. For example, introducing suitable functions to be optimized on the basis of the techniques presented in the field of graph theory. This will substantially help the understanding of still unknown biological mechanisms of structure formation associated with cell-cell interfaces, such the ones described in Comolli and Banfield (2014) for *archaea*.

In conclusion, our results show that since the environmental conditions constantly change microorganisms are responding not just to the changes in external factors but in concomitance

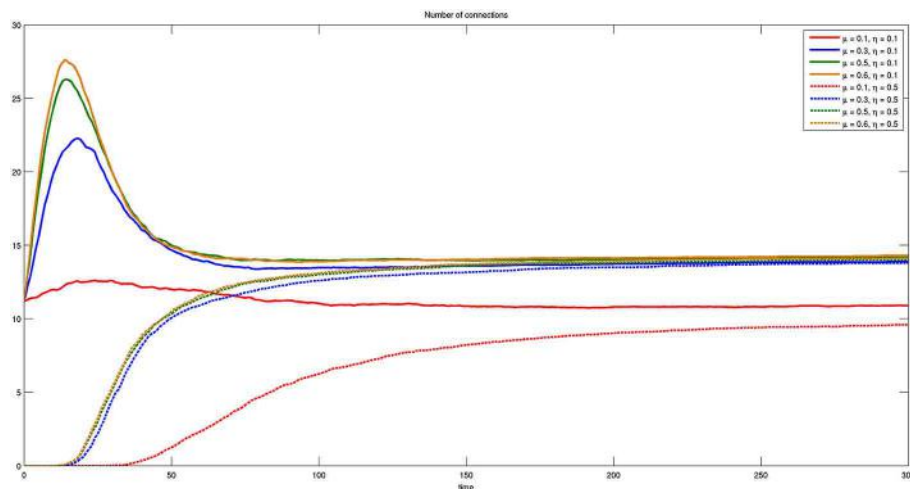


FIGURE 12 | Time course of the number of connections for different values of η and μ . Here $\eta = \{0.1, 0.5\}$ and $\mu = \{0.1, 0.3, 0.5, 0.6\}$. The presence of initial connections and transient behavior are evident for $\eta = 0.1$.

with the changes adopted by the entire system of microbes. The network thus provides a mechanism of resilience and robustness. In addition, the network of connections we show, linking organisms across a dynamic range of physical connections, should provide the basis for linked evolutionary changes under pressure from a changing environment.

AUTHOR CONTRIBUTIONS

Luis R. Comolli, Dario Madeo, and Chiara Mocenni contributed to the original motivation, ideas, and exploration of modeling strategies for the study. Dario Madeo and Chiara Mocenni worked on conceptualization, development and analysis of the mathematical model, and performed numerical simulations. Luis R. Comolli, Dario Madeo, and Chiara Mocenni analyzed the results and their conceptualization. Luis R. Comolli, Dario Madeo, and Chiara Mocenni contributed equally to the writing of the manuscript.

FUNDING

The study is partially funded by the project “Evolutionary Games on Networks for Modeling Complex Biological and Socio-Economic Phenomena” financed by CNPq (Program Science without Borders, N. 401795/2013-6).

ACKNOWLEDGMENT

Chiara Mocenni and Dario Madeo acknowledge Prof. Mustafa Khammash for the fruitful discussions on systems biology.

SUPPLEMENTARY MATERIAL

The Supplementary Material for this article can be found online at: <http://www.frontiersin.org/journal/10.3389/fmicb.2014.00407/abstract>

REFERENCES

- Baker, B. J., Comolli, L. R., Dick, G. J., Hauser, L., Land, M., VerBerkmoes, N. C., et al. (2010). Enigmatic, ultra-small uncultivated archaea. *Proc. Natl. Acad. Sci. U.S.A.* 107, 8806–8811. doi: 10.1073/pnas.0914470107
- Ben-Jacob, E., and Cohen, I. (1997). “Cooperative formation of bacterial patterns,” in *Bacteria as Multicellular Organisms*, eds J. A. Shapiro and M. Dworkin (New York, NY: Oxford University Press), 394–416.
- Ben-Jacob, E., Cohen, I., and Golding, I. (2000). Bacterial cooperative organization under antibiotic stress. *Physica A* 282, 247–282. doi: 10.1016/S0378-4371(00)00093-5
- Comolli, L. R., and Banfield, J. F. (2014). Inter-species interconnections in acid mine drainage microbial communities. *Front. Microbiol.* 5:367. doi: 10.3389/fmicb.2014.00367
- Dubey, G. P., and Ben-Yehuda, S. S. (2011). Intercellular nanotubes mediate bacterial communication. *Cell* 144, 590–600. doi: 10.1016/j.cell.2011.01.015
- Dwyer, D., Kohanski, M., and Collins, J. (2008). Networking opportunities for bacteria. *Cell* 135, 1153–1156. doi: 10.1016/j.cell.2008.12.016
- Eichinger, L., and Noegel, A. A. (2003). Crawling into a new era—the dictyostelium genome project. *EMBO J.* 22, 1941–1946. doi: 10.1093/emboj/cdg214
- Frey, E. (2010). Evolutionary game theory: theoretical concepts and applications to microbial communities. *Physica A* 389, 4265–4298. doi: 10.1016/j.physa.2010.02.047
- Fuhrman, J. A. (2009). Microbial community structure and its functional implications. *Nature* 459, 193–198. doi: 10.1038/nature08058
- Gure, T. (2009). Driving biofuels from field to fuel tank. *Cell* 138, 9–12. doi: 10.1016/j.cell.2009.06.038
- Hall-Stoodley, L., Costerton, J. W., and Stoodley, P. (2004). Bacterial biofilms: from the natural environment to infectious diseases. *Nat. Rev. Microbiol.* 2, 95–108. doi: 10.1038/nrmicro821
- Hansen, S. K., Rainey, P. B., Haagensen, J. A. J., and Molin, S. (2009). Evolution of species interactions in a biofilm community. *Nature* 445, 533–536. doi: 10.1038/nature05514
- Hofbauer, J., and Sigmund, K. (1998). *Evolutionary Games and Population Dynamics*. Cambridge: Cambridge University Press. doi: 10.1017/CBO9781139173179
- Kantor, R. S., Wrighton, K. C., Handley, K. M., Sharon, I., Hug, L. A., Castelle, C. J., et al. (2013). Small genomes and sparse metabolisms of sediment-associated bacteria from four candidate phyla. *mBio* 4, e708–e713. doi: 10.1128/mBio.00708-13
- Mitri, S., Xavier, J. B., and Foster, K. R. (2011). Social evolution in multispecies biofilms. *Proc. Natl. Acad. Sci. U.S.A.* 108, 10839–10846. doi: 10.1073/pnas.1100292108
- Nowak, M. A. (2006a). Five rules for the evolution of cooperation. *Science* 314, 1560–1563. doi: 10.1126/science.1133755
- Nowak, M. A. (2006b). *Evolutionary Game Theory, Exploring the Equations of Life*. Cambridge, MA: Harvard University Press.

- Shimoyama, T., Kato, S., Ishii, S., and Watanabe, K. (2009). Flagellum mediates symbiosis. *Science* 23, 1574. doi: 10.1126/science.1170086
- Weibull, J. W. (1995). *Evolutionary Game Theory*. Cambridge: MIT Press.
- Wrighton, K. C., Thomas, B. C., Sharon, I., Miller, C. S., Castelle, C. J., VerBerkmoes, N. C., et al. (2012). Fermentation, hydrogen, and sulfur metabolism in multiple uncultivated bacterial phyla. *Science* 337, 1661–1665. doi: 10.1126/science.1224041

Conflict of Interest Statement: The authors declare that the research was conducted in the absence of any commercial or financial relationships that could be construed as a potential conflict of interest.

Received: 08 April 2014; accepted: 18 July 2014; published online: 19 August 2014.
Citation: Madeo D, Comolli LR and Mocenni C (2014) Emergence of microbial networks as response to hostile environments. *Front. Microbiol.* 5:407. doi: 10.3389/fmicb.2014.00407

This article was submitted to Terrestrial Microbiology, a section of the journal *Frontiers in Microbiology*.

Copyright © 2014 Madeo, Comolli and Mocenni. This is an open-access article distributed under the terms of the Creative Commons Attribution License (CC BY). The use, distribution or reproduction in other forums is permitted, provided the original author(s) or licensor are credited and that the original publication in this journal is cited, in accordance with accepted academic practice. No use, distribution or reproduction is permitted which does not comply with these terms.

5. APPENDIX

The details of the game underlying the model presented in the Materials and Methods Section are provided. In particular, the strategies of the game correspond to the willingness of the players to become connected to one or more other players. For this reason, the payoffs of the game are calculated on the basis of the energy that each player is allowed to share. Thereupon, the payoffs as well as energy are functions of time.

5.1 CALCULATING THE PAYOFFS OF THE GAME

According to the approach proposed in Madeo and Mocenni (under revision), we need a matricial definition of payoff functions p_{v,s_v}^G and ϕ_v^G in order to describe the model using the replicator equation on a networked population. To this aim, we define the payoff obtained by v when he plays with w and strategies used are s_v and s_w , respectively:

$$b_{s_v, s_w}^{v,w} = \begin{cases} \mathcal{E}(w, v) & \text{if } v = s_w \wedge w = s_v \\ 0 & \text{otherwise} \end{cases}. \quad (\text{A11})$$

In other words, player v will earn a payoff (energy) when playing with player w if and only if both v and w decide to connect to each other (i.e., $s_v = w$ and $s_w = v$). The total payoff (energy) obtained by player $v \in \mathcal{V}_i$ is defined as the sum of all energy obtained from players $w \notin \mathcal{V}_i$. Namely:

$$\bar{\pi}_v(s_1, \dots, s_N) = \sum_{w \notin \mathcal{V}_i} b_{s_v, s_w}^{v,w}. \quad (\text{A12})$$

In the model developed in this paper, pure strategies are chosen by players that are willing to connect to only one other player, while mixed strategies are such that eventually an individual will share its energy with more than one individual. Notice that in this case sharing all the available energy with only one player corresponds to adoption of a pure strategy. The pure strategy s_v of player v can be described by the unitary vector $\mathbf{e}_{s_v} = (0, \dots, 1, \dots, 0)$, where 1 is placed at the s_v -th position. Using Equation (A11),

we can define the payoff matrix for each couple of bacteria v and w :

$$\mathbf{B}^{v,w} = \{b_{s,r}^{v,w}\}_{s,r=1,\dots,N}. \quad (\text{A13})$$

Thereafter, we can make use of Equation (A13) to rewrite Equation (A12) in a matricial fashion:

$$\bar{\pi}_v(s_1, \dots, s_N) = \pi_v(\mathbf{e}_{s_1}, \dots, \mathbf{e}_{s_N}) = \sum_{w \notin \mathcal{V}_i} \mathbf{e}_{s_v}^T \mathbf{B}^{v,w} \mathbf{e}_{s_w}, \quad (\text{A14})$$

where $\mathbf{e}_{s_v}^T \mathbf{B}^{v,w} \mathbf{e}_{s_w} = b_{s_v, s_w}^{v,w}$.

Mixed strategies describe how player v distributes his energy. This distribution is described by vector $\mathbf{x}_v = (x_{v,1}, \dots, x_{v,N})$, where $x_{v,s_v} \in [0, 1]$ and $\sum_{s_v=1}^N x_{v,s_v} = 1$. Practically, x_{v,s_v} represents the percentage of T_v that v wants to share with $s_v \neq v$. x_{v,s_v} can be also read as the propensity of v to create a link with a player $w = s_v$. $x_{v,s_v} \in [0, 1]$, for which $v = s_v$, is the fraction of energy that v does not share. In this case $x_{v,v}$ can also be read as the propensity of v to remain unlinked. The previous notation allows us to calculate the payoff, hereafter indicated by p_{v,s_v}^G , that player v obtains when he decides to use pure strategy s_v against a player that uses mixed strategy \mathbf{x}_w :

$$p_{v,s_v}^G = \pi_v(\mathbf{x}_1, \dots, \mathbf{e}_{s_v}, \dots, \mathbf{x}_N) = \sum_{w \notin \mathcal{V}_i} \mathbf{e}_{s_v}^T \mathbf{B}^{v,w} \mathbf{x}_w, \quad (\text{A15})$$

where the superscript G indicates the presence of a graph of possible connections. The model developed in this paper will be mainly used to recover the graph topology.

The average payoff obtained by player v when it plays a mixed strategy \mathbf{x}_v is:

$$\begin{aligned} \phi_v^G &= \pi_v(\mathbf{x}_1, \dots, \mathbf{x}_v, \dots, \mathbf{x}_N) \\ &= \sum_{s_v=1}^N x_{v,s_v} p_{v,s_v}^G = \sum_{w \notin \mathcal{V}_i} \mathbf{x}_v^T \mathbf{B}^{v,w} \mathbf{x}_w. \end{aligned} \quad (\text{A16})$$



Methane production from protozoan endosymbionts following stimulation of microbial metabolism within subsurface sediments

Dawn E. Holmes^{1,2*}, Ludovic Giloteaux¹, Roberto Orellana¹, Kenneth H. Williams³, Mark J. Robbins³ and Derek R. Lovley¹

¹ Department of Microbiology, University of Massachusetts, Amherst, MA, USA

² Physical and Biological Sciences, Western New England University, Springfield, MA, USA

³ Lawrence Berkeley National Laboratory, Berkeley, CA, USA

Edited by:

Luis Raul Comolli, Lawrence Berkeley National Laboratory, USA

Reviewed by:

Marc Gregory Dumont,
Max-Planck-Institute for Terrestrial Microbiology, Germany
Osnat Gillor, Ben Gurion University, Israel

***Correspondence:**

Dawn E. Holmes, Physical and Biological Sciences, Western New England University, 1215 Wilbraham Rd., Springfield, MA 01119, USA
e-mail: dholmes@wne.edu

Previous studies have suggested that protozoa prey on Fe(III)- and sulfate-reducing bacteria that are enriched when acetate is added to uranium contaminated subsurface sediments to stimulate U(VI) reduction. In order to determine whether protozoa continue to impact subsurface biogeochemistry after these acetate amendments have stopped, 18S rRNA and β -tubulin sequences from this phase of an *in situ* uranium bioremediation field experiment were analyzed. Sequences most similar to *Metopus* species predominated, with the majority of sequences most closely related to *M. palaformis*, a ciliated protozoan known to harbor methanogenic symbionts. Quantification of *mcrA* mRNA transcripts in the groundwater suggested that methanogens closely related to *Metopus* endosymbionts were metabolically active at this time. There was a strong correlation between the number of *mcrA* transcripts from the putative endosymbiotic methanogen and *Metopus* β -tubulin mRNA transcripts during the course of the field experiment, suggesting that the activity of the methanogens was dependent upon the activity of the *Metopus* species. Addition of the eukaryotic inhibitors cyclohexamide and colchicine to laboratory incubations of acetate-amended subsurface sediments significantly inhibited methane production and there was a direct correlation between methane concentration and *Metopus* β -tubulin and putative symbiont *mcrA* gene copies. These results suggest that, following the stimulation of subsurface microbial growth with acetate, protozoa harboring methanogenic endosymbionts become important members of the microbial community, feeding on moribund biomass and producing methane.

Keywords: anaerobic protozoa, methanogenesis, *in situ* transcriptomics, uranium bioremediation, endosymbiont

INTRODUCTION

Methanogenic microbial communities exemplify the importance of interspecies interactions. These include not only the various forms of interspecies electron transfer between bacteria and methanogens (Stams and Plugge, 2009; Malvankar and Lovley, 2014; Rotaru et al., 2014), but also the symbiotic association of protozoa and endosymbiotic methanogens (van Hoek et al., 2000; Fenchel and Finlay, 2010). Endosymbiotic methanogens make significant contributions to methane production in many environments including marine sediments (Fenchel, 1993), anaerobic landfills (Finlay and Fenchel, 1991), recently flooded rice paddy soils (Schwarz and Frenzel, 2005), wastewater reactors (Narayanan et al., 2007; Priya et al., 2008) and the rumen (Newbold et al., 1995; Ushida et al., 1997).

The majority of methanogenic endosymbionts are associated with ciliated protozoa, but methanogens have also been found in the cytoplasm of anaerobic amoebae and flagellates (Vogels et al., 1980; Vanbruggen et al., 1983; van Hoek et al., 2006; Nowack and

Melkonian, 2010; Hackstein, 2011). Methanogen-harboring ciliates contain specialized organelles called hydrogenosomes that ferment pyruvate, forming acetate, H₂ and CO₂ (Yarlett and Hackstein, 2005; Fenchel and Finlay, 2010). The acetate formed by this fermentation reaction is then used by the ciliate as an energy and carbon source, while the symbiont can utilize the H₂ and CO₂ for methanogenesis.

Recent studies have emphasized the importance of protozoa in influencing microbial growth and activity in uranium-contaminated aquifers in which microbial U(VI) reduction is stimulated with the addition of organic electron donors (Holmes et al., 2013). The addition of acetate to groundwater promotes the activity of bacteria such as *Geobacter* species that reduce highly soluble U(VI) to less soluble U(IV) (Anderson et al., 2003; Wall and Krumholz, 2006; Wu et al., 2007; Williams et al., 2011) and the growth of *Geobacter* populations is followed by a bloom of protozoa that feed on the *Geobacter* (Holmes et al., 2013). With continued addition of acetate, sulfate-reducing bacteria also

increase in abundance (Vrionis et al., 2005; Miletto et al., 2011), specifically inducing the growth of a different family of protozoa that appear to specialize in predation of the sulfate reducers (Holmes et al., 2013).

In addition to the benefit of precipitating uranium from contaminated groundwater, stimulating anaerobic respiration in the subsurface may have unintended negative consequences. For example, as U(VI) was reductively precipitated from the groundwater, arsenic was also released (Giloteaux et al., 2013), presumably as the result of microbial reduction of Fe(III) minerals that adsorb arsenic in the subsurface (Dowdle et al., 1996; Redman et al., 2002; Islam et al., 2004; Rowland et al., 2007; Hery et al., 2010; Giloteaux et al., 2013). It has already been shown that high levels of organic contaminants in groundwater can promote methanogenesis (Lovley, 1997; Bekins et al., 2001; Kleikemper et al., 2005). Therefore, it might be expected that long-term acetate additions to the subsurface could also promote methanogenesis by providing a substrate for growth of acetoclastic methanogens, or indirectly from the subsequent degradation of the biomass of acetate-oxidizing microorganisms that accumulates in the subsurface (N'Guessan et al., 2008; Wrighton et al., 2012, 2014; Hug et al., 2013). Methane production during *in situ* uranium bioremediation is undesirable because methane may reduce hydraulic transmissivity, disrupting the delivery of electron donor to contaminated zones. Furthermore, the production of methane, a strong greenhouse gas, has a negative impact on the overall environmental benefit of the bioremediation process.

Therefore, in our continuing investigation of the impact of protozoa on *in situ* bioremediation of uranium-contaminated groundwater, the potential for methanogen-harboring ciliates to contribute to methane production was investigated. The results suggest that this could be a source of methane production in the subsurface after acetate amendments have been discontinued.

MATERIALS AND METHODS

SITE AND DESCRIPTION OF FIELD SITE

In 2011, a small-scale *in situ* bioremediation experiment was conducted on the grounds of a former uranium ore processing facility in Rifle, Colorado (USA) during the months of August–October as previously described (Giloteaux et al., 2013). Subsurface microbial activity was stimulated by acetate additions during the months of August–October in a manner consistent with previous such experiments at the site (Anderson et al., 2003; Vrionis et al., 2005; Williams et al., 2011). The monitoring array consisted of an injection gallery with 6 injection wells, 9 down-gradient wells, and 1 background monitoring well located upstream from the injection gallery (See Supplementary Material, Figure S1). Groundwater for the experiments was collected from well CD-01.

During the field experiment, a concentrated acetate/bromide solution (150/20 mM) mixed with native groundwater was injected into the subsurface to provide approximately 15 mM acetate to the groundwater over the course of 68 days as previously described (Anderson et al., 2003; Williams et al., 2011). Bromide was utilized as a non-reactive tracer to enable injectate delivery to down-gradient monitoring locations.

RIFLE SEDIMENT INCUBATIONS AND ENRICHMENT CULTURES

Background subsurface sediments were collected near the acetate-injection test plot with a backhoe, placed in sealed mason jars, and stored at 16°C until use. Unfiltered background groundwater for sediment incubations was pumped to the surface into 5-gallon carboys with a peristaltic pump and stored at 4°C.

For sediment incubations, 40 g of the background sediments described above, 16 ml groundwater and acetate (~20 mM) were added to 60 ml serum bottles in an anaerobic chamber under an N₂ atmosphere and incubated at 18°C. Six acetate-amended (3 with eukaryotic inhibitors cycloheximide and colchicine; final concentration 200 mg/L each) and 3 control (no acetate additions) incubations were monitored over the course of 50 days. Fe(III) reduction, sulfate reduction, or methanogenesis was not observed in control incubations.

ANALYTICAL TECHNIQUES

Groundwater samples for geochemical analyses were collected after purging 12 l of groundwater from the wells with a peristaltic pump. Ferrous iron was measured spectrophotometrically immediately after sampling using the phenanthroline method (AccuVac ampules; Hach Company) for ferrous iron. After filtration through a 0.2 μm pore size polytetrafluoroethylene [PTFE (Teflon)] filter (Alltech Associates, Inc., Deerfield, IL), acetate, bromide, chloride, sulfate, and thiosulfate were measured using an ion chromatograph (ICS-2100, Dionex, CA) equipped with an AS18 column under isocratic elution with 32 mM KOH as the eluent.

Samples for dissolved gas analysis were collected using a passive gas sampler consisting of a 5 cm length of gas permeable silicone tubing affixed to the end of a 10 mL valve sealable, gas-tight syringe (Valco Instruments Co. Inc.; Baton Rouge, LA) patterned on that described by Spalding and Watson (Spalding and Watson, 2006). Syringes were affixed to rigid tubing and emplaced within the monitoring wells (CU01, CD01) at a depth of ca. 5 m below top of casing. Groundwater elevations at the time of sampling were recorded at each well in order to calculate the hydrostatic pressure associated with each measurement time point. Partitioning of dissolved gases in groundwater across the permeable silicon tubing results in equilibration of gases within the syringe over a period of 2–3 days (Spalding and Watson, 2006) thus reflecting an averaged value between sampling time points. Prior to analysis, syringes were removed from the well bores and the gas-tight valves closed before being analyzed on site via gas chromatography (GC) using an SRI Model 8610 GC equipped with multiple detectors: a helium ionization detector (HID) running in parallel with a thermal conductivity detector (TCD) discharging to a reductive gas detector (RGD). Helium (HID) and argon (TCD, RGD) were used as the carrier gases for the detectors, as indicated, with gas volumes of 1 mL and 9 mL used for the HID and TCD/RGD, respectively. Gas concentrations in the aqueous phase were calculated as described (Spalding and Watson, 2006) using a methane gas solubility of 1.23×10^{-3} mol/L/atm.

In the laboratory sediment incubations Fe(II) was monitored over time with a ferrozine assay in a split-beam dual-detector spectrophotometer (Spectronic Genosys2; Thermo Electron Corp., Mountain View, CA) at an absorbance of 562 nm

after a 1 h extraction with 0.5 N HCl (Lovley et al., 1987; Lovley and Phillips, 1988). The remaining Fe(III) in the sediments that was not HCl-extractable was then converted to Fe(II) with the addition of 0.25 M hydroxylamine (Lovley et al., 1987). After addition of hydroxylamine, samples were incubated for an additional hour, and then measured with the ferrozine assay. Methane in the headspace of sediment incubations was measured by gas chromatography with a flame ionization detector (Shimadzu, GC-8A), and hydrogen sulfide concentrations were determined by the methylene blue method (Truper and Schlegel, 1964).

EXTRACTION OF NUCLEIC ACIDS FROM SAMPLES

DNA and RNA were extracted from groundwater collected from the U(VI) contaminated aquifer during the bioremediation field experiments. In order to obtain sufficient biomass from the groundwater, it was necessary to concentrate 50 l of groundwater by impact filtration on 293 mm diameter Supor membrane disc filters with pore sizes of 1.2 and 0.2 μm (Pall Life Sciences), which took about 3 min. All filters were placed into whirl-pack bags, flash frozen in a dry ice/ethanol bath, and shipped back to the laboratory where they were stored at -80°C . RNA was extracted from filters as previously described (Holmes et al., 2005) and DNA was extracted with the FastDNA SPIN Kit for Soil (MP Biomedicals, Santa Ana, CA). DNA was also extracted from groundwater collected from the sediment incubations with the FastDNA SPIN Kit for Soil, however, it was not necessary to concentrate samples on membrane disc filters.

Analysis of nucleic acids by spectrophotometry (NanoDrop, Thermo Scientific), microfluidic analysis (Experion, BioRad), and gel electrophoresis showed that high quality DNA and RNA were extracted from the groundwater samples. In order to ensure that RNA samples were not contaminated with DNA, PCR amplification with primers targeting the 16S rRNA gene was conducted on RNA samples that had not undergone reverse transcription.

A DuraScript enhanced avian RT single strand synthesis kit (Sigma) was used to generate cDNA as previously described (Holmes et al., 2005).

PCR AMPLIFICATION PARAMETERS AND CLONE LIBRARY CONSTRUCTION

Several previously described primer pairs were used for amplification of 16S bacterial and archaeal rRNA, 18S rRNA, *mcrA*, and β -tubulin gene fragments from genomic DNA and cDNA constructed from mRNA extracted from groundwater. Gene fragments from the bacterial 16S rRNA gene were amplified with 8F (Eden et al., 1991) and 519R (Lane et al., 1985); 344F and 915R (Casamayor et al., 2002) amplified archaeal 16S rRNA gene fragments; 515F (Giovannoni et al., 1988) and 1209R (Reysenbach et al., 1992) amplified eukaryotic 18S rRNA gene fragments; BT107F and BT261R (Baker et al., 2004) amplified protozoan β -tubulin gene fragments; and MLF (Luton et al., 2002) and ME2 (Juutonen et al., 2006) amplified *mcrA* gene fragments (See Supplementary Material, Table S1). The 18S rRNA and β -tubulin primer sets were both non-specific and amplified both protozoan and non-protozoan eukaryotic gene sequences. Some of the non-protozoan gene sequences detected at this site came from plant, fungal, and animal species which accounted for ca. 5 and

15% of the 18S rRNA and β -tubulin clone libraries. This study focused exclusively on the protozoan sequences detected in these eukaryotic libraries.

A 50 μl PCR reaction consisted of the following solutions: 10 μl Q buffer (Qiagen), 0.4 mM of each dNTP, 1.5 mM MgCl₂, 0.2 μM of each primer, 5 μg bovine serum albumin (BSA), 2.5 U Taq DNA polymerase (QIAGEN) and 10 ng of DNA template. Amplification was performed with a minicycler PTC 200 (MJ Research) starting with 5 min at 94°C , followed by 35 cycles consisting of denaturation (45 s at 94°C), annealing (see Table S1), extension (90 s at 72°C), and a final extension at 72°C for 10 min.

After PCR amplification of these gene fragments, PCR products were purified with the Gel Extraction Kit (Qiagen), and cloned into the TOPO TA cloning vector, version M (Invitrogen, Carlsbad, CA). One hundred plasmid inserts from each of these clone libraries were sequenced with the M13F primer at the University of Massachusetts Sequencing Facility.

TESTING AND DESIGN OF qPCR PRIMERS

Quantitative PCR primer sets targeting the β -tubulin gene from *in situ* *Metopus* species and the *mcrA* gene from *in situ* Methanomicrobiales species were designed according to the manufacturer's specifications (Applied Biosystems) and had amplicon sizes ranging from 100 to 200 bp (See Supplementary Table S1). The *Metopus* specific primer set (Met_bt_60f/155r) was designed from *Metopus* β -tubulin clone 9 (KJ609554) which accounted for 90% of the sequences from the β -tubulin cDNA clone library assembled with groundwater collected on day 95 of the field experiment and shared 99% of its nucleotides with the β -tubulin gene from *Metopus palaformis*. The Methanomicrobiales specific primer set (Rifle_mcrA_379f/489r) was designed from Rifle *mcrA* clone 6 (KJ609576) and accounted for 52% of the *mcrA* cDNA clone library assembled with groundwater collected on day 95.

QUANTIFICATION OF GENE AND TRANSCRIPT ABUNDANCE BY qPCR

Quantitative PCR amplification and detection were performed with the 7500 Real Time PCR System (Applied Biosystems) using genomic DNA and cDNA made by reverse transcription from mRNA extracted from groundwater collected during the bioremediation experiment. All qPCR assays had triplicate biological and technical replicates. Each reaction mixture consisted of a total volume of 25 μL and contained 1.5 μL of the appropriate primers (stock concentrations, 1.5 μM), 5 ng cDNA, and 12.5 μL Power SYBR Green PCR Master Mix (Applied Biosystems). Standard curves covering 8 orders of magnitude were constructed with serial dilutions of known amounts of purified cDNA quantified with a NanoDrop ND-1000 spectrophotometer at an absorbance of 260 nm. Transcript abundances and qPCR efficiencies (90–99%) were calculated from appropriate standard curves and all qPCR experiments followed MIQE guidelines (Bustin et al., 2009). Optimal thermal cycling parameters consisted of an activation step at 50°C for 2 min, an initial 10 min denaturation step at 95°C followed by 40 cycles of 95°C for 15 s and 58 – 60°C for 1 min. After 40 cycles of PCR amplification, dissociation curves were made for all qPCR products by increasing the temperature from 58 to 95°C at a ramp rate of 2%. The curves

all yielded a single predominant peak, further supporting the specificity of the PCR primer pairs.

PHYLOGENETIC ANALYSIS

16S and 18S rRNA and functional gene sequences were assembled with Geneious 5.6 and compared to GenBank nucleotide and protein databases with the blastn and blastx algorithms (Altschul et al., 1998). Alignments were made in ClustalX (Thompson et al., 1997) and corrected with ProSeq v2.9 (Filatov, 2002) before phylogenetic trees were constructed with Mega v6 (Tamura et al., 2013). The Maximum likelihood algorithm with the Nearest-Neighbor Interchange was used to construct all phylogenetic trees. All evolutionary distances were computed with the Tamura-Nei substitution model (Tamura and Nei, 1993) with 100 bootstrap replicates.

The nucleotide sequences of 18S rRNA, β -tubulin, and 16S rRNA genes amplified from the uranium-contaminated aquifer have been deposited in the GenBank database under accession numbers KJ609533-KJ609576.

RESULTS

METHANE PRODUCTION FOLLOWING INJECTION OF ACETATE INTO THE SUBSURFACE

Acetate was pumped into the subsurface for 68 days to promote *in situ* uranium bioremediation. The initial accumulation of Fe(II), followed by an accumulation of sulfide, indicated a typical succession (Anderson et al., 2003; Vrionis et al., 2005) of Fe(III) reduction followed by sulfate reduction in response to the acetate amendment (Figures 1A,B). Although acetate was no longer being pumped into the subsurface after day 68, low

concentrations of acetate continued to be detected until day 88 (Figure 1A).

Methane analysis initiated on day 79 detected methane in the groundwater, which declined over time, but remained detectable well after acetate had been depleted (Figure 1C). Methane was not detected (detection limit 0.1 μ M) in the groundwater up-gradient of the acetate injection site.

PROTOZOA KNOWN TO HARBOR METHANOGENIC ENDOSYMBIONTS DETECTED IN GROUNDWATER

As previously reported (Holmes et al., 2013), the Fe(III) reduction phase of the bioremediation process was associated with the growth of *Geobacter* species and a specific enrichment of protozoa from the genus *Breviata*. The subsequent growth of sulfate-reducing bacteria was accompanied by a bloom in protozoa from the family Hexamitidae (Holmes et al., 2013). Following the Fe(III) and sulfate reducing phases of the experiment, when acetate concentrations were negligible, 18S rRNA and β -tubulin mRNA transcripts most similar to *Metopus* species (Figure 2) as well as *Metopus* β -tubulin gene copies (Supplementary Figure S2), increased dramatically. These results demonstrated that *Metopus*, which are ciliated protozoa known to harbor methanogens, became predominant members of the protozoan community.

The majority (42 and 88%) of the *Metopus* 18S rRNA and β -tubulin mRNA transcript sequences were most similar to *M. palaformis* (96 and 99% identical respectively; represented by *Metopus* clones C and 9) (Supplementary Figures S3, S4). Sequences from other methanogen harboring ciliates from the genera *Cyclidium*, *Nyctotherus*, and *Caenomorpha* were also detected but never accounted for more than 4% of the protozoan

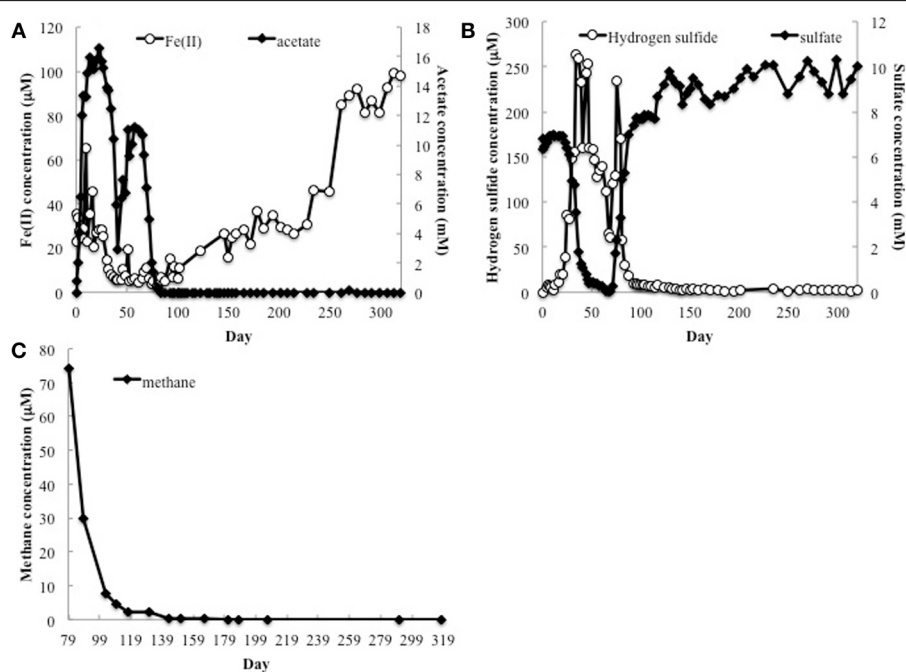


FIGURE 1 | (A) Fe(II), acetate, **(B)** sulfate and H₂S concentrations in groundwater collected from well CD-01 over the course of 320 days. **(C)** Methane concentrations in the subsurface starting 79 days after initial acetate injections (day 0).

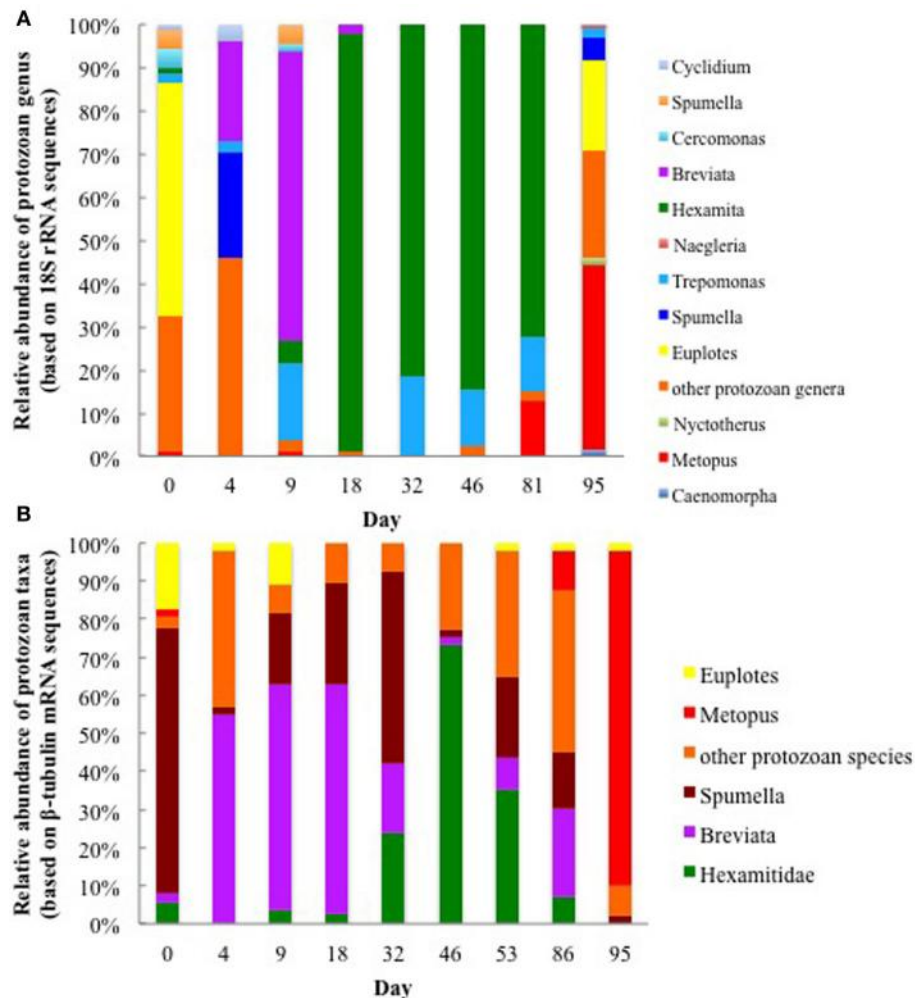


FIGURE 2 | Relative abundance of various protozoan taxa found in groundwater collected on various days during the 2011 field experiment based on (A) protozoan 18S rRNA transcripts and (B) β -tubulin mRNA transcripts.

community, making it unlikely that they made a significant contribution to methane production in the subsurface.

METHANOGEN ENDOSYMBIONT SEQUENCES DETECTED IN THE GROUNDWATER

In addition to expression of genes specific to methanogen-harboring protozoa in the groundwater during the 2011 field experiment, a gene specific to methanogens, *mcrA* (methyl coenzyme M reductase A), was also being actively transcribed in the subsurface following the sulfate reducing phase of the experiment. When acetate concentrations were high, the majority of *mcrA* mRNA transcripts (58.3%) clustered with Methanosaecinales (Figure 3). However, when acetate concentrations dropped below detectable levels on day 95, 60% of the *mcrA* transcripts clustered with Methanomicrobiales, an order that is frequently associated with methanogen-harboring ciliates found in freshwater environments (Fenchel and Finlay, 2010). The dominant Methanomicrobiales sequence (*mcrA* clone 6; 52% of the cDNA clone library) shared 87% of its nucleotides with an

endosymbiont of *Metopus contortus* (Supplementary Figure S5) (Vanbruggen et al., 1983).

CORRELATION BETWEEN METOPUS AND METHANOMICROBIALES ACTIVITY IN URANIUM CONTAMINATED SUBSURFACE SEDIMENTS

In order to evaluate the association of the dominant putative methanogenic symbiont (represented by *mcrA* clone 6) and the dominant *Metopus* species (represented by β -tubulin clone 9), transcripts from methanogen- and protozoan-related genes were quantified over time (Figure 4). There was a strong correlation (Pearson's correlation, $r = 0.95$, $p = 0.005$) between the number of transcripts from clone 6 *mcrA* and *Metopus* β -tubulin genes during the course of the field experiment. Transcription of both genes was low ($2.04 \times 10^1 - 9.6 \times 10^2$ mRNA transcripts per gene copies) until day 81, when the number of mRNA transcripts increased by two orders of magnitude (Figure 4). These results suggest that the growth and activity of this Methanomicrobiales species was directly related to the growth and activity of this *Metopus* protozoan species.

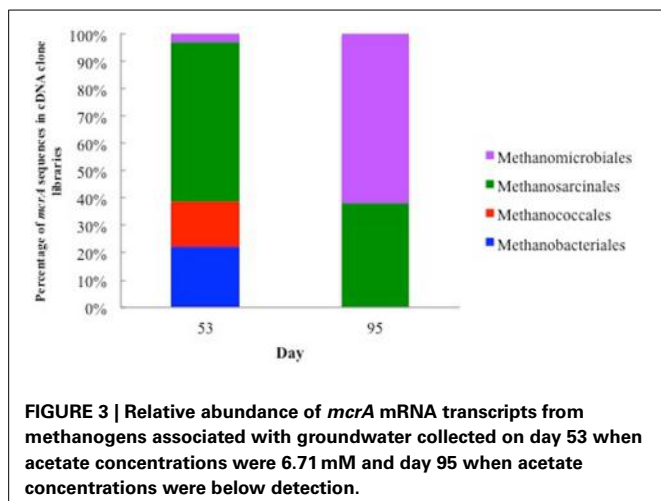


FIGURE 3 | Relative abundance of *mcrA* mRNA transcripts from methanogens associated with groundwater collected on day 53 when acetate concentrations were 6.71 mM and day 95 when acetate concentrations were below detection.

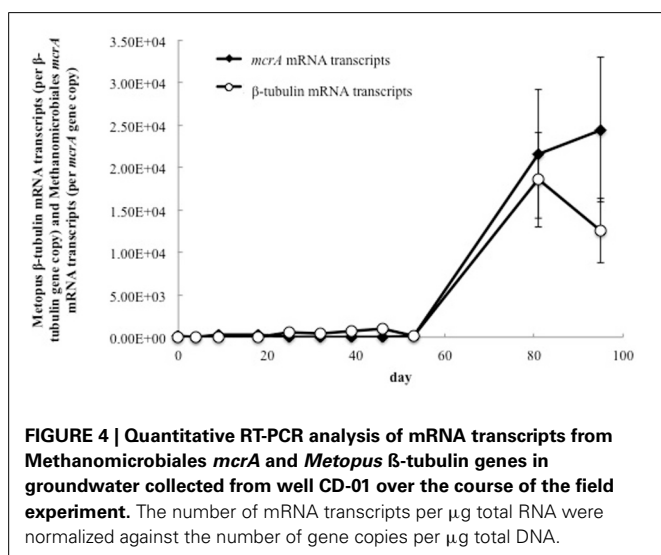


FIGURE 4 | Quantitative RT-PCR analysis of mRNA transcripts from Methanomicrobiales *mcrA* and *Metopus* β -tubulin genes in groundwater collected from well CD-01 over the course of the field experiment. The number of mRNA transcripts per μ g total RNA were normalized against the number of gene copies per μ g total DNA.

LABORATORY SEDIMENT INCUBATIONS

In order to further evaluate the potential contribution of methanogenic endosymbionts to methane production, *in situ* uranium bioremediation was mimicked in anaerobic subsurface sediment incubations (Figure 5). Previous studies (Barlett et al., 2012a) have demonstrated that the addition of acetate to subsurface sediments incubated under anaerobic conditions results in microbiological and geochemical changes similar to those observed during *in situ* uranium bioremediation.

As expected (Anderson et al., 2003; Miletto et al., 2011; Barlett et al., 2012b), the pattern of Fe(II) and sulfide accumulation in the sediment incubations suggested that Fe(III) reduction was initially the predominant terminal electron accepting process, followed by sulfate reduction (Figure 5A). Methane production was not significant until acetate concentrations dropped below 275 μ M and concentrations were \sim 2.5 times lower in the sediment incubations than they were in the field experiment (Figure 5B). This difference can be attributed to the fact that acetate was continuously pumped into the subsurface for the

field experiments whereas acetate was only provided once at the beginning of the sediment incubation experiment.

Methanogenesis was significantly inhibited in sediments in which the eukaryotic inhibitors cycloheximide and colchicine were added at the start of incubation (Figure 5B), suggesting that most of the methane production was related to protozoan activity, and presumably methanogens associated with these protozoa.

Analysis of gene copies for *Metopus* β -tubulin, demonstrated that *Metopus* species began to increase in abundance as acetate was depleted (Figure 5C). After a brief lag this was followed by an increase in gene copies of clone 6 *mcrA*, the sequence that was correlated with *Metopus* species abundance in the field experiment. The factors responsible for the lag in the increase in the symbiotic methanogenic partner are not known. However, there was a direct correlation between Methanomicrobiales *mcrA* and *Metopus* β -tubulin gene copies ($r = 0.87$, $p = 0.0004$), and between methane production and *Metopus* β -tubulin ($r = 0.97$, $p = 0.0003$) and putative symbiont *mcrA* ($r = 0.89$, $p = 0.02$) gene copies.

DISCUSSION

These results demonstrate that stimulating *in situ* bioremediation of uranium-contaminated groundwater with the addition of high concentrations of acetate can have the unintended negative consequence of stimulating methanogenesis. Endosymbiotic methanogens harbored in protozoa appeared to be responsible for much of the methane produced after acetate additions stopped. These studies further emphasize the importance of protozoa in influencing microbial community dynamics and subsurface geochemistry during the bioremediation process.

Both the field experiment and laboratory incubation studies indicated that the enrichment of protozoa harboring endosymbiotic methanogens took place after acetate injections stopped and acetate concentrations had significantly declined in the aquifer. Previous studies showed that high concentrations of acetate stimulate the growth of Fe(III)-reducing and sulfate-reducing microorganisms, and specific protozoan populations that appear to specialize in predation of those actively growing microbes (Holmes et al., 2013). When acetate declined, the same rates of microbial growth could no longer be sustained and it is likely that moribund biomass then served as the primary energy source for a microbial community in which fermentative microorganisms became more important (N'Guessan et al., 2008). The lack of these ciliates or their symbionts at the site up-gradient of the acetate injection wells suggests that their prevalence following acetate injection is related to this increased availability of organic matter.

Metopus species are known to feed both on detritus as well as intact bacterial cells (Esteban et al., 1995; Dewdney, 2010). Although other protozoa also have this ability, protozoa such as *Metopus* species that possess symbiotic methanogens may have a competitive advantage as the growth rate of protozoa is increased when they harbor methanogens (Finlay and Fenchel, 1991; Biagini et al., 1998; Shinzato et al., 2007). The ciliate provides protection, energy and a carbon source for the methanogen, while the methanogen can excrete dissolved organics that can be used by the host (Nowack and Melkonian, 2010).

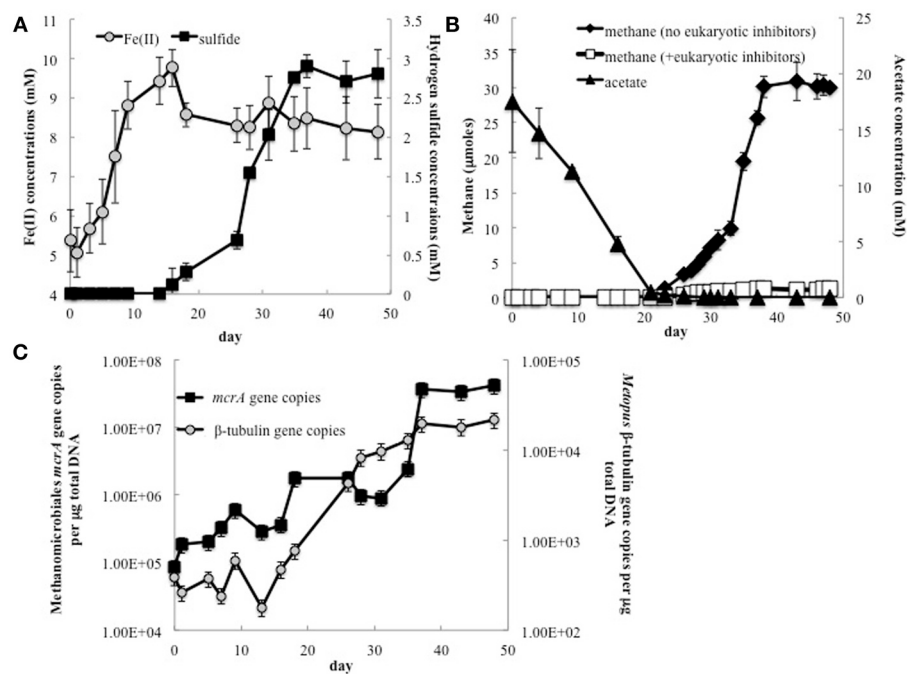


FIGURE 5 | (A) Fe(II) and H₂S concentrations in groundwater collected from Rifle sediment microcosms; **(B)** Methane and acetate concentrations in sediment incubations with and without addition of the eukaryotic inhibitors

cycloheximide and colchicine; **(C)** The number of Methanomicrobiales *mcrA* and *Metopus* β-tubulin gene copies detected in groundwater collected from sediment incubations.

Fermentative microorganisms are also expected to be actively involved in degrading the biomass that accumulates following acetate injection (N'Guessan et al., 2008), producing H₂ that can be consumed by free-living bacteria. This study showed that, without acetate additions to the subsurface, there was not sufficient electron donor supply to deplete sulfate from the groundwater (Figure 1B). Free-living methanogens cannot effectively compete with sulfate reducers for electron donors under these conditions (Lovley et al., 1982; Lovley and Klug, 1983). However, the endosymbionts have exclusive access to H₂ produced within the hydrogenosome of the host protozoan. A comparable benefit to methanogens has been reported in marine sediments in which methanogen endosymbionts can account for 90% of the methane produced in the subsurface (Fenchel, 1993). In a similar manner, endosymbiotic methanogens produce a substantial amount of methane when rice paddy soils are first flooded and alternative electron acceptors such as Fe(III) and sulfate are available, but once Fe(III) and sulfate are depleted free-living methanogens account for most of the methane (Schwarz and Frenzel, 2005).

These results further demonstrate the important impact that protozoa can have on the ecology and biogeochemistry of *in situ* uranium bioremediation. It is likely that protozoa have similar influences in other bioremediation strategies that rely on stimulating microbial metabolism with organic electron donors.

ACKNOWLEDGMENTS

This research was supported by the Office of Science (BER), U. S. Department of Energy, Award No. DE-SC0006790.

SUPPLEMENTARY MATERIAL

The Supplementary Material for this article can be found online at: <http://www.frontiersin.org/journal/10.3389/fmich.2014.00366/abstract>

REFERENCES

- Altschul, S., Madden, T., Schaffer, A., Zhang, J., Zhang, Z., Miller, W., et al. (1998). Gapped blast and psi-blast: a new generation of protein database search programs. *Nucleic Acids Res.* 25, 3389–3402. doi: 10.1093/nar/25.17.3389
- Anderson, R. T., Vrionis, H. A., Ortiz-Bernad, I., Resch, C. T., Long, P. E., Dayvault, R., et al. (2003). Stimulating the *in situ* activity of Geobacter species to remove uranium from the groundwater of a uranium-contaminated aquifer. *Appl. Environ. Microbiol.* 69, 5884–5891. doi: 10.1128/AEM.69.10.5884-5891.2003
- Baker, B. J., Lutz, M. A., Dawson, S. C., Bond, P. L., and Banfield, J. F. (2004). Metabolically active eukaryotic communities in extremely acidic mine drainage. *Appl. Environ. Microbiol.* 70, 6264–6271. doi: 10.1128/AEM.70.10.6264-6271.2004
- Barlett, M., Moon, H. S., Peacock, A. A., Hedrick, D. B., Williams, K. H., Long, P. E., et al. (2012a). Uranium reduction and microbial community development in response to stimulation with different electron donors. *Biodegradation* 23, 535–546. doi: 10.1007/s10532-011-9531-8
- Barlett, M., Zhuang, K., Mahadevan, R., and Lovley, D. (2012b). Integrative analysis of Geobacter spp. and sulfate-reducing bacteria during uranium bioremediation. *Biogeosciences* 9, 1033–1040. doi: 10.5194/bg-9-1033-2012
- Bekins, B. A., Cozzarelli, I. M., Godsy, E. M., Warren, E., Essaid, H. I., and Tuccillo, M. E. (2001). Progression of natural attenuation processes at a crude oil spill site: II. Controls on spatial distribution of microbial populations. *J. Contam. Hydrol.* 53, 387–406. doi: 10.1016/S0169-7722(01)00175-9
- Biagini, G. A., Finlay, B. J., and Lloyd, D. (1998). Protozoan stimulation of anaerobic microbial activity: enhancement of the rate of terminal decomposition of organic matter. *FEMS Microbiol. Ecol.* 27, 1–8. doi: 10.1111/j.1574-6941.1998.tb00520.x
- Bustin, S. A., Benes, V., Garson, J. A., Hellemans, J., Huggett, J., Kubista, M., et al. (2009). The MIQE guidelines: minimum information for publication

- of quantitative real-time PCR experiments. *Clin. Chem.* 55, 611–622. doi: 10.1373/clinchem.2008.112797
- Casamayor, E. O., Massana, R., Benlloch, S., Ovreas, L., Diez, B., Goddard, V. J., et al. (2002). Changes in archaeal, bacterial and eukaryal assemblages along a salinity gradient by comparison of genetic fingerprinting methods in a multipond solar saltern. *Environ. Microbiol.* 4, 338–348. doi: 10.1046/j.1462-2920.2002.00297.x
- Dewdney, A. K. (2010). “The structure of benthic microbial communities in the old Ausable River Channel,” in *Biotic Communities of a River in a Dune Watershed*, eds M. A. Maun, R. A. Schincariol (Ottawa, ON: NRC Research Press), 61.
- Dowdle, P. R., Laverman, A. M., and Oremland, R. S. (1996). Bacterial dissimilatory reduction of arsenic(V) to arsenic(III) in Anoxic Sediments. *Appl. Environ. Microbiol.* 62, 1664–1669.
- Eden, P. A., Schmidt, T. M., Blakemore, R. P., and Pace, N. R. (1991). Phylogenetic analysis of *Aquaspirillum magnetotacticum* using polymerase chain reaction amplified 16S ribosomal RNA specific DNA. *Int. J. Syst. Bacteriol.* 41, 324–325. doi: 10.1099/00207713-41-2-324
- Esteban, G., Fenchel, T., and Finlay, B. (1995). Diversity of free-living morphospecies in the ciliate genus Metopus. *Arch. Protistenkd.* 146, 137–164. doi: 10.1016/S0003-9365(11)80106-5
- Fenchel, T. (1993). Methanogenesis in marine shallow water sediments- The quantitative role of anaerobic protozoa with endosymbiotic methanogenic bacteria. *Ophelia* 37, 67–82.
- Fenchel, T., and Finlay, B. J. (2010). “Free-living protozoa with endosymbiotic methanogens,” in *(Endo)symbiotic Methanogenic Archaea*, ed J. H. P. Hackstein (Heidelberg: Springer-Verlag Heidelberg), 1–11. doi: 10.1007/978-3-642-13615-3_1
- Filatov, D. A. (2002). PROSEQ: a software for preparation and evolutionary analysis of DNA sequence data sets. *Mol. Ecol. Notes* 2, 621–624. doi: 10.1046/j.1471-8286.2002.00313.x
- Finlay, B. J., and Fenchel, T. (1991). An anaerobic protozoan, with symbiotic methanogens, living in municipal landfill material. *FEMS Microbiol. Ecol.* 85, 169–179. doi: 10.1111/j.1574-6968.1991.tb04709.x-i1
- Giloteaux, L., Holmes, D. E., Williams, K. H., Wrighton, K. C., Wilkins, M. J., Montgomery, A. P., et al. (2013). Characterization and transcription of arsenic respiration and resistance genes during *in situ* uranium bioremediation. *ISME J.* 7, 370–383. doi: 10.1038/ismej.2012.109
- Giovannoni, S. J., Delong, E. F., Olsen, G. J., and Pace, N. R. (1988). Phylogenetic group-specific oligodeoxynucleotide probes for identification of single microbial-cells. *J. Bacteriol.* 170, 720–726.
- Hackstein, J. H. P. (2011). Anaerobic ciliates and their methanogenic endosymbionts. *Microbiol. Monogr.* 19, 12–23. doi: 10.1007/978-3-642-13615-3_2
- Hery, M., van Dongen, B. E., Gill, F., Mondal, D., Vaughan, D. J., Pancost, R. D., et al. (2010). Arsenic release and attenuation in low organic carbon aquifer sediments from West Bengal. *Geobiology* 8, 155–168. doi: 10.1111/j.1472-4669.2010.00233.x
- Holmes, D. E., Giloteaux, L., Williams, K. H., Wrighton, K. C., Wilkins, M. J., Thompson, C. A., et al. (2013). Enrichment of specific protozoan populations during *in situ* bioremediation of uranium-contaminated groundwater. *ISME J.* 7, 1286–1298. doi: 10.1038/ismej.2013.20
- Holmes, D. E., Nevin, K. P., O’Neil, R. A., Ward, J. E., Adams, L. A., Woodard, T. L., et al. (2005). Potential for quantifying expression of the Geobacteraceae citrate synthase gene to assess the activity of Geobacteraceae in the subsurface and on current-harvesting electrodes. *Appl. Environ. Microbiol.* 71, 6870–6877. doi: 10.1128/AEM.71.11.6870-6877.2005
- Hug, L. A., Castelle, C. J., Wrighton, K. C., Thomas, B. C., Sharon, I., Frischkorn, K. R., et al. (2013). Community genomic analyses constrain the distribution of metabolic traits across the Chloroflexi phylum and indicate roles in sediment carbon cycling. *Microbiome* 1:22. doi: 10.1186/2049-2618-1-22
- Islam, F. S., Gault, A. G., Boothman, C., Polya, D. A., Charnock, J. M., Chatterjee, D., et al. (2004). Role of metal-reducing bacteria in arsenic release from Bengal delta sediments. *Nature* 430, 68–71. doi: 10.1038/nature02638
- Juutonen, H., Galand, P. E., and Yrjala, K. (2006). Detection of methanogenic Archaea in peat: comparison of PCR primers targeting the *mcrA* gene. *Res. Microbiol.* 157, 914–921. doi: 10.1016/j.resmic.2006.08.006
- Kleikemper, J., Pombo, S. A., Schroth, M. H., Sigler, W. V., Pesaro, M., and Zeyer, J. (2005). Activity and diversity of methanogens in a petroleum hydrocarbon-contaminated aquifer. *Appl. Environ. Microbiol.* 71, 149–158. doi: 10.1128/AEM.71.1.149-158.2005
- Lane, D. J., Pace, B., Olsen, G. J., Stahl, D. A., Sogin, M. L., and Pace, N. R. (1985). Rapid determination of 16S ribosomal RNA sequences for phylogenetic analyses. *Proc. Natl. Acad. Sci. U.S.A.* 82, 6955–6959. doi: 10.1073/pnas.82.20.6955
- Lovley, D. R. (1997). Potential for anaerobic bioremediation of BTEX in petroleum-contaminated aquifers. *J. Ind. Microbiol. Biotechnol.* 18, 75–81. doi: 10.1038/sj.jim.2900246
- Lovley, D. R., Dwyer, D. F., and Klug, M. J. (1982). Kinetic-analysis of competition between sulfate reducers and methanogens for hydrogen in sediments. *Appl. Environ. Microbiol.* 43, 1373–1379.
- Lovley, D. R., and Klug, M. J. (1983). Sulfate reducers can out-compete methanogens at fresh-water sulfate concentrations. *Appl. Environ. Microbiol.* 45, 187–192.
- Lovley, D. R., and Phillips, E. J. (1988). Novel mode of microbial energy metabolism: organic carbon oxidation coupled to dissimilatory reduction of iron or manganese. *Appl. Environ. Microbiol.* 54, 1472–1480.
- Lovley, D. R., Stoltz, J. F., Nord, G. L., and Phillips, E. J. P. (1987). Anaerobic production of magnetite by a dissimilatory iron-reducing microorganism. *Nature* 330, 252–254. doi: 10.1038/330252a0
- Luton, P. E., Wayne, J. M., Sharp, R. J., and Riley, P. W. (2002). The *mcrA* gene as an alternative to 16S rRNA in the phylogenetic analysis of methanogen populations in landfill. *Microbiology* 148(Pt 11), 3521–3530.
- Malvankar, N. S., and Lovley, D. R. (2014). Microbial nanowires for bioenergy applications. *Curr. Opin. Biotechnol.* 27, 88–95. doi: 10.1016/j.copbio.2013.12.003
- Miletto, M., Williams, K. H., N’Guessan, A. L., and Lovley, D. R. (2011). Molecular analysis of the metabolic rates of discrete subsurface populations of sulfate reducers. *Appl. Environ. Microbiol.* 77, 6502–6509. doi: 10.1128/AEM.00576-11
- Narayanan, N., Priya, M., Haridas, A., and Manilal, V. B. (2007). Isolation and culturing of a most common anaerobic ciliate, *Metopus* sp. *Anaerobe* 13, 14–20. doi: 10.1016/j.anaerobe.2006.10.003
- Newbold, C. J., Lassalas, B., and Jouany, J. P. (1995). The importance of methanogens associated with ciliate protozoa in ruminal methane production *in vitro*. *Lett. Appl. Microbiol.* 21, 230–234. doi: 10.1111/j.1472-765X.1995.tb1048.x
- N’Guessan, A. L., Vrionis, H. A., Resch, C. T., Long, P. E., and Lovley, D. R. (2008). Sustained removal of uranium from contaminated groundwater following stimulation of dissimilatory metal reduction. *Environ. Sci. Technol.* 42, 2999–3004. doi: 10.1021/es071960p
- Nowack, E. C. M., and Melkonian, M. (2010). Endosymbiotic associations within protists. *Philos. Trans. R Soc. Biol.* 365, 699–712. doi: 10.1098/rstb.2009.0188
- Priya, M., Haridas, A., and Manilal, V. B. (2008). Anaerobic protozoa and their growth in biomethanation systems. *Biodegradation* 19, 179–185. doi: 10.1007/s10532-007-9124-8
- Redman, A. D., Macalady, D. L., and Ahmann, D. (2002). Natural organic matter affects arsenic speciation and sorption onto hematite. *Environ. Sci. Technol.* 36, 2889–2896. doi: 10.1021/es0112801
- Reysenbach, A. L., Giver, L. J., Wickham, G. S., and Pace, N. R. (1992). Differential amplification of ribosomal-RNA genes by polymerase chain reaction. *Appl. Environ. Microbiol.* 58, 3417–3418.
- Rotaru, A. E., Shrestha, P. M., Liu, F. H., Shrestha, M., Shrestha, D., Embree, M., et al. (2014). A new model for electron flow during anaerobic digestion: direct interspecies electron transfer to *Methanosaeta* for the reduction of carbon dioxide to methane. *Energy Environ. Sci.* 7, 408–415. doi: 10.1039/c3ee42189a
- Rowland, H. A. L., Pederick, R. L., Polya, D. A., Pancost, R. D., Van Dongen, B. E., Gault, A. G., et al. (2007). The control of organic matter on microbially mediated iron reduction and arsenic release in shallow alluvial aquifers, Cambodia. *Geobiology* 5, 281–292. doi: 10.1111/j.1472-4669.2007.00100.x
- Schwarz, M. V. J., and Frenzel, P. (2005). Methanogenic symbionts of anaerobic ciliates and their contribution to methanogenesis in an anoxic rice field soil. *FEMS Microbiol. Ecol.* 52, 93–99. doi: 10.1016/j.femsec.2004.10.009
- Shinzato, N., Watanabe, I., Meng, X. Y., Sekiguchi, Y., Tamaki, H., Matsui, T., et al. (2007). Phylogenetic analysis and fluorescence *in situ* hybridization detection of archaeal and bacterial endosymbionts in the anaerobic ciliate *Trimyema compressum*. *Microb. Ecol.* 54, 627–636. doi: 10.1007/s00248-007-9218-1

- Spalding, B. P., and Watson, D. B. (2006). Measurement of dissolved H-2, O-2, and CO2 in groundwater using passive samplers for gas chromatographic analyses. *Environ. Sci. Technol.* 40, 7861–7867. doi: 10.1021/es0613310
- Stams, A. J., and Plugge, C. M. (2009). Electron transfer in syntrophic communities of anaerobic bacteria and archaea. *Nat. Rev. Microbiol.* 7, 568–577. doi: 10.1038/nrmicro2166
- Tamura, K., and Nei, M. (1993). Estimation of the number of nucleotide substitutions in the control region of mitochondrial-DNA in humans and chimpanzees. *Mol. Biol. Evol.* 10, 512–526.
- Tamura, K., Stecher, G., Peterson, D., Filipski, A., and Kumar, S. (2013). MEGA6: molecular evolutionary genetics analysis version 6.0. *Mol. Biol. Evol.* 30, 2725–2729. doi: 10.1093/molbev/mst197
- Thompson, J. D., Gibson, T. J., Plewniak, F., Jeanmougin, F., and Higgins, D. G. (1997). The CLUSTAL X windows interface: flexible strategies for multiple sequence alignment aided by quality analysis tools. *Nucleic Acids Res.* 25, 4876–4882. doi: 10.1093/nar/25.24.4876
- Truper, H. G., and Schlegel, H. G. (1964). Sulphur metabolism in thiorhodaceae. I. quantitative measurements on growing cells of chromatium okenii. *Antonie Van Leeuwenhoek.* 30, 225–238. doi: 10.1007/BF02046728
- Ushida, K., Tokura, M., Takenaka, A., and Itabashi, H. (1997). “Ciliate protozoa and ruminal methanogenesis,” in *Rumen Microbes and Digestive Physiology in Ruminants. Satellite Symposium of the 8th Animal Science Congress*, eds R. Onodera, H. Itabashi, K. Ushida, H. Yano, and Y. Sasaki (Tokyo: Japan Scientific Societies Press), 209–220.
- Vanbruggen, J. J. A., Stumm, C. K., and Vogels, G. D. (1983). Symbiosis of methanogenic bacteria and sapropelic protozoa. *Arch. Microbiol.* 136, 89–95. doi: 10.1007/BF00404779
- van Hoek, A., van Alen, T. A., Sprakel, V. S. I., Leunissen, J. A. M., Brigge, T., Vogels, G. D., et al. (2000). Multiple acquisition of methanogenic archaeal symbionts by anaerobic ciliates. *Mol. Biol. Evol.* 17, 251–258. doi: 10.1093/oxfordjournals.molbev.a026304
- van Hoek, A. H. A. M., van Alen, T. A., Vogels, G. D., and Hackstein, J. H. P. (2006). Contribution by the methanogenic endosymbionts of anaerobic ciliates to methane production in Dutch freshwater sediments. *Acta Protozool.* 45, 215–224. Available online at: <http://repository.ubn.ru.nl/handle/2066/58777>
- Vogels, G. D., Hoppe, W. F., and Stumm, C. K. (1980). Association of methanogenic bacteria with rumen ciliates. *Appl. Environ. Microbiol.* 40, 608–612.
- VRIONIS, H. A., ANDERSON, R. T., ORTIZ-BERNAD, I., O'NEILL, K. R., RESCH, C. T., PEACOCK, A. D., et al. (2005). Microbiological and geochemical heterogeneity in an *in situ* uranium bioremediation field site. *Appl. Environ. Microbiol.* 71, 6308–6318. doi: 10.1128/AEM.71.10.6308-6318.2005
- Wall, J. D., and Krumholz, L. R. (2006). Uranium reduction. *Annu. Rev. Microbiol.* 60, 149–166. doi: 10.1146/annurev.micro.59.030804.121357
- Williams, K. H., Long, P. E., Davis, J. A., Wilkins, M. J., N'Guessan, A. L., Steefel, C. I., et al. (2011). Acetate availability and its influence on sustainable bioremediation of uranium-contaminated groundwater. *Geomicrobiol. J.* 28, 519–539. doi: 10.1080/01490451.2010.520074
- Wrighton, K. C., Castelle, C. J., Wilkins, M. J., Hug, L. A., Sharon, I., Thomas, B. C., et al. (2014). Metabolic interdependencies between phylogenetically novel fermenters and respiratory organisms in an unconfined aquifer. *ISME J.* 8, 1452–1463. doi: 10.1038/ismej.2013.249
- Wrighton, K. C., Thomas, B. C., Sharon, I., Miller, C. S., Castelle, C. J., VerBerkmoes, N. C., et al. (2012). Fermentation, hydrogen, and sulfur metabolism in multiple uncultivated bacterial phyla. *Science* 337, 1661–1665. doi: 10.1126/science.1224041
- Wu, W. M., Carley, J., Luo, J., Ginder-Vogel, M. A., Cardenas, E., Leigh, M. B., et al. (2007). *In situ* bioreduction of uranium (VI) to submicromolar levels and reoxidation by dissolved oxygen. *Environ. Sci. Tech.* 41, 5716–5723. doi: 10.1021/es062657b
- Yarlett, N., and Hackstein, J. H. P. (2005). Hydrogenosomes: one organelle, multiple origins. *Bioscience* 55, 657–668. doi: 10.1641/0006-3568(2005)055[0657:HOOOMO]2.0.CO;2
- Conflict of Interest Statement:** The Associate Editor declares that despite having collaborated with author Kenneth H. Williams, the review process was handled objectively. The authors declare that the research was conducted in the absence of any commercial or financial relationships that could be construed as a potential conflict of interest.

Received: 24 April 2014; accepted: 01 July 2014; published online: 06 August 2014.

Citation: Holmes DE, Giloteaux L, Orellana R, Williams KH, Robbins MJ and Lovley DR (2014) Methane production from protozoan endosymbionts following stimulation of microbial metabolism within subsurface sediments. *Front. Microbiol.* 5:366. doi: 10.3389/fmicb.2014.00366

This article was submitted to Terrestrial Microbiology, a section of the journal *Frontiers in Microbiology*.

Copyright © 2014 Holmes, Giloteaux, Orellana, Williams, Robbins and Lovley. This is an open-access article distributed under the terms of the Creative Commons Attribution License (CC BY). The use, distribution or reproduction in other forums is permitted, provided the original author(s) or licensor are credited and that the original publication in this journal is cited, in accordance with accepted academic practice. No use, distribution or reproduction is permitted which does not comply with these terms.



Grappling archaea: ultrastructural analyses of an uncultivated, cold-loving archaeon, and its biofilm

Alexandra K. Perras^{1†}, Gerhard Wanner^{2†}, Andreas Klingl^{2,3,4}, Maximilian Mora¹, Anna K. Auerbach¹, Veronika Heinz¹, Alexander J. Probst¹, Harald Huber¹, Reinhard Rachel¹, Sandra Meck¹ and Christine Moissl-Eichinger^{1*}

¹ Department of Microbiology and Archaea Center, University of Regensburg, Regensburg, Germany

² Department of Biology I, Biozentrum Ludwig Maximilian University of Munich, Planegg-Martinsried, Germany

³ Zellbiologie, Philipps-Universität Marburg, Marburg, Germany

⁴ LOEWE Research Centre for Synthetic Microbiology (Synmikro), Marburg, Germany

Edited by:

Luis Raul Comolli, Lawrence Berkeley National Laboratory, USA

Reviewed by:

Luis Raul Comolli, Lawrence Berkeley National Laboratory, USA
Ariane Briegel, Caltech, USA

***Correspondence:**

Christine Moissl-Eichinger,
Department of Microbiology and Archaea Center, University of Regensburg, Universitätsstr. 31,
93053 Regensburg, Germany
e-mail: christine.moissl-eichinger@ur.de

[†]These authors have contributed equally to this work.

Similarly to Bacteria, Archaea are microorganisms that interact with their surrounding environment in a versatile manner. To date, interactions based on cellular structure and surface appendages have mainly been documented using model systems of cultivable archaea under laboratory conditions. Here, we report on the microbial interactions and ultrastructural features of the uncultivated SM1 Euryarchaeon, which is highly dominant in its biotope. Therefore, biofilm samples taken from the Sippenauer Moor, Germany, were investigated via transmission electron microscopy (TEM; negative staining, thin-sectioning) and scanning electron microscopy (SEM) in order to elucidate the fine structures of the microbial cells and the biofilm itself. The biofilm consisted of small archaeal cocci ($0.6\text{ }\mu\text{m}$ diameter), arranged in a regular pattern ($1.0\text{--}2.0\text{ }\mu\text{m}$ distance from cell to cell), whereas each archaeon was connected to 6 other archaea on average. Extracellular polymeric substances (EPS) were limited to the close vicinity of the archaeal cells, and specific cell surface appendages (hami, Moissl et al., 2005) protruded beyond the EPS matrix enabling microbial interaction by cell-cell contacts among the archaea and between archaea and bacteria. All analyzed hami revealed their previously described architecture of nano-grappling hooks and barb-wire basal structures. Considering the archaeal cell walls, the SM1 Euryarchaea exhibited a double-membrane, which has rarely been reported for members of this phylogenetic domain. Based on these findings, the current generalized picture on archaeal cell walls needs to be revisited, as archaeal cell structures are more complex and sophisticated than previously assumed, particularly when looking into the uncultivated majority.

Keywords: archaea, biofilm, ultrastructure, hami, EPS, SEM, TEM, microbial interaction

INTRODUCTION

Understanding the microbial “dark matter” has become one of the driving desires of the scientific community (Rinke et al., 2013). In particular, deep-branching, uncultivated archaea have attracted the interest, being largely unexplored but widespread and likely major drivers of the nutrient cycles in various ecosystems (Cavicchioli et al., 2007). Systems that allow unbiased and direct analyses of uncultivated microorganisms on microscopic and macroscopic levels due to one organism’s predominance are extremely rare. However, such systems are of utmost importance to understand the functioning of microorganisms in the environment, their natural cellular composition, their actual metabolic activity and their interactions with the abiotic and biotic environment (Morris et al., 2013).

The majority of microorganisms seems to be uncultivable using standard methods (Amann et al., 1995). The unsatisfying success in this regard might be rooted in the interwoven interactivity of microorganisms in their natural biotope, such as

natural ecosystems, or macrobes, such as plants or the human body. The human body itself is colonized by 10–100 times more microbial cells than own cells (Schleifer, 2004). Analyzing the (human) microbiome has become a major scientific focus, benefitting from state-of-the-art, cultivation-independent methods which include next generation sequencing of 16S rRNA genes and –OMICS technologies (Zhang et al., 2010). Altogether, these methods allow first glances at the diversity and function of an entire microbial community, which interacts closely with its host, forming a “superorganism”: the holobiont (Margulis, 1993; Rohwer et al., 2002). It is assumed, that the cooperation of host and microbes represents a unit of selection in evolution and changes in composition and function have severe impact on further development or even next host generations (Zilber-Rosenberg and Rosenberg, 2008). As a consequence, evolution appears to be a coordinated process of entire (microbial) communities, which need to be scientifically addressed as a whole.

The effects of microbial interactions for the different partners can vary. In symbiotic relationships all partners benefit, whereas commensal interaction is beneficial for one partner and not harmful for the other. Parasites, however, strongly affect the fitness of one partner (Moissl-Eichinger and Huber, 2011). A well-documented model system of a bacterial symbiotic interaction is “*Chlorochromatium aggregatum*,” a clearly structured consortium of immobile green sulfur bacteria epibionts and a motile beta-proteobacterium (Müller and Overmann, 2011). This association provides mobility to the epibionts and, in exchange, amino acids and 2-oxoglutarate to the inner partner. Detailed ultrastructural analyses revealed that hair-like filaments protrude from the epibionts and directly interconnect with the central bacterium. The latter connects with the epibionts via periplasmic tubes, which attach to the epibiont’s outer membrane (Wanner et al., 2008).

In general, structural analyses of syntrophic and interactive consortia and communities that include an archaeal partner have rarely been reported, and information on the structure of natural archaeal populations in the literature is scarce. A likely syntrophic interaction between two hyperthermophilic archaea was artificially established under laboratory conditions: during co-culture conditions, *Pyrococcus furiosus* attaches to *Methanopyrus kandleri* forming an unusual bi-species biofilm on provided surfaces (“fried-egg colonies”; Schopf et al., 2008). The contact between the two types of archaeal cells is mediated by flagella and possibly by extracellular polymeric substances (EPS). One example for a natural and uncultivated archaeal-archaeal interactive community is the ARMAN (archaeal Richmond Mine acidophilic nanoorganisms) system, where the ARMAN cells interact closely with *Thermoplasmatales* cells leading to a potential nutrient or molecule exchange (Comolli et al., 2009; Baker et al., 2010; see also article in this issue).

A model system for archaeal interspecies relationships is represented by the “intimate association” of *Ignicoccus hospitalis* and its partner *Nanoarchaeum equitans* (Huber et al., 2002; Jahn et al., 2008). The relationship is based on the attachment of *N. equitans* to the outer cellular membrane (OCM) of *I. hospitalis* (Jahn et al., 2004). It has been shown that this obligate dependence on *I. hospitalis* is a consequence of the transfer of membrane lipids, amino acids and probably even ATP from *I. hospitalis* to *N. equitans* (Huber et al., 2012). Other investigations gave evidence for the lateral transfer of genetic material in both directions, during the co-evolution of these two archaeal cells (Podar et al., 2008). While *I. hospitalis* is able to grow in pure culture, *N. equitans* still resists cultivation without its host. This system can be maintained in the laboratory, and since one of the microorganisms is strictly dependent on the other, it actually reflects the interaction of two archaea in the natural biotope, where both species thrive.

Moreover, interactive microbial communities of Bacteria and Archaea are known, such as the anaerobic methane oxidizing (AMO) consortia, consisting of anaerobic, methanotrophic archaea (ANME) in loose association with sulfate reducing bacteria (SRB) of the *Desulfococcus/Desulfosarcina* group (Hoehler et al., 1994; Elvert et al., 1999; Hinrichs et al., 1999; Thiel et al., 1999).

Another bacterial/archaeal consortium was detected in the sulfidic springs of the Sippenauer Moor (SM), a cold (~10°C) swamp area, located in the southeast of Germany. Coccoid archaea, designated as “SM1 Euryarchaeon,” were found to be the major constituents of macroscopically visible whitish pearls, floating in the surface waters of the springs. The outer sheath of these pearls is formed by a sulfur-oxidizing, filamentous bacterial partner (*Thiothrix* sp.; Rudolph et al., 2001; Moissl et al., 2002). The pearls are connected by thin threads, exclusively formed by *Thiothrix* sp. (Moissl et al., 2002), giving the microbial community a “string-of-pearls” like appearance. The SM1 Euryarchaeon was also detected in another, distinct sulfidic setting, the Mühlbacher Schwefelquelle (MSI; nearby Regensburg, Germany), where the string-of-pearls community (SOPC) can be found in a similar microbial composition (Rudolph et al., 2004).

Interestingly, subsequent studies revealed that the MSI-SM1 Euryarchaeon seeks the vicinity to sulfide-oxidizers only in (oxygenated) surface waters, whereas in the deeper, anaerobic subsurface it grows as an almost pure biofilm (Henneberger et al., 2006). Within the biofilm, the MSI-SM1 Euryarchaeon predominates a minor bacterial community, which is mostly composed of sulfate-reducing bacteria (Henneberger et al., 2006; Probst et al., 2013). Since the SM1 Euryarchaeon remains uncultured under laboratory conditions, many features, including its metabolic capability, are yet to be fully understood. The archaeal biofilms are transported with the water flow from the subsurface to the spring outflow, where biomass can be harvested in sufficient quantities for further analyses (Henneberger et al., 2006; Probst et al., 2013). Similar biofilms, mainly consisting of coccoid SM1 Euryarchaeota and a minor fraction of bacteria, were also observed in upwelling, anoxic waters of the SM (Henneberger et al., 2006).

The SM1 Euryarchaeon has revealed extraordinary properties, clearly distinguishing it from the archaeal strains characterized in the literature. Firstly, the SM1 Euryarchaeon is one of a few reported archaea capable of biofilm formation in its natural biotope. Additionally, it is the only archaeon known to clearly dominate a low-temperature biotope: the literature suggests that ecosystems are either dominated by bacteria or mixtures of diverse archaea (i.e., Schrenk et al., 2003, 2004; Koch et al., 2006; Webster and Negri, 2006; Weidler et al., 2008; Briggs et al., 2011; Couradeau et al., 2011; Ionescu et al., 2012). The appearance of the SM1 Euryarchaeon in a variety of ecosystems (Rudolph et al., 2004) and in extremely high density (as almost pure biofilms, “hot spots”) suggests an important role in the subsurface with a vast impact on local biogeochemistry. Thirdly, the SM1 Euryarchaeon carries a novel type of cell surface appendages. Being as thin as pili, these appendages (up to 4 μm long) exhibit barb-wire like prickles (which might function as distance holders in the biofilm) and small nano-hooks at their distal end. These structures were described as “hami” (latin for anchors, hooks; Moissl et al., 2005). So far no comparable microbial or artificial similar structures of similar size have been described. These unique properties of the SM1 Euryarchaeon biofilm have made the ecosystems, the microbial assemblages, and the archaeon itself a model system for studying cold-loving archaea in a natural biotope.

The SM1 euryarchaeal biofilms from the two biotopes SM and MSI were compared in a very recent study via genetic and chemical microbiome profiling, which revealed that both biofilms are different in their bacterial composition and are thus unlikely to originate from one single biotope in the subsurface. The archaea of both biofilms were initially judged to be identical - based on an identical 16S rRNA gene of both populations. However, the SM and MSI cells were different in size, showed strong variations in membrane lipid composition and in their genomic information, and revealed also minor differences in ultrastructure (EPS and hami). Thus, we concluded that the two biofilms are dominated by the same archaeal species, but by two different strains thereof (Probst et al., 2014).

Based on this finding, a deeper ultrastructural investigation of the SM population became warranted, which was conducted in this study. Here, we provide novel insights into the multifarious aspects of the SM1 Euryarchaeon lifestyle from structural biofilm organization and the interactions with the bacterial and archaeal neighbors via its unique cell surface appendages to cell wall architecture.

MATERIALS AND METHODS

SAMPLING AND SAMPLE PROCESSING

Samples for ultrastructural analyses were taken in a cold sulfidic spring in close vicinity to Regensburg, Germany (SM; Rudolph et al., 2001, 2004). Archaeal biofilms were harvested from raw-meshed nets, placed right within the spring outflow (Henneberger et al., 2006). The samples were collected using sterile syringes and transported on ice to the laboratory.

ULTRASTRUCTURAL ANALYSIS

Freshly taken biofilms were fixed in original spring water including 0.1% glutardialdehyde (w/v). Scanning electron microscopy was carried out as described elsewhere (Probst et al., 2014). Samples were examined using a Zeiss Auriga scanning electron microscope operated at 1–2 kV. For TEM, the sample preparation and procedure is described in Probst et al. (2014). Samples were examined using a CM12 transmission electron microscope (FEI Co., Eindhoven, The Netherlands) operated at 120 kV. All images were digitally recorded using a slow-scan charge-coupled device camera that was connected to a computer with TVIPS software (TVIPS GmbH, Gauting, Germany).

RESULTS

THE SM1 EURYARCHAEON FORMS A BIOFILM WITH EPS AND CELL SURFACE APPENDAGES

The SM SM1 Euryarchaeon forms a biofilm, which is dominated by a single species. Macroscopically, the biofilm droplets (diameter up to 2 cm) appear milky and viscous, and show strong attachment to various types of surfaces. Using different microscopy techniques, a homogenous cell-population was observed (e.g., Figure 1A). The rare (less than 5%, Probst et al., 2014), mostly unflagellated and unpiliated bacterial cells were embedded within the biofilms and morphologies ranged from short rods, spirilla and cocci to several μm -long filaments (Figures 1B,C). Viruses were not detected in any of the preparations. The archaeal cells were visible as regular cocci, although many cells appeared to be actively dividing at the time point of sampling, with an oval morphology and a clear, central contraction (Figure 2). The average cell diameter of non-dividing cells was determined to be about $0.6 \mu\text{m}$ ($\pm 0.1 \mu\text{m}$), corresponding to a cell volume of $0.11 \mu\text{m}^3$ on average (Probst et al., 2014).

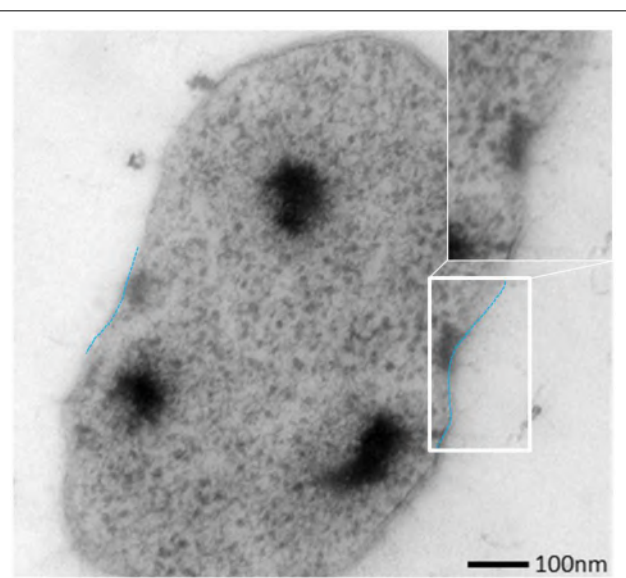


FIGURE 2 | Ultrathin section of one dividing SM1 coccus with a visible invagination.

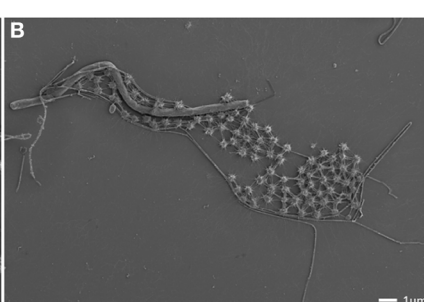
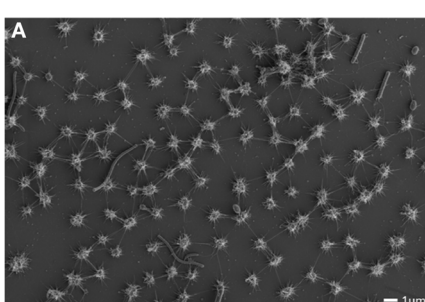


FIGURE 1 | Scanning electron micrographs of the SM biofilm. Overview, showing the homogenous archaeal population (small coccoid shaped cells; **A,B**) and large, spiral-shaped bacterium (**C**).

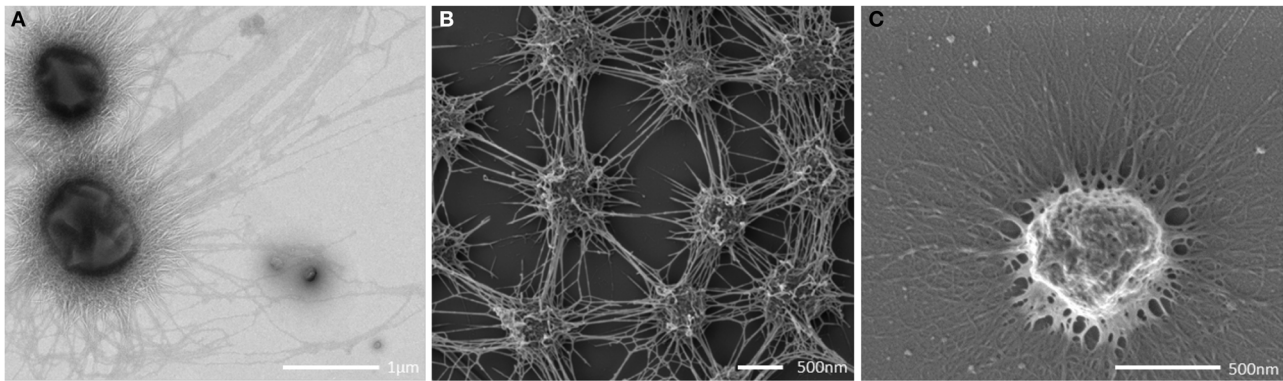


FIGURE 3 | Transmission electron (A) and scanning electron (B,C) micrographs. (A,B) show intraspecies contact via the cell appendages (bars: A: 500 nm; B: 400 nm). (C) shows a single coccus embedded in a thick EPS layer.

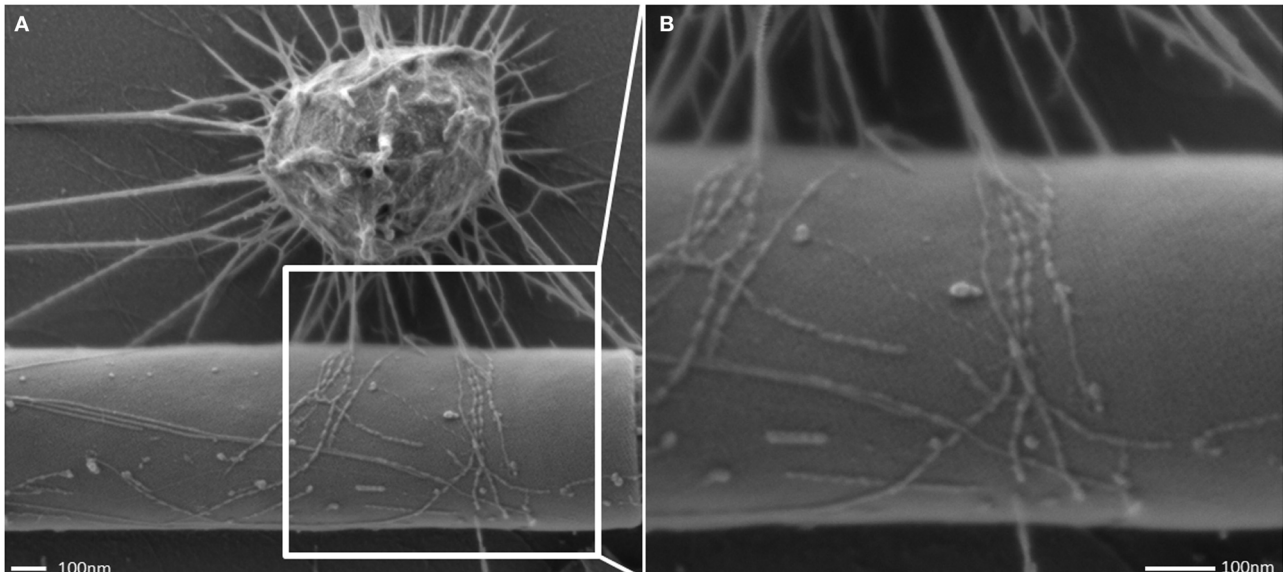


FIGURE 4 | Scanning electron micrograph of the cell appendages: "hami." Hami attaching to a filamentous bacterium (A) and close up view (B).

The archaeal cells were arranged in mostly regular distances [$\sim 1.0\text{--}2.0 \mu\text{m}$, mean: $1.26 \mu\text{m}$, standard deviation (*SD*): $0.5 \mu\text{m}$], forming a spacious, penetrable, but strongly connected cell-to-cell network (Figures 3A,B). Each cell within the biofilm was linked to 1–7 (mostly 6) cells by a dense web of cell-cell contact threads (Figures 3B and 1A). These connections occasionally appeared like tubes or bars (not shown), caused by drying artifacts due to a high amount of EPS, often covering the fine structures. This EPS layer resulted in the smooth appearance of cell surfaces and their surface appendages (Figure 3C). However, in different areas of the biofilm, where the EPS was thinner or absent, the fine-structures of cell-cell connections (the homi; Moissl et al., 2005) could be visualized in more detail (Figure 4). The EPS was shown to form a $\sim 400 \text{ nm}$ wide matrix around the cells (Figure 5). The homi protruded beyond the EPS,

still allowing the cells to contact other cells or abiotic surfaces (Figure 6). In contrast to the regularly organized pattern between the archaeal cocci, bacteria did not have a certain distance to the archaea but were embedded in an irregular manner - they were either directly attached to an archaeal cell, located between several archaeal cells, or not attached to other cells at all (Figure 1), leading to the assumption that the interacting homi, and not the EPS, are the driving force to maintain the archaeal biofilm structure with defined cell-cell distances.

The interconnected coccoid archaea seemed to seek additional contact to bacterial cells (Figures 4, 7) via their homi. Noteworthy, some bacterial morphotypes (filament-forming rods) within the biofilm appeared to be cocooned by homi (Figure 7, Probst et al., 2014), whereas other bacteria (such as spirilla, Figure 7B) were only sparsely contacted.

THE SM1 EURYARCHAEAL CELL APPENDAGES: THE HAMI

All archaeal cells revealed the presence of hundreds of hamis that protrude from their cell surfaces (**Figures 5, 6, 8A**). All hamis analyzed (incl. TEM following negative-staining and unstained by cryo-TEM; Moissl et al., 2005) showed nano-grappling hooks at their distal ends (**Figures 5, 8B**). The hamis architecture was clearly distinguishable in hook- and prickle-regions, where three prickles were formed in regular distances by the major filament (**Figure 8B**). These prickles are shaped by local bending of the three basic proteinaceous fibers (Moissl et al., 2005). The hooks were on average 60 nm in diameter (**Figures 5, 8B**) and were found to attach to the surfaces of other cells and to the

prickle-regions or hooks of hamis belonging to neighboring cells. The length of single hamis was determined to be in the range of 0.4–3.7 μm , with an average length of 1.3 μm ($SD: 0.6 \mu\text{m}$).

THE SM1 EURYARCHAEAL CELL WALL IS COMPOSED OF AN INNER AND OUTER MEMBRANE

SM biofilm samples were subjected to thin sectioning in order to analyze their ultrastructure in more detail. The outer sheath was identified as an additional membrane (**Figure 9**) and not, as often seen within the Archaea, as an S-layer. The SM1 euryarchaeal cell wall thus is composed of an inner membrane, periplasm, and an outer membrane. The inner and outer

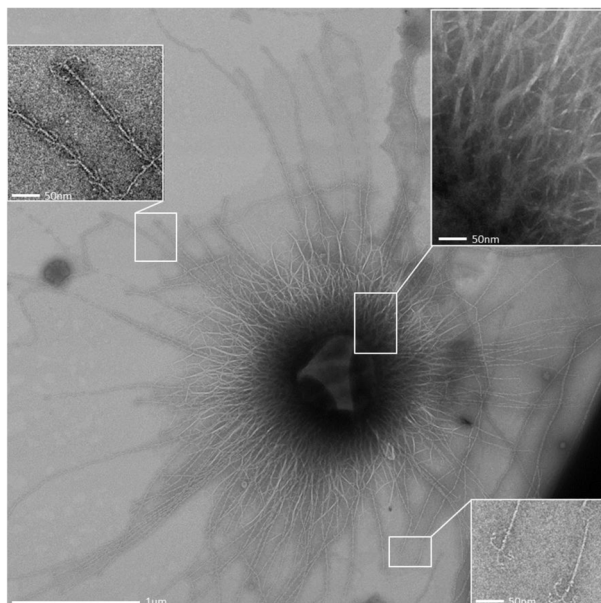


FIGURE 5 | Overview transmission electron micrograph (negative staining) of a SM1 euryarchaeal cell embedded in the EPS layer. The architecture of the hamis is shown in the close up views.

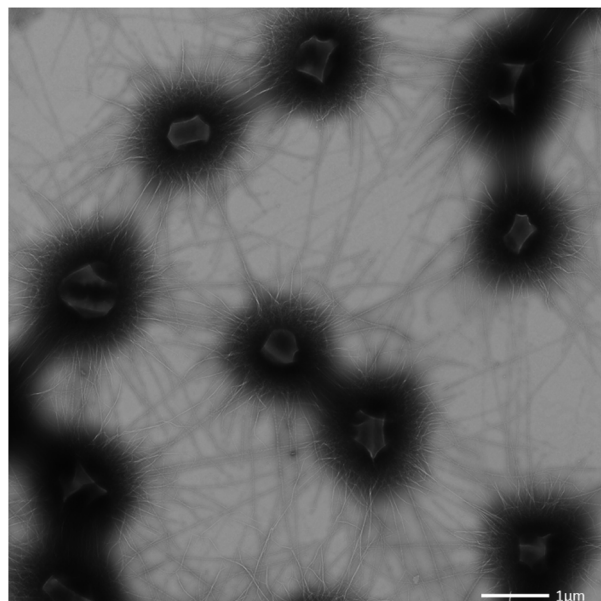


FIGURE 6 | Transmission electron micrograph (negative staining) of the SM1 euryarchaeal biofilm.

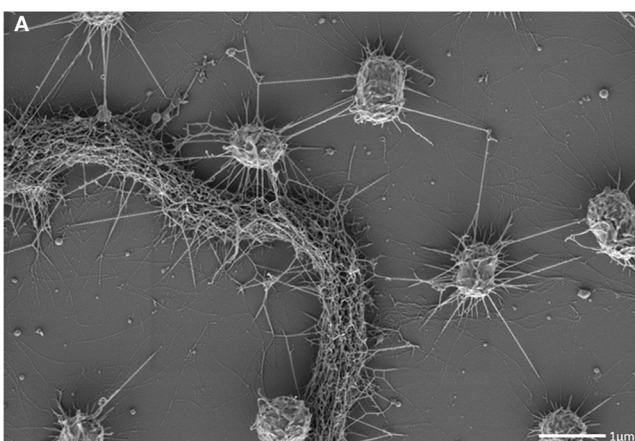


FIGURE 7 | Scanning electron micrograph. Archaeal cocci of the SM1 biofilm with numerous hamis, cocooning bacterial filaments of varying diameter (A,B).

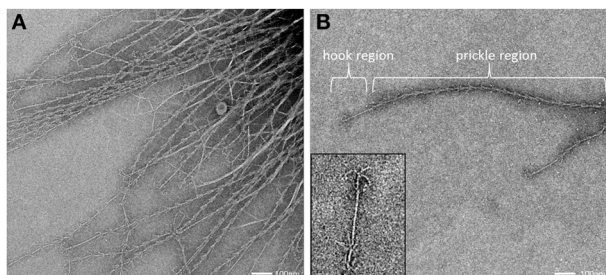


FIGURE 8 | Transmission electron micrograph (negative staining) of cell appendages (hami) protruding from a cell (**A**). The hamus architecture is distinguishable into a prickle region and a hook region (**B**), (see also Moissl et al., 2005).

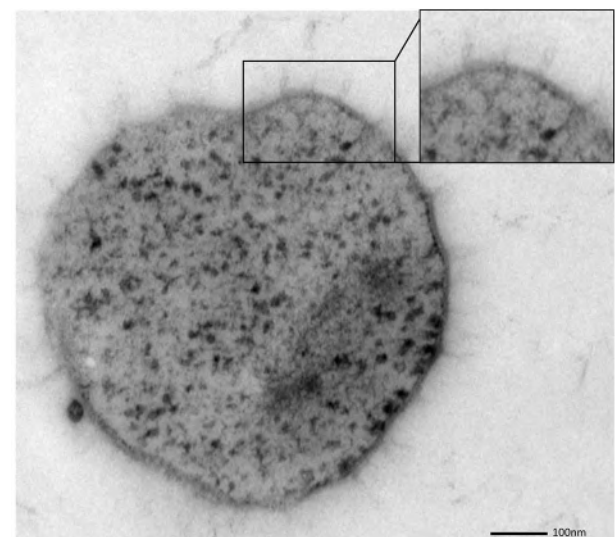


FIGURE 10 | Thin section of a single, coccoid, SM1 euryarchaeal cell. The close-up view highlights several structures, possibly hami, which might cross both membranes.

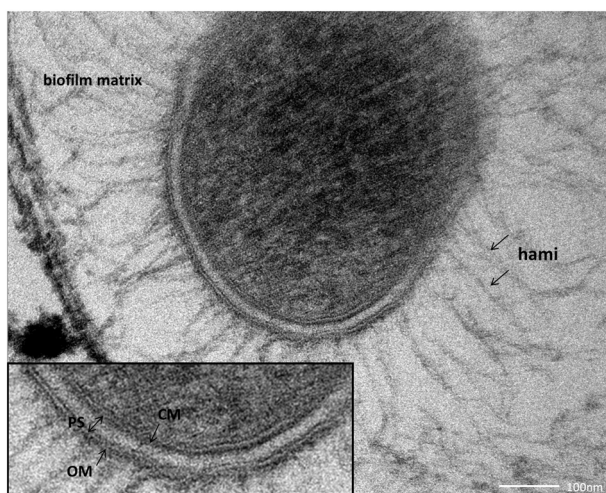


FIGURE 9 | Thin section of a single coccus, embedded in the biofilm matrix. The close-up view reveals the clearly visible cellular membrane (CM), the periplasmic space (PS) and the outer membrane (OM).

membranes revealed a typical structure (electron-dense, electron-lucent, electron-dense) and each showed an average thickness of 5–6 nm. The periplasm was determined to span 25 nm on average. The periplasm did not include any particles or other larger conglomerates or vesicles, as analyzed so far. Thin sections of cells further confirmed the presence of an EPS-layer and the hami forming a dense network around the cells (Figure 9). Although the anchorage of the hami could not be resolved so far, these filaments seemed to span both membranes (Figure 10). Within dividing cells, right at the central contraction site, belt-like structures were visible, suggesting protein aggregations involved in cell division machineries, such as FtsZ (Figure 2). The cytoplasm appeared packed with ribosomes and dark regions, which could display the chromosome or the location of storage substances (Figure 2).

DISCUSSION

The SM1 Euryarchaeon is a unique organism that shows many features not observed in other microorganisms. Its distinct position within the phylogenetic tree (Rudolph et al., 2004), the ability

for biofilm-formation, and its predominance over associated bacteria, as well as the biofilms' origin in the subsurface of sulfidic springs warranted a detailed analysis of the ultrastructure. In this communication, we focused on the biofilms found in upwelling waters of sulfidic springs in the SM. Besides the discovery of the hami (Moissl et al., 2005), this current study provides the first detailed ultrastructural analyses of the SM1 biofilm population. Most of the knowledge about the SM1 euryarchaeal biofilms, however, was so far retrieved from the MSI environment (Henneberger et al., 2006; Probst et al., 2013, 2014), including preliminary ultrastructural insights (Henneberger et al., 2006).

The archaeal biofilm fine-structure appeared to be similar to described bacterial biofilm architecture (Sutherland, 2001), where the microbial cells are typically enclosed in a matrix of EPS (Costerton et al., 1995). Generally, this matrix is composed of DNA, proteins and polysaccharides and forms a slimy layer around the cells (Wingender et al., 1999). Data on the EPS composition of the SM SM1 biofilm are not available yet. DNA, however, was not detected in the highly hydrated MSI biofilm EPS, and the protein component was attributed to the presence of hami (Henneberger et al., 2006). Noteworthy, the amount of EPS was found to be variable: some cells were completely covered by EPS, whereas others were without detectable matrix.

In the bacterial domain, biofilm-formation is highly common and can cause severe problems in, e.g., medical environments (Donlan, 2001) or industrial facilities (Mattila-Sandholm and Wirtanen, 1992). On the other hand, biofilms are highly beneficial for food production or wastewater treatment (Park et al., 1990; Nicolella et al., 2000). EPS generally mediates the surface attachment, and forms a protection-shield against harmful chemical compounds (Bridier et al., 2011). Besides other important advantages, the biofilm matrix entraps excreted enzymes in close proximity to the cell ("external digestion system"; Flemming and

Wingender, 2010). Water channels have been observed frequently in bacterial biofilms, which can support the distribution of nutrients and signal molecules, as well as the removal of inhibitory metabolic products (Costerton et al., 1994). The cells within the SM biofilms are organized in a strikingly regular pattern, in a spacious but strong and very sticky network, hinting at (1) a rapid flowing stream in its natural biotope in the subsurface, (2) the necessity of being attached to a surface, and (3) a requirement for a permanent water flow through the biofilm. Strikingly, compared to natural, non-medical bacterial biofilms, the purity and predominance of one species is extraordinary and was observed in both biofilms studied so far (Probst et al., 2014).

During the course of this analysis, numerous samples were taken from the sulfidic spring environment, transported under cool conditions and prepared for ultrastructural analyses as soon as possible. Due to the close vicinity of the two sampling sites to the Regensburg laboratory, transportation time was minimal (<1 h). However, due to the origin of the biofilms in the deeper subsurface of the sulfidic springs, which cannot be assessed at the moment, we have no information on the age or status of the biofilm pieces welled up with the spring water. In a previous study, the viability of the cells was found to be extraordinarily high (up to 90%), and cells exhibited excellent FISH (fluorescence *in situ* hybridization) signals due to the high content of ribosomes (Moissl et al., 2003), which are indications for a physiologically healthy status of the archaeal cells. Although precautions were taken in order to avoid preparation artifacts, caused by sampling or subsequent preparation for electron microscopy, alterations and damages cannot completely be avoided. This could be overcome by an immediate, on-site freezing of the samples for, e.g., cryo-electron tomographical analyses. This technique would allow for the detailed study of the cell division machinery, the hamí anchorage, and the two-membrane system itself and thus is a desirable goal for subsequent studies.

All of the cells analyzed by electron microscopy carried about 150 hamí on their surface, with an average length of 1.3 μm . This is within to the reported length-range of pili found on the surface of *Escherichia coli* (1.0–2.0 μm ; Russell and Orndorff, 1992), which usually carries 100–300 pili (Neidhardt et al., 1990). Obviously the unique hamí are well suited for the formation of such a biofilm, being responsible for cell-cell and cell-surface attachment. In addition, the hamí, and in particular the prickle region, seem to facilitate the regular distance pattern, forming spacers between the cells (Moissl et al., 2005). Noteworthy, the SM biofilm cells were found to be significantly smaller than those of the MSI biofilms (0.60 μm vs. 0.72 μm ; Probst et al., 2014). Based on SEM, the distances of SM cells to each other were 1.3 μm (on average), which is in strong contrast to confocal laser scanning microscopy data from the MSI population (4 μm distance). Currently it is unknown, whether this difference is based on strain-specific properties, or on method-specific preparation.

At this point of research, additional function(s) of the hamí, besides attachment to surfaces, remain speculative. The energetic cost of hamí synthesis appears higher than the production of simple, filamentous pili (which could also mediate surface adhesion), so that additional tasks might be envisaged. Thus, hamí could be involved in cell motility, such as mediated by some

bacterial type IV pili (Mattick, 2002; Ayers et al., 2010). Those can be retractile, and thus allow the bacterial cells to move on surfaces (“twitching motility,” Semmler et al., 1999; Maier, 2005). Although motility on a surface has not been observed for the SM1 Euryarchaeon so far, the cells might be able to control and regulate the attachment and the cell-cell distance via directed assembly and disassembly of the filaments. Another function could be electron-transfer, as observed for bacterial *Geobacter* species, which could allow cell-surface and cell-cell interactions (Reguera et al., 2005). Noteworthy, the SM1 Euryarchaeon seems to seek contact to bacteria of a specific morphotype: filament-forming, rod-shaped bacterial cells are frequently grappled by hamí, and sometimes even completely cocooned by the surface appendages (see also Probst et al., 2014). This observation might pinpoint at a specific interspecies interaction (e.g., Náther et al., 2006; Fröls et al., 2008; Ajon et al., 2011; Bellack et al., 2011; Jarrell et al., 2011), but remains speculative at this point.

The SM1 Euryarchaeon possesses two membranes, which has rarely been described for Archaea. A typical archaeal cell wall is composed of a single membrane and an attached outer proteinaceous sheath (the S-layer), whose crystalline pattern can be used as a marker for certain genera and groups of Archaea (König et al., 2007; Rachel, 2010). It has been proposed that the S-layer represents the oldest cell wall structure (Albers and Meyer, 2011), since only few archaeal groups, such as several methanogens, members of the recently proposed *Methanomassiliicoccales* species [former classified as *Thermoplasmatales*, the seventh order of methanogens (Iino et al., 2012; Borrel et al., 2013)] and *Ignicoccus* species lack this protein layer. The latter possesses two membranes, where the outer cellular membrane (OCM) harbors the H₂:sulfur oxidoreductase as well as the ATP synthase, and therefore appears to be energized (Küper et al., 2010; see Supplementary Figure S1). *Ignicoccus hospitalis* is in direct physical contact with its ectosymbiont/ectoparasite *Nanoarchaeum equitans*, which obtains several cell components from its host in order to compensate for its own biosynthetic shortcomings. The nano-sized archaeon is interacting with the host's OCM, facilitating the transport of amino acids, lipids and—although not experimentally proven yet—ATP molecules and cofactors in an yet unknown process (Huber et al., 2012). The unique cell architecture of all *Ignicoccus* species (Rachel et al., 2002; Junglas et al., 2008; Huber et al., 2012) in combination with the energized OCM demarcates *Ignicoccus* clearly from all known prokaryotic cell envelopes. To date, it is unknown whether the outer membranes of the Euryarchaeota *Methanomassiliicoccus* or SM1 are energized. This also remains unknown for the ultrasmall ARMAN cells, whose ultrastructure was interpreted as possessing an inner and OCM instead of an archaea-typical cell wall (Comolli et al., 2009; Baker et al., 2010). Except for the lipid composition, these membranes distantly resemble the dimensions and appearance of bacterial Gram-negative cell walls. It is not known whether such a cell wall architecture is rather a general feature of many archaea and was not recognized as such so far, or is an exception within this domain of life.

Strikingly, all archaea that possess a double membrane-based cell wall are involved in close interaction with other archaea, bacteria or their eukaryotic host. Bacteria which are participating

in syntrophic partnerships are often found to be equipped with unique multiple membrane complexes (Orphan, 2009), and thus a positive effect on such interactions could be envisaged for several reasons: (1) An outer membrane is a suitable surface for anchoring proteins, lipids and carbohydrates, which could serve as contact sites for interactions (Mashburn-Warren et al., 2008). In contrast to S-layers, membrane architecture can be changed and regulated internally, allowing flexible responses to environmental changes. Within the SM1 Euryarchaeon, the double membrane also anchors the ham1, which represent the major contact site of the cell toward biotic and abiotic surfaces. (2) The spanned periplasm provides additional space for metabolic products, chemosensors, signal cascades, storage compounds, and other molecules possibly involved in microbial interactions (Davidson et al., 1992; Wadham and Armitage, 2004). Additionally two compartments provide the possibility of generating gradients and allow compartmentalization even within one single prokaryotic cell.

The finding of an increasing number of archaea with double-membrane cell walls could suggest this feature to be a general characteristic of a predecessor archaeon, and questions the S-layer as the (proposed) ancient cell wall type for Archaea. It shall be noted, however, that sample preparation and clear visualization of the undisrupted cell wall is challenging and, in most cases, has to include a careful interpretation of the obtained data. The question whether the double membrane is a general feature of Archaea emphasizes the need for more detailed ultrastructural analyses of cultivated and uncultivated archaea, but also asks the community to reconsider the proposed models for archaeal cell division and formation of cell surface appendages. The latter includes the involvement of other (novel?) translocation machineries for cell surface molecules, including the transfer across two membranes and the periplasm. Overall, it becomes again clear that the archaeal domain is not humble in structure, organization, and function. The more we learn about this group of microorganisms, the more we recognize the sophisticated, complex, and clever way of archaeal living.

ACKNOWLEDGMENTS

This research was funded by the DFG (grant MO 1977 3-1; HU 703/2-1/2). Alexander J. Probst was supported by the German National Academic Foundation (Studienstiftung des Deutschen Volkes). We thank Reinhard Wirth, Robert Huber and Michael Thomm for critical discussions and support and Uwe-G. Maier for allocation of the EM facility in Marburg. Technical assistance by Silvia Dobler and Marion Debus is gratefully acknowledged.

SUPPLEMENTARY MATERIAL

The Supplementary Material for this article can be found online at: <http://www.frontiersin.org/journal/10.3389/fmicb.2014.00397/abstract>

REFERENCES

- Ajon, M., Fröls, S., van Wolferen, M., Stoecker, K., Teichmann, D., Driessens, A. J. M., et al. (2011). UV-inducible DNA exchange in hyperthermophilic archaea mediated by type IV pili. *Mol. Microbiol.* 82, 807–817. doi: 10.1111/j.1365-2958.2011.07861.x
- Albers, S.-V., and Meyer, B. H. (2011). The archaeal cell envelope. *Nat. Rev. Microbiol.* 9, 414–426. doi: 10.1038/nrmicro2576
- Amann, R. I., Ludwig, W., and Schleifer, K.-H. (1995). Phylogenetic identification and *in situ* detection of individual microbial cells without cultivation. *Microbiol. Rev.* 59, 143–169.
- Ayers, M., Howell, P. L., and Burrows, L. L. (2010). Architecture of the type II secretion and type IV pilus machineries. *Future Microbiol.* 5, 1203–1218. doi: 10.2217/fmb.10.76
- Baker, B. J., Comolli, L. R., Dick, G. J., Hauser, L. J., Hyatt, D., Dill, B. D., et al. (2010). Enigmatic, ultrasmall, uncultivated Archaea. *Proc. Natl. Acad. Sci. U.S.A.* 107, 8806–8811. doi: 10.1073/pnas.0914470107
- Bellack, A., Huber, H., Rachel, R., Wanner, G., and Wirth, R. (2011). Methanocaldococcus villosum sp. nov., a heavily flagellated archaeon that adheres to surfaces and forms cell-cell contacts. *Int. J. Syst. Evol. Microbiol.* 61, 1239–1245. doi: 10.1099/ijss.0.023663-0
- Borrel, G., O'Toole, P. W., Harris, H. M. B., Peyret, P., Brugère, J.-F., and Gribaldo, S. (2013). Phylogenomic data support a seventh order of methylotrophic methanogens and provide insights into the evolution of methanogenesis. *Genome Biol. Evol.* 5, 1769–1780. doi: 10.1093/gbe/evt128
- Bridier, A., Briandet, R., Thomas, V., and Dubois-Brissonnet, F. (2011). Resistance of bacterial biofilms to disinfectants: a review. *Biofouling* 27, 1017–1032. doi: 10.1080/08927014.2011.626899
- Briggs, B. R., Pohlman, J. W., Torres, M., Riedel, M., Brodie, E. L., and Colwell, F. S. (2011). Macroscopic biofilms in fracture-dominated sediment that anaerobically oxidize methane. *Appl. Environ. Microbiol.* 77, 6780–6787. doi: 10.1128/AEM.00288-11
- Cavicchioli, R., DeMaere, M. Z., and Thomas, T. (2007). Metagenomic studies reveal the critical and wide-ranging ecological importance of uncultivated archaea: the role of ammonia oxidizers. *Bioessays* 29, 11–14. doi: 10.1002/bies.20519
- Comolli, L. R., Baker, B. J., Downing, K. H., Siegerist, C. E., and Banfield, J. F. (2009). Three-dimensional analysis of the structure and ecology of a novel, ultra-small archaeon. *ISME J.* 3, 159–167. doi: 10.1038/ismej.2008.99
- Costerton, J. W., Lewandowski, Z., Caldwell, D. E., Korber, D. R., and Lappin-Scott, H. M. (1995). Microbial biofilms. *Annu. Rev. Microbiol.* 49, 711–745. doi: 10.1146/annurev.mi.49.100195.003431
- Costerton, J. W., Lewandowski, Z., DeBeer, D., Caldwell, D., Korber, D., and James, G. (1994). Biofilms, the customized microniches. *J. Bacteriol.* 176, 2137.
- Couradeau, E., Benzerara, K., Moreira, D., Gerard, E., Kaźmierczak, J., Tavera, R., et al. (2011). Prokaryotic and eukaryotic community structure in field and cultured microbialites from the alkaline Lake Alchichica (Mexico). *PLoS ONE* 6:e28767. doi: 10.1371/journal.pone.0028767
- Davidson, A. L., Shuman, H. A., and Nikaido, H. (1992). Mechanism of maltose transport in *Escherichia coli*: transmembrane signaling by periplasmic binding proteins. *Proc. Natl. Acad. Sci. U.S.A.* 89, 2360–2364. doi: 10.1073/pnas.89.6.2360
- Donlan, R. M. (2001). Biofilm formation: a clinically relevant microbiological process. *Clin. Infect. Dis.* 33, 1387–1392. doi: 10.1086/322972
- Elvert, M., Suess, E., and Whiticar, M. J. (1999). Anaerobic methane oxidation associated with marine gas hydrates: superlight C-isotopes from saturated and unsaturated C20 and C25 irregular isoprenoids. *Naturwissenschaften* 86, 295–300. doi: 10.1007/s001140050619
- Flemming, H.-C., and Wingender, J. (2010). The biofilm matrix. *Nat. Rev. Microbiol.* 8, 623–633. doi: 10.1038/nrmicro2415
- Fröls, S., Ajon, M., Wagner, M., Teichmann, D., Zolghadr, B., Folea, M., et al. (2008). UV-inducible cellular aggregation of the hyperthermophilic archaeon Sulfolobus solfataricus is mediated by pili formation. *Mol. Microbiol.* 70, 938–952. doi: 10.1111/j.1365-2958.2008.06459.x
- Henneberger, R., Moissl, C., Amann, T., Rudolph, C., and Huber, R. (2006). New insights into the lifestyle of the cold-loving SM1 euryarchaeon: natural growth as monospecies biofilm in the subsurface. *Appl. Environ. Microbiol.* 72, 192–199. doi: 10.1128/AEM.72.1.192-199.2006
- Hinrichs, K.-U., Hayes, J. M., Sylva, S. P., Brewer, P. G., and DeLong, E. F. (1999). Methane-consuming archaeabacteria in marine sediments. *Nature* 398, 802–805. doi: 10.1038/19751
- Hoehler, T. M., Alperin, M. J., Albert, D. B., and Martens, C. S. (1994). Field and laboratory studies of methane oxidation in an anoxic marine sediment: evidence for a methanogen–sulfate reducer consortium. *Global Biogeochem. Cycles* 8, 451–463. doi: 10.1029/94GB01800

- Huber, H., Hohn, M. J., Rachel, R., Fuchs, T., Wimmer, V. C., and Stetter, K. O. (2002). A new phylum of Archaea represented by a nanosized hyperthermophilic symbiont. *Nature* 417, 63–67. doi: 10.1038/417063a
- Huber, H., Küper, U., Daxer, S., and Rachel, R. (2012). The unusual cell biology of the hyperthermophilic Crenarchaeon *Ignicoccus hospitalis*. *Antonie Van Leeuwenhoek* 102, 203–219. doi: 10.1007/s10482-012-9748-5
- Iino, T., Tamaki, H., Tamazawa, S., Ueno, Y., Ohkuma, M., Suzuki, K.-I., et al. (2012). *Candidatus Methanogranum caenicola*: a novel methanogen from the anaerobic digested sludge, and proposal of *Methanomassiliicoccaceae* fam. nov. and *Methanomassiliicoccales* ord. nov., for a methanogenic lineage of the class Thermoplasmata. *Microbes Environ.* 28, 244–250. doi: 10.1264/jmee.ME12189
- Ionescu, D., Siebert, C., Polerecky, L., Munwes, Y. Y., Lott, C., Häusler, S., et al. (2012). Microbial and chemical characterization of underwater fresh water springs in the Dead Sea. *PLoS ONE* 7:e38319. doi: 10.1371/journal.pone.0038319
- Jahn, U., Gallenberger, M., Junglas, B., Eisenreich, W., Stetter, K. O., Rachel, R., et al. (2008). Nanoarchaeum equitans and *Ignicoccus hospitalis*: new insights into a unique, intimate association of two archaea. *J. Bacteriol.* 190, 1743–1750. doi: 10.1128/JB.01731-07
- Jahn, U., Summons, R., Sturt, H., Grosjean, E., and Huber, H. (2004). Composition of the lipids of *Nanoarchaeum equitans* and their origin from its host *Ignicoccus* sp. strain KIN4/I. *Arch. Microbiol.* 182, 404–413. doi: 10.1007/s00203-004-0725-x
- Jarrell, K. F., Stark, M., Nair, D. B., and Chong, J. P. J. (2011). Flagella and pili are both necessary for efficient attachment of *Methanococcus maripaludis* to surfaces. *FEMS Microbiol. Lett.* 319, 44–50. doi: 10.1111/j.1574-6968.2011.02264.x
- Junglas, B., Briegel, A., Burghardt, T., Walther, P., Wirth, R., Huber, H., et al. (2008). *Ignicoccus hospitalis* and *Nanoarchaeum equitans*: ultrastructure, cell-cell interaction, and 3D reconstruction from serial sections of freeze-substituted cells and by electron cryotomography. *Arch. Microbiol.* 190, 395–408. doi: 10.1007/s00203-008-0402-6
- Koch, M., Rudolph, C., Moissl, C., and Huber, R. (2006). A cold-loving crenarchaeon is a substantial part of a novel microbial community in cold sulfidic marsh water. *FEMS Microbiol. Ecol.* 57, 55–66. doi: 10.1111/j.1574-6941.2006.00088.x
- König, H., Rachel, R., and Claus, H. (2007). “Proteinaceous surface layers of archaea: ultrastructure and biochemistry,” in *Archaea: Molecular and Cellular Biology*, ed R. Cavicchioli (Washington, DC: ASM Press), 315–340.
- Küper, U., Meyer, C., Müller, V., Rachel, R., and Huber, H. (2010). Energized outer membrane and spatial separation of metabolic processes in the hyperthermophilic Archaeon *Ignicoccus hospitalis*. *Proc. Natl. Acad. Sci. U.S.A.* 107, 3152–3156. doi: 10.1073/pnas.0911711107
- Maier, B. (2005). Using laser tweezers to measure twitching motility in *Neisseria*. *Curr. Opin. Microbiol.* 8, 344–349. doi: 10.1016/j.mib.2005.04.002
- Margulis, L. (1993). *Symbiosis in Cell Evolution: Microbial Communities in The Archean and Proterozoic Eons*. 2nd Edn. New York, NY: W H Freeman.
- Mashburn-Warren, L., Howe, J., Garidel, P., Richter, W., Steiniger, F., Roessle, M., et al. (2008). Interaction of quorum signals with outer membrane lipids: insights into prokaryotic membrane vesicle formation. *Mol. Microbiol.* 69, 491–502. doi: 10.1111/j.1365-2958.2008.06302.x
- Mattick, J. S. (2002). Type IV pili and twitching motility. *Annu. Rev. Microbiol.* 56, 289–314. doi: 10.1146/annurev.micro.56.012302.160938
- Mattila-Sandholm, T., and Wirtanen, G. (1992). Biofilm formation in the industry: a review. *Food Rev. Int.* 8, 573–603. doi: 10.1080/87559129209540953
- Moissl, C., Rachel, R., Briegel, A., Engelhardt, H., and Huber, R. (2005). The unique structure of archaeal hami, highly complex cell appendages with nano-grappling hooks. *Mol. Microbiol.* 56, 361–370. doi: 10.1111/j.1365-2958.2005.04294.x
- Moissl, C., Rudolph, C., and Huber, R. (2002). Natural communities of novel archaea and bacteria with a string-of-pearls-like morphology: molecular analysis of the bacterial partners. *Appl. Environ. Microbiol.* 68, 933–937. doi: 10.1128/AEM.68.2.933-937.2002
- Moissl, C., Rudolph, C., Rachel, R., Koch, M., and Huber, R. (2003). *In situ* growth of the novel SM1 euryarchaeon from a string-of-pearls-like microbial community in its cold biotope, its physical separation and insights into its structure and physiology. *Arch. Microbiol.* 180, 211–217. doi: 10.1007/s00203-003-0580-1
- Moissl-Eichinger, C., and Huber, H. (2011). Archaeal symbionts and parasites. *Curr. Opin. Microbiol.* 14, 364–370. doi: 10.1016/j.mib.2011.04.016
- Morris, B. E. L., Henneberger, R., Huber, H., and Moissl-Eichinger, C. (2013). Microbial syntrophy: interaction for the common good. *FEMS Microbiol. Rev.* 37, 384–406. doi: 10.1111/1574-6976.12019
- Müller, J., and Overmann, J. (2011). Close interspecies interactions between prokaryotes from sulfurous environments. *Front. Microbiol.* 2:146. doi: 10.3389/fmicb.2011.00146
- Näther, D. J., Rachel, R., Wanner, G., and Wirth, R. (2006). Flagella of *Pyrococcus furiosus*: multifunctional organelles, made for swimming, adhesion to various surfaces, and cell-cell contacts. *J. Bacteriol.* 188, 6915–6923. doi: 10.1128/JB.00527-06
- Neidhardt, F. C., Ingraham, J. L., and Schaechter, M. (1990). *Physiology of the Bacterial Cell*. Sunderland: Sinauer Associates Inc.
- Nicolella, C., van Loosdrecht, M. C., and Heijnen, J. J. (2000). Wastewater treatment with particulate biofilm reactors. *J. Biotechnol.* 80, 1–33. doi: 10.1016/S0168-1656(00)00229-7
- Orphan, V. J. (2009). Methods for unveiling cryptic microbial partnerships in nature. *Curr. Opin. Microbiol.* 12, 231–237. doi: 10.1016/j.mib.2009.04.003
- Park, Y. S., Ohtake, H., and Toda, K. (1990). A kinetic study of acetic acid production by liquid-surface cultures of *Acetobacter aceti*. *Appl. Microbiol. Biotechnol.* 33, 259–263. doi: 10.1007/BF00164518
- Podar, M., Anderson, I., Makarova, K. S., Elkins, J. G., Ivanova, N., Wall, M. A., et al. (2008). A genomic analysis of the archaeal system *Ignicoccus hospitalis-Nanoarchaeum equitans*. *Genome Biol.* 9:R158. doi: 10.1186/gb-2008-9-11-r158
- Probst, A. J., Birarda, G., Holman, H.-Y. N., DeSantis, T. Z., Wanner, G., Andersen, G. L., et al. (2014). Coupling genetic and chemical microbiome profiling reveals heterogeneity of archaeome and bacteriome in subsurface biofilms that are dominated by the same archaeal Species. *PLoS ONE* 9:e99801. doi: 10.1371/journal.pone.0099801
- Probst, A. J., Holman, H.-Y. N., DeSantis, T. Z., Andersen, G. L., Birarda, G., Bechtel, H. A., et al. (2013). Tackling the minority: sulfate-reducing bacteria in an archaea-dominated subsurface biofilm. *ISME J.* 7, 635–651. doi: 10.1038/ismej.2012.133
- Rachel, R. (2010). “Cell envelopes of crenarchaeota and nanoarchaeota,” in *Prokaryotic Cell Wall Compounds*, eds H. König, A. Varma, and H. Claus (Berlin; Heidelberg: Springer), 271–291. doi: 10.1007/978-3-642-05062-6_9
- Rachel, R., Wyschkony, I., Riehl, S., and Huber, H. (2002). The ultrastructure of *Ignicoccus*: evidence for a novel outer membrane and for intracellular vesicle budding in an archaeon. *Archaea* 1, 9–18. doi: 10.1155/2002/307480
- Reguera, G., McCarthy, K. D., Mehta, T., Nicoll, J. S., Tuominen, M. T., and Lovley, D. R. (2005). Extracellular electron transfer via microbial nanowires. *Nature* 435, 1098–1101. doi: 10.1038/nature03661
- Rinke, C., Schwientek, P., Sczyrba, A., Ivanova, N. N., Anderson, I. J., Cheng, J.-F., et al. (2013). Insights into the phylogeny and coding potential of microbial dark matter. *Nature* 499, 431–437. doi: 10.1038/nature12352
- Rohwer, F., Seguritan, V., Azam, F., and Knowlton, N. (2002). Diversity and distribution of coral-associated bacteria. *Mar. Ecol. Prog. Ser.* 243, 1–10. doi: 10.3354/meps243001
- Rudolph, C., Moissl, C., Henneberger, R., and Huber, R. (2004). Ecology and microbial structures of archaeal/bacterial strings-of-pearls communities and archaeal relatives thriving in cold sulfidic springs. *FEMS Microbiol. Ecol.* 50, 1–11. doi: 10.1016/j.femsec.2004.05.006
- Rudolph, C., Wanner, G., and Huber, R. (2001). Natural communities of novel archaea and bacteria growing in cold sulfurous springs with a string-of-pearls-like morphology. *Appl. Environ. Microbiol.* 67, 2336–2344. doi: 10.1128/AEM.67.5.2336-2344.2001
- Russell, P. W., and Orndorff, P. E. (1992). Lesions in two *Escherichia coli* type 1 pilus genes alter pilus number and length without affecting receptor binding. *J. Bacteriol.* 174, 5923–5935.
- Schleifer, K.-H. (2004). Microbial diversity: facts, problems and prospects. *Syst. Appl. Microbiol.* 27, 3–9. doi: 10.1078/0723-2020-00245
- Schopf, S., Wanner, G., Rachel, R., and Wirth, R. (2008). An archaeal bi-species biofilm formed by *Pyrococcus furiosus* and *Methanopyrus kandleri*. *Arch. Microbiol.* 190, 371–377. doi: 10.1007/s00203-008-0371-9
- Schrenk, M. O., Kelley, D. S., Bolton, S. A., and Baross, J. A. (2004). Low archaeal diversity linked to subseafloor geochemical processes at the Lost City Hydrothermal Field, Mid-Atlantic Ridge. *Environ. Microbiol.* 6, 1086–1095. doi: 10.1111/j.1462-2920.2004.00650.x

- Schrenk, M. O., Kelley, D. S., Delaney, J. R., and Baross, J. A. (2003). Incidence and diversity of microorganisms within the walls of an active deep-sea sulfide chimney. *Appl. Environ. Microbiol.*, 69, 3580–3592. doi: 10.1128/AEM.69.6.3580-3592.2003
- Semmler, A. B. T., Whitchurch, C. B., and Mattick, J. S. (1999). A re-examination of twitching motility in *Pseudomonas aeruginosa*. *Microbiology*, 145, 2863–2873.
- Sutherland, I. W. (2001). The biofilm matrix—an immobilized but dynamic microbial environment. *Trends Microbiol.* 9, 222–227. doi: 10.1016/S0966-842X(01)02012-1
- Thiel, V., Peckmann, J., Seifert, R., Wehrung, P., Reitner, J., and Michaelis, W. (1999). Highly isotopically depleted isoprenoids: molecular markers for ancient methane venting. *Geochim. Cosmochim. Acta* 63, 3959–3966. doi: 10.1016/S0016-7037(99)00177-5
- Wadhams, G. H., and Armitage, J. P. (2004). Making sense of it all: bacterial chemotaxis. *Nat. Rev. Mol. Cell Biol.* 5, 1024–1037. doi: 10.1038/nrm1524
- Wanner, G., Vogl, K., and Overmann, J. (2008). Ultrastructural characterization of the prokaryotic symbiosis in “Chlorochromatium aggregatum.” *J. Bacteriol.* 190, 3721–3730. doi: 10.1128/JB.00027-08
- Webster, N. S., and Negri, A. P. (2006). Site-specific variation in Antarctic marine biofilms established on artificial surfaces. *Environ. Microbiol.* 8, 1177–1190. doi: 10.1111/j.1462-2920.2006.01007.x
- Weidler, G. W., Gerbl, F. W., and Stan-Lotter, H. (2008). Crenarchaeota and their role in the nitrogen cycle in a subsurface radioactive thermal spring in the Austrian Central Alps. *Appl. Environ. Microbiol.* 74, 5934–5942. doi: 10.1128/AEM.02602-07
- Wingender, J., Neu, T. R., and Flemming, H.-C. (1999). “What are bacterial extracellular polymeric substances?,” in *Microbial Extracellular Polymeric Substances*, eds J. Wingender, T. Neu, and H.-C. Flemming (Berlin; Heidelberg: Springer), 1–19.
- Zhang, W., Li, F., and Nie, L. (2010). Integrating multiple omics analysis for microbial biology: application and methodologies. *Microbiology* 156, 287–301. doi: 10.1099/mic.0.034793-0
- Zilber-Rosenberg, I., and Rosenberg, E. (2008). Role of microorganisms in the evolution of animals and plants: the hologenome theory of evolution. *FEMS Microbiol. Rev.* 32, 723–735. doi: 10.1111/j.1574-6976.2008.00123.x

Conflict of Interest Statement: The authors declare that the research was conducted in the absence of any commercial or financial relationships that could be construed as a potential conflict of interest.

Received: 02 June 2014; accepted: 14 July 2014; published online: 05 August 2014.

Citation: Perras AK, Wanner G, Klingl A, Mora M, Auerbach AK, Heinz V, Probst AJ, Huber H, Rachel R, Meck S and Moissl-Eichinger C (2014) Grappling archaea: ultrastructural analyses of an uncultivated, cold-loving archaeon, and its biofilm. *Front. Microbiol.* 5:397. doi: 10.3389/fmicb.2014.00397

This article was submitted to Terrestrial Microbiology, a section of the journal *Frontiers in Microbiology*.

Copyright © 2014 Perras, Wanner, Klingl, Mora, Auerbach, Heinz, Probst, Huber, Rachel, Meck and Moissl-Eichinger. This is an open-access article distributed under the terms of the Creative Commons Attribution License (CC BY). The use, distribution or reproduction in other forums is permitted, provided the original author(s) or licensor are credited and that the original publication in this journal is cited, in accordance with accepted academic practice. No use, distribution or reproduction is permitted which does not comply with these terms.



Identification of a cyclic-di-GMP-modulating response regulator that impacts biofilm formation in a model sulfate reducing bacterium

Lara Rajeev^{1†}, Eric G. Luning^{1†}, Sara Altenburg², Grant M. Zane³, Edward E. K. Baidoo¹, Michela Catena¹, Jay D. Keasling^{1,4}, Judy D. Wall³, Matthew W. Fields^{2,5} and Aindrila Mukhopadhyay^{1*}

¹ Physical Biosciences Division, Lawrence Berkeley National Laboratory, Berkeley, CA, USA

² Center for Biofilm Engineering, Montana State University, Bozeman, MT, USA

³ Department of Biochemistry, University of Missouri, Columbia, MO, USA

⁴ Department of Chemical and Biomolecular Engineering, Department of Bioengineering, University of California, Berkeley, CA, USA

⁵ Department of Microbiology and Immunology, Montana State University, Bozeman, MT, USA

Edited by:

Luis Raul Comolli, Lawrence Berkeley National Laboratory, USA

Reviewed by:

Xizhu Dong, Chinese Academy of Sciences, China

Michael Y. Galperin, National Institutes of Health, USA

*Correspondence:

Aindrila Mukhopadhyay, Lawrence Berkeley Lab, 1 Cyclotron Road MS-978-4121, Berkeley, CA 94720, USA

e-mail: amukhopadhyay@lbl.gov

[†]These authors have contributed equally to this work.

We surveyed the eight putative cyclic-di-GMP-modulating response regulators (RRs) in *Desulfovibrio vulgaris* Hildenborough that are predicted to function via two-component signaling. Using purified proteins, we examined cyclic-di-GMP (c-di-GMP) production or turnover *in vitro* of all eight proteins. The two RRs containing only GGDEF domains (DVU2067, DVU0636) demonstrated c-di-GMP production activity *in vitro*. Of the remaining proteins, three RRs with HD-GYP domains (DVU0722, DVUA0086, and DVU2933) were confirmed to be Mn²⁺-dependent phosphodiesterases (PDEs) *in vitro* and converted c-di-GMP to its linear form, pGpG. DVU0408, containing both c-di-GMP production (GGDEF) and degradation domains (EAL), showed c-di-GMP turnover activity *in vitro* also with production of pGpG. No c-di-GMP related activity could be assigned to the RR DVU0330, containing a metal-dependent phosphohydrolase HD-OD domain, or to the HD-GYP domain RR, DVU1181. Studies included examining the impact of overexpressed cyclic-di-GMP-modulating RRs in the heterologous host *E. coli* and led to the identification of one RR, DVU0636, with increased cellulose production. Evaluation of a transposon mutant in DVU0636 indicated that the strain was impaired in biofilm formation and demonstrated an altered carbohydrate:protein ratio relative to the *D. vulgaris* wild type biofilms. However, grown in liquid lactate/sulfate medium, the DVU0636 transposon mutant showed no growth impairment relative to the wild-type strain. Among the eight candidates, only the transposon disruption mutant in the DVU2067 RR presented a growth defect in liquid culture. Our results indicate that, of the two diguanylate cyclases (DGCS) that function as part of two-component signaling, DVU0636 plays an important role in biofilm formation while the function of DVU2067 has pertinence in planktonic growth.

Keywords: cyclic-di-GMP, biofilm, *Desulfovibrio*, HD-GYP, GGDEF, GGDEF-EAL, response regulator, two-component system

INTRODUCTION

Many inter- and intra- species interactions are mediated by small molecule signals. Of these, cyclic-di-GMP (c-di-GMP) has come to be recognized as a ubiquitous second messenger in bacteria. Discovered in 1987 in *Gluconacetobacter xylinus*, the first established function of c-di-GMP was in the allosteric activation of a cellulose synthase for the biosynthesis of extracellular cellulose (Ross et al., 1987). C-di-GMP is now known to play a role in a large number of phenotypes ranging from attachment, motility, biofilm formation, quorum sensing to numerous other developmental, pathogenic, and virulence responses (for a recent review see Romling et al., 2013). In general, accumulation of c-di-GMP results in greater sessility, attachment and improved biofilm formation, while reduction of the same results in greater motility and

other associated growth characteristics (Simm et al., 2004). Not surprisingly, enzymes that modulate c-di-GMP levels have been annotated in most bacteria (Galperin et al., 2010) and have been well reviewed (Hengge, 2009; Schirmer and Jenal, 2009). Levels of c-di-GMP in the cell are modulated through the function of GGDEF motif-containing proteins that act as diguanylate cyclases (DGCS) with GTP as substrate (Paul et al., 2004; Ryjenkov et al., 2005), and EAL (Ross et al., 1987; Simm et al., 2004; Schmidt et al., 2005) or HD-GYP motif-containing proteins (Ryan et al., 2006; Stelitano et al., 2013) that act as phosphodiesterases (PDEs) that degrade c-di-GMP to pGpG or GMP (**Figure 1A**).

C-di-GMP modulating domains are most commonly found in combination with other signaling domains, such as PAS or GAF, or as output domains in the receiver portion of two-component

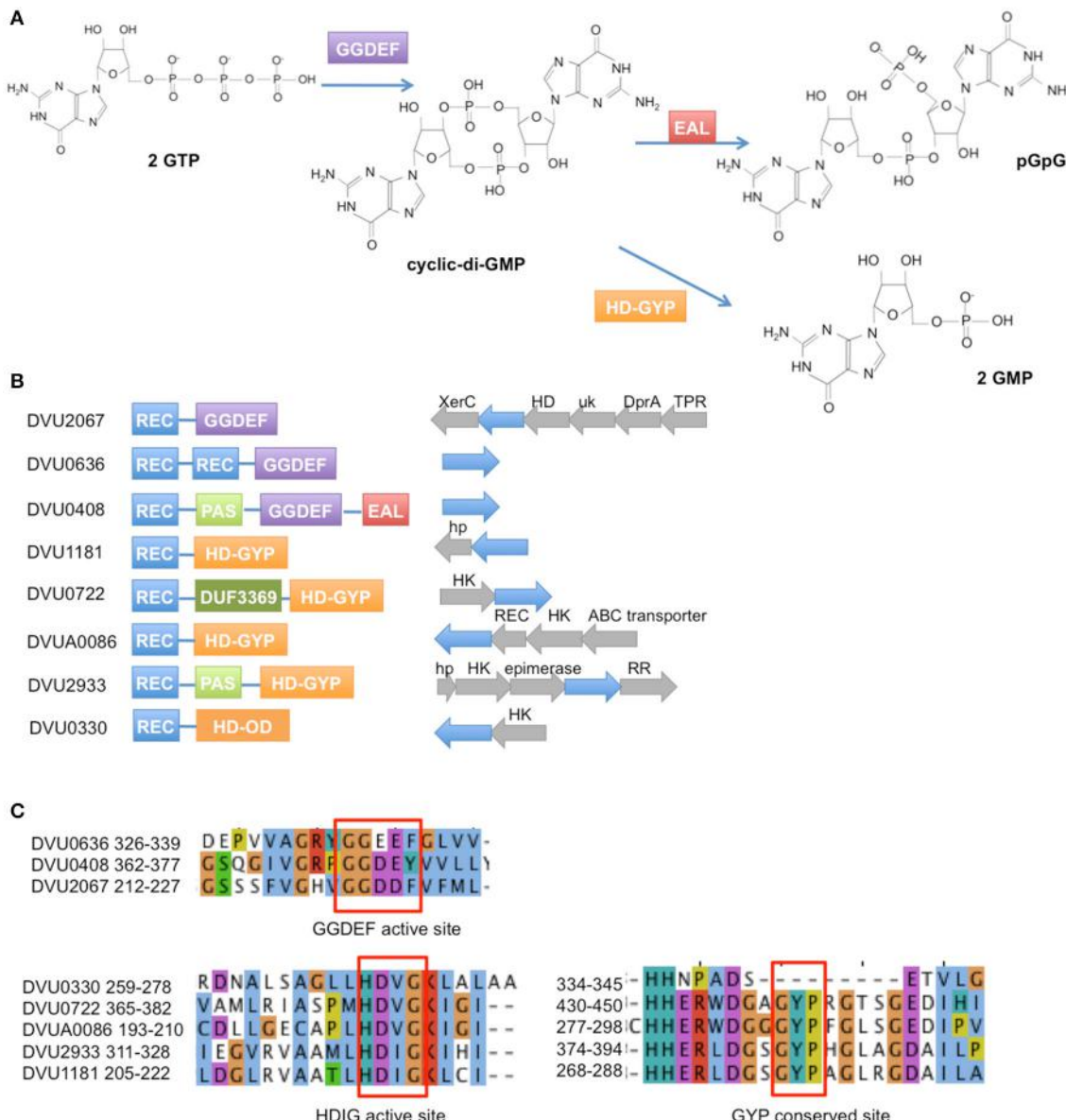


FIGURE 1 | Response regulators in *D. vulgaris* Hildenborough with GGDEF, EAL, and HD domains. (A) The GGDEF domain synthesizes c-di-GMP from GTP, while the EAL and HD-GYP domains hydrolyze c-di-GMP to pGpG and GMP, respectively. **(B)** Domain structures are shown for the 2 GGDEF domain RRs, 1 GGDEF-EAL RR, 4 HD-GYP RRs, and 1 HDOD RR (REC = receiver domain). To the right of the domain structures are shown the operon arrangements of each RR with the RR gene shown in blue.

(Abbreviations: XerC, integrase domain; HD, HD domain; uk, unknown domain; DprA, DNA processing protein A; TPR, Tetratricopeptide domain protein; hp, hypothetical protein; HK, histidine kinase; REC, receiver domain). **(C)** Amino acid sequence alignment of the conserved active site residues for the GGDEF domain RRs (top) and the HD domain RRs (bottom). Note that DVU0408 has a Y instead of the conserved F in its GGDEF domain. Also DVU0330 is an HDOD domain that lacks the GYP motif.

system response regulators (RRs) (Romling et al., 2013). Signaling systems that use second messenger signaling are critical to survival in different environments and provide a competitive advantage to biological systems under different environmental constraints. However, few such sets of enzymes have been functionally explored (Solano et al., 2009; Wang et al., 2010; Tan et al., 2014).

Here we examine all presumptive c-di-GMP-modulating RRs that are part of two-component signaling in the sulfate-reducing

bacterium *Desulfovibrio vulgaris* Hildenborough. Sequenced in 2003 (Heidelberg et al., 2004), this bacterium serves as a model organism to study sulfate reduction and carbon oxidation as well as metal reduction (Beyenal et al., 2004), metal corrosion (Lee et al., 1995), biofilm formation (Clark et al., 2012), and bioimmobilization in superfund sites (Faybushenko et al., 2008). *D. vulgaris* Hildenborough has been extensively studied for a variety of stress responses (Zhou et al., 2011), syntrophic interactions (Hillesland and Stahl, 2010), regulatory motifs (Rodionov et al.,

2004; Kazakov et al., 2013b), and signal transduction (Rajeev et al., 2011). The genome of *D. vulgaris* Hildenborough has a high “microbial sensory IQ” (Galperin et al., 2010) encoding a total of 41 genes containing GGDEF/EAL/HD-GYP domains. Of these, eight are linked to two-component system response regulator receiver domains (**Figure 1B**) and none have been functionally characterized. We used purified proteins to evaluate the predicted function of all eight candidates. We also conducted *in vivo* assays to test certain phenotypes that are known to be associated with c-di-GMP modulation. We identified DVU0636 to be involved in biofilm formation in *D. vulgaris* Hildenborough.

MATERIALS AND METHODS

CLONING OF RESPONSE REGULATOR GENES

Full-length genes for the eight RRs were cloned by Gateway technology into the destination vector pETDEST42 (Life Technologies, Grand Island, NY, USA) as previously described (Rajeev et al., 2011), such that the protein is expressed with a C-terminal V5 epitope and 6X-His tag. The HD-GYP domains of DVUA0086 (164–363 aa) and DVU2933 (282–458 aa) were cloned into pSKB3 (Kan^R) with an N-terminal cleavable 6X-His tag. The HD-GYP domains of DVU1181 (176–356 aa), DVU0722 (336–518 aa) and DVU0330 (230–412) were cloned into pSKB3 with a cleavable N-terminal 8x-His-tag, Strep Tag II, and a maltose binding protein tag. The genes were amplified from *D. vulgaris* Hildenborough genomic DNA with iProof HiFidelity polymerase (BioRad, Hercules, CA, USA) and primers that were designed to have 40 bp overlap between the insert and the vector backbone. The vector was similarly amplified and treated with DpnI, followed by agarose gel extraction and purification. The vector and insert were mixed in a 1:1 molar ratio and assembled with a modified Gibson reagent (Gibson et al., 2009) that lacked the Taq ligase. The Gibson reaction was used to transform *E. coli* BL21 (DE3) electrocompetent cells and transformants were selected on Yeast Tryptone agar plates with kanamycin (50 µg/ml). The presence of the insert was verified by sequencing. Note on DVU2067 cloning: Sequencing of the cloned DVU2067 revealed an extra 39 bp sequence at the C-terminus that appeared to be a repetition of the last 19–20 bp of the gene.

PROTEIN OVEREXPRESSION

Expression constructs were grown in 10 ml Terrific Broth (TB) (Tartof and Hobbs, 1987) containing kanamycin (50 µg/ml) at 37°C until an OD₆₀₀ of 1.5. Protein expression was induced with 0.25 mM IPTG, and cells were grown at 22°C overnight. The cells were harvested, resuspended in 1× PBS buffer and lysed by sonication. The lysates were centrifuged at 15,000 × g for 30 min at 4°C. The clarified lysate was examined for protein overexpression by SDS-PAGE followed by Western blotting with mouse anti-His monoclonal antibodies.

PROTEIN PURIFICATION

The expression strain was grown in 1 L of TB with kanamycin (50 µg/ml) at 37°C until OD₆₀₀ of 1.5. IPTG (0.25 mM) was added and cells were grown at 22°C overnight. Cells were harvested and lysed by sonication in 150 ml of cold Buffer A (20 mM sodium phosphate, 0.5 M NaCl, 40 mM imidazole, pH 7.4) with

lysozyme (1 mg/ml) and 1× benzonase nuclease (New England Biolabs, Ipswich, MA, USA). Lysate was clarified by centrifugation at 15,000 × g for 30 min at 4°C and filtered on a 0.45-µm pore-sized syringe filter. The lysate was loaded onto a 5 ml HisTrapFF column (GE Life Sciences, Piscataway, NJ) in an Akta Explorer 100 FPLC instrument (GE Life Sciences, Piscataway, NJ) and eluted with a gradient of 0–100% Buffer B (20 mM sodium phosphate, 0.5 M NaCl, 500 mM imidazole, pH 7.4) over 30 min with a flow rate of 2 ml/min. Purified fractions were pooled and buffer exchanged on a 26/10 desalting column (GE Life Sciences) into a desalting buffer (20 mM sodium phosphate pH 7.4, 300 mM NaCl). The tags were removed by incubating overnight with purified His-tagged TEV protease at 4°C with rocking. The TEV protease, cleaved tags, and uncleaved proteins were removed by passing the mixture through a 5 ml HisTrapFF column. Tagless proteins were buffer exchanged on a 26/10 desalting column into 20 mM Tris-HCl pH 8.0 and 20 mM NaCl. Proteins were concentrated to ~0.5–1 mg/ml, glycerol was added to 10% (vol/vol), aliquots were flash frozen in liquid nitrogen and stored at –80°C.

For the HD-GYP domains of DVU1181, DVU0722, and DVU0330, a second round of affinity purification was performed by eluting from the first HisTrapFF column onto a 5 ml StrepTrapFF (GE Life Sciences). The column was washed with Buffer C (20 mM sodium phosphate pH 7.4, 280 mM NaCl, 6 mM KCl) and eluted with Buffer D (Buffer C + 2.5 mM desthiobiotin). Then, 50 mM L-arginine and 50 mM L-glutamic acid buffered in Tris-HCl were added to stabilize proteins (Golovanov et al., 2004). This was followed by TEV cleavage and purification of tagless protein as described above.

DGC ASSAY FOR DVU0636, DVU2067, AND DVU0408

Full length DVU0636, DVU2067, and DVU0408 with a C-terminal V5 epitope and 6x His tag were purified from *E. coli*. Purified protein (1.6–1.8 µM) was mixed with 0.5 mM GTP in 50 mM Tris HCl pH 8.0, 100 mM NaCl, and either 2 mM MgCl₂ or 2 mM MnCl₂ in a total volume of 100 µl. The reactions were incubated at 30°C for 24 h. The proteins were denatured by heating at 95°C for 5 min. The samples were centrifuged at 15,000 × g for 10 min, and the supernatant was filtered through a 10 K molecular weight cutoff centrifugal filter prior to HPLC analysis. Samples (3 µl) were injected into an Inertsil ODS-3 column (3 µ, 250 × 2.1 mm; GL Sciences, Torrance, CA) equipped with a guard column (Inertsil ODS-3, 3 µ, 50 × 2.1 mm; GL Sciences) on an HPLC system (Agilent Technologies, Santa Clara, CA). Buffer A: 100 mM Potassium phosphate buffer pH 6.0; Buffer B = 100% (vol/vol) methanol. The samples were run for 25 min at a flow rate of 0.2 ml/min, with the following gradient: 0 min – 2% (vol/vol) B; 2 min – 2% B; 14 min – 30% B; 17 min – 30% B; 18 min – 2% B; 25 min – 2% B.

PDE ACTIVITY ASSAY: WITH bis-pNPP

Triplicate enzyme reactions for each protein were set up in a 96-well microplate (Costar, black with clear flat bottom, polystyrene; Corning Incorporated, Corning, NY). Proteins (7–10 µg) were mixed in a total volume of 100 µl with 5 mM bis-pNPP in 25 mM Tris-HCl pH 8.0, 100 mM NaCl, 1 mM DTT, and either 1 or 10 mM MnCl₂ or 10 mM MgCl₂. Absorbance was measured

at 410 nm every 10 min in a SpectraMax Plus plate reader (Molecular Devices, Sunnyvale, CA, USA). A reaction that lacked bis-*p*NPP served as the blank, while a reaction with no protein served as a negative control.

PDE ACTIVITY ASSAY WITH c-di-GMP

Each protein (7–10 µg) was mixed with 100 µM c-di-GMP in 25 mM Tris HCl pH 8.0, 10 mM MnCl₂, 100 mM NaCl, 1 mM DTT in a total volume of 100 µl HPLC grade water. Reactions were carried out in triplicate and incubated at room temperature for 24 h. The reactions were stopped and proteins denatured by heating to 95°C for 5 min. The samples were centrifuged at 15,000 × g for 10 min, and the supernatant was filtered through a 10 K molecular weight cutoff spin filter before HILIC-TOF MS (hydrophilic interaction liquid chromatography and time of flight mass spectrometry) analysis. The proteins were also tested for activity against 100 µM of cyclic-di-AMP, cyclic-AMP, cyclic-GMP, and pGpG. Samples were injected onto a SeQuant Zic pHILIC (150 mM length × 2.1 mM diameter column together with a 20 × 2.1 mM Zic pHILIC guard column; EMD Millipore, Billerica, MA, USA). For a full description of the analytical method, please refer to Bokinsky et al. (2013).

CONGO RED *E. COLI* ASSAY

E. coli BL21 Star DE3 strains expressing the full-length RR genes were grown overnight in 3 ml LB containing carbenicillin (100 µg/ml). Each strain was diluted 1:100 in fresh medium, grown until OD₆₀₀ of 0.5 at 37°C, and then streaked out on LB-carbenicillin plates containing Congo Red (CR) 5 µg/ml (±0.5 mM IPTG). Plates were incubated at room temperature for 4 days.

TRANSPOSON MUTANT LIBRARY

The transposon mutants were obtained from the *D. vulgaris* transposon mutant collection (Zane and Wall, 2013) constructed at the University of Missouri, which have been used in other studies (Fels et al., 2013; Kazakov et al., 2013a; Ray et al., 2014). Strain descriptions are provided in Table 1.

GROWTH ASSAYS FOR *D. VULGARIS* STRAINS

D. vulgaris was grown in a defined medium containing 8 mM MgCl₂, 20 mM NH₄Cl, 2.2 mM K₂PO₄, 0.6 mM CaCl₂, 30 mM Tris, 1 ml/liter of Thauer's vitamins (Brandis and Thauer, 1981),

Table 1 | Transposon mutant strains used in this study.

Name	Description
GZ0620	DVU0330-496::Tn5-RL27; insertion at bp 496/1239; Km ^r
GZ2490	DVU2067-828::Tn5-RL27; insertion at bp 828/1122; Km ^r
GZ3062	DVU0636-506::Tn5-RL27; insertion at bp 506/1314; Km ^r
GZ4281	DVU0408-857::Tn5-RL27; insertion at bp 857/2148; Km ^r
GZ4944	DVU1181-479::Tn5-RL27; insertion at bp 479/1071; Km ^r
GZ5161	DVUA0086-105::Tn5-RL27; insertion at bp 105/1092; Km ^r
GZ5218	DVU0722-279::Tn5-RL27; insertion at bp 279/1557; Km ^r
GZ2493	DVU2933-215::Tn5-RL27; insertion at bp 215/1377; Km ^r

12.5 ml/liter of trace element solution (Rajeev et al., 2012), 640 µl/liter of resazurin (0.1% wt/vol), and supplemented with 50 mM Na₂SO₄ and 60 mM sodium lactate (LS4D medium). The pH of the medium was adjusted to 7.2 with 1 N HCl. Cultures were grown at 30°C in an anaerobic growth chamber (COY Laboratory Products, Grass Lake, MI, USA) in an atmosphere of 85% N₂, 10% CO₂, and 5% H₂. For transposon mutants, the medium was supplemented with the antibiotic G418 (400 µg/ml) (Sigma Aldrich, St. Louis, MO, USA). *D. vulgaris* strains were grown from freezer stocks in LS4D supplemented with 0.1% (wt/vol) yeast extract in 15 ml centrifuge tubes and then transferred to LS4D medium with a 2% (vol/vol) inoculum. 400 µl of cultures were transferred (4 replicates each) into 100-well honeycomb well plates (Growth Curves USA, Piscataway, NJ, USA) and growth measurements were conducted on the Bioscreen C instrument (Growth Curves USA, Piscataway, NJ, USA) at 30°C within the anaerobic chamber.

COMPLEMENTATION OF Tn5::DVU0636

DVU0636 was cloned into the *E. coli*-*D. vulgaris* shuttle vector pMO9075 (Keller et al., 2014) under a constitutive kanamycin promoter, and with a C-terminal His-tag. Strain GZ3062 (Tn5::DVU0636) was grown overnight from a freezer stock in 10 ml MOYLS4 (+G418). Five milliliter of the overnight culture was used to inoculate 45 ml of fresh MOYLS4 (+G418) and allowed to grow overnight. Electrocompetent cells were prepared as previously described (Zane et al., 2010), and cells (50 µl) were transformed with pMO9075::DVU0636. Transformants were allowed to recover in 1 ml MOYLS4 overnight and then were plated on MOYLS4 containing spectinomycin (100 µg/ml). Colonies were obtained after 4–5 days. Colonies were inoculated into 1 ml MOYLS4 (+G418 and spectinomycin), grown overnight, and transferred to 5 ml MOYLS4 (+G418 and spectinomycin). The resulting culture was used for plasmid preparations and to make freezer stocks. The plasmids were verified by sequencing and the complemented strain was designated as GZ3062(pMO9075::DVU0636).

BIOFILM ASSAYS

Frozen stocks of *D. vulgaris* Hildenborough WT (from Montana State University), GZ3062, and the complemented strain were grown to approximately 0.6 OD₆₀₀ in LS4D medium before transfer. The mutant and complement were maintained under appropriate antibiotics for the duration of the study. Once transferred, the cells were again grown to 0.6 OD₆₀₀ before inoculation (approximately 10% vol/vol inoculum) into the biofilm reactor. The culture was allowed to grow for approximately 24 h before constant medium flow was introduced at a dilution rate of 0.10 h⁻¹. Biofilm samples were grown in a CDC biofilm reactor (Biosurface Technologies, Bozeman, MT, USA) at 30°C in LS4D under constant sparging (~0.85 kPa/min) with anoxic N₂ as previously described (Clark et al., 2012). Coupon holders fitted with glass microscope slides (cut in half) were removed at approximately 120 h, and samples were washed with chilled phosphate buffered saline (50 mM phosphate, 0.7% NaCl, pH 7.2) to remove loosely attached cells. The biofilm was then scraped from each slide into sterile tubes and stored at –80°C. Biofilm samples for

electron microscopy were treated as previously described (Clark et al., 2007). Glass slide sections were mounted on aluminum stubs, coated with iridium, and viewed on a SUPRA 55VP field emission scanning electron microscope (Carl Zeiss Microscopy, Peabody, MA, USA) at 1.0 kV. To determine carbohydrate and protein levels for the different cultures, hexose sugars were measured by the colorimetric cysteine-sulfuric acid method with glucose as the standard (Chaplin, 1986). Protein was measured with the Qubit® Protein Assay Kit (Life Technologies, Grand Island, NY, USA) and Qubit® Fluorometer (Life Technologies, Grand Island, NY, USA) according to the manufacturer's instructions.

RESULTS

BIOCHEMICAL ANALYSIS OF THE c-di-GMP MODULATING RRs

In order to confirm the putative functions of the annotated RRs with c-di-GMP modulating domains, genes encoding the eight RRs were cloned into *E. coli*, the encoded proteins produced and purified.

DVU0636 and DVU2067 have DGC activity, DVU0408 has PDE activity

The three RRs with GGDEF domains were subjected to DGC activity assays by incubation with GTP followed by HPLC analysis (Figures 2, 3).

Purified tagged full length DVU0636 protein converted nearly all of the GTP into c-di-GMP within 24 h of incubation with Mg²⁺ ions (2 mM) (Figure 2A). Interestingly when incubated with Mn²⁺ ions (2 mM), although the GTP was completely consumed, other peaks were present in addition to that of c-di-GMP (Figure 2B). We suspect that these are secondary products rather than reaction intermediates since incubation of the reaction with Mg²⁺ for a shorter time (4 h) did not produce these intermediate

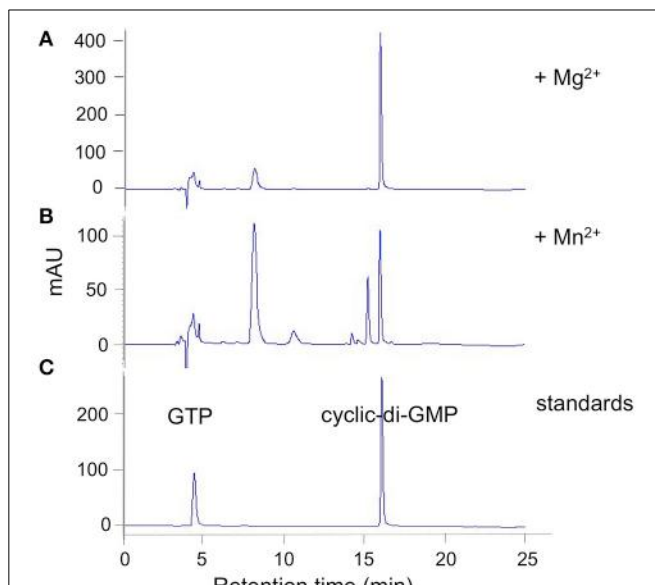


FIGURE 2 | DVU0636 has DGC activity. HPLC traces for DGC activity assays with purified DVU0636 (with C-terminal V5 epitope and 6X His tags) and 500 μ M GTP in the presence of 2 mM MgCl₂ (A), or 2 mM MnCl₂ (B). 100 μ M GTP and 100 μ M c-di-GMP were used as standards (C).

peaks (except for a small peak at 8 min), and extending the incubation time with Mn²⁺ to 40 h still resulted in the alternate product peaks (not shown). No product formed in the absence of either Mg²⁺ or Mn²⁺.

When full length purified tagged DVU2067 protein was incubated with GTP, there was very little product formed with either Mn²⁺ or Mg²⁺ ions. The small peak seen appears to be c-di-GMP as it was absent when no metal ions were added to the reaction (Figure 3). The addition of acetyl phosphate to stimulate phosphorylation did not increase the activity of either DVU0636 or DVU2067 (not shown).

Purified full length DVU0408 protein possessed no detectable DGC activity (not shown). However, it did have PDE activity against c-di-GMP (Figure 4). The amount of product, 5'-pGpG, was greater with Mn²⁺ than with Mg²⁺, whereas no product was formed without a divalent cation. An inactive GGDEF domain

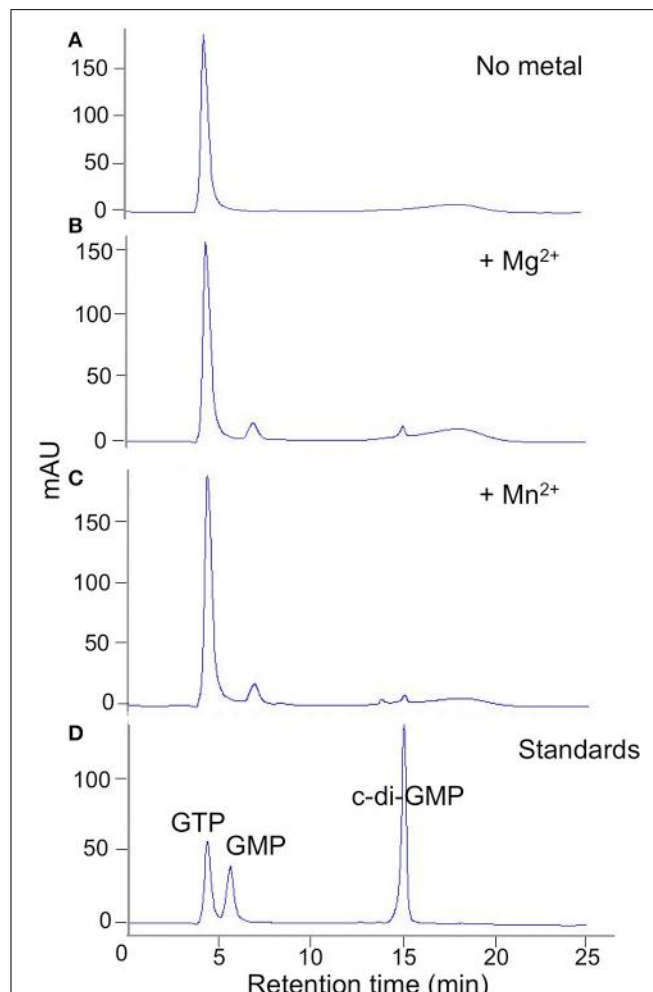


FIGURE 3 | DVU2067 has very low DGC activity. HPLC traces for diguanylate cyclase assay with purified DVU2067. Purified DVU2067 (with C-terminal V5 epitope and 6X-His tags) was mixed with 500 μ M GTP in the presence of (A) no metal; (B) 2 mM MgCl₂; (C) 2 mM MnCl₂; and incubated for 40 h. A mixture of 100 μ M GTP, 100 μ M GMP, and 100 μ M c-di-GMP were run as standards (D).

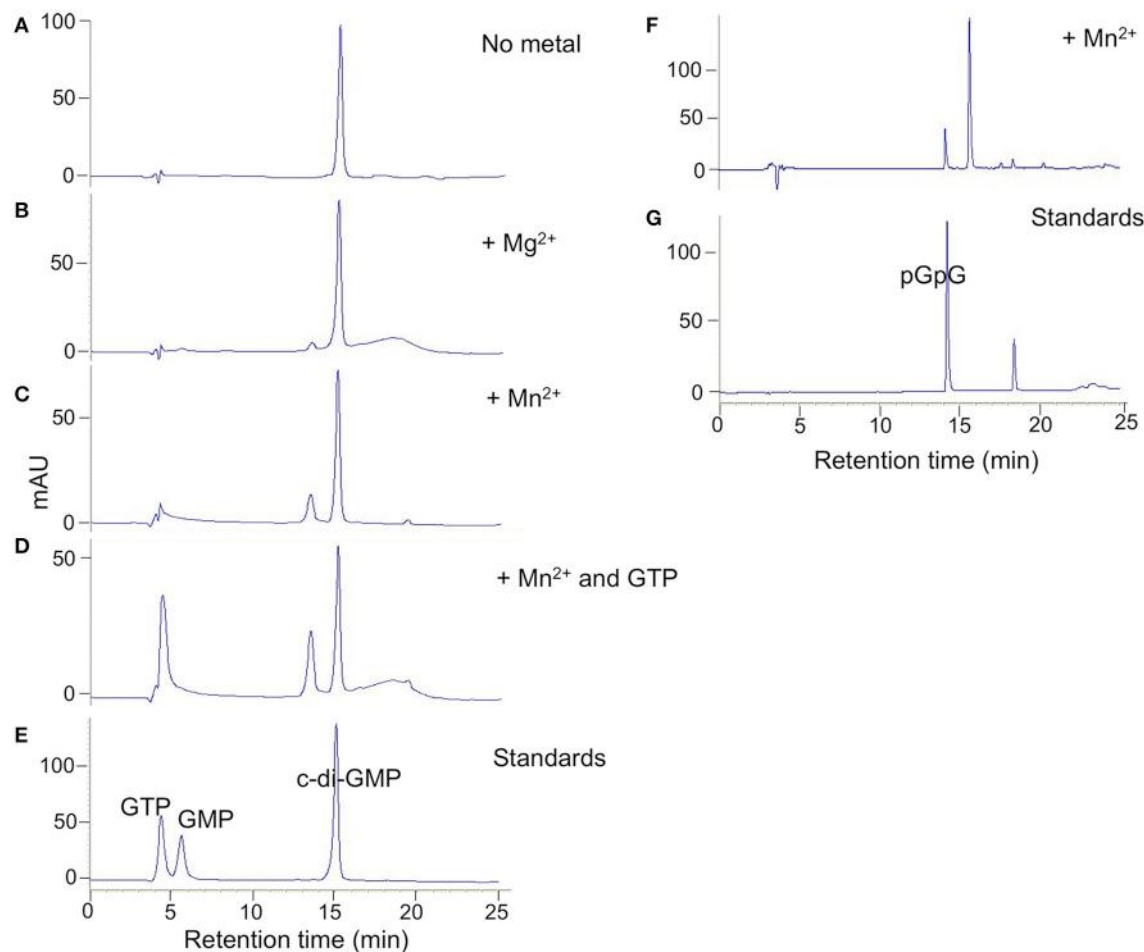


FIGURE 4 | DVU0408 has PDE activity. HPLC traces for PDE activity assays with purified DVU0408 and 100 μM c-di-GMP in the presence of no metal (A); 2 mM MgCl₂ (B); 2 mM MnCl₂ (C,F); 2 mM MnCl₂ and 100 μM GTP (D). Standards run in (E) were a mix of 100 μM GTP,

100 μM GMP, and 100 μM c-di-GMP, while standards run in (G) were 100 μM pGpG alone. HPLC traces (F,G) were from separate runs than (A–E), and hence the slight shifting of the c-di-GMP and pGpG peaks.

is often associated with allosteric activity upon GTP binding (Christen et al., 2005; Kazmierczak et al., 2006); therefore, we tested c-di-GMP hydrolysis activity with Mn²⁺ and GTP. There was an increase in the pGpG peak upon addition of GTP.

RRs with HD-GYP domains have PDE activity

Full length tagged HD-domain containing RRs were purified and tested for activity against the synthetic substrate bis-pNPP as well as against c-di-GMP. The proteins had slow activity against bis-pNPP but no activity on c-di-GMP (not shown). For hydrolysis of bis-pNPP, the proteins required Mn²⁺ and not Mg²⁺. We attempted to activate the proteins by phosphorylation with acetyl phosphate, however acetyl phosphate reacted with the Mn²⁺ and precipitated. Therefore, we cloned and purified only the respective tagless HD domains. All five purified HD domains showed PDE activity against bis-pNPP in the presence of Mn²⁺, but not with Mg²⁺ and not in the absence of any divalent cation (Figure 5). The activity varied among the proteins. DVU2933 and DVUA0086 reached saturation in less than 2 h, DVU0722 and

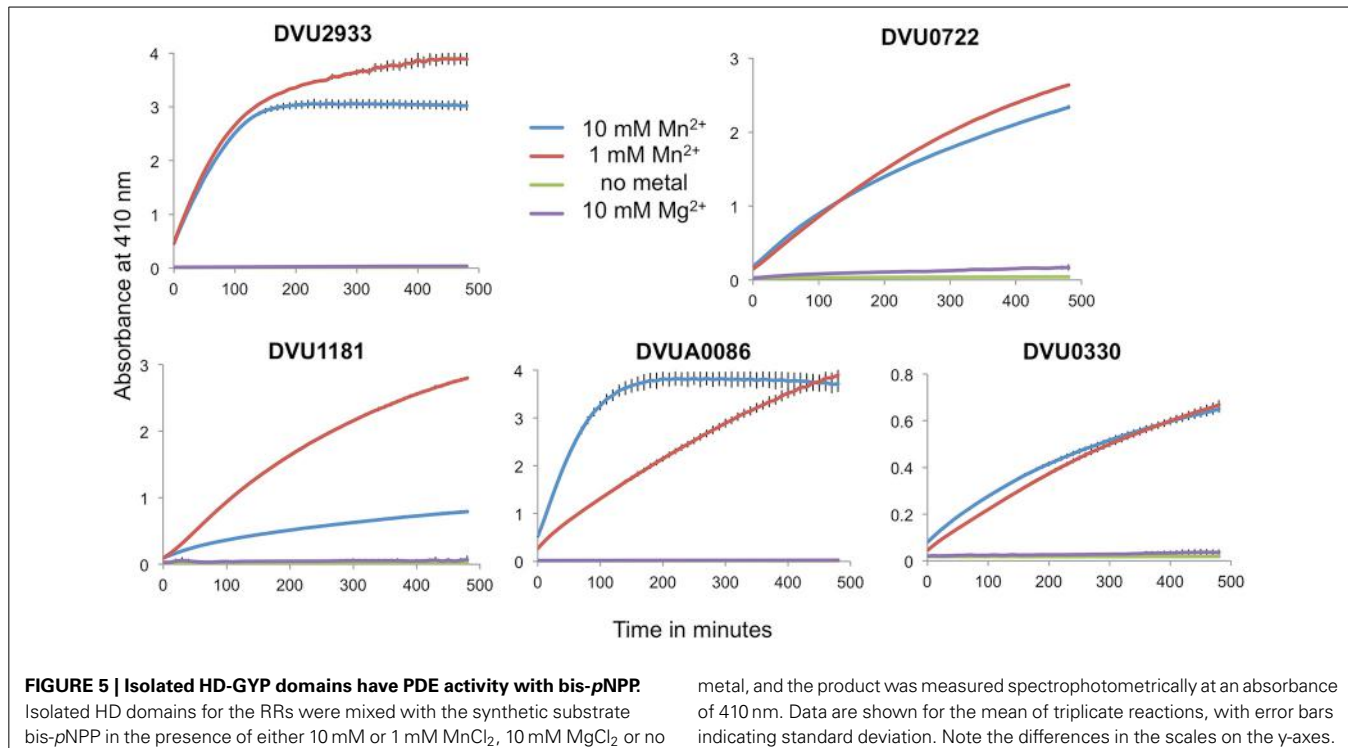
DVU1181 showed slower activity, and DVU0330 that lacks the GYP motif showed very low activity.

We then tested the purified HD domains for hydrolysis of c-di-GMP (Figure 6). DVUA0086 protein had maximum activity and completely hydrolyzed c-di-GMP, with pGpG as the main product and a small amount of GMP. DVU0722 protein also hydrolyzed most of the c-di-GMP to pGpG. DVU2933 protein had lower activity, but again pGpG was the main product formed. DVU1181 and DVU0330 proteins had no activity against c-di-GMP under the conditions tested.

All five proteins were also tested against other possible substrates such as cyclic-di-AMP, cyclic-AMP, and cyclic-GMP. We did not detect any activity against these substrates (not shown). Providing pGpG as a substrate also showed only as much hydrolysis to GMP as was observed with c-di-GMP as a substrate.

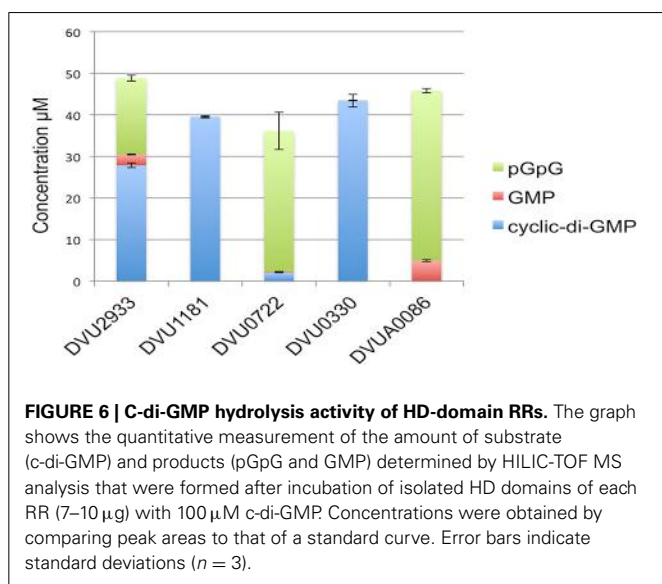
Congo Red assay

We also tested all eight proteins for their ability to affect cellulose production in *E. coli* with a CR plate assay (Zogaj et al., 2001;

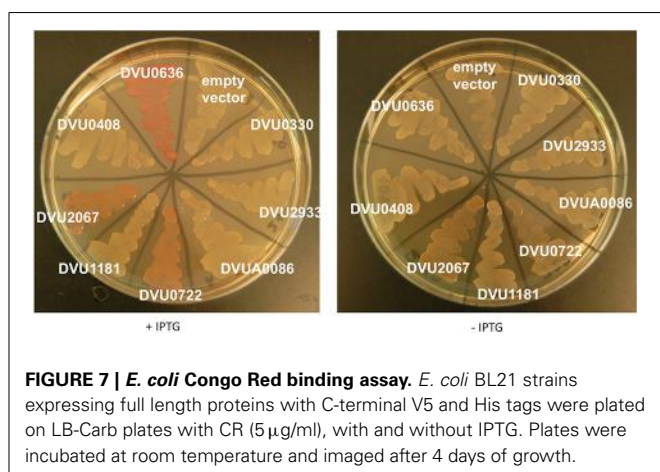
**FIGURE 5 | Isolated HD-GYP domains have PDE activity with bis-pNPP.**

Isolated HD domains for the RRs were mixed with the synthetic substrate bis-pNPP in the presence of either 10 mM or 1 mM $MnCl_2$, 10 mM $MgCl_2$ or no

metal, and the product was measured spectrophotometrically at an absorbance of 410 nm. Data are shown for the mean of triplicate reactions, with error bars indicating standard deviation. Note the differences in the scales on the y-axes.

**FIGURE 6 | C-di-GMP hydrolysis activity of HD-domain RRs.** The graph shows the quantitative measurement of the amount of substrate (c-di-GMP) and products (pGpG and GMP) determined by HILIC-TOF MS analysis that were formed after incubation of isolated HD domains of each RR (7–10 μ g) with 100 μ M c-di-GMP. Concentrations were obtained by comparing peak areas to that of a standard curve. Error bars indicate standard deviations ($n = 3$).

Da Re and Ghigo, 2006). A negative result in this assay cannot be used conclusively; a positive response correlates with DGC activity of the expressed gene, and has been reported to evaluate heterologous proteins in *E. coli* (Liu et al., 2010; Ruiz et al., 2011). BL21 strains expressing tagged full length proteins were plated on CR plates \pm IPTG (Figure 7). The GGDEF domain containing DVU0636 formed bright pink colonies with CR when induced with IPTG, indicating that DVU0636 had DGC activity *in vivo* as well. The GGDEF domain containing RR DVU2067 formed orange colonies when induced with IPTG, although a

**FIGURE 7 | *E. coli* Congo Red binding assay.** *E. coli* BL21 strains expressing full length proteins with C-terminal V5 and His tags were plated on LB-Carb plates with CR (5 μ g/ml), with and without IPTG. Plates were incubated at room temperature and imaged after 4 days of growth.

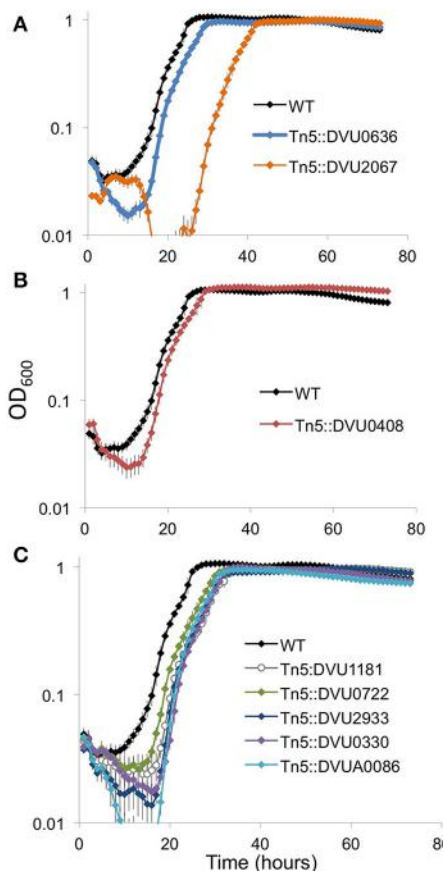
slight orange tinge was visible in the absence of IPTG as well. Interestingly, the HD-GYP containing DVU0722 that we showed above to have PDE activity also showed orange colonies on CR plates + IPTG and, similar to DVU2067, a slight coloration was present in the absence of IPTG too.

TRANSPOSON INSERTION MUTANT ANALYSIS

To further examine physiological roles of these genes, we used mutants with transposon insertions into each of the 8 RR genes that were available from a transposon mutant library.

DVU2067 is required for optimal growth on LS4D

We examined the strains for growth defects on LS4D medium. Of the two RRs with DGC activity, the strain with an insertion in

**FIGURE 8 | Growth on LS4D for the transposon insertion mutants.**

Transposon mutants in the two GGDEF domain RR genes (**A**), the GGDEF-EAL RR (**B**), and the five HD domain RR genes (**C**) were compared to WT during growth on LS4D. Error bars indicate standard deviations ($n = 4$).

DVU2067 showed a prominent growth defect with a longer lag than WT (**Figure 8A**). Transposon mutant in DVU0636 showed a slightly slower growth and decreased cell mass yields than WT. An insertion mutant in DVU0408 (GGDEF-EAL) showed slightly higher maximal ODs than WT (**Figure 8B**). All mutants in HD-domain RRs grew similarly with a slightly longer lag and reduced cell densities than WT (**Figure 8C**).

DVU0636 is required for optimal biofilm formation

Biofilm formation is a common target of c-di-GMP regulation for numerous bacterial groups (Romling et al., 2013), but a relationship between second messenger molecules and biofilm formation has not been investigated previously in δ -Proteobacteria. In general, proteins with GGDEF domains that synthesize c-di-GMP promote biofilm formation (Romling et al., 2013). We had strong biochemical evidence for DGC activity with DVU0636 and therefore we examined the transposon mutant in DVU0636 for an effect on biofilm formation. We observed that although the mutant made some biofilm on glass slides, it made less total biofilm and the composition was very different compared to WT biofilm under steady-state conditions (**Figure 9**). The DVU0636

mutant biofilm had >20-fold lower protein ($\mu\text{g}/\text{cm}^2$) compared to WT biofilm. Even though there was less biofilm, the mutant biofilm had approximately 2.3-fold more carbohydrate (hexose equivalents, $\mu\text{g}/\text{cm}^2$) compared to WT biofilm (**Figure 9A**). *D. vulgaris* WT makes biofilms that are composed more of protein filaments rather than carbohydrates (Clark et al., 2007) and these filaments were not observed in the mutant biofilm. Compared to WT biofilm that has a low carbohydrate to protein ratio ($\sim 0.03 \mu\text{g}/\mu\text{g}$), the Δ DVU0636 biofilm had an elevated ratio of $1.7 \mu\text{g}/\mu\text{g}$ (**Figure 9B**). The FEM images of WT and mutant biofilm also showed biofilm that were drastically different (**Figures 9C,D**). The WT biofilms contained many more cells that likely accounted for the elevated protein levels, and carbohydrate was not obviously visible. However, the Δ DVU0636 biofilm had fewer visible cells with increased extracellular material that appeared to be carbohydrate. We complemented the mutant strain with a plasmid that expressed DVU0636 under a constitutive promoter. The complemented strain produced a biofilm that was more similar in composition to that of WT with more protein and less carbohydrate (C:P ratio of $0.2 \mu\text{g}/\mu\text{g}$) (**Figure 9B**). Electron micrographs of the complemented mutant biofilm also showed more cells than the mutant (**Figure 9E**).

DISCUSSION

The main finding of this study is the identification of a two-component signaling regulator, DVU0636, with significance in biofilm production. Previous work has demonstrated the importance of intracellular interactions and communication for the formation, maintenance, and structuring of biofilms (Burmolle et al., 2014) and this in turn can impact function, stability, and resiliency. However, little is known about anaerobic biofilms that respond differently to mass transport limitations of energy sources other than oxygen. *D. vulgaris* does not produce biofilms with much exopolysaccharide, rather the biofilms are composed of long protein filaments that appear to be flagella or modified flagella (Clark et al., 2007). *In vitro*, we confirmed DVU0636 to be a DGC, where we observed a metal dependence (Mn^{+2} vs. Mg^{+2}) on the products formed, though the identity and significance of these peaks remain to be explored. *In vivo*, the overexpression of DVU0636 heterologously in *E. coli* results in a predictable outcome of increased extracellular cellulose production as indicated by increased binding of the CR dye. In *D. vulgaris*, the role of DVU0636 may be in regulating other biofilm related enzymes, suggested by low protein levels in Δ DVU0636 biofilms, leading to a much greater C:P ratio relative to the WT or the complemented mutant (**Figure 9**). Possibly as a result of the non-optimal C:P ratio, the Δ DVU0636 biofilm has a “slimier” appearance and is easily disrupted (**Figure 9D**). There is likely an optimal ratio of protein and carbohydrate for biofilms that is required to maintain biofilm integrity yet maximize transfer of nutrients, and further work is needed to elucidate the environmental cues and regulated systems that bacteria use to coordinate biofilm growth with local environment.

The *D. vulgaris* genome encodes eight two-component RRs with putative c-di-GMP modulating domains. Aside from DVU0636, the other putative cyclase is DVU2067. Of these two RR DGCs, DVU2067 is more highly conserved (**Table 2**) and is

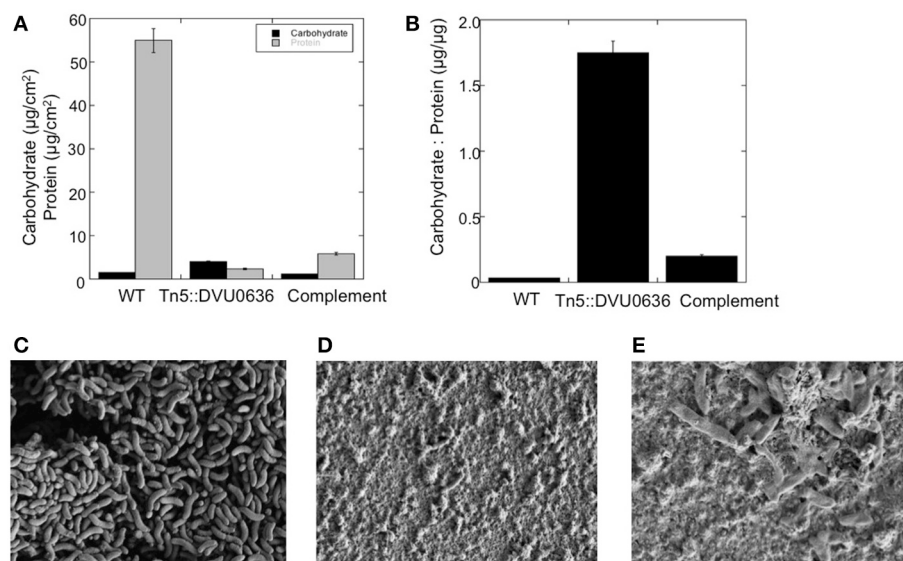


FIGURE 9 | Inactivation of DVU0636 affects biofilm formation. **(A)** The carbohydrate (black) and protein (gray) measurements for WT, Tn5::DVU0636 mutant and complemented strains. Measurements for carbohydrate and protein levels were measured in triplicate for biological duplicates. Error bars indicate standard error of the mean. **(B)** The carbohydrate to protein ratio (μg

hexose/ μg protein) for wild-type, Tn5::DVU0636 and complemented mutant as steady-state biofilm. **(C–E)** Electron micrographs of biofilms of wild-type at 17,700 \times (**C**), mutant at 16,700 \times (**D**), and complemented mutant at 22,900 \times biofilms showing increased cells and decreased extracellular material for WT biofilm compared to mutant biofilm.

also the enzyme needed for optimal growth typically observed under laboratory cultivation in LS4D medium. None of the other RR transposon mutants presented a significant growth defect in liquid culture. We observed very little *in vitro* activity for DVU2067, and it is possible that this protein requires phosphorylation. The *in vivo* CR plate assay showed that cells expressing DVU2067 gave orange coloration relative to cells expressing DVU0636, which were the more typically reported bright pink. The phenotypes observed for the two RR DGCs suggest that production of c-di-GMP does modulate important functions during both biofilm and planktonic growth.

Of the remaining six RRs, we confirmed PDE function for all but DVU0330. DVU0408, which contains both GGDEF and EAL domains, demonstrated turn over of c-di-GMP *in vitro*. The GGDEF domain of DVU0408 has a tyrosine instead of the conserved phenylalanine (**Figure 1C**), which could explain why this domain is inactive (Malone et al., 2007). However, DVU0408 has an active EAL domain that hydrolyses c-di-GMP into pGpG. Higher activity may be observed in an activated RR. Approximately 33% of GGDEF- or EAL-containing proteins are hybrid proteins with both domains, and, among these hybrid proteins, more than 30% have an active EAL domain combined with an inactive GGDEF domain (Seshasayee et al., 2010). For DVU0408, we observed increased product formation in the presence of GTP, which supports the possibility that the inactive GGDEF domain may bind GTP and provide GTP-dependent control of PDE activity (Christen et al., 2005; Kazmierczak et al., 2006).

With the 4 HD-GYP domain RRs, we observed robust PDE activity with the synthetic bis-pNPP for all but activity with c-di-GMP for only 3. We also observed higher activity with

the isolated domains rather than the full-length proteins suggesting that RR activation is necessary for maximal activity. The non-phosphorylated receiver domain of a *Pseudomonas* HD-GYP RR was shown to limit accessibility of the active site to c-di-GMP (Stelitano et al., 2013). The isolated HD-GYP domain for DVU1181 was not active with c-di-GMP although it showed activity against bis-pNPP. Perhaps a more active conformation involving the receiver domain is required for activity with c-di-GMP. The HDOD domain, as present in DVU0330, is related to the HD superfamily of phosphohydrolases (Aravind and Koonin, 1998) but lacks the key active site residues (Galperin, 2006). An HDOD RR, GsmR, was recently characterized from *Xanthomonas campestris*, and found to regulate the expression of motility related genes. GsmR lacked the conserved His in the active site, and also lacked phosphatase or phosphodiesterase activity (Liu et al., 2013). DVU0330 has the conserved HD active site residues (**Figure 1C**), and here we showed that the isolated domain has weak PDE activity with bis-pNPP and none with c-di-GMP or any of the other substrates.

We also observed that for DVU0408, as well as the three active HD-GYP RRs, the hydrolysis product was primarily pGpG. For EAL domains it has been reported that pGpG is the primary product, however GMP is reported as the predominant product for HD-GYP domains (Ryan et al., 2006; Romling et al., 2013). Some recent studies on other HD-GYP proteins also report on pGpG being the main product (Stelitano et al., 2013), and they suggest the possibility of pGpG being a signaling molecule in its own right. *D. vulgaris* Hildenborough is among the genomes with the highest number of HD-GYP domain genes encoded (Galperin et al., 2010) with a total of 14 genes, and it would be interesting to

Table 2 | Conservation of RRs across sequenced *Desulfovibrio*.

Genome name	DVU0636	DVU2067	DVU0408	DVU1181	DVU0722	DVU2933	DVU0086	DVU0330
<i>Desulfovibrio acrylicus</i>			+					
<i>Desulfovibrio aespoeensis</i> Aspo-2	+			+				+
<i>Desulfovibrio africanus</i> DSM 2603	+					+		
<i>Desulfovibrio africanus</i> PCS	+					+		
<i>Desulfovibrio africanus</i> Walvis Bay	+					+		
<i>Desulfovibrio alaskensis</i> DSM 16109	+	+	+	+	+	+		
<i>Desulfovibrio alaskensis</i> G20	+	+	+	+	+	+		
<i>Desulfovibrio aminophilus</i>	+		+			+	+	+
<i>Desulfovibrio bastinii</i>	+				+	+	+	
<i>Desulfovibrio desulfuricans</i> aestuarii			+					
<i>Desulfovibrio desulfuricans</i> desulfuricans 27774								
<i>Desulfovibrio desulfuricans</i> desulfuricans DSM 642	+							
<i>Desulfovibrio fructosovorans</i> JJ	+	+				+	+	+
<i>Desulfovibrio gigas</i>	+	+				+		+
<i>Desulfovibrio hydrothermalis</i>	+	+			+	+	+	+
<i>Desulfovibrio inopinatus</i>	+					+		
<i>Desulfovibrio longus</i>	+	+						+
<i>Desulfovibrio magneticus</i> Maddingley	+	+				+		
<i>Desulfovibrio magneticus</i> RS-1	+	+				+	+	+
<i>Desulfovibrio oxyclinae</i>	+							+
<i>Desulfovibrio piezophilus</i>	+							
<i>Desulfovibrio piger</i>								
<i>Desulfovibrio putealis</i>	+	+	+	+		+		+
<i>Desulfovibrio salexigens</i>	+	+	+		+	+	+	
<i>Desulfovibrio</i> sp. 3_1_syn3								
<i>Desulfovibrio</i> sp. 6_1_46AFAA								
<i>Desulfovibrio</i> sp. A2		+	+	+				+
<i>Desulfovibrio</i> sp. FW1012B	+	+				+		+
<i>Desulfovibrio</i> sp. ND132								
<i>Desulfovibrio</i> sp. U5L	+	+				+		+
<i>Desulfovibrio</i> termitidis HI1			+	+				
<i>Desulfovibrio vulgaris</i> Miyazaki F			+	+		+		
<i>Desulfovibrio vulgaris</i> vulgaris DP4	+	+	+	+	+	+	+	+
<i>Desulfovibrio vulgaris</i> vulgaris Hildenborough	+	+	+	+	+	+	+	+
<i>Desulfovibrio zosterae</i>	+	+			+	+	+	+

Orthologs were determined using the "find homolog" tool on the IMG website (Integrated Microbial Genomes) (Markowitz et al., 2012).

know which perform the incomplete hydrolysis of c-di-GMP to pGpG vs. completely to GMP.

As expected, the CR plate assay with *E. coli* strains expressing PDE RRs gave white colonies with or without IPTG. The interesting exception was the strain expressing DVU0722, which had orange coloration. This was unexpected as DVU0722 has PDE activity *in vitro* and hydrolyzes c-di-GMP. We speculate that DVU0722 interacts with other proteins in *E. coli* and ultimately leads to increased cellulose production.

Gene knockout strains of PDE RRs resulted in no impact on growth in liquid cultures. Additional experimentation is required to identify the phenotypes that involve the other RRs. Genetic data are available for only a few HD-GYP proteins from

pathogens, and none from environmental isolates. RpfG from *Xanthomonas campestris* promotes synthesis of virulence factors and affects biofilm formation and motility (Ryan et al., 2010, 2012). The *Borrelia burgdorferi* PdeB controls motility and promotes virulence in ticks (Sultan et al., 2011). Two HD-GYP domain proteins from *Pseudomonas aeruginosa* control swarming motility and production of virulence factors (Ryan et al., 2009). However, other studies conducted in *D. vulgaris* Hildenborough do shed some light on potential conditions under which the function of these RRs may be relevant. For example, in a recent evaluation of all transcriptionally acting two-component RRs in *D. vulgaris* (Rajeev et al., 2011), DVU0408 was found to be the target for the RR DVU1063, which also targets several flagellar genes.

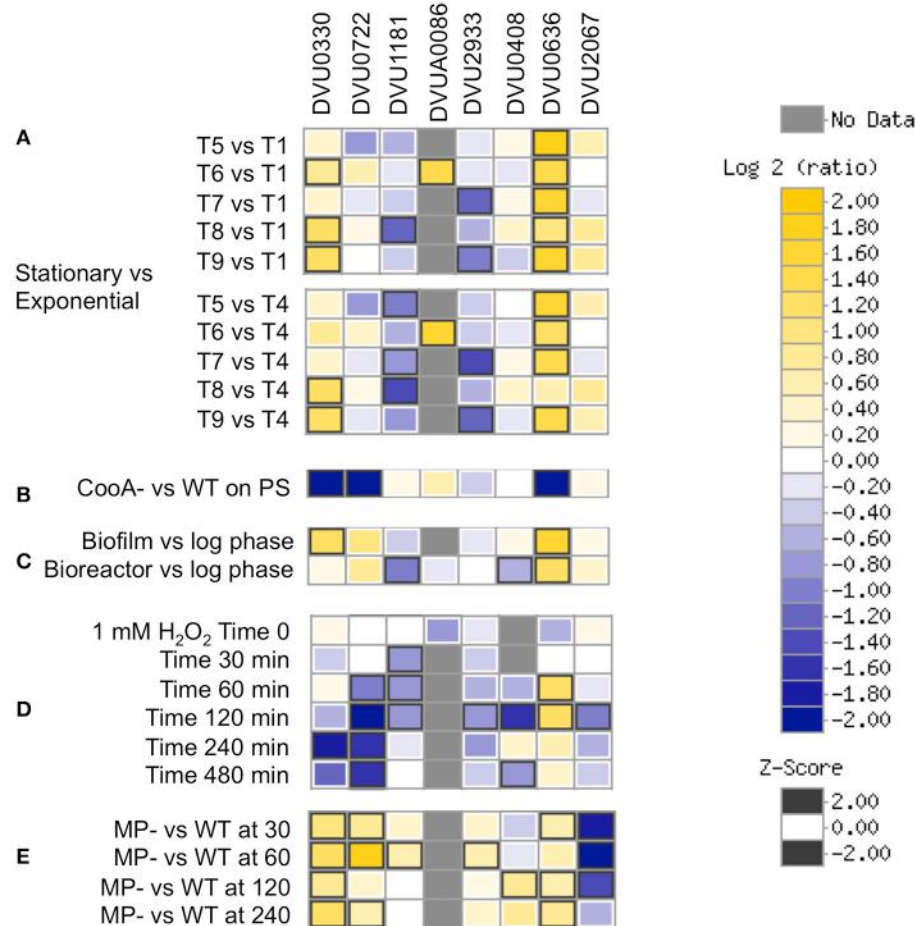


FIGURE 10 | Transcriptomics data showing relevant conditions for differential expression of the 8 RRs. (A) Stationary vs. Exponential phase where T1-T2 are exponential phases, T3-T4 are late exponential phases, T5 is early stationary, and T9 is late stationary (Clark et al., 2006). **(B)** CooA mutant (Deletion in DVU2097) vs. WT on pyruvate

sulfate (Rajeev et al., 2012). **(C)** Biofilm and bioreactor samples vs. log phase cells (Clark et al., 2012). **(D)** Temporal analysis of exposure to 1 mM hydrogen peroxide (Zhou et al., 2010). **(E)** pDV1- strain vs. WT (unpublished). Data were visualized using MicrobesOnline (Dehal et al., 2010).

DVU0408 may thus be involved indirectly in cellular motility. A knockout of this gene however had motility in wet mounts as well as in soft agar plates (data not shown). In the same study (Rajeev et al., 2011), DVU2933 was found to be part of a five-gene operon that also encodes a histidine kinase and another RR, DVU2934, which is a DNA binding RR that targets the *lpxC* gene involved in lipid A synthesis.

A review of available transcriptomics measurements in *D. vulgaris* (Figure 10) shows increased expression of DVU0636 (and DVU0330) transcripts in stationary phase vs. exponential growth stages (Clark et al., 2006). DVU0636 was also upregulated during biofilm growth (Clark et al., 2012), which is again consistent with our results. DVU0636 was also increased in expression during peroxide exposure, in contrast to DVU1181, DVU0722, and DVU2933, which were decreased in expression in this condition (Zhou et al., 2010). In a more environmentally relevant growth regime, defense against peroxide and other oxidative stresses may include the production of biofilms and may explain the increase in DVU0636 transcripts. Further, DVU0636 (and DVU0330,

DVU0722) were decreased in expression, while DVU2067 was increased in expression in a CooA mutant, which lacks the gene DVU2097 that acts as a carbon monoxide sensor. Transcriptomic analysis of the CooA mutant showed changes similar to that seen in WT when exposed to CO including a decrease in expression of Fur regulon genes, and was suggested to have been due to increased levels of endogenous CO and oxidative stress (Rajeev et al., 2012). Conversely, DVU0636 is upregulated, while DVU2067 is downregulated in the pDV1-minus strain, relative to the wild type. The pDV1 minus strain lacks the native 200-kb plasmid present in wild type *D. vulgaris* Hildenborough and has a reported defect in attachment and biofilm formation (Clark et al., 2007) and is also missing the DVUA0086 RR. More experimentation is required to prove if the regulation and function of these RRs are interconnected or interdependent.

CONCLUSIONS

This is the first demonstration of PDE and DGC activity in a sulfate-reducing bacterium. We were most successful in

identifying conditions under which the two DGC RRs are important, though they may have a role in other conditions also. The most conserved candidate, DVU2067, generated a growth defective strain in planktonic cultures. The less conserved, DVU0636, had no impact during growth in liquid cultures but had a clear role in biofilm production. The impact on biofilm growth manifested in altered macromolecular composition that caused decreased biofilm maintenance with elevated carbohydrate levels. The PDE RRs have no clear roles in WT planktonic growth, though some ancillary data links the dual domain DVU0408 with flagellar genes and PDEs to stress responses. Further studies will reveal the roles they play in other aspects of *D. vulgaris* physiology.

ACKNOWLEDGMENTS

We would like to thank Amy Chen and Kavya Siddartha for technical assistance. This work is part of ENIGMA, a Scientific Focus Area Program supported by the US Department of Energy, Office of Science, Office of Biological and Environmental Research, Genomics: GTL Foundational Science through contract DE-AC02-05CH11231 between Lawrence Berkeley National Laboratory and the U.S. Department of Energy. A portion of this work was supported by the U.S. Department of Energy Office of Science, Office of Biological and Environmental Research, Genomics Program:GTL BioHydrogen Production and BioEthanol contract DE-FG02-08346469.

REFERENCES

- Aravind, L., and Koonin, E. V. (1998). The HD domain defines a new superfamily of metal-dependent phosphohydrolases. *Trends Biochem. Sci.* 23, 469–472. doi: 10.1016/S0968-0004(98)01293-6
- Beyenal, H., Sani, R. K., Peyton, B. M., Dohnalkova, A. C., Amonette, J. E., and Lewandowski, Z. (2004). Uranium immobilization by sulfate-reducing biofilms. *Environ. Sci. Technol.* 38, 2067–2074. doi: 10.1021/es0348703
- Bokinsky, G., Baidoo, E. E., Akella, S., Burd, H., Weaver, D., Alonso-Gutierrez, J., et al. (2013). HipA-triggered growth arrest and β -lactam tolerance in *Escherichia coli* are mediated by RelA-dependent ppGpp synthesis. *J. Bacteriol.* 195, 3173–3182. doi: 10.1128/JB.02210-12
- Brandis, A., and Thauer, R. K. (1981). Growth of *Desulfovibrio* species on hydrogen and sulfate as sole energy-source. *J. Gen. Microbiol.* 126, 249–252. doi: 10.1099/00221287-126-1-249
- Burmolle, M., Ren, D., Bjarnsholt, T., and Sorensen, S. J. (2014). Interactions in multispecies biofilms: do they actually matter? *Trends Microbiol.* 22, 84–91. doi: 10.1016/j.tim.2013.12.004
- Chaplin, M. F. (1986). “Monosaccharides,” in *Carbohydrate Analysis*, eds M. F. Chaplin and J. F. Kennedy (Oxford: IRL Press), 1–4.
- Christen, M., Christen, B., Folcher, M., Schauerte, A., and Jenal, U. (2005). Identification and characterization of a cyclic di-GMP-specific phosphodiesterase and its allosteric control by GTP. *J. Biol. Chem.* 280, 30829–30837. doi: 10.1074/jbc.M504429200
- Clark, M. E., Edelmann, R. E., Duley, M. L., Wall, J. D., and Fields, M. W. (2007). Biofilm formation in *Desulfovibrio vulgaris* Hildenborough is dependent upon protein filaments. *Environ. Microbiol.* 9, 2844–2854. doi: 10.1111/j.1462-2920.2007.01398.x
- Clark, M. E., He, Q., He, Z., Huang, K. H., Alm, E. J., Wan, X. F., et al. (2006). Temporal transcriptomic analysis as *Desulfovibrio vulgaris* Hildenborough transitions into stationary phase during electron donor depletion. *Appl. Environ. Microbiol.* 72, 5578–5588. doi: 10.1128/AEM.00284-06
- Clark, M. E., He, Z., Redding, A. M., Joachimiak, M. P., Keasling, J. D., Zhou, J. Z., et al. (2012). Transcriptomic and proteomic analyses of *Desulfovibrio vulgaris* biofilms: carbon and energy flow contribute to the distinct biofilm growth state. *BMC Genomics* 13:138. doi: 10.1186/1471-2164-13-138
- Da Re, S., and Ghigo, J. M. (2006). A CsgD-independent pathway for cellulose production and biofilm formation in *Escherichia coli*. *J. Bacteriol.* 188, 3073–3087. doi: 10.1128/JB.188.8.3073-3087.2006
- Dehal, P. S., Joachimiak, M. P., Price, M. N., Bates, J. T., Baumohl, J. K., Chivian, D., et al. (2010). MicrobesOnline: an integrated portal for comparative and functional genomics. *Nucleic Acids Res.* 38, D396–D400. doi: 10.1093/nar/gkp919
- Faybishenko, B., Hazen, T. C., Long, P. E., Brodie, E. L., Conrad, M. E., Hubbard, S. S., et al. (2008). In situ long-term reductive bioimmobilization of Cr(VI) in groundwater using hydrogen release compound. *Environ. Sci. Technol.* 42, 8478–8485. doi: 10.1021/es801383r
- Fels, S. R., Zane, G. M., Blake, S. M., and Wall, J. D. (2013). Rapid transposon liquid enrichment sequencing (TnLE-seq) for gene fitness evaluation in underdeveloped bacterial systems. *Appl. Environ. Microbiol.* 79, 7510–7517. doi: 10.1128/AEM.02051-13
- Galperin, M. Y. (2006). Structural classification of bacterial response regulators: diversity of output domains and domain combinations. *J. Bacteriol.* 188, 4169–4182. doi: 10.1128/JB.01887-05
- Galperin, M. Y., Higdon, R., and Kolker, E. (2010). Interplay of heritage and habitat in the distribution of bacterial signal transduction systems. *Mol. Biosyst.* 6, 721–728. doi: 10.1039/b908047c
- Gibson, D. G., Young, L., Chuang, R. Y., Venter, J. C., Hutchison, C. A. 3rd, and Smith, H. O. (2009). Enzymatic assembly of DNA molecules up to several hundred kilobases. *Nat. Methods* 6, 343–345. doi: 10.1038/nmeth.1318
- Golovanov, A. P., Hautbergue, G. M., Wilson, S. A., and Lian, L. Y. (2004). A simple method for improving protein solubility and long-term stability. *J. Am. Chem. Soc.* 126, 8933–8939. doi: 10.1021/ja049297h
- Heidelberg, J. F., Seshadri, R., Haveman, S. A., Hemme, C. L., Paulsen, I. T., Kolonay, J. F., et al. (2004). The genome sequence of the anaerobic, sulfate-reducing bacterium *Desulfovibrio vulgaris* Hildenborough. *Nat. Biotechnol.* 22, 554–559. doi: 10.1038/nbt959
- Hengge, R. (2009). Principles of c-di-GMP signalling in bacteria. *Nat. Rev. Microbiol.* 7, 263–273. doi: 10.1038/nrmicro2109
- Hillesland, K. L., and Stahl, D. A. (2010). Rapid evolution of stability and productivity at the origin of a microbial mutualism. *Proc. Natl. Acad. Sci. U.S.A.* 107, 2124–2129. doi: 10.1073/pnas.0908456107
- Kazakov, A. E., Rajeev, L., Luning, E. G., Zane, G. M., Siddartha, K., Rodionov, D. A., et al. (2013a). New family of tungstate-responsive transcriptional regulators in sulfate-reducing bacteria. *J. Bacteriol.* 195, 4466–4475. doi: 10.1128/JB.00679-13
- Kazakov, A. E., Rodionov, D. A., Price, M. N., Arkin, A. P., Dubchak, I., and Novickov, P. S. (2013b). Transcription factor family-based reconstruction of singleton regulons and study of the Crp/Fnr, ArsR, and GntR families in *Desulfovibrionales* genomes. *J. Bacteriol.* 195, 29–38. doi: 10.1128/JB.01977-12
- Kazmierczak, B. I., Lebron, M. B., and Murray, T. S. (2006). Analysis of FimX, a phosphodiesterase that governs twitching motility in *Pseudomonas aeruginosa*. *Mol. Microbiol.* 60, 1026–1043. doi: 10.1111/j.1365-2958.2006.05156.x
- Keller, K. L., Rapp-Giles, B. J., Semkiw, E. S., Porat, I., Brown, S. D., and Wall, J. D. (2014). New model for electron flow for sulfate reduction in *Desulfovibrio alaskensis* G20. *Appl. Environ. Microbiol.* 80, 855–868. doi: 10.1128/AEM.02963-13
- Lee, W., Lewandowski, Z., Nielsen, P. H., and Hamilton, W. A. (1995). Role of sulfate-reducing bacteria in corrosion of mild steel: a review. *Biofouling* 8, 165–194. doi: 10.1080/08927019509378271
- Liu, N., Pak, T., and Boon, E. N. (2010). Characterization of a diguanylate cyclase from *Shewanella woodyi* with cyclase and phosphodiesterase activities. *Mol. Biosyst.* 6, 1561–1564. doi: 10.1039/C002246B
- Liu, Y.-F., Liao, C.-T., Song, W.-L., Hsu, P.-C., Du, S.-C., Lo, H.-H., et al. (2013). GsmR, a response regulator with an HD-related output domain in *Xanthomonas campestris*, is positively controlled by Clp and is involved in the expression of genes responsible for flagellum synthesis. *FEBS J.* 280, 199–213. doi: 10.1111/febs.12061
- Malone, J. G., Williams, R., Christen, M., Jenal, U., Spiers, A. J., and Rainey, P. B. (2007). The structure-function relationship of WspR, a *Pseudomonas fluorescens* response regulator with a GGDEF output domain. *Microbiology* 153, 980–994. doi: 10.1099/mic.0.2006/002824-0
- Markowitz, V. M., Chen, I. M., Palaniappan, K., Chu, K., Szeto, E., Grechkin, Y., et al. (2012). IMG: the Integrated Microbial Genomes database and comparative analysis system. *Nucleic Acids Res.* 40, D115–D122. doi: 10.1093/nar/gkr1044

- Paul, R., Weiser, S., Amiot, N. C., Chan, C., Schirmer, T., Giese, B., et al. (2004). Cell cycle-dependent dynamic localization of a bacterial response regulator with a novel di-guanylate cyclase output domain. *Genes Dev.* 18, 715–727. doi: 10.1101/gad.289504
- Rajeev, L., Hillesland, K. L., Zane, G. M., Zhou, A., Joachimiak, M. P., He, Z., et al. (2012). Deletion of the *Desulfovibrio vulgaris* carbon monoxide sensor invokes global changes in transcription. *J. Bacteriol.* 194, 5783–5793. doi: 10.1128/JB.00749-12
- Rajeev, L., Luning, E. G., Dehal, P. S., Price, M. N., Arkin, A. P., and Mukhopadhyay, A. (2011). Systematic mapping of two component response regulators to gene targets in a model sulfate reducing bacterium. *Genome Biol.* 12, R99. doi: 10.1186/gb-2011-12-10-r99
- Ray, J., Keller, K. L., Catena, M., Juba, T. R., Zemla, M., Rajeev, L., et al. (2014). Exploring the role of CheA3 in *Desulfovibrio vulgaris* Hildenborough motility. *Front. Microbiol.* 5:77. doi: 10.3389/fmicb.2014.00077
- Rodionov, D. A., Dubchak, I., Arkin, A., Alm, E., and Gelfand, M. S. (2004). Reconstruction of regulatory and metabolic pathways in metal-reducing delta-proteobacteria. *Genome Biol.* 5:R90. doi: 10.1186/gb-2004-5-11-r90
- Romling, U., Galperin, M. Y., and Gomelsky, M. (2013). Cyclic di-GMP: the first 25 years of a universal bacterial second messenger. *Microbiol. Mol. Biol. Rev.* 77, 1–52. doi: 10.1128/MMBR.00043-12
- Ross, P., Weinhouse, H., Aloni, Y., Michaeli, D., Weinberger-Ohana, P., Mayer, R., et al. (1987). Regulation of cellulose synthesis in *Acetobacter xylinum* by cyclic diguanylic acid. *Nature* 325, 279–281.
- Ruiz, L. M., Castro, M., Barriga, A., Jerez, C. A., and Giuliani, N. (2011). The extremophile *Acidithiobacillus ferrooxidans* possesses a cyclic-di-GMP signaling pathway that could play a significant role during bioleaching of minerals. *Lett. Appl. Microbiol.* 54, 133–139. doi: 10.1111/j.1472-765X.2011.03180.x
- Ryan, R. P., Fouhy, Y., Lucey, J. F., Crossman, L. C., Spiro, S., He, Y. W., et al. (2006). Cell-cell signaling in *Xanthomonas campestris* involves an HD-GYP domain protein that functions in cyclic di-GMP turnover. *Proc. Natl. Acad. Sci. U.S.A.* 103, 6712–6717. doi: 10.1073/pnas.0600345103
- Ryan, R. P., Lucey, J., O'donovan, K., McCarthy, Y., Yang, L., Tolker-Nielsen, T., et al. (2009). HD-GYP domain proteins regulate biofilm formation and virulence in *Pseudomonas aeruginosa*. *Environ. Microbiol.* 11, 1126–1136. doi: 10.1111/j.1462-2920.2008.01842.x
- Ryan, R. P., McCarthy, Y., Andrade, M., Farah, C. S., Armitage, J. P., and Dow, J. M. (2010). Cell-cell signal-dependent dynamic interactions between HD-GYP and GGDEF domain proteins mediate virulence in *Xanthomonas campestris*. *Proc. Natl. Acad. Sci. U.S.A.* 107, 5989–5994. doi: 10.1073/pnas.0912839107
- Ryan, R. P., McCarthy, Y., Kiely, P. A., O'connor, R., Farah, C. S., Armitage, J. P., et al. (2012). Dynamic complex formation between HD-GYP, GGDEF and PilZ domain proteins regulates motility in *Xanthomonas campestris*. *Mol. Microbiol.* 86, 557–567. doi: 10.1111/mmi.12000
- Ryjenkov, D. A., Tarutina, M., Moskvin, O. V., and Gomelsky, M. (2005). Cyclic diguanylate is a ubiquitous signaling molecule in bacteria: insights into biochemistry of the GGDEF protein domain. *J. Bacteriol.* 187, 1792–1798. doi: 10.1128/JB.187.5.1792-1798.2005
- Schirmer, T., and Jenal, U. (2009). Structural and mechanistic determinants of c-di-GMP signalling. *Nat. Rev. Microbiol.* 7, 724–735. doi: 10.1038/nrmicro2203
- Schmidt, A. J., Ryjenkov, D. A., and Gomelsky, M. (2005). The ubiquitous protein domain EAL is a cyclic diguanylate-specific phosphodiesterase: enzymatically active and inactive EAL domains. *J. Bacteriol.* 187, 4774–4781. doi: 10.1128/JB.187.14.4774-4781.2005
- Seshasayee, A. S., Fraser, G. M., and Luscombe, N. M. (2010). Comparative genomics of cyclic-di-GMP signalling in bacteria: post-translational regulation and catalytic activity. *Nucleic Acids Res.* 38, 5970–5981. doi: 10.1093/nar/gkq382
- Simm, R., Morr, M., Kader, A., Nimtz, M., and Romling, U. (2004). GGDEF and EAL domains inversely regulate cyclic di-GMP levels and transition from sessility to motility. *Mol. Microbiol.* 53, 1123–1134. doi: 10.1111/j.1365-2958.2004.04206.x
- Solano, C., Garcia, B., Latasa, C., Toledo-Arana, A., Zorraquino, V., Valle, J., et al. (2009). Genetic reductionist approach for dissecting individual roles of GGDEF proteins within the c-di-GMP signaling network in *Salmonella*. *Proc. Natl. Acad. Sci. U.S.A.* 106, 7997–8002. doi: 10.1073/pnas.0812573106
- Stelitano, V., Giardina, G., Paiardini, A., Castiglione, N., Cutruzzola, F., and Rinaldo, S. (2013). C-di-GMP hydrolysis by *Pseudomonas aeruginosa* HD-GYP phosphodiesterases: analysis of the reaction mechanism and novel roles for pGpG. *PLoS ONE* 8:e74920. doi: 10.1371/journal.pone.0074920
- Sultan, S. Z., Pitzer, J. E., Boquoi, T., Hobbs, G., Miller, M. R., and Motaleb, M. A. (2011). Analysis of the HD-GYP domain cyclic dimeric GMP phosphodiesterase reveals a role in motility and the enzootic life cycle of *Borrelia burgdorferi*. *Infect. Immun.* 79, 3273–3283. doi: 10.1128/IAI.05153-11
- Tan, H., West, J. A., Ramsay, J. P., Monson, R. E., Griffin, J. L., Toth, I. K., et al. (2014). Comprehensive overexpression analysis of cyclic-di-GMP signalling proteins in the phytopathogen *Pectobacterium atrosepticum* reveals diverse effects on motility and virulence phenotypes. *Microbiology* 160, 1427–1439. doi: 10.1099/mic.0.076828-0
- Tartof, K. D., and Hobbs, C. A. (1987). Improved media for growing plasmid and cosmid clones. *Bethesda Res. Lab. Focus* 9, 12.
- Wang, Y., Xu, J., Chen, A., Wang, Y., Zhu, J., Yu, G., et al. (2010). GGDEF and EAL proteins play different roles in the control of *Sinorhizobium meliloti* growth, motility, exopolysaccharide production, and competitive nodulation on host alfalfa. *Acta Biochim. Biophys. Sin. (Shanghai)* 42, 410–417. doi: 10.1093/abbs/gmq034
- Zane, G. M., and Wall, J. D. (2013). *Desulfovibrio vulgaris* Hildenborough Transposon Mutant Library [Online]. Available online at: <http://desulfovibriomaps.biochem.missouri.edu/mutants/>
- Zane, G. M., Yen, H. C., and Wall, J. D. (2010). Effect of the deletion of *qmoABC* and the promoter-distal gene encoding a hypothetical protein on sulfate reduction in *Desulfovibrio vulgaris* Hildenborough. *Appl. Environ. Microbiol.* 76, 5500–5509. doi: 10.1128/AEM.00691-10
- Zhou, A., He, Z., Redding-Johanson, A. M., Mukhopadhyay, A., Hemme, C. L., Joachimiak, M. P., et al. (2010). Hydrogen peroxide-induced oxidative stress responses in *Desulfovibrio vulgaris* Hildenborough. *Environ. Microbiol.* 12, 2645–2657. doi: 10.1111/j.1462-2920.2010.02920.x
- Zhou, J., He, Q., Hemme, C. L., Mukhopadhyay, A., Hillesland, K., Zhou, A., et al. (2011). How sulphate-reducing microorganisms cope with stress: lessons from systems biology. *Nat. Rev. Microbiol.* 9, 452–466. doi: 10.1038/nrmicro2575
- Zogaj, X., Nimtz, M., Rohde, M., Bokranz, W., and Romling, U. (2001). The multicellular morphotypes of *Salmonella typhimurium* and *Escherichia coli* produce cellulose as the second component of the extracellular matrix. *Mol. Microbiol.* 39, 1452–1463. doi: 10.1046/j.1365-2958.2001.02337.x
- Conflict of Interest Statement:** The authors declare that the research was conducted in the absence of any commercial or financial relationships that could be construed as a potential conflict of interest.
- Received:** 29 May 2014; **accepted:** 09 July 2014; **published online:** 29 July 2014.
- Citation:** Rajeev L, Luning EG, Altenburg S, Zane GM, Baidoo EEK, Catena M, Keasling JD, Wall JD, Fields MW and Mukhopadhyay A (2014) Identification of a cyclic-di-GMP-modulating response regulator that impacts biofilm formation in a model sulfate reducing bacterium. *Front. Microbiol.* 5:382. doi: 10.3389/fmicb.2014.00382
- This article was submitted to Terrestrial Microbiology, a section of the journal *Frontiers in Microbiology*.
- Copyright © 2014 Rajeev, Luning, Altenburg, Zane, Baidoo, Catena, Keasling, Wall, Fields and Mukhopadhyay. This is an open-access article distributed under the terms of the Creative Commons Attribution License (CC BY). The use, distribution or reproduction in other forums is permitted, provided the original author(s) or licensor are credited and that the original publication in this journal is cited, in accordance with accepted academic practice. No use, distribution or reproduction is permitted which does not comply with these terms.



Inter-species interconnections in acid mine drainage microbial communities

Luis R. Comolli^{1*} and Jill F. Banfield^{2*}

¹ Structural Biology and Imaging Department, Life Sciences Division, Lawrence Berkeley National Laboratory, Berkeley, CA, USA

² Department of Earth and Planetary Science, University of California, Berkeley, Berkeley, CA, USA

Edited by:

Lisa Stein, University of Alberta, Canada

Reviewed by:

Richard Webb, University of Queensland, Australia

Christine Moissl-Eichinger, University of Regensburg, Germany

***Correspondence:**

Luis R. Comolli, Lawrence Berkeley National Laboratory, Life Sciences Division, Structural Biology and Imaging Department, 1 Donner, 1 Cyclotron Road, Berkeley, CA 94720, USA
e-mail: lrcomolli@lbl.gov;

Jill F. Banfield, Department of Earth and Planetary Science, University of California, Berkeley, 336 Hilgard Hall, Berkeley, CA 94720, USA
e-mail: jbanfield@berkeley.edu

Metagenomic studies are revolutionizing our understanding of microbes in the biosphere. They have uncovered numerous proteins of unknown function in tens of essentially unstudied lineages that lack cultivated representatives. Notably, few of these microorganisms have been visualized, and even fewer have been described ultra-structurally in their essentially intact, physiologically relevant states. Here, we present cryogenic transmission electron microscope (cryo-TEM) 2D images and 3D tomographic datasets for archaeal species from natural acid mine drainage (AMD) microbial communities. Ultrastructural findings indicate the importance of microbial interconnectedness via a range of mechanisms, including direct cytoplasmic bridges and pervasive pili. The data also suggest a variety of biological structures associated with cell-cell interfaces that lack explanation. Some may play roles in inter-species interactions. Interdependences amongst the archaea may have confounded prior isolation efforts. Overall, the findings underline knowledge gaps related to archaeal cell components and highlight the likely importance of co-evolution in shaping microbial lineages.

Keywords: Cryo-TEM, Intact natural microbes, Archaea, Microbial inter-species connections, Metagenomics, Thermoplasmatales, ARMAN

INTRODUCTION

The fact that microbes shape the biosphere is well appreciated, but there are many blind spots in our understanding of the relevant processes because over half of all microbial phyla lack even a single characterized member (Baker and Dick, 2013). The tree of life is being constantly revised and expanded with the addition of new microbial genomes that have been obtained by cultivation-independent methods (Hall-Stoodley et al., 2004; Tyson et al., 2004; Fuhrman, 2009; Wrighton et al., 2012; Castelle et al., 2013; Di Rienzi et al., 2013; Kantor et al., 2013; Rinke et al., 2013). Systems-biology tools are being developed to uncover networks of interactions among microorganisms, and simulations begin to predict system-wide responses and adaptations (Dubey and Ben-Yehuda, 2011; Sanchez, 2011; Cremer et al., 2012). Yet, basic information about the nature and extent of microbial associations and ultrastructurally-resolved architecture of communities is lacking.

Direct sequencing of DNA extracted from natural microbial communities (metagenomics) provides a route to phylogenetic and functional insight without the requirement for laboratory cultivation or isolation. In some instances, the approach can yield near-complete and even complete genomes (Albertsen et al., 2013; Sharon et al., 2013; references therein). These genomes provide a context for functional information from cultivation-independent transcriptomic, proteomic, or metabolomic measurements. However, the utility of this approach is limited by genes and proteins of unknown function, which remain a massive knowledge gap in biology. In some cases ~50% of proteins in organisms from lineages lacking cultivated representatives have

no functional prediction (e.g., Kantor et al., 2013). Some of these proteins may be components of biochemically unknown ultrafine structures so far undetected in cultivated microorganisms or isolated organisms. Detection of such features by imaging methods provides a starting point for subsequent targeted investigations to uncover new structural features, appendages, or organelles. Even for structures that can be predicted (e.g., pili and flagella), imaging methods provide information that cannot be deduced from sequence information or expression assays (e.g., the distribution in cells or on cell surfaces, and certain structural characteristics).

Most current image data focuses on a subset of isolates, thus is restricted to a very small proportion of all microorganisms in nature. The effort to visually characterize and ultrastructurally describe microbes in their near intact, physiologically relevant states, within their natural communities has barely begun. Traditional fixation and dehydration methods cause significant artifacts that can be eliminated by using cryogenic TEM (cryo-TEM; see review by Milne and Subramaniam, 2009). Frozen hydrated samples, which are not stained, are imaged using low-dose techniques to minimize radiation damage and preserve structures in a “near native” state. Cryo-TEM provides two-dimensional (2D) images, including fairly high-dose, high signal-to-noise ratio views of selected areas. Cryogenic electron tomography provides three-dimensional (3D) ultrastructural information regarding cell organization and associations with inorganic phases at a resolution up to ~4 nm (Comolli et al., 2009, 2011; Luef et al., 2012). Morphology and ultrastructure are the physical scaffolds underlying and enabling the molecular physiology of the individual populations as well

as interrelationships between species in communities. Linking metagenomics, metaproteomics, and metabolomics information with near intact morphology, ultrastructure, and highly resolved spatial interactions and networks remains a grand challenge that must be solved if we want to understand microorganisms in natural context.

Acid mine drainage (AMD) biofilm microbial communities have provided a model system for our efforts to integrate the techniques of cryogenic sample preparation and cryo-transmission electron microscopy (cryo-TEM) and with “omics” data (Supplementary Information; Comolli et al., 2009; Baker et al., 2010; Yelton et al., 2013). Communities are dominated by *Leptospirillum* bacteria (related to *Leptospirillum ferriphilum* and *Leptospirillum ferrodiazotrophum*), with lower abundances of archaea, mostly from the *Thermoplasmatales* lineage. Species abundances vary. Relative to other microbial ecosystems, AMD communities are tractable for integrated “omics” and microscopy analysis because they are dominated by a relatively small number of different organism types. Extensive prior metagenomic analyses have documented the presence of novel acidophilic nanoarchaea (ARMAN; Baker et al., 2006, 2010) and *Thermoplasmatales* lineage archaea (Edwards et al., 2000; Yelton et al., 2013), in association with abundant Nitrospirae phylum (*Leptospirillum* spp., Tyson et al., 2004; Simmons et al., 2008; Aliaga-Goltzman et al., 2009) and less abundant bacteria. See also the review (Baker and Banfield, 2003) for community composition. 3D reconstructions of archaeal ARMAN-lineage cells have revealed intriguing features such as very low ribosome copy numbers and a completely novel cytoplasmic tubular structure (Comolli et al., 2009). These structures may be analogous to those used by bacteria, as discussed by Dubey and Ben-Yehuda (2011), enabling the transfer of macromolecules between individuals. Other studies of AMD biofilms uncovered direct cytoplasmic interaction between ARMAN and *Thermoplasmatales* lineage archaea, hinting at a solution to the mystery of how the ARMAN, with tiny genomes apparently lacking genes for many core biosynthetic pathways, survive (Baker et al., 2010). Certain *Thermoplasmatales* lineage archaea cells are decorated with pili, flagella, and S-layers. These features have been linked with genomic data to discriminate between closely related clades and spatially locate cells within communities (Yelton et al., 2013). While the presence of these ultrastructural features implies the expression of corresponding genes, their absence does not provide any conclusion; not all genes are expressed all the time.

Recently, metagenomic studies have opened new windows on microbial diversity, microbial roles in element cycling and responses to changing environmental conditions. Notably, many organisms very recently described by these methods are predicted to lack many (in some cases, most) core biosynthetic pathways (e.g., members of candidate phyla OD1, OP11, SR1, TM7, BD1-5; Wrighton et al., 2012; Albertsen et al., 2013; Campbell et al., 2013; Kantor et al., 2013), raising the possibility that they are symbionts or parasites as e.g., *Nanoarchaeum equitans* and *Ignicoccus hospitalis* (Jahn et al., 2008). Thus, it is important to pair functional predictions for individual organisms with information about organism associations and interdependences to understand how microorganisms mediate biogeochemical

processes. An early example of possibly key interdependences is the discovery of archaeal/bacterial strings-of-pearls communities (Rudolph et al., 2001; Moissl et al., 2002). However, no high-resolution, intact ultrastructural studies, nor linked metagenomics, metaproteomics, and metabolomics studies are yet available. Few methods have the ability to resolve microbial cells with sufficient detail to distinguish them from each other and to provide evidence for direct interconnections. Here, we extend our prior studies of AMD archaea, using cryo-TEM to provide further evidence for a fascinating, yet currently almost uninterpretable variety of ultrastructural features in uncultivated organisms. The findings underscore major gaps in our understanding of microbial biology, microbial community functioning, and by inference, microbial evolution. Fully understanding the role of these inter-species interconnections in providing metabolic complementarities across whole microbial communities is central to understanding how they modulate their adaptive and evolutionary responses to environmental pressures.

RESULTS

The AMD microbial community samples contain *Thermoplasmatales* lineage archaea referred to as Aplasma, Eplasma, Gplasma, Ferroplasmas Fer1 and Fer2 [related to previously described *Ferroplasma* and *Thermoplasma acidophilum* (Golyshina and Timmis, 2005)]; Iplasma from a sibling lineage to the *Thermoplasmatales* (Yelton et al., 2013); as well as ARMAN nanoarchaea (Baker et al., 2006). Whole ultrastructural characterization of ARMAN nanoarchaea was reported previously (Comolli et al., 2009); their cell walls are smooth and uniform in thickness ($\sim 30 \pm 2$ nm wide), with conspicuous inner and outer membranes (IM, OM) and no S-layer. The periplasmic space is studded with $\sim 5\text{--}8$ nm diameter high contrast features in close proximity to the IM and with physical connections through the IM into the cytoplasm (Figure 1; Comolli et al., 2009). Distinguishing *Thermoplasmatales* lineage archaea from the other archaea is straightforward on the basis of size and irregular and pleomorphic morphology and absence of cell wall (Yasuda et al., 1995; Golyshina and Timmis, 2005; Yelton et al., 2013 and references therein; Figures S2–S6). *Thermoplasmatales* lineage archaea cells are generally bounded by a single membrane; all of the AMD plasma genomes (except Fer 1) have putative S-layer genes, and also genes potentially involved in archaeal S-layer protein N-glycosylation (Figures 2, 3; Figures S2–S6; Movies 1, 2; Yelton et al., 2013). Most *Thermoplasmatales* lineage archaea lack flagella genes, except for A or E plasma, which have complete sets of flagella genes.

We surveyed the associations between ARMAN and *Thermoplasmatales* lineage archaea cells and detected a series of repeated patterns of physical associations. A striking physical interaction occurs via direct communication between cytoplasmic spaces through a “synapse-like” structure as the one shown in Figure 1. A protrusion in the cell wall of ARMAN with a hole approximately 30 nm in diameter is coupled to a hole through the S-layer and plasma membrane of the *Thermoplasma* lineage cell, or most likely a “bud” separated from a larger cell, providing a direct connection between the cytoplasmic spaces. The outer membrane of the cells interacting with ARMAN is typically

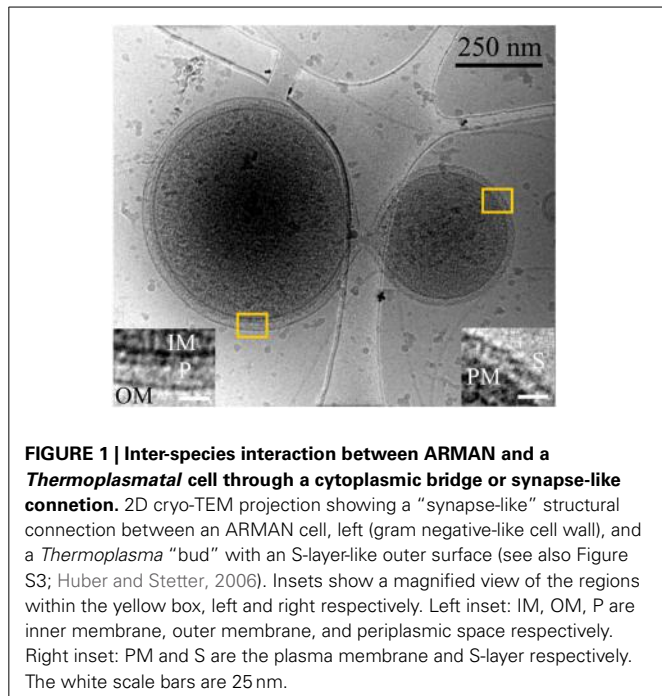


FIGURE 1 | Inter-species interaction between ARMAN and *Thermoplasmatal* cell through a cytoplasmic bridge or synapse-like connection. 2D cryo-TEM projection showing a “synapse-like” structural connection between an ARMAN cell, left (gram negative-like cell wall), and a *Thermoplasma* “bud” with an S-layer-like outer surface (see also Figure S3; Huber and Stetter, 2006). Insets show a magnified view of the regions within the yellow box, left and right respectively. Left inset: IM, OM, P are inner membrane, outer membrane, and periplasmic space respectively. Right inset: PM and S are the plasma membrane and S-layer respectively. The white scale bars are 25 nm.

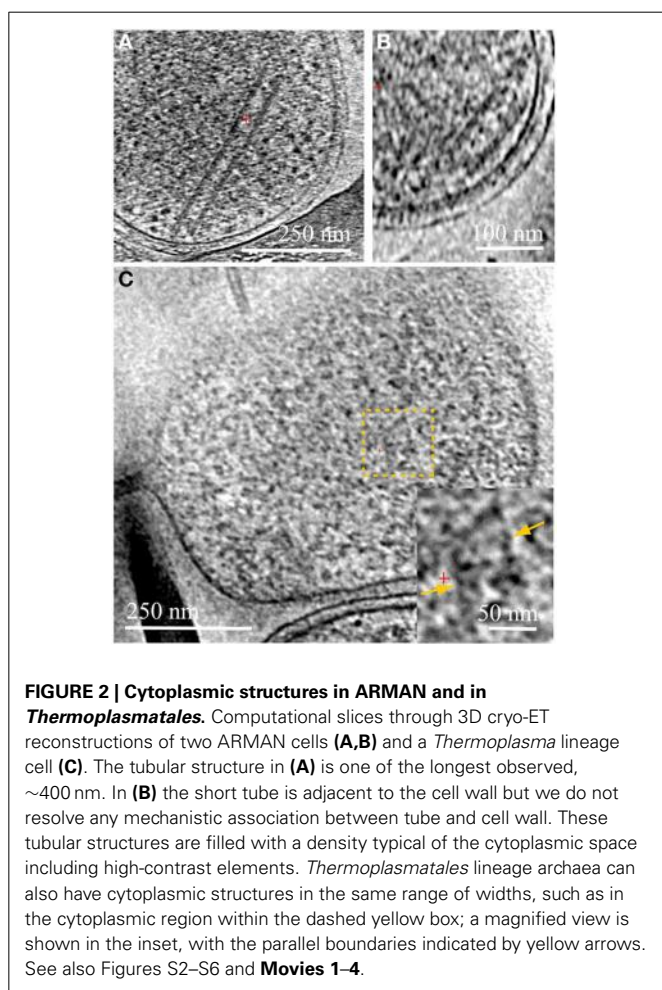


FIGURE 2 | Cytoplasmic structures in ARMAN and in *Thermoplasmatales*. Computational slices through 3D cryo-ET reconstructions of two ARMAN cells (**A,B**) and a *Thermoplasma* lineage cell (**C**). The tubular structure in (**A**) is one of the longest observed, ~400 nm. In (**B**) the short tube is adjacent to the cell wall but we do not resolve any mechanistic association between tube and cell wall. These tubular structures are filled with a density typical of the cytoplasmic space including high-contrast elements. *Thermoplasmatales* lineage archaea can also have cytoplasmic structures in the same range of widths, such as in the cytoplasmic region within the dashed yellow box; a magnified view is shown in the inset, with the parallel boundaries indicated by yellow arrows. See also Figures S2–S6 and **Movies 1–4**.

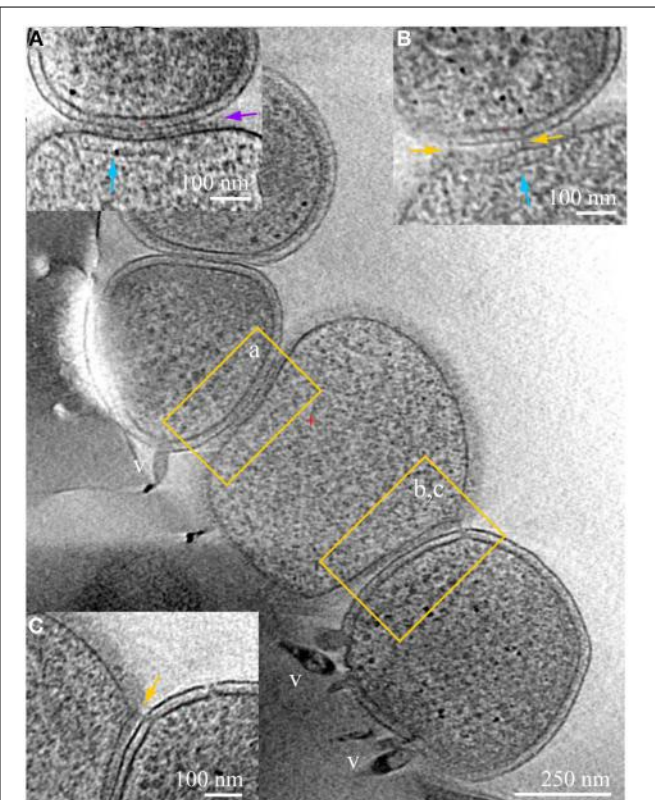


FIGURE 3 | ARMAN–*Thermoplasmatales* inter-species associations and viral infection processes. Slices from a 3D cryo-ET reconstruction of a colony of cells showing contacts and associations between a *Thermoplasmatal* lineage cell (center, no cell wall) and two ARMAN cells infected with viruses (gram-negative like cell wall, top left, and bottom right). Insets represent slices at different orientations, of the regions within yellow boxes in the main z-slice. In inset (**A**) the cell surfaces are in tight contact, with a distinct line of density at the interface pointed by the purple arrow. *Thermoplasma* lineage archaea cells engaged in this type of association typically have a cytoplasmic band of density parallel to the plasma membrane, indicated here by the vertical blue arrow. These features resemble, to some extent, bacterial chemotaxis apparatus (Milne and Subramaniam, 2009), but AMD *Thermoplasmatales* lineage archaea have no identified chemotaxis genes. Inset (**B**) is a slice at an orientation that exactly contains a filamentous connection between the cells that clearly crosses the cell wall; the same band of density as in (**B**) is indicated by a blue arrow. Inset (**C**) is another slice of the same region, at different coordinates (z-height and angles), with pili-like connections through the cell wall. The ARMAN cells involved in the interactions shown in insets (**A–C**) are infected by rod-shape and lemon shaped viruses some of which are clear and labeled “v.” See also Figures S2–S6 and **Movie 4**.

covered with a 5–7 nm thick periodic layer inferred to be an S-layer. *Thermoplasma* lineage cell typically form “buds” which are released from the original cell (Huber and Stetter, 2006). See also Figure S3.

We consistently observe large tubular structures within ARMAN (Comolli et al., 2009; **Figure 2**; **Movie 3**). We have also observed structures in the cytoplasmic space of *Thermoplasmatales* lineage archaea (**Figure 2**). However, we have not resolved whether they are involved in interspecies connections.

Physical contacts are commonly observed, often involving more than two cells (**Figure 3**). Large areas of cell surfaces are in very close contact in some instances. We detected Velcro-like or zipped surface densities at some interfaces, as in inset (a). The same surfaces in contact are also linked by pili-like fibers, as in inset (b), and by appendages connecting *Thermoplasmatales* lineage archaea that through ARMAN cell wall, as in inset (c).

Another type of prevalent association is established over sub-micron scale distances via a long tubular structure formed by a *Thermoplasmatales* lineage archaea cell, as in **Figures 4, 5A–C**. These tubular structures have a diameter equal or larger than the synapse of **Figure 1**, and they completely penetrate through the cell walls of ARMAN. In some cases, as in **Figure 5**, we have identified flagella on the *Thermoplasmatales* lineage archaea, narrowing the possible lineages to either A or E plasmas (based on genome prediction; Yelton et al., 2013). It is thus plausible that each lineage of *Thermoplasmatales* uses a specific mode of interaction.

We observed a variety of other intriguing, but still enigmatic associations. For example, some ARMAN cells are penetrated by long, thick pili that extend from other organisms

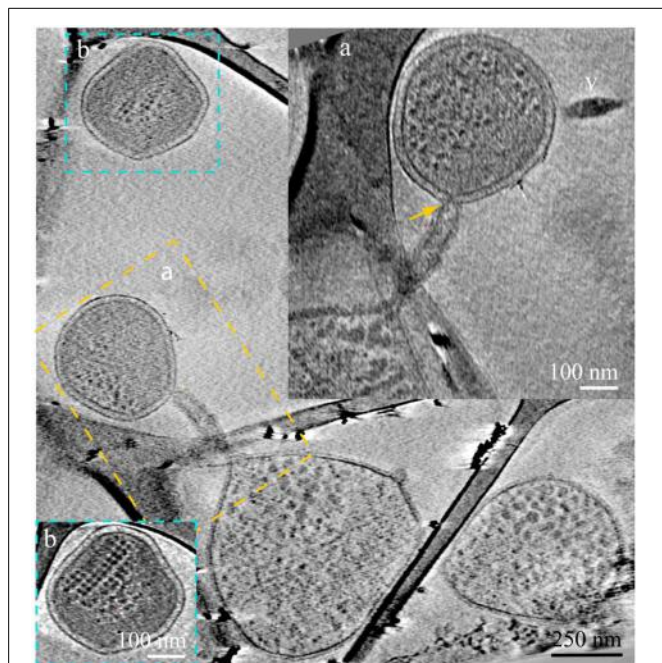


FIGURE 4 | ARMAN–*Thermoplasmatales* inter-species associations and viral infection processes. Slices from a 3D cryo-ET reconstruction. A *Thermoplasmatales* cell and an ARMAN cell—enclosed within the dash yellow box, are connected through a remarkable tubular appendage; the region within the dash yellow box is magnified as inset (A) in a slice at a different angle. The “arm-shape” connection extends the *Thermoplasmatales* cytoplasmic compartment and punctures the cell wall of ARMAN establishing an inter-species cytoplasmic bridge (yellow arrow). An elongated virus is partially in plane to the right (v). The cell within the blue box is shown in inset (B) in a slice at a different angle. The very regular ladder-like series of high contrast elements are putative polysomes. These cells are of an unknown species and are often found connected to *Thermoplasmatales* cells through pili, as shown in **Figure 6** with more detail.

(**Figures 6A–C**). Other very small, compact cells of unknown identity, studded with cytoplasmic ladder-like structures (hypothetically polysomes, **Figure 6**), were observed to establish connections with much larger cells (**Figures 6C,D**).

We very frequently detected viruses infecting the ARMAN cells, in general of two different morphotypes, based on distinct virus particle morphology. In some cases we observe a thick surface density layer on the *Thermoplasmatales* lineage archaea cells that are associated with ARMAN cells infected by viruses, but no regular S-layers (**Figure 3**). *Thermoplasmatales* lineage archaea cells also often had surface-attached viral particles. The viruses that infect ARMAN and the viruses that infect *Thermoplasmatales* lineage archaea are morphologically distinct.

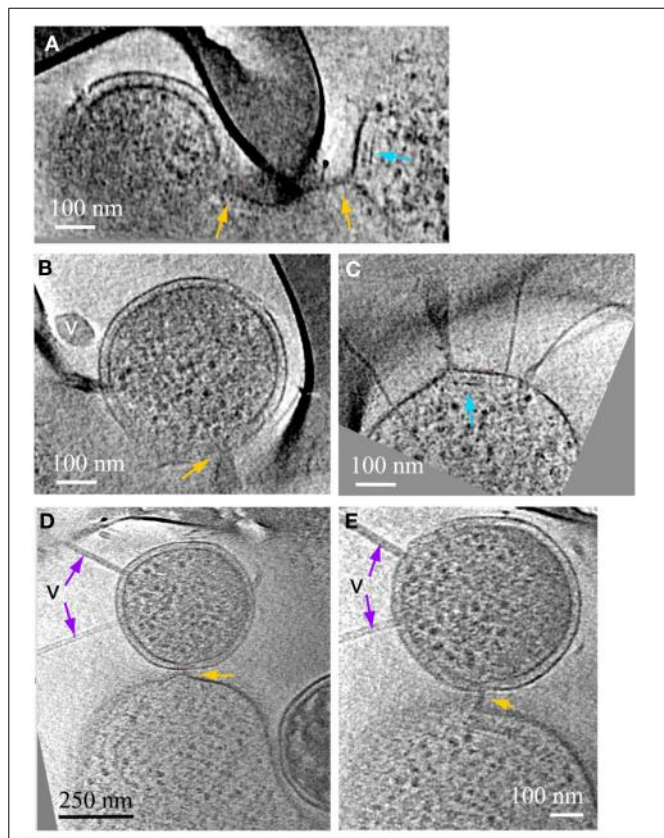


FIGURE 5 | ARMAN–*Thermoplasmatales* inter-species associations and viral infection processes. Slices from a 3D cryo-ET reconstruction. (A–C) are computational slices at different orientations through an ARMAN and a *Thermoplasmatales* lineage archaea cell connected through a cytoplasmic bridge. In (A) the cytoplasmic bridge is directly under a grid bar with ARMAN to the left and the plasma cell to the right respectively. The blue arrow points to a band, within the cytoplasmic space, adjacent to the connection. (B) The ARMAN cell in (A); the yellow arrow points to the cytoplasmic side of the connection; the ARMAN cell is infected by a virus (v) of a different morphotype than in **Figure 4**. (C) The *Thermoplasmatales* lineage cell in (A); the putative flagella indicates the plasma cell is either (A or E); for instance, see above and to the right of the feature indicated with the blue arrow. (D,E) Are slices through a different type of ARMAN (top)-*Thermoplasmatales* (bottom) lineage archaea association. The ARMAN cell, top, is infected by rod-shape viruses (v) indicated by purple arrows and the connection (yellow arrow) is a short and thick line of density.

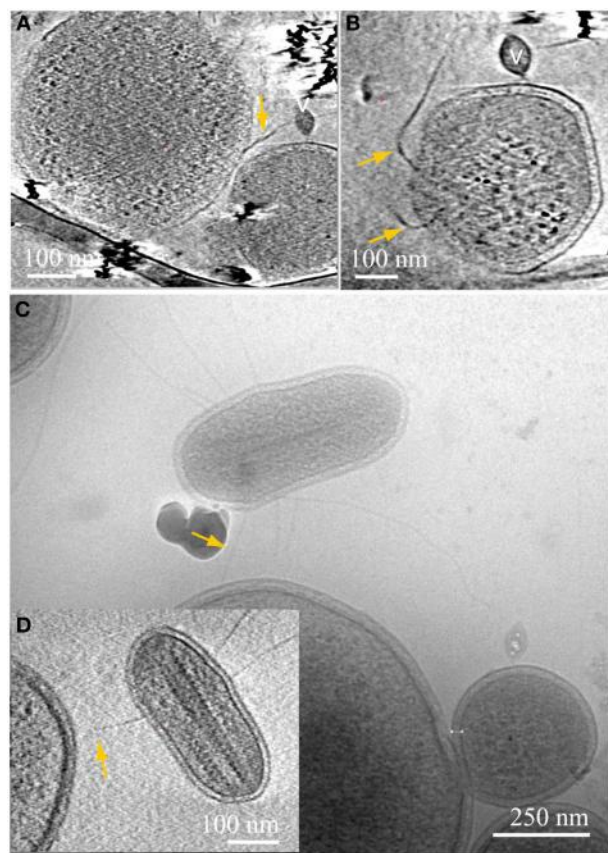


FIGURE 6 | Inter-species associations through pili. Computational slices through 3D cryo-ET reconstructions of an archaea (**A**), connected to the center of an ARMAN cell, bottom right, through thick pili; the ARMAN cell sliced through a different angle is magnified in (**B**). The complete trajectory can be followed in 3D but falls out of plane in these sections. (**C**) 2D cryo-TEM projection and inset (**D**) slice through 3D cryo-ET reconstruction of an unknown archaeal cell with large putative polysomes, as in inset (**B**) of **Figure 4**. The microorganism is connected through putative pili indicated by yellow arrows to a large cell. See also **Movies 5, 6**.

The Thermoplasmatales-related cells also had viruses attached to their putative pili (**Figure 7**).

DISCUSSION

Because thin, small samples were obtained directly from the natural environment and instantly frozen as fragments of biofilm, the cryo-TEM imaging and 3D cryo-ET reconstructions show us microorganisms in their mutual relationships with the intact ultrastructure, in the full context of their mutual relationships. We detected a variety of physical connections amongst uncultivated archaeal cells, include synapse-like connections, connections between cytoplasmic spaces through tubular structures, needle-like penetration of ARMAN's cell wall by *Thermoplasmatales* lineage archaea (Comolli et al., 2009), Velcro-like contacts and string-like attachments between their cell boundaries. These may enable cells from distinct phyla to share small molecules as well as larger proteins. Alternatively, rather than symbiotic, the association may be predatory. All

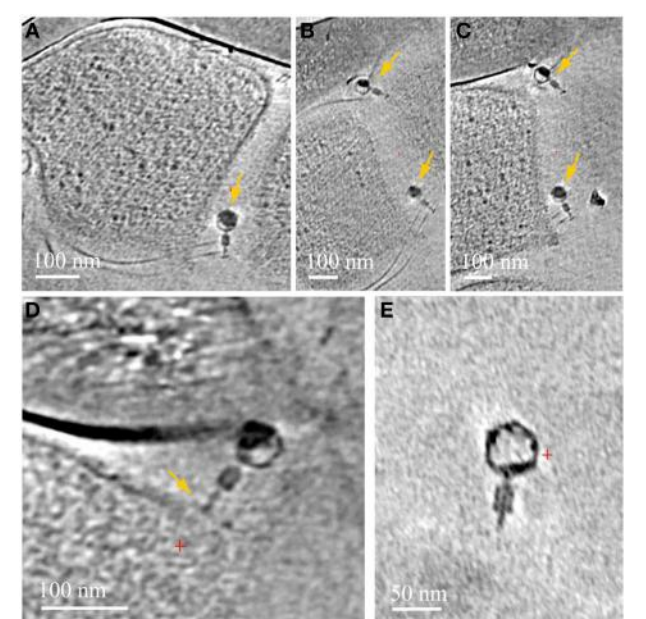


FIGURE 7 | Associations between viruses and *Thermoplasmatales* pili. Computational slices through 3D cryo-ET reconstructions of *Thermoplasmatales* lineage archaea associated with viruses. (**A**) A virus attached to pili, close to the cell surface; (**B,C**) two slices at different heights and angles through the same reconstruction as in (**A**), with two viruses attached to pili, yellow arrows. Pili are very thin and a series of slices are needed to capture them, and the viruses, in-plane of the slices respectively. The top and bottom viruses are shown in Supplementary Information **Movies 7, 8** respectively. (**D**) a virus attached to a cell surface. (**E**) A free virus.

Thermoplasmatales lineage archaea except for Fer1 have S-layer genes and most lack flagella genes; cells in **Figures 5, 6** can only be A or E plasma, which have complete sets of flagella genes.

ARMAN cells are typically found in AMD microbial communities that include *Thermoplasmatales* lineage archaea cells. Given the tiny size of the ARMAN genome (~1 Mb), and it's apparently lack of many biosynthetic pathways, some level of dependence of ARMAN on the larger archaea seems likely. Systems-biology tools are revealing networks of interacting microorganisms (e.g., Fuhrman, 2009). A pivotal question in evolutionary biology is the emergence of cooperative traits and their sustainment in the presence of free-riders. In order to understand how cooperation can emerge and be maintained, Cremer et al. proposed various strategies of spatial distribution within biofilms (Cremer et al., 2012). They found that "demographic noise during population bottlenecks creates a broad distribution in the relative abundance of cooperators and free riders. The growth advantage of more cooperative subpopulations implies an asymmetric amplification of fluctuations and possibly yields to an increase of cooperation in the whole population (group-growth mechanism)." Their analysis shows that this can enable a single cooperative mutant to spread in the population which then, mediated by the dynamics, reaches a stationary state with coexisting cooperators and free-riders (Cremer et al., 2012). It seems unlikely that ARMAN behave as free-riders, since *Thermoplasmatales* lineage cells create many of the physical connections; at the same time,

ARMAN likely depends on other archaea as discussed above. The ultrastructural survey presented here establishes physical architectures underlying networks and enabling metabolic exchange between microorganisms. A new capability will be needed to prove, with subcellular resolution, the exact molecular nature of these interactions.

The capacity for recognition, which must be essential for formation of the associations observed here, is likely embedded in the macromolecular surface assemblies, pili, and other sensory apparatus. Tackling questions related to interspecies interactions is important for understanding the environmentally and medically important process of biofilm formation. There, a cooperating collective of microorganisms runs the risk to be undermined by members that do not contribute to the metabolically costly task of biofilm polymer formation. It is notable that the findings of the current study center on interspecies interactions that do not produce a “common good” (such as the constituents of the biofilm architecture). Rather, all associations are cell-to-cell. An implication of the observed associations is that the microorganisms involved almost certainly co-evolve.

The tendency of certain archaeal cells to establish inter-species interactions has gone largely undetected until recently. *Pyrococcus furiosus* and *Pyrodictium* have been shown to connect through flagella and cannulae respectively (Nickell et al., 2003; Nätter et al., 2006). The two archaea *Ignicoccus hospitalis* and *Nanoarchaeum equitans* form an intimate association, the character of which is not yet fully understood (Jahn et al., 2008). Cryo-TEM show that at least two modes of cell-cell interactions exist: (i) the two cells are interconnected via thin fibers; and (ii) the two cell surfaces are in direct contact with each other (Junglas et al., 2008). Although *N. equitans* obtains lipids and aminoacids from its host, no direct cytoplasmic connection has been observed (Jahn et al., 2008). It is often the case with archaea, extremophiles, and intact microbial communities that singular novel observations precede our ability to provide complete functional interpretations; another intriguing example in this context is the structural appendage named “hamus” (Moissl et al., 2005), involved in archaeal cells adhesion and anchoring.

Dubey and Ben-Yehuda (2011) showed that nanotubes can form between *Bacillus subtilis* cells, enabling bacteria to transfer proteins and genetic material between them. They also show the capacity of *Bacillus subtilis* to transfer proteins to *Staphylococcus aureus* and to *Escherichia coli*, different species of bacteria. While this was shown in *in-vitro* experiments these results clearly suggest the potential for this type of communication is present in biofilms, enabling bacteria to adapt to adverse conditions collectively.

Archaea can have unique cell envelopes, lacking any component outside the cytoplasmic membrane other than surface proteins, S-layers, or glycoproteins (Albers and Meyer, 2011). One of the possible consequences or attributes of the unique archaeal cell wall structure may be this ability to recognize interacting partners, to readily and actively deform and extend through space, crossing through occluding objects in biofilms, and to puncture into the cytoplasmic space of interacting partners. These structures suggest an active mechanism of reaching out, searching and penetrating ARMAN cells by *Thermoplasmatales* lineage archaea.

We observed many archaeal pili associated with viruses. Laboratory work has shown the capacity of bacteriophage to use bacterial pili as an “alternative mechanism” available for infection (Guerrero-Ferreira et al., 2011). Our cryo-TEM data suggest this interaction may also occur between archaea and their viruses. Pili have been known to mediate in cell-to-cell connections, genetic recombination, and attachments. Yet we find the extent of the physical contacts established by pili, and the range of inter-species bridged by them, including viral-microbes interaction, to warrant a new examination from an ecological and evolutionary perspective. Pili may guide them toward the host cell or provide a direct access route for viral DNA. Alternatively, pili may trap viral particles and thus serve as part of the viral defense mechanism of the host cells.

The findings of the current study reinforce the idea that our limited ability to cultivate microorganisms, and thus to understand them, rests with interdependence on other organisms. The study of microbes in their intact natural context enables evidence for such associations to be detected. Ultrastructural characterization of uncultivated cells from novel lineages also reveals the existence of features (possibly organelles) whose functions and biosynthetic capacities are unknown.

METHODS

CRYO-EM SPECIMEN PREPARATION

For cryo-transmission electron microscope characterization, aliquots of 5 μ l were taken directly from fresh biofilm samples and placed onto lacey carbon grids (Ted Pella 01881) that were pre-treated by glow-discharge. The support grids were pre-loaded with 10 nm colloidal gold particles. The Formvar support was not removed from the lacey carbon. The grids were manually blotted and plunged into liquid ethane by a compressed air piston, then stored in liquid nitrogen. For electron microscopy at room temperature, 5 μ l aliquots were placed on glow-discharged Formvar carbon coated grids (Ted Pella 01811), then the grids were blotted and air dried. Samples were carefully transported to the laboratory bench for cryo-plunging within the same day; samples were also cryo-plunged inside the IMM, as previously described (Supplementary Information; Comolli et al., 2011; Knierim et al., 2011). For more details see Comolli et al. (2009, 2011); Baker et al. (2010); Yelton et al. (2013). Supplementary Information Figures S1–S6 provide a useful survey from sampling to cryo-TEM images of complex regions with healthy and dead cells.

CRYO-ELECTRON TOMOGRAPHIC IMAGING

Samples were transferred from the liquid nitrogen storage to the electron microscope sample holder for data acquisition. Images were acquired on a JEOL-3100 transmission electron microscope equipped a FEG electron source operating at 300 kV, an Omega energy filter, a Gatan 795 2 \times 2 K CCD camera, and cryo-transfer stage. The stage was cooled using liquid nitrogen to 80 K.

In order to have a statistically relevant survey of cell sizes and morphologies, over 800 images or 2D projections were recorded using magnifications of 36, 30, and 25 Kx at the CCD, giving a pixel size of 0.83, 1.0, or 1.2 nm at the specimen, respectively. Underfocus values ranged between $8 \pm 0.5 \mu\text{m}$ and $14 \pm 0.5 \mu\text{m}$, and energy filter widths were typically around $22 \pm 2 \text{ eV}$. The survey of the grids and the selection of suitable targets for tilt series

acquisition were done in low dose diffraction mode through the acquisition of hundreds of images. For a discussion on electron dose and radiation damage see (Knierim et al., 2011).

Tomographic tilt series were acquired under low dose conditions, typically over an angular range between +65 and -65°, ± 5° with increments of 1 or 2°. Between 70 and 124 images were recorded for each series. A total of 69 3D data sets were obtained: 11 tilt series were acquired manually with the program Digital Micrograph (Gatan, Inc.), and 58 tilt series were acquired semi-automatically with the program Serial-EM (<http://bio3d.colorado.edu/>) adapted to JEOL microscopes. All images were recorded using a magnification of 36, 30, or 25 Kx at the CCD giving a pixel size of 0.833, 1.0, or 1.2 nm at the specimen respectively. Underfocus values ranged between 9 ± 0.5 μm to 16 ± 0.5 μm, depending on the goal of the data set, and energy filter widths ranged between 22 to 28 eV, also depending on the data set. For all data sets the maximum dose used per complete tilt series was ~150 e-/Å², with typical values of ~100 e-/Å².

It is important to clarify that cryo-TEM imaging is limited to a thickness of ~750 nm or less; while ARMAN and small bacteria fall well within this range, larger microorganisms can exceed this limit; complex, rich areas of biofilms are certainly thicker and thus not accessible to this methodology. Although in the current sampling we have observed a percentage of ~30% ARMAN involved in interactions and inter-connections, only a large scale effort using different technologies can provide a reliable estimate. The signal-to-noise for a fixed dose is in inverse relationship to sample thickness; consequently our resolution is lower for larger microorganisms and complex regions of biofilms. Many of these limitations could be overcome in the future with cryo-sectioning. It would currently not be scientifically rigorous to extrapolate from direct cryo-TEM of sufficiently transparent, microscopic areas of biofilms, to the whole system of biofilms covering geographical scales. Instead, these observations and the linking between genomics and cryo-TEM advanced in this manuscript underlie the need to leverage a multidisciplinary approach to these questions (the core motivation of this Frontiers Special Topic). For instance, a large scale effort linking cryo-TEM, FIB sections and cryo-TEM, FIB SEM milling, plastic sections TEM, light microscopy and correlative FISH-cryo-TEM would be a natural next step.

IMAGE PROCESSING AND ANALYSES

All tomographic reconstructions were obtained with the program Imod (<http://bio3d.colorado.edu/>). The program ImageJ (NIH, <http://rsb.info.nih.gov/ij/>) was used for analysis of the two-dimensional image projections. Volume rendering and image analysis of tomographic reconstructions was done using the program VisIt (<http://www.llnl.gov/visit>). All movies were done with the package ffmpeg (www.ffmpeg.org).

AUTHOR CONTRIBUTIONS

Study conception and experimental design: Luis R. Comolli and Jill F. Banfield. Cryo-TEM data acquisition, processing, and analysis: Luis R. Comolli. Linking “Omics” with imaging data: Jill F. Banfield. Integrated data survey and analysis: Jill F. Banfield and Luis R. Comolli. Writing and editing of the manuscript: Luis R. Comolli and Jill F. Banfield.

ACKNOWLEDGMENTS

This work was performed at Lawrence Berkeley National Laboratory, with support from the Office of Science, Office of Basic Energy Sciences, Biological and Environmental Research, of the U.S. Department of Energy under Contract No. DE-AC02-05CH11231. This work was funded by Laboratory Directed Research and Development support from the University of California, Lawrence Berkeley National Laboratory and by the US Department of Energy’s Office of Science, Biological and Environmental Research Program (DOE Genomics: GTL project Grant DE-FG02-05ER64134), the National Aeronautics and Space Administration Astrobiology Institute, The sequencing was provided through the Community Sequencing Program at the Department of Energy Joint Genome Institute.

SUPPLEMENTARY MATERIAL

The Supplementary Material for this article can be found online at: <http://www.frontiersin.org/journal/10.3389/fmicb.2014.00367/abstract>

Movie 1 | Compressed view of the cryo-ET reconstruction of a *Thermoplasmatales* cell; a high quality slice through the 3D reconstruction is shown in Figure S1A.

Movie 2 | Compressed view of the cryo-ET reconstruction of a *Thermoplasmatales* cell; a high quality slice through the 3D reconstruction is shown in Figure S1B.

Movie 3 | Volumen-rendered view of a 3D section from a cryo-ET reconstruction of ARMAN cells. A large tubular structure is seen in the center. See also main text **Figure 2**.

Movie 4 | *Thermoplasmatales*, ARMAN, and interconnections. Compressed view of the cryo-ET reconstruction of associated and inter-connected Tpl and ARMAN shown in **Figure 3** of the main manuscript.

Movie 5 | Compressed view of the cryo-ET reconstruction from which the slices shown in Figures 6A,B of were extracted.

Movie 6 | Compressed view of the cryo-ET reconstruction from which the slice shown in Figure 6D of was extracted.

Movie 7 | Compressed view of the cryo-ET reconstruction from which the slices shown in Figures 7A-C of were extracted. The virus is the top virus in those panels.

Movie 8 | Compressed view of the cryo-ET reconstruction from which the slices shown in Figures 7A-C of were extracted. The virus is the bottom virus in those panels.

REFERENCES

- Albers, S.-V., and Meyer, B. H. (2011). The archaeal cell envelope. *Nat. Rev. Microbiol.* 9, 414–425. doi: 10.1038/nmicro2576
- Albertsen, M., Hugenholtz, P., Skarszewski, A., Nielsen, K. L., Tyson, G. W., and Nielsen, P. H. (2013). Genome sequences of rare, uncultured bacteria obtained by differential coverage binning of multiple metagenomes. *Nat. Biotechnol.* 31, 533–538. doi: 10.1038/nbt.2579
- Aliaga-Goltsman, D. S., Denef, V. J., Singer, S. W., VerBerkmoes, N. C., Lefsrud, M., Mueller, R. S., et al. (2009). Community genomic and proteomic analyses of chemoautotrophic iron-oxidizing “*Leptospirillum rubarum*” (Group II) and “*Leptospirillum ferrodiazotrophum*” (Group III) Bacteria in acid mine drainage biofilms. *Appl. Environ. Microbiol.* 75, 4599–4615. doi: 10.1128/AEM.02943-08
- Baker, B. J., and Banfield, J. F. (2003). Microbial communities in acid mine drainage. *FEMS Microbiol. Ecol.* 44, 139–152. doi: 10.1016/S0168-6496(03)00028-X

- Baker, B. J., Comolli, L. R., Dick, G. J., Hauser, L., Land, M., VerBerkmoes, N. C., et al. (2010). Enigmatic, ultra-small uncultivated Archaea. *Proc. Natl. Acad. Sci. U.S.A.* 107, 8806–8811. doi: 10.1073/pnas.0914470107
- Baker, B. J., and Dick, G. J. (2013). Omic approaches in microbial ecology: charting the unknown. *Microbe* 8, 353–360. doi: 10.1128/microbe.8.353
- Baker, B. J., Tyson, G. W., Webb, R. I., Flanagan, J., Hugenholtz, P., and Banfield, J. F. (2006). Lineages of acidophilic archaea revealed by community genomic analysis. *Science* 314, 1933–1935. doi: 10.1126/science.1132690
- Campbell, J. H., O'Donoghue, P., Campbell, A. G., Schwientek, P., Sczyrba, A., Woyke, T., et al. (2013). UGA is an additional glycine codon in uncultured SR1 bacteria from the human microbiota. *Proc. Natl. Acad. Sci. U.S.A.* 110, 5540–5545. doi: 10.1073/pnas.1303090110
- Castelle, C. J., Hug, L. A., Wrighton, K. C., Thomas, B. C., Williams, K. H., Wu, D., et al. (2013). Extraordinary phylogenetic diversity and metabolic versatility in aquifer sediment. *Nat. Commun.* 4, 2120. doi: 10.1038/ncomms3120
- Comolli, L. R., Baker, B., Downing, K. H., Siegerist, C. E., and Banfield, J. (2009). Three-dimensional analysis of the structure and ecology of a novel, ultra-small archaeon. *ISME J.* 3, 159–167. doi: 10.1038/ismej.2008.99
- Comolli, L. R., Duarte, R., Baum, D., Luef, B., Downing, K. H., Larson, D., et al. (2011). A portable cryo-plunger for on-site intact cryogenic microscopy sample preparation in natural environments. *Microsc. Res. Techniq.* 75, 829–836. doi: 10.1002/jemt.22001
- Cremer, J., Melbinger, A., and Frey, E. (2012). Growth dynamics and the evolution of cooperation in microbial populations. *Sci. Rep.* 2, 281. doi: 10.1038/srep00281
- Di Renzi, S. C., Sharon, I., Wrighton, K. C., Koren, O., Hug, L. A., Ley, R. E. et-al (2013). The human gut and groundwater harbor non-photosynthetic bacteria belonging to a new candidate phylum sibling to Cyanobacteria. *ELife* 2:e01102. doi: 10.7554/eLife.01102
- Dubey, G. P., and Ben-Yehuda, S. (2011). Intercellular nanotubes mediate bacterial communication. *Cell* 144, 590–600. doi: 10.1016/j.cell.2011.01.015
- Edwards, K. J., Bond, L. P., Gehrung, T. M., and Banfield, J. F. (2000). An archaeal iron-oxidizing extreme acidophile important in acid mine drainage. *Science* 287, 1796–1799. doi: 10.1126/science.287.5459.1796
- Fuhrman, J. A. (2009). Microbial community structure and its functional implications. *Nature* 459, 193–198. doi: 10.1038/nature08058
- Golyshina, O. V., and Timmis, K. N. (2005). *Ferroplasma* and relatives, recently discovered cell wall-lacking archaea making a living in extremely acid, heavy metal-rich environments. *Environ. Microbiol.* 7, 1277–1288. doi: 10.1111/j.1462-2920.2005.00861.x
- Guerrero-Ferreira, R. C., Viollier, P. H., Elyc, B., Poindexter, J. S., Georgieva, M., Jensen, G. J., et al. (2011). Alternative mechanism for bacteriophage adsorption to the motile bacterium Caulobacter crescentus. *Proc. Natl. Acad. Sci. U.S.A.* 108, 9963–9968. doi: 10.1073/pnas.1012388108
- Hall-Stoodley, L., Costerton, J. W., and Stoodley, P. (2004). Bacterial biofilms: from the natural environment to infectious diseases. *Nat. Rev. Microbiol.* 2, 95–108. doi: 10.1038/nrmicro821
- Huber, H., and Stetter, K. O. (2006). “Thermoplasmatales,” in *The Prokaryotes*, eds S. Falkow, E. Rosenberg, K.-H. Schleifer, and E. Stackebrandt (M. Dworkin, Editor-in-Chief) (Berlin: Springer-Verlag), 101–112.
- Jahn, U., Gallenberger, M., Paper, W., Junglas, B., Eisenreich, W., Stetter, K. O., et al. (2008). *Nanoarchaeum equitans* and *Ignicoccus hospitalis*: new insights into a unique, intimate association of two archaea. *J. Bacteriol.* 190, 1743–1750. doi: 10.1128/JB.01731-07
- Junglas, B., Briegel, A., Burghardt, T., Walther, P., Wirth, R., Huber, H., et al. (2008). *Ignicoccus hospitalis* and *Nanoarchaeum equitans*: ultrastructure, cell-cell interaction, and 3D reconstruction from serial sections of freeze-substituted cells and by electron cryotomography. *Arch. Microbiol.* 190, 395–408. doi: 10.1007/s00203-008-0402-6
- Kantor, R. S., Wrighton, K. C., Handley, K. M., Sharon, I., Hug, L. A., Castelle, C. J., et al. (2013). Bacteria from four candidate phyla metabolisms of sediment-associated bacteria from four candidate phyla. *mBio* 4, e00708–e00713. doi: 10.1128/mBio.00708-13
- Knierim, B., Luef, B., Wilmes, P., Auer, M., Webb, R. I., Comolli, L. R., et al. (2011). Correlative microscopy for phylogenetic and ultrastructural characterization of microbial communities. *Environ. Microbiol. Rep.* 4, 36–41. doi: 10.1111/j.1758-2229.2011.00275.x
- Luef, B., Fakra, S. C., Csencsits, R., Wrighton, K. C., Williams, K. H., Wilkins, M. J., et al. (2012). Iron-reducing bacteria accumulate ferric oxyhydroxide nanoparticle aggregates that may support planktonic growth. *ISME J.* 7, 338–350. doi: 10.1038/ismej.2012.103
- Milne, J., and Subramaniam, S. (2009). Cryo-electron tomography of bacteria: progress, challenges and future prospects. *Nat. Rev. Microbiol.* 7, 666–675. doi: 10.1038/nrmicro2183
- Moissl, C., Rachel, R., Ariane Briegel, A., Engelhardt, A., and Huber, R. (2005). The unique structure of archaeal ‘hami’, highly complex cell appendages with nano-grappling hooks. *Mol. Microbiol.* 56, 361–370. doi: 10.1111/j.1365-2958.2005.04294.x
- Moissl, C., Rudolph, C., and Huber, R. (2002). Natural communities of novel archaea and bacteria with a string-of-pearls-like morphology: molecular analysis of the bacterial partners. *Appl. Environ. Microbiol.* 68, 933–937. doi: 10.1128/AEM.68.2.933-937.2002
- Näther, D. J., Reinhard, R., Wanner, G., and Wirth, R. (2006). Flagella of *Pyrococcus furiosus*: multifunctional organelles, made for swimming, adhesion to various surfaces, and cell-cell contacts. *J. Bacteriol.* 188, 6915. doi: 10.1128/JB.00527-06
- Nickell, S., Hegerl, R., Baumeister, W., and Reinhard, R. (2003). *Pyrodictium caninulae* enter the periplasmic space but do not enter the cytoplasm, as revealed by cryo-electron tomography. *J. Struct. Biol.* 141, 34–42. doi: 10.1016/S1047-8477(02)00581-6
- Rinke, C., Schwientek, P., Sczyrba, A., Ivanova, N. N., Anderson, I. J., Cheng, J.-F., et al. (2013). Insights into the phylogeny and coding potential of microbial dark matter. *Nature* 99, 431–437. doi: 10.1038/nature12352
- Rudolph, C., Wanner, G., and Huber, R. (2001). Natural communities of novel archaea and bacteria growing in cold sulfurous springs with a string-of-pearls-like Morphology. *Appl. Environ. Microbiol.* 67, 2336–2344. doi: 10.1128/AEM.67.5.2336-2344.2001
- Sanchez, C. (2011). Cellular microbiology: bacterial networking. *Nat. Rev. Microbiol.* 9, 229. doi: 10.1038/nrmicro2543
- Simmons, S. L., DiBartolo, G., Denef, V. J., Goltsman, D. S. A., Thelen, M. P., and Banfield, J. F. (2008). Population genomic analysis of strain variation in Leptospirillum group II bacteria involved in acid mine drainage formation. *PLoS Biol.* 6:e177. doi: 10.1371/journal.pbio.0060177
- Sharon, I., Morowitz, M. J., Thomas, B. C., Costello, E. K., Relman, D. A., and Banfield, J. F. (2013). Time series community genomics analysis reveals rapid shifts in bacterial species, strains, and phage during infant gut colonization. *Genome Res.* 23, 111–120. doi: 10.1101/gr.142315.112
- Tyson, G. W., Chapman, J., Hugenholtz, P., Allen, E. E., Ram, J. R., Richardson, P. M., et al. (2004). Community structure and metabolism through reconstruction of microbial genomes from the environment. *Nature* 428, 37–43. doi: 10.1038/nature02340
- Yasuda, M., Oyaizu, H., Yamagishi, A., and Oshima, T. (1995). Morphological variation of new *Thermoplasma acidophilum* isolates from Japanese hot springs. *Appl. Environ. Microbiol.* 61, 3482–3485.
- Wrighton, K. C., Thomas, B. C., Sharon, I., Miller, C. S., Castelle, C. J., VerBerkmoes, N. C., et al. (2012). Fermentation, hydrogen, and sulfur metabolism in multiple uncultivated bacterial phyla. *Science* 337, 1661–1665. doi: 10.1126/science.1224041
- Yelton, A. P., Comolli, L. R., Castelle, C., Justice, N., Denef, V. J., Thomas, B. C., et al. (2013). Comparative genomics in acid mine drainage biofilm communities reveals metabolic and structural differentiation of co-occurring archaea. *BMC Genomics* 14:485. doi: 10.1186/1471-2164-14-485
- Conflict of Interest Statement:** The authors declare that the research was conducted in the absence of any commercial or financial relationships that could be construed as a potential conflict of interest.
- Received:** 11 March 2014; **accepted:** 01 July 2014; **published online:** 25 July 2014.
- Citation:** Comolli LR and Banfield JF (2014) Inter-species interconnections in acid mine drainage microbial communities. *Front. Microbiol.* 5:367. doi: 10.3389/fmicb.2014.00367
- This article was submitted to Terrestrial Microbiology, a section of the journal *Frontiers in Microbiology*.
- Copyright © 2014 Comolli and Banfield. This is an open-access article distributed under the terms of the Creative Commons Attribution License (CC BY). The use, distribution or reproduction in other forums is permitted, provided the original author(s) or licensor are credited and that the original publication in this journal is cited, in accordance with accepted academic practice. No use, distribution or reproduction is permitted which does not comply with these terms.



Temporal dynamics of fibrolytic and methanogenic rumen microorganisms during *in situ* incubation of switchgrass determined by 16S rRNA gene profiling

Hailan Piao¹, Medora Lachman², Stephanie Malfatti³, Alexander Sczyrba⁴, Bernhard Knierim⁵, Manfred Auer⁵, Susannah G. Tringe⁶, Roderick I. Mackie⁷, Carl J. Yeoman² and Matthias Hess^{1,6,8*}

¹ Systems Microbiology and Biotechnology Group, School of Molecular Biosciences, Washington State University, Richland, WA, USA

² Department of Animal and Range Sciences, Montana State University, Bozeman, MT, USA

³ Lawrence Livermore National Laboratory, Biosciences and Biotechnology Division, Livermore, CA, USA

⁴ Faculty of Technology and Center for Biotechnology, Bielefeld University, Bielefeld, Germany

⁵ Lawrence Berkeley National Laboratory, Life Sciences Division, Berkeley, CA, USA

⁶ Prokaryote Super Program, DOE Joint Genome Institute, Walnut Creek, CA, USA

⁷ Department of Animal Sciences and Institute for Genomic Biology, University of Illinois, Urbana-Champaign, IL, USA

⁸ Energy and Efficiency Division, Chemical and Biological Process Development Group, Pacific Northwest National Laboratory, Richland, WA, USA

Edited by:

Luis Raul Comolli, Lawrence Berkeley National Laboratory, USA

Reviewed by:

William John Kelly, AgResearch Ltd., New Zealand

Etinosa Igbinosa, University of Benin, Nigeria

***Correspondence:**

Matthias Hess, Systems Microbiology and Biotechnology Group, School of Molecular Biosciences, Washington State University, 2710 Crimson Way, Richland, WA 99354-1671, USA
e-mail: mhess@lbl.gov

The rumen microbial ecosystem is known for its biomass-degrading and methane-producing phenotype. Fermentation of recalcitrant plant material, comprised of a multitude of interwoven fibers, necessitates the synergistic activity of diverse microbial taxonomic groups that inhabit the anaerobic rumen ecosystem. Although interspecies hydrogen (H_2) transfer, a process during which bacterially generated H_2 is transferred to methanogenic Archaea, has obtained significant attention over the last decades, the temporal variation of the different taxa involved in *in situ* biomass-degradation, H_2 transfer and the methanogenesis process remains to be established. Here we investigated the temporal succession of microbial taxa and its effect on fiber composition during rumen incubation using 16S rRNA amplicon sequencing. Switchgrass filled nylon bags were placed in the rumen of a cannulated cow and collected at nine time points for DNA extraction and 16S pyrotag profiling. The microbial community colonizing the air-dried and non-incubated (0 h) switchgrass was dominated by members of the *Bacilli* (recruiting 63% of the pyrotag reads). During *in situ* incubation of the switchgrass, two major shifts in the community composition were observed: *Bacilli* were replaced within 30 min by members belonging to the *Bacteroidia* and *Clostridia*, which recruited 34 and 25% of the 16S rRNA reads generated, respectively. A second significant shift was observed after 16 h of rumen incubation, when members of the *Spirochaetes* and *Fibrobacteria* classes became more abundant in the fiber-adherent community. During the first 30 min of rumen incubation ~13% of the switchgrass dry matter was degraded, whereas little biomass degradation appeared to have occurred between 30 min and 4 h after the switchgrass was placed in the rumen. Interestingly, methanogenic members of the *Euryarchaeota* (i.e., *Methanobacteria*) increased up to 3-fold during this period of reduced biomass-degradation, with peak abundance just before rates of dry matter degradation increased again. We hypothesize that during this period microbial-mediated fibrolysis was temporarily inhibited until H_2 was metabolized into CH_4 by methanogens. Collectively, our results demonstrate the importance of inter-species interactions for the biomass-degrading and methane-producing phenotype of the rumen microbiome—both microbially facilitated processes with global significance.

Keywords: rumen microbiology, microbe-microbe interactions, cellulolytic bacteria, methanogenic archaea, interspecies H_2 transfer

INTRODUCTION

The microbial community (microbiota) inhabiting the cow rumen has been described as “the most elegant and highly evolved cellulose-digesting system in nature” (Weimer et al., 2009). Cellulose, the most abundant natural polymer on earth

(Klemm et al., 2005), and a major component of plant biomass (Heredia et al., 1995) is degraded within the rumen by various bacteria (Weimer, 1996), fungi (Bauchop and Mountfort, 1981; Theodorou et al., 1996), and protozoa (Coleman, 1992). The efficacy of cellulose-degradation, and ultimately fiber-degradation, is

mediated by important microbial enzymatic and metabolic interactions and it has been shown that major cellulolytic bacteria, such as *Fibrobacter succinogenes*, *Ruminococcus flavefaciens*, and *Ruminococcus albus* (Weimer, 1996), exhibit suboptimal cellulolytic activity if they are not able to synergistically engage with non-cellulolytic microorganisms (Kudo et al., 1987; Fondevila and Dehority, 1996). In particular methanogenic archaea have been described to boost the carbohydrate-degrading activity of cellulolytic rumen bacteria (Joblin et al., 1989). The role of rumen methanogens is unique in that these organisms do not degrade or ferment any portion of plant biomass, but instead obtain their energy from byproducts, principally H₂ and CO₂, of fibrolytic organisms (Janssen and Kirs, 2008). By using hydrogen to reduce CO₂, methanogens remove otherwise inhibitory levels of H₂ (Janssen and Kirs, 2008), increase ATP yields by redirecting reducing equivalents toward acetate (Latham and Wolin, 1977) and thereby promote growth (Rychlik and May, 2000) and the ability to produce higher concentrations of fibrolytic enzymes. Physical co-aggregation between fibrolytic and methanogenic populations are commonly observed (i.e., Leahy et al., 2010) and this is thought to be important for both the efficient transfer of H₂ and maintaining the low H₂ partial pressures necessary to sustain active growth of the fermentative bacteria (Stams, 1994; Ishii et al., 2006).

To this end, the temporal dynamics of fibrolytic bacteria and methanogenic archaea remain to be systematically explored during *in situ* colonization and degradation of plant biomass within the rumen. Previous studies have shown temporal changes in bacterial (Edwards et al., 2007; Huws et al., 2013) and fungal (Edwards et al., 2008) populations during ruminal incubation of fresh perennial rye grass (*Lolium perenne*). Specifically, these studies revealed a rapid colonization of the plant material within 5 min of rumen-incubation by both bacterial (Edwards et al., 2007) and fungal populations, followed by a compositional shift in bacterial populations between 2 and 4 h following incubation (Huws et al., 2013). Compositional dynamics may vary among forage types based on observed differences in fiber disappearance and fibrolytic enzyme activities (Bowman and Firkins, 1993) and the observed temporal changes in microbiota may be affected by residual plant metabolism of fresh forages (Huws et al., 2013). Here we provide evidence that similar temporal changes occur during the *in situ* incubation of dried switchgrass and correspond to changes in methanogen abundance. Furthermore, these changes in microbiota also correspond to notable differences in the rate of forage degradation.

MATERIALS AND METHODS

SAMPLE COLLECTION

To enrich for fiber-adherent rumen microorganisms, air-dried switchgrass (*Panicum virgatum*) was ground into 2 mm pieces using a Wiley mill and weighed into individual *in situ* nylon bags (50 µm pores; Ankom Technology, Macedon, NY, USA). A total of 18 nylon bags, each containing 5 g of air-dried switchgrass, were placed in the rumen of one cannulated Friesian cow, fed on a mixed diet containing 60% fiber (Hess et al., 2011). Nylon bags were retrieved from the cow's rumen at 0.5, 1, 2, 4, 6, 16, 24, 48, and 72 h and washed immediately with

2 × 50 ml PBS buffer (pH7) to remove rumen fluid containing loosely adherent microbes, placed on dry-ice and transported immediately to the laboratory where DNA extraction and fiber degradation analysis were performed. Non-incubated nylon bags filled with ground switchgrass were used as control (0 h). To account for biological variation during the fiber colonization process, nylon bags were retrieved from the cow's rumen in duplicates. All animal procedures were carried out under an approved protocol with the University of Illinois Institutional Animal Care and Use of Animals Committee (IUCAC #06081).

FIBER DEGRADATION ANALYSIS

Relative biomass (switchgrass) degradation during rumen-incubation was determined by dry matter, organic matter, neutral detergent fiber (NDF), acid detergent fiber (ADF), and acid detergent lignin (ADL) analysis. NDF, ADF, and ADL were determined using the procedures of Goering and Van Soest (1970). Cellulose content was estimated as ADF–ADL and hemicellulose as NDF–ADF.

DNA EXTRACTION AND 16S rRNA GENE AMPLIFICATION

Total microbial genomic DNA was extracted from 100 mg of the non-incubated control sample and from each rumen-incubated biomass sample using a FastDNA SPIN Kit for Soil (MP Biomedical, Solon, OH) according to the manufacturer's instructions. Extracted DNA was quantified with a spectrophotometer (Nanodrop ND1000; Thermo Scientific, USA). The hypervariable V6 to V8 region of the 16S ribosomal RNA (rRNA) gene was amplified from the environmental DNA using the primer set 926F/1392R (926F: 5'- cct atc ccc tgt gtg cct tgg cag tct cag AAA CTY AAA KGA ATT GRC GG- 3' and 1392R: 5' - cca tct cat ccc tgc gtg tct ccg act cag xxxxx ACG GGC GGT GTG TRC – 3') described by Engelbrektson et al. (2010). Primer sequences were modified by the addition of 454 A or B adapter sequences (lower case). In addition, the reverse primer included a 5 bp barcode, indicated by xxxxx in the reverse primer sequence above, for multiplexing of samples during sequencing. The barcode sequence for each sample is listed in Table 1. The generated raw reads were deposited in NCBI's Short Read Archive under the accession number SRP042121.

Twenty-microliter PCR reactions were performed in duplicate and pooled to minimize PCR bias. PCR reaction was performed using 0.4 µl Advantage GC 2 Polymerase Mix (Advantage-2 GC PCR Kit, Clontech), 4 µl 5x GC PCR buffer, 2 µl 5 M GC Melt Solution, 0.4 µl 10 mM dNTP mix (MBI Fermentas), 1.0 µl of each 25 nM primer, and 10 ng sample DNA. The thermal cycler protocol was 95°C for 3 min, 25 cycles of 95°C for 30 s, 50°C for 45 s, and 68°C for 90 s, and a final 10 min extension at 68°C. PCR amplicons were purified using Solid Phase Reversible Immobilization (SPRI) beads and quantified using a Qubit fluorometer (Invitrogen). Samples were diluted to 10 ng/µl and mixed in equal concentrations. Emulsion PCR and sequencing of the PCR amplicons were performed following the Roche 454 GS FLX Titanium technology instructions provided by the manufacturer.

PYROTAG SEQUENCE ANALYSIS

Pyrosequencing data from the 20 samples were demultiplexed and processed using QIIME version 1.7.0 (Caporaso et al., 2010) according to the standard operating procedure described at <http://qiime.org/tutorials/tutorial.html>. Primers and barcodes were removed before the raw reads were quality filtered. Sequences were removed if they had long homopolymeric regions (>6 nt), were smaller than 200 nt, had quality scores lower than 25, or if they were identified as being chimeric. This resulted in a total of 198,037 high quality 16S rRNA gene sequences. Sequences generated from each of the biological duplicates were combined prior to sequence analysis to account for biological variation.

OTU-BASED SEQUENCE ANALYSIS

Sequences were clustered into operational taxonomic units (OTUs) at a 97% sequence identity cut-off using UCLUST (Edgar, 2010). The most abundant sequence of each OTU was picked as representative sequence. Singleton and doubleton abundance, Shannon, Simpson, Simpson reciprocal, and Chao1 estimators were calculated using the QIIME software. Representative sequences were aligned using the PyNAST algorithm and the alignment was filtered to remove common gaps. Following the quality filtering and grouping steps, 7,168 unique sequences (representing 198,037 total sequences) were used for OTU analyses. QIIME scripts were used to calculate α -diversity metrics for OTU representative sequences and to generate a Principal Coordinate

Analysis plot according to the standard operating procedure described at <http://qiime.org/tutorials/tutorial.html>.

TAXONOMIC CLASSIFICATION OF UNIQUE REPRESENTATIVE SEQUENCES

Taxonomic classification of the final set of representative sequences was performed using QIIME. Each sequence was normalized to contain six taxonomic levels, ranging from the domain to the genus level.

SCANNING ELECTRON MICROSCOPY

For scanning electron microscopy (SEM) pieces of switchgrass taken from the cow rumen as described above were immediately fixed with glutaraldehyde. The samples were washed several times with phosphate buffered saline, treated with 1% OsO₄ for 1 h on ice, prior to dehydration and critical point drying using a Tousimis Autosamdry-815 critical point dryer. The dried samples were then mounted on precut brass sample stubs using double sided carbon tape and sputter coated with approximately 30 Angstrom of Au/Pd. SEM imaging was performed on a Hitachi S-5000 microscope at 10 kV accelerating voltage.

RESULTS

TEMPORAL CHANGES IN α -DIVERSITY OF FIBER-ADHERENT RUMEN MICROBIOME

To determine α -diversity within the fiber-adherent community the quality-filtered pyrotag reads of each sample were clustered

Table 1 | Barcode sequences.

Sample ID	0h_A	0h_B	0.5h_A	0.5h_B	1h_A	1h_B	2h_A	2h_B	4h_A	4h_B
Barcode sequence	TGTAG	ATATG	CTACT	CATGC	CTGCG	CGATG	CGTAC	CACAG	TACTG	CGATG
Sample ID	6h_A	6h_B	16h_A	16h_B	24h_A	24h_B	48h_A	48h_B	72h_A	72h_B
Barcode sequence	TAGAG	TCTCG	TCATC	AGCAC	TCTAT	CACAG	TGCTG	CATGC	ATGCT	CACAG

Table 2 | Summary of pyrosequencing reads generated and OTUs observed for each time point sampled during this study.

Incubation time [h]	0	0.5	1	2	4	6	16	24	48	72	Total count
Raw reads	30,150	22,165	14,104	33,037	16,966	15,441	34,313	34,459	33,850	28,216	262,701
Quality filtered reads	26,888	16,119	10,270	23,892	12,234	11,690	26,059	25,771	25,373	19,741	198,037
OTUs observed	788	1,782	1,470	2,257	1,679	1,827	2,524	2,758	2,589	1,985	7,168

Table 3 | Phylogenetic assignment of OTUs at domain level.

Incubation time [h]	0	0.5	1	2	4	6	16	24	48	72	Total OTU count
Archaea	2	7	8	8	8	6	7	6	5	11	17
Bacteria	703	1,740	1,448	2,221	1,636	1,809	2,505	2,741	2,562	1,940	7,005
Unclassified	83	35	13	27	35	12	12	11	22	34	146
Number of OTUs observed	788	1,782	1,469	2,256	1,679	1,827	2,524	2,758	2,589	1,985	7,168

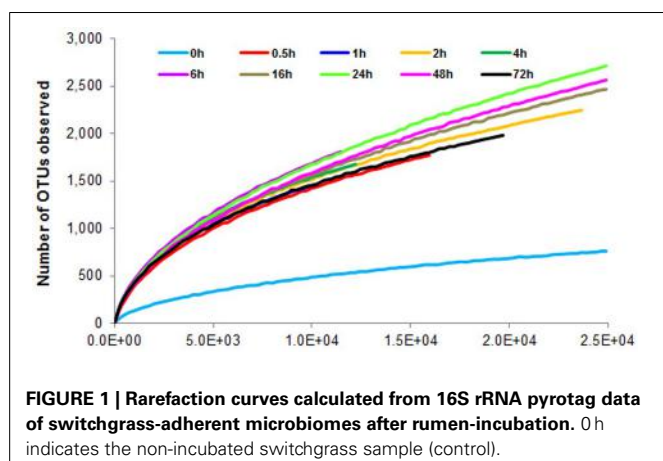
Table 4 | Distinct OTUs observed.

Incubation time [h]	0 h	0.5 h	1 h	2 h	4 h	6 h	16 h	24 h	48 h	72 h
Number of distinct OTUs observed	260	289	180	358	224	308	563	727	689	296

into OTUs at a sequence identify level of 97%. This resulted in a total of 7,168 distinct OTUs, with a range of 788–2,758 OTUs observed for each community. **Table 2** summarizes the number of raw reads, quality filtered reads, and OTUs that were obtained for each time point. Of the observed 7,168 OTUs, 7,005 (97.7%) were determined to be unambiguously of bacterial origin, while 0.2% (17 OTUs) were assigned to be archaeal (**Table 3**). **Table 4** summarizes the number of OTUs unique to each time point sampled. A complete list of all OTUs observed during this study and an OTU count for each sample is provided in Supplementary Table 1. Analysis of the successional appearance of OTUs suggests an initial increase in community richness within the first 30 min of rumen incubation (**Tables 2, 3**) and a second increase in richness of the bacterial community associated with the switchgrass samples subjected to rumen-incubation for 16, 24, and 48 h (**Table 3**). This finding is supported by the calculated rarefaction curves (**Figure 1**) and Chao 1 indices (**Table 5**). Likewise the Shannon and Simpson Reciprocal indices increased noticeably for all rumen-incubated samples (**Table 5**). An average Good's coverage estimator of 94.9% was calculated for all samples, with 92% (6 h) being the lowest and 98.6% (non-incubated switchgrass) being the highest (**Table 5**).

TEMPORAL CHANGES IN β -DIVERSITY OF FIBER-ADHERENT RUMEN MICROBIOME

Principal coordinates analysis comparing the temporal dynamics of switchgrass-associated microbiota indicated that the



community associated with the air-dried switchgrass sample (0 h) was distinct from the microbiomes of all rumen-incubated samples (**Figure 2**). After 30 min of rumen incubation the switchgrass-associated microbiota exhibited clearly noticeable changes: for example, members of the *Archaea*, which were essentially absent in the non-incubated microbiome, were detected in all rumen-incubated samples. In total, 17 distinct archaeal OTUs were detected (**Table 3**), with 14 (82%) of them categorized as *Methanobacteriaceae*, a family belonging to the methanogenic *Euryarchaeota* (Supplementary Table 1). Of the reads derived from the *Archaea*, the majority ($\geq 76\%$) was recruited for each sample (median 88%) by two OTUs both categorized as *Methanobrevibacter* following rumen incubation. Abundance of members belonging to the genus *Methylobacterium* was notably high in the samples retrieved after 30 min of rumen incubation. The bacterial phylum *Bacteroidetes*, represented primarily by members of the *Sphingobacteria* in the 0 h sample, increased up

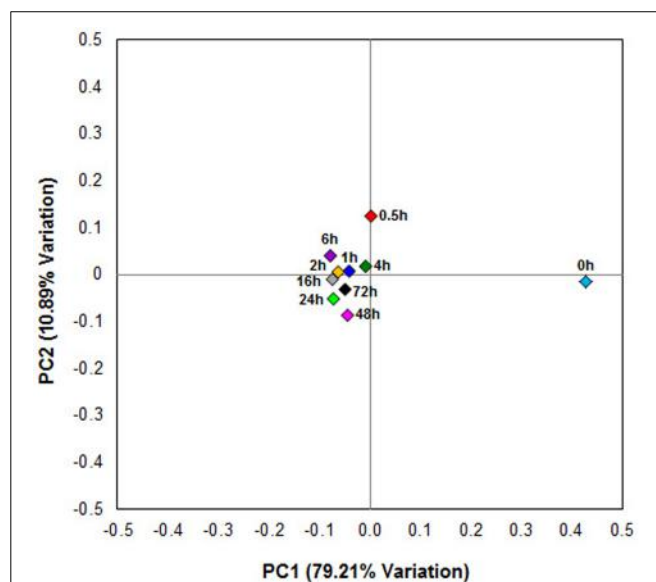


FIGURE 2 | Principal coordinate analysis of switchgrass-adherent microbiomes. Each point corresponds to one of nine rumen-incubated samples (0.5, 1, 2, 4, 6, 16, 24, 48, and 72 h) and one control sample (0 h). The percentage of variation explained by the plotted principal coordinates is indicated on the axes.

Table 5 | Estimated OTU richness and diversity metrics and estimated sample coverage of rarefied bacterial and archaeal 16S rRNA sequences.

Incubation time [h]	0	0.5	1	2	4	6	16	24	48	72
Sequences sampled	24,910	15,946	10,219	23,665	12,211	11,464	24,910	24,910	24,910	19,681
Observed species	760.5	1,771.5	1,466.2	2,248.1	1,678.0	1,809.8	2,468.3	2,714.8	2,565.5	1,982.6
Goods coverage (%)	98.6	95.0	93.8	95.9	94.1	92.0	95.2	94.4	94.8	95.6
Singles	352.7	800.5	635.2	978.2	718.6	922.4	1,202.7	1,384.3	1,303.0	861.2
Doubles	124.9	285.7	212.2	305.9	261.3	253.3	332.0	398.6	376.8	293.6
Chao1	1,253.6	2,888.0	2,411.1	3,805.8	2,661.0	3,481.2	4,639.3	5,111.3	4,811.2	3,239.9
Shannon	4.0	7.9	8.9	9.0	8.9	9.0	8.9	8.9	8.8	8.9
Simpson	0.7	1.0	1.0	1.0	1.0	1.0	1.0	1.0	1.0	1.0
Simpson reciprocal	3.8	23.6	204.2	189.0	160.2	202.5	135.5	126.6	122.9	183.7

to five fold throughout rumen incubation, mainly through large increases in *Bacteroidia* populations and in particular of increases in members belonging to the genus *Prevotella* (**Tables 6–8**). This overall increase in *Bacteroidetes* was accompanied by increased abundance of *Cyanobacteria*, *Fibrobacteres*, *Spirochaetes*, and *Tenericutes* and decreases in *Actinobacteria* (i.e., *Kineosporiaceae* and *Microbacteriaceae*), *Firmicutes*, and *Proteobacteria* abundance (**Table 8**).

Observed decreases in *Firmicutes* were driven by a 460-fold reduction in the *Bacilli* (mostly *Bacillus* spp.), which initially accounted for 97% of the *Firmicutes* phylum and 63% of all bacteria prior to rumen incubation. Decreases in *Bacilli* were partially offset by large increases in the *Clostridia* including the *Lachnospiraceae* (particularly *Butyrivibrio* spp., *Pseudobutyrivibrio* spp., and *Clostridium* spp.) and the *Ruminococcaceae* (almost entirely *Ruminococcus* spp.) families. The *Clostridia* continued to increase to become the predominant class and made *Firmicutes* the predominant phylum after a brief peak in *Proteobacteria* abundance within the initial 30 min of rumen-incubation (**Figure 3**, **Tables 6, 8**). The

switchgrass-associated microbiota stabilized at the phylum level after 1 h of rumen incubation (**Figure 3**), and only modest phylum- and class-level changes were observed for most taxonomic groups between 1 and 72 h of rumen incubation (**Tables 6, 8**). The only exceptions to this observation were the *Fibrobacteres* and *Spirochaetes*, which both increased considerably in abundance in samples collected between 6 and 16 h, peaking around 24 h before returning to their 1 h levels after a total of 72 h of rumen-incubation (**Figure 3, Table 8**). Each of these phylum-level changes was driven by a single genus: the *Fibrobacteres* driven exclusively by *Fibrobacter*, while changes in the *Spirochaetes* were driven by *Treponema* (**Table 7**).

BIOMASS-DEGRADATION COORDINATED WITH MICROBIAL COLONIZATION

Biomass degradation following rumen incubation appeared to be biphasic; each phase corresponding to notable changes in microbial communities. Biomass degradation began rapidly following rumen incubation with 13% of the total biomass being degraded within 30 min (**Figure 4**). Biomass-degradation then

Table 6 | Community composition of switchgrass-adherent microbiome at the class level based on 16S rRNA pyrotag data.

	Percentage of sequences									
	0 h	0.5 h	1 h	2 h	4 h	6 h	16 h	24 h	48 h	72 h
BACTERIA										
Actinobacteria;c__Actinobacteria	3.77	0.60	0.39	0.48	0.70	0.28	0.20	0.23	0.35	0.43
Bacteroidetes;c__Bacteroidia	2.31	33.87	31.93	36.65	27.90	36.77	34.94	35.13	32.22	34.30
Bacteroidetes;c__Flavobacteriia	0.63	0.03	0.01	0.00	0.00	0.01	0.00	0.00	0.00	0.00
Bacteroidetes;c__Sphingobacteriia	4.34	0.13	0.03	0.05	0.04	0.03	0.02	0.00	0.00	0.03
Chloroflexi;c__Anaerolineae	0.01	0.13	0.35	0.33	0.23	0.15	0.26	0.29	0.38	0.35
Cyanobacteria;c__4C0d-2	0.01	0.90	1.48	0.80	1.30	0.82	0.97	0.65	0.33	0.95
Elusimicrobia;c__Elusimicrobia	0.01	0.23	0.21	0.08	0.13	0.09	0.07	0.07	0.04	0.06
Elusimicrobia;c__Endomicrobia	0.02	0.18	0.19	0.15	0.18	0.16	0.22	0.19	0.23	0.20
Fibrobacteres;c__Fibrobacteria	0.11	0.35	1.35	2.14	0.63	2.30	6.87	7.54	6.23	2.11
Firmicutes;c__Bacilli	63.26	0.11	0.12	0.05	0.03	0.22	0.02	0.06	0.07	0.04
Firmicutes;c__Clostridia	1.91	24.65	41.64	42.54	43.10	38.86	37.29	38.95	42.94	42.96
Firmicutes;c__Erysipelotrichi	0.02	0.09	0.10	0.26	0.23	0.20	0.18	0.22	0.32	0.21
Firmicutes;c__RF3	0.03	0.32	0.36	0.55	0.41	0.28	0.43	0.45	0.48	0.53
Lentisphaerae;c__[Lentisphaera]	0.02	0.34	0.79	0.55	0.58	0.51	0.60	0.39	0.58	0.71
Planctomycetes;c__Planctomycetia	0.01	0.25	0.53	0.50	0.49	0.26	0.28	0.38	0.62	0.60
Proteobacteria;c__Alphaproteobacteria	12.93	22.76	1.31	0.90	1.79	0.88	0.63	0.40	0.44	0.81
Proteobacteria;c__Betaproteobacteria	5.51	0.22	0.16	0.11	0.47	0.14	0.01	0.02	0.02	0.06
Proteobacteria;c__Deltaproteobacteria	0.03	0.09	0.32	0.26	0.23	0.31	0.38	0.48	0.42	0.30
Proteobacteria;c__Gammaproteobacteria	4.28	2.28	4.11	2.09	3.00	4.57	3.23	1.78	1.49	1.79
Spirochaetes;c__Spirochaetes	0.23	1.78	2.03	1.62	1.21	2.68	4.40	4.58	3.70	2.18
Synergistetes;c__Synergistia	0.00	0.03	0.18	0.06	0.06	0.13	0.12	0.09	0.15	0.10
Tenericutes;c__Mollicutes	0.21	7.46	6.18	5.10	10.34	5.78	4.60	3.47	3.17	4.61
TM7;c__TM7-3	0.02	0.06	0.17	0.03	0.26	0.05	0.04	0.00	0.03	0.03
Verrucomicrobia;c__Verruco-5	0.01	0.32	0.49	0.47	0.54	0.35	0.31	0.25	0.25	0.60
Bacteria classes <0.1%	0.11	0.11	0.18	0.16	0.14	0.09	0.13	0.09	0.23	0.20
Unclassified bacteria classes	0.20	2.42	4.73	3.56	5.06	3.67	3.55	4.09	5.00	5.11
ARCHAEA										
Euryarchaeota;c__Methanobacteria	0.01	0.28	0.61	0.47	0.91	0.34	0.21	0.20	0.30	0.69
Archaea classes <0.1%	0.00	0.01	0.06	0.03	0.05	0.09	0.02	0.02	0.01	0.05

Table 7 | Community composition of switchgrass-adherent microbiome at the genus level based on 16S rRNA pyrotag data.

	Percentage of sequences									
	0 h	0.5 h	1 h	2 h	4 h	6 h	16 h	24 h	48 h	72 h
BACTERIA										
Actinobacteria;c_Actinobacteria;o_Actinomycetales;f_Microbacteriaceae;g_Microbacterium	0.21	0.04	0.01	0.00	0.04	0.00	0.00	0.00	0.00	0.01
Actinobacteria;c_Actinobacteria;o_Actinomycetales;f_Propionibacteriaceae;g_Propionibacterium	0.01	0.11	0.00	0.00	0.00	0.00	0.03	0.00	0.00	0.00
Actinobacteria;c_Actinobacteria;o_Actinomycetales;f_Pseudonocardiaceae;g_Saccharopolyspora	0.02	0.03	0.14	0.25	0.16	0.08	0.09	0.16	0.20	0.21
Bacteroidetes;c_Bacteroidia;o_Bacteroidales;f_Bacteroidaceae;g_BF311	0.06	0.63	1.06	1.37	0.80	0.92	1.54	1.67	1.91	1.46
Bacteroidetes;c_Bacteroidia;o_Bacteroidales;f_Porphyromonadaceae;g_Paludibacter	0.04	2.21	1.03	1.36	1.53	1.08	0.86	0.53	0.40	0.88
Bacteroidetes;c_Bacteroidia;o_Bacteroidales;f_Prevotellaceae;g_Prevotella	1.21	18.25	14.09	14.60	12.79	19.68	15.59	13.12	9.40	12.30
Bacteroidetes;c_Bacteroidia;o_Bacteroidales;f_[Paraprevotellaceae];g_CF231	0.03	0.37	0.53	0.49	0.42	0.68	0.70	0.67	0.39	0.43
Bacteroidetes;c_Bacteroidia;o_Bacteroidales;f_[Paraprevotellaceae];g_YRC22	0.10	1.19	1.23	1.14	0.93	1.49	1.36	1.20	0.84	1.15
Bacteroidetes;c_Flavobacterii;a_O_Flavobacteriales;f_Flavobacteriaceae;g_Chryseobacterium	0.21	0.01	0.00	0.00	0.00	0.01	0.00	0.00	0.00	0.00
Bacteroidetes;c_Sphingobacterii;a_O_Sphingobacteriales;f_Chitinophagaceae;g_Chitinophaga	0.24	0.01	0.00	0.00	0.00	0.00	0.00	0.00	0.00	0.01
Bacteroidetes;c_Sphingobacterii;a_O_Sphingobacteriales;f_Flexibacteraceae;g_Hymenobacter	1.00	0.03	0.01	0.00	0.01	0.00	0.00	0.00	0.00	0.00
Bacteroidetes;c_Sphingobacterii;a_O_Sphingobacteriales;f_Sphingobacteriaceae;g_Pedobacter	0.32	0.03	0.00	0.00	0.00	0.00	0.00	0.00	0.00	0.00
Bacteroidetes;c_Sphingobacterii;a_O_Sphingobacteriales;f_Sphingobacteriaceae;g_Sphingobacterium	0.77	0.02	0.00	0.00	0.00	0.00	0.01	0.00	0.00	0.00
Chloroflexi;c_Anaerolineae;o_Anaerolineales;f_Anaerolinaceae;g_SHD-231	0.01	0.10	0.27	0.28	0.21	0.13	0.24	0.27	0.34	0.30
Fibrobacteres;c_Fibrobacteria;o_Fibrobacterales;f_Fibrobacteraceae;g_Fibrobacter	0.07	0.32	1.32	2.07	0.62	2.28	6.79	7.51	6.19	2.01
Firmicutes;c_Bacilli;o_Bacillales;f_Bacillaceae;g_Bacillus	62.05	0.04	0.00	0.00	0.00	0.00	0.00	0.00	0.00	0.00
Firmicutes;c_Bacilli;o_Lactobacillales;f_Streptococcaceae;g_Streptococcus	0.00	0.00	0.03	0.01	0.03	0.21	0.00	0.01	0.00	0.00
Firmicutes;c_Clostridia;o_Clostridiales;f_Clostridiaceae;g_Clostridium	0.19	0.98	1.76	2.24	1.86	1.54	2.17	2.64	3.27	2.33
Firmicutes;c_Clostridia;o_Clostridiales;f_Dehalobacteriaceae;g_Dehalobacterium	0.00	0.03	0.11	0.40	0.07	0.07	0.14	0.15	0.33	0.58
Firmicutes;c_Clostridia;o_Clostridiales;f_Lachnospiraceae;g_Anastostipes	0.02	0.18	0.49	0.43	0.30	0.33	0.31	0.25	0.25	0.40
Firmicutes;c_Clostridia;o_Clostridiales;f_Lachnospiraceae;g_Butyryvibrio	0.22	2.21	3.33	3.49	4.40	3.11	2.68	2.70	2.81	3.34
Firmicutes;c_Clostridia;o_Clostridiales;f_Lachnospiraceae;g_Coprococcus	0.05	0.46	0.98	0.99	1.02	0.91	0.76	0.72	0.75	0.88
Firmicutes;c_Clostridia;o_Clostridiales;f_Lachnospiraceae;g_Moryella	0.01	0.12	0.20	0.21	0.18	0.13	0.14	0.10	0.15	0.14
Firmicutes;c_Clostridia;o_Clostridiales;f_Lachnospiraceae;g_Pseudobutyryvibrio	0.01	0.49	0.83	0.70	0.66	1.45	0.65	0.76	0.61	0.73
Firmicutes;c_Clostridia;o_Clostridiales;f_Ruminococcaceae;g_Oscillospira	0.01	0.37	0.40	0.53	0.47	0.28	0.29	0.41	0.50	0.67
Firmicutes;c_Clostridia;o_Clostridiales;f_Ruminococcaceae;g_Ruminococcus	0.08	1.90	3.23	2.72	2.52	2.74	2.34	2.46	2.64	2.82

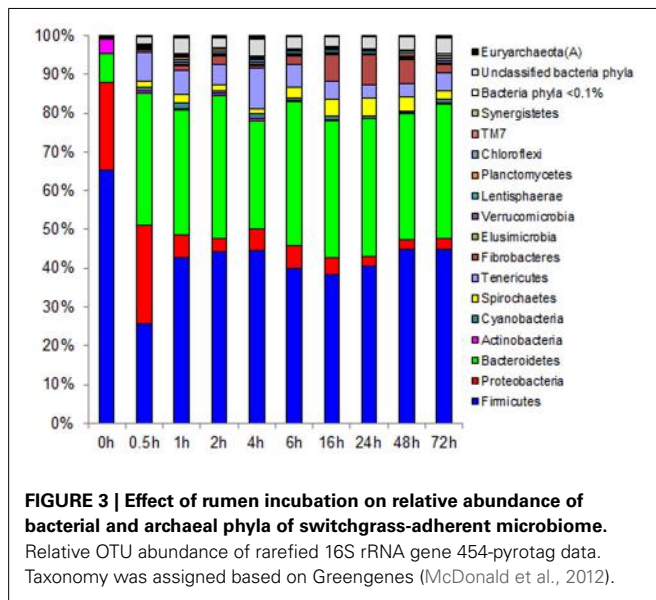
(Continued)

Table 7 | Continued

	Percentage of sequences									
	0 h	0.5 h	1 h	2 h	4 h	6 h	16 h	24 h	48 h	72 h
Firmicutes;c_Clostridia;o_Clostridiales; f_Veillonellaceae;g_Anaerovibrio	0.00	0.02	0.13	0.06	0.08	0.07	0.05	0.08	0.07	0.05
Firmicutes;c_Clostridia;o_Clostridiales; f_Veillonellaceae;g_Selenomonas	0.01	0.16	0.28	0.20	0.19	0.43	0.10	0.09	0.05	0.12
Firmicutes;c_Clostridia;o_Clostridiales; f_Veillonellaceae;g_Succinibacter	0.05	0.20	0.39	0.38	0.35	0.54	0.30	0.32	0.32	0.45
Firmicutes;c_Erysipelotrichi;o_Erysipelotrichales; f_Erysipelotrichaceae;g_L7A_E11	0.00	0.04	0.04	0.16	0.08	0.07	0.09	0.12	0.25	0.13
Proteobacteria;c_Alphaproteobacteria;o_Rhizobiales; f_Hyphomicrobiaceae;g_Devosia	1.62	0.08	0.03	0.01	0.06	0.02	0.02	0.01	0.02	0.00
Proteobacteria;c_Alphaproteobacteria;o_Rhizobiales; f_Methylobacteriaceae;g_Methylobacterium	0.32	20.14	0.00	0.02	0.00	0.02	0.00	0.00	0.00	0.01
Proteobacteria;c_Alphaproteobacteria;o_Rhizobiales; f_Rhizobiaceae;g_Agrobacterium	0.74	0.04	0.09	0.00	0.03	0.02	0.00	0.00	0.00	0.06
Proteobacteria;c_Alphaproteobacteria;o_Rhizobiales; f_Rhizobiaceae;g_Rhizobium	0.05	0.00	0.00	0.00	0.00	0.00	0.00	0.00	0.00	0.01
Proteobacteria;c_Alphaproteobacteria;o_Rhodobacterales; f_Rhodobacteraceae;g_Paracoccus	0.15	0.01	0.01	0.00	0.03	0.00	0.00	0.00	0.00	0.01
Proteobacteria;c_Alphaproteobacteria;o_Rhodobacterales; f_Rhodobacteraceae;g_Rhodobacter	0.18	0.01	0.00	0.00	0.00	0.00	0.00	0.00	0.00	0.00
Proteobacteria;c_Alphaproteobacteria;o_Rhodospirillales; f_Aacetobacteraceae;g_Roseomonas	0.38	0.03	0.01	0.01	0.03	0.02	0.00	0.00	0.00	0.02
Proteobacteria;c_Alphaproteobacteria; o_Sphingomonadales;f_Sphingomonadaceae; g_Sphingomonas	0.98	0.08	0.01	0.03	0.06	0.01	0.00	0.01	0.00	0.01
Proteobacteria;c_Deltaproteobacteria;o_Desulfovibrionales; f_Desulfovibrionaceae;g_Desulfovibrio	0.00	0.04	0.24	0.14	0.13	0.20	0.20	0.26	0.18	0.17
Proteobacteria;c_Gammaproteobacteria;o_Aeromonadales; f_Succinivibrionaceae;g_Ruminobacter	0.04	0.58	0.83	0.77	0.50	0.69	0.98	0.48	0.53	0.59
Proteobacteria;c_Gammaproteobacteria; o_Enterobacteriales;f_Enterobacteriaceae; g_Erwinia	0.61	0.07	0.01	0.00	0.00	0.00	0.00	0.00	0.00	0.01
Proteobacteria;c_Gammaproteobacteria; o_Pseudomonadales;f_Pseudomonadaceae; g_Pseudomonas	2.46	0.12	0.03	0.02	0.09	0.01	0.00	0.00	0.00	0.02
Proteobacteria;c_Gammaproteobacteria; o_Xanthomonadales;f_Xanthomonadaceae; g_Stenotrophomonas	0.15	0.00	0.01	0.00	0.02	0.00	0.00	0.00	0.00	0.01
Spirochaetes;c_Spirochaetes;o_Sphaerochaetales; f_Sphaerochaetaceae;g_Sphaerochaeta	0.01	0.83	0.56	0.62	0.54	0.62	0.37	0.34	0.48	0.49
Spirochaetes;c_Spirochaetes;o_Spirochaetales; f_Spirochaetaceae;g_Treponema	0.22	0.83	1.11	0.81	0.52	1.81	3.89	4.06	2.92	1.42
Synergistetes;c_Synergistia;o_Synergistales; f_Dethiosulfonvibrionaceae;g_Pyramidobacter	0.00	0.01	0.08	0.02	0.03	0.09	0.07	0.06	0.11	0.04
Tenericutes;c_Mollicutes;o_Anaeroplasmatales; f_Anaeroplasmataceae;g_Anaeroplasma	0.02	0.49	0.49	0.27	0.63	0.85	0.63	0.28	0.15	0.20
Tenericutes;c_Mollicutes;o_Anaeroplasmatales; f_Anaeroplasmataceae;g_RFN20	0.07	5.11	2.30	2.31	5.27	1.64	1.40	1.37	1.22	1.98
Bacteria genera <0.1%	0.81	0.30	0.37	0.30	0.40	0.36	0.23	0.22	0.30	0.40
Unclassified bacteria genera	24.16	40.37	61.27	60.08	60.98	55.00	54.71	56.78	62.09	62.43
ARCHAEA										
Euryarchaeota;c_Methanobacteria;o_Methanobacteriales; f_Methanobacteriaceae;g_Methanobrevibacter	0.01	0.27	0.56	0.45	0.86	0.33	0.21	0.19	0.30	0.66
Archaeal genera <0.1%	0.00	0.03	0.11	0.06	0.09	0.10	0.02	0.02	0.01	0.07

Table 8 | Community composition of switchgrass-adherent microbiome at the phylum level based on 16S rRNA pyrotag data.

	Percentage of sequences									
	0 h	0.5 h	1 h	2 h	4 h	6 h	16 h	24 h	48 h	72 h
BACTERIA										
Firmicutes	65.27	25.57	42.79	44.25	44.47	39.93	38.41	40.41	45.00	44.78
Proteobacteria	22.75	25.36	5.91	3.39	5.52	5.91	4.26	2.67	2.41	2.96
Bacteroidetes	7.29	34.09	32.02	36.84	28.02	37.00	35.08	35.37	32.47	34.54
Actinobacteria	3.79	0.60	0.39	0.48	0.70	0.28	0.20	0.23	0.36	0.43
Cyanobacteria	0.01	0.90	1.48	0.80	1.30	0.82	0.97	0.65	0.33	0.95
Spirochaetes	0.23	1.80	2.07	1.66	1.24	2.72	4.42	4.61	3.75	2.21
Tenericutes	0.21	7.46	6.18	5.10	10.34	5.78	4.59	3.47	3.17	4.61
Fibrobacteres	0.14	0.36	1.35	2.14	0.63	2.30	6.86	7.54	6.23	2.11
Elusimicrobia	0.03	0.40	0.39	0.23	0.30	0.25	0.29	0.26	0.26	0.27
Verrucomicrobia	0.01	0.37	0.52	0.50	0.58	0.36	0.32	0.26	0.27	0.64
Lentisphaerae	0.02	0.34	0.79	0.55	0.58	0.52	0.59	0.39	0.58	0.72
Planctomycetes	0.01	0.25	0.54	0.51	0.50	0.26	0.29	0.39	0.62	0.60
Chloroflexi	0.01	0.13	0.36	0.34	0.23	0.16	0.27	0.29	0.39	0.36
TM7	0.02	0.06	0.17	0.03	0.26	0.05	0.05	0.00	0.03	0.03
Synergistetes	0.00	0.03	0.18	0.06	0.06	0.13	0.12	0.09	0.15	0.10
Bacteria phyla <0.1%	0.04	0.04	0.07	0.04	0.04	0.01	0.05	0.05	0.11	0.10
Unclassified bacteria phyla	0.15	1.95	4.11	2.57	4.28	3.11	2.72	3.11	3.56	3.86
ARCHAEA										
Euryarchaeota	0.01	0.29	0.67	0.50	0.96	0.43	0.23	0.22	0.31	0.73



appeared to stall between 30 min and 4 h, with no significant change to biomass during this period. Corresponding to this period, we observed noticeable increases in *Methanobrevibacter* spp. and changes in some bacterial taxa. The *Butyrivibrio* spp. increased, while *Prevotella* spp. decreased between 30 min and 4 h. Following 4 h, biomass degradation proceeded somewhat linearly at a rate of $\sim 0.81\%$ biomass h^{-1} for the next 20 h of incubation, before gradually slowing over the following two measurements ($\sim 0.41\%$ biomass h^{-1} between 24 and 48 h and

0.17% biomass h^{-1} between 48 and 72 h). The increase in rate of biomass degradation between 4 and 24 h occurred simultaneously with increased numbers of reads assigned to *Fibrobacter* and *Treponema* species (Figure 4, Table 7). Biomass-degradation and colonization of switchgrass was also detectable by SEM with significant fiber degradation being visible for samples incubated within the rumen for 24 h and longer (Figure 5).

DISCUSSION

In the present study we observed temporal shifts in the plant biomass-associated microbiota and in the rates of biomass degradation during the *in situ* rumen-incubation of dried switchgrass. Changes in the microbiome were in particular prevailing immediately within the first 30 min and after 4 h onwards. These observations are consistent with analogous trials on rumen-incubated fresh perennial ryegrass, where denaturing gradient gel electrophoresis (DGGE)-based analyses identified discrete microbial profiles at 0–2 h and after 4 h onwards (Huws et al., 2013). Notable similarities and differences were observed in several findings between these two studies. Consistent with our findings, Huws and colleagues reported increases in richness and diversity following rumen incubation (Huws et al., 2013). The authors of the former study also found the major ruminal genus *Prevotella* (Stevenson and Weimer, 2007) increased after 4 h. In our study, *Prevotella* spp. growth was biphasic, increasing dramatically within the first 30 min following rumen incubation and decreasing between 30 min and 4 h, before increasing again. In our study, *Prevotella* spp. were most abundant at 6 h and did not return to 4 h levels until after 24 h of incubation. In contrast to our observations, Huws et al. reported a loss of a band corresponding

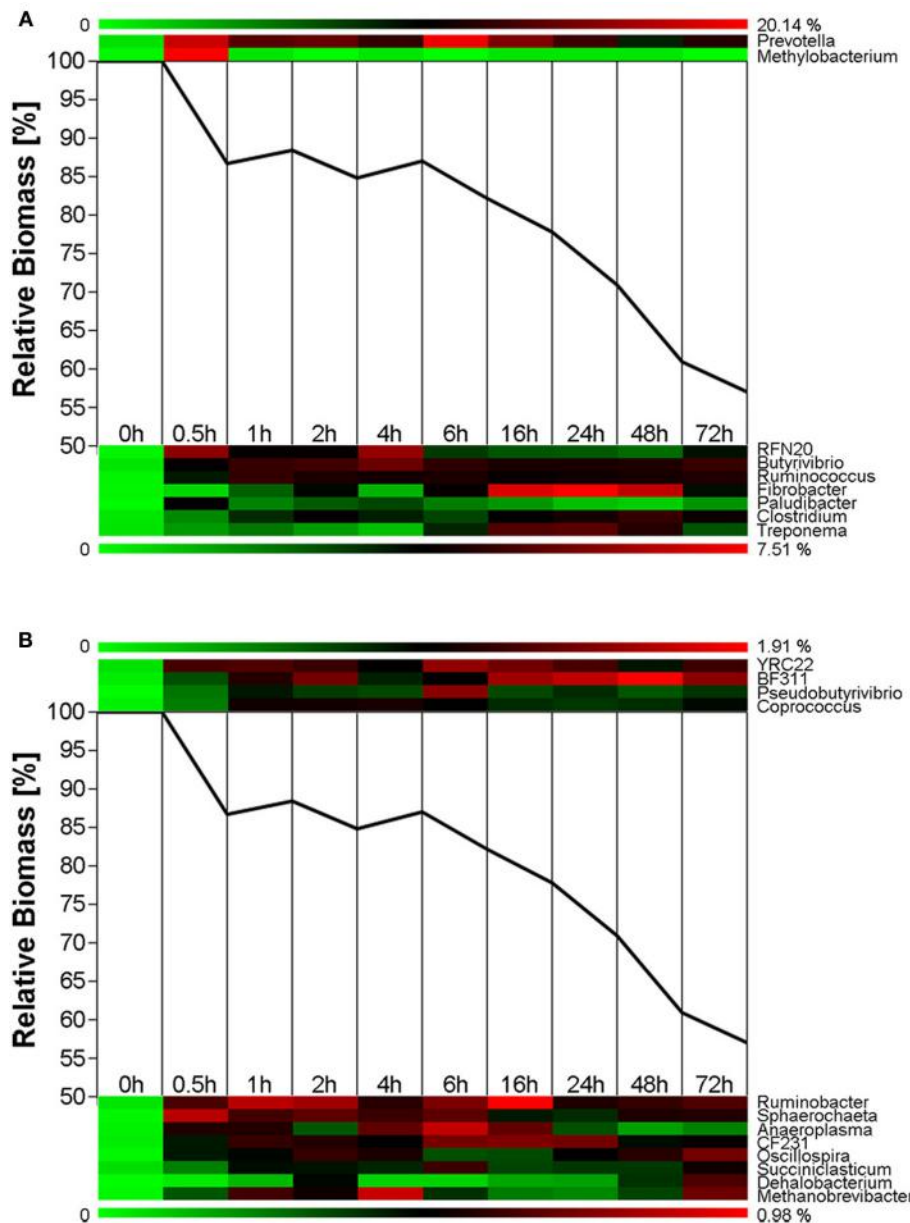


FIGURE 4 | Microbial succession and biomass-degradation during rumen-incubation. Heat map show succession of genera recruiting >0.5% of the generated sequences. Line graphs show the relative dry mater change during rumen-incubation. **(A)** Upper panel shows genera with >10% relative

abundance, lower panel shows genera with a relative abundance between 2 and 10%; **(B)** Upper panel shows genera with relative abundance between 1 and 2%, lower panel shows genera with a relative abundance between 0.5 and 1%.

to *Treponema* spp. after 4 h rumen incubation (Huws et al., 2013), whereas we saw great increases in this genus between 6 and 16 h. This discrepancy likely reflects differences in analytical techniques (DGGE vs. next-generation sequencing), where loss of a single *Treponema* band may not reflect all members of that taxonomic group. Direct sequencing of 16S rRNA amplicons also facilitated the detection of a significant increase of *Methylobacterium* in switchgrass samples retrieved after 30 min of rumen incubation (**Figure 4**). Members of the genus *Methylobacterium* are strictly aerobic, can utilize C₁ compounds such as formate, methanol and

methyamine and a variety of C₂ (including acetate), C₃, and C₄ compounds (Green, 2006) as sole carbon source, and have been found in association with a variety of plants (Corpe, 1985). We hypothesize that members of the *Methylobacterium* were associated with the switchgrass fibers and introduced into the rumen, where they metabolized common fermentation intermediates, such as formate and acetate (Sabine and Johnson, 1964; Hungate et al., 1970), until all oxygen that might have been introduced with the ground switchgrass was depleted. Overall many similarities exist between the two studies and may indicate that the

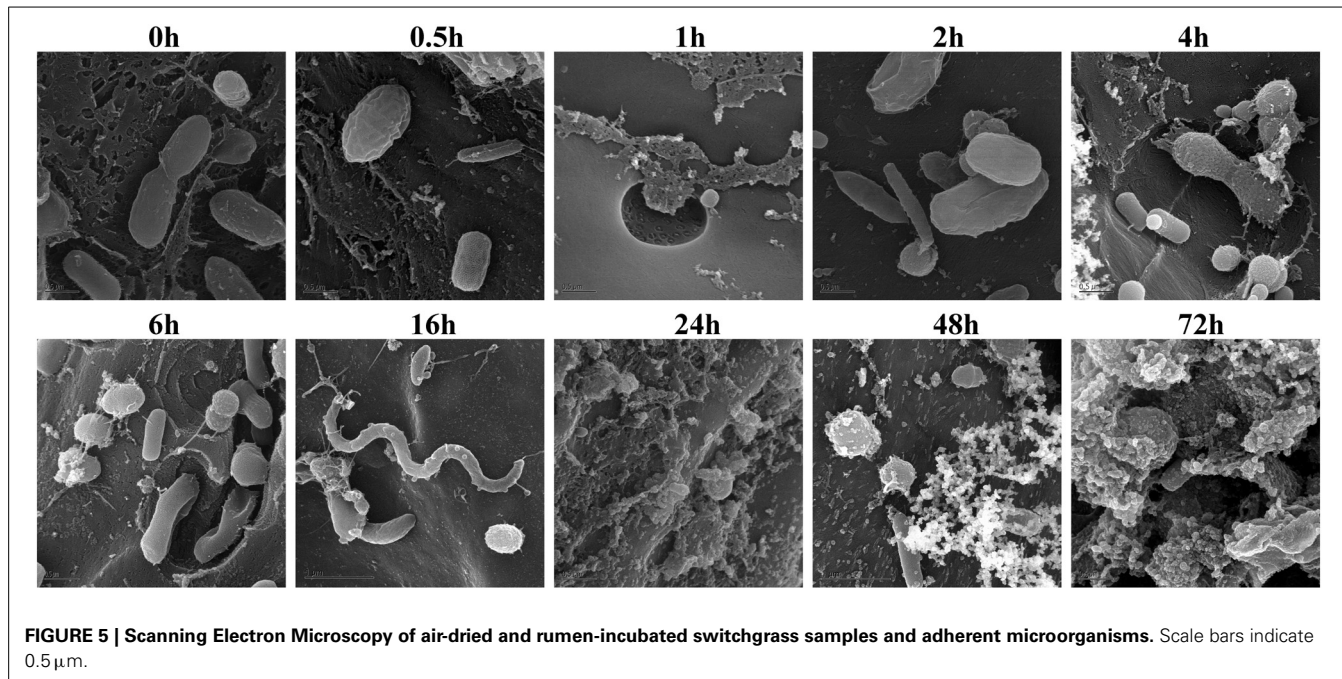


FIGURE 5 | Scanning Electron Microscopy of air-dried and rumen-incubated switchgrass samples and adherent microorganisms. Scale bars indicate 0.5 μm.

temporal changes in microbiota during the first 30 min following rumen-incubation and then after 4 h may be common features of rumen-microbial digestion among multiple plant species in various states (fresh vs. dried). Changes in the microbiota corresponded with differences in the rates of switchgrass degradation. The rate of switchgrass degradation was greatest within the first 30 min of rumen-incubation during which 13% of the total biomass was lost. This may reflect rapid utilization of soluble sugars and other easily fermentable nutrients that were unabated by proximal H₂ partial pressures. However, the rate of degradation stalled between 30 min and 4 h. During this period we observed a dramatic increase in methanogen density such that the total abundance of methanogens at 4 h post-incubation increased 3.3-fold compared to 30 min incubation. We hypothesize that these two observations were linked and related to a dramatic increase in proximal H₂ partial pressure caused by the rapid initial fermentation of easily accessible plant polysaccharides. Methanogen numbers swelled, most likely in response to the hypothesized high H₂ partial pressures and were eventually able to overcome these and create an environment that was favorable to the energetically-efficient growth of the fibrolytic microbial consortia, as has been proposed based on *in vitro* evidence (Stams, 1994; Ishii et al., 2006). Although the community was largely established by 1 h, as evidenced by less dramatic changes in the overall microbiota 16S rRNA profile following this period, it was not until after 4 h before their collective metabolism was operating efficiently.

In summary the findings presented here support the hypothesis that the hydrogenotrophic metabolism of methanogens is an essential part of the fibrolytic activity of the rumen ecosystem and is essential for the degradation of the more recalcitrant plant polysaccharides by rumen microbes. Additional *in situ* work during which methane emission, fiber composition and community

are monitored more stringently will be essential for obtaining a better holistic understanding of the rumen microbiome and the contribution of particular community members to the fibrolytic and methanogenic rumen phenotype.

AUTHOR CONTRIBUTIONS

Conceived and designed the experiments: Matthias Hess, Susannah G. Tringe, and Roderick I. Mackie. Performed the experiments: Matthias Hess, Hailan Piao, Roderick I. Mackie. Generated and analyzed the data: Matthias Hess, Hailan Piao, Medora Lachman, Stephanie Malfatti, Alexander Sczryba, Bernhard Knierim, Manfred Auer, Susannah G. Tringe, and Carl J. Yeoman. Wrote the paper: Matthias Hess, Hailan Piao, Medora Lachman, and Carl J. Yeoman.

ACKNOWLEDGMENTS

The work conducted by the US Department of Energy Joint Genome Institute is supported by the Office of Science of the US Department of Energy under Contract No. DE-AC02-05CH11231. MH was partially funded by the Energy Biosciences Institute at the University of California, Berkeley. We would like to thank Dr. Edward Rubin at the DOE Joint Genome Institute and Dr. Philip Hugenholtz at the University of Queensland for their help and guidance during this project as well as Dr. Anthony Yannarell at the University of Illinois Urbana-Champaign and Anna Engelbrektson for helping us with the DNA extraction and sample preparation.

SUPPLEMENTARY MATERIAL

The Supplementary Material for this article can be found online at: <http://www.frontiersin.org/journal/10.3389/fmicb.2014.00307/abstract>

REFERENCES

- Bauchop, T., and Mountfort, D. O. (1981). Cellulose fermentation by a rumen anaerobic fungus in both the absence and presence of rumen methanogens. *Appl. Environ. Microbiol.* 42, 1103–1110.
- Bowman, J. G., and Firkins, J. L. (1993). Effects of forage species and particle size on bacterial cellulolytic activity and colonization *in situ*. *J. Anim. Sci.* 71, 1623–1633.
- Caporaso, J. G., Kuczynski, J., Stombaugh, J., Bittinger, K., Bushman, F. D., Costello, E. K., et al. (2010). QIIME allows analysis of high-throughput community sequencing data. *Nat. Methods* 7, 335–336. doi: 10.1038/nmeth.f.303
- Coleman, G. S. (1992). The rate of uptake and metabolism of starch grains and cellulose particles by *Entodinium* species, *Eudiplodinium maggi*, some other entodiniomorphid protozoa and natural protozoal populations taken from the ovine rumen. *J. Appl. Bacteriol.* 73, 507–513. doi: 10.1111/j.1365-2672.1992.tb05013.x
- Corpe, W. A. (1985). A method for detecting methylotrophic bacteria on solid-surfaces. *J. Microbiol. Methods* 3, 215–221. doi: 10.1016/0167-7012(85)90049-1
- Edgar, R. C. (2010). Search and clustering orders of magnitude faster than BLAST. *Bioinformatics* 26, 2460–2461. doi: 10.1093/bioinformatics/btq461
- Edwards, J. E., Huws, S. A., Kim, E. J., and Kingston-Smith, A. H. (2007). Characterization of the dynamics of initial bacterial colonization of nonconserved forage in the bovine rumen. *FEMS Microbiol. Ecol.* 62, 323–335. doi: 10.1111/j.1574-6941.2007.00392.x
- Edwards, J. E., Kingston-Smith, A. H., Jimenez, H. R., Huws, S. A., Skot, K. P., Griffith, G. W., et al. (2008). Dynamics of initial colonization of nonconserved perennial ryegrass by anaerobic fungi in the bovine rumen. *FEMS Microbiol. Ecol.* 66, 537–545. doi: 10.1111/j.1574-6941.2008.00563.x
- Engelbrektson, A., Kunin, V., Wrighton, K. C., Zvenigorodsky, N., Chen, F., Ochman, H., et al. (2010). Experimental factors affecting PCR-based estimates of microbial species richness and evenness. *ISME J.* 4, 642–647. doi: 10.1038/ismej.2009.153
- Fondevila, M., and Dehority, B. A. (1996). Interactions between *Fibrobacter succinogenes*, *Prevotella ruminicola*, and *Ruminococcus flavefaciens* in the digestion of cellulose from forages. *J. Anim. Sci.* 74, 678–684.
- Goering, H. K., and Van Soest, P. J. (1970). *Forage Fiber Analysis*. Vol. 379. Washington, DC: Agricultural Research Service, US Department of Agriculture.
- Green, P. N. (2006). Methylobacterium. *Prokaryotes* 5, 257–265. doi: 10.1007/0-387-30745-1_14
- Heredia, A., Jimenez, A., and Guillen, R. (1995). Composition of plant-cell walls. *Zeitschrift für Lebensmittel-Untersuchung -Forschung* 200, 24–31. doi: 10.1007/BF01192903
- Hess, M., Sczryba, A., Egan, R., Kim, T. W., Chokhawala, H., Schroth, G., et al. (2011). Metagenomic discovery of biomass-degrading genes and genomes from cow rumen. *Science* 331, 463–467. doi: 10.1126/science.1200387
- Hungate, R. E., Smith, W., Bauchop, T., Yu, I., and Rabinowitz, J. C. (1970). Formate as an intermediate in the bovine rumen fermentation. *J. Bacteriol.* 102, 389–397.
- Huws, S. A., Mayorga, O. L., Theodorou, M. K., Onime, L. A., Kim, E. J., Cookson, A. H., et al. (2013). Successional colonization of perennial ryegrass by rumen bacteria. *Lett. Appl. Microbiol.* 56, 186–196. doi: 10.1111/lam.12033
- Ishii, S., Kosaka, T., Hotta, Y., and Watanabe, K. (2006). Simulating the contribution of coaggregation to interspecies hydrogen fluxes in syntrophic methanogenic consortia. *Appl. Environ. Microbiol.* 72, 5093–5096. doi: 10.1128/AEM.00333-06
- Janssen, P. H., and Kirs, M. (2008). Structure of the archaeal community of the rumen. *Appl. Environ. Microbiol.* 74, 3619–3625. doi: 10.1128/AEM.02812-07
- Joblin, K. N., Campbell, G. P., Richardson, A. J., and Stewart, C. S. (1989). Fermentation of barley straw by anaerobic rumen bacteria and fungi in axenic culture and in co-culture with methanogens. *Lett. Appl. Microbiol.* 9, 195–197. doi: 10.1111/j.1472-765X.1989.tb00323.x
- Klemm, D., Heublein, B., Fink, H.-P., and Bohn, A. (2005). Cellulose: fascinating biopolymer and sustainable raw material. *Angew. Chem. Int. Ed.* 44, 3358–3393. doi: 10.1002/anie.200460587
- Kudo, H., Cheng, K. J., and Costerton, J. W. (1987). Interactions between *Treponema bryantii* and cellulolytic bacteria in the *in vitro* degradation of straw cellulose. *Can. J. Microbiol.* 33, 244–248. doi: 10.1139/m87-041
- Latham, M. J., and Wolin, M. J. (1977). Fermentation of cellulose by *Ruminococcus flavefaciens* in the presence and absence of *Methanobacterium ruminantium*. *Appl. Environ. Microbiol.* 34, 297–301.
- Leahy, S. C., Kelly, W. J., Altermann, E., Ronimus, R. S., Yeoman, C. J., Pacheco, D. M., et al. (2010). The genome sequence of the rumen methanogen *Methanobrevibacter ruminantium* reveals new possibilities for controlling ruminant methane emissions. *PLoS ONE* 5:e8926. doi: 10.1371/journal.pone.0008926
- McDonald, D., Price, M. N., Goodrich, J., Nawrocki, E. P., DeSantis, T. Z., Probst, A., et al. (2012). An improved Greengenes taxonomy with explicit ranks for ecological and evolutionary analyses of bacteria and archaea. *ISME J.* 6, 610–618. doi: 10.1038/ismej.2011.139
- Rychlik, J. L., and May, T. (2000). The effect of a methanogen, *Methanobrevibacter smithii*, on the growth rate, organic acid production, and specific ATP activity of three predominant ruminal cellulolytic bacteria. *Curr. Microbiol.* 40, 176–180. doi: 10.1007/s002849910035
- Sabine, J. R., and Johnson, B. C. (1964). Acetate metabolism in the ruminant. *J. Biol. Chem.* 239, 89–93.
- Stams, A. J. M. (1994). Metabolic interactions between anaerobic-bacteria in methanogenic environments. *Antonie van Leeuwenhoek* 66, 271–294. doi: 10.1007/BF00871644
- Stevenson, D. M., and Weimer, P. J. (2007). Dominance of *Prevotella* and low abundance of classical ruminal bacterial species in the bovine rumen revealed by relative quantification real-time PCR. *Appl. Microbiol. Biotechnol.* 75, 165–174. doi: 10.1007/s00253-006-0802-y
- Theodorou, M. K., Mennim, G., Davies, D. R., Zhu, W. Y., Trinci, A. P., and Brookman, J. L. (1996). Anaerobic fungi in the digestive tract of mammalian herbivores and their potential for exploitation. *Proc. Nutr. Soc.* 55, 913–926. doi: 10.1093/PNS/19960088
- Weimer, P. J. (1996). Why don't ruminal bacteria digest cellulose faster? *J. Dairy Sci.* 79, 1496–1502. doi: 10.3168/jds.S0022-0302(96)76509-8
- Weimer, P. J., Russell, J. B., and Muck, R. E. (2009). Lessons from the cow: what the ruminant animal can teach us about consolidated bioprocessing of cellulosic biomass. *Bioresource Technol.* 100, 5323–5331. doi: 10.1016/j.biortech.2009.04.075

Conflict of Interest Statement: The authors declare that the research was conducted in the absence of any commercial or financial relationships that could be construed as a potential conflict of interest.

Received: 09 May 2014; accepted: 03 June 2014; published online: 22 July 2014.

Citation: Piao H, Lachman M, Malfatti S, Sczryba A, Knierim B, Auer M, Tringe SG, Mackie RI, Yeoman CJ and Hess M (2014) Temporal dynamics of fibrolytic and methanogenic rumen microorganisms during *in situ* incubation of switchgrass determined by 16S rRNA gene profiling. *Front. Microbiol.* 5:307. doi: 10.3389/fmicb.2014.00307

This article was submitted to Terrestrial Microbiology, a section of the journal Frontiers in Microbiology.

Copyright © 2014 Piao, Lachman, Malfatti, Sczryba, Knierim, Auer, Tringe, Mackie, Yeoman and Hess. This is an open-access article distributed under the terms of the Creative Commons Attribution License (CC BY). The use, distribution or reproduction in other forums is permitted, provided the original author(s) or licensor are credited and that the original publication in this journal is cited, in accordance with accepted academic practice. No use, distribution or reproduction is permitted which does not comply with these terms.



Persistence in the shadow of killers

Robert M. Sinclair*

Mathematical Biology Unit, Okinawa Institute of Science and Technology, Okinawa, Japan

Edited by:

Luis Raul Comolli, Lawrence Berkeley National Laboratory, USA

Reviewed by:

Chiara Mocenni, University of Siena, Italy

Franz Luef, NTNU Trondheim, Norway

***Correspondence:**

Robert M. Sinclair, Mathematical Biology Unit, Okinawa Institute of Science and Technology Graduate University, 1919-1 Tancha, Onna-son, Okinawa 904-0495, Japan

e-mail: sinclair@oist.jp

Killing is perhaps the most definite form of communication possible. Microbes such as yeasts and gut bacteria have been shown to exhibit killer phenotypes. The killer strains are able to kill other microbes occupying the same ecological niche, and do so with impunity. It would therefore be expected that, wherever a killer phenotype has arisen, all members of the population would soon be killers or dead. Surprisingly, (1) one can find both killer and sensitive strains in coexistence, both in the wild and in *in vitro* experiments, and (2) the absolute fitness cost of the killer phenotype often seems to be very small. We present an explicit model of such coexistence in a fragmented or discrete environment. A killer strain may kill all sensitive cells in one patch (one piece of rotting fruit, one cave or one human gut, for example), allowing sensitives to exist only in the absence of killer strains on the same patch. In our model, populations spread easily between patches, but in a stochastic manner: one can imagine spores borne by the wind over a field of untended apple trees, or enteric disease transmission in a region in which travel is effectively unrestricted. What we show is that coexistence is not only possible, but that it is possible even if the absolute fitness advantage of the sensitive strain over the killer strain is arbitrarily small. We do this by performing a specifically targeted mathematical analysis on our model, rather than via simulations. Our model does not assume large population densities, and may thus be useful in the context of understanding the ecology of extreme environments.

Keywords: intra-species interaction, killer phenotype, competitive exclusion, coexistence, mathematical analysis

INTRODUCTION

The Purpose of Computing Is Insight, Not Numbers (Hamming, 1987).

It will be useful to begin with a clear statement of what this work is really about. The central question being addressed is whether killer and sensitive phenotypes could in theory coexist in the same environment even if the absolute fitness penalty for the killer phenotype were arbitrarily small. The question is motivated by experimental and field observations to be described below, but is to be approached here from a theoretical point of view. This immediately implies that what is needed is a theoretical framework which has two apparently contradictory properties: First, it must capture important aspects of the relevant biology. Second, it must be simple enough that the question can be answered. This theoretical framework will therefore necessarily be a compromise between realism and tractability. Furthermore, what is actually needed is only a single affirmative result, since that proves the theoretical possibility of coexistence. The phrase “arbitrarily small” excludes some standard approaches, and it is best to make this point now rather than later, because it is this compact phrase which drags us into what will be unfamiliar territory for many readers. If the theoretical framework were to be in the form of a standard numerical simulation of a model, then the best one could do would be to show that coexistence is possible for given small absolute fitness penalties for the killer phenotype. This is not the same as “arbitrarily small”: if a simulation

were to show coexistence to be possible for a fitness penalty of 0.1, it would still leave open the question of whether coexistence could be possible for a fitness penalty of 0.01 and so on ad infinitum. We are thus motivated, by the question we have chosen to investigate, to search outside of the box of standard scientific computing tools until a truly suitable approach is found. The field of mathematical analysis (Ross, 1980) offers itself at this point, since it includes powerful techniques for dealing with the arbitrarily small. Moreover, we can apply elementary methods of mathematical analysis to mathematical models. We are now ready to sketch our approach: we will analyse a model which captures much of the biology but is simple enough to allow a mathematical analysis to be performed. If we can show that coexistence of killer and sensitive phenotypes is possible, for arbitrarily small absolute fitness penalties for the killer phenotype, for this single model, then we will have answered our question in the affirmative. Once this has been done, the particular model is no longer of direct importance (in the same sense that a certain telescope may be used to make an important astronomical observation, but it is almost always the observation which has lasting importance, not the telescope), although we hope it may be useful in other investigations. To paraphrase Hamming, the purpose of our analysis is insight, not the establishment of a computational model *per se*. In other words, the reader should not be expecting to see the standard modeling approach of computational biology, with all of the standard parameter fitting and graph plotting that entails. Instead, the reader should expect to find here something rather unusual, a more truly mathematical approach, but

something which has already been proposed in a related context (Silva, 2011).

The phenomenon of killer phenotypes, which possess the ability to kill conspecifics while being themselves immune (Marquina et al., 2002; Breinig et al., 2006), is widespread in the microbial world (Schmitt and Breinig, 2006; Schrallhammer, 2010; Holt et al., 2013). As more such systems are studied, it is becoming increasingly clear that the evolutionary contexts are so varied (Cornejo et al., 2009 provide a surprising example) that it may be impossible to encompass all that is relevant (such as biodiversity Czárán et al., 2002) in a single, simple model. Classical theory predicts that competition for a single resource should result in the survival of only one competitor (Hardin, 1960), and yet sensitive strains can be more common than killers (Riley and Gordon, 1999; Pieczynska et al., 2013), and it has been observed that there can be coexistence between killer and sensitive strains, necessitating the development of new models (Czárán and Hoekstra, 2003; Vadasz et al., 2003). Here, we provide a novel explicitly solvable mathematical model of the population dynamics of a species with killer and sensitive strains inhabiting a fragmented but potentially highly interconnected environment. Our model includes only killer and sensitive phenotypes. While we were originally inspired by the image of fallen, over-ripe fruits beneath a grove of fruit trees, with spores providing the mechanism of connectivity, the mathematical structure of the model allows it to be applied to many other situations: enteric pathogens live in isolated environments (within the digestive tracts of their individual hosts), but transmission between hosts does occur and can represent a high degree of connectivity in the case of a pandemic. Also, intraterrestrial microbial communities living in largely isolated caves or niches may be sporadically connected by flooding events (Hawes, 1939), as could psychrophilic microbial communities living in niches in or on ice (Margesin and Miteva, 2011) be connected during annual thawing or via other dispersal mechanisms.

Rather surprisingly, it has been shown that the cost of toxin production can be negligible (Garbeva et al., 2011), and is presumably only a few percent when measurable (Wloch-Salamon et al., 2008). We asked whether, in a model, coexistence of killer and sensitive phenotypes is possible for any difference in absolute fitness between killer and sensitive phenotypes, however small. That requires analysis rather than simulation, and this point has therefore decisively influenced our approach.

MATERIALS AND METHODS

We describe here an explicitly solvable model of yeast population dynamics on an infinite number of patches, in which killer and sensitive strains can coexist. Our model includes killer and sensitive strains only. In the following, we will use the example of a killer yeast in our verbal descriptions of the model. A full mathematical treatment would not be appropriate here. We will instead provide what may be called a sketch of the model and our analysis of it. The Supplementary Material contains details of the most important part of the mathematical analysis, but it is also best described as a sketch rather than a formal proof.

Each patch is intended to represent a single piece of fruit. A patch can be colonized by spores from any patch. If a patch is colonized only by spores of the sensitive yeast strain, then the patch

will emit only spores of the sensitive strain. If a killer yeast spore lands on a patch, then any sensitive yeast colony will be eradicated, and the patch will emit only spores of the killer yeast. If a sensitive yeast spore lands on a patch colonized by killer yeast, it will not survive nor influence the (killer yeast) spore production of the patch. The number of spores emitted by a patch depends only upon the type of yeast that has successfully colonized it. If no spores have landed on a patch then that patch will emit no spores. Sporulation occurs in all patches simultaneously, leaving all patches barren and ready for the next cycle, initialized by the dispersal of the spores.

Let $f_S \geq 1$ and $f_K \geq 1$ denote the average number of spores emitted per patch colonized by sensitive (S) or killer (K) strains, where these are to be understood as effective rather than absolute values, since the model assumes that all spores are viable and eventually find a patch. As expected, these numbers play the role of absolute fitnesses. Also, let $0 \leq x_S \leq 1$ and $0 \leq x_K \leq 1$ denote the respective fractions of patches successfully colonized (at the time of sporulation) by the two strains.

The dynamics of the killer yeast strain is not in any way influenced or restricted by the sensitive strain, and so can be treated independently. The probability of a given patch not being reached by any killer strain spore is

$$e^{-f_K x_K}.$$

The reason for this can be understood by first considering a finite number of patches, and then taking the limit as that number goes to infinity. Let n denote the (finite) number of patches. The probability that any given spore will not land on any given patch is $1 - 1/n$, assuming random dispersal. The total number of colonized patches is $n f_K x_K$, so the average number of spores emitted in total is $n f_K x_K$. The probability that none of these land on any given patch is $(1 - 1/n)^{n f_K x_K}$. If we now let n go to infinity, we find that we can quite directly use one of the standard definitions of the exponential function:

$$\lim_{n \rightarrow \infty} \left(1 - \frac{1}{n}\right)^{n f_K x_K} = \lim_{n \rightarrow \infty} \left[\left(1 - \frac{1}{n}\right)^n\right]^{f_K x_K} \\ = [e^{-1}]^{f_K x_K} = e^{-f_K x_K}.$$

This will be, for an infinite number of patches, the fraction of patches which are not reached by any spore. On the other hand, the fraction of patches which are reached by a spore must be the remainder, or $1 - e^{-f_K x_K}$. The killer strain population dynamics is therefore described by the map

$$x_K \mapsto \left(1 - e^{-f_K x_K}\right). \quad (1)$$

Since we can write

$$x_K \mapsto f_K x_K + O(f_K^2 x_K^2),$$

we can state that f_K plays the role of absolute fitness for small $f_K x_K$. In other words, our model includes the phenomenon of

exponential growth when resources are not a limiting factor, and this exponential growth can be used to define an absolute fitness.

According to standard theory, the map (Equation 1) has an unstable fixed point at $x_K = 0$ and a stable fixed point at

$$x_K = X_K = 1 + \frac{W(-f_K e^{-f_K})}{f_K},$$

where W is the principal branch of the Lambert W function (Corless et al., 1996).

The dynamics of the sensitive strain is governed by the same equations in the complete absence of spores of the killer strain. The reason for this assumption is the observation (discussed above) that the difference in absolute fitness between the killer and sensitive strains can be very small. In the presence of an established killer strain population occupying a fixed fraction (X_K) of all patches, the sensitive strain population dynamics is determined by the map

$$x_S \mapsto (1 - e^{-f_S x_S})(1 - X_K),$$

which has an unstable fixed point at $x_S = 0$ and a stable fixed point at

$$x_S = X_S = (1 - X_K) + \frac{W(-(1 - X_K)f_S e^{-(1 - X_K)f_S})}{f_S}$$

if and only if

$$f_S > \frac{-f_K}{W(-f_K e^{-f_K})}. \quad (2)$$

One can construct (details are in the Supplementary Material and see also **Figure 1**) the upper bounds

$$5f_K - 4 > \frac{f_K^2}{3 - 2f_K} \geq \frac{-f_K}{W(-f_K e^{-f_K})} \quad (3)$$

for $1 < f_K < 1.09$. If the cost of the killer phenotype is $\delta > 0$, so that $f_K = f_S - \delta$, and we set $f_S = 5f_K - 4$, then for any very small choice of $0 < \delta < 0.36$, we can state that coexistence is possible in our model, and can provide an explicit family of examples, with $f_K = 1 + \delta/4$ and $f_S = 1 + 5\delta/4$.

Given a stable subpopulation of the killer strain, a necessary condition for establishment of a subpopulation of the sensitive strain from a finite number of sensitive spores is

$$f_S(1 - X_K) > 1,$$

which is identical to the previous inequality (Equation 2). We omit the technical details here, but the product $f_S(1 - X_K)$ is the effective absolute fitness of the sensitive strain in the presence of an established population of the killer strain. For each patch successfully colonized by a sensitive strain, an average of f_S spores will be emitted, but only $1 - X_K$ of patches are free of the killer strain, so only this fraction is will survive to sporulation. These considerations apply equally to an initial exponential growth phase or a

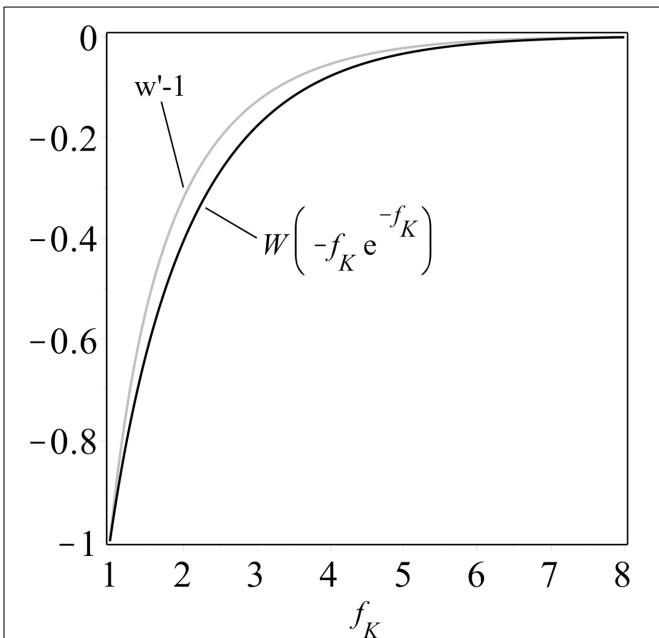


FIGURE 1 | A comparison of the composition of an exponential function and the Lambert W function, $W(-f_K e^{-f_K})$, and the upper bound derived in the Supplementary Material, both plotted as functions of $f_K \geq 1$. Note that both curves are monotonically increasing, a property which facilitates analysis.

stable state, and therefore the agreement with Equation (2) is to be expected.

The total fraction of patches stably colonized by either strain is

$$X_K + X_S = 1 + \frac{W(-(1 - X_K)f_S e^{-(1 - X_K)f_S})}{f_S} < 1.$$

Note that

$$X_K + X_S > X_K$$

if Equation (2) is satisfied, meaning that the sensitive strain, when present, only contributes to total population.

Can any ratio of killer to sensitive phenotypes be achieved in this model? Furthermore, can any total fraction of patches be stably colonized? Since X_K and X_S are continuous functions of f_K and f_S , and

$$\lim_{f_K \rightarrow \infty} X_K = 1,$$

$$\lim_{f_S \rightarrow \infty} X_S = 1 - X_K,$$

$$\lim_{f_K \rightarrow 0} X_K = \lim_{f_S \rightarrow -f_K/W(-f_K e^{-f_K})} X_S = 0$$

and

$$\lim_{f_K \rightarrow \infty} (X_K + X_S) = \lim_{f_S \rightarrow \infty} (X_K + X_S) = 1,$$

all pairs (X_K, X_S) for which $X_K + X_S < 1$ holds can be achieved by suitable choices of f_K or f_S .

As a numerical example, if $f_K = 2$ and $f_S = 5$, then Equation (2) is satisfied, and two subpopulations of sizes $X_K \approx 0.797$ (i.e., 79.7% of patches) and $X_S \approx 0.006$ (i.e., 0.6% of patches) can stably coexist. If one were interested in trying to fit a minimalist model of this type to real data, note that it would not be enough to know the ratio of killer-dominated patches to sensitive-colonized patches. One also needs the fraction of patches which are colonized by neither strain, data which is not always reported in the literature.

RESULTS

Two direct consequences of the model are (1) that killer and sensitive strains can coexist in any given proportion, and (2) that the presence of a sensitive subpopulation increases the total population size of yeast (including both strains) without reducing the population size of the virus population maintained by the killer yeast strain. Taking a broader point of view, the second consequence means that the species benefits from having both sensitive and killer strains.

COEXISTENCE FOR ARBITRARILY SMALL COST OF KILLER PHENOTYPE

Since our model is explicitly solvable, we are able to perform a mathematical analysis which showed (see the Equation 3 and the associated comments above) that coexistence is possible for any extra fitness cost of the killer phenotype, *however small*.

As a numerical example, if $f_S = 1.0001$, then we have coexistence for $f_K = 1.000049$, and the very small fitness cost represented by $\delta = 0.000051$. The corresponding fractions are $X_K \approx 0.0000996$ and $X_S \approx 0.00000399$. One notices that very small differences in fitness are achieved by populations for which the total fraction of colonized patches is also very small. This is the reason to suggest that this model may best be suited to extreme environments.

Using the explicit formulae from our analysis, $f_K = 1 + \delta/4$ and $f_S = 1 + 5\delta/4$, for a target cost of $\delta = 0.00004$, we have $f_K = 1.00001$ and $f_S = 1.00005$, with the respective fractions being $X_K \approx 0.00002$ and $X_S \approx 0.00006$. Here we see the power of the analysis: we are able to construct infinitely many further such examples for even smaller values of δ , without lower limit.

Therefore, we are able to construct pairs (f_K, f_S) for which coexistence is guaranteed, and, furthermore, do so for any given fitness cost δ for the killer phenotype, *however small*.

DISCUSSION

It is not intuitively obvious that sensitive strains can survive in the presence of killers, given that our model has no fixed barriers to prevent the sensitive strains from being eradicated by encounters with killers. The value of our model lies not only in this prediction, which is consistent with other, related, models (the semi-analytical configuration-field approximations for the one- and two-species SCA models of Czárán and Hoekstra, 2003 in particular), but also in the fact that it is *explicitly solvable*, a property which allows types of analysis to be performed which are truly complementary to what is possible with simulations alone (Silva, 2011).

We have been able to prove that killer-sensitive coexistence is possible for any fitness penalty of the killer phenotype, *however small*. This is important because it has been shown that there does not have to be any measurable fitness cost for antibiotic production (Garbeva et al., 2011). The fact that our model applies naturally to communities with low total population densities suggests that it may be applicable to microbial communities in extreme environments.

SUPPLEMENTARY MATERIAL

The Supplementary Material for this article can be found online at: <http://www.frontiersin.org/journal/10.3389/fmicb.2014.00342/abstract>

REFERENCES

- Breinig, F., Sendzik, T., Eisfeld, K., and Schmitt, M. J. (2006). Dissecting toxin immunity in virus-infected killer yeast uncovers an intrinsic strategy of self-protection. *Proc. Natl. Acad. Sci. U.S.A.* 103, 3810–3815. doi: 10.1073/pnas.0510070103
- Corless, R. M., Gonnet, G. H., Hare, D. E. G., Jeffrey, D. J., and Knuth, D. E. (1996). On the Lambert W Function. *Adv. Comput. Math.* 5, 329–359. doi: 10.1007/BF02124750
- Cornejo, O. E., Rozen, D. E., May, R. M., and Levin, B. R. (2009). Oscillations in continuous culture populations of *Streptococcus pneumoniae*: population dynamics and the evolution of clonal suicide. *Proc. Biol. Sci.* 276, 999–1008. doi: 10.1098/rspb.2008.1415
- Czárán, T. L., and Hoekstra, R. F. (2003). Killer-sensitive coexistence in metapopulations of micro-organisms. *Proc. Biol. Sci.* 270, 1373–1378. doi: 10.1098/rspb.2003.2338
- Czárán, T. L., Hoekstra, R. F., and Pagie, L. (2002). Chemical warfare between microbes promotes biodiversity. *Proc. Natl. Acad. Sci. U.S.A.* 99, 786–790. doi: 10.1073/pnas.012399899
- Garbeva, P., Tyc, O., Remus-Emsermann, M. N. P., van der Wal, A., Vos, M., Silby, M., et al. (2011). No apparent costs for facultative antibiotic production by the soil bacterium *Pseudomonas fluorescens* Pf0-1. *PLoS ONE* 6:e27266. doi: 10.1371/journal.pone.0027266
- Hamming, R. W. (1987). *Numerical Methods for Scientists and Engineers*, 2nd Edn. New York, NY: Dover Publications.
- Hardin, G. (1960). The competitive exclusion principle. *Science* 131, 1292–1297. doi: 10.1126/science.131.3409.1292
- Hawes, R. S. (1939). The flood factor in the ecology of caves. *J. Anim. Ecol.* 8, 1–5. doi: 10.2307/1248
- Holt, K. E., Nga, T. V. T., Thanh, D. P., Vinh, H., Kim, D. W., Tra, M. P. V., et al. (2013). Tracking the establishment of local endemic populations of an emergent enteric pathogen. *Proc. Natl. Acad. Sci. U.S.A.* 110, 17522–17527. doi: 10.1073/pnas.1308632110
- Margesin, R., and Miteva, V. (2011). Diversity and ecology of psychrophilic microorganisms. *Res. Microbiol.* 162, 346–361. doi: 10.1016/j.resmic.2010.12.004
- Marquina, D., Santos, A., and Peinado, J. (2002). Biology of killer yeasts. *Int. Microbiol.* 5, 65–71. doi: 10.1007/s10123-002-0066-z
- Pieczynska, M. D., Visser, J., and Korona, R. (2013). Incidence of symbiotic dsRNA killer viruses in wild and domesticated yeast. *FEMS Yeast Res.* 13, 856–859. doi: 10.1111/1567-1364.12086
- Riley, M. A., and Gordon, D. M. (1999). The ecological role of bacteriocins in bacterial competition. *Trends Microbiol.* 7, 129–133. doi: 10.1016/S0966-842X(99)01459-6
- Ross, K. A. (1980). *Elementary Analysis: The Theory of Calculus*. Berlin: Springer Verlag.
- Schmitt, M. J., and Breinig, F. (2006). Yeast viral killer toxins: lethality and self-protection. *Nat. Rev. Microbiol.* 4, 212–221. doi: 10.1038/nrmicro1347
- Schrallhammer, M. (2010). The killer trait of Paramecium and its causative agents. *Palaeodiversity* 3, 79–88. Available online at: http://www.palaeodiversity.org/pdf/03Suppl/Supplement_Schrallhammer.pdf
- Silva, G. A. (2011). The need for the emergence of mathematical neuroscience: beyond computation and simulation. *Front. Comput. Neurosci.* 5:51. doi: 10.3389/fncom.2011.00051

- Vadasz, A. S., Vadasz, P., Gupthar, A. S., and Abashar, M. E. (2003). Theoretical and experimental evidence of extinction and coexistence of killer and sensitive strains of yeast grown as a mixed culture in water. *Int. J. Food Microbiol.* 84, 157–174. doi: 10.1016/S0168-1605(02)00417-8
- Wloch-Salamon, D. M., Gerla, D., Hoekstra, R. F., and de Visser, J. A. G. (2008). Effect of dispersal and nutrient availability on the competitive ability of toxin-producing yeast. *Proc. Biol. Sci.* 275, 535–541. doi: 10.1098/rspb.2007.1461

Conflict of Interest Statement: The author declares that the research was conducted in the absence of any commercial or financial relationships that could be construed as a potential conflict of interest.

Received: 31 March 2014; accepted: 20 June 2014; published online: 14 July 2014.

Citation: Sinclair RM (2014) Persistence in the shadow of killers. *Front. Microbiol.* 5:342. doi: 10.3389/fmicb.2014.00342

This article was submitted to Terrestrial Microbiology, a section of the journal *Frontiers in Microbiology*.

Copyright © 2014 Sinclair. This is an open-access article distributed under the terms of the Creative Commons Attribution License (CC BY). The use, distribution or reproduction in other forums is permitted, provided the original author(s) or licensor are credited and that the original publication in this journal is cited, in accordance with accepted academic practice. No use, distribution or reproduction is permitted which does not comply with these terms.



Nutrient cross-feeding in the microbial world

Erica C. Seth and Michiko E. Taga*

Department of Plant and Microbial Biology, University of California, Berkeley, Berkeley, CA, USA

Edited by:

Luis Raul Comolli, Lawrence Berkeley National Laboratory, USA

Reviewed by:

Yasuyoshi Sakai, Graduate School of Agriculture, Kyoto University, Japan
Ulas Karaoz, Lawrence Berkeley National Laboratory, USA

***Correspondence:**

Michiko E. Taga, Department of Plant and Microbial Biology, University of California, Berkeley, 111 Koshland Hall, Berkeley, CA 94720-3102, USA
e-mail: taga@berkeley.edu

The stability and function of a microbial community depends on nutritional interactions among community members such as the cross-feeding of essential small molecules synthesized by a subset of the population. In this review, we describe examples of microbe-microbe and microbe–host cofactor cross-feeding, a type of interaction that influences the forms of metabolism carried out within a community. Cofactor cross-feeding can contribute to both the health and nutrition of a host organism, the virulence and persistence of pathogens, and the composition and function of environmental communities. By examining the impact of shared cofactors on microbes from pure culture to natural communities, we stand to gain a better understanding of the interactions that link microbes together, which may ultimately be a key to developing strategies for manipulating microbial communities with human health, agricultural, and environmental implications.

Keywords: nutrient cross-feeding, cofactor, microbial interactions, corrinoid, microbial communities

INTRODUCTION

Life in the microbial world exists as a dynamic network of interactions among microbes that fuels a complex web of interconnected metabolisms (Faust and Raes, 2012). Ignorance of what microbes gain via these interactions impedes our ability to cultivate the vast majority of microbes (Leadbetter, 2003; Tyson and Banfield, 2005). In addition, by failing to elicit a microbe's full range of metabolic responses to the presence of other organisms, the metabolic potential of microbes grown in isolation may not accurately reflect a microbe's ecological role (Moller et al., 1998; Traxler et al., 2013). Three broad categories of nutritional interactions that govern a microbe's ability to carry out specific forms of metabolism within a microbial community are illustrated in **Figure 1**.

The ability to compete for nutrients can determine whether a microbe will be able to persist in a particular niche (Hibbing et al., 2010; Johnson et al., 2012; **Figure 1A**). Specialized ability to gain access to a limiting nutrient (for example, iron acquisition via siderophore production) may give a microbe a competitive advantage in colonization. In contrast, metabolic cooperation between microbes engaged in syntrophic partnerships can allow access to substrates that neither microbe could metabolize alone (**Figure 1B**). For example, the presence of a partner that actively consumes intermediates such as hydrogen (H_2) allows secondary fermentation of products such as propionate to become energetically favorable (Sieber et al., 2012; Morris et al., 2013). Finally, nutrient cross-feeding – the production of a molecule such as a vitamin or amino acid that is used by both the producing organism and other microbes in the environment – relaxes the metabolic burden on any one microbe in the community (Freilich et al., 2011; **Figure 1C**). Given the complexity of microbial communities, each form of nutritional interaction may have ripple effects on other community members.

COFACTOR CROSS-FEEDING

In this review, we focus on cross-feeding of cofactors as a model for nutritional interactions between microbes. While cofactor

cross-feeding is not necessarily mutualistic, the availability of exogenously produced cofactors can have a profound impact on a microbe's mode of growth and metabolite production. (Graber and Breznak, 2005; Pedersen et al., 2012). Examining cofactor cross-feeding can inform our understanding of the scope and relevance of metabolic interdependences in microbial communities.

CROSS-FEEDING OF HEME AND QUINONES ALLOWS LACTIC ACID BACTERIA TO RESPIRE

A striking example of the impact of cofactor cross-feeding on metabolism comes from studies of the lactic acid bacteria, (LAB). Though LAB were long considered to be exclusively dependent on fermentative growth, physiological changes in cultures grown with heme led to the hypothesis that some LAB are capable of aerobic respiration (Bryan-Jones and Whittenbury, 1969). Examination of sequenced environmental and host-associated LAB predicts that the majority have the genetic capacity for respiratory growth if heme, and in some cases, quinones, are supplied. The ability to respire in the presence of these cofactors are supplied has been experimentally verified in several LAB. Respiratory metabolism in LAB has been associated with increased growth rate, long-term survival, and a variety of metabolic changes that may impact other organisms in the environment (Pedersen et al., 2012). For example, in *Lactococcus lactis* (strains of which are frequently isolated from plants) and a number of other LAB, switching from fermentation to respiratory metabolism leads to a decrease in the amount of lactic acid produced and a large increase in the production of acetoin, a volatile compound known to stimulate growth and induce the stringent response in plants (Duwat et al., 2001; Ryu et al., 2003; Rudrappa et al., 2010; Siezen et al., 2010; Jaaskelainen et al., 2013). In the opportunistic pathogen *Streptococcus agalactiae*, the ability to perform respiratory metabolism in the presence of heme and quinones enhances virulence and persistence (Rezaiki et al., 2008). Examples such as these, in which respiratory metabolism is determined

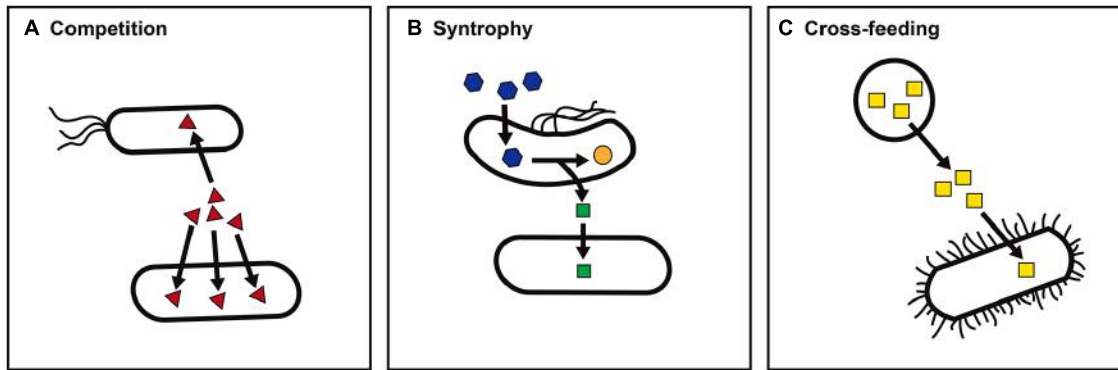


FIGURE 1 | Nutritional interactions between microbes. Nutritional interactions may shape a microbe's metabolic capacity within a microbial community. Three general categories of nutritional interactions are illustrated. **(A)** Nutrient competition. The ability of a microbe to compete for limiting nutrients such as iron (red triangles) may determine survival and persistence within a particular niche. **(B)** Syntrophic metabolism. The

consumption of an intermediate or end product such as hydrogen (green squares) by a partner organism allows an otherwise energetically unfavorable reaction, for example, propionate (blue hexagons) to acetate (orange circles) to support growth. **(C)** Nutrient cross-feeding. The presence of a microbe that produces an essential nutrient such as folate (yellow squares) enables auxotrophs to survive.

by the availability of exogenous cofactors, challenge our understanding of the metabolic capacity of microbes in their natural environments.

COFACTOR CROSS-FEEDING IN THE TERMITE GUT: *Treponema primitia* AS BOTH A DONOR AND RECIPIENT OF COFACTORS

Investigations of the termite gut-associated bacterium *Treponema primitia* illustrate the complex web of interactions that can exist within a host's microbiota. *T. primitia* contributes to the host's nutrition by producing acetate, the major carbon and energy source for the termite, by consuming H₂ and CO₂, which are generated as waste products by cellulolytic protists. The process of homoacetogenesis requires folate, yet *T. primitia* is incapable of synthesizing this cofactor (Graber and Breznak, 2004). Given that insects are not known to synthesize folate, and the folate content of the termite's diet is very low, *T. primitia*'s folate requirements must be fulfilled by other members of the termite gut microbiota. *L. lactis* and *Serratia grimesii* isolated from the termite gut were identified as candidates for this role, as both bacteria secrete 5-formyltetrahydrofolate, the dominant folate compound found in the gut, at levels capable of supporting *T. primitia* growth *in vitro* (Graber and Breznak, 2005).

T. primitia is likely to function as a donor of cofactors as well as a recipient. Cofactors produced by *T. primitia* enhance the growth of another important member of the termite gut microbiota, *Treponema azotonutricium*, which supplements the host's nitrogen-poor wood diet through nitrogen fixation (Graber et al., 2004). In co-culture, *T. primitia* and *T. azotonutricium* achieve higher growth rates and yields than either species grown in isolation. RNA-seq data suggest that in addition to inter-species hydrogen transfer between the two organisms, growth enhancement seen in *T. azotonutricium* may also be influenced by the production of the cofactors biotin, pyridoxal phosphate and co-enzyme A by *T. primitia* (Rosenthal et al., 2011). These findings undoubtedly represent only a small fraction of the complex

interactions between members of a very diverse microbiota and provide clues about how microbes that are essential to a host's nutritional status support and are supported by other members of the microbial community.

MODELS OF COFACTOR CROSS-FEEDING: CORRINOID SHARING IN MUTUALISTIC PAIRS AND MICROBIAL COMMUNITIES

Of the many documented examples of nutrient cross-feeding, one group of cofactors, the corrinoids, has been particularly informative for understanding cross-feeding mechanisms. Corrinoid-dependent reactions function in diverse metabolic processes across all three domains of life, yet corrinoids are produced solely by a subset of prokaryotes. While the majority of bacteria (75%) are predicted to encode corrinoid-dependent enzymes, at least half of these lack the ability to produce corrinoids *de novo* (Rodionov et al., 2003; Zhang et al., 2009). As such, corrinoid cross-feeding is prevalent and may reflect the advantage of acquiring these complex cofactors from the environment rather than by *de novo* biosynthesis which requires approximately 30 enzymatic steps (Roth et al., 1996; Warren et al., 2002; Zhang et al., 2009). The availability of corrinoids and corrinoid precursors can have profound effects on a microbe's metabolism and its ability to occupy a specific niche (Matthews, 2009). For instance, the ability to utilize ethanolamine as a sole carbon and nitrogen source relies on the corrinoid-dependent enzyme ethanolamine ammonia lyase, which converts ethanolamine into ammonia and acetaldehyde (Garsin, 2010). In enterohemorrhagic *Escherichia coli*, ethanolamine utilization – enabled by corrinoid cross-feeding – provides a competitive advantage for colonization and persistence in the bovine intestine, a main reservoir for this pathogen (Bertin et al., 2011; Kendall et al., 2012). Ethanolamine utilization is also important in other human pathogens that rely on exogenously produced corrinoids or corrinoid precursors including *Listeria monocytogenes* and *Enterococcus faecalis* (Joseph et al., 2006; Del Papa and Perego, 2008; Garsin,

2010). The mechanism by which corrinoids are released from corrinoid-producing microbes into the environment is unclear. As yet, no active means of corrinoid export has been identified.

Sixteen distinct corrinoids with structural differences in the lower ligand have been identified and the array of corrinoids that can serve as cofactors differs from organism to organism (Barker et al., 1960; Renz, 1999; Hibbing et al., 2010; Yi et al., 2012). Given that microbial communities have been found to contain multiple corrinoids (Allen and Stabler, 2008; Girard et al., 2009; Men et al., 2014), how do corrinoid-dependent microbes acquire the specific corrinoids that function in their metabolism? As described below, some organisms form mutualisms with corrinoid-producing partners. Others may selectively import corrinoids from the environment or modify imported corrinoids or corrinoid precursors intracellularly (**Figure 2**).

EXAMPLES OF SPECIFIC MUTUALISTIC INTERACTIONS INVOLVING CORRINOID

Phytoplankton are of great ecological importance in their roles in the global carbon cycle, as primary producers in the marine food web, and occasionally as producers of toxins in harmful algal blooms (HABs). Half of eukaryotic algal species are predicted to require exogenously produced corrinoids for growth (Croft et al., 2005; Helliwell et al., 2011). Algal corrinoid requirements can be fulfilled via symbiotic relationships with corrinoid-producing bacteria that colonize the algal surface (Croft et al., 2005; Grant et al., 2014). The availability of corrinoids may play an important role in the occurrence of HABs, as corrinoid auxotrophy is especially prevalent among HAB species (Tang et al., 2010).

Symbiotic relationships can also be fueled by cross-feeding of products of corrinoid-dependent enzymes. Genomic studies of the cicada endosymbiotic bacteria, *Hodgkinia cicadicola* and

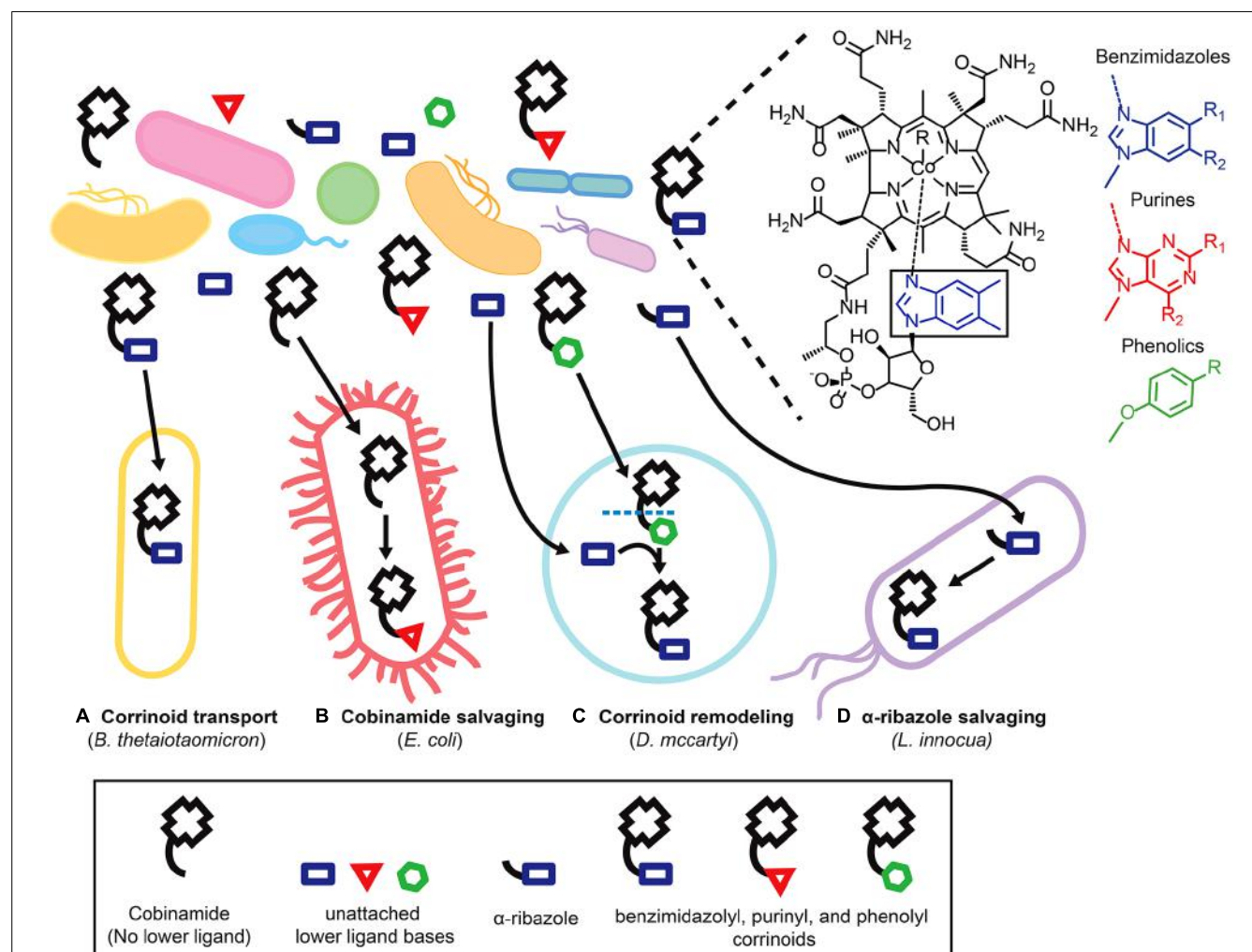


FIGURE 2 | Microbial strategies for fulfilling corrinoid requirements.

Microbes employ various strategies to obtain specific corrinoids from environments that contain a variety of corrinoids and corrinoid precursors. The structure of cobalamin, a corrinoid with the lower ligand 5,6-dimethylbenzimidazole (boxed) is shown, as are the structures of the three

classes of lower ligand bases of other corrinoids. Specific strategies for obtaining corrinoids are illustrated with representative bacteria listed in parentheses. **(A)** Corrinoid transport in *Bacteroides thetaiotaomicron*.

(B) Cobinamide salvaging in *Escherichia coli*. **(C)** Corrinoid remodeling in *Dehalococcoides mccartyi*. **(D)** α -ribazole salvaging in *Listeria innocua*.

Sulcia muelleri, indicate that the ability to produce a corrinoid is vital for maintaining this tripartite symbiosis (McCutcheon et al., 2009). *H. cicadicola* and *S. muelleri* together produce essential amino acids that are cross-fed between the co-symbionts and provided to the host. The burden of methionine production rests on *H. cicadicola*, which devotes 7% of its 144 kb genome to corrinoid biosynthesis because the methionine synthase it encodes requires a corrinoid cofactor. Interestingly, the corrinoid biosynthesis pathway in *H. cicadicola* is incomplete, and lacks genes involved in the production of precursors common to the biosynthesis of corrinoids as well as other tetrapyrroles such as heme (McCutcheon et al., 2009). We speculate that *H. cicadicola* may acquire tetrapyrrole precursors from the host, completing a loop between organisms which allows maintenance of the symbiotic relationship.

STRATEGIES USED BY BACTERIA THAT SCAVENGE CORRINOID PRECURSORS FROM ENVIRONMENTAL SOURCES

The ability of bacteria to selectively transport specific corrinoids has been largely unexplored, yet may play an important role in ensuring that bacteria acquire the specific corrinoids that function in their metabolism. The corrinoid transporter – BtuBFCD in gram negative bacteria, and BtuFCD in gram positive bacteria - allows bacteria to import corrinoids from the environment (Figure 2A) and is present in an estimated 76% of bacterial genomes (Zhang et al., 2009). A recent study of the human gut microbiome found that many bacteria encode multiple copies of the BtuBFCD corrinoid transporter, and that the three homologs of the outer membrane transporter BtuB encoded by the model gut bacterium *Bacteroides thetaiotaomicron*, though apparently redundant, have distinct preferences for different corrinoids (Degnan et al., 2014). The presence of multiple corrinoid transport systems with different affinities for specific corrinoids may allow bacteria to fine-tune their responses to the array of corrinoids present in the environment.

In contrast to obtaining specific corrinoids through selective transport, the ability to remodel corrinoids (that is, to remove the lower ligand of an imported corrinoid and attach a preferred lower ligand in its place) can enable microbes to make use of many different corrinoids present in a community (Gray and Escalante-Semerena, 2009). For instance, our recent work showed that *Dehalococcoides mccartyi*, which has an obligate requirement for exogenously produced corrinoids as cofactors in the reductive dehalogenation of the common groundwater pollutants tetrachloroethene (PCE) and trichloroethene (TCE), is restricted to the use of just three benzimidazolyl corrinoids (Maymo-Gatell et al., 1997; He et al., 2007; Yi et al., 2012). However, if an appropriate benzimidazole lower ligand base is supplied, *D. mccartyi* can fulfill its corrinoid requirements by remodeling other corrinoids (Figure 2C; Yi et al., 2012). Since benzimidazolyl corrinoids represent only a fraction of the corrinoids present in a community containing *D. mccartyi*, the ability to remodel corrinoids may be essential to its survival in the environment (Men et al., 2014). Corrinoid remodeling is also performed by some bacteria capable of producing a corrinoid *de novo* (Gray and Escalante-Semerena, 2009), and has been

observed in the human gut, where examination of fecal corrinoid profiles before and after ingestion of cobalamin suggests that at least some members of the gut microbiota are engaged in active modification of exogenous corrinoids (Allen and Stabler, 2008).

In addition to importing complete corrinoids (i.e., those containing a lower ligand), some microbes are capable of importing corrinoid precursors from the environment and carrying out the remaining biosynthetic steps to produce a complete corrinoid. For example, though *E. coli* is incapable of *de novo* corrinoid biosynthesis, it possesses the ability to take up cobinamide (a corrinoid precursor that lacks a lower ligand) and convert it to a complete corrinoid through a process known as cobinamide salvaging (Figure 2B; Di Girolamo and Bradbeer, 1971; Raux et al., 1996; Escalante-Semerena, 2007). In contrast, *Listeria spp.* encode a nearly complete corrinoid biosynthesis pathway, but apparently lack the genes necessary for lower ligand activation, a step that must be completed before the lower ligand can be attached. *Listeria innocua* was shown instead to rely on the *cblT* encoded transporter to take up activated lower ligands such as α -ribazole from the environment, which it then phosphorylates and attaches to produce a complete corrinoid (Gray and Escalante-Semerena, 2010; Figure 2D). CblT homologs have been identified in a variety of human pathogens including *L. monocytogenes* and *Clostridium botulinum* (Gray and Escalante-Semerena, 2010).

Microbes that produce corrinoids *de novo* can also be affected by the presence of corrinoid precursors. Guided biosynthesis, the process of controlling which corrinoid a microbe produces by providing an excess of a particular lower ligand base, can be a useful tool for determining the specific corrinoids required in different metabolic pathways (Stupperich et al., 1987; Keller et al., 2013). For example, in *Sporomusa ovata*, which produces phenolyl corrinoids, the addition of benzimidazoles and their subsequent incorporation into benzimidazolyl corrinoids inhibits growth to different degrees on substrates that require a corrinoid-dependent methyltransferase for utilization (Stupperich and Konle, 1993; Mok and Taga, 2013). We have detected free lower ligand bases in a variety of environmental samples, which raises the question of whether the production of a free lower ligand base by one organism is capable of affecting the corrinoid production of another; that is, whether guided biosynthesis occurs in nature. Evidence from our recent study of the corrinoid and lower ligand profiles in a TCE-dechlorinating community containing *D. mccartyi* suggests that this indeed may be the case (Men et al., 2014).

CORRINOID AS LYNCHPIN OF MICROBIAL COMMUNITY DYNAMICS?

Given that the majority of bacteria depend on corrinoids for their metabolism, and that only a fraction of available corrinoids may be suitable for use by a particular organism, could it be possible to manipulate microbial communities by targeting corrinoid-dependent metabolism? Recent work has shown that manipulation of the composition of a TCE-dechlorinating community can result in a shift in corrinoid composition, and conversely, that the addition of a corrinoid causes a dramatic shift in marine algal community

composition (Koch et al., 2011; Men et al., 2014). With growing interest in developing methods for targeted manipulation of microbial communities to benefit human health and the environment, the utility of altering the composition and/or metabolism occurring in microbial communities via corrinoid supplementation or guided biosynthesis deserves further investigation.

CONCLUSION

From obligate requirements for exogenously supplied cofactors in *T. primitia* and *D. mccartyi* to unlocking cryptic modes of growth in LAB, examples of cofactor cross-feeding provide a glimpse into the impact of nutritional interactions on individual species as well as entire communities. Cofactor cross-feeding undoubtedly deserves further examination; one need look no further than the vitamin amendments required for microbes growing in pure culture to obtain examples of nutrients that must be supplied by other organisms in their natural environment. Advances in imaging mass spectrometry and multiple “omics” approaches, in combination with pure culture studies of individual microbes and defined consortia, bring us closer to understanding the molecular details of metabolic interactions at new levels (Nakanishi et al., 2011; Phelan et al., 2012).

ACKNOWLEDGMENT

This work was supported by National Science Foundation grant MCB1122046 to Michiko E. Taga.

REFERENCES

- Allen, R. H., and Stabler, S. P. (2008). Identification and quantitation of cobalamin and cobalamin analogs in human feces. *Am. J. Clin. Nutr.* 87, 1324–1335.
- Barker, H. A., Smyth, R. D., Weissbach, H., Toohey, J. I., Ladd, J. N., and Volcani, B. E. (1960). Isolation and properties of crystalline cobamide coenzymes containing benzimidazole or 5, 6-dimethylbenzimidazole. *J. Biol. Chem.* 235, 480–488.
- Bertin, Y., Girardeau, J. P., Chaucheyras-Durand, F., Lyan, B., Pujos-Guillot, E., Harel, J., et al. (2011). Enterohaemorrhagic *Escherichia coli* gains a competitive advantage by using ethanolamine as a nitrogen source in the bovine intestinal content. *Environ. Microbiol.* 13, 365–377. doi: 10.1111/j.1462-2920.2010.02334.x
- Bryan-Jones, D. G., and Whittenbury, R. (1969). Haematin-dependent oxidative phosphorylation in *Streptococcus faecalis*. *J. Gen. Microbiol.* 58, 247–260. doi: 10.1099/00221287-58-2-247
- Croft, M. T., Lawrence, A. D., Raux-Deery, E., Warren, M. J., and Smith, A. G. (2005). Algae acquire vitamin B12 through a symbiotic relationship with bacteria. *Nature* 438, 90–93. doi: 10.1038/nature04056
- Degnan, P. H., Barry, N. A., Mok, K. C., Taga, M. E., and Goodman, A. L. (2014). Human gut microbes use multiple transporters to distinguish vitamin B12 analogs and compete in the gut. *Cell Host Microbe* 15, 47–57. doi: 10.1016/j.chom.2013.12.007
- Del Papa, M. F., and Perego, M. (2008). Ethanolamine activates a sensor histidine kinase regulating its utilization in *Enterococcus faecalis*. *J. Bacteriol.* 190, 7147–7156. doi: 10.1128/JB.00952-08
- Di Girolamo, P. M., and Bradbeer, C. (1971). Transport of vitamin B12 in *Escherichia coli*. *J. Bacteriol.* 106, 745–750.
- Duwat, P., Source, S., Cesselin, B., Lamberet, G., Vido, K., Gaudu, P., et al. (2001). Respiration capacity of the fermenting bacterium *Lactococcus lactis* and its positive effects on growth and survival. *J. Bacteriol.* 183, 4509–4516. doi: 10.1128/JB.183.15.4509-4516.2001
- Escalante-Semerena, J. C. (2007). Conversion of cobinamide into adenosylcobamide in bacteria and archaea. *J. Bacteriol.* 189, 4555–4560. doi: 10.1128/JB.00503-07
- Faust, K., and Raes, J. (2012). Microbial interactions: from networks to models. *Nat. Rev. Microbiol.* 10, 538–550. doi: 10.1038/nrmicro2832
- Freilich, S., Zarecki, R., Eilam, O., Segal, E. S., Henry, C. S., Kupiec, M., et al. (2011). Competitive and cooperative metabolic interactions in bacterial communities. *Nat. Commun.* 2:589. doi: 10.1038/ncomms1597
- Garsin, D. A. (2010). Ethanolamine utilization in bacterial pathogens: roles and regulation. *Nat. Rev. Microbiol.* 8, 290–295. doi: 10.1038/nrmicro2334
- Girard, C. L., Santschi, D. E., Stabler, S. P., and Allen, R. H. (2009). Apparent ruminal synthesis and intestinal disappearance of vitamin B12 and its analogs in dairy cows. *J. Dairy Sci.* 92, 4524–4529. doi: 10.3168/jds.2009-2049
- Graber, J. R., and Breznak, J. A. (2004). Physiology and nutrition of *Treponema primitia*, an H2/CO2-acetogenic spirochete from termite hindguts. *Appl. Environ. Microbiol.* 70, 1307–1314. doi: 10.1128/AEM.70.3.1307-1314.2004
- Graber, J. R., and Breznak, J. A. (2005). Folate cross-feeding supports symbiotic homoacetogenic spirochetes. *Appl. Environ. Microbiol.* 71, 1883–1889. doi: 10.1128/AEM.71.4.1883-1889.2005
- Graber, J. R., Leadbetter, J. R., and Breznak, J. A. (2004). Description of *Treponema azotonutricium* sp. nov. and *Treponema primitia* sp. nov., the first spirochetes isolated from termite guts. *Appl. Environ. Microbiol.* 70, 1315–1320. doi: 10.1128/aem.70.3.1315-1320.2004
- Grant, M. A., Kazamia, E., Cicuta, P., and Smith, A. G. (2014). Direct exchange of vitamin B12 is demonstrated by modeling the growth dynamics of algal-bacterial cocultures. *ISME J.* 8, 1418–1427. doi: 10.1038/ismej.2014.9
- Gray, M. J., and Escalante-Semerena, J. C. (2009). The cobinamide amidohydrolase (cobyric acid-forming) CbiZ enzyme: a critical activity of the cobamide remodeling system of *Rhodobacter sphaeroides*. *Mol. Microbiol.* 74, 1198–1210. doi: 10.1111/j.1365-2958.2009.06928.x
- Gray, M. J., and Escalante-Semerena, J. C. (2010). A new pathway for the synthesis of alpha-ribazole-phosphate in *Listeria innocua*. *Mol. Microbiol.* 77, 1429–1438. doi: 10.1111/j.1365-2958.2010.07294.x
- He, J., Holmes, V. F., Lee, P. K., and Alvarez-Cohen, L. (2007). Influence of vitamin B12 and cocultures on the growth of *Dehalococcoides* isolates in defined medium. *Appl. Environ. Microbiol.* 73, 2847–2853. doi: 10.1128/AEM.02574-06
- Helliwell, K. E., Wheeler, G. L., Leptos, K. C., Goldstein, R. E., and Smith, A. G. (2011). Insights into the evolution of vitamin B12 auxotrophy from sequenced algal genomes. *Mol. Biol. Evol.* 28, 2921–2933. doi: 10.1093/molbev/msr124
- Hibbing, M. E., Fuqua, C., Parsek, M. R., and Peterson, S. B. (2010). Bacterial competition: surviving and thriving in the microbial jungle. *Nat. Rev. Microbiol.* 8, 15–25. doi: 10.1038/nrmicro2259
- Jaaskelainen, E., Johansson, P., Kostianoinen, O., Nieminen, T., Schmidt, G., Somervuo, P., et al. (2013). Significance of heme-based respiration in meat spoilage caused by *Leuconostoc gasicomitatum*. *Appl. Environ. Microbiol.* 79, 1078–1085. doi: 10.1128/AEM.02943-12
- Johnson, D. R., Goldschmidt, F., Lilja, E. E., and Ackermann, M. (2012). Metabolic specialization and the assembly of microbial communities. *ISME J.* 6, 1985–1991. doi: 10.1038/ismej.2012.46
- Joseph, B., Przybilla, K., Stuhler, C., Schauer, K., Slaghuis, J., Fuchs, T. M., et al. (2006). Identification of *Listeria monocytogenes* genes contributing to intracellular replication by expression profiling and mutant screening. *J. Bacteriol.* 188, 556–568. doi: 10.1128/JB.188.2.556–568.2006
- Keller, S., Ruett, M., Kunze, C., Krautler, B., Diekert, G., and Schubert, T. (2013). Exogenous 5,6-dimethylbenzimidazole caused production of a non-functional tetrachloroethene reductive dehalogenase in *Sulfurospirillum multivorans*. *Environ. Microbiol.* doi: 10.1111/1462-2920.12268 [Epub ahead of print].
- Kendall, M. M., Gruber, C. C., Parker, C. T., and Sperandio, V. (2012). Ethanolamine controls expression of genes encoding components involved in interkingdom signaling and virulence in enterohemorrhagic *Escherichia coli* O157:H7. *MBio* 3. doi: 10.1128/mBio.00050-12
- Koch, F., Alejandra Marcoval, M., Panzeca, C., Bruland, K. W., Sañudo-Wilhelmy, S. A., and Gobler, C. J. (2011). The effect of vitamin B12 on phytoplankton growth and community structure in the Gulf of Alaska. *Limnol. Oceanogr.* 56, 1023–1034. doi: 10.4319/lo.2011.56.3.1023
- Leadbetter, J. R. (2003). Cultivation of recalcitrant microbes: cells are alive, well and revealing their secrets in the 21st century laboratory. *Curr. Opin. Microbiol.* 6, 274–281. doi: 10.1016/s1369-5274(03)00041-49
- Matthews, R. G. (2009). Cobalamin- and corrinoid-dependent enzymes. *Met. Ions Life Sci.* 6, 53–114. doi: 10.1039/BK9781847559159-00053
- Maymo-Gatell, X., Chien, Y., Gossett, J. M., and Zinder, S. H. (1997). Isolation of a bacterium that reductively dechlorinates tetrachloroethene

- to ethene. *Science* 276, 1568–1571. doi: 10.1126/science.276.5318.1568
- McCutcheon, J. P., McDonald, B. R., and Moran, N. A. (2009). Convergent evolution of metabolic roles in bacterial co-symbionts of insects. *Proc. Natl. Acad. Sci. U.S.A.* 106, 15394–15399. doi: 10.1073/pnas.0906424106
- Men, Y., Seth, E. C., Yi, S., Crofts, T. S., Allen, R. H., Taga, M. E., et al. (2014). Identification of specific corrinoids reveals corrinoid modification in dechlorinating microbial communities. *Environ. Microbiol.* doi: 10.1111/1462-2920.12500 [Epub ahead of print].
- Mok, K. C., and Taga, M. E. (2013). Growth inhibition of *Sporomusa ovata* by incorporation of benzimidazole bases into cobamides. *J. Bacteriol.* 195, 1902–1911. doi: 10.1128/JB.01282-12
- Moller, S., Sternberg, C., Andersen, J. B., Christensen, B. B., Ramos, J. L., Givskov, M., et al. (1998). In situ gene expression in mixed-culture biofilms: evidence of metabolic interactions between community members. *Appl. Environ. Microbiol.* 64, 721–732.
- Morris, B. E., Henneberger, R., Huber, H., and Moissl-Eichinger, C. (2013). Microbial syntrophy: interaction for the common good. *FEMS Microbiol. Rev.* 37, 384–406. doi: 10.1111/1574-6976.12019
- Nakanishi, Y., Fukuda, S., Chikayama, E., Kimura, Y., Ohno, H., and Kikuchi, J. (2011). Dynamic omics approach identifies nutrition-mediated microbial interactions. *J. Proteome Res.* 10, 824–836. doi: 10.1021/pr100989c
- Pedersen, M. B., Gaudu, P., Lechardeur, D., Petit, M. A., and Gruss, A. (2012). Aerobic respiration metabolism in lactic acid bacteria and uses in biotechnology. *Annu. Rev. Food Sci. Technol.* 3, 37–58. doi: 10.1146/annurev-food-022811-101255
- Phelan, V. V., Liu, W. T., Pogliano, K., and Dorrestein, P. C. (2012). Microbial metabolic exchange—the chemotype-to-phenotype link. *Nat. Chem. Biol.* 8, 26–35. doi: 10.1038/nchembio.739
- Raux, E., Lanois, A., Levillayer, F., Warren, M. J., Brody, E., Rambach, A., et al. (1996). *Salmonella typhimurium* cobalamin (vitamin B12) biosynthetic genes: functional studies in *S. typhimurium* and *Escherichia coli*. *J. Bacteriol.* 178, 753–767.
- Renz, P. (1999). “Biosynthesis of the 5,6-dimethylbenzimidazole moiety of cobalamin and of the other bases found in natural corrinoids,” in *Chemistry and Biochemistry of B12*, ed. R Banerjee (New York, NY: John Wiley & Sons, Inc.), 557–575.
- Rezaiki, L., Lamberet, G., Derre, A., Gruss, A., and Gaudu, P. (2008). *Lactococcus lactis* produces short-chain quinones that cross-feed Group B *Streptococcus* to activate respiration growth. *Mol. Microbiol.* 67, 947–957. doi: 10.1111/j.1365-2958.2007.06083.x
- Rodionov, D. A., Vitreschak, A. G., Mironov, A. A., and Gelfand, M. S. (2003). Comparative genomics of the vitamin B12 metabolism and regulation in prokaryotes. *J. Biol. Chem.* 278, 41148–41159. doi: 10.1074/jbc.M305837200 [Epub ahead of print].
- Rosenthal, A. Z., Matson, E. G., Eldar, A., and Leadbetter, J. R. (2011). RNA-seq reveals cooperative metabolic interactions between two termite-gut spirochete species in co-culture. *ISME J.* 5, 1133–1142. doi: 10.1038/ismej.2011.3
- Roth, J. R., Lawrence, J. G., and Bobik, T. A. (1996). Cobalamin (coenzyme B12): synthesis and biological significance. *Annu. Rev. Microbiol.* 50, 137–181. doi: 10.1146/annurev.micro.50.1.137
- Rudrappa, T., Biedrzycki, M. L., Kunjeti, S. G., Donofrio, N. M., Czummek, K. J., Pare, P. W., et al. (2010). The rhizobacterial elicitor acetoin induces systemic resistance in *Arabidopsis thaliana*. *Commun. Integr. Biol.* 3, 130–138. doi: 10.4161/cib.3.2.10584
- Ryu, C. M., Farag, M. A., Hu, C. H., Reddy, M. S., Wei, H. X., Pare, P. W., et al. (2003). Bacterial volatiles promote growth in *Arabidopsis*. *Proc. Natl. Acad. Sci. U.S.A.* 100, 4927–4932. doi: 10.1073/pnas.0730845100
- Sieber, J. R., Mcinerney, M. J., and Gunsalus, R. P. (2012). Genomic insights into syntrophy: the paradigm for anaerobic metabolic cooperation. *Annu. Rev. Microbiol.* 66, 429–452. doi: 10.1146/annurev-micro-090110-102844
- Siezen, R. J., Bayjanov, J., Renckens, B., Wels, M., Van Huijum, S. A., Molenaar, D., et al. (2010). Complete genome sequence of *Lactococcus lactis* subsp. *lactis* KF147, a plant-associated lactic acid bacterium. *J. Bacteriol.* 192, 2649–2650. doi: 10.1128/JB.00276-210
- Stupperich, E., and Konle, R. (1993). Corrinoid-dependent methyl transfer reactions are involved in methanol and 3,4-dimethoxybenzoate metabolism by *Sporomusa ovata*. *Appl. Environ. Microbiol.* 59, 3110–3116.
- Stupperich, E., Steiner, I., and Eisinger, H. J. (1987). Substitution of Co alpha-(5-hydroxybenzimidazolyl)cobamide (factor III) by vitamin B12 in *Methanobacterium thermoautotrophicum*. *J. Bacteriol.* 169, 3076–3081.
- Tang, Y. Z., Koch, F., and Gobler, C. J. (2010). Most harmful algal bloom species are vitamin B1 and B12 auxotrophs. *Proc. Natl. Acad. Sci. U.S.A.* 107, 20756–20761. doi: 10.1073/pnas.1009566107
- Traxler, M. F., Watrous, J. D., Alexandrov, T., Dorrestein, P. C., and Kolter, R. (2013). Interspecies interactions stimulate diversification of the *Streptomyces coelicolor* secreted metabolome. *MBio* 4. doi: 10.1128/mBio.00459-13
- Tyson, G. W., and Banfield, J. F. (2005). Cultivating the uncultivated: a community genomics perspective. *Trends Microbiol.* 13, 411–415. doi: 10.1016/j.tim.2005.07.003
- Warren, M. J., Raux, E., Schubert, H. L., and Escalante-Semerena, J. C. (2002). The biosynthesis of adenosylcobalamin (vitamin B12). *Nat. Prod. Rep.* 19, 390–412. doi: 10.1039/b108967f
- Yi, S., Seth, E. C., Men, Y. J., Stabler, S. P., Allen, R. H., Alvarez-Cohen, L., et al. (2012). Versatility in corrinoid salvaging and remodeling pathways supports corrinoid-dependent metabolism in *Dehalococcoides mccartyi*. *Appl. Environ. Microbiol.* 78, 7745–7752. doi: 10.1128/AEM.02150-12
- Zhang, Y., Rodionov, D. A., Gelfand, M. S., and Gladyshev, V. N. (2009). Comparative genomic analyzes of nickel, cobalt and vitamin B12 utilization. *BMC Genomics* 10:78. doi: 10.1186/1471-2164-10-78

Conflict of Interest Statement: The authors declare that the research was conducted in the absence of any commercial or financial relationships that could be construed as a potential conflict of interest.

Received: 30 May 2014; accepted: 23 June 2014; published online: 08 July 2014.

Citation: Seth EC and Taga ME (2014) Nutrient cross-feeding in the microbial world. *Front. Microbiol.* 5:350. doi: 10.3389/fmicb.2014.00350

This article was submitted to Terrestrial Microbiology, a section of the journal *Frontiers in Microbiology*.

Copyright © 2014 Seth and Taga . This is an open-access article distributed under the terms of the Creative Commons Attribution License (CC BY). The use, distribution or reproduction in other forums is permitted, provided the original author(s) or licensor are credited and that the original publication in this journal is cited, in accordance with accepted academic practice. No use, distribution or reproduction is permitted which does not comply with these terms.



Variations in the identity and complexity of endosymbiont combinations in whitefly hosts

Einat Zchori-Fein¹, Tamar Lahav² and Shiri Freilich^{2*}

¹ The Agricultural Research Organization, Newe Ya'ar Research Center, Institute of Plant Protection, Ramat Yishay, Israel

² The Agricultural Research Organization, Newe Ya'ar Research Center, Institute of Plant Sciences, Ramat Yishay, Israel

Edited by:

Luis Raul Comolli, Lawrence Berkeley National Laboratory, USA

Reviewed by:

Joana Falcão Salles, University of Groningen, Netherlands

Mark Radosevich, University of Tennessee, USA

***Correspondence:**

Shiri Freilich, The Agricultural Research Organization, Newe Ya'ar Research Center, Institute of Plant Sciences, PO Box 1021, Ramat Yishay 30095, Israel
e-mail: shiri.freilich@gmail.com

The target of natural selection is suggested to be the holobiont - the organism together with its associated symbiotic microorganisms. The well-defined endosymbiotic communities of insects make them a useful model for exploring the role of symbiotic interactions in shaping the functional repertoire of plants and animals. Here, we studied the variations in the symbiotic communities of the sweet potato whitefly *Bemisia tabaci* (Hemiptera: Aleyrodidae) by compiling a dataset of over 2000 individuals derived from several independent screenings. The secondary endosymbionts harbored by each individual were clustered into entities termed Facultative Endosymbiont Combinations (FECs), each representing a natural assemblage of co-occurring bacterial genera. The association of FECs with whitefly individuals stratified the otherwise homogeneous population into holobiont units. We both identified bacterial assemblages that are specific to whitefly groups sharing unique genetic backgrounds, and characterized the FEC variations within these groups. The analysis revealed that FEC complexity is positively correlated with both distance from the equator and specificity of the genetic clade of the host insect. These findings highlight the importance of symbiotic combinations in shaping the distribution patterns of *B. tabaci* and possibly other insect species.

Keywords: bacteriome, *Bemisia tabaci*, facultative endosymbionts, holobiont

INTRODUCTION

The term “holobiont” was coined to describe a central, multi-cellular organism and all of its associated symbiotic microbes, including parasites, mutualists, synergists, and amensalists (Rosenberg and Zilber-Rosenberg, 2011). Variations in the structure and composition of holobiont communities have been shown to affect the fitness of the host, suggesting that the target of natural selection is not only the organism itself but also its associated community of microorganisms (Rosenberg et al., 2007). Simple symbiotic systems such as those formed between many arthropods and a limited-size community of bacterial endosymbionts (i.e., bacteria that reside within the cells of their hosts, as opposed to gut bacteria for example) can provide useful models for exploring the functional variations among holobiont units (Ferrari and Vavre, 2011).

Many insects, mainly those feeding on a nutrient-imbalanced diet (e.g., plant sap, wood, or vertebrate blood), possess a specialized organ termed bacteriome that hosts endosymbiotic bacteria (Buchner, 1965; Baumann, 2005). Within the bacteriome, insect cells provide nutrients and shelter for their tenants; in exchange, bacteria, that are classified as “primary” or “obligated” endosymbionts, complement the insect’s diet by providing essential and otherwise missing nutrients such as vitamins, amino acids and carotenoids (McCutcheon and Moran, 2010; Sloan and Moran, 2012; Russell et al., 2013). Such obligatory endosymbionts are strictly maternally inherited, their phylogeny is congruent with that of their host and they tend to be fixed in insect species,

genera and families (Zchori-Fein and Bourtzis, 2011). Alongside the primary endosymbionts, insects often carry non-essential bacterial associates termed “facultative” or “secondary” endosymbionts that can also be housed within the bacteriome, as well as in various other tissues (Zchori-Fein and Bourtzis, 2011). Unlike the primary endosymbionts, facultative associates are transmitted not only vertically, through maternal inheritance, but also through occasional events of horizontal transmission. Such transfer, spreading and loss events lead to dynamic variations in bacterial communities within insect populations. These variations are suggested to form a “horizontal gene pool” which may provide fitness benefits to the insect host (Moran, 2007; Gueguen et al., 2010; Jaenike, 2012; Henry et al., 2013). Studying the ecological factors that are associated with such variations can point at the functional significance and the selective pressures that promote the sustainability of different holobiont units assembled around a single central species.

In the past decade, the emergence of new genomic sequencing techniques has allowed the characterization of specific microbial communities across significant number of insect individuals. Two recent surveys of symbionts associated with aphids (Henry et al., 2013) and whiteflies (Gueguen et al., 2010) individuals have pointed at a dynamic process of community assemblage resulting from horizontal transfers and reflecting ecological similarities (e.g., host plant) among individuals carrying specific symbionts. The symbiotic communities of the phloem-sap feeding sweetpotato whitefly *Bemisia tabaci* (Hemiptera: Aleyrodidae)—a

major pest of several key crops worldwide (Stansly and Steven, 2010)—have been extensively documented. *B. tabaci* is a species complex consisting of as many as 34 genetically distinct but morphologically indistinguishable, delimited genetic groups (De Barro et al., 2011; Liu et al., 2012; Tay et al., 2012). Most of these genetic groups are equivalent to the “biotypes” of earlier works, and for the sake of simplicity, we will use this definition hereafter. Like the entire Aleyrodidae family, all *B. tabaci* individuals carry the primary endosymbiotic bacterium *Portiera aleyrodidarum* (Thao and Baumann, 2004). Frequently, individuals also carry varying combinations of one to four facultative endosymbionts out of seven bacterial genera (*Wolbachia*, *Cardinium*, *Rickettsia*, *Arsenophonus*, *Hamiltonella*, *Fritschea*, and *Hemipterophilus*). Occurrence patterns of facultative endosymbionts have been attributed to several aspects of the insect’s biology, including host reproduction (Zchori-Fein et al., 2001; Hunter et al., 2003; Zchori-Fein and Perlman, 2004; Himler et al., 2011), survival and fecundity (Liu et al., 2007; Kotsosalov et al., 2008; Gottlieb et al., 2010; Thierry et al., 2011), resistance to insecticides (Kotsosalov et al., 2008) and capacity to transmit diseases to the host plant (Gottlieb et al., 2010). Variations among biotypes in their association patterns with facultative endosymbionts are repeatedly reported (e.g., Chiel et al., 2007; Gueguen et al., 2010). In previous screening efforts, the strong biotype-endosymbiont associations impede the characterization of additional, possibly more subtle determinants of facultative endosymbiont distribution, beyond biotype identity. In order to delineate possible environmental factors that are associated with community variations we compiled the results from several independent screens, reporting the distribution patterns of facultative endosymbionts across over 2000 *B. tabaci* individuals. Taking advantage of environmental diversity of the sampling sites, we used this collection for characterizing the diversity of bacterial assemblages *within* genetic groups.

MATERIALS AND METHODS

DATABASE

Information from six worldwide screening projects of bacterial abundance within *B. tabaci* was combined to obtain the most comprehensive database to date in terms of the number of individuals sampled and the geographical range of their habitats. Overall, individuals were sampled from 20 host plants across 11 geographical locations that fall into 7 climatic zones and are classified into 13 distinct biotypes (Figure 1). The numbers of individuals sampled in the independent projects were: Project A: 330 (Tsagkarakou et al., 2012); Project B: 262 (Bing et al., 2013); Project C: 430 (Zchori-Fein’s lab, unpublished); Project D: 237 (Gueguen et al., 2010); Project E: 393 (Thierry et al., 2011); and Project F: 378 (Gnankine et al., 2012). The biotype classifications of individuals from each project and the endosymbiont they harbor are provided at the Supplementary Material. All laboratories applied almost identical protocols for species’ detection, detailed at the Supplementary Material. Briefly, biotype recognition generally relies on sequence-based phylogenetic analyses using numerous sequences of the mitochondrial gene cytochrome oxidase I (COI) (Boykin et al., 2007). The presence of *Portiera* was determined as an internal control for DNA

quality. All individuals were screened for the presence of five facultative endosymbionts (*Arsenophonus*, *Cardinium*, *Hamiltonella*, *Rickettsia*, and *Wolbachia*) using PCR primers targeting the 16S rRNA gene for *Cardinium*, *Hamiltonella*, and *Rickettsia*, the 23S rRNA gene for *Arsenophonus* and the wsp gene or the 16S rRNA gene for *Wolbachia* (Supplementary Material). *Fritschea* and *Hemipterophilus* were not screened by all groups and hence were not considered in the analysis. We verified that all screens allow the identification of each of the five endosymbionts by counting the number of individuals from a specific biotype carrying a specific endosymbiont in each project (Supplementary Materials). All five endosymbionts were identified in three of the projects (projects B, D, F); four out of five endosymbionts were identified in two of the projects (projects C, E); and in a single project, three out of five endosymbionts were identified (project A). Overall, out of 30 laboratory procedures of endosymbiont identification (5 endosymbionts X 6 projects), only four procedures did not result in the identification of an endosymbiont (Supplementary Material). Three out of these four procedures can be explained by the biotype identity of the individuals screened in the project: (1) *Cardinium* was not identified in project (C), but only individuals from B and Q2 were screened and *Cardinium* was not detected in these biotypes in any of the other projects. (2) *Wolbachia* was not identified in project (E), but only individuals from Ms and B were screened and *Wolbachia* was not detected in these biotypes in any of the other projects. (3) *Arsenophonus* was not identified in project (A), but only individuals from Q1 were screened and *Arsenophonus* was not detected in that biotype in of the other projects. Hence, though the screens were carried independently by different groups, the use of a common procedures and the consistency of the variations in the endosymbiont-biotype associations across projects (Supplementary Materials) support the integration of the data and its further use for delineating intra-biotype variations.

STATISTICAL ANALYSES

The probability that the number of individuals classified to a given biotype and harboring a specific Facultative Endosymbiont Combination (FEC) will be collected from a given host plant or geographical location was higher than chance, was determined by calculating a cumulative hypergeometric *P*-value. The corresponding size of the population was calculated as the sum of individuals collected for a given biotype; the number of items with the desired characteristic in the population, *K*, was the number of individuals in the population carrying a given FEC, and number of samples drawn, *N*, was the number of individuals in the population that were collected on a given host plant or in a given geographical region. Cumulative hypergeometric probability and partial correlations were calculated using Matlab.

RESULTS

CHARACTERIZATION OF INFECTION RICHNESS OF WHITEFLY INDIVIDUALS WITH FACULTATIVE ENDOSYMBIONTS

Information on the rate of occurrence of key facultative endosymbionts was collected by compiling data derived from independent projects. The analysis of the combined dataset reinforced past phylogenetic reports, derived from smaller-scale screens, which



FIGURE 1 | Description of the dataset. Top: Collection sites of *B. tabaci* included in the dataset. In some cases, small samples from proximal locations were grouped (e.g., location 4 in West Africa). The plot on the left shows the mean genera richness of facultative endosymbionts co-infesting whitefly individuals in each location (Pearson correlation: 0.65, *P*-value 0.03). Circle sizes indicate the number of sampled individuals. **Bottom:** Distribution of *B. tabaci* biotypes, plants, and facultative symbionts in each geographical location. FS, facultative symbiont; FEC, facultative symbiont combination; #, sample size. Scientific names of the host plants: cotton (*Gossypium* sp.), poinsettia (*Euphorbia pulcherrima*), tomato (*Solanum lycopersicum*), sweet potato (*Ipomoea batatas*), eggplant (*Solanum melongena*), tobacco (*Nicotiana tabacum*), zucchini (*Cucurbita pepo* var. *cylindrica*), lantana (*Lantana* sp.), cucumber (*Cucumis sativa*), bean (*Phaseolus vulgaris*), melon (*Cucumis melo*), cassava (*Manihot esculenta*), pepper (*Capsicum annuum*), croton (*Codiaeum variegatum*), hibiscus (*Hibiscus mutabilis*), marrow (*Cucurbita pepo* var. *pepo*), garden spurge (*Euphorbia* sp.), black nightshade (*Solanum nigrum*), amaranthus (*Amaranthus retroflexus*), and okra (*Abelmoschus esculentus*).

have delineated patterns of non-random occurrence of facultative endosymbionts among well-resolved *B. tabaci* genetic clades (Supplementary Materials). *Hamiltonella* is abundant in biotypes B and Q1 and *Arsenophonus* in other biotypes, mainly Ms and Q2; *Wolbachia* was not detected in individuals from biotype B, despite the large number of whiteflies included in the dataset. Most individuals were found to harbor at least one facultative endosymbiont (88%), with nearly half of the individuals surveyed (49%) harboring more than one, in agreement with previous observations (Gueguen et al., 2010). Analysis of the mean infection richness (number of genera) per individual across the different locations showed that community complexity increases with distance from the equator (Figure 1). We verified that this geographical gradient of infection richness does not reflect biases introduced by sensitivity differences between laboratory equipment and protocols by further grouping whitefly individuals not only according to their geographical locations but also according to their contributing groups. Reassuringly, high similarity in the mean infection richness among populations collected at a common geographic location and analyzed by different groups was observed (Supplementary Material). Similarly, we observe a richness gradient in *B. tabaci* populations collected at different locations and analyzed by a single group.

CHARACTERIZATION OF FACULTATIVE ENDOSYMBIONT COMBINATIONS (FECs) AND THEIR DISTRIBUTION ACROSS BIOTYPES

The analysis of the factors associated with community variations is hampered by the complexity of the ecological system: the insects that host the endosymbionts are classified into several genetic clades and were collected from different host-plants at different locations (Figure 1). Individuals might harbor none, single or several facultative symbionts forming a range of possible combinations. To gain a community perspective and to simplify the association analyses by reducing the number of factors analyzed, we clustered all of the facultative symbionts harbored by an individual insect into entities termed Facultative Endosymbiont Combinations (FECs), each representing a natural assemblage of microbial genera that co-occur within distinct boundaries. Nineteen such FEC entities were detected across the database, including five, eight, and six combinations of single-, two- and three-genera combinations, respectively (Figure 2). FEC are termed according to the initials of their genera members (A, C, H, R, and W represent *Arsenophonus*, *Cardinium*, *Hamiltonella*, *Rickettsia*, and *Wolbachia*, respectively) where the number of letters represents the number of genera members. That is, FEC H represents a single member combination grouping together individuals for which *Hamiltonella* is the only facultative endosymbiont detected; FEC HW represents a two-members combination grouping together individuals for which *Hamiltonella* and *Wolbachia* are the only facultative endosymbionts detected. A strong negative correlation between FEC complexity (number of genera) and the number of biotypes harboring that specific FEC was observed (Spearman's Rho -0.83 , P -value $5e-6$, Figure 2). These results clearly show that the FEC–biotype association was stronger for multi-member combinations than for single-member ones, with most multi-member combinations being harbored exclusively by a single biotype. For example, as

a single-genus combination, *Hamiltonella* (FEC H) was the only bacterium in the dataset that could be found in both Q1 and B biotypes. In contrast, the distribution ranges of H-containing multi-member communities were limited to either the Q1 biotype (combinations HC, HW, HCR, and HCW) or the B biotype (combinations HR and HRA) (Figure 2). Similarly, 62% of the FEC C (*Cardinium* only combination) were found in the Ms biotype. The association of C with this biotype was more pronounced when that bacterium was part of multi-member FECs; 90 and 83% of the CA combinations (CA and CRA, respectively) were harbored by the Ms biotype; CW combinations (CW, CWA) were limited to the Asia II 7 biotype, and HC combinations (HC, HCR) were limited to the Q1 biotype (Figure 2).

CHARACTERIZATION OF THE INTRA-BIOTYPE DIVERSITY IN FECs

Although previous screening studies have indicated that biotypes differ in their association patterns with facultative endosymbionts, the current analysis reports also an intra-biotype diversity of associated FECs. With the exception of Asia II 7, all biotypes harbor multiple FECs (up to 9, Figure 2). Overall, 58 unique biotype-FEC associations were identified in the dataset. The biotype-FEC entities stratify an otherwise homogeneous population (a biotype) into different holobiont units. To explore the functional significance of alternative combinations associated with a single biotype, we compared the plant and geographical preferences associated with the presence of a specific FEC. Focus was placed on B and Q1 insect individuals, as these were the two most extensively sampled biotypes across diverse locations (Supplementary Materials). Because the other key biotypes sampled (Ms, ASL, and Q2) were collected in a single geographical location with an almost exclusive host plant, the data did not allow carrying out a comparative analysis (Figure 2).

The distribution of a specific FEC-carrying individuals from biotypes Q1 and B across 9 and 5 geographical locations, and 15 and 6 host plants, respectively, is shown in Table 1. The distribution of Q1-associated FECs across host plants revealed that Q1_H (Q1-biotype individuals harboring *Hamiltonella* only—the FEC “H”) was sampled from cotton at a significantly higher frequency than expected by chance, considering the frequency of H FEC in Q1 individuals and the number of Q1 individuals collected from cotton plants ($P < 0.05$ in a cumulative hypergeometric distribution test; Table 1); Q1_{HW} were most often found on cucumber, melon and zucchini (all belonging to the family Cucurbitaceae), and Q1_{HC} individuals were significantly overrepresented in tomato samplings. Similarly, B_H individuals were significantly associated with cotton whereas B_{HR} individuals were associated with eggplant and tomato (both belonging to the family Solanaceae). As in similar surveys (Tsuchida et al., 2002; Brady et al., 2014), the association patterns of biotype-FEC geographical categories overlapped with the crops sampled at each location, where the synchronization between the categories (host plant, geographical location) impeded the stratification of the unique effect of each of these factors. The sampling of Q1-associated FECs from tomato was the only case of a multiple-geographical origin for the sampling of a biotype on a crop in the database (Supplementary Materials). Most Q1 individuals sampled at geographical locations 1 and 4 carried communities HW and H,

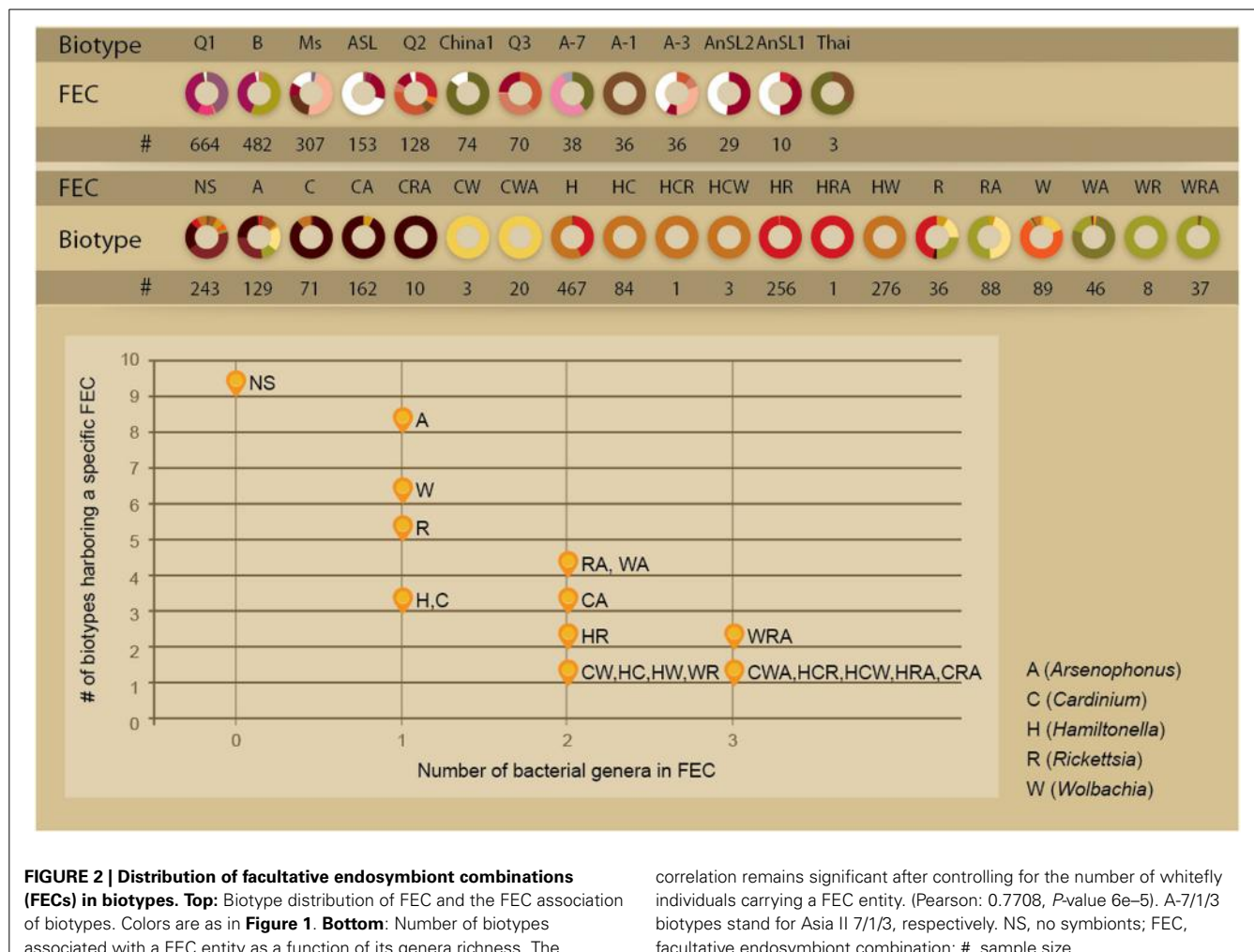


FIGURE 2 | Distribution of facultative endosymbiont combinations (FECs) in biotypes. Top: Biotype distribution of FEC and the FEC association of biotypes. Colors are as in Figure 1. **Bottom:** Number of biotypes associated with a FEC entity as a function of its genera richness. The correlation remains significant after controlling for the number of whitefly individuals carrying a FEC entity. (Pearson: 0.7708, P-value 6e-5). A-7/1/3 biotypes stand for Asia II 7/1/3, respectively. NS, no symbionts; FEC, facultative endosymbiont combination; #, sample size.

respectively, in accordance with the general FEC preference at these sites (Table 1). This FEC preference of Q1 individuals was not plant-specific: a majority of HW combinations was observed for eight out of nine sampled crops in region 1; a majority of H combinations was observed for all five crops sampled in region 4. Hence, the symbionts found in Q1 *B. tabaci* collected from tomato point to geographical origin over crop as the key factor associated with specific FECs.

DISCUSSION

The abundance of facultative endosymbionts has been extensively studied in many arthropods. To the best of our knowledge, the dataset used in this study represents both the largest collection of insects for which communities of facultative endosymbionts have been described and the most comprehensive collection in terms of range of environmental conditions sampled. For example, recent surveys of facultative endosymbionts in whiteflies and aphids are based on approximately 350 and 1100 individuals, respectively (Gueguen et al., 2010; Henry et al., 2013). When compiling such data it is important to bear in mind that biases might be introduced by technical inconsistencies among the independent screening laboratories. In support of the biological relevance

of this collection, we verified that all screens were conducted using highly similar protocols and their ability to detect the various endosymbionts is comparable both qualitatively and quantitatively (sensitivity) (Supplementary Material). Here, we used this data to point at environmental and biological factors associated with variations in the diversity and identity of endosymbiont bacteria harbored by whiteflies individuals. Though most insects harbor two or more facultative endosymbionts, the majority of studies focus on the phenotypical significance of an insect–single bacterium association (Zchori-Fein and Bourtzis, 2011). Unlike complex ecosystems such as gut microbiomes, the bacteriome of *B. tabaci* contains a limited number of bacterial members. These include the obligatory endosymbiont as well as an extensively characterized collection of facultative endosymbionts that are repeatedly reported as the key species in this well-defined ecosystem. Hence, basic fingerprinting techniques combined with species-specific sequencing approaches provide a close to full description of the microbial diversity within that niche. This high-coverage description of bacterial genera, allows taking a community view to explore the role of endosymbiont combinations in shaping the distribution patterns of *B. tabaci* individuals. Yet, the presence of screened endosymbionts in low titters (below

Table 1 | Distribution pattern of biotype-specific facultative endosymbiont combinations (FECs) across collection sites and crops.

	Q1										B						
	NS	C	H	HC	HCR	HCW	HR	HW	W	T	NS	A	H	HR	HRA	R	T
HOST-PLANT																	
Amaranthus			1					15*		16							
Bean			1					19*		20							
Sweet potato																	
Cucumber			16					42*		58							
Melon				7				39*		46							
Zucchini				24			2	28		54			9*		1	10	
Croton																	
Poinsettia											2		36*		9*	47	
Garden spurge											1		2			3	
Hibiscus			4					29*		33							
Cotton	7*		72*	2	1	1	1	5	89	6	1*	191*	102	1	1	302	
Okra	1		11*					1		13							
Marrow	2		17*					1		20							
Black nightshade	1							13*	4	18							
Eggplant			3					31*		34	5*		55*		1	61	
Tobacco			22					18	2	42							
Tomato	6	1	28	51*			2	32		120		4	33*		3	40	
pepper			38*							38							
Cassava																	
Lantana			11*														
Unknown	1	7*	10	31*					3	52		1	16*		2	19	
GEOGRAPHIC LOCATION																	
1		1	79					1	244*	5	330						
2			38*								38		40*			40	
3											6	1	191*	102	1	1	302
4	16*		121*	2	1	3	1	9	1	154			1	8		9	
5			11*							11			1	88*	16*	113	
6											8*		1	15*		18	
7													3				
8	1	7*	2	22*													
9		1	2	48*					20		71						
10			8	9*					3		20						
11			4	3*			1				8						
GEOGRAPHIC LOCATION - TOMATO																	
1			5					1	10		17						
4	6		17						2		25						
9		1	2	48*					20		71						
11			4	3			1				8						

Within each cell, numbers indicate the count of individual whiteflies infected with a FEC. Shades of gray indicate the relative abundance of each bacteria within a given sampling category (row) ranging from white (0–10%) to dark gray (90–100%). A, Arsenophonus; C, Cardinium; H, Hamiltonella; R, Rickettsia; W, Wolbachia; NS, no secondary symbionts; T, total.

*Number of individuals from a given biotype-FEC (column) in a category (host plant/collection site; row) is higher than random. Significant enrichment in an ecological category was determined by calculating a cumulative hypergeometric P-value (Methods). Significant cut-offs were determined by setting a False Discovery Rate (FDR) threshold of 10%.

PCR detectable level) or the occurrence of other bacterial genera cannot be entirely ruled out and might influence the outcome of analysis. First, we observed that the associations are more biotype-specific for multi-member vs. single-member communities. Second, within a biotype, variations in the composition

of the symbiotic communities are typically associated with ecological patterns. This is consistent with observations from a smaller-scale global survey of facultative endosymbionts in the cowpea aphid *Aphis craccivora* (Brady et al., 2014) and surveys of facultative endosymbiont populations of the pea aphid

Acyrthosiphon pisum (Tsuchida et al., 2002; Henry et al., 2013). Third, the analysis revealed a geographical gradient of increasing facultative endosymbiont richness at extreme latitudes. This observation, consistent among highly remote sampling areas, points at the possibility that an evolutionary pressure might be associated with community diversity. A similar increase in complexity correlated with decreasing mean annual temperature and precipitation was previously reported (Tsuchida et al., 2002). Since even two-member multiple infections are suggested to have deleterious effects on fecundity (Oliver et al., 2006), the trade-off between contribution and cost to fitness seems to vary with dependence on climatic factors. Moreover, whereas the geographical distribution preferences of FECs might reflect the historical invasion and spread of the host, the geographical gradient is not composition-specific and is observed independently at a few locations, supporting the role of FEC–insect interactions in shaping the functional repertoire of individuals and hence affecting their pattern of distribution. Finally, the biotype specificity of multiple-member FECs further suggests that the cost of such communities involves highly specific adaptation between host and symbiotic community. These complementary interactions might occur at two different levels: multiple independent host–bacteria interactions and/or interactions between the microorganisms themselves. For example, the complementation of the H combinations with R (HR combinations) is unique to B biotype individuals, whereas the complementation with C or W (HC/HW combinations) is unique to individuals of the Q1 biotype, suggesting a biotype-specific functional adaptation. The scarcity of Q1 individuals carrying both W and C suggests that these genera might have overlapping roles, reducing the likelihood of their co-occurrence.

Complementation of the functional capabilities by insect–symbiont associations is gaining more and more documentation due to the emergence of new genomic sequencing techniques and analytical approaches. In particular, symbiotic microorganisms have been shown to complete partial metabolic pathways in the host, enabling the conductance of otherwise lacking functions (e.g., McCutcheon and Moran, 2010; Sloan and Moran, 2012; Russell et al., 2013). Future exploration of the functional repertoire of different communities, together with the parallel exploration of the functional repertoire in the host insect and host plant, will shed light on the role of mutual complementation in shaping insect ecology. Considering the growing interest in the role of symbiotic interactions in shaping the fitness of plants and animals, the limited size of the communities in this study and the co-localization of their members in a designated organ mark them as a useful model system for such explorations.

ACKNOWLEDGMENTS

We are grateful to Liu Shu Sheng, Fabrice Vavre, Anastasia Tsagkaruku, Laurence Moton, Helene Dellatte, and their teams for generously providing raw data from their screening efforts. Thanks are extended to Netta Mozes Daube for technical help, Itai Opatovsky for discussion, Itay Mayrose for instructive comments and two reviewers for highly valuable suggestions. This research was supported by The Israel Science Foundation (grant no. 1481/13 to Shiri Freilich and Einat Zchori-Fein).

SUPPLEMENTARY MATERIAL

The Supplementary Material for this article can be found online at: <http://www.frontiersin.org/journal/10.3389/fmicb.2014.00310/abstract>

REFERENCES

- Baumann, P. (2005). Biology bacteriocyte-associated endosymbionts of plant sap-sucking insects. *Annu. Rev. Microbiol.* 59, 155–189. doi: 10.1146/annurev.micro.59.030804.121041
- Bing, X. L., Ruan, Y. M., Rao, Q., Wang, X. W., and Liu, S. S. (2013). Diversity of secondary endosymbionts among different putative species of the whitefly *Bemisia tabaci*. *Insect Sci.* 20, 194–206. doi: 10.1111/j.1744-7917.2012.01522.x
- Boykin, L. M., Shatters, R. G. Jr., Rosell, R. C., McKenzie, C. L., Bagnall, R. A., De Barro, P., et al. (2007). Global relationships of *Bemisia tabaci* (Hemiptera: Aleyrodidae) revealed using Bayesian analysis of mitochondrial COI DNA sequences. *Mol. Phylogenet. Evol.* 44, 1306–1319. doi: 10.1016/j.ympev.2007.04.020
- Brady, C. M., Asplen, M. K., Desneux, N., Heimpel, G. E., Hopper, K. R., Linnen, C. R., et al. (2014). Worldwide populations of the aphid *Aphis craccivora* are infected with diverse facultative bacterial symbionts. *Microb. Ecol.* 67, 195–204. doi: 10.1007/s00248-013-0314-0
- Buchner, P. (1965). *Endosymbiosis of Animals with Plant Microorganisms*. New York, NY: Interscience Publishers Inc.
- Chiel, E., Gottlieb, Y., Zchori-Fein, E., Mozes-Daube, N., Katzir, N., Inbar, M., et al. (2007). Biotype-dependent secondary symbiont communities in sympatric populations of *Bemisia tabaci*. *Bull. Entomol. Res.* 97, 407–413. doi: 10.1017/S0007485307005159
- De Barro, P. J., Liu, S. S., Boykin, L. M., and Dinsdale, A. B. (2011). *Bemisia tabaci*: a statement of species status. *Annu. Rev. Entomol.* 56, 1–19. doi: 10.1146/annurev-ento-112408-085504
- Ferrari, J., and Vavre, F. (2011). Bacterial symbionts in insects or the story of communities affecting communities. *Philos. Trans. R. Soc. Lond. B. Biol. Sci.* 366, 1389–1400. doi: 10.1098/rstb.2010.0226
- Gnankine, O., Mouton, L., Henri, H., Terraz, G., Houndete, T., Martin, T., et al. (2012). Distribution of *Bemisia tabaci* (Homoptera: Aleyrodidae) biotypes and their associated symbiotic bacteria on host plants in West Africa. *Insect Conserv. Diver.* 6, 411–421. doi: 10.1111/j.1752-4598.2012.00206.x
- Gottlieb, Y., Zchori-Fein, E., Mozes-Daube, N., Kontsedalov, S., Skaljac, M., Brumin, M., et al. (2010). The transmission efficiency of tomato yellow leaf curl virus by the whitefly *Bemisia tabaci* is correlated with the presence of a specific symbiotic bacterium species. *J. Virol.* 84, 9310–9317. doi: 10.1128/JVI.00423-10
- Gueguen, G., Vavre, F., Gnankine, O., Peterschmitt, M., Charif, D., Chiel, E., et al. (2010). Endosymbiont metacommunities, mtDNA diversity and the evolution of the *Bemisia tabaci* (Hemiptera: Aleyrodidae) species complex. *Mol. Ecol.* 19, 4365–4376. doi: 10.1111/j.1365-294X.2010.04775.x
- Henry, L. M., Peccoud, J., Simon, J. C., Hadfield, J. D., Maiden, M. J., Ferrari, J., et al. (2013). Horizontally transmitted symbionts and host colonization of ecological niches. *Curr. Biol.* 23, 1713–1717. doi: 10.1016/j.cub.2013.07.029
- Himler, A. G., Adachi-Hagimori, T., Bergen, J. E., Kozuch, A., Kelly, S. E., Tabashnik, B. E., et al. (2011). Rapid spread of a bacterial symbiont in an invasive whitefly is driven by fitness benefits and female bias. *Science* 332, 254–256. doi: 10.1126/science.1199410
- Hunter, M. S., Perlman, S. J., and Kelly, S. E. (2003). A bacterial symbiont in the Bacteroidetes induces cytoplasmic incompatibility in the parasitoid wasp *Encarsia pergandiella*. *Proc. Biol. Sci.* 270, 2185–2190. doi: 10.1098/rspb.2003.2475
- Jaenike, J. (2012). Population genetics of beneficial heritable symbionts. *Trends Ecol. Evol.* 27, 226–232. doi: 10.1016/j.tree.2011.10.005
- Kontsedalov, S., Zchori-Fein, E., Chiel, E., Gottlieb, Y., Inbar, M., and Ghanim, M. (2008). The presence of *Rickettsia* is associated with increased susceptibility of *Bemisia tabaci* (Homoptera: Aleyrodidae) to insecticides. *Pest Manag. Sci.* 64, 789–792. doi: 10.1002/ps.1595
- Liu, S., Chougule, N. P., Vijayendran, D., and Bonning, B. C. (2012). Deep sequencing of the transcriptomes of soybean aphid and associated endosymbionts. *PLoS ONE* 7:e45161. doi: 10.1371/journal.pone.0045161
- Liu, S. S., De Barro, P. J., Xu, J., Luan, J. B., Zang, L. S., Ruan, Y. M., et al. (2007). Asymmetric mating interactions drive widespread invasion and displacement in a whitefly. *Science* 318, 1769–1772. doi: 10.1126/science.1149887

- McCutcheon, J. P., and Moran, N. A. (2010). Functional convergence in reduced genomes of bacterial symbionts spanning 200 My of evolution. *Genome Biol. Evol.* 2, 708–718. doi: 10.1093/gbe/evq055
- Moran, N. A. (2007). Symbiosis as an adaptive process and source of phenotypic complexity. *Proc. Natl. Acad. Sci. U.S.A.* 104(Suppl. 1), 8627–8633. doi: 10.1073/pnas.0611659104
- Oliver, K. M., Moran, N. A., and Hunter, M. S. (2006). Costs and benefits of a super-infection of facultative symbionts in aphids. *Proc. Biol. Sci.* 273, 1273–1280. doi: 10.1098/rspb.2005.3436
- Rosenberg, E., Koren, O., Reshef, L., Efrony, R., and Zilber-Rosenberg, I. (2007). The role of microorganisms in coral health, disease and evolution. *Nat. Rev. Microbiol.* 5, 355–362. doi: 10.1038/nrmicro1635
- Rosenberg, E., and Zilber-Rosenberg, I. (2011). Symbiosis and development: the hologenome concept. *Birth Defects Res. C Embryo Today* 93, 56–66. doi: 10.1002/bdrc.20196
- Russell, C. W., Bouvaine, S., Newell, P. D., and Douglas, A. E. (2013). Shared metabolic pathways in a coevolved insect-bacterial symbiosis. *Appl. Environ. Microbiol.* 79, 6117–6123. doi: 10.1128/AEM.01543-13
- Sloan, D. B., and Moran, N. A. (2012). Endosymbiotic bacteria as a source of carotenoids in whiteflies. *Biol. Lett.* 8, 986–989. doi: 10.1098/rsbl.2012.0664
- Stansly, P. A. N., Steven, E. (2010). *Bemisia: Bionomics and Management of a Global Pest*. Amsterdam: Springer.
- Tay, W. T., Evans, G. A., Boykin, L. M., and De Barro, P. J. (2012). Will the real *Bemisia tabaci* please stand up? *PLoS ONE* 7:e50550. doi: 10.1371/journal.pone.0050550
- Thao, M. L., and Baumann, P. (2004). Evolutionary relationships of primary prokaryotic endosymbionts of whiteflies and their hosts. *Appl. Environ. Microbiol.* 70, 3401–3406. doi: 10.1128/AEM.70.6.3401-3406.2004
- Thierry, M., Becker, N., Hajri, A., Reynaud, B., Lett, J. M., and Delatte, H. (2011). Symbiont diversity and non-random hybridization among indigenous (Ms) and invasive (B) biotypes of *Bemisia tabaci*. *Mol. Ecol.* 20, 2172–2187. doi: 10.1111/j.1365-294X.2011.05087.x
- Tsagkarakou, A., Mouton, L., Kristoffersen, J. B., Dokianakis, E., Grispou, M., and Bourtzis, K. (2012). Population genetic structure and secondary endosymbionts of Q *Bemisia tabaci* (Hemiptera: Aleyrodidae) from Greece. *Bull. Entomol. Res.* 102, 353–365. doi: 10.1017/S0007485311000757
- Tsuchida, T., Koga, R., Shiba, H., Matsumoto, T., and Fukatsu, T. (2002). Diversity and geographic distribution of secondary endosymbiotic bacteria in natural populations of the pea aphid, *Acyrthosiphon pisum*. *Mol. Ecol.* 11, 2123–2135. doi: 10.1046/j.1365-294X.2002.01606.x
- Zchori-Fein, E., and Bourtzis, K. (2011). *Manipulative Tenants—Bacteria Associated with Arthropods*. Boca Raton, FL; London; New York, NY: CRC press.
- Zchori-Fein, E., Gottlieb, Y., Kelly, S. E., Brown, J. K., Wilson, J. M., Karr, T. L., et al. (2001). A newly discovered bacterium associated with parthenogenesis and a change in host selection behavior in parasitoid wasps. *Proc. Natl. Acad. Sci. U.S.A.* 98, 12555–12560. doi: 10.1073/pnas.221467498
- Zchori-Fein, E., and Perlman, S. J. (2004). Distribution of the bacterial symbiont *Cardiniinum* in arthropods. *Mol. Ecol.* 13, 2009–2016. doi: 10.1111/j.1365-294X.2004.02203.x

Conflict of Interest Statement: The authors declare that the research was conducted in the absence of any commercial or financial relationships that could be construed as a potential conflict of interest.

Received: 31 March 2014; accepted: 06 June 2014; published online: 04 July 2014.

Citation: Zchori-Fein E, Lahav T and Freilich S (2014) Variations in the identity and complexity of endosymbiont combinations in whitefly hosts. *Front. Microbiol.* 5:310. doi: 10.3389/fmicb.2014.00310

This article was submitted to Terrestrial Microbiology, a section of the journal *Frontiers in Microbiology*.

Copyright © 2014 Zchori-Fein, Lahav and Freilich. This is an open-access article distributed under the terms of the Creative Commons Attribution License (CC BY). The use, distribution or reproduction in other forums is permitted, provided the original author(s) or licensor are credited and that the original publication in this journal is cited, in accordance with accepted academic practice. No use, distribution or reproduction is permitted which does not comply with these terms.



Intercellular communications in multispecies oral microbial communities

Lihong Guo, Xuesong He and Wenyuan Shi*

School of Dentistry, University of California-Los Angeles, Los Angeles, CA, USA

Edited by:

Manfred Auer, Lawrence Berkeley Lab, USA

Reviewed by:

Hui Wu, University of Alabama at Birmingham, USA

Richard Lamont, University of Louisville, USA

***Correspondence:**

Wenyuan Shi, School of Dentistry, University of California-Los Angeles, 10833 Le Conte Avenue, Los Angeles, CA 90095, USA

e-mail: wenyuan@ucla.edu

The oral cavity contains more than 700 microbial species that are engaged in extensive cell-cell interactions. These interactions contribute to the formation of highly structured multispecies communities, allow them to perform physiological functions, and induce synergistic pathogenesis. Co-adhesion between oral microbial species influences their colonization of oral cavity and effectuates, to a large extent, the temporal and spatial formation of highly organized polymicrobial community architecture. Individual species also compete and collaborate with other neighboring species through metabolic interactions, which not only modify the local microenvironment such as pH and the amount of oxygen, making it more suitable for the growth of other species, but also provide a metabolic framework for the participating microorganisms by maximizing their potential to extract energy from limited substrates. Direct physical contact of bacterial species with its neighboring co-habitants within microbial community could initiate signaling cascade and achieve modulation of gene expression in accordance with different species it is in contact with. In addition to communication through cell-cell contact, quorum sensing (QS) mediated by small signaling molecules such as competence-stimulating peptides (CSPs) and autoinducer-2 (AI-2), plays essential roles in bacterial physiology and ecology. This review will summarize the evidence that oral microbes participate in intercellular communications with co-inhabitants through cell contact-dependent physical interactions, metabolic interdependencies, as well as coordinative signaling systems to establish and maintain balanced microbial communities.

Keywords: oral microbial community, coadhesion, signaling transduction, metabolic interactions, cell-cell communication

INTRODUCTION

With the respect to microbial flora, the human oral cavity is one of the most densely populated sites of the human body, consisting of as many as 600–800 bacterial species (Paster et al., 2006; Dewhirst et al., 2010). Extensive clinical studies have indicated that the oral microbial flora is responsible for two major human diseases: dental caries and periodontitis (Marsh, 1994). The environmental diversity of the oral cavity promotes the establishment of distinct microbial communities. For example, the supragingival plaque is known to be dominated by Gram-positive streptococci and the subgingival plaque is populated with mainly Gram-negative anaerobic bacteria (Marsh, 1994). These microbial inhabitants have co-evolved not only with their host, but also with each other, leading to extensive intercellular communications across species. The ecological equilibrium of a well-organized multispecies oral microbial community is maintained through competitive and cooperative interactions between microorganisms of the same or different species at the cellular and molecular levels.

Intercellular communications are essential for the development of temporal and spatial organization of oral microbial communities, and are involved in processes such as provision of attachment sites, modification of local microenvironment, cooperative nutrient utilization, as well as synergistic and competitive interactions

(Kuramitsu et al., 2007). In addition, intercellular signaling initiated by cell-cell contact, quorum sensing, and other diffusible signaling molecules allow oral microbial species to coordinate their physiological behaviors and pathogenesis (Jenkinson and Lamont, 2005; Kolenbrander et al., 2006). All of these intercellular interactions between oral microbes enable them to select co-residents, promote the establishment of a highly structured and diverse microbial community, and play an essential role in microbial pathogenesis.

PHYSICAL INTERACTIONS

The ability of species to adhere to salivary pellicles or to bacteria that are already attached to the surface is among the key factors that determine whether a species can perpetuate in the oral cavity. Initial adhesion of the early colonizers of oral microbial communities invariably involves binding to saliva components that are adsorbed to solid surfaces such as teeth or to desquamating surfaces such as epithelial tissue. Oral streptococci are believed to be among the earliest inhabitants on tooth surfaces due to their capability to adhere directly to salivary pellicle and comprise about 80% of the early colonizers (Avila et al., 2009). Meanwhile, *Actinomyces* has also been identified in the inner portion of the dental biofilms, suggesting their early colonizer nature (Palmer et al., 2003; Dige et al., 2009). Other early colonizers are

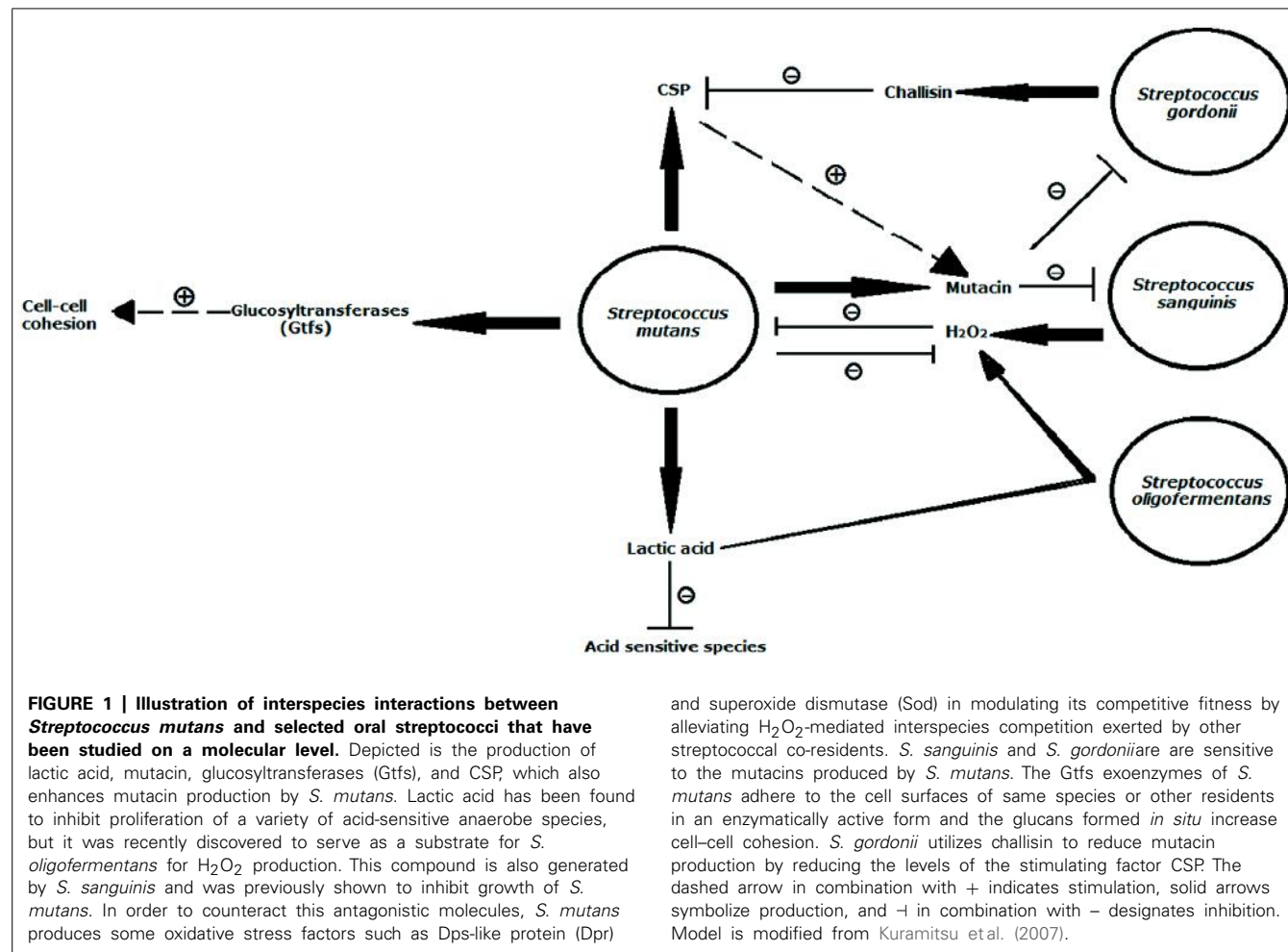
comprised of *Veillonella* and *Neisseria* (Li et al., 2004). Several studies have identified adhesins and receptors for early colonizing microorganisms to adhere specifically to salivary pellicle and even determine the unique domains on these molecules involved in binding. For example, it has been shown that Hsa mediated binding of *Streptococcus gordonii* to sialic acid-containing receptors in salivary pellicle (Ding et al., 2010) and the region containing lysine in the salivary components may have binding activity to *S. gordonii* and *Streptococcus sanguinis*. Meanwhile, the scavenger receptor cysteine-rich domain peptide 2 (SRCRP 2) region may also function as a receptor for the binding of streptococci (Hamada et al., 2004).

Biofilm matrix also plays a role in maintaining microbial colonization, therefore contributing to oral biofilm development. *Streptococcus mutans*, a predominantly prevalent caries-associated species in humans (Loesche, 1986), utilizes extracellular polysaccharides synthesized by glucosyltransferases (Gtfs) to facilitate its firm attachment to teeth and promote tight cell clustering (Koo et al., 2010; Xiao et al., 2012). The Gtfs exoenzymes of *S. mutans* were shown to adhere strongly not only to the salivary pellicle that covers the surface of teeth but also to bacterial surfaces, and could produce glucans in the adsorbed state (Vacca-Smith and Bowen, 1998; Bowen and Koo, 2011). In view of the cohesive attribute (Loesche, 1986; Tamesada et al., 2004), glucans synthesized on the pellicle provides additional bacterial binding sites, while the polymers on the cell surfaces of same species or other residents increase cell–cell cohesion (Figure 1). For example, GtfB, one of Gtfs, binds effectively to both yeast and hyphae cell forms of *Candida albicans* in an enzymatically active form and the glucans formed *in situ* not only enhances the binding of *S. mutans* cells to *C. albicans* cells but also promotes the colonization of *C. albicans* on the tooth surface (Gregoire et al., 2011). Among the numerous types, the rigid alpha 1, 3 linked glucans are particularly suited for cohesion (Rölla et al., 1985). Due to its important role in promoting microbial adherence and clustering, many oral bacterial species modulate their behavior within biofilm by interfering with matrix structure. *Actinobacillus actinomycetemcomitans*, the predominant pathogen in aggressive periodontitis was reported to be able to produce a matrix-degrading enzyme dispersin B for degrading poly-N-acetylglucosamine (PNAG), a major polysaccharide component of biofilm matrix, and thus, caused detachment and dispersion of *A. actinomycetemcomitans* biofilm cells (Kaplan et al., 2003). *Streptococcus salivarius* produces a fructosyltransferase (FTF) and an exo-beta-D-fructosidase (FruA) to hinder further polymicrobial community development with other oral bacteria such as *S. mutans* (Ogawa et al., 2011).

After the initial attachment of early colonizers to salivary receptors, the early colonizers could transform teeth or oral soft tissue surface to a bacterial surface. The adhesins on cell surface of early colonizers enable the sequential addition of the partner species. Oral streptococci express a diversity of cell surface molecules functioning as adhesins that recognize diverse bacterial receptors, such as pili, surface fibrils and Antigen I/II family protein, indicating that streptococci have a broad pairwise match with succeeding colonizers. It has been documented that oral streptococci recruit strains of *Actinomyces* by a highly selective cell surface interactions

between specific streptococcal cell wall polysaccharides and *Actinomyces* sp. type 2 fimbriae (Cisar et al., 1979). Additionally, an inducible high-affinity Mn²⁺ transporter of *S. gordonii* (Kolenbrander et al., 1998a) was found to mediate its coadhesion with *Actinomyces naeslundii* (Kolenbrander et al., 1994). The close spatial association between streptococci and *Actinomyces*, as well as between streptococci and *Veillonella* was visualized in early stage of dental biofilms *in vivo* (Palmer et al., 2003; Chalmers et al., 2007).

The bacteria that can recruit subsequent colonizing species through binding to early and late colonizers constitute middle colonizers. *Fusobacterium nucleatum* is considered a “bridge-organism” that links early commensal colonizers and late colonizing species including periodontal pathogens and is important in the succession of genera in oral multispecies communities. Multivalent adhesins on the cell surface of *F. nucleatum*, with their distinct selectivity to early and late colonizers, contribute greatly to the development of polymicrobial communities within the oral cavity. It has been shown that the distinctive corncob structure visible in mature plaque is formed by the coadhesion between *F. nucleatum* and streptococci (Lancy et al., 1983). In addition to streptococci, other early colonizers such as *A. naeslundii* and *Veillonella parvula* also bind to *F. nucleatum* (Biyikoğlu et al., 2012). Among the multiple adhesins of *F. nucleatum*, an arginine-inhibitable adhesin (RadD) is responsible for its adherence to streptococci; while some serotype-specific adhesins are involved in binding to periodontopathogens including *Porphyromonas gingivalis*, *A. actinomycetemcomitans* and *Treponema denticola* (Rosen and Sela, 2006; Rosen et al., 2008; Rupani et al., 2008; Kaplan et al., 2009). The coadhesion between *F. nucleatum* and these late colonizing Gram-negative species are usually mediated by lectin–carbohydrate interactions. For instance, the recognition between a galactose-specific lectin-like adhesin expressed by *F. nucleatum* and the sugar moiety present in the capsule and lipopolysaccharide of *P. gingivalis* contributes to coadhesion between the two species (Rosen and Sela, 2006). Similar galactose-containing receptors are also found on cell surface of *A. actinomycetemcomitans* (Rupani et al., 2008) and *T. denticola* (Rosen et al., 2008). As for *Tannerella forsythia* which is associated with severe and chronic periodontitis, its cell surface glycoproteins in S-layer act as adhesins in coadhesion with *F. nucleatum* (Shimotahira et al., 2013). Apart from protein–carbohydrate interactions, some researchers have reported that leucine-rich repeat in proteins from *T. denticola* and *T. forsythia* are involved in protein–protein interactions with each other and with *F. nucleatum* (Ikegami et al., 2004; Sharma et al., 2005). Even though *T. forsythia* possesses an S-layer at the outermost cell surface, a portion of the protein is exposed on the cell surface, one of them being OmpA-like protein, which was proposed to play a role in intercellular adhesion (Abe et al., 2011). Through selective recognition of adhesins on cell surface of *F. nucleatum*, these periodontitis associated species are integrated into microbial communities. For example, *Filifactor alocis*, an emerging important periodontal pathogen was found to preferentially accumulate at sites rich in *F. nucleatum* (Wang et al., 2013).



Besides *F. nucleatum*, *P. gingivalis* also exhibits a broad range of pairwise interactions with other microbial community members. *P. gingivalis* was shown to be able to assemble into a heterotypic microbial complex with *S. gordonii* and *F. nucleatum* (Lamont et al., 2002; Periasamy and Kolenbrander, 2009b). The specific molecular interactions between *P. gingivalis* and *S. gordonii* have been well characterized and occur through Mfa-Ssp and fimbrial adhesin (FimA)-GAPDH adhesin-receptor pairs (Maeda et al., 2004; Kuboniwa and Lamont, 2010). *P. gingivalis*' short fimbriae (Mfa) bind to *S. gordonii* AgI/II family proteins SspA and SspB (Lamont et al., 2002; Park et al., 2005), whereas *P. gingivalis* long fimbriae (FimA) mediate its attachment to glyceraldehyde-3-phosphate dehydrogenase (GAPDH) of *Streptococcus cristatus* (Maeda et al., 2004). Further researches revealed that the region defined by residues 1167–1250 of *S. gordonii* SspB protein was essential motif for *P. gingivalis* binding (Brooks et al., 1997), and both NITVK motif and the nuclear receptor box of SspB contributed to the Mfa–SspB interaction (Demuth et al., 2001; Daep et al., 2011). The binding domain of GAPDH present on the streptococcal surface specific for *P. gingivalis* long fimbriae exists within the region encompassing amino acid residues 166–183 of GAPDH (Nagata et al., 2009). Although Mfa and FimA participate in the coadhesion of *P. gingivalis* to streptococci,

another *P. gingivalis* surface molecule InlJ retards the development of *P. gingivalis*–*S. gordonii* community (Capestanay et al., 2006), which allows *P. gingivalis* to fine-tune the extent of buildup of microbial communities. Besides, Kuboniwa et al. (2009) reported that *P. gingivalis* had a decreased ability to partner with *S. gordonii* and *F. nucleatum* when being defective in HmuR, a major hemin uptake protein. Consistent with the interspecies interaction described above, biofilm visualization by confocal microscopy confirmed that *P. gingivalis* colonized *in vitro* biofilms mainly within regions where *S. gordonii* accumulated (Kuboniwa et al., 2006).

Late colonizers are species with weak colonizing ability that require partner species to integrate into microbial communities and are comprised primarily of anaerobic, Gram-negative bacteria (Kolenbrander et al., 2006; Zijnge et al., 2010). As a late colonizer, *T. denticola* is unable to adhere to oral surfaces such as teeth or epithelial tissue; however, in the presence of *P. gingivalis*, it could colonize oral biofilms. In sub-gingival dental biofilms, *T. denticola* is always found more external relative to *P. gingivalis* (Ishihara et al., 2004). The chymotrypsin-like proteinase (CTLP), found within a high-molecular-mass complex on the cell surface of *T. denticola*, mediates its adherence to other potential periodontal pathogens including *P. gingivalis*, *F. nucleatum*,

Prevotella intermedia and *Parvimonas micra*, and thus is crucial for *T. denticola* to integrate into multispecies oral microbial communities (Cogoni et al., 2012).

PHYSIOLOGICAL INTERACTIONS

METABOLITES MEDIATED COOPERATION

The high cell density of the oral microbial community impels individual resident to compete and collaborate with its neighboring species in order to survive in a hostile environment. An important factor in determining the microbial colonization in multispecies communities is the availability of nutrients. Metabolic communications among oral microbes may occur through the excretion of a metabolite by one bacterium that can be utilized as a nutrient by another species (Takahashi et al., 2010; Liu et al., 2012), or through syntrophic biochemical enzymes to cooperatively metabolize a substrate (Kolenbrander et al., 2002).

In the oral cavity, the short-chain acids such as lactate and acetate produced by early colonizers *via* sugar metabolism serve as carbon and energy sources for succeeding colonizers. This cross-feeding ensures sequential microbial colonization (Kolenbrander, 2011). Oral streptococci are well known by its ability to generate lactic acid as a by-product of sugar fermentation, whereas some neighboring species, such as *Veillonellae* sp. (Kumar et al., 2005; Chalmers et al., 2008) are unable to ferment sugars, but use lactic acid as a preferred source of carbon and energy. The ability of *A. actinomycetemcomitans* to utilize L-lactate, a carbohydrate metabolic by-product of *S. gordonii* as nutrient source allows it to integrate and become much more competitive within oral polymicrobial communities (Brown and Whiteley, 2007; Ramsey et al., 2011; Figure 2). The consumption of lactic acid by these lactic acid-utilizing bacteria minimizes lactic acid accumulation, which otherwise would cause streptococci to repress amylase synthesis and reduce the utilization efficiency of fermentable sugars by both partners (Egland et al., 2004). *P. gingivalis* and *T. denticola* are also metabolically connected. Succinate produced by *T. denticola* supports the growth of *P. gingivalis*, which, in turn, enhances the growth of *T. denticola* by providing isobutyric acid and proteinaceous substrates (Grenier, 1992; Nilius et al., 1993). Besides short-chain acids, *Porphyromonas* sp. can acquire vitamin K-like growth factors from *Veillonella* (Hojo et al., 2009).

Another type of metabolic interaction involves the complementary substrate utilization. Individual species in the oral cavity usually do not contain complete metabolic pathways to degrade complex salivary components. However, the breakdown of these compounds can be achieved through cooperation among multiple species. The synergistic and concerted action of *Streptococcus mitis*, *S. gordonii*, *Streptococcus crostatus*, and *A. naeslundii* with overlapping patterns of enzyme activity in salivary mucin catabolism has been reported (Wickström et al., 2009). Similarly, co-culture of *S. sanguinis* and *S. oralis* obtains significantly higher degradation efficiency of mucin than in monospecies culture (van der Hoeven and Camp, 1991). Therefore, this type of metabolic cooperation can benefit the participating species through maximizing their potential to extract energy from limited substrates.

Metabolic synergistic partnership usually occurs among community residents that often co-localize within the same niche and are metabolically compatible. In a three-species flow cell, *P. gingivalis* could not grow together with *Streptococcus oralis*–*A. actinomycetemcomitans* and *S. oralis*–*F. nucleatum* two-species community but displayed mutualistic growth when paired with *S. gordonii*–*S. oralis*, or *V. parvula*–*A. actinomycetemcomitans*, as well as with *V. parvula*–*F. nucleatum* two-species community (Periasamy and Kolenbrander, 2009a,b). The results indicated that *P. gingivalis* and *S. oralis* are incompatible, whereas *S. gordonii* could assist *P. gingivalis* to overcome this incompatibility, which also indicated that *S. oralis* was much more restricted in its successful partnership compared to its relative *S. gordonii*. Furthermore, in the presence of *V. parvula*, *S. oralis* displays positive partnership either with *P. gingivalis* or *F. nucleatum*. These findings illustrate the high species selectivity during multispecies community development.

METABOLITES MEDIATED COMPETITION

Interspecies antagonism reflects the competition among bacterial species for limited space and nutritional resources, and is the fundamental driving force in defining the structure and activity of polymicrobial oral communities. H_2O_2 secreted by viridans streptococci, including *S. sanguinis*, *S. oralis*, *S. mitis*, *S. gordonii*, *Streptococcus parasanguinis*, and a few *S. mutans* strains, plays an important role in interspecies competitive interaction (Figure 1). An inverse correlation between *Streptococcus oligofermentans* and *S. mutans* has been reported and thus suggested a possible antagonistic interaction between the two species (Tong et al., 2003). Tong et al. (2007) showed that *S. oligofermentans* possesses the capacity to convert its competitor's main "weapon" (lactic acid) into an inhibitory chemical (H_2O_2) against *S. mutans* in order to gain a competitive growth advantage. This fascinating ability may be an example of a counteroffensive strategy used during chemical warfare within the oral microbial community. Furthermore, the inhibitory nature of H_2O_2 helps to structure the microbial composition of multispecies communities and contributes to an overall ecological homeostasis. It has been known that high levels of cariogenic *S. mutans* in the oral cavity correlate with low levels of *S. sanguinis* (Caufield et al., 2000). An epidemiological survey demonstrated the presence of putative periodontopathogens such as *P. gingivalis*, *A. actinomycetemcomitans*, and *Eikenella corrodens* in a destructive periodontitis site was correlated with the absence of certain viridans streptococci including *S. sanguinis* and *Streptococcus intermedius*, and vice versa (Hillman et al., 1985).

In addition to H_2O_2 , bacteriocin or bacteriocin-like activities in multispecies communities play an essential role in modulating the ecological balance of oral microbial communities (Figure 1). Some oral commensal streptococci, such as *S. sanguinis*, *S. gordonii*, and *S. oligofermentans*, can suppress the overgrowth of cariogenic species *S. mutans* through the production of bacteriocins (Kreth et al., 2005a; Heng et al., 2007; Tong et al., 2008). *S. mutans*, in turn, gains competitive edge by producing lactic acid and mutacin to antagonize the growth of other oral commensal streptococci (Loesche, 1986; Qi et al., 2001). *Lactobacillus paracasei* can also produce bacteriocin to

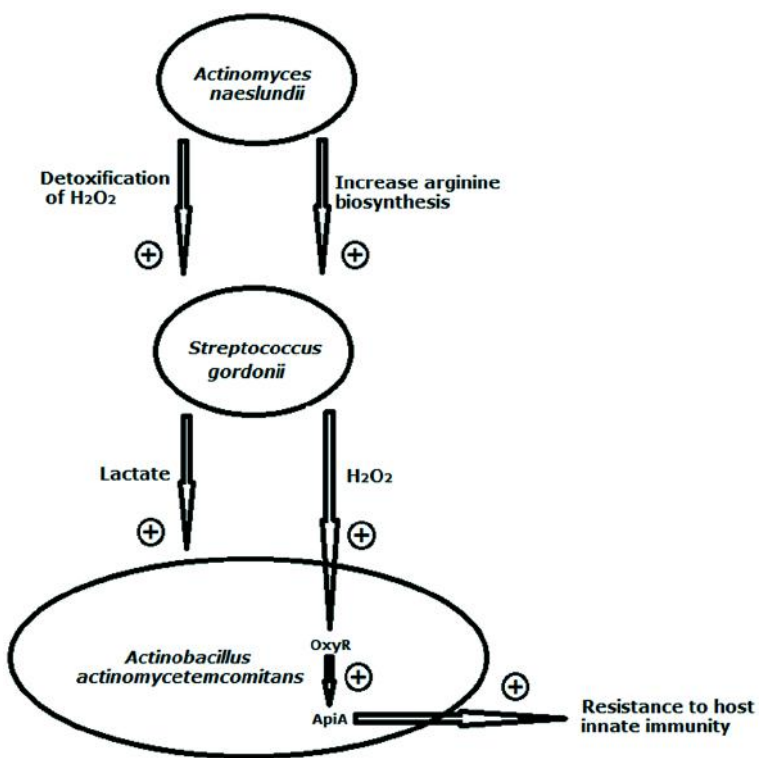


FIGURE 2 | Illustration of interspecies interactions between *Streptococcus gordonii* and its co-residents *Actinomyces naeslundii* and *Actinobacillus actinomycetemcomitans*. *S. gordonii* benefits from its coaggregation with *A. naeslundii* both in tolerating protein oxidation by H₂O₂ and in upregulating arginine biosynthesis. *A. actinomycetemcomitans* utilizes L-lactate, a carbohydrate metabolic by-product of *S. gordonii* as nutrient source. The consumption of lactic acid by the lactic acid-utilizing

bacteria minimizes lactic acid accumulation, which otherwise would inhibit streptococcal growth. *S. gordonii*-generated H₂O₂ can stimulate activation of the *A. actinomycetemcomitans* OxyR regulator to increase transcription of *apiA* that leads to enhanced resistance to host innate immunity. The arrow in combination with + indicates stimulation. Model compiled from Brown and Whiteley (2007), Jakubovics et al. (2008a,b), and Ramsey and Whiteley (2009).

inhibit the growth of *P. gingivalis*, *P. intermedia*, *T. forsythia*, *S. salivarius*, and *S. sanguinis* (Pangsomboon et al., 2006, 2009). *Prevotella nigrescens* (*P. nigrescens*) ATCC 25261 was reported to produce a novel bacteriocin Nigrescin against *P. gingivalis*, *P. intermedia*, *T. forsythia*, and *Actinomyces* sp. (Kaewsrichan et al., 2004). More recently, it has been suggested that *P. gingivalis* gingipains secreted in the subgingival environment are the main inhibitor in promoting the detachment of antecedent *A. actinomycetemcomitans* cells from the surface (Takasaki et al., 2013).

Some species have evolved specific mechanisms to counteract the antagonistic molecules such as H₂O₂ and bacteriocin (Figure 1). For example, *S. mutans* produces Dps-like protein (Dpr), superoxide dismutase (Sod) and glutathione synthetase (GshAB) in modulating its competitive fitness by alleviating H₂O₂-mediated interspecies competition exerted by other streptococcal co-residents, thus promoting its survival and persistence within the oral microbial communities (Fujishima et al., 2013; Zheng et al., 2013). Meanwhile, *S. mutans* expresses a cell-envelope associated eukaryotic serine/threonine protein kinase (STPK) to resist peroxide (Zhu and Kreth, 2010). Another example is that *S. gordonii* secrets challisin to inhibit bacteriocin production through interfering with competence-stimulating peptide

(CSP)-dependent quorum sensing system in *S. mutans* (Wang and Kuramitsu, 2005).

pH/OXYGEN MEDIATED INTERACTIONS

The co-inhabitants within the oral microbial community usually favor mutual growth in harsh conditions by modifying surrounding pH or oxygen tension. For example, as pH drops caused by acid-producing bacteria such as streptococci and actinomycetes following sugar fermentation, acid-tolerant bacteria, including *S. mutans* and lactobacilli, will out-compete acid-sensitive bacteria and have great impact on the microbial composition within community (Figure 1). Meanwhile, the lactic acid-utilizing bacteria such as *Veillonella atypica* and *A. actinomycetemcomitans* could prevent the acid buildup in dental biofilms, thus restoring microenvironment pH toward neutrality even in the presence of lactic acid bacteria and fermentable carbohydrates. As a result, the acid-sensitive species such as *P. gingivalis* are protected from acid attack (Takahashi, 2003). Acid-neutralizing activity could also be derived from the decrease in acidity during the fermentation of amino acid into organic acids and ammonia by certain periodontopathogens (Takahashi, 2003). For instance, it has been shown that *F. nucleatum* can grow at a wide pH range of 5.0–7.0, while *P. gingivalis* is susceptible to pH below 6.5. A study by Takahashi

(2003) demonstrated that *F. nucleatum* can generate ammonia from glutamic and aspartic acid, subsequently elevating the pH to favor *P. gingivalis* growth. Besides adjusting local pH, *F. nucleatum* is also aerotolerant and its metabolic activity can reduce the concentration of oxygen to levels that can be tolerated by obligate anaerobes such as *P. gingivalis*, *P. Nigrescens*, and *T. denticola* (Bradshaw and Marsh, 1998; Bradshaw et al., 1998; Kolenbrander et al., 1998b). Without *F. nucleatum*, the number of obligate anaerobes would decrease sharply in oxygenated environments (Bradshaw et al., 1998). Meanwhile, *F. nucleatum* can support *P. gingivalis* growth by providing a capnophilic microenvironment when growing in a CO₂ depleted environment (Diaz et al., 2002).

DNA MEDIATED INTERACTIONS

Cell lysis resulting from H₂O₂ and bacteriocin has been conjectured to provide genomic DNAs to the microbial communities (Zhu and Kreth, 2012). Extracellular DNA can be trapped within microbial biofilm matrix (Nadell et al., 2009) and might help to stabilize the biofilm structure (Barnes et al., 2012). Perry et al. (2009) found that treating *S. mutans* biofilms with DNase I reduced the surface-associated biomass by approximately 20%.

Genetic exchange occurs within oral microbial communities because residents are in close proximity. Horizontal gene transfer is the main driving force in bacterial evolution of antibiotic resistance and pathogenicity (Roberts and Mullany, 2010). Genome sequencing of several oral bacteria has revealed the presence of “pathogenicity islands” on the chromosomes of species such as *P. gingivalis* (Curtis et al., 1999). Conjugation, transformation, and transduction have been commonly observed in a variety of oral bacterial species (LeBlanc et al., 1978; Kuramitsu and Trapa, 1984; Yeung, 1999; Li et al., 2001b). Many genera of oral bacteria, including *Actinomyces*, *Bifidobacterium*, *Fusobacterium*, *Haemophilus*, *Peptostreptococcus*, *Streptococcus*, and *Veillonella* contain conjugative transposons that facilitate intercellular DNA transfer through conjugation (Rice, 1998). It is well known that oral streptococci are naturally competent, and it is possible that the DNA in the extracellular matrix is transmitted among them (Warburton et al., 2007). A study reported by Kreth et al. (2005b) proposed that *S. mutans* might utilize competence-induced bacteriocin to kill and lyse the neighboring species colonizing the same ecological niche and take up their DNA. Besides streptococci, *P. gingivalis* is able to exchange fimbrial allele types I and IV via natural competence as an adaptive process to modify behavior (Kerr et al., 2014). *A. actinomycetemcomitans* isolates from periodontal pockets have also been found to contain bacteriophages (Sandmeier et al., 1995).

MICROBIAL INTERCELLULAR SIGNALING

Within dense and constricted oral microbial community, intercellular signaling allows residents to regulate their gene expressions in accordance with their environments, and coordinate their behaviors in virulence factors regulation, metabolic adaptation, competence initiation and polymicrobial biofilm development.

CONTACT-DEPENDENT SIGNALING

In response to physical association with host tissues or bacterial cell surface, bacteria could initiate signal transduction cascades to regulate the expression of genes involved in adherence (Zainal-Abidin

et al., 2012; Sarkar et al., 2014). For example, attachment of *S. gordonii* to salivary pellicle on the tooth surface triggers upregulated expression of AgI/II family protein Ssp (Dü and Kolenbrander, 2000), which are adhesins to salivary proteins (Demuth et al., 1996), as well as *Actinomyces* and *P. gingivalis* (Lamont et al., 2002). Further study revealed that this transcriptional regulation was mediated by a two-component system BrfAB (Zhang et al., 2004). Thus, the direct contact with saliva enhances *S. gordonii*'s adherence to tooth surface and the recruitment of late colonizing species such as *Actinomyces*, which will contribute to the spatiotemporal development of multispecies communities. Meanwhile, signaling can also be triggered when different bacterial species are in direct physical contact. *P. gingivalis* was reported to acquire increased adhesive capacities on various substrata through up-regulated expression of gingipain upon contact with *T. denticola* (Meuric et al., 2013). The transcriptional responses as a result of cell–cell contact often are not limited to a few genes. A study showed that thirty-three genes were differentially regulated during accretion of *P. gingivalis* in heterotypic biofilms with *S. gordonii* (Simionato et al., 2006). The functions of the regulated genes were predominantly related to metabolism and energy production. Another study on *P. gingivalis* assembled into a mixed community with *F. nucleatum* and *S. gordonii* revealed that over 400 genes were differentially regulated in response to cell–cell contact (Kuboniwa et al., 2009). Such signaling is important in the integration of *P. gingivalis* into early biofilms dominated by Gram-positive bacteria. In addition to facilitating bacteria colonization of microbial community, contact-inducible gene expression could also enhance microbial growth. *S. gordonii* was shown to benefit from its coaggregation with *A. naeslundii* in arginine-restricted conditions through three fold changes in the expression of the genes involved in arginine biosynthesis (Jakubovics et al., 2008a; Figure 2). This signaling was not observed in co-cultures where there was no coaggregation between the two species, suggesting that there is a specific transcriptional response after cell–cell contact. Contact-inducible transcriptional change could prepare bacteria to better cope with the environmental stress, such as the exposure to H₂O₂ within the multispecies communities. An example comes from our observation of *S. sanguinis* and *F. nucleatum* (He et al., 2012). We found that upon contact with *S. sanguinis*, *F. nucleatum* acquired increased resistance to H₂O₂ and also significantly inhibited H₂O₂ production by *S. sanguinis*. This event was not observed in a *F. nucleatum* mutant deficient in *radD*, which encodes an outer membrane protein adhesin responsible for coadhesion with streptococci. This defense strategy of *F. nucleatum* prevents antagonism by other oral bacteria and allows integration into the developing oral microbial community. Similarly, coaggregation with *A. naeslundii* protects *S. gordonii* from oxidative damage by H₂O₂ (Jakubovics et al., 2008b; Figure 2).

On the other hand, cell contact-dependent signaling has also been shown to reduce adhesion. Park et al. (2006) observed that following contact with *S. gordonii*, the short fimbriae adhesin Mfa of *P. gingivalis* was down-regulated. Moreover, a cascade of tyrosine phosphorylation/dephosphorylation events in *P. gingivalis* initiated by contact with *S. gordonii* constrains the heterotypic community development between the two species

(Maeda et al., 2008; Chawla et al., 2010). Similarly, cell–cell contact between *T. forsythia* and *F. nucleatum* or *T. forsythia* and *P. gingivalis* also initiates a signal transduction cascade that causes down-regulated expression of BspA leucine-rich repeat protein adhesin in *T. forsythia* (Inagaki et al., 2005), resulting in reduced adherence ability. There is a signaling down-regulation in microbial biosynthesis pathway as well. A study showed *S. gordonii* and *F. nucleatum* reduced the abundance of *P. gingivalis* proteins responsible for several vitamin synthesis and pyrimidine biosynthesis in a contact-dependent manner (Kuboniwa et al., 2009).

Some degree of specificity exists in response to contact-dependent signaling. The study of Hendrickson et al. (2012) demonstrated that, when in contact with *P. gingivalis*, *S. gordonii* up-regulates the expression of the glycolysis pathway while when in contact with *F. nucleatum* the pentose phosphate pathway is up-regulated.

QUORUM SENSING

In addition to contact-dependent signaling, microbial intercellular signaling can also be mediated by secreted diffusible molecules. Quorum sensing mediated by autoinducing diffusible molecules (autoinducer) is a system of stimulus and response correlated to population density, which allows bacteria to coordinate gene expression on a population-wide scale. A significant portion of a bacterial genome (4–10%) and proteome (20% or more) can be influenced by quorum sensing signaling (Dunman et al., 2001; Arevalo-Ferro et al., 2003; Schuster et al., 2003; Wagner et al., 2003). Common classes of autoinducer are *N*-Acyl Homoserine Lactones (*N*-AHL) found in Gram-negative bacteria, autoinducing peptides (AIPs) produced by Gram-positive bacteria, and a family of autoinducers known as autoinducer-2 (AI-2) which is widespread among both Gram-negative and Gram-positive bacteria (Miller and Bassler, 2001) and is known as the most conserved quorum sensing signal molecule.

In Gram-negative bacteria, *N*-AHL signal is mainly generated by an *N*-AHL synthase of the LuxI family of proteins, and is recognized by an *N*-AHL receptor protein belonging to the LuxR family of transcriptional regulators (Ryan and Dow, 2008). Most Gram-negative bacteria use analogous LuxI/LuxR-type circuits for intraspecies signaling in which only members of the same species are able to recognize and respond to the signal. Meanwhile, there are reports suggesting their involvement in interspecies signaling (Huber et al., 2001; Riedel et al., 2001). The *N*-AHL intra- and interspecies signaling role of oral microbes needs to be further investigated. In this review we mainly focus on cell–cell signaling via AIPs and AI-2.

AIPs

In Gram-positive bacteria, recognition of and response to the AIPs occur not by direct binding to a cognate receptor but through a two-component signal transduction system, in which AIPs binds to a membrane-bound histidine kinase sensor and the binding leads to phosphorylation of response regulator proteins that ultimately bind to the promoter of target genes to regulate gene expression (Senadheera and Cvitkovitch, 2008).

Competence-stimulating peptide-mediated quorum sensing has been identified in various oral streptococcal species including *S. mutans*, *S. gordonii*, and *S. intermedius* (Håvarstein et al., 1997; Cvitkovitch, 2001; Petersen et al., 2004). The proposed role of CSP-mediated quorum sensing is to alter genes transcription and proteins synthesis involved in biofilm formation, competence development, bacteriocin synthesis, stress resistance, and autolysis (Petersen et al., 2004; Senadheera and Cvitkovitch, 2008; Perry et al., 2009; Senadheera et al., 2009).

Although AIPs are generally species-specific and sometimes strain-specific, they can be detected by and induce response in other species. A study showed that *S. mutans* CSP could be sensed by *C. albicans* and resulted in induction of its germ tube formation (Jarosz et al., 2009). In *Enterococcus faecalis* (*E. faecalis*), Fsr quorum-sensing system exerts inhibitive effect on *C. albicans* hyphal morphogenesis (Cruz et al., 2013). These two observations demonstrate the potential signaling role of AIPs in interkingdom communication. In order to perpetuate in complex oral multispecies community, microbial species can contend with its competitor by decreasing the concentration of the extracellular AIPs secreted by the competitor. *P. gingivalis* was found to be able to inactivate *S. mutans* CSP and abolish CSP-induced natural transformation (Wang et al., 2011a). Wang and Kuramitsu (2005) reported that *S. gordonii*, *S. sanguinis*, *S. mitis*, and *S. oralis* inhibited *S. mutans*' mutacin production by degrading its CSP. *S. gordonii* can secrete serine protease challeisin to inactivate *S. mutans* CSP, subsequently impairing *S. mutans* biofilm formation (Wang et al., 2011b; **Figure 1**). *S. salivarius* was also reported to strongly inhibit *S. mutans* biofilm formation via inactivating CSP produced by *S. mutans*, which provides a competitive advantage to *S. salivarius* against its competing bacteria (Tamura et al., 2009).

AI-2

AI-2 is a group of molecules derived from spontaneous rearrangement of *S*-4,5-dihydroxy-2,3-pentanedione (DPD), whose production is the catabolism of *S*-adenosylhomocysteine by conserved LuxS (Schäuder et al., 2001b). It is widely distributed in Gram-positive and Gram-negative bacteria and plays a widespread role in bacterial communication across species boundaries (Hardie and Heurlier, 2008; Jayaraman and Wood, 2008). AI-2 has been well-characterized as a universal interspecies signal molecule in regulating formation of multispecies biofilms (Bassler et al., 1997; Schäuder and Bassler, 2001a; Whitmore and Lamont, 2011). For example, mixed biofilm formation by *A. naeslundii* and *S. oralis* in flowing saliva was shown to be dependent on the production of AI-2 by *S. oralis* (Rickard et al., 2006). A *luxS* mutant of *S. oralis*, which cannot produce AI-2, does not form dual-species biofilms with *A. naeslundii*. This defect can be restored with either genetic complementation or supplementation with synthetic AI-2. *Streptococcus*-derived AI-2 can also regulate gene expression in *P. gingivalis* (Chung et al., 2001). Meanwhile, *S. gordonii* and *F. nucleatum* can sense *P. gingivalis* AI-2 as well and translate the signal into a biofilm phenotype (McNab et al., 2003; Saito et al., 2008). In addition to streptococcal AI-2, *P. gingivalis* can response to AI-2 signal secreted by *A. actinomycetemcomitans* (Fong et al., 2001). AI-2 secreted by *F. nucleatum* is

able to elicit changes in the expression of the representative adhesins of the so-called “red-complex” (*P. gingivalis*, *T. denticola*, and *T. forsythia*), and thus, increase the colonization of these periodontopathogens in oral multispecies biofilms (Jang et al., 2013a).

The concentration of AI-2 is critical for interspecies mutualism. It has been reported that above and below optimal AI-2 concentration dual-species biofilm formation of *S. oralis* and *A. naeslundii* was suppressed (Rickard et al., 2006). *F. nucleatum*, a middle colonizer of oral microbial communities, applies differential regulation of AI-2 on biofilm growth of two oral streptococci by exerting a stimulatory effect on *S. gordonii* and an inhibitory effect on *S. oralis* (Jang et al., 2013b). Cuadra-Saenz et al. (2012) found that *S. gordonii* produce more AI-2 than *S. oralis*. They suggested that AI-2 could alter the structure and composition of pioneering oral streptococcal population, thereafter influencing the subsequent succession of other species into oral microbial communities (Cuadra-Saenz et al., 2012). Commensal bacteria such as *S. oralis* and *A. naeslundii* have been shown to respond to AI-2 levels that are below those produced by species associated with oral disease, for example *F. nucleatum* (Frias et al., 2001). Commensal species produce and respond to AI-2 signals at picomolar concentrations, which are much lower than that of periodontopathogens (Kolenbrander et al., 2006). *Fusobacteria* are usually detectable in oral microbial biofilms after 8 h of biofilm development (Li et al., 2004). As entry of *Fusobacteria* increases on the tooth surface and local AI-2 concentration rises, *Fusobacteria* would initiate signal-dependent changes in gene expression regulated by AI-2. By contrast, commensal bacteria are inhibited by the increasing concentration of AI-2. Accordingly, high levels of AI-2 increase the accumulation of periodontopathogens and reduce the growth of commensal bacteria. Considering the different AI-2 concentrations, some researchers propose AI-2 as a modulator for multispecies microbial communities in transition from a beneficial community to a pathogenic community (Kolenbrander et al., 2010).

In addition to interspecies interaction, AI-2 has been reported to play a role in interkingdom signaling. *C. albicans* can sense AI-2 produced by *S. gordonii* to induce numerous transcriptional changes, including increased production of hyphae and the activation or repression of three mitogen-activated protein kinases involved in morphogenetic switching (Bamford et al., 2009).

During the development of highly organized microbial communities, individual species must be able to overcome antagonistic effects from other community co-inhabitants in order to perpetuate in the multispecies community (Vollaard and Clasener, 1994; He et al., 2012). Xavier et al. (2007) found that some species of enteric bacteria can degrade AI-2 signaling and interfere with other competing species’ ability to assess and respond correctly to changes in cell population density. No such interactions have yet been observed for oral microbial community members.

Recent studies also have demonstrated an emerging role for AI-2 as an intraspecies signal molecule besides its well-characterized function in interspecies signaling. In *A. actinomycetemcomitans* and *S. mutans*, AI-2 is required in modulating their biofilm development and virulence (Merritt et al., 2003; Shao et al., 2007;

Torres-Escobar et al., 2013). While in *P. gingivalis*, AI-2 regulates iron (hemin) acquisition (James et al., 2006) and oxidative stress-related genes (Yuan et al., 2005).

NON-AUTOINDUCING MOLECULES DEPENDENT SIGNALING

In addition to autoinducers, oral microbial species can sense and respond to extracellular non-autoinducing diffusible molecules to achieve gene regulation. It has been shown that a diffusible molecule dependent signaling exists between *S. gordonii* and *V. atypica* besides their cross-feeding through lactic acid. *S. gordonii* responds to maltose or a related sugar from the lipopolysaccharide released by *V. atypica* by up-regulating the expression of streptococcal transcription factor CcpA, which is required for amylase synthesis (Egland et al., 2004; Johnson et al., 2009). Increased amylase activity on a starch substrate causes *S. gordonii* to generate more lactate, the primary energy source for *V. atypica*. Thus, one or both species involved in this event benefit from this metabolic requirements-driven interspecies interaction. Furthermore, this type of signaling occurred only in *S. gordonii* cells located within a few micrometers of *V. atypica*, emphasizing that diffusible signals between species are designed to function over very short distances, on the order of 1 μm. In addition to coordinative effect, metabolites can induce antagonistic signaling as well. For example, extracellular arginine deiminase of *S. cristatus* and *S. intermedius* downregulates expression of FimA of *P. gingivalis*, and consequently *P. gingivalis* cannot integrate into communities together with these organisms (Xie et al., 2007; Christopher et al., 2010). In contrast, lack of the similar signaling pathway in *S. gordonii* makes it more compatible with *P. gingivalis* compared to *S. cristatus* and *S. intermedius*.

Acidic pH and H₂O₂ could play a role in interspecies signaling, which may affect gene expression patterns of bacteria cells growing within oral microbial communities (Li and Burne, 2001a; Deng et al., 2007). Under low microenvironmental pH, 14% of the *S. mutans* genome displays altered gene expression including quorum sensing systems (Gong et al., 2009). In response to H₂O₂-induced oxidative stress, there were three major protein systems of *F. nucleatum* changed (Steeves et al., 2011). *S. gordonii*-generated H₂O₂ can stimulate activation of the *A. actinomycetemcomitans* OxyR regulator to increase transcription of *apiA* that leads to enhanced resistance to host innate immunity (Ramsey and Whiteley, 2009; **Figure 2**).

Other than growth inhibition, antibiotics at sub-inhibitory concentration were reported to be potent global regulators of transcription for bacteria within microbial communities (Yim et al., 2006). In *S. mutans* GS5, low concentrations of antibiotics could up-regulate expression of bacteriocin immunity protein gene, which affected its sensitivity to a variety of antimicrobial agents (Matsumoto-Nakano and Kuramitsu, 2006).

CONCLUSION

Recently, there is an increasing appreciation of the essential roles of inter-cellular communications in polymicrobial oral biofilm development, environmental adaptation, and virulent factors regulation. Adhesins and receptors-mediated binding benefits microbial community residents by providing a broader habitat range and influences the temporal and spatial formation of

highly organized polymicrobial community architecture. Furthermore, the close physical association allows residents to obtain metabolic support from their neighboring species. Cooperative metabolic interactions either via cross-feeding or through cooperatively metabolizing substrate maximize co-residents' potential to extract energy from limited substrates. In addition to synergistic interactions, oral bacterial species are also engaged in intense competition for limited space and nutritional resources using compounds such as bacteriocin and H₂O₂, which plays a crucial role in defining the structure and activity of oral microbial communities. Intercellular signaling within the same or between different bacterial species can be achieved by contact dependent mechanisms or mediated by diffusible signal molecules. These signaling events play significant roles in coordinating gene expression involved in microbial physiology and pathobiology. Among the secreted signaling molecules, AIPs and AI-2 appear to be involved in both intra-species quorum sensing and a variety of interspecies interactions across oral species. More comprehensive investigations of microbial intercellular interactions will shed light on the complexity of multispecies oral microbial communities and may provide novel approaches for controlling microbial community-based pathogenesis.

ACKNOWLEDGMENTS

This work was supported by a NIH grant DE020102 and DE021108.

REFERENCES

- Abe, T., Murakami, Y., Nagano, K., Hasegawa, Y., Moriguchi, K., Ohno, N., et al. (2011). OmpA-like protein influences cell shape and adhesive activity of *Tannerella forsythia*. *Mol. Oral Microbiol.* 26, 374–387. doi: 10.1111/j.2041-1014.2011.00625.x
- Arevalo-Ferro, C., Hentzer, M., Reil, G., Görg, A., Kjelleberg, S., Givskov, M., et al. (2003). Identification of quorumsensing regulated proteins in the opportunistic pathogen *Pseudomonas aeruginosa* by proteomics. *Environ. Microbiol.* 5, 1350–1369. doi: 10.1046/j.1462-2920.2003.00532.x
- Avila, M., Ojcius, D. M., and Yilmaz, Ö. (2009). The oral microbiota: living with a permanent guest. *DNA Cell Biol.* 28, 405–411. doi: 10.1089/dna.2009.0874
- Bamford, C. V., d'Mello, A., Nobbs, A. H., Dutton, L. C., Vickerman, M. M., and Jenkinson, H. F. (2009). *Streptococcus gordonii* modulates *Candida albicans* biofilm formation through intergeneric communication. *Infect. Immun.* 77, 3696–3704. doi: 10.1128/IAI.00438-09
- Barnes, A. M., Ballering, K. S., Leibman, R. S., Wells, C. L., and Dunny, G. M. (2012). *Enterococcus faecalis* produces abundant extracellular structures containing DNA in the absence of cell lysis during early biofilm formation. *MBio* 3, e00193–e00212. doi: 10.1128/mBio.00193-12
- Bassler, B. L., Greenberg, E. P., and Stevens, A. M. (1997). Cross-species induction of luminescence in the quorum-sensing bacterium *Vibrio harveyi*. *J. Bacteriol.* 179, 4043–4045.
- Biyikoğlu, B., Ricker, A., and Diaz, P. I. (2012). Strain-specific colonization patterns and serum modulation of multi-species oral biofilm development. *Anaerobe* 18, 459–470. doi: 10.1016/j.anaerobe.2012.06.003
- Bowen, W. H., and Koo, H. (2011). Biology of *Streptococcus mutans*-derived glucosyltransferases: role in extracellular matrix formation of cariogenic biofilms. *Caries Res.* 45, 69–86. doi: 10.1159/000324598
- Bradshaw, D. J., and Marsh, P. D. (1998). Analysis of pH-driven disruption of oral microbial communities in vitro. *Caries Res.* 32, 456–462. doi: 10.1159/00016487
- Bradshaw, D. J., Marsh, P. D., Watson, G. K., and Allison, C. (1998). Role of *Fusobacterium nucleatum* and coaggregation in anaerobe survival in planktonic and biofilm oral microbial communities during aeration. *Infect. Immun.* 66, 4729–4732.
- Brooks, W., Demuth, D. R., Gil, S., and Lamont, R. J. (1997). Identification of a *Streptococcus gordonii* SspB domain that mediates adhesion to *Porphyromonas gingivalis*. *Infect. Immun.* 65, 3753–3758.
- Brown, S. A., and Whiteley, M. (2007). A novel exclusion mechanism for carbon resource partitioning in *Aggregatibacter actinomycetemcomitans*. *J. Bacteriol.* 189, 6407–6414. doi: 10.1128/JB.00554-07
- Capestaný, C. A., Kuboniwa, M., Jung, I. Y., Park, Y., Tribble, G. D., and Lamont, R. J. (2006). Role of the *Porphyromonas gingivalis* InlJ protein in homotypic and heterotypic biofilm development. *Infect. Immun.* 74, 3002–3005. doi: 10.1128/IAI.74.5.3002-3005.2006
- Caufield, P. W., Dasanayake, A. P., Li, Y., Pan, Y., Hsu, J., and Hardin, J. M. (2000). Natural history of *Streptococcus sanguinis* in the oral cavity of infants: evidence for a discrete window of infectivity. *Infect. Immun.* 68, 4018–4023. doi: 10.1128/IAI.68.7.4018-4023.2000
- Chalmers, N. I., Palmer, R. J., Cisar, J. O., and Kolenbrander, P. E. (2008). Characterization of a *Streptococcus* sp.–*Veillonella* sp. community micromanipulated from dental plaque. *J. Bacteriol.* 190, 8145–8154. doi: 10.1128/JB.00983-08
- Chalmers, N. I., Palmer, R. J. Jr., Du-Thumm, L., Sullivan, R., Shi, W., and Kolenbrander, P. E. (2007). Use of quantum dot luminescent probes to achieve single-cell resolution of human oral bacteria in biofilms. *Appl. Environ. Microbiol.* 73, 630–636. doi: 10.1128/AEM.02164-06
- Chawla, A., Hirano, T., Bainbridge, B. W., Demuth, D. R., Xie, H., and Lamont, R. J. (2010). Community signaling between *Streptococcus gordonii* and *Porphyromonas gingivalis* is controlled by the transcriptional regulator CdhR. *Mol. Microbiol.* 78, 1510–1522. doi: 10.1111/j.1365-2958.2010.07420.x
- Christopher, A. B., Arndt, A., Cugini, C., and Davey, M. E. (2010). A streptococcal effector protein that inhibits *Porphyromonas gingivalis* biofilm development. *Microbiology* 156, 3469–3477. doi: 10.1099/mic.0.042671-0
- Chung, W. O., Park, Y., Lamont, R. J., McNab, R., Barbieri, B., and Demuth, D. R. (2001). Signaling system in *Porphyromonas gingivalis* based on a LuxS protein. *J. Bacteriol.* 183, 3903–3909. doi: 10.1128/JB.183.13.3903-3909.2001
- Cisar, J. O., Kolenbrander, P. E., and McIntire, F. C. (1979). Specificity of coaggregation reactions between human oral streptococci and strains of *Actinomyces viscosus* or *Actinomyces naeslundii*. *Infect. Immun.* 24, 742–752.
- Cogoni, V., Morgan-Smith, A., Fenno, J. C., Jenkinson, H. F., and Dymock, D. D. (2012). *Treponema denticola* chymotrypsin-like proteinase (CTLP) integrates spirochaetes within oral microbial communities. *Microbiology* 158, 759–770. doi: 10.1099/mic.0.055939-0
- Cruz, M. R., Graham, C. E., Gagliano, B. C., Lorenz, M. C., and Garsin, D. A. (2013). *Enterococcus faecalis* inhibits hyphal morphogenesis and virulence of *Candida albicans*. *Infect. Immun.* 81, 189–200. doi: 10.1128/IAI.00914-12
- Cuadra-Saenz, G., Rao, D. L., Underwood, A. J., Belapure, S. A., Campagna, S. R., Sun, Z., et al. (2012). Autoinducer-2 influences interactions amongst pioneer colonizing streptococci in oral biofilms. *Microbiology* 158, 1783–1795. doi: 10.1099/mic.0.057182-0
- Curtis, M. A., Hawley, S. A., and Aduse-Opoku, J. (1999). The rag locus of *Porphyromonas gingivalis*: a novel pathogenicity island. *J. Periodontol. Res.* 34, 400–440. doi: 10.1111/j.1600-0765.1999.tb02273.x
- Cvitkovitch, D. G. (2001). Genetic competence and transformation in oral streptococci. *Crit. Rev. Oral Biol. Med.* 12, 217–243. doi: 10.1177/104544110120030201
- Daep, C. A., Novak, E. A., Lamont, R. J., and Demuth, D. R. (2011). Structural dissection and in vivo effectiveness of a peptide inhibitor of *Porphyromonas gingivalis* adherence to *Streptococcus gordonii*. *Infect. Immun.* 79, 67–74. doi: 10.1128/IAI.00361-10
- Demuth, D. R., Duan, Y., Brooks, W., Holmes, A. R., McNab, R., and Jenkinson, H. F. (1996). Tandem genes encode cell-surface polypeptides SspA and SspB which mediate adhesion of the oral bacterium *Streptococcus gordonii* to human and bacterial receptors. *Mol. Microbiol.* 20, 403–413. doi: 10.1111/j.1365-2958.1996.tb02627.x
- Demuth, D. R., Irvine, D. C., Costerton, J. W., Cook, G. S., and Lamont, R. J. (2001). Discrete protein determinant directs the species-specific adherence of *Porphyromonas gingivalis* to oral streptococci. *Infect. Immun.* 69, 5736–5741. doi: 10.1128/IAI.69.9.5736-5741.2001

- Deng, D. M., Liu, M. J., ten Cate, J. M., and Crielaard, W. (2007). The VicRK system of *Streptococcus mutans* responds to oxidative stress. *J. Dent. Res.* 86, 606–610. doi: 10.1177/154405910708600705
- Dewhirst, F. E., Chen, T., Izard, J., Paster, B. J., Tanner, A. C. R., Yu, W. H., et al. (2010). The human oral microbiome. *J. Bacteriol.* 192, 5002–5017. doi: 10.1128/JB.00542-10
- Diaz, P. I., Zilm, P. S., and Rogers, A. H. (2002). *Fusobacterium nucleatum* supports the growth of *Porphyromonas gingivalis* in oxygenated and carbon dioxide-depleted environments. *Microbiology* 148, 467–472.
- Dige, I., Raarup, M. K., Nyengaard, J. R., Kilian, M., and Nyvad, B. (2009). *Actinomyces naeslundii* in initial dental biofilm formation. *Microbiology* 155, 2116–2126. doi: 10.1099/mic.0.027706-0
- Ding, A. M., Palmer, R. J. Jr., Cisar, J. O., and Kolenbrander, P. E. (2010). Shear-enhanced oral microbial adhesion. *Appl. Environ. Microbiol.* 76, 1294–1297. doi: 10.1128/AEM.02083-09
- Dù, L. D., and Kolenbrander, P. E. (2000). Identification of saliva-regulated genes of *Streptococcus gordonii* DL1 by differential display using random arbitrarily primed PCR. *Infect. Immun.* 68, 4834–4837. doi: 10.1128/IAI.68.8.4834-4837.2000
- Dunman, P. M., Murphy, E., Haney, S., Palacios, D., Tucker-Kellogg, G., Wu, S., et al. (2001). Transcription profiling-based identification of *Staphylococcus aureus* genes regulated by the agr and/or sarA loci. *J. Bacteriol.* 183, 7341–7353. doi: 10.1128/JB.183.24.7341-7353.2001
- Egland, P. G., Palmer, R. J., and Kolenbrander, P. E. (2004). Interspecies communication in *Streptococcus gordonii*–*Veillonella atypica* biofilms: signaling in flow conditions requires juxtaposition. *Proc. Natl. Acad. Sci. U.S.A.* 101, 16917–16922. doi: 10.1073/pnas.0407457101
- Fong, K. P., Chung, W. O., Lamont, R. J., and Demuth, D. R. (2001). Intra- and interspecies regulation of gene expression by *Actinobacillus actinomycetemcomitans* LuxS. *Infect. Immun.* 69, 7625–7634. doi: 10.1128/IAI.69.12.7625-7634.2001
- Frias, J., Olle, E., and Alsina, M. (2001). Periodontal pathogens produce quorum sensing signal molecules. *Infect. Immun.* 69, 3431–3434. doi: 10.1128/IAI.69.5.3431-3434.2001
- Fujishima, K., Kawada-Matsuo, M., Oogai, Y., Tokuda, M., Torii, M., and Komatsuwa, H. (2013). dpr and sod in *Streptococcus mutans* are involved in coexistence with *S. sanguinis*, and PerR is associated with resistance to H2O2. *Appl. Environ. Microbiol.* 79, 1436–1443. doi: 10.1128/AEM.03306-12
- Gong, Y., Tian, X. L., Sutherland, T., Sisson, G., Mai, J., Ling, J., et al. (2009). Global transcriptional analysis of acid-inducible genes in *Streptococcus mutans*: multiple two-component systems involved in acid adaptation. *Microbiology* 155, 3322–3332. doi: 10.1099/mic.0.031591-0
- Gregoire, S., Xiao, J., Silva, B. B., Gonzalez, I., Agidi, P. S., Klein, M. I., et al. (2011). Role of glucosyltransferase B in interactions of *Candida albicans* with *Streptococcus mutans* and with an experimental pellicle on hydroxyapatite surfaces. *Appl. Environ. Microbiol.* 77, 6357–6367. doi: 10.1128/AEM.05203-11
- Grenier, D. (1992). Nutritional interactions between two suspected periodontopathogens, *Treponema denticola* and *Porphyromonas gingivalis*. *Infect. Immun.* 60, 5298–5301.
- Hamada, T., Kawashima, M., Watanabe, H., Tagami, J., and Senpuku, H. (2004). Molecular interactions of surface protein peptides of *Streptococcus gordonii* with human salivary components. *Infect. Immun.* 72, 4819–4826. doi: 10.1128/IAI.72.8.4819-4826.2004
- Hardie, K. R., and Heurlier, K. (2008). Establishing bacterial communities by “word of mouth”: LuxS and autoinducer 2 in biofilm development. *Nat. Rev. Microbiol.* 6, 635–643. doi: 10.1038/nrmicro1916
- Håvarstein, L. S., Hakenbeck, R., and Gaustad, P. (1997). Natural competence in the genus *Streptococcus*: evidence that streptococci can change phenotype by interspecies recombinational exchanges. *J. Bacteriol.* 179, 6589–6594.
- He, X., Hu, W., Kaplan, C. W., Guo, L., Shi, W., and Lux, R. (2012). Adherence to streptococci facilitates *Fusobacterium nucleatum* integration into an oral microbial community. *Microb. Ecol.* 63, 532–542. doi: 10.1007/s00248-011-9989-2
- Hendrickson, E. L., Wang, T., Dickinson, B. C., Whitmore, S. E., Wright, C. J., Lamont, R. J., et al. (2012). Proteomics of *Streptococcus gordonii* within a model developing oral microbial community. *BMC Microbiol.* 12:211. doi: 10.1186/1471-2180-12-211
- Heng, N. C. K., Tagg, J. R., and Tompkins, G. R. (2007). Competence-dependent bacteriocin production by *Streptococcus gordonii* DL1 (Challis). *J. Bacteriol.* 189, 1468–1472. doi: 10.1128/JB.01174-06
- Hillman, J. D., Socransky, S. S., and Shivers, M. (1985). The relationships between streptococcal species and periodontopathic bacteria in human dental plaque. *Arch. Oral Biol.* 30, 791–795. doi: 10.1016/0003-9969(85)90133-5
- Hojo, K., Nagaoka, S., Ohshima, T., and Maeda, N. (2009). Bacterial interactions in dental biofilm development. *J. Dent. Res.* 88, 982–990. doi: 10.1177/0022034509346811
- Huber, B., Riedel, K., Hentzer, M., Heydorn, A., Gotschlich, A., Givskov, M., et al. (2001). The cep quorumsensing system of *Burkholderia cepacia* H111 controls biofilm formation and swarming motility. *Microbiology* 147, 2517–2528.
- Ikegami, A., Honma, K., Sharma, A., and Kuramitsu, H. K. (2004). Multiple functions of the leucine-rich repeat protein LrrA of *Treponema denticola*. *Infect. Immun.* 72, 4619–4627. doi: 10.1128/IAI.72.8.4619-4627.2004
- Inagaki, S., Kuramitsu, H. K., and Sharma, A. (2005). Contact-dependent regulation of a *Tannerella forsythia* virulence factor, BspA, in biofilms. *FEMS Microbiol. Lett.* 249, 291–296. doi: 10.1016/j.femsle.2005.06.032
- Ishihara, K., Nabuchi, A., Ito, R., Miyachi, K., Kuramitsu, H. K., and Okuda, K. (2004). Correlation between detection rates of periodontopathic bacterial DNA in carotid coronary stenotic artery plaque and in dental plaque samples. *J. Clin. Microbiol.* 42, 1313–1315. doi: 10.1128/JCM.42.3.1313-1315.2004
- Jakubovics, N. S., Gill, S. R., Iobst, S. E., Vickerman, M. M., and Kolenbrander, P. E. (2008a). Regulation of gene expression in a mixed-genus community: stabilized arginine biosynthesis in *Streptococcus gordonii* by coaggregation with *Actinomyces naeslundii*. *J. Bacteriol.* 190, 3646–3657. doi: 10.1128/JB.00088-08
- Jakubovics, N. S., Gill, S. R., Vickerman, M. M., and Kolenbrander, P. E. (2008b). Role of hydrogen peroxide in competition and cooperation between *Streptococcus gordonii* and *Actinomyces naeslundii*. *FEMS Microbiol. Ecol.* 66, 637–644. doi: 10.1111/j.1574-6941.2008.00585.x
- James, C. E., Hasegawa, Y., Park, Y., Yeung, V., Tribble, G. D., Kuboniwa, M., et al. (2006). LuxS involvement in the regulation of genes coding for hemin and iron acquisition systems in *Porphyromonas gingivalis*. *Infect. Immun.* 74, 3834–3844. doi: 10.1128/IAI.01768-05
- Jang, Y. J., Choi, Y. J., Lee, S. H., Jun, H. K., and Choi, B. K. (2013a). Autoinducer 2 of *Fusobacterium nucleatum* as a target molecule to inhibit biofilm formation of periodontopathogens. *Arch. Oral Biol.* 58, 17–27. doi: 10.1016/j.archoralbio.2012.04.016
- Jang, Y. J., Sim, J., Jun, H. K., and Choi, B. K. (2013b). Differential effect of autoinducer 2 of *Fusobacterium nucleatum* on oral streptococci. *Arch. Oral Biol.* 58, 1594–1602. doi: 10.1016/j.archoralbio.2013.08.006
- Jarosz, L. M., Deng, D. M., van der Mei, H. C., Crielaard, W., and Krom, B. P. (2009). *Streptococcus mutans* competence-stimulating peptide inhibits *Candida albicans* hypha formation. *Eukaryot. Cell* 8, 1658–1664. doi: 10.1128/EC.00070-09
- Jayaraman, A., and Wood, T. K. (2008). Bacterial quorum sensing: signals, circuits, and implications for biofilms and disease. *Annu. Rev. Biomed. Eng.* 10, 145–167. doi: 10.1146/annurev.bioeng.10.061807.160536
- Jenkinson, H. F., and Lamont, R. J. (2005). Oral microbial communities in sickness and in health. *Trends Microbiol.* 13, 589–595. doi: 10.1016/j.tim.2005.09.006
- Johnson, B. P., Jensen, B. J., Ransom, E. M., Heinemann, K. A., Vannatta, K. M., Egland, K. A., et al. (2009). Interspecies signaling between *Veillonella atypica* and *Streptococcus gordonii* requires the transcription factor CcpA. *J. Bacteriol.* 191, 5563–5565. doi: 10.1128/JB.01226-08
- Kaewsrichan, J., Douglas, C. W. I., Nissen-Meyer, J., Fimland, G., and Teanpaisan, R. (2004). Characterization of a bacteriocin produced by *Prevotella nigrescens* ATCC 25261. *Lett. Appl. Microbiol.* 39, 451–458. doi: 10.1111/j.1472-765X.2004.01608.x
- Kaplan, C. W., Lux, R., Haake, S. K., and Shi, W. (2009). The *Fusobacterium nucleatum* outer membrane protein RadD is an arginine-inhibitable adhesin required for inter-species adherence and the structured architecture of multi-species biofilm. *Mol. Microbiol.* 71, 35–47. doi: 10.1111/j.1365-2958.2008.06503.x
- Kaplan, J. B., Ragunath, C., Ramasubbu, N., and Fine, D. H. (2003). Detachment of *Actinobacillus actinomycetemcomitans* biofilm cells by an endogenous beta-hexosaminidase activity. *J. Bacteriol.* 185, 4693–4698. doi: 10.1128/JB.185.16.4693-4698.2003

- Kerr, J. E., Abramian, J. R., Dao, D. H., Rigney, T. W., Fritz, J., Pham, T., et al. (2014). Genetic exchange of fimbrial alleles exemplifies the adaptive virulence strategy of *Porphyromonas gingivalis*. *PLoS ONE* 13:e91696. doi: 10.1371/journal.pone.0091696
- Kolenbrander, P. E. (2011). Multispecies communities: interspecies interactions influence growth on saliva as sole nutritional source. *Int. J. Oral* 3, 49–54. doi: 10.4248/IJOS11025
- Kolenbrander, P. E., Andersen, R. N., Baker, R. A., Jenkinson, H. F. (1998a). The adhesion-associated sca operon in *Streptococcus gordonii* encodes an inducible high-affinity ABC transporter for Mn²⁺ uptake. *J. Bacteriol.* 180, 290–295.
- Kolenbrander, P. E., Andersen, R. N., and Moore, L. V. (1998b). Coaggregation of *Fusobacterium nucleatum*, *Selenomonas flueggei*, *Selenomonas infelix*, *Selenomonas noxia*, and *Selenomonas sputigena* with strains from 11 genera of oral bacteria. *Infect. Immun.* 57, 3194–3203.
- Kolenbrander, P. E., Andersen, R. N., Blehert, D. S., Egland, P. G., Foster, J. S., and Palmer, R. J. Jr. (2002). Communication among oral bacteria. *Microbiol. Mol. Biol. Rev.* 66, 486–505. doi: 10.1128/MMBR.66.3.486-505.2002
- Kolenbrander, P. E., Andersen, R. N., and Ganeshkumar, N. (1994). Nucleotide sequence of the *Streptococcus gordonii* PK488 coaggregation adhesin gene, scaA, and ATP-binding cassette. *Infect. Immun.* 62, 4469–4480.
- Kolenbrander, P. E., Palmer, R. J. Jr., Periasamy, S., and Jakubovics, N. S. (2010). Oral multispecies biofilm development and the key role of cell–cell distance. *Nat. Rev. Microbiol.* 8, 471–480. doi: 10.1038/nrmicro2381
- Kolenbrander, P. E. Jr., Palmer, R. J., Rickard, A. H., Jakubovics, N. S., Chalmers, N. I., and Diaz, P. I. (2006). Bacterial interactions and successions during plaque development. *Periodontol. 2000* 42, 47–79. doi: 10.1111/j.1600-0757.2006.00187.x
- Koo, H., Xiao, J., Klein, M. I., and Jeon, J. G. (2010). Exopolysaccharides (EPS) produced by *Streptococcus mutans* glucosyltransferases modulate the establishment of microcolonies within multispecies biofilms. *J. Bacteriol.* 192, 3024–3032. doi: 10.1128/JB.01649-09
- Kreth, J., Merritt, J., Shi, W., and Qi, F. (2005a). Competition and coexistence between *Streptococcus mutans* and *Streptococcus sanguinis* in the dental biofilm. *J. Bacteriol.* 187, 7193–203. doi: 10.1128/JB.187.21.7193-7203.2005
- Kreth, J., Merritt, J., Shi, W., and Qi, F. (2005b). Co-ordinated bacteriocin production and competence development: a possible mechanism for taking up DNA from neighbouring species. *Mol. Microbiol.* 57, 392–404. doi: 10.1111/j.1365-2958.2005.04695.x
- Kuboniwa, M., Hendrickson, E. L., Xia, Q., Wang, T., Xie, H., Hackett, M., et al. (2009). Proteomics of *Porphyromonas gingivalis* within a model oral microbial community. *BMC Microbiol.* 9:98. doi: 10.1186/1471-2180-9-98
- Kuboniwa, M., and Lamont, R. J. (2010). Subgingival biofilm formation. *Periodontol. 2000* 52, 38–52. doi: 10.1111/j.1600-0757.2009.00311.x
- Kuboniwa, M., Tribble, G. D., Lamer, C. E., Killic, A. O., Tao, L., Herzberg, M., et al. (2006). *Streptococcus gordonii* utilizes several distinct gene functions to recruit *Porphyromonas gingivalis* into a mixed community. *Mol. Microbiol.* 60, 121–139. doi: 10.1111/j.1365-2958.2006.05099.x
- Kumar, P. S., Griffen, A. L., Moeschberger, M. L., and Ley, E. J. (2005). Identification of candidate periodontal pathogens and beneficial species by quantitative 16S clonal analysis. *J. Clin. Microbiol.* 43, 3944–3955. doi: 10.1128/JCM.43.8.3944-3955.2005
- Kuramitsu, H. K., He, X., Lux, R., Anderson, M. H., and Shi, W. (2007). Interspecies interactions within oral microbial communities. *Microbiol. Mol. Biol. Rev.* 71, 653–670. doi: 10.1128/MMBR.00024-07
- Kuramitsu, H. K., and Trapa, V. (1984). Genetic exchange between oral streptococci during mixed growth. *J. Gen. Microbiol.* 130, 2497–2500.
- Lamont, R. J., El-Sabaeny, A., Park, Y., Cook, G. S., Costerton, J. W., and Demuth, D. R. (2002). Role of the *Streptococcus gordonii* SspB protein in the development of *Porphyromonas gingivalis* biofilms on streptococcal substrates. *Microbiology* 148, 1627–1636.
- Lancy, P. Jr., Dirienzo, J. M., Appelbaum, B., Rosan, B., and Holt, S. C. (1983). Corncob formation between *Fusobacterium nucleatum* and *Streptococcus sanguis*. *Infect. Immun.* 40, 303–309.
- LeBlanc, D. J., Hawley, R. J., Lee, L. N., and Martin, E. J. St. (1978). “Conjugal” transfer of plasmid DNA among oral streptococci. *Proc. Natl. Acad. Sci. U.S.A.* 75, 3484–3487. doi: 10.1073/pnas.75.7.3484
- Li, J., Helmerhorst, E. J., Leone, C. W., Troxler, R. F., Yaskell, T., Haffajee, A. D., et al. (2004). Identification of early microbial colonizers in human dental biofilm. *J. Appl. Microbiol.* 97, 1311–1318. doi: 10.1111/j.1365-2672.2004.02420.x
- Li, Y., and Burne, R. A. (2001a). Regulation of the gtfBC and ftf genes of *Streptococcus mutans* in biofilms in response to pH and carbohydrate. *Microbiology* 147, 2841–2848.
- Li, Y. H., Lau, P. C. Y., Lee, J. H., Ellen, R. P., and Cvitkovitch, D. G. (2001b). Natural genetic transformation of *Streptococcus mutans* growing in biofilms. *J. Bacteriol.* 183, 897–908. doi: 10.1128/JB.183.3.897-908.2001
- Liu, B., Faller, L. L., Klitgord, N., Mazumdar, V., Ghodsi, M., Sommer, D. D., et al. (2012). Deep sequencing of the oral microbiome reveals signatures of periodontal disease. *PLoS ONE* 7:e37919. doi: 10.1371/journal.pone.0037919
- Loesche, W. J. (1986). Role of *Streptococcus mutans* in human dental decay. *Microbiol. Infect.* 50, 353–380.
- Maeda, K., Nagata, H., Nonaka, A., Kataoka, K., Tanaka, M., and Shizukuishi, S. (2004). Oral streptococcal glyceraldehyde-3-phosphate dehydrogenase mediates interaction with *Porphyromonas gingivalis* fimbriae. *Microbes Infect.* 6, 1163–1170. doi: 10.1016/j.micinf.2004.06.005
- Maeda, K., Tribble, G. D., Tucker, C. M., Anaya, C., Shizukuishi, S., Lewis, J. P., et al. (2008). A *Porphyromonas gingivalis* tyrosine phosphatase is a multi-functional regulator of virulence attributes. *Mol. Microbiol.* 69, 1153–1164. doi: 10.1111/j.1365-2958.2008.06338.x
- Marsh, P. D. (1994). Microbial ecology of dental plaque and its significance in health and disease. *Adv. Dent. Res.* 8, 263–271.
- Matsumoto-Nakano, M., and Kuramitsu, H. K. (2006). Role of bacteriocin immunity proteins in the antimicrobial sensitivity of *Streptococcus mutans*. *J. Bacteriol.* 188, 8095–8102. doi: 10.1128/JB.00908-06
- McNab, R., Ford, S. K., El-Sabaeny, A., Barbieri, B., Cook, G. S., and Lamont, R. J. (2003). LuxS-based signaling in *Streptococcus gordonii*: autoinducer 2 controls carbohydrate metabolism and biofilm formation with *Porphyromonas gingivalis*. *J. Bacteriol.* 185, 274–284. doi: 10.1128/JB.185.1.274-284.2003
- Merritt, J., Qi, F., Goodman, S. D., Anderson, M. H., and Shi, W. (2003). Mutation of luxS affects biofilm formation in *Streptococcus mutans*. *Infect. Immun.* 71, 1972–1979. doi: 10.1128/IAI.71.4.1972-1979.2003
- Meuric, V., Martin, B., Guyodo, H., Rouillon, A., Tamanai-Shacoori, Z., Barloy-Hubler, F., et al. (2013). *Treponema denticola* improves adhesive capacities of *Porphyromonas gingivalis*. *Mol. Oral Microbiol.* 28, 40–53. doi: 10.1111/omi.12004
- Miller, M. B., and Bassler, B. L. (2001). Quorum sensing in bacteria. *Annu. Rev. Microbiol.* 55, 165–199. doi: 10.1146/annurev.micro.55.1.165
- Nadell, C. D., Xavier, J. B., and Foster, K. R. (2009). The sociobiology of bio-films. *FEMS Microbiol. Rev.* 33, 206–224. doi: 10.1111/j.1574-6976.2008.00150.x
- Nagata, H., Iwasaki, M., Maeda, K., Kuboniwa, M., Hashino, E., Toe, M., et al. (2009). Identification of the binding domain of *Streptococcus oralis* glyceraldehyde-3-phosphate dehydrogenase for *Porphyromonas gingivalis* major fimbriae. *Infect. Immun.* 77, 5130–5138. doi: 10.1128/IAI.00439-09
- Nilius, A. M., Spencer, S. C., and Simonson, L. G. (1993). Stimulation of in vitro growth of *Treponema denticola* by extracellular growth factors produced by *Porphyromonas gingivalis*. *J. Dent. Res.* 72, 1027–1031. doi: 10.1177/00220345930720060601
- Ogawa, A., Furukawa, S., Fujita, S., Mitobe, J., Kawarai, T., Narisawa, N., et al. (2011). Inhibition of *Streptococcus mutans* biofilm formation by *Streptococcus salivarius* FruA. *Appl. Environ. Microbiol.* 77, 1572–1580. doi: 10.1128/AEM.02066-10
- Palmer, R. J. Jr., Gordon, S. M., Cisar, J. O., and Kolenbrander, P. E. (2003). Co-aggregation-mediated interactions of streptococci and actinomycetes detected in initial human dental plaque. *J. Bacteriol.* 185, 3400–3409. doi: 10.1128/JB.185.11.3400-3409.2003
- Pangsomboon, K., Bansal, S., Martin, G. P., Suntinanalert, P., Kaewnopparat, S., and Srichana, T. (2009). Further characterization of a bacteriocin produced by *Lactobacillus paracasei* HL32. *J. Appl. Microbiol.* 106, 1928–1940. doi: 10.1111/j.1365-2672.2009.04146.x
- Pangsomboon, K., Kaewnopparat, S., Pitakpornpreecha, T., and Srichana, T. (2006). Antibacterial activity of a bacteriocin from *Lactobacillus paracasei* HL32 against *Porphyromonas gingivalis*. *Arch. Oral Biol.* 51, 784–793. doi: 10.1016/j.archoralbio.2006.03.008

- Park, Y., James, C. E., Yoshimura, F., and Lamont, R. J. (2006). Expression of the short fimbriae of *Porphyromonas gingivalis* is regulated in oral bacterial consortia. *FEMS Microbiol. Lett.* 262, 65–71. doi: 10.1111/j.1574-6968.2006.00357.x
- Park, Y., Simionato, M. R., Sekiya, K., Murakami, Y., James, D., Chen, W., et al. (2005). Short fimbriae of *Porphyromonas gingivalis* and their role in coadhesion with *Streptococcus gordonii*. *Infect. Immun.* 73, 3983–3989. doi: 10.1128/IAI.73.7.3983-3989.2005
- Paster, B. J., Olsen, I., Aas, J. A., and Dewhirst, F. E. (2006). The breadth of bacterial diversity in the human periodontal pocket and other oral sites. *Periodontol. 2000* 2, 80–87. doi: 10.1111/j.1600-0757.2006.00174.x
- Periasamy, S., and Kolenbrander, P. E. (2009a). *Aggregatibacter actinomycetemcomitans* builds mutualistic biofilm communities with *Fusobacterium nucleatum* and *Veillonella* species in saliva. *Infect. Immun.* 77, 3542–3551. doi: 10.1128/IAI.00345-09
- Periasamy, S., and Kolenbrander, P. E. (2009b). Mutualistic biofilm communities develop with *Porphyromonas gingivalis* and initial, early, and late colonizers of enamel. *J. Bacteriol.* 191, 6804–6811. doi: 10.1128/JB.01006-09
- Perry, J. A., Cvitkovitch, D. G., and Levesque, C. M. (2009). Cell death in *Streptococcus mutans* biofilms: a link between CSP and extracellular DNA. *FEMS Microbiol. Lett.* 299, 261–266. doi: 10.1111/j.1574-6968.2009.01758.x
- Petersen, F. C., Pecharki, D., and Scheie, A. A. (2004). Biofilm mode of growth of *Streptococcus intermedius* favored by a competence-stimulating signaling peptide. *J. Bacteriol.* 186, 6327–6331. doi: 10.1128/JB.186.18.6327-6331.2004
- Qi, F., Chen, P., and Caufield, P. W. (2001). The group I strain of *Streptococcus mutans*, UA140, produces both the lantibiotic mutacin I and a nonlantibiotic bacteriocin, mutacin IV. *Appl. Environ. Microbiol.* 67, 15–21. doi: 10.1128/AEM.67.1.15-21.2001
- Ramsey, M. M., Rumbaugh, K. P., and Whiteley, M. (2011). Metabolite cross-feeding enhances virulence in a model polymicrobial infection. *PLoS Pathog.* 7:e1002012. doi: 10.1371/journal.ppat.1002012
- Ramsey, M. M., and Whiteley, M. (2009). Polymicrobial interactions stimulate resistance to host innate immunity through metabolite perception. *Proc. Natl. Acad. Sci. U.S.A.* 106, 1578–1583. doi: 10.1073/pnas.0809533106
- Rice, L. B. (1998). Tn916 family conjugative transposons and dissemination of antimicrobial resistance determinants. *Antimicrob. Agents Chemother.* 42, 1871–1877.
- Rickard, A. H., Palmer, R. J., Blehert, D. S., Campagna, S. R., Semmelhack, M. F., Egland, P. G., et al. (2006). Autoinducer 2: a concentration-dependent signal for mutualistic bacterial biofilm growth. *Mol. Microbiol.* 60, 1446–1456. doi: 10.1111/j.1365-2958.2006.05202.x
- Riedel, K., Hentzer, M., Geisenberger, O., Huber, B., Steidle, A., Wu, H., et al. (2001). N-acylhomoserine-lactone-mediated communication between *Pseudomonas aeruginosa* and *Burkholderia cepacia* in mixed biofilms. *Microbiology* 147, 3249–3262.
- Roberts, A. P., and Mullany, P. (2010). Oral biofilms: a reservoir of transferable, bacterial, antimicrobial resistance. *Expert Rev. Anti Infect. Ther.* 8, 1441–1450. doi: 10.1586/eri.10.106
- Rölla, G., Scheie, A. A., and Ciardi, J. E. (1985). Role of sucrose in plaque formation. *Scand. J. Dent. Res.* 93, 105–111.
- Rosen, G., Genzler, T., and Sela, M. N. (2008). Coaggregation of *Treponema denticola* with *Porphyromonas gingivalis* and *Fusobacterium nucleatum* is mediated by the major outer sheath protein of *Treponema denticola*. *FEMS Microbiol. Lett.* 289, 59–66. doi: 10.1111/j.1574-6968.2008.01373.x
- Rosen, G., and Sela, M. N. (2006). Coaggregation of *Porphyromonas gingivalis* and *Fusobacterium nucleatum* PK 1594 is mediated by capsular polysaccharide and lipopolysaccharide. *FEMS Microbiol. Lett.* 256, 304–310. doi: 10.1111/j.1574-6968.2006.00131.x
- Rupani, D., Izano, E. A., Schreiner, H. C., Fine, D. H., and Kaplan, J. B. (2008). *Aggregatibacter actinomycetemcomitans* serotype fO-polysaccharide mediates coaggregation with *Fusobacterium nucleatum*. *Oral Microbiol. Immunol.* 23, 127–130. doi: 10.1111/j.1399-302X.2007.00399.x
- Ryan, R. P., and Dow, J. M. (2008). Diffusible signals and interspecies communication in bacteria. *Microbiology* 154, 1845–1858. doi: 10.1099/mic.0.2008/017871-0
- Saito, Y., Fujii, R., Nakagawa, K. I., Kuramitsu, H. K., Okuda, K., and Ishihara, K. (2008). Stimulation of *Fusobacterium nucleatum* biofilm formation by *Porphyromonas gingivalis*. *Oral Microbiol. Immunol.* 23, 1–6. doi: 10.1111/j.1399-302X.2007.00380.x
- Sandmeier, H., van Winkelhoff, A. J., Bär, K., Ankli, E., Maeder, M., and Meyer, J. (1995). Temperate bacteriophages are common among *Actinobacillus actinomycetemcomitans* isolates from periodontal pockets. *J. Periodontol. Res.* 30, 418–425. doi: 10.1111/j.1600-0765.1995.tb01296.x
- Sarkar, J., McHardy, I. H., Simanian, E. J., Shi, W., and Lux, R. (2014). Transcriptional responses of *Treponema denticola* to other oral bacterial species. *PLoS ONE* 9:e88361. doi: 10.1371/journal.pone.0088361
- Schauder, S., and Bassler, B. L. (2001a). The languages of bacteria. *Genes Dev.* 15, 1468–1480. doi: 10.1101/gad.899601
- Schauder, S., Shokat, K., Surette, M. G., and Bassler, B. B. (2001b). The LuxS family of bacterial autoinducers: biosynthesis of a novel quorum-sensing signal molecule. *Mol. Microbiol.* 41, 463–476. doi: 10.1046/j.1365-2958.2001.02532.x
- Schuster, M., Lostroh, C. P., Ogi, T., and Greenberg, E. P. (2003). Identification, timing, and signal specificity of *Pseudomonas aeruginosa* quorum-controlled genes: a transcriptome analysis. *J. Bacteriol.* 185, 2066–2079. doi: 10.1128/JB.185.7.2066-2079.2003
- Senadheera, D., and Cvitkovitch, D. G. (2008). Quorum sensing and biofilm formation by *Streptococcus mutans*. *Adv. Exp. Med. Biol.* 631, 178–188. doi: 10.1007/978-0-387-78885-2_12
- Senadheera, D., Krastel, K., Mair, R., Persadmeir, A., Abranach, J., Burne, R. A., et al. (2009). Inactivation of VicK affects acid production and acid survival of *Streptococcus mutans*. *J. Bacteriol.* 191, 6415–6424. doi: 10.1128/JB.00793-09
- Shao, H., Lamont, R. J., and Demuth, D. R. (2007). Autoinducer 2 is required for biofilm growth of *Aggregatibacter (Actinobacillus) actinomycetemcomitans*. *Infect. Immun.* 75, 4211–4218. doi: 10.1128/IAI.00402-07
- Sharma, A., Inagaki, S., Sigurdson, W., and Kuramitsu, H. K. (2005). Synergy between *Tannerella forsythia* and *Fusobacterium nucleatum* in biofilm formation. *Oral Microbiol. Immunol.* 20, 39–42. doi: 10.1111/j.1399-302X.2004.00175.x
- Shimotahira, N., Oogai, Y., Kawada-Matsuo, M., Yamada, S., Fukutsuji, K., Nagano, K., et al. (2013). The surface layer of *Tannerella forsythia* contributes to serum resistance and oral bacterial coaggregation. *Infect. Immun.* 81, 1198–1206. doi: 10.1128/IAI.00983-12
- Simionato, M. R., Tucker, C. M., Kuboniwa, M., Lamont, G., Demuth, D. R., Tribble, G. D., et al. (2006). *Porphyromonas gingivalis* genes involved in community development with *Streptococcus gordonii*. *Infect. Immun.* 74, 6419–6428. doi: 10.1128/IAI.00639-06
- Steeves, C. H., Potrykus, J., Barnett, D. A., and Bearne, S. L. (2011). Oxidative stress response in the opportunistic oral pathogen *Fusobacterium nucleatum*. *Proteomics* 11, 2027–2037. doi: 10.1002/pmic.201000631
- Takahashi, N. (2003). Acid-neutralizing activity during amino acid fermentation by *Porphyromonas gingivalis*, *Prevotella intermedia* and *Fusobacterium nucleatum*. *Oral Microbiol. Immunol.* 18, 109–113. doi: 10.1034/j.1399-302X.2003.00054.x
- Takasaki, K., Fujise, O., Miura, M., Hamachi, T., and Maeda, K. (2013). *Porphyromonas gingivalis* displays a competitive advantage over *Aggregatibacter actinomycetemcomitans* in co-cultured biofilm. *J. Periodontol. Res.* 48, 286–292. doi: 10.1111/jre.12006
- Takahashi, N., Washio, J., and Mayanagi, G. (2010). Metabolomics of supragingival plaque and oral bacteria. *J. Dent. Res.* 89, 1383–1388. doi: 10.1177/0022034510377792
- Tamesada, M., Kawabata, S., Fujiwara, T., and Hamada, S. (2004). Synergistic effects of streptococcal glucosyltransferases on adhesive biofilm formation. *J. Dent. Res.* 83, 874–879. doi: 10.1177/154405910408301110
- Tamura, S., Yonezawa, H., Motegi, M., Nakao, R., Yoneda, S., Watanabe, H., et al. (2009). Inhibiting effects of *Streptococcus salivarius* on competence-stimulating peptide-dependent biofilm formation by *Streptococcus mutans*. *Oral Microbiol. Immunol.* 24, 152–161. doi: 10.1111/j.1399-302X.2008.00489.x
- Tong, H., Chen, W., Merritt, J., Qi, F., Shi, W., and Dong, X. (2007). *Streptococcus oligofermentans* inhibits *Streptococcus mutans* through conversion of lactic acid into inhibitory H₂O₂: a possible counteroffensive strategy for interspecies competition. *Mol. Microbiol.* 63, 872–880. doi: 10.1111/j.1365-2958.2006.05546.x
- Tong, H., Chen, W., Shi, W., Qi, F., and Dong, X. (2008). SO-LAAO, a novel L-amino acid oxidase that enables *Streptococcus oligofermentans* to outcompete *Streptococcus mutans* by generating H₂O₂ from peptone. *J. Bacteriol.* 190, 4716–4721. doi: 10.1128/JB.00363-08

- Tong, H., Gao, X., and Dong, X. (2003). *Streptococcus oligofermentans* sp. nov., a novel oral isolate from caries-free humans. *Int. J. Syst. Evol. Microbiol.* 53, 1101–1104. doi: 10.1099/ijss.0.02493-0
- Torres-Escobar, A., Juárez-Rodríguez, M. D., Lamont, R. J., and Demuth, D. R. (2013). Transcriptional regulation of *Aggregatibacter actinomycetemcomitans* *lslACDBFG* and *lslRK* operons and their role in biofilm formation. *J. Bacteriol.* 195, 56–65. doi: 10.1128/JB.01476-12
- Vacca-Smith, A. M., and Bowen, W. H. (1998). Binding properties of streptococcal glucosyltransferases for hydroxyapatite, saliva-coated hydroxyapatite, and bacterial surfaces. *Arch. Oral Biol.* 43, 103–110. doi: 10.1016/S0003-9969(97)00111-8
- van der Hoeven, J. S., and Camp, P. J. (1991). Synergistic degradation of mucin by *Streptococcus oralis* and *Streptococcus sanguis* in mixed chemostat cultures. *J. Dent. Res.* 70, 1041–1044. doi: 10.1177/00220345910700070401
- Vollaard, E., and Clasener, H. (1994). Colonization resistance. *Antimicrob. Agents Chemother.* 38, 409–414. doi: 10.1128/AAC.38.3.409
- Wagner, V. E., Bushnell, D., Passador, L., Brooks, A. I., and Iglesias, B. H. (2003). Microarray analysis of *Pseudomonas aeruginosa* quorum-sensing regulators: effects of growth phase and environment. *J. Bacteriol.* 185, 2080–2095. doi: 10.1128/JB.185.7.2080-2095.2003
- Wang, B. Y., Alvarez, P., Hong, J., and Kuramitsu, H. K. (2011a). Periodontal pathogens interfere with quorum-sensing-dependent virulence properties in *Streptococcus mutans*. *J. Periodontol. Res.* 46, 105–110. doi: 10.1111/j.1600-0765.2010.01319.x
- Wang, B. Y., Deutch, A., Hong, J., and Kuramitsu, H. K. (2011b). Proteases of an early colonizer can hinder *Streptococcus mutans* colonization in vitro. *J. Dent. Res.* 90, 501–505. doi: 10.1177/0022034510388808
- Wang, B. Y., and Kuramitsu, H. K. (2005). Interactions between oral bacteria: inhibition of *Streptococcus mutans* bacteriocin production by *Streptococcus gordonii*. *Appl. Environ. Microbiol.* 71, 354–362. doi: 10.1128/AEM.71.1.354-362.2005
- Wang, Q., Wright, C. J., Dingming, H., Uriarte, S. M., Lamont, R. J. (2013). Oral community interactions of *Filifactor alocis* in vitro. *PLoS ONE* 8:e76271. doi: 10.1371/journal.pone.0076271
- Warburton, P. J., Palmer, R. M., Munson, M. A., and Wade, W. G. (2007). Demonstration of in vivo transfer of doxycycline resistance mediated by a novel transposon. *J. Antimicrob. Chemother.* 60, 973–980. doi: 10.1093/jac/dkm331
- Whitmore, S. E., and Lamont, R. J. (2011). The pathogenic persona of community-associated oral streptococci. *Mol. Microbiol.* 81, 305–314. doi: 10.1111/j.1365-2958.2011.07707.x
- Wickström, C., Herzberg, M. C., Beighton, D., and Svensäter, G. (2009). Proteolytic degradation of human salivary MUC5B by dental biofilms. *Microbiology* 155, 2866–2872. doi: 10.1099/mic.0.030536-0
- Xavier, K. B., Bassler, B. L., Xavier, K. B., Miller, S. T., Lu, W., Kim, J. H., et al. (2007). Phosphorylation and processing of the quorum-sensing molecule autoinducer-2 in enteric bacteria. *ACS Chem. Biol.* 2, 128–136. doi: 10.1021/cb600444h
- Xiao, J., Klein, M. I., Falsetta, M. L., Lu, B., Delahunty, C. M., and Yates, J. R. III, et al. (2012). The exopolysaccharide matrix modulates the interaction between 3D architecture and virulence of a mixed-species oral biofilm. *PLoS Pathog.* 8:e1002623. doi: 10.1371/journal.ppat.1002623
- Xie, H., Lin, X., Wang, B. Y., Wu, J., and Lamont, R. J. (2007). Identification of a signalling molecule involved in bacterial intergeneric communication. *Microbiology* 153, 3228–3234. doi: 10.1099/mic.0.2007/009050-0
- Yeung, M. K. (1999). Molecular and genetic analysis of *Actinomyces* species. *Oral Biol. Med.* 10, 120–138. doi: 10.1177/1045441199010020101
- Yim, G., Wang, H. H., and Davies, J. (2006). The truth about antibiotics. *Int. J. Med. Microbiol.* 296, 163–170. doi: 10.1016/j.ijmm.2006.01.039
- Yuan, L., Hillman, J. D., and Progulske-Fox, A. (2005). Microarray analysis of quorum sensing regulated genes in *Porphyromonas gingivalis*. *Infect. Immun.* 73, 4146–4154. doi: 10.1128/IAI.73.7.4146-4154.2005
- Zainal-Abidin, Z., Veith, P. D., Dashper, S. G., Zhu, Y., Catmull, D. V., Chen, Y. Y., et al. (2012). Differential proteomic analysis of a polymicrobial biofilm. *J. Proteome Res.* 11, 4449–4464. doi: 10.1021/pr300201c
- Zhang, Y., Lei, Y., Khammanivong, A., and Herzberg, M. C. (2004). Identification of a novel two-component system in *Streptococcus gordonii* V288 involved in biofilm formation. *Infect. Immun.* 72, 3489–3494. doi: 10.1128/IAI.72.6.3489-3494.2004
- Zheng, X., Zhang, K., Zhou, X., Liu, C., Li, M., Li, Y., et al. (2013). Involvement of gshAB in the interspecies competition within oral biofilm. *J. Dent. Res.* 92, 819–824. doi: 10.1177/0022034513498598
- Zhu, L., and Kreth, J. (2010). Role of *Streptococcus mutans* eukaryotic-type serine/threonine protein kinase in interspecies interactions with *Streptococcus sanguinis*. *Arch. Oral Biol.* 55, 385–390. doi: 10.1016/j.archoralbio.2010.03.012
- Zhu, L., and Kreth, J. (2012). The role of hydrogen peroxide in environmental adaptation of oral microbial communities. *Oxid. Med. Cell Longev.* 2012:717843. doi: 10.1155/2012/717843
- Zijnghe, V., van Leeuwen, M. B., Degener, J. E., Abbas, F., Thurnheer, T., Gmür, R., et al. (2010). Oral biofilm architecture on natural teeth. *PLoS ONE* 5:e9321. doi: 10.1371/journal.pone.0009321

Conflict of Interest Statement: Dr. Shi is a part time chief science officer of C3 Jian Inc., which has licensed technologies from UC regents.

Received: 29 March 2014; paper pending published: 16 May 2014; accepted: 14 June 2014; published online: 01 July 2014.

Citation: Guo L, He X and Shi W (2014) Intercellular communications in multispecies oral microbial communities. Front. Microbiol. 5:328. doi: 10.3389/fmicb.2014.00328

This article was submitted to Terrestrial Microbiology, a section of the journal Frontiers in Microbiology.

Copyright © 2014 Guo, He and Shi. This is an open-access article distributed under the terms of the Creative Commons Attribution License (CC BY). The use, distribution or reproduction in other forums is permitted, provided the original author(s) or licensor are credited and that the original publication in this journal is cited, in accordance with accepted academic practice. No use, distribution or reproduction is permitted which does not comply with these terms.



Volatile-mediated interactions between phylogenetically different soil bacteria

Paolina Garbeva^{1*}, Cornelis Hordijk¹, Saskia Gerards¹ and Wietse de Boer^{1,2}

¹ Department Microbial Ecology, Netherlands Institute of Ecology (NIOO-KNAW), Wageningen, Netherlands

² Department of Soil Quality, Wageningen University and Research Centre, Wageningen, Netherlands

Edited by:

Luis Raul Comolli, Lawrence Berkeley National Laboratory, USA

Reviewed by:

Osnat Gillor, Ben Gurion University, Israel

Gabriele Berg, Graz University of Technology, Austria

***Correspondence:**

Paolina Garbeva, Department Microbial Ecology, Netherlands Institute of Ecology (NIOO-KNAW), Droevedaalsesteeg 10, 6708 PB Wageningen, Netherlands
e-mail: p.garbeva@nioo.knaw.nl

There is increasing evidence that organic volatiles play an important role in interactions between micro-organisms in the porous soil matrix. Here we report that volatile compounds emitted by different soil bacteria can affect the growth, antibiotic production and gene expression of the soil bacterium *Pseudomonas fluorescens* Pf0-1. We applied a novel cultivation approach that mimics the natural nutritional heterogeneity in soil in which *P. fluorescens* grown on nutrient-limited agar was exposed to volatiles produced by 4 phylogenetically different bacterial isolates (*Collimonas pratensis*, *Serratia plymuthica*, *Paenibacillus* sp., and *Pedobacter* sp.) growing in sand containing artificial root exudates. Contrary to our expectation, the produced volatiles stimulated rather than inhibited the growth of *P. fluorescens*. A genome-wide, microarray-based analysis revealed that volatiles of all four bacterial strains affected gene expression of *P. fluorescens*, but with a different pattern of gene expression for each strain. Based on the annotation of the differently expressed genes, bacterial volatiles appear to induce a chemotactic motility response in *P. fluorescens*, but also an oxidative stress response. A more detailed study revealed that volatiles produced by *C. pratensis* triggered antimicrobial secondary metabolite production in *P. fluorescens*. Our results indicate that bacterial volatiles can have an important role in communication, trophic - and antagonistic interactions within the soil bacterial community.

Keywords: bacterial volatiles, inter-specific interactions, transcriptional responses, sand microcosm, infochemicals

INTRODUCTION

Most soil bacteria occur in multi-species communities, in which a variety of interactions influences their behavior and performance. Recent years have shown an explosion of research on “communication” between different soil bacterial species (Keller and Surette, 2006; Ryan and Dow, 2008; Shank and Kolter, 2009; Garbeva et al., 2011b). Most attention has been paid to the perception of other bacterial species via signaling compounds diffusing in liquid or semi-solid media. However, an important characteristic of most soils is the occurrence of air-filled pores. Hence, the gaseous phase forms an integral part of the natural surroundings of soil microorganisms. It has been estimated that the area of soil particles covered by microorganisms is less than 1% implying that the distance between microbial neighbors can be considerable (Young et al., 2008). Volatile molecules can act over a wider range of scale than non-volatiles as they can diffuse through both the liquid and gaseous phases of the soil (Effmert et al., 2012). Therefore, volatiles are thought to play an important role in communication and competition between physically separated soil microorganisms (Kai et al., 2009; Chernin et al., 2011; Garbeva et al., 2011a, 2014; Effmert et al., 2012).

It is well known that many soil microorganisms produce volatile organic compounds (VOC). In a recent review by Effmert et al. (2012) an overview is given of the wide variety of volatiles emitted by bacterial strains isolated from soils. From this review

as well as from other papers it is clear that the spectrum of volatile compounds differs between bacterial species, even between closely related ones (Groenhagen et al., 2013; Garbeva et al., 2014). In addition, environmental conditions, in particular nutrient availability, do influence the composition of bacterial volatiles (Blom et al., 2011; Garbeva et al., 2014).

With respect to the functioning of soil microbial volatiles, most attention has been given to suppressive effects of bacterial volatiles on soil eukaryotes that are harmful to agricultural crops, e.g., plant-pathogenic fungi and plant-parasitic nematodes (Gu et al., 2007; Kai et al., 2007; Zou et al., 2007; Verginer et al., 2010; Garbeva et al., 2014). However, the role of volatiles in interactions between soil bacterial species has been hardly studied. Given the physically separated distribution of bacterial populations (micro-colonies) in the porous soil matrix we hypothesize that volatiles play key roles in interspecific bacterial interactions. In the current study, our aim was to test volatile-mediated interactions between soil bacterial species under conditions that are realistic to soil conditions. To this end we applied a novel cultivation approach where we tried to mimic volatile-mediated interactions between bacteria in the rhizosphere and bacteria outside the rhizosphere. As model bacteria we selected five phylogenetically different soil isolates that do occur in natural rhizosphere communities. The main research questions we addressed were (1) Do rhizobacteria protect their “territory” against potential rhizosphere invaders

by producing volatiles that suppress bacteria outside the rhizosphere or (2) Can bacteria outside the rhizosphere profit from the volatiles produced by rhizosphere-inhabiting bacteria? Our expectation was that rhizosphere-inhabiting bacteria will invest part of the energy obtained from metabolizing root-exudates in the production of suppressing volatiles.

MATERIALS AND METHODS

BACTERIAL ISOLATES AND GROWTH MEDIA USED IN THIS WORK

Collimonas pratensis Ter91 (β -Proteobacteria), *Paenibacillus* sp. P4 (Bacilli) and *Pedobacter* sp. V48 (Sphingobacteria) have been isolated isolates from the rhizosphere of Marram grass in sandy dune soils in The Netherlands (De Boer et al., 1998, 2004); *Serratia plymuthica* PRI-2C strain (Y-Proteobacteria) was isolated from maize rhizosphere, The Netherlands (Garbeva et al., 2004). *Pseudomonas fluorescens* Pf0-1 was isolated from an agricultural soil in Massachusetts, USA (Compeau et al., 1988). All strains were pre-cultured from frozen glycerol stocks on 1/10 strength Tryptone Soya Broth agar (CMO129, Oxoid).

BIOASSAY FOR TESTING THE EFFECT OF BACTERIAL VOLATILES ON *PSEUDOMONAS FLUORESCENS* PF0-1

The bioassay was performed as described in the Figure S1. The top area of the glass Petri dish contained 12 ml water-agar medium (20 g L⁻¹ of Agar, 5 g L⁻¹ of NaCl, 1 g L⁻¹ of KH₂PO₄ and 0.1 g L⁻¹ (NH₄)₂SO₄; pH 6.5.). This carbon-limited medium was used to represent the situation in the bulk soil where bacterial growth is limited by availability of easily degradable carbon compounds. The water-agar medium was inoculated with *Pseudomonas fluorescens* Pf0-1 of which 5.0 × 10⁶ cells were spread over the water-agar surface. The bottom area of the glass Petri dish contained 45 g of sterile washed sea sand (Honeywell Specialty Chemicals Seelze GmbH, Germany) supplemented with 4.5 ml artificial root exudates and bacterial inoculum (3.0 × 10⁶/gr sand) from monocultures of *Collimonas pratensis* Ter 91; *Paenibacillus* sp. P4; *Pedobacter* sp. V48; *Serratia plymuthica* PRI-2C or a mixture of these soil bacteria. As control treatment *P. fluorescens* Pf0-1 was exposed only to sand with artificial root exudates without bacterial inoculum. The artificial root exudates (ARE) stock solution contained 18.4 mM glucose; 18.4 mM fructose; 9.2 mM saccharose; 4.6 mM citric acid; 9.2 mM lactic acid; 6.9 mM succinic acid; 18.4 mM L-serine; 11 mM L-glutamic acid and 18.4 mM L-alanine (C/N 10.4). To each plate 4.5 ml of ARE working solution consisting of 1.5 ml of stock solution mixed with 3 ml of 10 mM phosphate buffer (pH 6.5) was added as described in Baudoin et al. (2003). The plates were incubated at 20°C while packed in aluminium foil. After 3 days of incubation bacterial numbers in the top and bottom compartments were determined. *P. fluorescens* Pf0-1 cells that had developed on the top water-agar area were scraped and suspended in 3 ml 10 mM phosphate buffer (pH 6.5). One hundred and fifty micro liter of this bacterial suspension was used for OD measurements and plating of serial dilutions on 1/10 TSBA medium (the remaining 2.85 ml were used for RNA extraction, see below). For enumeration of bacteria growing in the bottom area 1 g of sand was taken from each plate and transferred into a 20 ml Greiner tube. Ten milli liter of 10 mM phosphate buffer (pH 6.5) were added and the tubes

were shaken on a rotary shaker at 350 rpm for 30 min at 20°C. Subsequently, serial dilutions were plated in triplicate on 1/10 TSBA. All plates were incubated at 20°C and bacterial colonies were counted after 48 h.

TRANSCRIPTIONAL ANALYSIS

For total RNA extraction all suspensions retrieved from agar (see above) were diluted in sterile phosphate buffer to the same optical density (OD; 600 nm) to obtain equal amounts of cells for RNA extraction. The cell suspensions were centrifuged at 16,000 × g for 3 min. RNA was extracted from the cell pellets with the Artrum Total RNA Mini Kit (BIO-RAD cat# 732-6820) according to the manufacturer's recommendations. The extracted total RNA was treated with the TURBO DNA-free Kit to remove DNA (Ambion cat#1907).

Transcriptomic analyses were performed using high-density, multiplex (12x72K) microarrays designed and produced by Roche NimbleGen (Cat# A7241-00-01). Arrays consisted of 60-mer probes covering 5735 genes, 6 probes per gene, 2 replicates. cDNA synthesis, labeling of cDNA with Cy3 dye and hybridization were performed by the Micro Array Department (MAD), University of Amsterdam, The Netherlands (www.microarray.nl).

Each treatment and control were performed in triplicates. The lists of differential expressed genes were extracted by comparison of each interaction with the control. The Robust Microarray Analysis (RMA)-normalized gene expression data were analyzed with the Array Star 2 software for microarray analysis (DNASTAR, Madison, Wisconsin, USA). Analysis was performed, with application of false discovery rate (FDR; Benjamini Hochberg) and multiple testing corrections.

Quantitative RT-PCR was performed to verify the gene expression detected by microarray analysis. First strand cDNA was synthesized with random hexamer primers from Invitrogen (cat# 48190-011) using SuperScript™ Double-Stranded cDNA Synthesis kits (Invitrogen cat#11917-010). Two μ L of cDNA was subjected to real-time PCR using SYBR Green PCR master mix (Applied Biosystem). For each target gene [five differentially expressed genes: catalase; sulfotransferase, methyl-accepting chemotaxis sensory transducer, cytochrome C oxidase, chemotaxis sensory transducer and two non-differentially expressed control housekeeping genes: 16S rRNA and RNA polymerase (rpoB)], forward and reverse primers were designed using Primer Express software (PE Applied Biosystem, Warrington, UK). All primers used for real-time PCR were first tested using conventional PCR with DNA isolated from *P. fluorescens* Pf0-1. Real-time PCR was performed using a Corbett Research Rotor-Gene 3000 thermal cycler (Westburg, Leusden, The Netherlands) with the following conditions: initial cycle 95°C for 15 min and 40 cycles of: 95°C for 15 s; 56°C for 50 s and 72°C for 50 s. The relative expression of the genes was normalized to that of the house keeping genes.

BACTERIAL VOLATILES TRAPPING AND GC/MS ANALYSIS

For the collection of bacterial volatiles that were produced in sand containing artificial root exudates, glass Petri dishes with leads, to which a steel trap containing 150 mg Tenax TA and 150 mg Carbopack B (Markes International Ltd., Llantrisant, UK) could

be fixed, were used (Figure S1b). Volatiles were collected during 72 h of incubation at 20°C, traps were removed, capped and stored at 4°C until analysis.

Volatile compounds were desorbed from the traps using an automated thermodesorption unit (model Unity, Markes International Ltd., Llantrisant, UK) at 200°C for 12 min (He flow 30 ml/min). The trapped volatiles were introduced into the GC-MS (model Trace, ThermoFinnigan, Austin, TX, USA) by heating the cold trap for 3 min to 270°C. Split ratio was set to 1:4, and the column used was a 30 × 0.32 mm ID RTX-5 Silms, film thickness 0.33 μm (Restek, Bellefonte, PA, USA). Temperature program used was as follows: from 40 to 95°C at 3°C/min, then to 165°C at 2°C/min, and finally to 250°C at 15°C/min. The VOCs were detected by the MS operating at 70 eV in EI mode. Mass spectra were acquired in full scan mode (33–300 AMU, 0.4 scan/s). Compounds were identified by their mass spectra using deconvolution software (AMDIS) in combination with NIST 2008 (National Institute of Standards and Technology, USA, <http://www.nist.gov>) and Wiley 7th edition spectral libraries and by their linear retention indexes (lri).

The lri values were compared with those found in the NIST and the NIOO lri database. Mass spectra and lri values for identification were also checked by analysis of pure compounds.

TEST OF PURE INDIVIDUAL VOLATILES

Several volatiles produced by *Collimonas pratensis* Ter91 and *Serratia plymuthica* PRI-2C were commercially available. A number of these compounds, namely methanethiosulfonate ($\text{CH}_3\text{SO}_2\text{SCH}_3$); S-methyl thioacetate ($\text{C}_3\text{H}_6\text{OS}$); dimethyldisulfide ($\text{CH}_3\text{S}_2\text{CH}_3$) and benzonitrile ($\text{C}_6\text{H}_5\text{CN}$), were tested for their individual effect on *P. fluorescens* Pf0-1 growth. Each volatile was applied in concentrations ranging from 3, 12, 30 to 60 μmol as a droplet on a filter paper on the bottom of the Petri dish. The effect of these pure compounds on *P. fluorescens* Pf0-1 growth was determined by CFU enumeration as described above.

EXTRACTION OF SECONDARY METABOLITES FROM *P. FLUORESCENS* Pf0-1

For extraction of secondary metabolites the water-agar inoculated with *P. fluorescens* Pf0-1 was removed carefully from the plate and cut in small (1-cm-diameter) pieces. These pieces were vigorously shaken in 20 mL of 80% (v/v) acetone for 1 h at room temperature. The acetone solution was centrifuged for 10 min at 4000 × g and the acetone was evaporated under air flow. The water fraction was acidified with trifluoroacetic acid [0.1% (v/v)], mixed with 2 volumes of ethylacetate and shaken vigorously for 5 min. After incubation overnight at –20°C the unfrozen (ethylacetate) fraction that contains the active compounds was carefully transferred to a new flask and dried under air flow. The dried extract was dissolved in 150 μL of 50% (v/v) methanol and subjected to reverse phase high pressure liquid chromatography (RP-HPLC) analysis and test for antimicrobial activity.

The antimicrobial compounds dissolved in 50% methanol were tested for activity against the fungi *Rhizoctonia solani* AG2.2IIIB and *Fusarium oxysporum*, and the bacteria *Bacillus* sp. V102 and *Collimonas pratensis* Ter91 (as described in Garbeva et al., 2011a,b).

STATISTICAL ANALYSIS

All experiments were performed in triplicate with three independent replicates for each treatment and controls. ArrayStar 2 (DNASTAR, Madison, WI) was used for statistical analysis of differentially expressed genes applying Student's *t*-test with Benjamini-Hochberg false discovery rate correction. The statistical analyses of fungal biomass, bacterial enumeration, antagonistic tests and qRT-PCR were carried out with XLStat 2010 (Addinsoft, New York, USA) using a Student's *t*-Test. Data were considered to be statistically different at $p \leq 0.05$.

RESULTS

EFFECT OF BACTERIAL VOLATILES ON *P. FLUORESCENS* Pf0-1 GROWTH

After 3 days of incubation, the four bacterial strains that were grown in sand containing artificial root exudates had reached similar cell densities (number of CFUs) (Figure 1). All four strains and also the mixture of strains produced volatiles in the sand microcosms (see next section), but the effect of these volatiles on the growth of *P. fluorescens* was different (Figure 2A). Volatiles produced by *C. pratensis* and *S. plymuthica* stimulated the growth of *P. fluorescens*, whereas volatiles emitted by *Paenibacillus* sp., *Pedobacter* sp. and the mix of all 4 bacteria did not affect *P. fluorescens* growth.

VOLATILES PRODUCED BY BACTERIA GROWING IN SAND MICROCOSSMS

GC-MS analysis revealed that besides commonly known bacterial VOCs such as dimethylsulfide, 2-pentanone, 4-heptanone, 2-heptanol, and 2-undecanone, each bacterial species produced a different blend of volatiles in sand supplied with artificial root exudates (Table 1). The highest numbers of unique volatile compounds were emitted by *C. pratensis* and *S. plymuthica*. Several of these volatiles (like S-methyl thioacetate, methyl thiocyanate, dimethyl disulfide, benzonitrile) were produced by both bacteria. *Paenibacillus* sp. and *Pedobacter* sp. produced less different volatile compounds and this was also the case for the mixture of

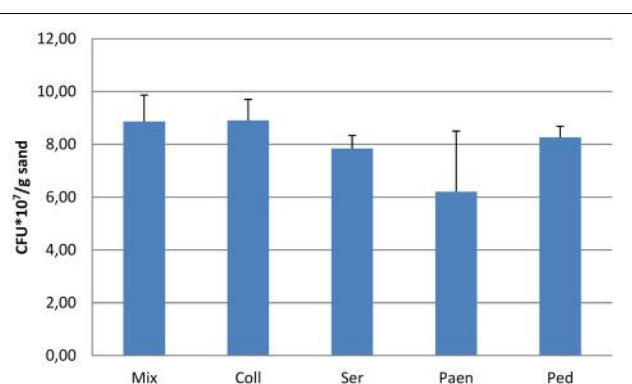


FIGURE 1 | Number of bacteria (CFUs) after 3 days of incubation in sand containing artificial root exudates. Coll- *Collimonas pratensis* Ter 91; Ser- *Serratia plymuthica* PRI-2C; Paen- *Paenibacillus* sp. P4; Ped- *Pedobacter* sp. V48 and Mix mix of all four bacteria. Inoculation densities were 3.0×10^6 /gr sand. Presented values are means of three replicates and error bars indicate standard deviation. No significant differences were found between the different bacterial inoculums.

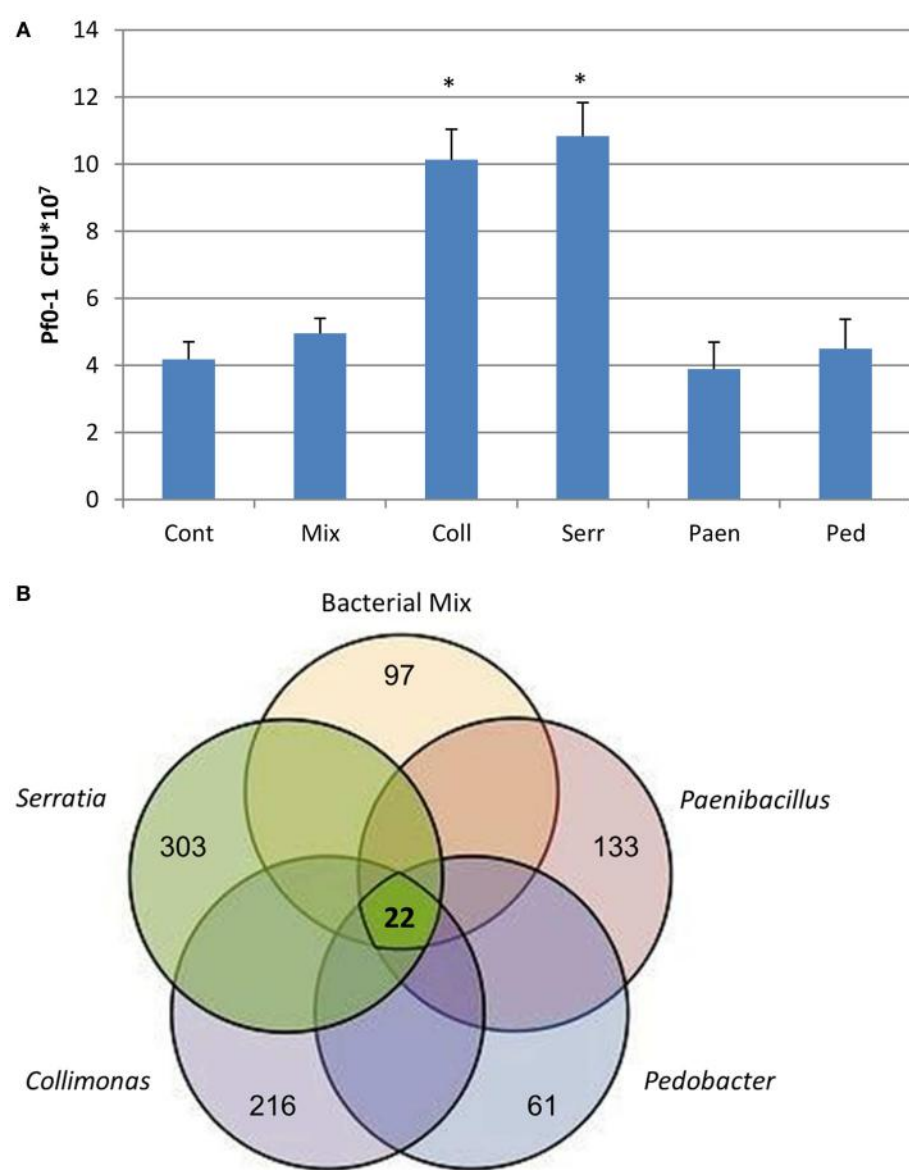


FIGURE 2 | (A) Number of *P. fluorescens* Pf0-1 colony forming units (CFUs) developed after 3 days of incubation on water-agar while exposed to volatiles emitted by different bacteria growing in sand containing artificial root exudates: Coll- *Collimonas pratensis* Ter 91; Serr- *Serratia plymuthica* PRI-2C; Paen- *Paenibacillus* sp. P4; Ped- *Pedobacter* sp. V48 and Mix- mix of all 4 bacteria. Cont- control is sand with artificial root exudates but without bacteria. Inoculation density of *P. fluorescens* Pf0-1 is 5.0×10^6 cells. Presented data are means of three replicates, error bars indicate standard deviation and *indicates significant differences in CFUs between control and treatments ($P < 0.05$). **(B)** Venn diagram representing the number of differentially expressed genes in *P. fluorescens*

fluorescens Pf0-1 in response to volatiles emitted by different bacteria grown in sand containing artificial root exudates. The bold number in the middle of the diagram represents the common differentially expressed genes in all treatments as listed in **Table 1**. Other numbers indicate treatment-specific differences in gene expression: *Paenibacillus* sp. P4 total 133 genes (63 up-regulated and 70 down regulated); *Pedobacter* sp. V48 total 61 genes (50 up-regulated and 11 down regulated); *Collimonas pratensis* Ter91 total 216 genes (73 up-regulated and 143 down regulated); *Serratia plymuthica* PRI-2C total 303 genes (93 up-regulated and 210 down regulated) and bacterial mix of all 4 strains total 97 genes (31 up-regulated and 66 down regulated).

four bacterial species. Interestingly, the volatiles produced by the bacterial mix included compounds that were not detected in the spectrum of volatiles produced by the different bacterial monocultures (like 1-tetradecanol, isopropyl dodecanoate, branched alkanes, and unknowns).

TRANSCRIPTIONAL RESPONSE OF *P. FLUORESCENS* Pf0-1 TO BACTERIAL VOLATILES

Microarray-based analyses did reveal strong differences in expression of *P. fluorescens* gene when exposed to volatiles emitted by the different bacterial species (**Figure 2B**). Only a small set of 22 genes

Table 1 | Volatile organic compounds produced by 4 bacterial strains growing in sterile sand containing artificial root exudates.

Compound name	RI
PRODUCED IN ALL TREATMENTS	
Dimethyl sulfide	<600
2-pentanone	688
3-pentanone	702
2,4 pentadione	779
4-heptanone	868
2-heptanol	900
beta pinene	969
nonanal	1102
2-decanone	1193
decanal	1203
2-undecanol	1301
6-dodecanone	1371
Octylcyclohexane	1443
PRODUCED BY SERRATIA PLYMUTHICA PRI-2C	
S-methyl thioacetate	703
Methyl thiocyanate	713
Dimethyl disulfide	740
1H-pyrrole	751
Methyl 3-methylbutanoate	775
Ethyl butanoate	802
Chlorobenzene	838
2,4 dithiapentane	882
3-heptanol	895
Dimethyl sulfone	922
Benzonitrile	978
2-octanone	989
5-dodecanone	1372
2-pentadecanone	1697
PRODUCED BY COLIMONAS PRATENSIS TER91	
2- methyl propanal	<600
Ethenyl acetate	<600
S-methyl thioacetate	703
Methyl thiocyanate	713
Dimethyl disulfide	740
3-methyl 2-pentanoene	749
Methyl 2-methylbutanoate	774
Methyl 3-methylbutanoate	775
3-hexanone	789
4-methyl 3-penten-2-one	808
2-acetyl 1-pyrroline	922
Methyl hexanoate	923
3-methyl 2-heptanone	940
Benzonitrile	978
7-methyl-3-methylene-1,6-octadiene (myrcene)	987
Ethyl hexanoate	1001
Methyl 2-ethylhexanoate	1044
1-methyl 4-(1-methylethyl) 1,4-cyclohexadiene (terpinene)	1056
Methyl 2-methylbenzoate	1179
Methyl salicylate	1190
Methyl 3-methylbenzoate	1199
Methyl 4-methylbenzoate	1207
Methyl 2,6-dimethylbenzoate	1239

(Continued)

Table 1 | Continued

Compound name	RI
PRODUCED BY PAENIBACILLUS SP. P4	
3-methyl-2-hexanone	840
Pentalactone	947
Hexanoic-acid	981
Carene isomer	1007
Tridecane	1300
PRODUCED BY PEDOBACTER SP. V48	
1,3-butadiene, 2-methyl-	<600
Cyclohexanone	891
Oxime methoxy phenyl	907
Benzaldehyde	958
Camphepane	940
Hexanoic-acid	981
Unknown	1145
Diphenylsulfide	1574
PRODUCED ONLY IN BACTERIAL MIX	
Sulfur dioxide	<600
Branched alcane	1021
Isopropyl dodecanoate	1628
Salicylic acid hexyl ester	1672
Unknown	1674
1-tetradecanol	1675

RI- Linear retention index Rtx-5 ms column.

The table excludes volatiles that were also present in the controls (non-inoculated sand with artificial root exudates).

was differentially expressed by volatiles of all bacteria, including the mixture. These genes were mainly involved in amino acid transport and—metabolism, energy production and conversion, signal transduction mechanisms, inorganic ion transport and—metabolism, secretion and cell motility (**Table 2**). In addition, all exposures to bacterial volatiles resulted in increased expression of a gene encoding catalase, an enzyme involved in the protection of cells against damage by reactive oxygen species. The RT-PCR analysis of 5 selected differentially expressed genes confirmed the microarray data (Figure S2). The highest number of differentially expressed genes in *P. fluorescens* was obtained when exposed to volatiles produced by *C. pratensis*, *Paenibacillus* sp. and *S. plymuthica* (Tables S1–S3) whereas volatiles emitted by *Pedobacter* sp. and the bacterial mix affected the expression of much less genes (Tables S4, S5). There was high similarity in the effect of volatiles of *C. pratensis* and *S. plymuthica* on gene expression (116 common differentially expressed genes) of *P. fluorescens* which corresponds to the high similarity in the composition of volatiles produced by these two bacteria (Tables S1, S3).

EFFECT OF INDIVIDUAL VOLATILES ON *P. FLUORESCENS* Pf0-1 GROWTH

Four volatiles produced by *C. pratensis* and *S. plymuthica* namely methanthiosulfonate; S-methyl thioacetate; dimethyldisulfide and benzonitrile, were tested individually for their effect on *P. fluorescens*. Benzonitrile and dimethyldisulfide stimulated the growth of *P. fluorescens* growth when applied in

Table 2 | Common genes differentially expressed in *P. fluorescens* Pf0–1 exposed to volatiles produced by four bacterial species and a mixture of these species in sand containing artificial root exudates.

SEQ_ID	Gene description	Fold change	Fold change	Fold change	Fold change	Fold change	Possible function
		(1)	(2)	(3)	(4)	(5)	
UP-REGULATED GENES WITH > 2-FOLD CHANGE							
Pfl_0064	Catalase	6.3	6.7	7.1	3.6	6.4	Inorganic ion transport and metabolism
Pfl_0157	Sulfotransferase	2.6	3.2	4.3	2.3	3.1	Amino acid transport and metabolism
Pfl_0378	Methyl-accepting chemotaxis sensory transducer	3.3	3.2	3.9	2.6	2.4	Signal transduction mechanisms
Pfl_0623	Putative diguanylate cyclase (GGDEF domain)	5.4	7.3	4.1	2.7	3.1	Signal transduction mechanisms
Pfl_1076	Hypothetical protein	2.9	2.6	3.6	2.1	4.6	Function unknown
Pfl_1813	Coproporphyrinogen III oxidase	2.4	6.8	3.1	2.6	3.1	Coenzyme metabolism
Pfl_1824	Cytochrome c oxidase cbb3-type, subunit III	2.8	4.6	2.7	3.1	2.3	Energy production and conversion
Pfl_1826	Cytochrome C oxidase, mono-heme subunit/FixO	2.9	4.8	2.5	4.2	3.3	Energy production and conversion
Pfl_1827	Cytochrome c oxidase cbb3-type, subunit I	2.3	5.8	2.6	3.6	3.2	Energy production and conversion
Pfl_2904	D-isomer specific 2-hydroxyacid dehydrogenase, NAD-binding	2.1	2.7	2.7	2.4	2.4	Amino acid transport and metabolism
Pfl_2907	Chemotaxis sensory transducer	6.3	6.6	7.1	6.5	6.1	Cell motility and secretion
Pfl_4382	Chemotaxis sensory transducer	2.1	6.2	2.6	2.5	3.7	Cell motility and secretion
Pfl_4989	Aldehyde dehydrogenase (NAD ⁺)	3.1	2.8	4.3	2.9	4.2	Energy production and conversion
Pfl_5345	Aldehyde dehydrogenase	2.7	2.1	2.6	2.4	6.5	Energy production and conversion
DOWN-REGULATED GENES WITH > 2-FOLD CHANGE							
Pfl_0044	Protein of unknown function DUF1328	2.1	4.1	3.2	2.2	4.2	Function unknown
Pfl_0045	Hypothetical protein	2.8	6.9	2.4	2.4	2.9	Function unknown
Pfl_1337	Amidase	2.1	5.8	5.7	1.9	4.3	Energy production and conversion
Pfl_1779	Assimilatory nitrat reductase (NADH) alpha apoprotein	4.7	3.3	2.8	2.7	5.3	Inorganic ion transport and metabolism
Pfl_1780	Assimilatory nitrite reductase NAD(P)H small subunit	5.7	2.3	3.4	3.1	5.8	Inorganic ion transport and metabolism
Pfl_1781	Nitrite and sulphite reductase 4Fe-4S region	7.1	2.5	3.6	3.2	3.3	Energy production and conversion
Pfl_4818	Transport-associated	2.8	3.6	2.7	2.3	4.5	General function prediction only
Pfl_4819	General secretion pathway protein H	1.9	2.8	3.1	2.9	3.3	Cell motility and secretion

Fold change of differentially expressed genes in *P. fluorescens* Pf0–1 exposed to volatiles produced by (1) *Collimonas pratensis* (2) *Serratia plymuthica* (3) *Paenibacillus* sp. (4) *Pedobacter* sp., and (5) Mixture of four bacterial species. The differentially expressed genes were identified using the false discovery rate (Benjamini-Hochberg) correction method with 99% confidence ($P < 0.05$).

concentrations above 3 μmol (Figure S3). Methanethiosulfonate and S-methyl thioacetate did not reveal any effect on the Pf0–1 growth.

EFFECT OF BACTERIAL VOLATILES ON *P. FLUORESCENS* Pf0–1 SECONDARY METABOLITES PRODUCTION

To test if bacterial volatiles triggered *P. fluorescens* Pf0–1 secondary metabolites production, ethylacetate extracts were made from water-agar on which *P. fluorescens* had been grown while exposed to volatiles emitted by *C. pratensis*. Comparison of the HPLC profiles and activities of these extracts with those extracts obtained from controls revealed that *P. fluorescens* Pf0–1 produced many more secondary metabolites (11 vs. 7) with higher intensity when exposed to volatiles produced by *C. pratensis* (Figure S4). Furthermore, these extracts showed antimicrobial activity against a Gram-positive bacterium (*Bacillus* sp.) and the plant pathogenic fungus (*Fusarium oxysporum*) but did not affect growth of *C. pratensis*.

DISCUSSION

The role of bacterial volatiles in microbial interactions is increasingly recognized in the last years. However, most work on bacterial volatiles to date is done *in vitro* under nutrient-rich conditions (Beck et al., 2003; Chun et al., 2010; Kai et al., 2010; Weise et al., 2012; Kim et al., 2013) and may not be representative for the conditions that occur in the soil environment. In the present study, we developed an experimental set-up that is approaching a situation which is likely to occur in soils namely the volatile-mediated interactions between bacteria growing in the rhizosphere with bacteria present outside the rhizosphere. Since the latter are experiencing starvation conditions we hypothesized that volatiles produced by rhizosphere bacteria could act as a chemoattractant to the nutrient-richer conditions nearby. On the other hand production of volatiles by rhizosphere-inhabiting bacteria could also be used to suppress other bacteria which would prevent invasion of the rhizosphere by potentially new competitors.

It is known that bacterial volatiles can have antimicrobial activity and inhibit the growth of other microorganisms (Kai et al., 2007, 2009; Garbeva et al., 2014). However, none of the four rhizobacteria appeared to produce volatiles that were inhibiting the starved model bacterium *P. fluorescens*. It is plausible that similar to what has been reported for effects of antibiotics, bacteria are becoming highly tolerant to volatiles when they are under nutrient limitation (Nguyen et al., 2011). Volatiles emitted by *C. pratensis* and *S. plymuthica* did even stimulate *Pseudomonas* growth and were probably used as energy source. Some volatiles produced by these two bacteria were applied as pure substances and did also result in increased *P. fluorescens* growth. Growth of microbes in the area surrounding the rhizosphere is limited by carbon availability and, therefore, carbon-containing volatiles produced by rhizosphere microbes may be important energy resources for such microbes (Owen et al., 2007). Kleinheinz et al. (1999) revealed that *P. fluorescens* were able to degrade alpha-pinene released by plants and to use it as a sole energy source.

Although bacterial volatiles did not inhibit the growth of *P. fluorescens* they caused expression of genes that indicate a stress response, e.g., Pfl_0064 Catalase. It is known that catalase can be induced under conditions of oxidative stress which may have been caused by some of the volatiles (Lushchak, 2001; Kwon et al., 2010).

The genome-wide microarray-based analyses revealed that *P. fluorescens* had a different response in gene expression to volatiles emitted by the different bacterial species. Only a small set of 22 genes was differentially expressed in all treatments. Among these common differentially expressed genes were Pfl_0064 Catalase, an important enzyme in protecting the cell against damage by reactive oxygen species; Pfl_0157 Sulfotransferase, belonging to a group of enzymes that catalyze the transfer of a sulfo group from a donor molecule to an acceptor alcohol or amine; Pfl_2907 and Pfl_4382 Chemotaxis sensory transducer genes, genes that are important for regulation of bacterial chemotaxis, and Pfl_0623 Diguanylate cyclase (GGDEF domain), a gene that has been indicated to be responsible for the wrinkly spreader phenotype in *P. fluorescens* (Malone et al., 2007; Silby et al., 2009). The difference in transcriptional response of *P. fluorescens* to different bacterial strains appeared to reflect the composition of volatiles. *C. pratensis* and *S. plymuthica*, producing similar sets of volatiles, caused similar changes in gene expression. Many differentially expressed genes were genes involved in *P. fluorescens* metabolic activity, signal transduction mechanisms, cell motility and secretion.

Soil bacteria including *Pseudomonas* possess many two-component signal transduction systems that help them to adapt to fluctuations in environmental conditions (Gao et al., 2007; Rodriguez et al., 2013; Willett et al., 2013). The set of differentially expressed genes involved in two-component signal transduction was not the same for the 4 volatile-producing bacterial species (Tables S1–S5) indicating that volatiles may act as an infochemicals providing information on the identity of surrounding microorganisms. Furthermore, *C. pratensis* and *S. plymuthica* triggered expression of several genes related to chemotaxis and motility indicating that part of their volatiles may act as

chemoattractants guiding *P. fluorescens* to a close-by environment with nutrient input.

Recent studies revealed that inter-specific interactions between phylogenetically unrelated soil bacteria often leads to production of antimicrobial compounds (Garbeva et al., 2011a,b; Onaka et al., 2011; Hopwood, 2013). Most antimicrobial compounds are produced in growth density-dependent manner and nutrient availability has a major impact on the expression of biosynthetic genes (Sanchez et al., 2010; Van Wezel and McDowell, 2011). Our results revealed that volatiles can have an effect on secondary metabolites production by *P. fluorescens*. When exposed to volatiles emitted by *C. pratensis*, *P. fluorescens* produced secondary metabolites that had inhibiting activity against a Gram positive bacterium and a fungus but not against the Gram negative volatile producer. It is plausible that the volatiles served as energy sources and/or signal inducing secondary metabolite production. The volatile-triggered antibiotic production in *P. fluorescens* could point a strategy to combine movement (chemotaxis- and motility genes) with increasing competitive strength (antibiotics) to invade into the nutrient-providing rhizosphere zone.

The volatile blend produced by soil bacteria growing in the sand microcosm containing artificial root exudates differed between different bacterial species. Several studies indicated that the numbers and spectrum of volatiles produced by bacteria depends on growth conditions and nutrient availability (Blom et al., 2011; Weise et al., 2012; Garbeva et al., 2014). Interestingly, the composition of volatiles produced by the mixture of 4 bacterial species was different from that produced by each of the bacterial monocultures which may be due to competitive interactions between the bacterial species. The blend of volatiles produced by bacterial mix had a smaller effect on the expression of genes in *P. fluorescens* than the volatiles produced by monocultures. The effect of volatiles produced by the bacterial mixture is probably more representative for the situation occurring in natural environment.

In conclusion, this work is the first to report that volatiles compounds emitted by different rhizobacteria can affect the growth and gene expression of other phylogenetically distinct and physically separated bacteria. The model bacteria *P. fluorescens* growing under nutrient limited conditions was able to sense bacterial activity based on volatile production. The results obtained here do not indicate that volatiles produced by rhizobacteria are inhibitory to the bacteria outside the rhizosphere. Bacteria outside the rhizosphere may even profit from the volatiles emitted by rhizobacteria. This work reveals novel information on the role of bacterial volatiles in long-distance microbial interactions in soil and indicates that bacterial volatiles may act as growth substrates and as infochemicals affecting gene expression, metabolism and triggering the production of other secondary metabolites in responding bacteria.

ACKNOWLEDGMENTS

This work is supported by The Netherlands Organization for Scientific Research (NWO) MEERVOUD personal grant to Paolina Garbeva (836.09.004). This is publication 5614 of the NIOO-KNAW.

SUPPLEMENTARY MATERIAL

The Supplementary Material for this article can be found online at: <http://www.frontiersin.org/journal/10.3389/fmicb.2014.00289/abstract>

REFERENCES

- Baudoin, E., Benizri, E., and Guckert, A. (2003). Impact of artificial root exudates on the bacterial community structure in bulk soil and maize rhizosphere. *Soil Biol. Biochem.* 35, 1183–1192. doi: 10.1016/S0038-0717(03)00179-2
- Beck, H. C., Hansen, A. M., and Lauritsen, F. R. (2003). Novel pyrazine metabolites found in polymyxin biosynthesis by *Paenibacillus polymyxa*. *FEMS Microbiol. Lett.* 220, 67–73. doi: 10.1016/S0378-1097(03)00054-5
- Blom, D., Fabbri, C., Connor, E. C., Schiestl, F. P., Klauser, D. R., Boller, T., et al. (2011). Production of plant growth modulating volatiles is widespread among rhizosphere bacteria and strongly depends on culture conditions. *Environ. Microbiol.* 13, 3047–3058. doi: 10.1111/j.1462-2920.2011.02582.x
- Chernin, L., Toklikishvili, N., Ovadis, M., Kim, S., Ben-Ari, J., Khmel, I., et al. (2011). Quorum-sensing quenching by rhizobacterial volatiles. *Environ. Microbiol. Rep.* 3, 698–704. doi: 10.1111/j.1758-2229.2011.00284.x
- Chun, S. C., Yoo, M. H., Moon, Y. S., Shin, M. H., Son, K. C., Chung, I. M., et al. (2010). Effect of bacterial population from rhizosphere of various foliage plants on removal of indoor volatile organic compounds. *Korean J. Hortic. Sci. Technol.* 28, 476–483.
- Compeau, G., Alachi, B. J., Platsouka, E., and Levy, S. B. (1988). Survival of rifampin-resistant mutants of *pseudomonas-fluorescens* and *pseudomonas-putida* in soil systems. *Appl. Environ. Microbiol.* 54, 2432–2438.
- De Boer, W., Gunnewiek, P., Lafeber, P., Janse, J. D., Spit, B. E., and Woldendorp, J. W. (1998). Anti-fungal properties of chitinolytic dune soil bacteria. *Soil Biol. Biochem.* 30, 193–203. doi: 10.1016/S0038-0717(97)00100-4
- De Boer, W., Leveau, J. H. J., Kowalchuk, G. A., Gunnewiek, P., Abeln, E. C. A., Figge, M. J., et al. (2004). *Collimonas fungivorans* gen. nov., sp nov., a chitinolytic soil bacterium with the ability to grow on living fungal hyphae. *Int. J. Syst. Evol. Microbiol.* 54, 857–864. doi: 10.1099/ijts.0.02920-0
- Effmert, U., Kalderas, J., Warnke, R., and Piechulla, B. (2012). Volatile mediated interactions between bacteria and fungi in the soil. *J. Chem. Ecol.* 38, 665–703. doi: 10.1007/s10886-012-0135-5
- Gao, R., Mack, T. R., and Stock, A. M. (2007). Bacterial response regulators: versatile regulatory strategies from common domains. *Trends Biochem. Sci.* 32, 225–234. doi: 10.1016/j.tibs.2007.03.002
- Garbeva, P., Hol, W. H. G., Termorshuizen, A. J., Kowalchuk, G. A., and De Boer, W. (2011a). Fungistasis and general soil biostasis—a new synthesis. *Soil Biol. Biochem.* 43, 469–477. doi: 10.1016/j.soilbio.2010.11.020
- Garbeva, P., Hordijk, C., Gerards, S., and De Boer, W. (2014). Volatiles produced by the mycophagous soil bacterium *Collimonas*. *FEMS Microbiol. Ecol.* 87, 639–649. doi: 10.1111/1574-6941.12252
- Garbeva, P., Silby, M. W., Raaijmakers, J. M., Levy, S. B., and De Boer, W. (2011b). Transcriptional and antagonistic responses of *Pseudomonas fluorescens* Pf0-1 to phylogenetically different bacterial competitors. *ISME J.* 5, 973–985. doi: 10.1038/ismej.2010.196
- Garbeva, P., Voesenek, K., and Van Elsas, J. D. (2004). Quantitative detection and diversity of the pyrrolnitrin biosynthetic locus in soil under different treatments. *Soil Biol. Biochem.* 36, 1453–1463. doi: 10.1016/j.soilbio.2004.03.009
- Groenhagen, U., Baumgartner, R., Bailly, A., Gardiner, A., Eberl, L., Schulz, S., et al. (2013). Production of bioactive volatiles by different *Burkholderia ambifaria* strains. *J. Chem. Ecol.* 39, 892–906. doi: 10.1007/s10886-013-0315-y
- Gu, Y.-Q., Mo, M.-H., Zhou, J.-P., Zou, C.-S., and Zhang, K.-Q. (2007). Evaluation and identification of potential organic nematicidal volatiles from soil bacteria. *Soil Biol. Biochem.* 39, 2567–2575. doi: 10.1016/j.soilbio.2007.05.011
- Hopwood, D. A. (2013). Imaging mass spectrometry reveals highly specific interactions between actinomycetes to activate specialized metabolic gene clusters. *Mbio* 4:e00612–13. doi: 10.1128/mBio.00612-13
- Kai, M., Crespo, E., Cristescu, S. M., Harren, F. J. M., Francke, W., and Piechulla, B. (2010). *Serratia odorifera*: analysis of volatile emission and biological impact of volatile compounds on *Arabidopsis thaliana*. *Appl. Microbiol. Biotechnol.* 88, 965–976. doi: 10.1007/s00253-010-2810-1
- Kai, M., Effmert, U., Berg, G., and Piechulla, B. (2007). Volatiles of bacterial antagonists inhibit mycelial growth of the plant pathogen *Rhizoctonia solani*. *Arch. Microbiol.* 187, 351–360. doi: 10.1007/s00203-006-0199-0
- Kai, M., Haustein, M., Molina, F., Petri, A., Scholz, B., and Piechulla, B. (2009). Bacterial volatiles and their action potential. *Appl. Microbiol. Biotechnol.* 81, 1001–1012. doi: 10.1007/s00253-008-1760-3
- Keller, L., and Surette, M. G. (2006). Communication in bacteria: an ecological and evolutionary perspective. *Nat. Rev. Microbiol.* 4, 249–258. doi: 10.1038/nrmicro1383
- Kim, K. S., Lee, S., and Ryu, C. M. (2013). Interspecific bacterial sensing through airborne signals modulates locomotion and drug resistance. *Nat. Commun.* 4:1809. doi: 10.1038/ncomms2789
- Kleinheinz, G. T., Bagley, S. T., St John, W. P., Rughani, J. R., and McGinnis, G. D. (1999). Characterization of alpha-pinene-degrading microorganisms and application to a bench-scale biofiltration system for VOC degradation. *Arch. Environ. Contam. Toxicol.* 37, 151–157. doi: 10.1007/s002449900500
- Kwon, Y. S., Ryu, C. M., Lee, S., Park, H. B., Han, K. S., Lee, J. H., et al. (2010). Proteome analysis of *Arabidopsis* seedlings exposed to bacterial volatiles. *Planta* 232, 1355–1370. doi: 10.1007/s00425-010-1259-x
- Lushchak, V. I. (2001). Oxidative stress and mechanisms of protection against it in bacteria. *Biochemistry* 66, 476–489. doi: 10.1023/A:1010294415625
- Malone, J. G., Williams, R., Christen, M., Jenal, U., Spiers, A. J., and Rainey, P. B. (2007). The structure-function relationship of WspR, a *Pseudomonas fluorescens* response regulator with a GGDEF output domain. *Microbiology* 153, 980–994. doi: 10.1099/mic.0.2006/002824-0
- Nguyen, D., Joshi-Datar, A., Lepine, F., Bauerle, E., Olakanmi, O., Beer, K., et al. (2011). Active starvation responses mediate antibiotic tolerance in biofilms and nutrient-limited bacteria. *Science* 334, 982–986. doi: 10.1126/science.1211037
- Onaka, H., Mori, Y., Igashiki, Y., and Furumai, T. (2011). Mycolic acid-containing bacteria induce natural-product biosynthesis in *Streptomyces* species. *Appl. Environ. Microbiol.* 77, 400–406. doi: 10.1128/AEM.01337-10
- Owen, S. M., Clark, S., Pompe, M., and Semple, K. T. (2007). Biogenic volatile organic compounds as potential carbon sources for microbial communities in soil from the rhizosphere of *Populus tremula*. *FEMS Microbiol. Lett.* 268, 34–39. doi: 10.1111/j.1574-6968.2006.00602.x
- Rodriguez, H., Rico, S., Diaz, M., and Santamaría, R. I. (2013). Two-component systems in *Streptomyces*: key regulators of antibiotic complex pathways. *Microb. Cell Fact.* 12:127. doi: 10.1186/1475-2859-12-127
- Ryan, R. P., and Dow, J. M. (2008). Diffusible signals and interspecies communication in bacteria. *Microbiology* 154, 1845–1858. doi: 10.1099/mic.0.2008/017871-0
- Sanchez, S., Chavez, A., Forero, A., Garcia-Huante, Y., Romero, A., Sanchez, M., et al. (2010). Carbon source regulation of antibiotic production. *J. Antibiot.* 63, 442–459. doi: 10.1038/ja.2010.78
- Shank, E. A., and Kolter, R. (2009). New developments in microbial interspecies signaling. *Curr. Opin. Microbiol.* 12, 205–214. doi: 10.1016/j.mib.2009.01.003
- Silby, M. W., Cerdeno-Tarraga, A. M., Vernikos, G. S., Giddens, S. R., Jackson, R. W., Preston, G. M., et al. (2009). Genomic and genetic analyses of diversity and plant interactions of *Pseudomonas fluorescens*. *Genome Biol.* 10:R51. doi: 10.1186/gb-2009-10-5-r51
- Van Wezel, G. P., and McDowell, K. J. (2011). The regulation of the secondary metabolism of Streptomyces: new links and experimental advances. *Nat. Prod. Rep.* 28, 1311–1333. doi: 10.1039/c1np00003a
- Verginer, M., Leitner, E., and Berg, G. (2010). Production of Volatile Metabolites by Grape-Associated Microorganisms. *J. Agric. Food Chem.* 58, 8344–8350. doi: 10.1021/jf100393w
- Weise, T., Kai, M., Gummesson, A., Troeger, A., Von Reuss, S., Piepenborn, S., et al. (2012). Volatile organic compounds produced by the phytopathogenic bacterium *Xanthomonas campestris* pv. *vesicatoria* 85-10. *Beilstein J. Org. Chem.* 8, 579–596. doi: 10.3762/bjoc.8.65
- Willett, J. W., Tiwari, N., Muller, S., Hummels, K. R., Houtman, J. C. D., Fuentes, E. J., et al. (2013). Specificity residues determine binding affinity for Two-Component Signal Transduction Systems. *Mbio* 4:e00420–13. doi: 10.1128/mBio.00420-13
- Young, I. M., Crawford, J. W., Nunan, N., Otten, W., and Spiers, A. (2008). “Microbial distribution in soils: physics and scaling,” in *Advances in Agronomy*, Vol. 100, ed D. L. Sparks (Elsevier), 81–121. doi: 10.1016/s0065-2113(08)00604-4

Zou, C.-S., Mo, M.-H., Gu, Y.-Q., Zhou, J.-P., and Zhang, K.-Q. (2007). Possible contributions of volatile-producing bacteria to soil fungistasis. *Soil Biol. Biochem.* 39, 2371–2379. doi: 10.1016/j.soilbio.2007.04.009

Conflict of Interest Statement: The authors declare that the research was conducted in the absence of any commercial or financial relationships that could be construed as a potential conflict of interest.

Received: 17 March 2014; accepted: 25 May 2014; published online: 14 June 2014.

Citation: Garbeva P, Hordijk C, Gerards S and de Boer W (2014) Volatile-mediated

interactions between phylogenetically different soil bacteria. *Front. Microbiol.* 5:289. doi: 10.3389/fmicb.2014.00289

This article was submitted to Terrestrial Microbiology, a section of the journal *Frontiers in Microbiology*.

Copyright © 2014 Garbeva, Hordijk, Gerards and de Boer. This is an open-access article distributed under the terms of the Creative Commons Attribution License (CC BY). The use, distribution or reproduction in other forums is permitted, provided the original author(s) or licensor are credited and that the original publication in this journal is cited, in accordance with accepted academic practice. No use, distribution or reproduction is permitted which does not comply with these terms.



Planctomycetes and macroalgae, a striking association

Olga M. Lage^{1,2*} and Joana Bondoso^{1,2}

¹ Department of Biology, Faculty of Sciences, University of Porto, Porto, Portugal

² CIMAR/CIIMAR – Interdisciplinary Centre for Marine and Environmental Research, University of Porto, Porto, Portugal

Edited by:

Luis Raul Comolli, Lawrence Berkeley National Laboratory, USA

Reviewed by:

Mia Bengtsson, University of Vienna, Austria

Onur Erbilgin, University of California, Berkeley, USA

***Correspondence:**

Olga M. Lage, Department of Biology, Faculty of Sciences, University of Porto, Rua do Campo Alegre, s/n, 4169-007 Porto, Portugal
e-mail: olga.lage@fc.up.pt

Planctomycetes are part of the complex microbial biofilm community of a wide range of macroalgae. Recently, some studies began to unveil the great diversity of Planctomycetes present in this microenvironment and the interactions between the two organisms. Culture dependent and independent methods revealed the existence of a great number of species but, so far, only less than 10 species have been isolated. Planctomycetes comprise the genera *Rhodopirellula*, *Blastopirellula*, and *Planctomyces*, *Phycisphaera* and the uncultured class OM190 and some other taxa have only been found in this association. Several factors favor the colonization of macroalgal surfaces by planctomycetes. Many species possess holdfasts for attachment. The macroalgae secrete various sulfated polysaccharides that are the substrate for the abundant sulfatases produced by planctomycetes. Specificity between planctomycetes and macroalgae seem to exist which may be related to the chemical nature of the polysaccharides produced by each macroalga. Furthermore, the peptidoglycan-free cell wall of planctomycetes allows them to resist the action of several antimicrobial compounds produced by the macroalgae or other bacteria in the biofilm community that are effective against biofouling by other microorganisms. Despite the increase in our knowledge on the successful planctomycetes-macroalgae association, a great effort to fully understand this interaction is needed.

Keywords: **planctomycetes, macroalgae, biofilm, association, macroalgae exudates**

INTRODUCTION

Planctomycetes are a peculiar group of bacteria within the *Planctomycetes*, *Verrucomicrobia*, *Chlamydiae* (PVC)—superphylum. They share with archaea or eukaryotes some distinctive characteristics such as peptidoglycan-less cell walls of proteic nature (Lage, 2013), a complex system of endomembranes forming a unique cell plan (Lage et al., 2013; Santarella-Mellwig et al., 2013), the presence of compartments like the anammoxosome (Van Teeseling et al., 2013), budding reproduction in many of their members (Ward et al., 2006) and the lack of the division protein FtsZ (Pilhofer et al., 2008), endocytosis (Lonhienne et al., 2010) and the presence of membrane coat (MC)—like proteins (Santarella-Mellwig et al., 2010). Some of these features place planctomycetes in the center of the discussion of the eukaryotic cell origin (Devos and Reynaud, 2010; Reynaud and Devos, 2011; Fuerst and Sagulenko, 2013).

Metabolically, planctomycetes are mainly aerobic, mesophilic, and neutrophilic organisms. A particular group of planctomycetes, the anaerobic ammonium oxidation (anammox) species, are strict anaerobes. Their diversified metabolism allows them to colonize a wide variety of ecosystems ranging from aquatic (marine, brackish, freshwater, sediments, and marine snow) to terrestrial habitats as well as several extreme environments such as desert soils (Abed et al., 2010; Andrew et al., 2012), hypersaline environments (Baumgartner et al., 2009; Schneider et al., 2013), hot springs (Tekere et al., 2011; Bohorquez et al., 2012), acidophilic habitats (Ivanova and Dedysh, 2012; Lucheta et al., 2013), glacial waters (Liu et al., 2006; Zeng et al., 2013) and

Antarctic soils and waters (Newsham et al., 2010; Piquet et al., 2010), hydrocarbon polluted environments (Abed et al., 2011) and other polluted habitats (Reed et al., 2002; Chouari et al., 2003; Caracciolo et al., 2005; Akob et al., 2007; Halter et al., 2011). Furthermore, their association with a great number of diverse eukaryotic organisms has been reported. These include sponges (Webster et al., 2001; Pimentel-Elardo et al., 2003; Zhu et al., 2008; Costa et al., 2013), ascidians (Oliveira et al., 2013), corals (Yakimov et al., 2006; Webster and Bourne, 2007; Duque-Alarcón et al., 2012), prawns (Fuerst et al., 1997), macrophytes (Hempel et al., 2008) and lichens (Grube et al., 2012). They were also found in sphagnum peat bogs (Kulichevskaia et al., 2006), the rock below the lichens (Bjelland et al., 2011) and in the rizosphere of several plants (Jensen et al., 2007; Zhao et al., 2010; Zhang et al., 2013).

Recently, various studies showed that planctomycetes are widespread in the biofilm community of several species of macroalgae and present a high diversity (Bengtsson and Ovreas, 2010; Lachnit et al., 2011; Lage and Bondoso, 2011). Besides a fundamental role in the primary production, beds of macroalgae along ocean coastlines provide the needed structure complexity, habitat and food for a huge and variable community of organisms which range from microscopic forms to larger organisms like fishes. Macroalgae are the dominant habitat-forming organisms on temperate coastlines (Campbell et al., 2014) and offer shelter for many forms of life that can thus avoid predation by higher forms in the food chain. This is particularly evident in the large brown algal kelp forests. At a

microscopic scale, macroalgal surfaces harbor a rich community composed by bacteria, fungi, diatoms, protozoa, spores and larvae of marine invertebrates (Lachnit et al., 2011) that can benefit from the availability of a range of organic carbon sources produced by algae (Armstrong et al., 2001). Bacteria are dominant among primary colonizers (Lachnit et al., 2009). The two major groups are *Bacteroidetes* and *Proteobacteria* followed by *Firmicutes*, *Actinobacteria*, *Verrucomicrobia*, and *Planctomycetes* (Goecke et al., 2013). In this review, we explore several aspects of the interaction between planctomycetes and macroalgae, a topic that recently started to be unveiled.

MACROALGAE THAT HARBOR PLANCTOMYCETES

Planctomycetes are frequent colonizers of macroalgae from the three phyla, Chlorophyta (green algae), Rhodophyta (red algae) and Heterokontophyta (brown algae). Planctomycetes colonization was observed for ulvacean algae like *Cladophora* sp. (Yoon et al., 2014), *Ulva compressa* (Hengst et al., 2010), *Ulva intestinalis* (Hengst et al., 2010; Lachnit et al., 2011; Lage and Bondoso, 2011), *Ulva australis* (Longford et al., 2007; Burke et al., 2011), *Ulva prolifera* (Liu et al., 2010), and *Ulva* sp. (Lage and Bondoso, 2011; Bondoso et al., 2013). This group was also reported to be present in the green macroalgae *Chara aspera* (Hempel et al., 2008) and *Caulerpa taxifolia* (Meusnier et al., 2001). Epiphytic planctomycetes were also found in the red algae *Porphyra umbilicalis* (Miranda et al., 2013), *Laurencia dendroidea* (De Oliveira et al., 2012), *Delisea pulchra* (Longford et al., 2007), and *Gracilaria vermiculophylla* (Lachnit et al., 2011). Isolates were retrieved from *Chondrus crispus*, *Mastocarpus stellatus*, *Gracilaria bursapastoris*, *Gelidium pulchellum*, *Gratelouzia turuturu*, and *Porphyra dioica* (Lage and Bondoso, 2011). The presence of planctomycetes on *Chondrus crispus*, *Mastocarpus stellatus*, and *Porphyra dioica* was detected by molecular methods (Bondoso et al., 2013). A novel order of planctomycetes containing one species isolated from *Porphyra* sp. was described (Fukunaga et al., 2009). 16S rRNA clone libraries from the brown algae *Fucus vesiculosus* revealed a great diversity of planctomycetes (Lachnit et al., 2011). Planctomycetes were isolated from other brown algae like *Fucus spiralis*, *Sargassum muticum*, *Laminaria* sp. (Lage and Bondoso, 2011), and *Laminaria hyperborea* (Bengtsson and Ovreas, 2010). The presence of planctomycetes has also been confirmed in *Fucus spiralis*, *Sargassum muticum* by Bondoso et al. (2013) and in *Saccharina latissima* and *L. digitata* (Bengtsson, unpublished results). These data suggest that planctomycetes are widespread among macroalgae which can be used for the discovery of novel planctomycetes species.

PLANCTOMYCETES ASSOCIATED WITH MACROALGAE

Although the abundance of planctomycetes is usually observed to be low in marine environments (Rusch et al., 2007) and some macroalgae (Burke et al., 2011; Lachnit et al., 2011; Miranda et al., 2013), Bengtsson and Ovreas (2010) showed, by FISH, that planctomycetes are dominant on *Laminaria hyperborea* where they can account for up to 51–53% of the bacterial biofilm cells.

About 30% of all the studies on macroalgae bacterial communities report the presence of planctomycetes and almost 4% of sequences from these studies belong to the phylum *Planctomycetes*

(Hollants et al., 2013). Planctomycete communities on macroalgae can be highly diverse varying from only one to 24 OTUs at a 97% cut-off in the 16S rRNA gene per macroalgae (**Table 1**). With the use of specific primers for planctomycetes, Bengtsson and Ovreas (2010) defined 16 OTUs associated with the kelp *Laminaria hyperborea*, each representing a different species and Bondoso et al. (2013), using PCR-DGGE, identified a total of 21 different OTUs associated with six macroalgae. In a pyrosequencing study, the red macroalga *Porphyra umbilicalis* was found to harbor 24 different OTUs belonging to planctomycetes (Miranda et al., 2013). In total, more than 60 potential different species of planctomycetes are associated with macroalgae and the majority were not isolated in pure culture (**Figure 1**). So far, only 10 species were isolated from macroalgae (Winkelmann and Harder, 2009; Bengtsson and Ovreas, 2010; Lage and Bondoso, 2011) on the basis of the 97% cut-off defined for species delineation (Stackebrandt, 2002) of which four were validly described (Fukunaga et al., 2009; Bondoso et al., 2014; Yoon et al., 2014). The communities of planctomycetes comprise mainly members related to the cultured genera *Blastopirellula*, *Rhodopirellula*, and *Planctomyces* (**Figure 1**) and to the class *Phycisphaerae* which contains the genera *Phycisphaera* and *Algiphysphaera*. The most abundant taxon reported in culture-independent studies is related to an isolate from *Fucus spiralis*, strain FC18 (Lage and Bondoso, 2011), and can be found in almost all the macroalgae studied but predominantly in the brown macroalgae *Fucus* sp. and *Laminaria hyperborea*. The uncultured class OM190 (SILVA taxonomy), a deeply branching group within the *Planctomycetes*, is also usually reported as being associated to macroalgae (**Figure 1, Table 1**).

The planctomycetes associated with red and brown macroalgae seem to have a higher diversity than the ones colonizing green algae (**Figure 1** and **Table 1**). This finding was reported by Lachnit et al. (2011) where only one OTU was associated with *Ulva intestinalis*, but 7 and 6 OTUs were, respectively, associated with *Delisea pulchra* and *Fucus vesiculosus*.

The communities of planctomycetes comprise taxa that were never found before in other habitats, suggesting a specific association with the macroalgae. Thirty nine out of 116 total sequences present in databases were found to be limited to macroalgal surfaces. Moreover, the study performed by Bondoso et al. (2013) also suggested that this association is host-specific and does not change with the geographical location of the macroalgae.

INTERACTIONS BETWEEN MACROALGAE AND PLANCTOMYCETES

The dynamic marine environments where macroalgae live are affected by diverse biotic and abiotic factors which contribute to, and influence the microbial community of their biofilms. Fundamental for this biofilm formation is the complex chemistry of macroalgal surfaces composed of exudates of secondary metabolites and extracellular exopolymeric substances (EPS) (Goecke et al., 2013). The chemistry varies among macroalgal species making each species a unique microenvironment, which induces a unique microbial community. Planctomycetes should be able to adapt easily to these complex environments. They are highly responsive to changes in environmental conditions through complex adaptation machinery. This was observed in

Table 1 | Abundance and phylogenetic affiliation of planctomycetes associated with macroalgae.

Macroalgae	Species/genus	Location	Used method	Planctomycetes				References
				Percentage genera ^a	Number of genera ^a	Number of species ^a	Phylogenetically related to	
Chlorophyta (Green)								
<i>Caulerpa taxifolia</i>	Philippines	16S rRNA gene libraries	ND	1	1	1	<i>Blastopirellula</i>	Meusnier et al., 2001
<i>Chara aspera</i>	Lake Constance	Fluorescence in situ hybridization (FISH)	2-3	ND	ND	ND		Hempel et al., 2008
<i>Cladophora sp.</i>	Sado Island, Japan	Isolation	ND	1	1	1	<i>Phycisphaera</i>	Yoon et al., 2014
<i>Ulva australis</i>	Bare Island, Australia	16S rRNA gene libraries	2	2	2	2	<i>Blastopirellula, Planctomycetes</i>	Longford et al., 2007
	Shark Point, Clovelly, Australia	16S rRNA gene libraries	3.4	ND	ND	ND		Burke et al., 2011
<i>Ulva compressa and intestinalis</i>	Chañaral Bay, Chile	T-RFLP	1.3	1	1	1	<i>Rhodopirellula</i> and planctomycete FC18	Hengst et al., 2010
<i>Ulva intestinalis</i>	Kiel fjord, Germany	16S rRNA gene libraries	ND	1	1	1	Planctomycete FC18	Lachnit et al., 2011
	Porto and Viana do Castelo, Portugal	Isolation	ND	1	1	1	<i>Planctomycetes</i>	Lage and Bondoso, 2011
<i>Ulva profilera</i>	Jiaozhou Bay, China	16S rRNA gene libraries	1	1	1	1	Planctomycete FC18	Liu et al., 2010
	Porto and Viana do Castelo, Portugal	Isolation	ND	2	5	5	<i>Rhodopirellula</i>	Lage and Bondoso, 2011
	Porto and Viana do Castelo, Portugal	DGGE	ND	1	2	1	Planctomycete FC18	Bondoso et al., 2013
Rhodophyt (Red) <i>Chondrus crispus</i>	Porto and Viana do Castelo, Portugal	Isolation	ND	1	2	2	<i>Rhodopirellula</i>	Lage and Bondoso, 2011
	Porto and Viana do Castelo, Portugal	DGGE	ND	1	2	2	Planctomycete FC18	Bondoso et al., 2013
<i>Delisea pulchra</i>	Bare Island, Australia	16S rRNA gene libraries	ND	1	2	2	<i>Rhodopirellula</i>	Lage and Bondoso, 2011
<i>Gelidium pulchellum</i>	Porto and Viana do Castelo, Portugal	Isolation	ND	1	1	1	<i>Rhodopirellula</i>	Lage and Bondoso, 2011
<i>Gracilaria bursa-pastoris</i>	Porto and Viana do Castelo, Portugal	Isolation	ND	2	2	2	<i>Rhodopirellula</i>	Lage and Bondoso, 2011
<i>Gracilaria vermiculophylla</i>	Kiel fjord, Germany	16S rRNA gene libraries	ND	3	6	6	<i>Blastopirellula, Rhodopirellula, Planctomycetes</i>	Lachnit et al., 2011

(Continued)

Table 1 | Continued

Macroalgae	Species/genus	Location	Used method	Planctomycetes				References
				Percentage	Number of genera ^a	Number of species ^a	Phylogenetically related to	
<i>Grateloupiā turuturu</i>	Porto and Viana do Castelo, Portugal	Isolation	ND	1	1	1	<i>Rhodopirellula</i>	Lage and Bondoso, 2011
<i>Laurencia dendroidea</i>	Búzios and Mangaratiba, Brasil	Transcriptome	ND	ND	ND	ND		De Oliveira et al., 2012
<i>Mastocarpus stellatus</i>	Porto and Viana do Castelo, Portugal	Isolation	ND	1	2	2	<i>Rhodopirellula</i>	Lage and Bondoso, 2011
<i>Porphyra dioica</i>	Porto and Viana do Castelo, Portugal	DGGE	ND	2	3	3	<i>Rhodopirellula</i> , OM190	Bondoso et al., 2013
<i>Porphyra dioica</i>	Porto and Viana do Castelo, Portugal	Isolation	ND	2	2	2	<i>Rhodopirellula</i> , <i>Planctomycetes</i>	Lage and Bondoso, 2011
<i>Porphyra umbilicalis</i>	Schoodic Point, USA	Pyrosequencing	0.03–4.06	ND	24	24	<i>Planctomycetes</i> , <i>Phycisphaera</i> , <i>Rhodopirellula</i>	Bondoso et al., 2013
<i>Porphyra</i> sp.	Mikura Island, Japan	Isolation	ND	1	1	1	<i>Phycisphaera</i>	Miranda et al., 2013
Heterokontophyt <i>Fucus spiralis</i> (Brown)	Porto and Viana do Castelo, Portugal	Isolation	ND	2	6	6	<i>Rhodopirellula</i> , FC18	Fukunaga et al., 2009
<i>Fucus vesiculosus</i>	Bare Island, Australia	16S rRNA gene libraries	ND	3	6	6	<i>Blastopirellula</i> , <i>Planctomycetes</i> , <i>Planctomycete</i> FC18	Lachnit et al., 2011
<i>Laminaria hyperborea</i>	Bergen, Norway	FISH and 16S rRNA gene libraries	23.7–52.5	4	16	16	<i>Blastopirellula</i> , <i>Planctomycetes</i> , <i>Planctomycete</i> FC18, <i>Rhodopirellula</i> , OM190	Bengtsson and Ovreas, 2010
<i>Fucus vesiculosus</i>	Bergen, Norway	DGGE	46.3	5	8	8	<i>Blastopirellula</i> , <i>Planctomycetes</i> , <i>Planctomycete</i> FC18, <i>Rhodopirellula</i> , OM190	Bengtsson et al., 2010
<i>Laminaria</i> sp.	Porto and Viana do Castelo, Portugal	454-pyrosequencing	55.7	ND	ND	ND	<i>Rhodopirellula</i> , <i>Planctomycete</i> FC18,	Bengtsson et al., 2012
<i>Sargassum muticum</i>	Porto and Viana do Castelo, Portugal	Isolation	ND	1	1	1	<i>Rhodopirellula</i>	Lage and Bondoso, 2011
<i>Sargassum muticum</i>	Porto and Viana do Castelo, Portugal	DGGE	ND	3	7	7	<i>Planctomycetes</i> , <i>Planctomycete</i> FC18, <i>Rhodopirellula</i>	Bondoso et al., 2013

^aThe sequences reported in the studies above were grouped using cdhit-test (Huang et al., 2010) based on 97% (species) or 95% (genus) cut-off similarity in the 16S rRNA gene.

ND, not determined.



FIGURE 1 | Maximum-Likelihood tree of 16S rRNA gene sequences of planctomycetes associated with macroalgae downloaded from NCBI database. The final set consisted of 116 sequences above 500 bp. Strains in bold represent the isolates from macroalgae described to date. The numbers

beside nodes are the percentages for bootstrap analyses; only values above 50% are shown. Scale bar = 0.02 substitutions per 100 nucleotides. The different groups are presented on the right. Anammox 16S rRNA gene sequences were used as outgroup.

Rhodopirellula baltica under stress response to temperature and salinity (Wecker et al., 2009).

Macroalgae produce or release many molecules that can be rich sources of substrates for planctomycetes nutrition. Algal macromolecules include sulfated polysaccharides like carrageenan and agar from red algae, alginate, fucan and laminarin from brown algae and cellulose and ulvan from green algae. Planctomycetes are well tailored for the utilization of sulfated polysaccharides as revealed by the analysis of the marine *R. baltica* SH1^T genome where the presence of 110 sulphatases was detected (Glockner et al., 2003). Furthermore, Wegner et al. (2013) also found an exceptionally high number of sulphatase genes in the recently sequenced genomes of nine *Rhodopirellula* strains. These authors also verified in *R. baltica* SH1^T sulphatase expression profiles in cells grown on different sulfated polysaccharides. Polysaccharide utilization was also confirmed by the work of Jeske et al. (2013) where *R. baltica* was checked for potential utilization of several polymers. It was able to utilize laminarin, mannitol, pectin, chondroitin sulfate, N-acetylgalactosamine, and D-glucuronic acid. Cellobiose, a product of cellulose degradation, could also be used as carbon source. Weak or moderate degradation was obtained for mannan and its monomer D-mannose, the disaccharide sucrose and D-xylose. The novel species *R. rubra* and *R. lusitana*, both isolated from macroalgae, were shown to utilize the majority of the monomers that constitute the main polysaccharides secreted by macroalgae such as fucose, galactose, xylose, rhamnose, and manitol (Bondoso et al., 2014). Agarolytic activity was also described in a novel representative of the class Phycisphaera, *Algisphaera agarilytica*, isolated from the marine alga *Cladophora* sp. (Yoon et al., 2014). As frequent inhabitants of phytodetrital macroaggregates in marine environments, planctomycetes mineralize organic matter, intervening in important transformations in the global carbon cycle in the sea (DeLong et al., 1993). Very recently, Erbilgin et al. (2014) provided evidence by a metabolic activity screen that Bacterial Microcompartments (BMCs) present in planctomycetes are involved in the degradation of a number of plant and algal cell wall sugars, namely L-fucose and L-rhamnose. This work further supports the great relevance of algal exudates on planctomycetes physiology especially for those associated with macroalgae.

The different substrates produced by each macroalga may explain the specificity of planctomycetes to the algal host. It was found that the same algal species from two localities demonstrated high similarities in the composition of associated planctomycetes (Bondoso et al., 2013). A core of evidence seems to point to the algal host as the main factor controlling the composition and structure of epiphytic bacterial communities (Wahl, 2008; Lachnit et al., 2009, 2011; Hengst et al., 2010). Comparable results were reported for the epibiotic bacterial communities living on corals which seemed to be determined by the nature and composition of host exudates due to strong seasonal effects (Guppy and Bythell, 2006).

Planctomycetes colonize macroalgal surfaces; an attached life style has been well recognized for these bacteria and when in pelagic environments they are mainly associated with particles like marine snow (DeLong et al., 1993). The presence of a holdfast of glycoproteic nature (Lage, 2013; Lage et al., 2013) favors

attachment and, thus, the colonization of surfaces (Gade et al., 2005; Lage, 2013; Lage et al., 2013).

Another factor that favors the colonization of macroalgal biofilms by planctomycetes is their ability to resist several antibiotics. These can be produced by the macroalgae or by other competing bacteria in the biofilm. One of the methods to achieve planctomycetes isolation in culture is precisely based on this resistance to antibiotics (Schlesner, 1994; Winkelmann and Harder, 2009; Lage and Bondoso, 2011). Resistance to β-lactam antibiotics that affect peptidoglycan biosynthesis is due to the absence of this molecule in their cell wall.

In a study of the behavior of planctomycetes toward antibiotics, Cayrou et al. (2010) showed that five reference strains of planctomycetes were resistant to β-lactams, to the quinolone nalidixic acid and to the glycopeptide vancomycin. The organisms were, however sensitive to tetracycline and doxycycline. Most were also resistant to chloramphenicol and the aminoglycoside gentamicin as well as rifampicin. A variable resistance to the association sulfomethoxazole/trimethoprim was obtained.

The potential benefits of the planctomycetes to the macroalgae can only be hypothesized. Being heterotrophs, planctomycetes can mineralize organic molecules producing inorganic compounds that meet the nutritional needs of macroalgae. These may also profit from the production of growth factors or antimicrobial molecules by the planctomycetes. It has been shown that morphogenetic factors like thallusin, isolated from an epiphytic marine bacterium, are indispensable to the foliaceous morphology of macroalgae (Matsuo et al., 2005). Unknown factors may be due to planctomycetes. The production of bioactive molecules by planctomycetes was initially searched by genome mining in *R. baltica* (Donadio et al., 2007) and subsequently in 13 genomes (Jeske et al., 2013). Two small nonribosomal peptide synthetases (NRPSs), two monomeric polyketide synthases (PKSs), and a bimodular hybrid NRPS–PKS were found in the genome of *R. baltica* which are probably involved in the synthesis of five different, unknown bioactive products (Donadio et al., 2007). In the 13 genomes analyzed, 102 genes or gene clusters putatively related with the production of secondary metabolites like bacteriocin encoding genes, putative lantibiotic-encoding gene, ectoine synthesis gene cluster, putative phenazine encoding gene cluster were found (Jeske et al., 2013). The potential production of these bioactive molecules may help the macroalgae to control their colonization by undesired bacteria or fungi. Furthermore, we can hypothesize that bioactive molecules should be important for planctomycetes in the process of macroalgal colonization and posterior defense against competitors.

Bacteria can also impact negatively on macroalgae. Members of Bacteroidetes and Gammaproteobacteria can induce several diseases like “shot hole disease” or “hole-rotten disease” (Goecke et al., 2013). Up to now, pathogenicity from planctomycetes on macroalgae was never reported.

CONCLUSIONS

As shown in this review, macroalgae are promising environments for in-depth study of planctomycetes. Macroalgae possess a relatively high number and a diverse community of planctomycetes in their biofilm. Thus, they represent great potential for

the discovery of new taxa that can be isolated from these habitats and their characterization could provide new knowledge on the morphology, physiology and ecology of planctomycetes and on this interaction. New research on the structure, succession and dynamics of the community in this relationship, namely the relation with the macroalgal life cycle, the temporality of planctomycetes diversity and composition and their association with other macroalgae will give new highlights in the ecology of this interaction. Metabolomic approaches will allow obtaining insights into the mechanisms of the nutritional relationship and the role of planctomycetes in biofilm formation and maintenance. The increasing scientific interest in the biology of planctomycetes and biofilms will, most certainly, generate new exciting knowledge that will allow a better comprehension of this association.

ACKNOWLEDGMENTS

This research was supported by the European Regional Development Fund (ERDF) through the COMPETE - Operational Competitiveness Programme and national funds through FCT – Foundation for Science and Technology, under the project PEst-C/MAR/LA0015/2013. The second author was financed by FCT (PhD grant SFRH/BD/35933/2007).

REFERENCES

- Abed, R. M. M., Al Kharusi, S., Schramm, A., and Robinson, M. D. (2010). Bacterial diversity, pigments and nitrogen fixation of biological desert crusts from the Sultanate of Oman. *FEMS Microbiol. Ecol.* 72, 418–428. doi: 10.1111/j.1574-6941.2010.00854.x
- Abed, R. M. M., Musat, N., Musat, F., and Mußmann, M. (2011). Structure of microbial communities and hydrocarbon-dependent sulfate reduction in the anoxic layer of a polluted microbial mat. *Mar. Pollut. Bull.* 62, 539–546. doi: 10.1016/j.marpolbul.2010.11.030
- Akob, D. M., Mills, H. J., and Kostka, J. E. (2007). Metabolically active microbial communities in uranium-contaminated subsurface sediments. *FEMS Microbiol. Ecol.* 59, 95–107. doi: 10.1111/j.1574-6941.2006.00203.x
- Andrew, D. R., Fitak, R. R., Munguia-Vega, A., Racolta, A., Martinson, V. G., and Dontsova, K. (2012). Abiotic factors shape microbial diversity in Sonoran desert soils. *Appl. Environ. Microbiol.* 78, 7527–7537. doi: 10.1128/AEM.01459-12
- Armstrong, E., Yan, L., Boyd, K. G., Wright, P. C., and Burgess, J. G. (2001). The symbiotic role of marine microbes on living surfaces. *Hydrobiologia* 461, 37–40. doi: 10.1023/A:1012756913566
- Baumgartner, L. K., Dupraz, C., Buckley, D. H., Spear, J. R., Pace, N. R., and Visscher, P. T. (2009). Microbial species richness and metabolic activities in hypersaline microbial mats: insight into biosignature formation through lithification. *Astrobiology* 9, 861–874. doi: 10.1089/ast.2008.0329
- Bengtsson, M. M., and Ovreas, L. (2010). Planctomycetes dominate biofilms on surfaces of the kelp *Laminaria hyperborea*. *BMC Microbiol.* 10:261. doi: 10.1186/1471-2180-10-261
- Bengtsson, M. M., Sjotun, K., Lanzen, A., and Ovreas, L. (2012). Bacterial diversity in relation to secondary production and succession on surfaces of the kelp *Laminaria hyperborea*. *ISME J.* 6, 2188–2198. doi: 10.1038/ismej.2012.67
- Bengtsson, M. M., Sjotun, K., and Ovreås, L. (2010). Seasonal dynamics of bacterial biofilms on the kelp *Laminaria hyperborea*. *Aquat. Microb. Ecol.* 60, 71–83. doi: 10.3354/ame01409
- Bjelland, T., Grube, M., Hoem, S., Jorgensen, S. L., Daae, F. L., Thorseth, I. H., et al. (2011). Microbial metacommunities in the lichen-rock habitat. *Environ. Microbiol. Rep.* 3, 434–442. doi: 10.1111/j.1758-2229.2010.00206.x
- Bohorquez, L. C., Delgado-Serrano, L., Lopez, G., Osorio-Forero, C., Klepac-Ceraj, V., Kolter, R., et al. (2012). In-depth characterization via complementing culture-independent approaches of the microbial community in an acidic hot spring of the Colombian Andes. *Microb. Ecol.* 63, 103–115. doi: 10.1007/s00248-011-9943-3
- Bondoso, J., Albuquerque, L., Lobo-Da-Cunha, A., Da Costa, M. S., Harder, J., and Lage, O. M. (2014). Rhodopirellula lusitana sp. nov. and Rhodopirellula rubra sp. nov., isolated from the surface of macroalgae. *Syst. Appl. Microbiol.* doi: 10.1016/j.syapm.2013.11.004
- Bondoso, J., Balagüé, V., Gasol, J. M., and Lage, O. M. (2013). Community composition of the Planctomycetes associated with different macroalgae. *FEMS Microbiol. Ecol.* doi: 10.1111/1574-6941.12258
- Burke, C., Thomas, T., Lewis, M., Steinberg, P., and Kjelleberg, S. (2011). Composition, uniqueness and variability of the epiphytic bacterial community of the green alga *Ulva australis*. *ISME J.* 5, 590–600. doi: 10.1038/ismej.2010.164
- Campbell, A. H., Marzinelli, E. M., Vergés, A., Coleman, M. A., and Steinberg, P. D. (2014). Towards restoration of missing underwater forests. *PLoS ONE* 9:e84106. doi: 10.1371/journal.pone.0084106
- Caracciolo, A. B., Grenni, P., Ciccoli, R., Di Landa, G., and Cremisini, C. (2005). Simazine biodegradation in soil: analysis of bacterial community structure by *in situ* hybridization. *Pest Manag. Sci.* 61, 863–869. doi: 10.1002/ps.1096
- Cayrou, C., Raoult, D., and Drancourt, M. (2010). Broad-spectrum antibiotic resistance of *Planctomycetes* organisms determined by Etest. *J. Antimicrob. Chemother.* 65, 2119–2122. doi: 10.1093/jac/dkq290
- Chouari, R., Le Paslier, D., Daegelen, P., Ginestet, P., Weissenbach, J., and Sghir, A. (2003). Molecular evidence for novel planctomycete diversity in a municipal wastewater treatment plant. *Appl. Environ. Microbiol.* 69, 7354–7363. doi: 10.1128/AEM.69.12.7354-7363.2003
- Costa, R., Keller-Costa, T., Gomes, N. C. M., Da Rocha, U. N., van Overbeek, L., and van Elsas, J. D. (2013). Evidence for selective bacterial community structuring in the freshwater sponge *Ephydatia fluviatilis*. *Microb. Ecol.* 65, 232–244. doi: 10.1007/s00248-012-0102-2
- De Oliveira, L. S., Gregoracci, G. B., Silva, G. G., Salgado, L. T., Filho, G. A., Alves-Ferreira, M., et al. (2012). Transcriptomic analysis of the red seaweed *Laurencia dendroidea* (*Florideophyceae, Rhodophyta*) and its microbiome. *BMC Genomics* 13:487. doi: 10.1186/1471-2164-13-487
- DeLong, E. F., Franks, D. G., and Alldredge, L. (1993). Phylogenetic diversity of aggregate-attached vs. free-living marine bacterial assemblages. *Limnol. Oceanogr.* 38, 924–934. doi: 10.4319/lo.1993.38.5.0924
- Devos, D. P., and Reynaud, E. G. (2010). Intermediate steps. *Science* 330, 1187–1188. doi: 10.1126/science.1196720
- Donadio, S., Monciardini, P., and Sosio, M. (2007). Polyketide synthases and non-ribosomal peptide synthetases: the emerging view from bacterial genomics. *Nat. Prod. Rep.* 24, 1073–1109. doi: 10.1039/b514050c
- Duque-Alarcón, A., Santiago-Vázquez, L. Z., and Kerr, R. G. (2012). A microbial community analysis of the octocoral *Eunicea fusca*. *Electron. J. Biotechnol.* 15, 1–9. doi: 10.2225/vol15-issue5-fulltext-11
- Erbilgin, O., McDonald, K. L., and Kerfeld, C. A. (2014). Characterization of a planctomycetal organelle: a novel bacterial microcompartment for the aerobic degradation of plant saccharides. *Appl. Environ. Microbiol.* 80, 2193–2205. doi: 10.1128/AEM.03887-13
- Fuerst, J. A., Gwilliam, H. G., Lindsay, M., Lichanska, A., Belcher, C., Vickers, J. E., et al. (1997). Isolation and molecular identification of planctomycete bacteria from postlarvae of the giant tiger prawn, *Penaeus monodon*. *Appl. Environ. Microbiol.* 63, 254–262.
- Fuerst, J. A., and Sagulenko, E. (2013). Nested bacterial boxes: nuclear and other intracellular compartments in planctomycetes. *J. Mol. Microbiol. Biotechnol.* 23, 95–103. doi: 10.1159/000346544
- Fukunaga, Y., Kurahashi, M., Sakiyama, Y., Ohuchi, M., Tokota, A., and Harayama, S. (2009). Phycisphaera mikurensis gen. nov., sp. nov., isolated from a marine alga, and proposal of phycisphaeraeace fam. nov., phycisphaerales ord. nov. and phycisphaerae classis nov. in the phylum planctomycetes. *J. Gen. Appl. Microbiol.* 55, 267–275. doi: 10.2323/jgam.55.267
- Gade, D., Stuhrmann, T., Reinhardt, R., and Rabus, R. (2005). Growth phase dependent regulation of protein composition in *Rhodopirellula baltica*. *Environ. Microbiol.* 7, 1074–1084. doi: 10.1111/j.1462-2920.2005.00784.x
- Glockner, F. O., Kube, M., Bauer, M., Teeling, H., Lombardot, T., Ludwig, W., et al. (2003). Complete genome sequence of the marine planctomycete *Pirellula* sp. strain 1. *Proc. Natl. Acad. Sci. U. S. A.* 100, 8298–8303. doi: 10.1073/pnas.1431443100
- Goecke, F., Thiel, V., Wiese, J., Labes, A., and Imhoff, J. F. (2013). Algae as an important environment for bacteria—phylogenetic relationships among new bacterial species isolated from algae. *Phycologia* 52, 14–24. doi: 10.2216/12-24.1
- Grube, M., Köberl, M., Lackner, S., Berg, C., and Berg, G. (2012). Host-parasite interaction and microbiome response: effects of fungal infections on the

- bacterial community of the Alpine lichen *Solorina crocea*. *FEMS Microbiol. Ecol.* 82, 472–481. doi: 10.1111/j.1574-6941.2012.01425.x
- Guppy, R., and Bythell, J. C. (2006). Environmental effects on bacterial diversity in the surface mucus layer of the reef coral *Montastraea faveolata*. *Mar. Ecol. Prog. Ser.* 328, 133–142. doi: 10.3354/meps328133
- Halter, D., Cordi, A., Gribaldo, S., Gallieni, S., Goulhen-Chollet, F., Heinrich-Salmeron, A., et al. (2011). Taxonomic and functional prokaryote diversity in mildly arsenic-contaminated sediments. *Res. Microbiol.* 162, 878–887. doi: 10.1016/j.resmic.2011.06.001
- Hempel, M., Blume, M., Blindow, I., and Gross, E. M. (2008). Epiphytic bacterial community composition on two common submerged macrophytes in brackish water and freshwater. *BMC Microbiol.* 8:58. doi: 10.1186/1471-2180-8-58
- Hengst, M. B., Andrade, S., Gonzalez, B., and Correa, J. A. (2010). Changes in epiphytic bacterial communities of intertidal seaweeds modulated by host, temporality, and copper enrichment. *Microb. Ecol.* 60, 282–290. doi: 10.1007/s00248-010-9647-0
- Hollants, J., Leliaert, F., De Clerck, O., and Willems, A. (2013). What we can learn from sushi: a review on seaweed-bacterial associations. *FEMS Microbiol. Ecol.* 83, 1–16. doi: 10.1111/j.1574-6941.2012.01446.x
- Huang, Y., Niu, B., Gao, Y., Fu, L., and Li, W. (2010). CD-HIT Suite: a web server for clustering and comparing biological sequences. *Bioinformatics* 26, 680–682. doi: 10.1093/bioinformatics/btq003
- Ivanova, A. O., and Dedysh, S. N. (2012). Abundance, diversity, and depth distribution of Planctomycetes in acidic northern wetlands. *Front. Microbiol.* 3:5. doi: 10.3389/fmicb.2012.00005
- Jensen, S. I., Kühl, M., and Priemé, A. (2007). Different bacterial communities associated with the roots and bulk sediment of the seagrass *Zostera marina*. *FEMS Microbiol. Ecol.* 62, 108–117. doi: 10.1111/j.1574-6941.2007.00373.x
- Jeske, O., Jogler, M., Petersen, J., Sikorski, J., and Jogler, C. (2013). From genome mining to phenotypic microarrays: Planctomycetes as source for novel bioactive molecules. *Antonie Van Leeuwenhoek* 104, 551–567. doi: 10.1007/s10482-013-0007-1
- Kulichevskaya, I. S., Pankratov, T. A., and Dedysh, S. N. (2006). Detection of representatives of the Planctomycetes in Sphagnum peat bogs by molecular and cultivation methods. *Mikrobiologiya*. 75, 389–396.
- Lachnit, T., Blümel, M., Imhoff, J. F., and Wahl, M. (2009). Specific epibacterial communities on macroalgae: phylogeny matters more than habitat. *Aquatic Biology* 5, 181–186. doi: 10.3354/ab00149
- Lachnit, T., Meske, D., Wahl, M., Harder, T., and Schmitz, R. (2011). Epibacterial community patterns on marine macroalgae are host-specific but temporally variable. *Environ. Microbiol.* 13, 655–665. doi: 10.1111/j.1462-2920.2010.02371.x
- Lage, O. (2013). Characterization of a planctomycete associated with the marine dinoflagellate *Prorocentrum micans* Her. *Antonie Van Leeuwenhoek* 104, 499–508. doi: 10.1007/s10482-013-9994-4
- Lage, O., Bondoso, J., and Lobo-Da-Cunha, A. (2013). Insights into the ultrastructural morphology of novel Planctomycetes. *Antonie van Leeuwenhoek*, 1–10. doi: 10.1007/s10482-013-9969-2
- Lage, O. M., and Bondoso, J. (2011). Planctomycetes diversity associated with macroalgae. *FEMS Microbiol. Ecol.* 78, 366–375. doi: 10.1111/j.1574-6941.2011.01168.x
- Liu, M., Dong, Y., Zhao, Y., Zhang, G., Zhang, W., and Xiao, T. (2010). Structures of bacterial communities on the surface of *Ulva prolifera* and in seawaters in an *Ulva* blooming region in Jiaozhou Bay, China. *World J. Microbiol. Biotechnol.* 27, 1703–1712. doi: 10.1007/s11274-010-0627-9
- Liu, Y., Yao, T., Jiao, N., Kang, S., Zeng, Y., and Huang, S. (2006). Microbial community structure in moraine lakes and glacial meltwaters, Mount Everest. *FEMS Microbiol. Lett.* 265, 98–105. doi: 10.1111/j.1574-6968.2006.00477.x
- Longford, S. R., Tujula, N. A., Crocetti, G. R., Holmes, A. J., Holmström, C., Kjelleberg, S., et al. (2007). Comparisons of diversity of bacterial communities associated with three sessile marine eukaryotes. *Aquat. Microb. Ecol.* 48, 217–229. doi: 10.3354/ame048217
- Lonhienne, T. G., Sagulenko, E., Webb, R. I., Lee, K. C., Franke, J., Devos, D. P., et al. (2010). Endocytosis-like protein uptake in the bacterium *Gemmata obscuriglobus*. *Proc. Natl. Acad. Sci. U.S.A.* 107, 12883–12888. doi: 10.1073/pnas.1001085107
- Lucheta, A. R., Otero, X. L., Macías, F., and Lambais, M. R. (2013). Bacterial and archaeal communities in the acid pit lake sediments of a chalcopyrite mine. *Extremophiles* 17, 941–951. doi: 10.1007/s00792-013-0576-y
- Matsuo, Y., Imagawa, H., Nishizawa, M., and Shizuri, Y. (2005). Isolation of an algal morphogenesis inducer from a marine bacterium. *Science* 307, 1598. doi: 10.1126/science.1105486
- Meusnier, I., Olsen, J. L., Stam, W. T., Destombe, C., and Valero, M. (2001). Phylogenetic analyses of *Caulerpa taxifolia* (Chlorophyta) and of its associated bacterial microflora provide clues to the origin of the Mediterranean introduction. *Mol. Ecol.* 10, 931–946. doi: 10.1046/j.1365-294X.2001.01245.x
- Miranda, L. N., Hutchison, K., Grossman, A. R., and Brawley, S. H. (2013). Diversity and abundance of the bacterial community of the red macroalga *Porphyra umbilicalis*: did bacterial farmers produce macroalgae? *PLoS ONE* 8:e58269. doi: 10.1371/journal.pone.0058269
- Newsham, K. K., Pearce, D. A., and Bridge, P. D. (2010). Minimal influence of water and nutrient content on the bacterial community composition of a maritime Antarctic soil. *Microbiol. Res.* 165, 523–530. doi: 10.1016/j.micres.2009.11.005
- Oliveira, F.a.S., Colares, G. B., Hissa, D. C., Angelim, A. L., Melo, V. M. M., and Lotufo, T.M.C. (2013). Microbial epibionts of the colonial ascidians *Didemnum galacteum* and *Cystodytes* sp. *Symbiosis* 59, 57–63. doi: 10.1007/s13199-012-0210-2
- Pilhofer, M., Rappl, K., Eckl, C., Bauer, A. P., Ludwig, W., Schleifer, K. H., et al. (2008). Characterization and evolution of cell division and cell wall synthesis genes in the bacterial phyla *Verrucomicrobia*, *Lentisphaerae*, *Chlamydiae*, and *Planctomycetes* and phylogenetic comparison with rRNA genes. *J. Bacteriol.* 190, 3192–3202. doi: 10.1128/JB.01797-07
- Pimentel-Elardo, S., Wehrli, M., Friedrich, A. B., Jensen, P. R., and Hentschel, U. (2003). Isolation of planctomycetes from *Aplysina* sponges. *Aquat. Microb. Ecol.* 33, 239–245. doi: 10.3354/ame033239
- Piquet, A. M. T., Bolhuis, H., Davidson, A. T., and Buma, A. G. J. (2010). Seasonal succession and UV sensitivity of marine bacterioplankton at an Antarctic coastal site. *FEMS Microbiol. Ecol.* 73, 68–82. doi: 10.1111/j.1574-6941.2010.00882.x
- Reed, D. W., Fujita, Y., Delwiche, M. E., Blackwelder, D. B., Sheridan, P. P., Uchida, T., et al. (2002). Microbial communities from methane hydrate-bearing deep marine sediments in a forearc basin. *Appl. Environ. Microbiol.* 68, 3759–3770. doi: 10.1128/AEM.68.8.3759-3770.2002
- Reynaud, E. G., and Devos, D. P. (2011). Transitional forms between the three domains of life and evolutionary implications. *Proc. Biol. Sci.* 278, 3321–3328. doi: 10.1098/rspb.2011.1581
- Rusch, D. B., Halpern, A. L., Sutton, G., Heidelberg, K. B., Williamson, S., Yooseph, S., et al. (2007). The sorcerer II global ocean sampling expedition: northwest atlantic through eastern tropical pacific. *PLoS Biol.* 5:e77. doi: 10.1371/journal.pbio.0050077
- Santarella-Mellwig, R., Franke, J., Jaedicke, A., Gorjanacz, M., Bauer, U., Budd, A., et al. (2010). The compartmentalized Bacteria of the *Planctomycetes-Verrucomicrobia-Chlamydiae* superphylum have membrane coat-like proteins. *PLoS Biol.* 8:e1000281. doi: 10.1371/journal.pbio.1000281
- Santarella-Mellwig, R., Prugnaller, S., Roos, N., Mattaj, I. W., and Devos, D. P. (2013). Three-dimensional reconstruction of bacteria with a complex endomembrane system. *PLoS Biol.* 11:e1001565. doi: 10.1371/journal.pbio.1001565
- Schlesner, H. (1994). The development of media suitable for the microorganisms morphologically resembling *Planctomyces* spp., *Pirellula* spp., and other *Planctomycetales* from various aquatic habitats using dilute media. *Syst. Appl. Microbiol.* 17, 135–145. doi: 10.1016/S0723-2020(11)80042-1
- Schneider, D., Arp, G., Reimer, A., Reitner, J., and Daniel, R. (2013). Phylogenetic analysis of a microbialite-forming microbial mat from a hypersaline lake of the kiritimati atoll, central pacific. *PLoS ONE* 8:e66662. doi: 10.1371/journal.pone.0066662
- Stackebrandt, E. (2002). Report of the ad hoc committee for the re-evaluation of the species definition in bacteriology. *Int. J. Syst. Evol. Microbiol.* 52, 1043–1047. doi: 10.1099/ijss.0.02360-0
- Tekere, M., Löttner, A., Olivier, J., Jonker, N., and Venter, S. (2011). Metagenomic analysis of bacterial diversity of siloam hot water spring, limpopo, South Africa. *Afr. J. Biotechnol.* 10, 18005–18012. doi: 10.5897/AJB11.899
- Van Teeseling, M. C. F., Neumann, S., and Van Niftrik, L. (2013). The anamoxosome organelle is crucial for the energy metabolism of anaerobic ammonium oxidizing bacteria. *J. Mol. Microbiol. Biotechnol.* 23, 104–117. doi: 10.1159/000346547
- Wahl, M. (2008). Ecological lever and interface ecology: epibiosis modulates the interactions between host and environment. *Biofouling* 24, 427–438. doi: 10.1080/08927010802339772

- Ward, N., Staley, J. T., Fuerst, J. A., Giovannoni, S., Schlesner, H., and Stackebrandt, E. (2006). "The order Planctomycetales, including the genera Planctomyces, Pirellula, Gemmata and Isosphaera and the Candidatus genera Brocadia, Kuenenia and Scalindua," in *The Prokaryotes: A Handbook on the Biology of Bacteria*, Vol. 7, eds M. Dworkin, S. Falkow, E. Rosenberg, K. H. Schleifer, and E. Stackebrandt (New York, NY: Springer), 757–793.
- Webster, N. S., and Bourne, D. (2007). Bacterial community structure associated with the Antarctic soft coral, *Alcyonium antarcticum*. *FEMS Microbiol. Ecol.* 59, 81–94. doi: 10.1111/j.1574-6941.2006.00195.x
- Webster, N. S., Wilson, K. J., Blackall, L. L., and Hill, R. T. (2001). Phylogenetic diversity of bacteria associated with the marine sponge *Rhopaloeides odorabile*. *Appl. Environ. Microbiol.* 67, 434–444. doi: 10.1128/AEM.67.1.434-44.4.2001
- Wecker, P., Klockow, C., Ellrott, A., Quast, C., Langhammer, P., Harder, J., et al. (2009). Transcriptional response of the model Planctomycete *Rhodopirellula baltica* SH1^(T) to changing environmental conditions. *BMC Genomics* 10:410. doi: 10.1186/1471-2164-10-410
- Wegner, C. E., Richter-Heitmann, T., Klindworth, A., Klockow, C., Richter, M., Achstetter, T., et al. (2013). Expression of sulfatases in *Rhodopirellula baltica* and the diversity of sulfatases in the genus *Rhodopirellula*. *Mar. Genomics* 9, 51–61. doi: 10.1016/j.margen.2012.12.001
- Winkelmann, N., and Harder, J. (2009). An improved isolation method for attached-living Planctomycetes of the genus *Rhodopirellula*. *J. Microbiol. Methods* 77, 276–284. doi: 10.1016/j.mimet.2009.03.002
- Yakimov, M. M., Cappello, S., Crisafi, E., Tursi, A., Savini, A., Corselli, C., et al. (2006). Phylogenetic survey of metabolically active microbial communities associated with the deep-sea coral *Lophelia pertusa* from the Apulian plateau, Central Mediterranean Sea. *Deep-Sea Res. I* 53, 62–75. doi: 10.1016/j.dsr.2005.07.005
- Yoon, J., Jang, J. H., and Kasai, H. (2014). *Algisiaphaera agarilytica* gen. nov., sp. nov., a novel representative of the class Phycisphaerae within the phylum Planctomycetes isolated from a marine alga. *Antonie Van Leeuwenhoek* 105, 317–324. doi: 10.1007/s10482-013-0076-1
- Zeng, Y. X., Yan, M., Yu, Y., Li, H. R., He, J. F., Sun, K., et al. (2013). Diversity of bacteria in surface ice of Austre Lovénbreen glacier, Svalbard. *Arch. Microbiol.* 195, 313–322. doi: 10.1007/s00203-013-0880-z
- Zhang, W., Wu, X., Liu, G., Chen, T., Zhang, G., Dong, Z., et al. (2013). Pyrosequencing reveals bacterial diversity in the rhizosphere of three *Phragmites australis* ecotypes. *Geomicrobiol. J.* 30, 593–599. doi: 10.1080/01490451.2012.740145
- Zhao, Z., Luo, K., Chen, G., Yang, Y., Mao, Z., Liu, E., et al. (2010). Analysis of bacterial diversity in rhizosphere of cucumber in greenhouse by the methods of metagenomic end-random sequencing and 16S rDNA technology. *Shengtai Xuebao/Acta Ecologica Sinica* 30, 3849–3857.
- Zhu, P., Li, Q., and Wang, G. (2008). Unique microbial signatures of the alien hawaiian marine sponge *Suberites zeteki*. *Microb. Ecol.* 55, 406–414. doi: 10.1007/s00248-007-9285-3

Conflict of Interest Statement: The authors declare that the research was conducted in the absence of any commercial or financial relationships that could be construed as a potential conflict of interest.

Received: 28 March 2014; accepted: 15 May 2014; published online: 03 June 2014.

Citation: Lage OM and Bondoso J (2014) Planctomycetes and macroalgae, a striking association. *Front. Microbiol.* 5:267. doi: 10.3389/fmicb.2014.00267

This article was submitted to Terrestrial Microbiology, a section of the journal *Frontiers in Microbiology*.

Copyright © 2014 Lage and Bondoso. This is an open-access article distributed under the terms of the Creative Commons Attribution License (CC BY). The use, distribution or reproduction in other forums is permitted, provided the original author(s) or licensor are credited and that the original publication in this journal is cited, in accordance with accepted academic practice. No use, distribution or reproduction is permitted which does not comply with these terms.



Plugging in or going wireless: strategies for interspecies electron transfer

Pravin Malla Shrestha^{1,2 *} and Amelia-Elena Rotaru³

¹ Department of Microbiology, University of Massachusetts, Amherst, MA, USA

² Energy Biosciences Institute, University of California, Berkeley, CA, USA

³ Nordic Center for Earth Evolution, University of Southern Denmark, Odense, Denmark

Edited by:

Luis Raul Comolli, Lawrence Berkeley National Laboratory, USA

Reviewed by:

Wei Shi, North Carolina State University, USA

Rizlan Bernier-Latmani, École Polytechnique Fédérale de Lausanne, Switzerland

***Correspondence:**

Pravin Malla Shrestha, Energy Biosciences Institute, University of California, Berkeley, CA 94704, USA
e-mail: pravin@berkeley.edu

Interspecies exchange of electrons enables a diversity of microbial communities to gain energy from reactions that no one microbe can catalyze. The first recognized strategies for interspecies electron transfer were those that relied on chemical intermediates that are recycled through oxidized and reduced forms. Well-studied examples are interspecies H₂ transfer and the cycling of sulfur intermediates in anaerobic photosynthetic communities. Direct interspecies electron transfer (DIET) in which two species establish electrical contact is an alternative. Electrical contacts documented to date include electrically conductive pili, as well as conductive iron minerals and conductive carbon moieties such as activated carbon and biochar. Interspecies electron transfer is central to the functioning of methane-producing microbial communities. The importance of interspecies H₂ transfer in many methanogenic communities is clear, but under some circumstances DIET predominates. It is expected that further mechanistic studies and broadening investigations to a wider range of environments will help elucidate the factors that favor specific forms of interspecies electron exchange under different environmental conditions.

Keywords: syntrophy, diet, interspecies electron transfer, conductive pili, coculture

INTRODUCTION

Interspecies electron transfer plays a key role in the functioning of methane-producing microbial communities, which have a significant impact on the global carbon cycle (Stams and Plugge, 2009; Sieber et al., 2012). Organic matter mineralization to methane by microbial processes contributes to 69% of the atmospheric CH₄ (Conrad, 2009) and it involves four major steps (Figure 1A):

(1) Hydrolytic bacteria break down complex compounds such as polysaccharides, proteins, nucleic acids, and lipids to monomeric substances (Schink and Stams, 2013), (2) Primary fermenters convert monomeric substances to H₂/formate, CO₂ and small organic molecules such as lactate, succinate, fatty acids, and acetate (Morris et al., 2013; Schink and Stams, 2013), (3) Syntrophic bacteria carryout secondary fermentation of small organic molecules to produce acetate, formate, H₂ and CO₂ (Morris et al., 2013; Schink and Stams, 2013), or releases electrons for direct electric connections (Summers et al., 2010; Rotaru et al., 2014), (4) Methanogenic Archaea uses electrons from H₂/formate/shuttles or directly to reduce CO₂ to CH₄ (Morris et al., 2013; Rotaru et al., 2014; Sieber et al., 2014).

Interspecies electron transfer via H₂/formate has been extensively reviewed in recent years (Morris et al., 2013; Schink and Stams, 2013; Sieber et al., 2014). Besides, H₂/formate, there are many important mechanisms of interspecies electron transfer reported, which include but are not limited to pili mediated direct interspecies electron transfer (DIET; Summers et al., 2010; Morita et al., 2011; Nagarajan et al., 2013; Shrestha et al., 2013a,b; Rotaru et al., 2014) and mineral mediated direct interspecies

electron transfer (Kato et al., 2012a,b; Liu et al., 2012, 2014; Chen et al., 2014), or by shuttle molecules like cysteine (Kaden et al., 2002), sulfur compounds (Biebl and Pfennig, 1978; Milucka et al., 2012), and humics (Lovley et al., 1999; Liu et al., 2012). This review discusses recent findings on interspecies electron transfer during syntrophic interactions, with the main focus on DIET mechanisms.

H₂ AND FORMATE AS ELECTRON TRANSFER MOLECULES

H₂ and formate are important electron transfer molecules that are reported in various methanogenic environments (Schink and Stams, 2006, 2013; Stams and Plugge, 2009), these are described briefly under separate headings below:

H₂ AS ELECTRON TRANSFER MOLECULE

Interspecies electron transfer via H₂ was first demonstrated almost four decades ago in a defined co-culture (Bryant et al., 1967) of the “S organism,” which converted ethanol to acetate and H₂, only in the presence of *Methanobacterium ruminantium*, which consumed H₂ for the reduction of CO₂ to CH₄ (Bryant et al., 1967). H₂ is a very powerful electron donor under anoxic conditions and must be continuously removed by partner organism in order for the syntrophic interaction to take place (Nedwell and Banat, 1981; Lovley and Ferry, 1985; Kleerebezem et al., 1999; Wintermute and Silver, 2010). The generation of H₂ is energetically unfavorable at H₂ partial pressures above 10⁻³ bar (Schink and Stams, 2013), however, syntrophic microorganisms bypass this energetic barrier by coupling the unfavorable H₂ production with

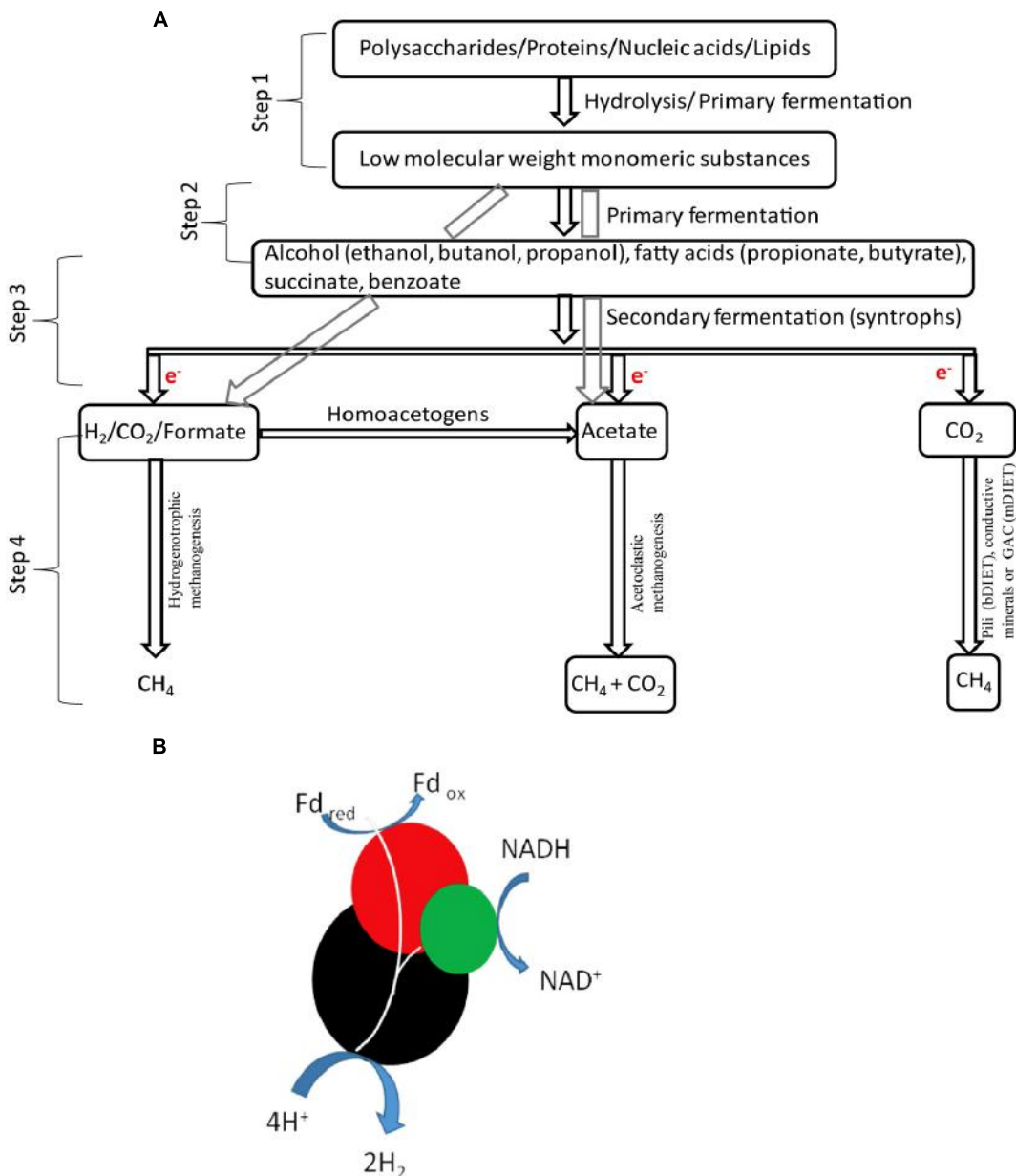


FIGURE 1 | Organic matter degradation in methanogenic environments (A). Sketch of the coupling of H_2 with the energetically favorable oxidation of a reduced ferredoxin in the presence of putative NADH-linked confurcating hydrogenases [modified from McInerney et al., 2011; (B)].

the energetically favorable oxidation of a reduced compound like ferredoxin (Figure 1B), a process known as electron confurcation (Schut and Adams, 2009; Sieber et al., 2010, 2012). Confurcating hydrogenases are found in the genomes of all H_2 generating syntrophs described to date (Sieber et al., 2010, 2012).

FORMATE AS ELECTRON TRANSFER MOLECULE

Formate is an alternative to H_2 and could also act as an electron carrier between syntrophic partners (Thiele and Zeikus, 1988; Boone et al., 1989; Hattori et al., 2001; de Bok et al., 2004;

Stams et al., 2006; Stams and Plugge, 2009). The use of formate as an electron transfer molecule has been noticed especially in co-cultures thriving on proteins (Zindel et al., 1988) or fatty acids like propionate and butyrate (de Bok et al., 2004; Sousa et al., 2007). Certain communities might favor formate transfer because formate has ca. three times higher diffusion coefficient as compared to H_2 , and allows larger mass transfer to methanogens (Boone et al., 1989). It has been also reported that some syntrophic interactions uses both formate and H_2 to transfer electrons between species (Boone et al., 1989; Dong and Stams, 1995; Stams et al., 2006; Rotaru et al., 2012). This dual mechanism of electron

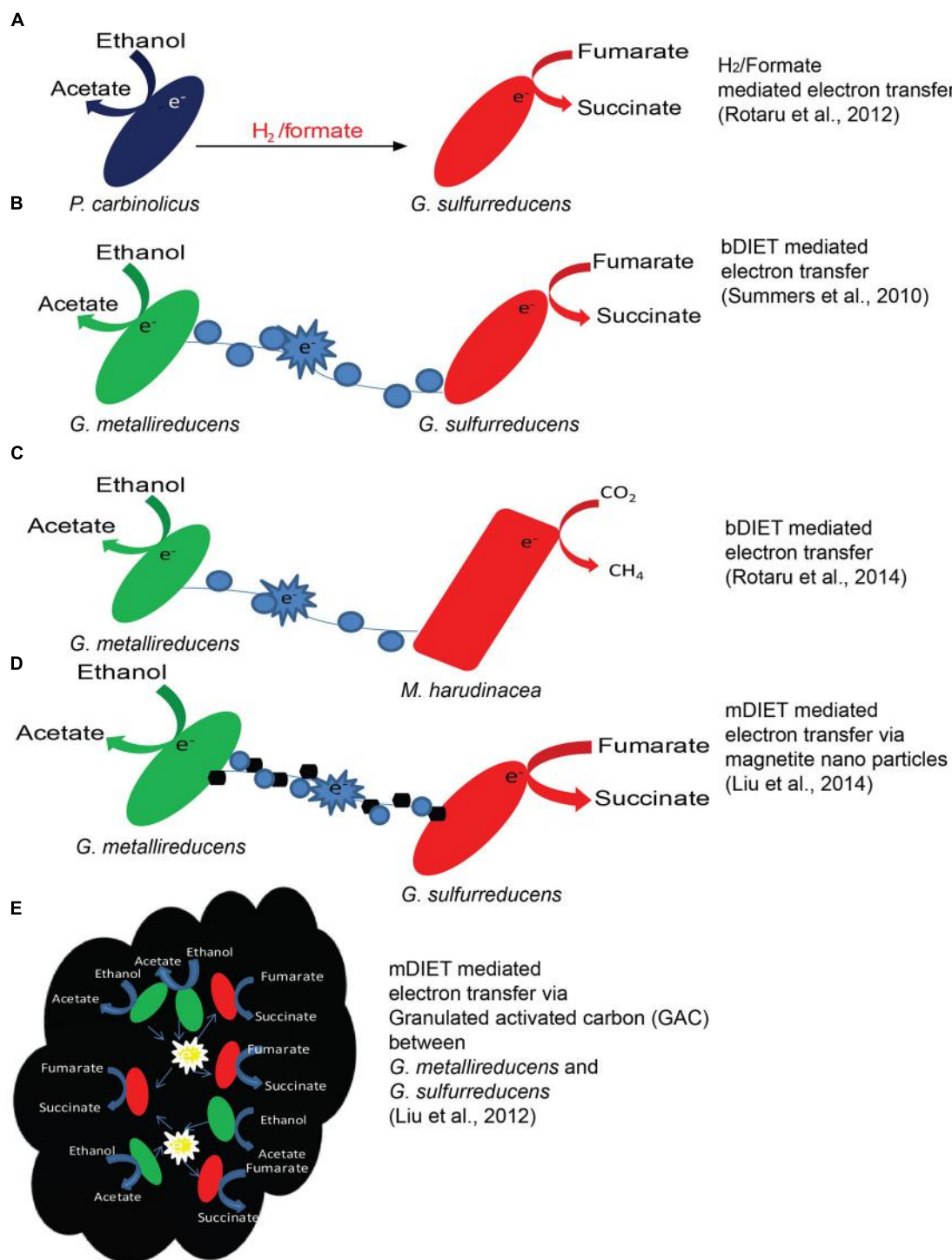


FIGURE 2 | Examples of mechanisms of electron transfer. H_2 transfer between *P. carbinolicus* and *G. sulfurreducens* (**A**), bDIET between *G. metallireducens* and *G. sulfurreducens* (**B**), mineral mediated mDIET between *G. metallireducens* and *G. sulfurreducens* with nano-sized minerals (**D**) or GAC (**E**) in the presence of ethanol as the electron

donor and fumarate as the electron acceptor. DIET in a co-culture of *G. metallireducens* and *Methanosaeta harudinacea* where ethanol was used as electron donor and CO_2 is reduced to CH_4 by *Methanosaeta* using electrons received directly from *G. metallireducens* via bDIET (**C**).

transfer using H₂ and formate (**Figure 2A**) has been studied in detail using deletion mutants, in a co-culture of *Pelobacter carbinolicus* and *Geobacter sulfurreducens* (Rotaru et al., 2012). For example, when a co-culture was established with a hydrogenase mutant (*hybL*) of *G. sulfurreducens*, the formate dehydrogenase (*fdnG*) gene of *G. sulfurreducens* was over-expressed (Rotaru et al., 2012).

ELECTRON TRANSFER VIA SHUTTLE MOLECULES

Electron shuttles are chemical compounds that facilitates the transfer of electrons to and from bacteria these may include sulfur compounds (Biebl and Pfennig, 1978), humic substances (Lovley et al., 1996, 1998, 1999; Newman and Kolter, 2000), and flavins (Marsili et al., 2008; von Canstein et al., 2008; Brutinel and Gralnick, 2012), etc.

SULFUR COMPOUNDS AS MEDIATORS FOR INTERSPECIES ELECTRON TRANSFER

Sulfur compounds as shuttle were first discovered between green sulfur bacteria and sulfate-reducing bacteria (SRB; Biebl and Pfennig, 1978). S(0) is converted to sulfide by a sulfate reducing bacteria and then recycled back to S(0) by a photosynthetic green-sulfur bacteria creating an interspecies S-cycle (Biebl and Pfennig, 1978). The second discovered S-based interspecies interaction used cysteine as electron shuttle between *G. sulfurreducens* and *Wolinella succinogenes*, growing with acetate as electron donor and nitrate as electron acceptor (Kaden et al., 2002). S-compounds were also found responsible for electron transfer between anaerobic methane oxidizing Archaea (ANME) and sulfate reducing bacteria (Boetius et al., 2000), which oxidizes methane with sulfate, one of the most studied, yet least understood interactions. The members of the anaerobic oxidation of methane consortium were initially thought to exchange electrons via methyl-sulfides (Moran et al., 2008), however, more recently the electron carrier within the consortium was revealed to be polysulfides (Milucka et al., 2012).

HUMICS AND HUMICS EQUIVALENTS AS ELECTRON SHUTTLES

Humic substances are ubiquitous in nature (Lovley et al., 1996; Bittner et al., 2007). The humic substance analog, anthraquinone disulphonate (AQDS) serves as an electron shuttles between *G. metallireducens* and *G. sulfurreducens* (Liu et al., 2012), or between *G. metallireducens* and *W. succinogenes* (Lovley et al., 1999). This came as no surprise because it is known that certain microorganisms can use AH₂QDS as electron donor (Lovley et al., 1999), while others use AQDS as electron acceptor (Lovley et al., 1996). However, AQDS cannot mediate electron transfer in *G. metallireducens* and *M. barkeri* co-cultures, likely because of the redox potential of the AQDS couple is too high to reduce carbon (E_{0'} = -184 mV) to reduce carbon dioxide to methane (E_{0'} = -240 mV; Liu et al., 2012).

FLAVINS AS ELECTRON SHUTTLES

Flavins were also noted to improve electron transfer to electrodes in *Shewanella* biofilms (Marsili et al., 2008; von Canstein et al., 2008; Brutinel and Gralnick, 2012) yet their impact on interspecies interactions remains to be reported.

DIRECT INTERSPECIES ELECTRON TRANSFER

To clearly distinguish between conductive mineral mediated DIET and direct cell contact DIET, we have subcategorized the pili mediated electron transfer, as biological DIET (bDIET), and the conductive mineral mediated DIET, as mineral DIET (mDIET).

BIOLOGICAL DIET

Biological DIET (**Figures 2B,C**) was first described in *G. metallireducens* and *G. sulfurreducens* co-cultures, growing in a defined minimal medium with ethanol as electron donor and fumarate as electron acceptor (Summers et al., 2010). Tightly associated aggregates were consistently noticed in co-cultures growing via bDIET (Summers et al., 2010; Shrestha et al., 2013a; Rotaru et al., 2014) but not during growth via H₂/formate electron transfer (Rotaru et al., 2012). The mechanism for bDIET in *Geobacter* co-cultures was intensely studied during the past few years, combining phenotypic, genetic, transcriptomics, proteomics analysis (Summers et al., 2010; Shrestha et al., 2013a,b). bDIET might be favored over H₂ or formate transfer under certain conditions (Lovley, 2011) as demonstrated using genome-scale models including genomic, transcriptomic and physiological data (Nagarajan et al., 2013). The absence of H₂/formate mediated electron transfer in the co-culture was best shown by the ability of *G. metallireducens* to generate successful syntrophic co-cultures with a double mutant of *G. sulfurreducens* ($\Delta hybL\Delta fdnG$) incapable of H₂ or formate uptake (Rotaru et al., 2012). Furthermore, bDIET is seemingly capable to produce successful co-cultures in the absence of acetate transfer as supportive mechanism of electron exchange as revealed in a recent study (Shrestha et al., 2013a) in co-cultures of *G. metallireducens* with strain of *G. sulfurreducens* depleted in acetate utilization capacity, a citrate synthase mutant ($\Delta gltA$; Ueki and Lovley, 2010). This study clearly revealed that bDIET alone is sufficient for energy conservation in syntrophic co-cultures.

Biological DIET interactions with fumarate as terminal electron acceptors are probably not ecologically relevant, but more recently bDIET was discovered in co-cultures of *G. metallireducens* with *Methanosaeta harudinacea* (Rotaru et al., 2014). These two genera of methanogens are responsible for the majority of methane emission in environments such as paddy soils (Grosskopf et al., 1998; Feng et al., 2013) or anaerobic digesters (Vavilin et al., 2008; Morita et al., 2011; Rotaru et al., 2014; Ying et al., 2014). Only these acetoclastic methanogens were capable of bDIET-interactions with *G. metallireducens*, whereas hydrogenotrophic methanogens were not (Rotaru et al., 2014). *Methanosaeta* was shown to use electrons directly for the reduction of CO₂ to methane because the methanogen converted 1/3 of the ¹⁴C-bicarbonate to ¹⁴C methane (Rotaru et al., 2014). Other shuttles were excluded as electron transferring mechanisms because a pili-deficient *G. metallireducens* could not produce successful co-cultures with *Methanosaeta* or *Methanosarcina* (Rotaru et al., 2014).

Role of pili in bDIET

Pili are known to have an important role in biofilm formation (Moreira et al., 2006; Reguera et al., 2007; Oxaran et al., 2012; Snider et al., 2012), but also for the conductive properties of *Geobacter* biofilms (Summers et al., 2010; Malvankar

et al., 2011; Malvankar and Lovley, 2012, 2014; Vargas et al., 2013). Co-cultures do not grow when initiated with a strain of either *G. metallireducens* (Summers et al., 2010) or *G. sulfurreducens* (Rotaru et al., 2014) in which the gene for PilA is deleted, confirming the importance of conductive pili (Reguera et al., 2005, 2006; Lovley, 2011; Malvankar et al., 2011) networks for bDIET. It has been proposed that the stacking of $\pi-\pi$ orbitals of five aromatic amino-acids in the carboxyl-terminus of PilA, the pilin monomer, contribute to the metallic-like conductivity similar to that of conductive organic polymers (Vargas et al., 2013). A *G. sulfurreducens* strain deficient in the five aromatic amino acids (ARO5), the pili were still produced with properly localized OmcS and yet the biofilms of ARO5 showed greatly diminished conductivity (Vargas et al., 2013). In another study, the gene for conductive pili in *G. sulfurreducens* was replaced with the non-conductive *pilA* gene of *Pseudomonas aeruginosa* PAO1 (Liu et al., 2013) generating a mutant strain PAO1, which can express properly assembled *P. aeruginosa* pili ornamented by outer surface c-type cytochromes. However, PAO1 biofilms had significantly lower conductivity than wild type *G. sulfurreducens* and was unable to reduce Fe^{3+} -oxides or produce current (Liu et al., 2013). The lack of conductivity in PAO1 biofilms indicates that three out of five aromatic amino acids at the C-terminus domain are necessary for conductivity (Liu et al., 2013). These findings validated that OmcS alone on scaffold-pili is insufficient to confer conductivity to *Geobacter* biofilms, in contrast to a recent hypothesis, which suggested that conductivity is the result of electron-hopping via cytochromes aligned on the pili of *G. sulfurreducens* (Strycharz-Glaven et al., 2011).

Role of cytochromes in bDIET

Geobacter sulfurreducens was used as model organism for the study of extracellular electron transfer, and several studies revealed that besides pili, *G. sulfurreducens* require a multitude of extracellular and periplasmic cytochromes for insoluble Fe^{3+} oxide reduction (Lloyd et al., 2003; Butler et al., 2004; Qian et al., 2007, 2011; Aklujkar et al., 2009; Lovley et al., 2011; Lovley, 2012), current production (Nevin et al., 2009; Inoue et al., 2010), or current uptake on electrodes (Holmes et al., 2006; Strycharz et al., 2011). However, there are slight differences in the types of cytochromes expressed during growth in electron-donating and electron up-taking modes (Strycharz et al., 2011).

Geobacter sulfurreducens growing via bDIET with *G. metallireducens* highly expresses an extracellular c-type cytochrome, OmcS (Summers et al., 2010; Shrestha et al., 2013a,b). OmcS decorates the pili of *G. sulfurreducens* (Leang et al., 2010; Summers et al., 2010) and is required for bDIET and Fe^{3+} reduction (Mehta et al., 2005; Ding et al., 2008; Qian et al., 2011) but not for current production (Nevin et al., 2009). OmcS is not necessary while growing via H_2 interspecies transfer with *P. carbinolicus* (Rotaru et al., 2012).

Another extracellular cytochrome OmcZ, which helps *G. sulfurreducens* achieve high current densities in single species biofilms (Nevin et al., 2009; Richter et al., 2009), was not required for bDIET in *G. sulfurreducens* – *G. metallireducens* co-cultures (Shrestha et al., 2013b) or during iron oxide reduction (Nevin et al., 2009).

There is no correspondence between the well studied extracellular cytochromes in *G. sulfurreducens* and *G. metallireducens*, and today we have yet no clear understanding, about the exact role of each cytochrome in *G. metallireducens* during extracellular electron transfer processes. And yet it must be noted that extracellular cytochrome like OmcS in the electron acceptor strain, *G. sulfurreducens* were highly relevant for the interspecies association. How exactly they aid the electron transfer process is yet to be uncovered.

bDIET in environmental communities

The possible existence of bDIET in the natural ecosystem was first reported by Morita et al. (2011), while studying the mechanism of interspecies electron exchange in the natural methanogenic communities that formed conductive aggregates in a simulated anaerobic wastewater digester converting brewery wastes to methane. The microbial community structure in up-flow anaerobic sludge blanket digester aggregates showed the predominance of *Geobacter* spp. (Morita et al., 2011; Rotaru et al., 2014). It is interesting to note that in most of the methanogenic environments where bDIET is reported, *Geobacter* spp. are abundant (Kato et al., 2012a; Aulenta et al., 2013; Zhou et al., 2013a; Rotaru et al., 2014), which is probably because *Geobacter* spp. form conductive networks using pili (Malvankar et al., 2011; Malvankar and Lovley, 2012) and transfer electrons to methanogens such as *Methanosaeta* (Morita et al., 2011; Rotaru et al., 2014). Similar species abundance has also been reported in enrichment culture converting coal to methane, where *Geobacter* and *Methanosaeta* were the dominant genera (Jones et al., 2010) possibly using coal as an electron donor and an electron transfer mediator.

MINERAL MEDIATED DIET (mDIET)

The need to produce biological conductive molecular networks can be averted by the addition of conductive minerals (Liu et al., 2012, 2014). mDIET could take place via non-biological conductive networks of semi-conductive minerals (**Figures 2D,E**) like nano-magnetite (Kato et al., 2012a,b; Liu et al., 2014), granulated activated carbon (GAC; Liu et al., 2012) or biochar (Chen et al., 2014) in the absence of molecular conduits.

For example, electrically conductive magnetite nano-particles facilitate mDIET from *G. sulfurreducens* to *Thiobacillus denitrificans*, accomplishing acetate oxidation coupled to nitrate reduction (Kato et al., 2012b). Recently, magnetite nano-particles were shown to compensate for the absence of OmcS on the pili of a deficient *G. sulfurreducens* co-cultured with *G. metallireducens* in the presence of ethanol and fumarate (Liu et al., 2014; **Figure 2D**). Another conductive material, GAC promotes mDIET, bypassing biologically produced electrical conduits (Liu et al., 2012), as evident from the ability to restore syntrophic metabolism in co-cultures deficient in pili or cytochromes (Liu et al., 2012).

mDIET in environmental communities

Although extracellular appendages are required for the respiration of extracellular electron acceptors (Reguera et al., 2005; Tremblay et al., 2012), they can be replaced with conductive materials which can mediate electron transfer between cells during mDIET. Naturally occurring minerals could offer ecological advantages

because of their abundance in natural ecosystems (Kato et al., 2012b), where they could aid mDIET in the absence of pre-evolved molecular conduits. Iron is one of the most ubiquitous metals in Earth's crust (Braunschweig et al., 2013) and could act as conductive mediator for mDIET, demanding less energetic investment from the species exchanging electrons because there would be no need to produce extracellular components for biological electrical connections (Kato et al., 2012b). For example, magnetite, a conductive iron (II&III)-oxide, stimulated methane production in rice paddy soils and enriched for *Geobacter* and *Methanosaerina* species, which likely exchanged electrons via magnetite minerals (Kato et al., 2012a; Zhou et al., 2013b). Electrically conductive magnetite (Fe_3O_4) nano-particles could also enhance reductive dechlorination of trichloroethane, an ubiquitous groundwater pollutant, by allowing electrons to be transferred extracellular from acetate oxidizing microorganisms to trichloroethane dechlorinating microorganisms (Aulenta et al., 2013). In this study the abundant microorganisms were also *Geobacter* spp., which accounted for 50% of the total bacterial population (Aulenta et al., 2013).

Similarly, it has been reported that poorly crystalline akaganeite (β -polymorph of FeOOH) enhanced mDIET to methanogens in slurries from river sediments (Jiang et al., 2013). In such slurries, *Clostridium* coupled Fe^{3+} -akaganeite reduction to Fe^{2+} with acetate oxidation. Partly, electrons from Fe^{2+} were used by the methanogen to convert bicarbonate to methane. Partly, Fe^{2+} ions were re-adsorbed onto akaganeite nano-rods, followed by re-precipitation as structural Fe^{3+} with the simultaneous formation of goethite (α -polymorph of FeOOH) nanofibres (Jiang et al., 2013).

Anthraquinone disulphonate was also suggested to facilitate mDIET between *Geobacter* spp. and *Methanosaerina* spp. in rice paddies (Zhou et al., 2013b). The impact of AQDS on methanogenesis is in contrast with studies in defined co-cultures of *Geobacter* and *Methanosaerina* (Liu et al., 2012). However, soils are not well-defined systems, and it is possible that in soil other interactions happen between humics and soil components, which should be further investigated.

IMPLICATIONS

The electron exchange between syntrophic partners growing together by bDIET requires cells to develop efficient conductive biological contacts via pili and cytochromes in the absence of conductive mediators (mDIET). However, little is known about the importance of bDIET/mDIET-based interactions in the environment or in man-made systems. A better understanding could help devise better strategies for wastewater digestion, or to control methane emission in environments where such emission are high, like landfills, or rice paddies.

ACKNOWLEDGMENTS

We would like to thank Prof. Derek R. Lovley for reading manuscript and providing valuable suggestions. Pravin Malla Shrestha was supported by U.S. Department of Energy grant no. DESC0004485. Amelia-Elena Rotaru was supported by a FNU grant no. DFF-1325-00025 awarded by the Danish Research Council.

REFERENCES

- Aklujkar, M., Krushkal, J., Dibartolo, G., Lapidus, A., Land, M. L., and Lovley, D. R. (2009). The genome sequence of *Geobacter metallireducens*: features of metabolism, physiology and regulation common and dissimilar to *Geobacter sulfurreducens*. *BMC Microbiol.* 9:109. doi: 10.1186/1471-2180-9-109
- Aulenta, F., Rossetti, S., Amalfitano, S., Majone, M., and Tandoi, V. (2013). Conductive magnetite nanoparticles accelerate the microbial reductive dechlorination of trichloroethene by promoting interspecies electron transfer processes. *ChemSusChem* 6, 433–436. doi: 10.1002/cssc.201200748
- Biebl, H., and Pfennig, N. (1978). Growth yields of green sulfur bacteria in mixed cultures with sulfur and sulfate reducing bacteria. *Arch. Microbiol.* 117, 9–16. doi: 10.1007/Bf00689344
- Bittner, M., Hilscherova, K., and Giesy, J. P. (2007). Changes of AhR-mediated activity of humic substances after irradiation. *Environ. Int.* 33, 812–816. doi: 10.1016/j.envint.2007.03.011
- Boetius, A., Ravenschlag, K., Schubert, C. J., Rickert, D., Widdel, F., Gieseke, A., et al. (2000). A marine microbial consortium apparently mediating anaerobic oxidation of methane. *Nature* 407, 623–626. doi: 10.1038/35036572
- Boone, D. R., Johnson, R. L., and Liu, Y. (1989). Diffusion of the interspecies electron carriers H-2 and formate in methanogenic ecosystems and its implications in the measurement of Km for H-2 or formate uptake. *Appl. Environ. Microbiol.* 55, 1735–1741.
- Braunschweig, J., Bosch, J., and Meckenstock, R. U. (2013). Iron oxide nanoparticles in geomicrobiology: from biogeochemistry to bioremediation. *N. Biotechnol.* 30, 793–802. doi: 10.1016/j.nbt.2013.03.008
- Brutinel, E. D., and Gralnick, J. A. (2012). Shutting happens: soluble flavin mediators of extracellular electron transfer in *Shewanella*. *Appl. Microbiol. Biotechnol.* 93, 41–48. doi: 10.1007/s00253-011-3653-0
- Bryant, M. P., Wolin, E. A., Wolin, M. J., and Wolfe, R. S. (1967). *Methanobacillus omelianskii*, a symbiotic association of two species of bacteria. *Arch. Mikrobiol.* 59, 20–31. doi: 10.1007/BF00406313
- Butler, J. E., Kaufmann, F., Coppi, M. V., Nunez, C., and Lovley, D. R. (2004). MacA, a diheme c-type cytochrome involved in Fe(III) reduction by *Geobacter sulfurreducens*. *J. Bacteriol.* 186, 4042–4045. doi: 10.1128/JB.186.12.4042-4045.2004
- Chen, S., Rotaru, A.-E., Shrestha, P. M., Malvankar, N., Liu, F., Fan, W., et al. (2014). Promoting interspecies electron transfer with biochar. *Sci. Rep.* (in press).
- Conrad, R. (2009). The global methane cycle: recent advances in understanding the microbial processes involved. *Environ. Microbiol. Rep.* 1, 285–292. doi: 10.1111/j.1758-2229.2009.00038.x
- de Bok, F. A., Plugge, C. M., and Stams, A. J. (2004). Interspecies electron transfer in methanogenic propionate degrading consortia. *Water Res.* 38, 1368–1375. doi: 10.1016/j.watres.2003.11.028
- Ding, Y. H. R., Hixson, K. K., Aklujkar, M. A., Lipton, M. S., Smith, R. D., Lovley, D. R., et al. (2008). Proteome of *Geobacter sulfurreducens* grown with Fe(III) oxide or Fe(III) citrate as the electron acceptor. *Biochim. Biophys. Acta* 1784, 1935–1941. doi: 10.1016/j.bbapap.2008.06.011
- Dong, X., and Stams, A. J. (1995). Evidence for H₂ and formate formation during syntrophic butyrate and propionate degradation. *Anaerobe* 1, 35–39. doi: 10.1016/S1075-9964(95)80405-6
- Feng, Y., Lin, X., Yu, Y., Zhang, H., Chu, H., and Zhu, J. (2013). Elevated ground-level O₃ negatively influences paddy methanogenic archaeal community. *Sci. Rep.* 3, 3193. doi: 10.1038/srep03193
- Grosskopf, R., Janssen, P. H., and Liesack, W. (1998). Diversity and structure of the methanogenic community in anoxic rice paddy soil microcosms as examined by cultivation and direct 16S rRNA gene sequence retrieval. *Appl. Environ. Microbiol.* 64, 960–969.
- Hattori, S., Luo, H., Shoun, H., and Kamagata, Y. (2001). Involvement of formate as an interspecies electron carrier in a syntrophic acetate-oxidizing anaerobic microorganism in coculture with methanogens. *J. Biosci. Bioeng.* 91, 294–298.
- Holmes, D. E., Chaudhuri, S. K., Nevin, K. P., Mehta, T., Methe, B. A., Liu, A., et al. (2006). Microarray and genetic analysis of electron transfer to electrodes in *Geobacter sulfurreducens*. *Environ. Microbiol.* 8, 1805–1815. doi: 10.1111/j.1462-2920.2006.01065.x
- Inoue, K., Qian, X., Morgado, L., Kim, B. C., Mester, T., Izallalen, M., et al. (2010). Purification and characterization of OmcZ, an outer-surface, octaheme c-type cytochrome essential for optimal current production by *Geobacter sulfurreducens*. *Appl. Environ. Microbiol.* 76, 3999–4007. doi: 10.1128/AEM.00027-10

- Jiang, S., Park, S., Yoon, Y., Lee, J. H., Wu, W. M., Phuoc Dan, N., et al. (2013). Methanogenesis facilitated by geobiochemical iron cycle in a novel syntrophic methanogenic microbial community. *Environ. Sci. Technol.* 47, 10078–10084. doi: 10.1021/es402412c
- Jones, E. J. P., Voytek, M. A., Corum, M. D., and Orem, W. H. (2010). Stimulation of methane generation from nonproductive coal by addition of nutrients or a microbial consortium. *Appl. Environ. Microbiol.* 76, 7013–7022. doi: 10.1128/Aem.00728-10
- Kaden, J., Galushko, A. S., and Schink, B. (2002). Cysteine-mediated electron transfer in syntrophic acetate oxidation by cocultures of *Geobacter sulfurreducens* and *Wolinella succinogenes*. *Arch. Microbiol.* 178, 53–58. doi: 10.1007/s00203-002-0425-3
- Kato, S., Hashimoto, K., and Watanabe, K. (2012a). Methanogenesis facilitated by electric syntropy via (semi)conductive iron-oxide minerals. *Environ. Microbiol.* 14, 1646–1654. doi: 10.1111/j.1462-2920.2011.02611.x
- Kato, S., Hashimoto, K., and Watanabe, K. (2012b). Microbial interspecies electron transfer via electric currents through conductive minerals. *Proc. Natl. Acad. Sci. U.S.A.* 109, 10042–10046. doi: 10.1073/pnas.1117592109
- Kleerebezem, R., Hulshoff Pol, L. W., and Lettinga, G. (1999). Anaerobic degradation of phthalate isomers by methanogenic consortia. *Appl. Environ. Microbiol.* 65, 1152–1160.
- Leang, C., Qian, X. L., Mester, T., and Lovley, D. R. (2010). Alignment of the c-type cytochrome Omcs along pili of *Geobacter sulfurreducens*. *Appl. Environ. Microbiol.* 76, 4080–4084. doi: 10.1128/Aem.00023-10
- Liu, F. H., Rotaru, A.-E., Shrestha, P. M., Malvankar, N. S., Nevin, K. P., and Lovley, D. R. (2012). Promoting direct interspecies electron transfer with activated carbon. *Energy Environ. Sci.* 5, 8982–8989. doi: 10.1039/C2ee22459c
- Liu, F., Rotaru, A.-E., Shrestha, P. M., Malvankar, N. S., Nevin, K., and Lovley, D. (2014). Magnetite compensates for the lack of a pilin-associated c-type cytochrome in extracellular electron exchange. *Environ. Microbiol.* doi: 10.1111/1462-2920.12485 [Epub ahead of print].
- Liu, X., Tremblay, P. L., Malvankar, N. S., Nevin, K. P., Lovley, D. R., and Vargas, M. (2013). *Geobacter sulfurreducens* strain expressing *Pseudomonas aeruginosa* type IV pili localizes Omcs on pili but is deficient in Fe(III) oxide reduction and current production. *Appl. Environ. Microbiol.* 80, 1219–1224. doi: 10.1128/AEM.0293813
- Lloyd, J. R., Leang, C., Hodges Myerson, A. L., Coppi, M. V., Cuiffo, S., Methe, B., et al. (2003). Biochemical and genetic characterization of PpcA, a periplasmic c-type cytochrome in *Geobacter sulfurreducens*. *Biochem. J.* 369, 153–161. doi: 10.1042/BJ20020597
- Lovley, D. R. (2011). Live wires: direct extracellular electron exchange for bioenergy and the bioremediation of energy-related contamination. *Energy Environ. Sci.* 4, 4896–4906. doi: 10.1039/C1ee02229f
- Lovley, D. R. (2012). Long-range electron transport to Fe(III) oxide via pili with metallic-like conductivity. *Biochem. Soc. Trans.* 40, 1186–1190. doi: 10.1042/BST20120131
- Lovley, D. R., Coates, J. D., Bluntharris, E. L., Phillips, E. J. P., and Woodward, J. C. (1996). Humic substances as electron acceptors for microbial respiration. *Nature* 382, 445–448. doi: 10.1038/382445a0
- Lovley, D. R., and Ferry, J. G. (1985). Production and consumption of H₂ during growth of *Methanosarcina* spp. on acetate. *Appl. Environ. Microbiol.* 49, 247–249.
- Lovley, D. R., Fraga, J. L., Blunt-Harris, E. L., Hayes, L. A., Phillips, E. J. P., and Coates, J. D. (1998). Humic substances as a mediator for microbially catalyzed metal reduction. *Acta Hydrochim. Hydrobiol.* 26, 152–157. doi: 10.1002/(Sici)1521-401x(199805)26:3<152::Aid-Aheh152>3.0.co;2-d
- Lovley, D. R., Fraga, J. L., Coates, J. D., and Blunt-Harris, E. L. (1999). Humics as an electron donor for anaerobic respiration. *Environ. Microbiol.* 1, 89–98. doi: 10.1046/j.1462-2920.1999.00009.x
- Lovley, D. R., Ueki, T., Zhang, T., Malvankar, N. S., Shrestha, P. M., Flanagan, K. A., et al. (2011). *Geobacter*: the microbe electric's physiology, ecology, and practical applications. *Adv. Microb. Physiol.* 59, 1–100. doi: 10.1016/B978-0-12-387661-4.00004-5
- Malvankar, N. S., and Lovley, D. R. (2012). Microbial nanowires: a new paradigm for biological electron transfer and bioelectronics. *ChemSusChem* 5, 1039–1046. doi: 10.1002/cssc.201100733
- Malvankar, N. S., and Lovley, D. R. (2014). Microbial nanowires for bioenergy applications. *Curr. Opin. Biotechnol.* 27, 88–95. doi: 10.1016/j.copbio.2013.12.003
- Malvankar, N. S., Vargas, M., Nevin, K. P., Franks, A. E., Leang, C., Kim, B. C., et al. (2011). Tunable metallic-like conductivity in microbial nanowire networks. *Nat. Nanotechnol.* 6, 573–579. doi: 10.1038/nnano.2011.119
- Marsili, E., Baron, D. B., Shikhare, I. D., Coursolle, D., Gralnick, J. A., and Bond, D. R. (2008). *Shewanella* secretes flavins that mediate extracellular electron transfer. *Proc. Natl. Acad. Sci. U.S.A.* 105, 3968–3973. doi: 10.1073/pnas.0710525105
- McInerney, M. J., Sieber, J. R., and Gunsalus, R. P. (2011). Microbial syntropy: ecosystem-level biochemical cooperation. *Microbe* 6, 479–485.
- Mehta, T., Coppi, M. V., Childers, S. E., and Lovley, D. R. (2005). Outer membrane c-type cytochromes required for Fe(III) and Mn(IV) oxide reduction in *Geobacter sulfurreducens*. *Appl. Environ. Microbiol.* 71, 8634–8641. doi: 10.1128/Aem.71.12.8634-8641.2005
- Milucka, J., Ferdelman, T. G., Polerecky, L., Franzke, D., Wegener, G., Schmid, M., et al. (2012). Zero-valent sulphur is a key intermediate in marine methane oxidation. *Nature* 491, 541–546. doi: 10.1038/Nature11656
- Moran, J. J., Beal, E. J., Vrentas, J. M., Orphan, V. J., Freeman, K. H., and House, C. H. (2008). Methyl sulfides as intermediates in the anaerobic oxidation of methane. *Environ. Microbiol.* 10, 162–173. doi: 10.1111/j.1462-2920.2007.01441.x
- Moreira, C. G., Palmer, K., Whiteley, M., Sircili, M. P., Trabulsi, L. R., Castro, A. F. P., et al. (2006). Bundle-forming pili and EspA are involved in biofilm formation by enteropathogenic *Escherichia coli*. *J. Bacteriol.* 188, 3952–3961. doi: 10.1128/Jb.00177-06
- Morita, M., Malvankar, N. S., Franks, A. E., Summers, Z. M., Giloteaux, L., Rotaru, A.-E., et al. (2011). Potential for direct interspecies electron transfer in methanogenic wastewater digester aggregates. *MBio* 2, e00159–e00111. doi: 10.1128/mBio.00159-11
- Morris, B. E., Henneberger, R., Huber, H., and Moissl-Eichinger, C. (2013). Microbial syntropy: interaction for the common good. *FEMS Microbiol. Rev.* 37, 384–406. doi: 10.1111/1574-6976.12019
- Nagarajan, H., Embree, M., Rotaru, A.-E., Shrestha, P. M., Feist, A. M., Palsson, B. O., et al. (2013). Characterization and modelling of interspecies electron transfer mechanisms and microbial community dynamics of a syntrophic association. *Nat. Commun.* 4, 2809. doi: 10.1038/ncomms3809
- Nedwell, D. B., and Banat, I. M. (1981). Hydrogen as an electron-donor for sulfate-reducing bacteria in slurries of salt-marsh sediment. *Microb. Ecol.* 7, 305–313. doi: 10.1007/Bf02341425
- Nevin, K. P., Kim, B. C., Glaven, R. H., Johnson, J. P., Woodard, T. L., Methe, B. A., et al. (2009). Anode biofilm transcriptomics reveals outer surface components essential for high density current production in *Geobacter sulfurreducens* fuel cells. *PLoS ONE* 4:e5628. doi: 10.1371/journal.pone.00005628
- Newman, D. K., and Kolter, R. (2000). A role for excreted quinones in extracellular electron transfer. *Nature* 405, 94–97. doi: 10.1038/35011098
- Oxaran, V., Ledue-Clier, F., Dieye, Y., Herry, J. M., Pechoux, C., Meylheuc, T., et al. (2012). Pilus biogenesis in *Lactococcus lactis*: molecular characterization and role in aggregation and biofilm formation. *PLoS ONE* 7:e50989. doi: 10.1371/journal.pone.0050989
- Qian, X. L., Mester, T., Morgado, L., Arakawa, T., Sharma, M. L., Inoue, K., et al. (2011). Biochemical characterization of purified Omcs, a c-type cytochrome required for insoluble Fe(III) reduction in *Geobacter sulfurreducens*. *Biochim. Biophys. Acta* 1807, 404–412. doi: 10.1016/j.bbabi.2011.01.003
- Qian, X. L., Reguera, G., Mester, T., and Lovley, D. R. (2007). Evidence that OmcsB and OmpB of *Geobacter sulfurreducens* are outer membrane surface proteins. *FEMS Microbiol. Lett.* 277, 21–27. doi: 10.1111/j.1574-6968.2007.00915.x
- Reguera, G., McCarthy, K. D., Mehta, T., Nicoll, J. S., Tuominen, M. T., and Lovley, D. R. (2005). Extracellular electron transfer via microbial nanowires. *Nature* 435, 1098–1101. doi: 10.1038/Nature03661
- Reguera, G., Nevin, K. P., Nicoll, J. S., Covalla, S. F., Woodard, T. L., and Lovley, D. R. (2006). Biofilm and nanowire production leads to increased current in *Geobacter sulfurreducens* fuel cells. *Appl. Environ. Microbiol.* 72, 7345–7348. doi: 10.1128/AEM.01444-06
- Reguera, G., Pollina, R. B., Nicoll, J. S., and Lovley, D. R. (2007). Possible nonconductive role of *Geobacter sulfurreducens* pilus nanowires in biofilm formation. *J. Bacteriol.* 189, 2125–2127. doi: 10.1128/Jb.01284-06
- Richter, H., Nevin, K. P., Jia, H., Lowy, D. A., Lovley, D. R., and Tender, L. M. (2009). Cyclic voltammetry of biofilms of wild type and mutant *Geobacter sulfurreducens* on fuel cell anodes indicates possible roles of OmcsB, OmcsZ, type IV pili, and protons in extracellular electron transfer. *Energy Environ. Sci.* 2, 506–516. doi: 10.1039/b816647a
- Rotaru, A.-E., Shrestha, P. M., Liu, F., Shrestha, M., Shrestha, D., Embree, M., et al. (2014). A new model for electron flow during anaerobic digestion: direct interspecies electron transfer to *Methanosaeta* for the reduction of carbon dioxide to methane. *Energy Environ. Sci.* 7, 408–415. doi: 10.1038/c3ee42189a

- Rotaru, A.-E., Shrestha, P. M., Liu, F., Ueki, T., Nevin, K., Summers, Z. M., et al. (2012). Interspecies electron transfer via hydrogen and formate rather than direct electrical connections in cocultures of *Pelobacter carbinolicus* and *Geobacter sulfurreducens*. *Appl. Environ. Microbiol.* 78, 7645–7651. doi: 10.1128/AEM.01946-12
- Schink, B., and Stams, A. J. M. (2006). *Syntrophism among Prokaryotes*. *Prokaryotes: A Handbook on the Biology of Bacteria*, 3rd Edn, Vol. 2, (New York: Springer Verlag), 309–335.
- Schink, B., and Stams, A. M. (2013). “Syntrophism Among Prokaryotes,” in *The Prokaryotes*, eds E. Rosenberg, E. Delong, S. Lory, E. Stackebrandt, and F. Thompson (New York: Springer Berlin Heidelberg), 471–493.
- Schut, G. J., and Adams, M. W. W. (2009). The iron-hydrogenase of *thermoga maritima* utilizes ferredoxin and NADH synergistically: a new perspective on anaerobic hydrogen production. *J. Bacteriol.* 191, 4451–4457. doi: 10.1128/Jb.01582-08
- Shrestha, P. M., Rotaru, A.-E., Aklujkar, M., Liu, F., Shrestha, M., Summers, Z. M., et al. (2013a). Syntrophic growth with direct interspecies electron transfer as the primary mechanism for energy exchange. *Environ. Microbiol. Rep.* 5, 904–910. doi: 10.1111/1758-2229.12093
- Shrestha, P. M., Rotaru, A.-E., Summers, Z. M., Shrestha, M., Liu, F., and Lovley, D. R. (2013b). Transcriptomic and genetic analysis of direct interspecies electron transfer. *Appl. Environ. Microbiol.* 79, 2397–2404. doi: 10.1128/AEM.03837-12
- Sieber, J. R., Le, H. M., and McInerney, M. J. (2014). The importance of hydrogen and formate transfer for syntrophic fatty, aromatic and alicyclic metabolism. *Environ. Microbiol.* 16, 177–188. doi: 10.1111/1462-2920.12269
- Sieber, J. R., McInerney, M. J., and Gunsalus, R. P. (2012). Genomic insights into syntrophy: the paradigm for anaerobic metabolic cooperation. *Annu. Rev. Microbiol.* 66, 429–452. doi: 10.1146/annurev-micro-090110-102844
- Sieber, J. R., Sims, D. R., Han, C., Kim, E., Lykidis, A., Lapidus, A. L., et al. (2010). The genome of *Syntrophomonas wolfei*: new insights into syntrophic metabolism and biohydrogen production. *Environ. Microbiol.* 12, 2289–2301. doi: 10.1111/j.1462-2920.2010.02237.x
- Snider, R. M., Strycharz-Glaven, S. M., Tsoi, S. D., Erickson, J. S., and Tender, L. M. (2012). Long-range electron transport in *Geobacter sulfurreducens* biofilms is redox gradient-driven. *Proc. Natl. Acad. Sci. U.S.A.* 109, 15467–15472. doi: 10.1073/pnas.1209829109
- Sousa, D. Z., Smidt, H., Alves, M. M., and Stams, A. J. M. (2007). *Syntrophomonas zehnderi* sp nov., an anaerobe that degrades long-chain fatty acids in co-culture with *Methanobacterium formicum*. *Int. J. Syst. Evol. Microbiol.* 57, 609–615. doi: 10.1099/ijss.0.647340
- Stams, A. J., De Bok, F. A., Plugge, C. M., Van Eekert, M. H., Dolfing, J., and Schraa, G. (2006). Exacellular electron transfer in anaerobic microbial communities. *Environ. Microbiol.* 8, 371–382. doi: 10.1111/j.1462-2920.2006.00989.x
- Stams, A. J., and Plugge, C. M. (2009). Electron transfer in syntrophic communities of anaerobic bacteria and archaea. *Nat. Rev. Microbiol.* 7, 568–577. doi: 10.1038/nrmicro2166
- Strycharz-Glaven, S. M., Snider, R. M., Guiseppi-Elie, A., and Tender, L. M. (2011). On the electrical conductivity of microbial nanowires and biofilms. *Energy Environ. Sci.* 4, 4366–4379. doi: 10.1039/c1ee01753e
- Strycharz, S. M., Glaven, R. H., Coppi, M. V., Gannon, S. M., Perpetua, L. A., Liu, A., et al. (2011). Gene expression and deletion analysis of mechanisms for electron transfer from electrodes to *Geobacter sulfurreducens*. *Bioelectrochemistry* 80, 142–150. doi: 10.1016/j.bioelechem.2010.07.005
- Summers, Z. M., Fogarty, H. E., Leang, C., Franks, A. E., Malvankar, N. S., and Lovley, D. R. (2010). Direct exchange of electrons within aggregates of an evolved syntrophic coculture of anaerobic bacteria. *Science* 330, 1413–1415. doi: 10.1126/science.1196526
- Thiele, J. H., and Zeikus, J. G. (1988). Control of interspecies electron flow during anaerobic digestion: significance of formate transfer versus hydrogen transfer during syntrophic methanogenesis in flocs. *Appl. Environ. Microbiol.* 54, 20–29.
- Tremblay, P. L., Aklujkar, M., Leang, C., Nevin, K. P., and Lovley, D. (2012). A genetic system for *Geobacter metallireducens*: role of the flagellin and pilin in the reduction of Fe(III) oxide. *Environ. Microbiol. Rep.* 4, 82–88. doi: 10.1111/j.1758-2229.2011.00305.x
- Ueki, T., and Lovley, D. R. (2010). Genome-wide gene regulation of biosynthesis and energy generation by a novel transcriptional repressor in *Geobacter* species. *Nucleic Acids Res.* 38, 810–821. doi: 10.1093/nar/gkp1085
- Vargas, M., Malvankar, N. S., Tremblay, P. L., Leang, C., Smith, J. A., Patel, P., et al. (2013). Aromatic amino acids required for pili conductivity and long-range extracellular electron transport in *Geobacter sulfurreducens*. *MBio* 4, e00105–e00113. doi: 10.1128/mBio.00105-13
- Vavilin, V. A., Qu, X., Mazeas, L., Lemunier, M., Duquennoi, C., He, P. J., et al. (2008). Methanoscincina as the dominant aceticlastic methanogens during mesophilic anaerobic digestion of putrescible waste. *Antonie Van Leeuwenhoek* 94, 593–605. doi: 10.1007/s10482-008-9279-2
- von Canstein, H., Ogawa, J., Shimizu, S., and Lloyd, J. R. (2008). Secretion of flavins by *Shewanella* species and their role in extracellular electron transfer. *Appl. Environ. Microbiol.* 74, 615–623. doi: 10.1128/Aem.01387-07
- Wintermute, E. H., and Silver, P. A. (2010). Dynamics in the mixed microbial concourse. *Genes Dev.* 24, 2603–2614. doi: 10.1101/gad.1985210
- Ying, Y., Yu, K., Xia, Y., Lau, F. T., Tang, D. T., Fung, W. C., et al. (2014). Metagenomic analysis of sludge from full-scale anaerobic digesters operated in municipal wastewater treatment plants. *Appl. Microbiol. Biotechnol.* doi: 10.1007/s00253-014-5648-0 [Epub ahead of print].
- Zhou, M., Chen, J., Freguia, S., Rabaeij, K., and Keller, J. (2013a). Carbon and electron fluxes during the electricity driven 1,3-propanediol biosynthesis from glycerol. *Environ. Sci. Technol.* 47, 11199–11205. doi: 10.1021/es402132r
- Zhou, S., Xu, J., Yang, G., and Zhuang, L. (2013b). Methanogenesis affected by the co-occurrence of iron(III) oxides and humic substances. *FEMS Microbiol. Ecol.* 88, 107–120. doi: 10.1111/1574-6941.12274
- Zindel, U., Freudenberg, W., Rieth, M., Andreessen, J. R., Schnell, J., and Widdel, F. (1988). *Eubacterium-acidaminophilum* Sp-nov, a versatile amino acid-degrading anaerobe producing or utilizing H-2 or formate – description and enzymatic studies. *Arch. Microbiol.* 150, 254–266. doi: 10.1007/Bf00407789

Conflict of Interest Statement: The authors declare that the research was conducted in the absence of any commercial or financial relationships that could be construed as a potential conflict of interest.

Received: 28 March 2014; accepted: 30 April 2014; published online: 16 May 2014.

Citation: Shrestha PM and Rotaru A-E (2014) Plugging in or going wireless: strategies for interspecies electron transfer. *Front. Microbiol.* 5:237. doi: 10.3389/fmicb.2014.00237

This article was submitted to Terrestrial Microbiology, a section of the journal *Frontiers in Microbiology*.

Copyright © 2014 Shrestha and Rotaru. This is an open-access article distributed under the terms of the Creative Commons Attribution License (CC BY). The use, distribution or reproduction in other forums is permitted, provided the original author(s) or licensor are credited and that the original publication in this journal is cited, in accordance with accepted academic practice. No use, distribution or reproduction is permitted which does not comply with these terms.